ROLE OF PHYTOCHEMICALS AND STRUCTURAL ANALOGS IN CANCER CHEMOPREVENTION AND THERAPEUTICS

EDITED BY: Jamal Arif, Farrukh Aqil and Raghuram Kandimalla

PUBLISHED IN: Frontiers in Pharmacology and Frontiers in Oncology

frontiers Research Topics

ISSN 1664-8714
ISBN 978-2-88974-873-0
DOI 10.3389/978-2-88974-873-0

About Frontiers

Frontiers is more than just an open-access publisher of scholarly articles: it is a pioneering approach to the world of academia, radically improving the way scholarly research is managed. The grand vision of Frontiers is a world where all people have an equal opportunity to seek, share and generate knowledge. Frontiers provides immediate and permanent online open access to all its publications, but this alone is not enough to realize our grand goals.

Frontiers Journal Series

The Frontiers Journal Series is a multi-tier and interdisciplinary set of open-access, online journals, promising a paradigm shift from the current review, selection and dissemination processes in academic publishing. All Frontiers journals are driven by researchers for researchers; therefore, they constitute a service to the scholarly community. At the same time, the Frontiers Journal Series operates on a revolutionary invention, the tiered publishing system, initially addressing specific communities of scholars, and gradually climbing up to broader public understanding, thus serving the interests of the lay society, too.

Dedication to Quality

Each Frontiers article is a landmark of the highest quality, thanks to genuinely collaborative interactions between authors and review editors, who include some of the world's best academicians. Research must be certified by peers before entering a stream of knowledge that may eventually reach the public - and shape society; therefore, Frontiers only applies the most rigorous and unbiased reviews.
Frontiers revolutionizes research publishing by freely delivering the most outstanding research, evaluated with no bias from both the academic and social point of view. By applying the most advanced information technologies, Frontiers is catapulting scholarly publishing into a new generation.

What are Frontiers Research Topics?

Frontiers Research Topics are very popular trademarks of the Frontiers Journals Series: they are collections of at least ten articles, all centered on a particular subject. With their unique mix of varied contributions from Original Research to Review Articles, Frontiers Research Topics unify the most influential researchers, the latest key findings and historical advances in a hot research area! Find out more on how to host your own Frontiers Research Topic or contribute to one as an author by contacting the Frontiers Editorial Office: frontiersin.org/about/contact

ROLE OF PHYTOCHEMICALS AND STRUCTURAL ANALOGS IN CANCER CHEMOPREVENTION AND THERAPEUTICS

Topic Editors:
Jamal Arif, Shaqra University, Saudi Arabia
Farrukh Aqil, University of Louisville, United States
Raghuram Kandimalla, James Graham Brown Cancer Center, United States

Citation: Arif, J., Aqil, F., Kandimalla, R., eds. (2022). Role of Phytochemicals and Structural Analogs in Cancer Chemoprevention and Therapeutics. Lausanne: Frontiers Media SA. doi: 10.3389/978-2-88974-873-0

Table of Contents

frontiers in Pharmacology

EDITORIAL
published: 16 March 2022
doi: 10.3389/fphar.2022.865619

Editorial: Role of Phytochemicals and Structural Analogs in Cancer Chemoprevention and Therapeutics

Jamal M. Arif[1]*, *Raghuram Kandimalla*[2]* and *Farrukh Aqil*[2,3]*

[1]Department of Biochemistry, College of Medicine, Shaqra University, Shaqra, Saudi Arabia, [2]UofL Health—Brown Cancer Center, University of Louisville, Louisville, KY, United States, [3]Department of Medicine, University of Louisville, Louisville, KY, United States

Keywords: phytochemicals, cancer, chemoprevention, structural analogous, chemotherapy—oncology

Editorial on the Research Topic

Editorial: Role of Phytochemicals and Structural Analogs in Cancer Chemoprevention and Therapeutics

Cancer is a multifactorial disease and a leading cause of deaths worldwide. An estimated 1.89 million new cancer cases and about 600,000 cancer related deaths were reported only in United Stated in the year 2021 (Siegel et al., 2021). A systematic and complicated mechanism is involved in the transformation of a normal cell into cancerous form. In human body, most cell functions are controlled by genes through cell growth, signal transduction, protein transcription, cell cycle, apoptosis and DNA repair. While proto-oncogenes are essential for the normal functioning of cells, mutations covert them into oncogenes and lead to uncontrolled cell growth. There are about 40 different proto-oncogenes discovered to date including RAS, HER2, Myc and cyclins. The treatment options for cancers involve surgery followed by chemotherapy and/or radiation. More than 100 chemotherapeutic drugs are in use to treat cancer of different types. However, the efficacy of chemotherapy of cancer is limited by the development of drug resistance and metastatic disease.

Lately, plant bioactives are gaining increased attention for their therapeutic activity against many cancers (nearly 2000 publications per year) as they possess versatile biological properties and target multiple pathways in cancer. Plant-derived compounds have historically led to some of our most useful cancer drugs (e.g., paclitaxel, vincristine, etc.). These chemopreventives can block initiation, reverse promotion and/or halt the progression of precancerous cells into malignant cells. Since advanced, recurrent and metastatic tumors are practically lethal and cannot be cured by any therapy, cancer chemoprevention of earlier lesions should be the definitive goal if we are to eradicate this deadly disease. To fulfil the unmet needs of cancer treatments, a scrupulous repurposing of plant-based phytochemicals such as chemical modification of the pharmacophores, development of target-based delivery strategies including nano formulations, and their uses in adjuvant settings need to be considered. In this regard, we launched the current special issue to highlight the current development in the anticancer drug research.

Most of the chemotherapy treatment failures occur due to drug resistance subsequently limiting its use and available treatment options. Several factors like tumor microenvironment, size, heterogeneity, involvement of immune system and undruggable genes necessitate in evoking the drug resistance (Vasan et al., 2019). For instance, over expression of myeloid cell leukemia 1 (Mcl-1) leads to resistance towards drugs used to treat multiple myeloma. Al-Odat et al. discuss the role of Mcl-1 inhibition in the management of multiple myeloma. They further highlight that the most prominent BH3 mimetic and semi-BH3 mimetic selectively inhibit Mcl-1 and could be used by itself or in combination with existing therapies for the management of multiple myeloma. In another article, Cui et al. showed that the tubulin Inhibitor VERU-111 in combination with vemurafenib, an

OPEN ACCESS

Edited and reviewed by:
Olivier Feron,
Université Catholique de Louvain, Belgium

Correspondence:
Jamal M. Arif
jmarif@gmail.com
Raghuram Kandimalla
raghuram.kandimalla@louisville.edu
Farrukh Aqil
farrukh.aqil@louisville.edu

Specialty section:
This article was submitted to Pharmacology of Anti-Cancer Drugs, a section of the journal Frontiers in Pharmacology

Received: *30 January 2022*
Accepted: *17 February 2022*
Published: *16 March 2022*

Citation:
Arif JM, Kandimalla R and Aqil F (2022) Editorial: Role of Phytochemicals and Structural Analogs in Cancer Chemoprevention and Therapeutics. Front. Pharmacol. 13:865619. doi: 10.3389/fphar.2022.865619

FDA-approved BRAF inhibitor, provides an effective treatment for vemurafenib-resistant A375 melanoma.

Besides repurposing the existing drugs, discovery of novel drug molecules is the most explored alternate option to overcome chemotherapy related drug constraints in cancer therapy. In this context, new plant bioactives fill the void of limited chemotherapy options. Uterine leiomyosarcoma is a rare gynecological malignancy with no standard approved drug at present. Wet et al. successfully demonstrated using *in vitro* and *in vivo* assays that curdione isolated from *Curcuma zedoary* suppressed uterine leiomyosarcoma cell proliferation by inducing G2/M phase arrest, apoptosis, and autophagy via targeting IDO1. In the similar line, Macleayins A and phenethyl isothiocyanate were shown to inhibit the growth of cervical cancer cells (Shoaib et al.; Sai et al.).

In a systematic review and meta-analysis of randomized clinical trials, Peng et al. concluded that ginsenoside Rg 3 isolated from Korean *Panax ginseng* in combination with first line chemotherapeutic drugs demonstrate enhanced efficacy towards advanced non-small cell lung cancer (NSCLC) patients. Ginsenoside Rg 3 also reduced the chemotherapy induced toxicity. Similarly, phyto-chemicals from banana also showed great potential for future development of drugs for cancer prevention and therapy (Mondal et al.).

Despite potential anticancer abilities, many novel anticancer drugs suffer from poor bioavailability to achieve therapeutic drug level. The review by Wagh et al., provides an up-to-date summary on the effect of celastrol and its nano formulations in cancer prevention. This review discusses a multitude of celastrol nanoformulations that have been developed and tested for various therapeutic applications. Outside the scope of this review, exosomal formulations using milk derived exosomes have been demonstrated against lung cancer using *in vitro* and *in vivo* models (Aqil et al., 2016). In another review, Aggrawal et al. highlights phytochemical-related research on human papilloma virus (HPV)-induced head and neck cancer (HNC) and concluded that the therapies to distinguish HPV-positive HNC from HPV-negative HNC could help to achieve better outcome. This HPV-associated HNC can be treated with well-established phytochemicals targeting the HPV-mediated carcinogenic mechanisms.

Plant polyphenols are known for their pharmacological activities and therapeutic benefits. A study conducted by Albini et al. demonstrate that the polyphenol-rich extract of olive mill waste water enhances the anticancer potentiality of chemotherapeutic drugs cisplatin and 5-fluorouracil while mitigating their dose related cardiotoxicity. In another study, Oxyresveratrol was shown to have the ability to alter the cancer-causing genes and subsequently inducing apoptosis and cell cycle arrest in breast cancer MCF-7 cells (Radapong et al.).

Growing body of evidence suggests that approaches like chemical synthesis, analogue modification and development of nano formulations might help to achieve better anticancer therapies. Otaibi et al. shed the light on this aspect in their study and show chemically synthesized biologically active α-amino amide analogs alone and in combination with T cells exhibit pronounced anticancer activity against leukemia cancer cell lines (HL-60 and K562). In another study, Rampogu et al. used chemically modified butein derivatives to inhibit breast cancer progression through modulation of PI3K/AKT signaling pathway and other molecular markers.

In summary, this research topic comprises eight informative research and five authoritative review articles written by expert scientists and expansively discusses various aspects of cancer prevention and control. This special issue highlights strategies for cancer prevention and therapy by plant therapeutics alone and in combination with already in use therapeutics drugs, repurposed molecules for other diseases, and various nanotechnology-based techniques to enhance efficacy, reduce dose related toxicity and to better manage resistant and metastatic cancers. While articles in this special issue show *in vitro* and *in vivo* data for cancer prevention, the review articles shed light on preclinical and clinical studies in cancer prevention and therapy.

AUTHOR CONTRIBUTIONS

All authors listed have made a substantial, direct, and intellectual contribution to the work and approved it for publication.

REFERENCES

Aqil, F., Kausar, H., Agrawal, A. K., Jeyabalan, J., Kyakulaga, A. H., Munagala, R., et al. (2016). Exosomal Formulation Enhances Therapeutic Response of Celastrol against Lung Cancer. *Exp. Mol. Pathol.* 101, 12–21. doi:10.1016/j.yexmp.2016.05.013

Siegel, R. L., Miller, K. D., Fuchs, H. E., and Jemal, A. (2021). Cancer Statistics, 2021. *CA Cancer J. Clin.* 71, 7–33. doi:10.3322/caac.21669

Vasan, N., Baselga, J., and Hyman, D. M. (2019). A View on Drug Resistance in Cancer. *Nature* 575, 299–309. doi:10.1038/s41586-019-1730-1

Conflict of Interest: The authors declare that the research was conducted in the absence of any commercial or financial relationships that could be construed as a potential conflict of interest.

frontiers in Oncology

ORIGINAL RESEARCH
published: 26 February 2021
doi: 10.3389/fonc.2021.637024

Curdione Induces Antiproliferation Effect on Human Uterine Leiomyosarcoma *via* Targeting IDO1

Chao Wei, Donghua Li, Yu Liu, Wenna Wang and Tiantian Qiu*

School of Traditional Chinese Medicine, Capital Medical University, Beijing, China

Objectives: Curdione is one of the active ingredients of a traditional Chinese herbal medicine-*Curcuma zedoary* and established anti-tumor effects. Uterine leiomyosarcoma (uLMS) is a rare gynecological malignancy, with no standard therapeutic regimen at present. The aim of this study was to explore the potential anti-tumor impact of curdione in uLMS and elucidate the underlying mechanisms.

Methods: *In vitro* functional assays were performed in the SK-UT-1 and SK-LMS-1 cell lines. The *in vivo* model of uLMS was established by subcutaneously injecting SK-UT-1 cells, and the tumor-bearing mice were intraperitoneally injected with curdione. Tumor weight and volume were measured at specific time points. The biosafety was evaluated by monitoring changes of body weight and the histopathology in the liver and kidney. The expression levels of relevant proteins were analyzed by western blotting and immunohistochemistry.

Results: Curdione decreased the viability and proliferation of uLMS cells in a concentration and time-dependent manner. In addition, the curdione-treated cells exhibited significantly higher rates of apoptosis and autophagic death. Curdione also decreased the tumor weight and volume in the SK-UT-1 xenograft model compared to the untreated control without affecting the body bodyweight or pathological injury of liver and kidney tissues. At the molecular level, the anti-tumor effects of curdione were mediated by indoleamine-2, 3-dioxygenase-1 (IDO1).

Conclusion: Curdione exhibited an anti-uLMS effect *in vitro* and *in vivo*; the underlying mechanism involved in IDO1 mediate apoptosis, autophagy, and G2/M phase arrest.

Keywords: curdione, uterine leiomyosarcoma, apoptosis, autophagy, Indoleamine-2, 3-dioxygenase-1

OPEN ACCESS

Edited by:
Jamal Arif,
Shaqra University, Saudi Arabia

Reviewed by:
Abdul Q. Khan,
Hamad Medical Corporation, Qatar
Mohtashim Lohani,
Jazan University, Saudi Arabia

****Correspondence:***
Donghua Li
donghuali@ccmu.edu.cn

Specialty section:
This article was submitted to Pharmacology of Anti-Cancer Drugs, a section of the journal Frontiers in Oncology

Received: *02 December 2020*
Accepted: *18 January 2021*
Published: *26 February 2021*

Citation:
Wei C, Li D, Liu Y, Wang W and Qiu T (2021) Curdione Induces Antiproliferation Effect on Human Uterine Leiomyosarcoma via Targeting IDO1. Front. Oncol. 11:637024. doi: 10.3389/fonc.2021.637024

INTRODUCTION

Uterine leiomyosarcoma (uLMS) is a rare and aggressive gynecological malignancy, which is characterized by high recurrence rate, low mortality rate, distant metastases, and poor prognosis (1, 2). It is the most common subtype of uterine sarcoma, and clinical manifestations are abnormal uterine bleeding, palpable pelvic mass, and lower abdominal pain. Since these symptoms mimic uterine leiomyoma, uLMS is often misdiagnosed (3–5).

In addition, no standardized therapeutic regimen has been available for uLMS due to its rare occurrence and rapid progression (6, 7), effective and standardized therapy is urgently needed.

Herbal medicine exhibits broad-spectrum antibacterial, anti-inflammatory, and anticancer activity with tolerable toxicity, which plays a pivotal role in preventing and treating disease. Currently, chemotherapy is one of the main strategies against cancer; herbal medicine gained considerable interest in recent years as an alternative to chemotherapy drugs. For instance, *Curcuma zedoary* has been reported with an anti-tumor effect (8–11), and its bioactive compounds of the essential oils including β-elemene, curcumol, curcumin, curdione, furanodiene, furanodienone, and germacrone exhibit anti-thromboric (12, 13), anti-inflammatory, (14) antibacterial (15), neuroprotective properties (16), cardio-protective (17), and anti-tumor effects (18). The therapeutic effects of curdione have been reported in breast cancer (19), while the potential anti-tumor effect in uLMS is still unclear.

Evading death and uncontrolled proliferation are hallmarks of the tumor. The death forms of tumor cells include but not limited to apoptosis, autophagy, and necrosis. Apoptosis is a form of programmed cell death (20), and the most common type of tumor cell death induced by natural plant-derived compounds in tumor cells (21). It can initiate cascade of caspases reaction through both intrinsic (mitochondrial) or extrinsic (death receptor) pathways, and eventually cell death (22). The intrinsic apoptosis pathway is commonly triggered by hypoxia, chemotherapy, and radiation. Phytochemicals have multi-target effects on tumor; in addition to activating apoptosis, they can also induce autophagy through epigenetic mechanisms (23). It is a self-catabolic process that is activated in response to stress and maintains cellular homeostasis by degrading unnecessary substances such as misfolded proteins or damaged organelles. In addition, autophagy is the second-most common form of tumor cell death induced by phytochemicals (24). Nevertheless, autophagy acts as a double-edged sword in tumor cells by fulfilling their nutrient and energy requirements in the hypoxic or energy shortage environment on one hand and inducing cell death after sustained hyper-activation on the other hand (25). Cell death is a complex and sophisticated process; typically, it may not be limited to a single form but involves multiple forms (24).

Indoleamine-2, 3-dioxygenase-1 (IDO1) is an immune checkpoint and a key rate-limiting enzyme that breaks down tryptophan into kynurenine, which plays an important regulatory effect in tumor immunity (26). It is overexpressed in many tumor types, but not all. Liu et al. (27) reported significantly higher expression of IDO1 in uterine carcinosarcoma and uterine corpus endometrial carcinoma tissues compared to the paired normal tissues. In addition, IDO1 overexpression is related to increased tumor progression and poor prognosis of tumors, which makes it a promising therapeutic strategy for malignant tumors (28). Generally, the effect of IDO1 on tumors depends on its mediate immunoregulatory effect; however, Thaker (29) found that IDO1 directly mediates the proliferation and progression of colon cancer independent of its immunoregulatory effects. In our preliminary experiments as well, we detected high IDO1 expression in uLMS cell lines. We speculated whether the effect of curdione on uLMS is through targeting IDO1. If so, how does IDO1 mediate the suppression effect of curdione on uLMS?

Thus, the goal of this study was to analyze the effect of curdione on uLMS cells and the possible mechanistic role of IDO1. In this work, curdione inhibited the growth of SK-UT-1 and SK-LMS-1 cells by inducing cell cycle arrest at the G2/M phase, as well as apoptosis and autophagic death. Intrinsic apoptosis induced by curdione was demonstrated by the increased levels of cleaved caspases 3, 6, and 9 but that of pro- and cleaved-caspase 8. *In vivo*, curdione suppressed the tumor growth in the SK-UT-1 xenograft model without adverse effects. In addition, it significantly down-regulated IDO1 expression in a dose and time-dependent manner. Pharmacological inhibition of IDO1 with epacadostat or its siRNA-mediated knockdown restored the viability of cells following curdione treatment. Likewise, co-treatment with epacadostat and curdione attenuated the curdione-induced apoptosis, autophagy, and G2/M phase arrest. This demonstrated that the suppressive effect of curdione on uLMS *via* targeting IDO1.

MATERIAL AND METHODS

Reagents and Materials

Curdione was purchased from Solarbio Science&Technology Co. Ltd. (Beijing, China). Modified Eagle's medium (MEM), Dulbecco's modified Eagle's medium (DMEM), fetal bovine serum (FBS), Non-Essential Amino Acids (NEAA), Pymvate Sodium (NaP), and penicillin–streptomycin (PS) were purchased from Gibco (Waltham, MA, USA). The IDO1 inhibitor epacadostat was purchased from Selleck (S7910, Texas, USA) and autophagy inhibitor 3- Methyladenine was purchased from Selleck (S2767, Texas, USA), CCk8 was purchased from Dojindo (CK04, Kumamoto, Japan), Beyo Click^{TM} Edu-594 Cell Proliferation Kit was purchased from Beyotime (C0078S, Shanghai, China), and Annexin V-fluorescein isothiocyanate (FITC) cell apoptosis kit was purchased from Invitrogen (V13241, New York, California, USA).

Cell Culture

SK-UT-1 and SK-LMS-1 cells were obtained from American Type Culture Collection (Manassas, VA, USA). The SK-UT-1 cells were cultured in MEM, supplemented with 10% FBS, 1% NEAA, 1% NaP, and 1% penicillin–streptomycin. The SK-LMS-1 cells were grown in DMEM supplemented with 10% FBS and 1% penicillin–streptomycin. Both cell lines were incubated in a humidified atmosphere with 5% CO_2 at 37°C.

Cell Viability Assay

The viability of the suitably treated cells was detected by the CCK-8 kit. Briefly, the SK-UT-1 and SK-LMS-1 cells were starved with serum-free and then incubated with gradient concentrations of

curdione for 24 h, or with 100 μM curdione for 24, 48, and 72 h. In another experiment, the serum-starved cells were pre-treated with 3-MA or eapacadostat for 2 h, and then with curdione or not for 24 h. 10μl CCK8 solution was added into each well, the cells were incubated for 2 h at 37°C. The optical density (OD) at 450 nm was measured at a microplate spectrophotometer (BioTek, USA).

Immunofluorescence

EdU assay was performed using Beyo ClickTM Edu-594 Cell Proliferation Kit (Beyotime, Shanghai, China), according to the manufacturer's instructions. Briefly, curdione-treated cells were incubated with EdU, fixed with 4% paraformaldehyde, and then permeabilized with 0.3% Triton X-100. Following incubation with click additive solution, the nucleus was counterstained with Hoechst33342 for 15 min. To detect Ki67 expression levels, the cells were incubated with the anti-Ki67 primary antibody (ab15580, Cambridge, UK) and then with fluorophore-conjugated secondary antibody for 1 h, followed by counterstaining with 4,6-diamino-2-phenyl indole (DAPI, Genview, Florida, USA) for 10 min. For the TUNEL assay, the cells were stained with the reagents provided with the TUNEL kit (KGA7072, KeyGen, Nanjing, China) according to the manufacturer's instructions. The stained cells were observed under laser confocal microscope (Leica DM60008, Kyoto, Japan) at a magnification of ×40, and the number of EdU, Ki67, and TUNEL positive cells from six random fields was used for quantitative analysis by Image J software.

Flow Cytometry Analysis

The serum-starved cells were exposed to curdione for 24 h and then were harvested and co-stained with Annexin V-FITC & PI cell apoptosis kit according to the manufacturer's instruction. In addition, the cell cycle distribution was analyzed using the Cell Cycle and Apoptosis Analysis Kit (C1052, Beyotime, Shanghai, China) according to the manufacturer's instructions. Briefly, the cells were fixed with 70% cold ethanol for 24 h and then incubated with 5 μl PI staining solution and 45 μl RNase water. Subsequently, all stained samples were analyzed by flow cytometry (BD Biosciences, CA, USA).

Transient Transfection

IDO1-specific siRNA (5′-GGATGTTCATTGCTAAACA-3′) was designed and synthesized by RiboBio Co. Ltd. (C10511-05, Beijing, China). The SK-UT-1 and SK-LMS-1 cells were transfected according to the manufacturer's instructions. The stably transfected cells were confirmed by analyzing the IDO1 protein and mRNA expression levels.

Western Blotting

Total protein was extracted from tumor tissues and uLMS cells and quantified by the BCA Protein Assay kit (Beyotime, Shanghai, China). Equal amounts of proteins (30 μg) per sample were separated by SDS-PAGE (Solarbio, Beijing, China) and then transferred to polyvinylidene fluoride microporous membranes (PVDF) (XLL093-3, Millipore, MA, USA). After blocking with 5% skimmed dry milk, the blots were incubated overnight with primary antibodies against: IDO1 (ab211017), caspase-3 (ab13847), cleaved-caspase-3 (ab2302), caspase-6 (ab185645), cleaved-caspase-6 (ab2326), caspase-9 (ab32539), cleaved-caspase-9 (ab2324), caspase-8 (ab108333), cleaved-caspase-8 (CST#9496), LC3 (ab48394), Beclin1 (ab210498), P62 (ab109012), and GAPDH (ab181602) at 4°C. Next, the membranes were then probed with HRP-conjugated secondary antibodies, and the positive bands were visualized using the enhanced Chemiluminescence (ECL) detection kit (GE2301-25ML, Genview, USA) on an imaging system (Bio-Rad, USA). The band densities were analyzed using Image J software, and the relative protein expression levels were normalized to that of GAPDH.

Real-Time Quantitative PCR

Total RNA was extracted from the uLMS cells using ES-science RNA-Quick Purification Kit, cDNA synthesized with the Fast All-in-One RT Kit, and RT-PCR was performed using 2×Super SYBR Green qPCR Master Mix (PN001, YiShan Biotech, Shanghai, China) according to the manufacturer's instructions on the ABI-7500 Sequence Detection System (Applied Biosystems, Foster City, CA, USA) with the following program: pre-incubation at 95°C for 5 min, followed by 40 cycles of denaturation at 95°C for 10 s, and then annealing and extension at 60°C for 30 s. The primers were designed as follows: IDO1 F: GCCAGCTTCGAGAAAGAGTTG; R: ATCCCAGAACTAGACGTGCAA, GAPDH F: GAGCGAGATCCCTCCAAAAT; R: GGCTGTTGTCA ACTTCTCATGG. The comparative cycle threshold (Ct) method (2−ΔΔCt) was used to calculate the fold change in RNA expression. The relative mRNA levels of IDO1 were normalized to that of GAPDH. Experiments were independently performed in triplicates.

Mouse Xenograft Tumor Model

BALB/c nude mice (6–7 weeks, female, 18 ± 2 g) were purchased from Beijing Vital River Laboratory Animal Technology (Beijing, China). Approximately 1×10^7 SK-UT-1 cells were suspended and injected subcutaneously into their right flanks and once the tumor volume reached approximately 0.5 cm^3, the mice were randomly divided into three groups (n = 5 per group) and injected intraperitoneally (i.p.) with 100 mg/kg or 200 mg/kg curdione or the same volume physiological saline (control) every day. The tumor volume (length × $width^2$/2) and body weight were calculated every three days. 21 days later, the mice were euthanized, and the tumor tissues were harvested for immunohistochemical staining and western blotting. All experimental protocols were performed according to the Guidelines for the Care and Use of Laboratory Animals by the National Institute of Health, and approved by the Ethics Committee of Capital Medical University.

Histopathology and Immunohistochemistry

The tumor, liver, and kidney tissues were harvested and embedded in 4% paraformaldehyde, dehydrated across an ethanol gradient, and cleared in xylene. The liver and kidney tissues were fixed with 4% formaldehyde, embedded with paraffin, sectioned, and stained with hematoxylin and eosin (H&E). The tumor tissue

sections were heated in citrate buffer for antigen retrieval and blocked with 10% bovine serum albumin (BSA, C1052, Beyotime, Shanghai, China). After incubating overnight with primary antibodies, the sections were probed with species-specific HRP-labeling secondary antibody. The stained cells were observed by a light microscope (Leica DM60008, Kyoto, Japan) at a magnification of ×200. The positive staining was scored according to the following criteria: (1) The positive rate: 0, less than 5%; 1, 5–25%; 2, 26–50%; 3, 51–75% and 4, greater than 75%. (2) The staining intensity: 0, negative; 1, low positive; 2, positive and 3, high positive. The expression score is the multiplication of the positive rate score and staining intensity score.

Statistical Analysis

Statistical analysis was performed using SPSS version 19.0 software (SPSS Inc., IL, USA) and GraphPad Prism 7.0 software. One-way analysis of variance ANOVA was used for comparative analysis of the significant differences among groups. Data are presented as mean ± SD of three independent experiments. P <0.05 was considered statistically significant.

RESULTS

Curdione Decreased the Viability of uLMS Cells

The effect of curdione on uLMS cells' viability was detected by CCK8 assay. As shown in **Figures 1A, B**, curdione significantly decreased cell viability in a concentration and time-dependent manner at a dose higher than 10 μM. Its half-maximal inhibitory concentration (IC50) and the corresponding 95% confidence intervals for (**Figure 1C**) SK-UT-1 were 327.0 (297.7–362.8) μM and (**Figure 1D**) SK-LMS-1 cells were 334.3 (309.9–362.5) μM respectively. Accordingly, less than one-third of IC50 curdione (100 μM) were used for the subsequent experiments. The chemical structure of curdione is shown in **Figure 1E**.

Curdione Inhibited the Proliferation of uLMS Cells

The anti-proliferative effect of curdione on SK-UT-1 and SK-LMS-1 cells were assessed by EdU incorporation, and ki67 expression levels using immunofluorescent techniques. As

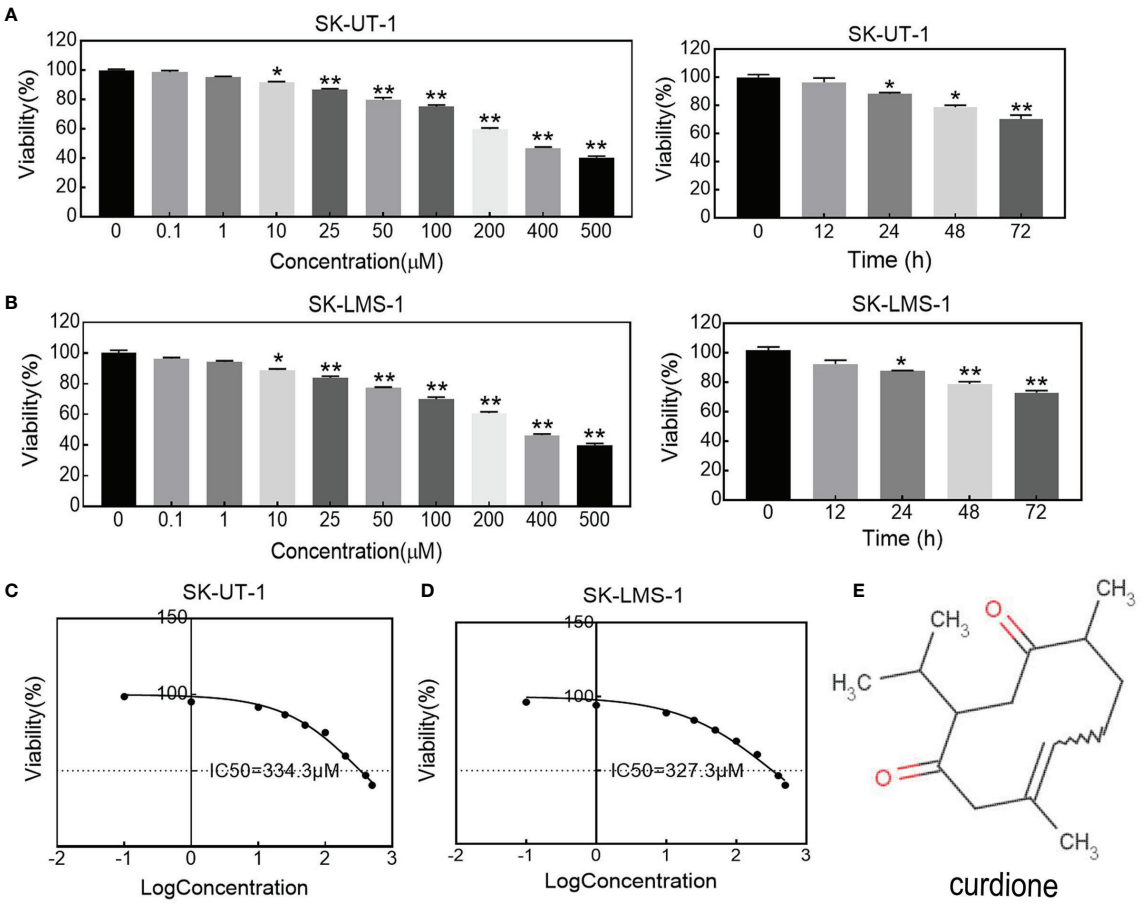

FIGURE 1 | Effect of curdione on the viability in uLMS cells. The dose and time response of curdione in **(A)** SK-UT-1 and **(B)** SK-LMS-1 cells. The viability of cells treated with varying concentrations of curdione for 24 h, or 100 μM curdione for 12, 24, 48 and 72 h were detected by CCK8. Accordingly, IC50 of **(C)** SK-UT-1 and **(D)** SK-LMS-1 cells were calculated by non-linear regression using GraphPad Prism7. **(E)** Chemical structure of curdione. All values were expressed as the mean ± SD, n = 3. *P < 0.05, **P < 0.01 compared with control.

shown in **Figures 2A, B**, curdione decreased the expression of both EdU and ki67 positive of SK-UT-1 and SK-LMS-1 cells in a concentration-dependent manner.

Curdione Induced G2/M Phase Arrest in uLMS Cells

Flow cytometry analysis and Western blotting were performed on uLMS cells to explore the effect of curdione on the cell cycle. As shown in **Figure 3A**, in SK-UT-1 cells, the G2/M phase proportion of the control, 25, 50, and 100μM curdione groups were 10.34 ± 1.54%, 14.03 ± 1.28%, 17.70 ± 1.48%, and 22.27 ± 1.05%; in SK-LMS-1 cells, the G2/M phase proportion of the control, 25, 50, and 100μM curdione groups were 9.84 ± 0.83%, 14.47 ± 0.97%, 19.10 ± 1.16% and 22.27 ± 1.05%; at the same time, the G1 phase proportion of both cell lines decreased. These data revealed that, curdione markedly increased the proportion of uLMS cells in the G2/M phase and decreased that in the G1 stage, compared with control. Consistent with this, curdione also up-regulated the cell cycle checkpoint proteins P21 and CyclinB1 and down-regulated Cdc2 in a concentration-dependent manner (**Figure 3B**). These results indicated that curdione arrested uLMS cells in the G2/M phase.

Curdione Induced Apoptosis in uLMS Cells

The apoptosis of SK-UT-1 and SK-LMS-1 cells exposed to varying concentrations of curdione was evaluated by Annexin V-FITC/PI and TUNEL assays. As shown in **Figure 4A**, in SK-UT-1 cells, the early apoptosis rates of the control, 25, 50, and 100μM curdione groups were 1.90 ± 0.25%, 2.77 ± 0.21%, 4.57 ± 0.39%, and 5.93 ± 0.77%, the late apoptosis rates of the control, 25, 50, and 100μM curdione groups were 1.70 ± 0.36%, 3.10 ± 0.16%, 4.83 ± 1.05% and 4.97 ± 1.08%; in SK-LMS-1 cells, the early apoptosis rates in the control, 25, 50, and 100μM curdione groups were 1.50 ± 0.29%, 5.20 ± 0.01%, 6.40 ± 1.01% and 6.87 ± 0.09%, the late apoptosis rates in the control, 25, 50, and 100μM curdione groups were 1.00 ± 0.36%, 2.67 ± 0.12%, 3.40 ± 0.80% and 4.77 ± 0.09% respectively. These data indicated that curdione markedly increased the percentage of both early and late apoptotic cells in a concentration-dependent manner. Likewise, the TUNEL assay further confirmed that curdione induced apoptosis (**Figure 4B**). Furthermore, curdione increased cleaved-caspase 3, 6, and 9 in a concentration-dependent manner without affecting that of caspase 8 (**Figure 4C**). Thus, curdione induced caspases mediate apoptosis through the intrinsic pathway.

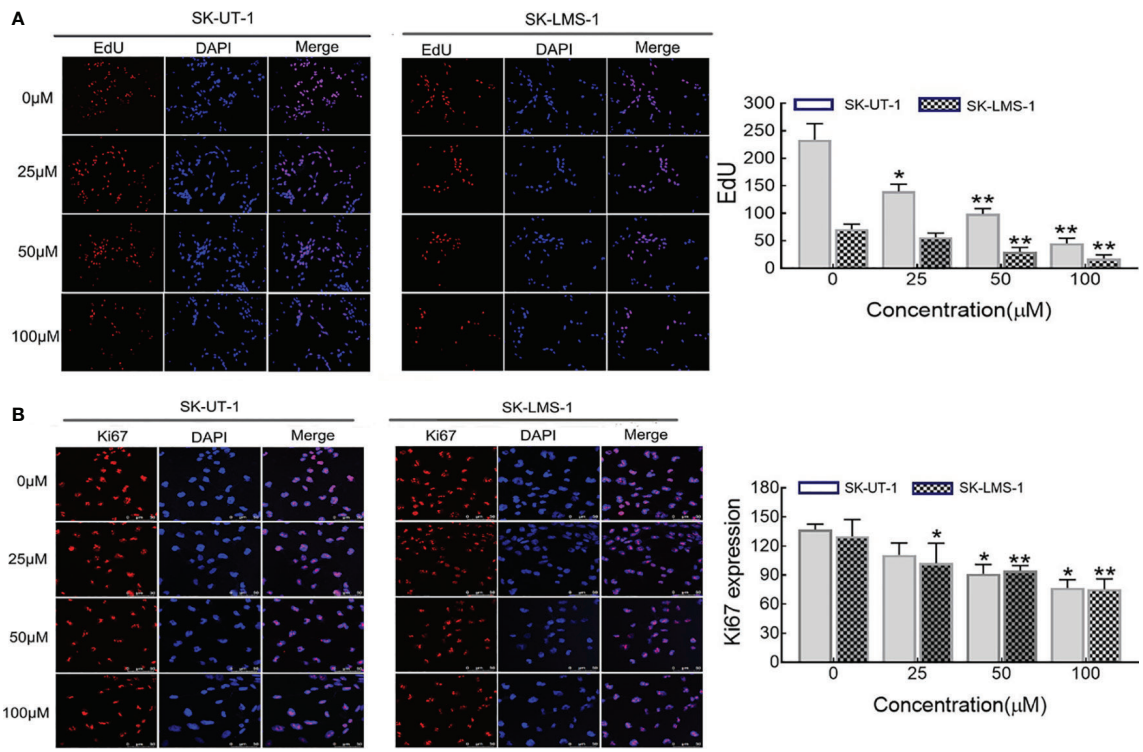

FIGURE 2 | Effect of curdione on the proliferation of uLMS cells. Immune fluorescence detection of the proliferation effect of curdione in uLMS cells. Cultured SK-UT-1 and SK-LMS-1 cells were treated with 0, 25, 50, and 100 μM curdione for 24h, and stained with **(A)** EdU and **(B)** Ki67, the stained cells were observed by fluorescence microscope (×40 magnification). Quantitative analysis of the positive fluorescence density by Image J, Independent experiments were performed three times. Data were presented as mean ± SD, n = 3. *$P < 0.05$, **$P < 0.01$ compared with control.

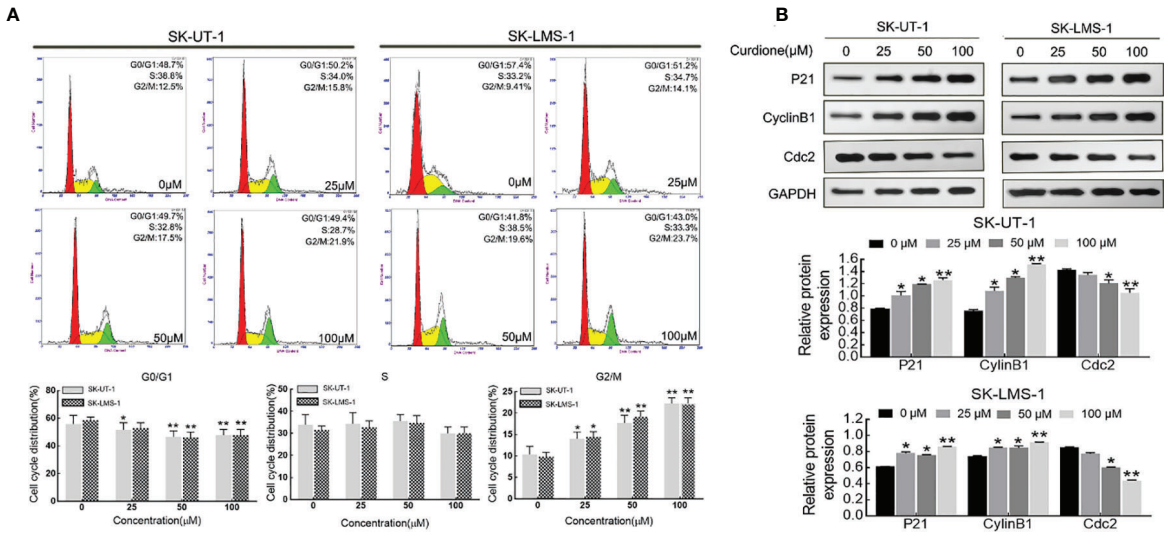

FIGURE 3 | Curdione induces G2/M phase arrest in uLMS cells. **(A)** Flow cytometry analyzes the cell cycle distribution in SK-UT-1 and SK-LMS-1 cells treated with 0, 25, 50, and 100 μM curdione for 24 h. **(B)** Western blotting detection of the P21, CylinB1, and Cdc2 expression in SK-UT-1 and SK-LMS-1 cells treated with 0, 25, 50, and 100 μM curdione for 24 h. Independent experiments were performed three times. All data were presented as mean ± SD, n = 3. $^{*}P < 0.05$, $^{**}P < 0.01$ compared with control.

Curdione Induced Autophagy in uLMS Cells

To examine whether curdione induced autophagy in SK-UT-1 and SK-LMS-1 cells, we analyzed the levels of characteristic markers including LC3, Beclin-1, and P62 by Western blotting. As shown in **Figure 5A**, curdione up-regulated LC3 and Beclin-1 and down-regulated P62 in a dose-dependent manner. To further clarify the autophagy was pro-survival or pro-death, CCK8 assay was performed in uLMS cells pre-treated with 3-MA for 2 h followed with curdione for 24 h. The viability of the curdione alone group and 3-MA pre-treated group was 71.21 ± 4.27% and 87.96 ± 1.44% in SK-UT-1 cells, 73.44 ± 2.11% and 82.94 ± 0.73% in SK-LMS-1 cells. This suggests that 3-MA partly alleviated the suppressive effect of curdione on the uLMS cells (**Figure 5B**). Taken together, the inhibitory effect of curdione on uLMS cells can also be attributed to autophagic death.

IDO1 Mediated the Suppressive Effect of Curdione in uLMS Cells

Western blotting was performed to evaluate the effect of curdione on IDO1 expression, the results showed that, curdione significantly down-regulated IDO1 expression of uLMS cells in a dose and time-dependent manner (**Figures 6A, B**). To study the effect of IDO1 on the proliferation of curdione, we transfected SK-UT-1 and SK-LMS-1 cells with siRNA to silence IDO1 expression. The stable transfection of IDO1 was confirmed by the mRNA (**Figure 6C**) and protein (**Figure 6D**) expression. In addition, the effect of IDO1 on uLMS cell viability was assessed by CCK8. The viability of the epacadostat pre-treated group and curdione alone group was 72.89 and 82.04% in SK-UT-1 cells, 75.26 and 89.41% in SK-LMS-1 cells. Similarly, IDO1-siRNA restored the viability reduced by curdione from 73.05 to 90.09% in SK-UT-1 cells, from 75.26 to 90.60% in SK-LMS-1 cells. These results suggested that, both pharmacological inhibitor epacadostat and IDO1-siRNA reversed the suppressive effect of curdione on uLMS cells (**Figures 6E, F**). Briefly, the suppressive effect of curdione on uLMS cells is mediated by IDO1.

IDO1 Mediated Apoptosis, Autophagy, and G2/M Phase Arrest Induced by Curdione in uLMS Cells

To clarify the mechanism underlying the ability of IDO1 to mediate the suppressive effect of curdione in uLMs cells, western blotting was performed. The result showed that, epacadostat markedly attenuated the curdione-induced changes in cleaved-caspase 3, cleaved-caspase 6, and cleaved-caspase 9 (**Figure 7A**), LC3, Beclin1, P62 (**Figure 7B**); P21, CyclinB1, and Cdc2 (**Figure 7C**), indicating that IDO1 mediates the suppressive effect of curdione in uLMs cells through regulating apoptosis, autophagy, and G2/M phase arrest.

Curdione Suppressed the Growth of uLMS *In Vivo*

To further explore the anti-uLMS effect of curdione *in vivo*, we established the subcutaneous xenograft models and administered them with (1) the control group: same value saline, (2) 100 mg/kg/day curdione, (3) 200 mg/kg/day curdione for 21 days. The anti-tumor effects were evaluated by tumor volume and tumor weight, and the *in vivo* safety was assessed in terms of body weight and histopathological changes. As shown in **Figures 8A–E**, after 21 days treatment, tumor weight of the control group, 100 mg/kg/day curdione and 200 mg/kg/day curdione group was (0.75 ± 0.18) g, (0.41 ± 0.11) g. and (0.10 ± 0.02) g,

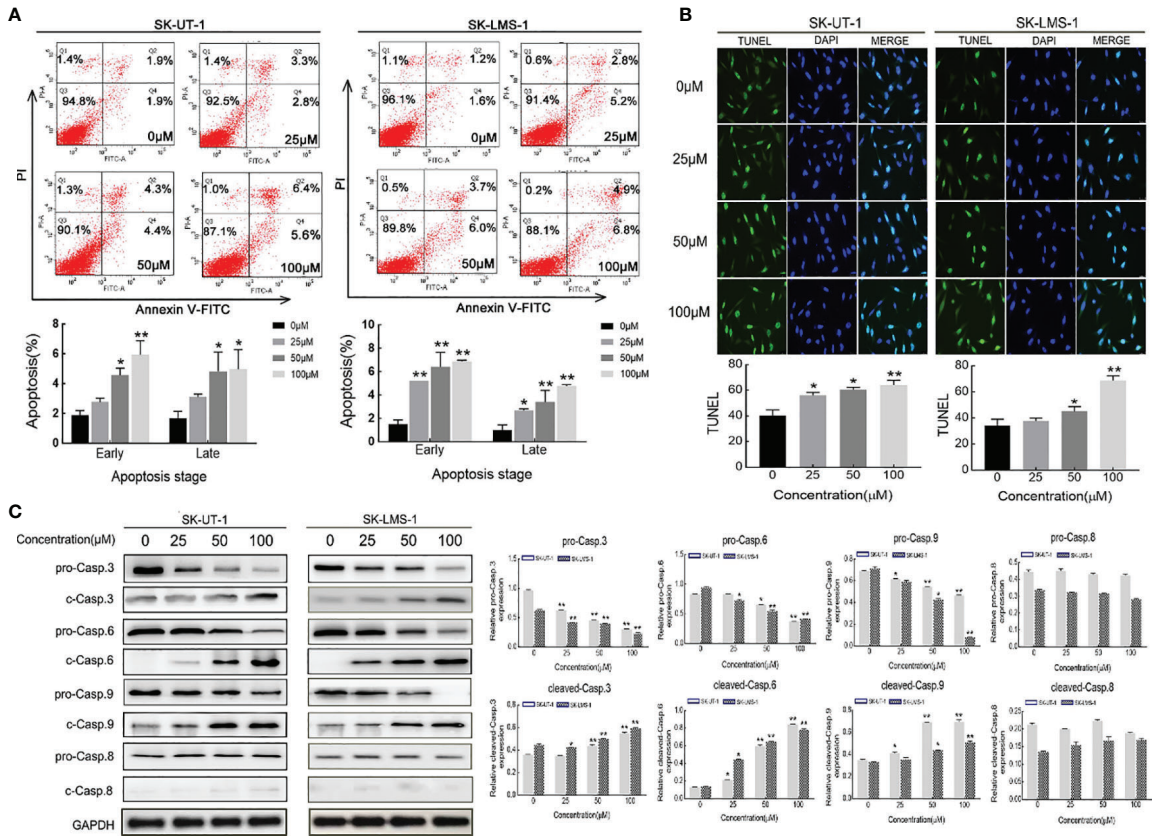

FIGURE 4 | Curdione induces caspases-mediate apoptosis in uLMS cells. SK-UT-1 and SK-LMS-1 cells were treated with 0, 25, 50, and 100 μM curdione for 24 h, **(A)** Flow cytometry with Annexin V-FITC/PI staining was conducted to analyze the apoptosis ratio. **(B)** Immunofluorescent analysis with TUNEL staining was performed to detected apoptosis using laser confocal microscopy (×40 magnification), Scale bars = 100 μm. **(C)** Western blotting detection of the pro-and cleaved-caspase 3, 6, 8, and 9 expressions. The relative protein expression level was normalized to that of GAPDH. Independent experiments were repeated three times, all data were present with means ± SD, n = 3. $^{*}P < 0.05$, $^{**}P < 0.01$ compared with control.

respectively; tumor volume of the control group, 100 mg/kg/day curdione and 200 mg/kg/day curdione group was (0.70 ± 0.07) cm^3, (0.29 ± 0.08) cm^3, and (0.17 ± 0.09) cm^3. These results indicated that curdione markedly reduced tumor volume and weight without affecting body weight. Furthermore, no histopathological lesions were observed in the liver and kidney tissues (**Figure 8F**). Thus, curdione exhibited anti-uLMS growth efficacy with minimal systemic toxicity *in vivo*.

IDO1 Mediated the Anti-Growth Effect of Curdione in the SK-UT-1 Xenograft Tumor Model

To determine the mechanism involved in the inhibitory effect of curdione on uLMS *in vivo*, western blotting and histological immunohistochemistry assay were performed. Consistent with the *in vitro* results, curdione down-regulated IDO1, ki67, and p62, and up-regulated the cleaved caspase-3, Beclin1 and LC3 in tumor tissues (**Figures 9A–C**). The above results showed that curdione suppressed the growth of uLMS *in vivo* by targeting IDO1 and activating apoptosis and autophagy.

DISCUSSION

Chemotherapy is a widely accepted strategy for treating cancers. However, conventional chemotherapeutic drugs have the disadvantages of high costs and adverse effects. Characteristiced by high efficacy, low toxicity, and relatively lower costs, natural plant derived compounds are favored in the field of cancer treatment, especially after the successful clinical application of paclitaxel and vinblastine (24). In fact, 80% of the chemotherapeutic drugs approved by the United States Food and Drug Administration in the past 30 years are either plant-derived compounds or their synthetic derivatives (30). *Curcuma zedoary*, a traditional Chinese medicine formulation that promotes blood circulation, removes blood stasis, and alleviates pain, has been widely used for treating gynecological diseases. Curcumin is one of the bioactive compounds of *Rhizoma Curcumae* with anti-proliferation effects on uterine sarcoma (18, 31), and uterine leiomyosarcoma (32, 33). Curdione is an active component of *Rhizoma Curcuma;* it has the same family and genus source with

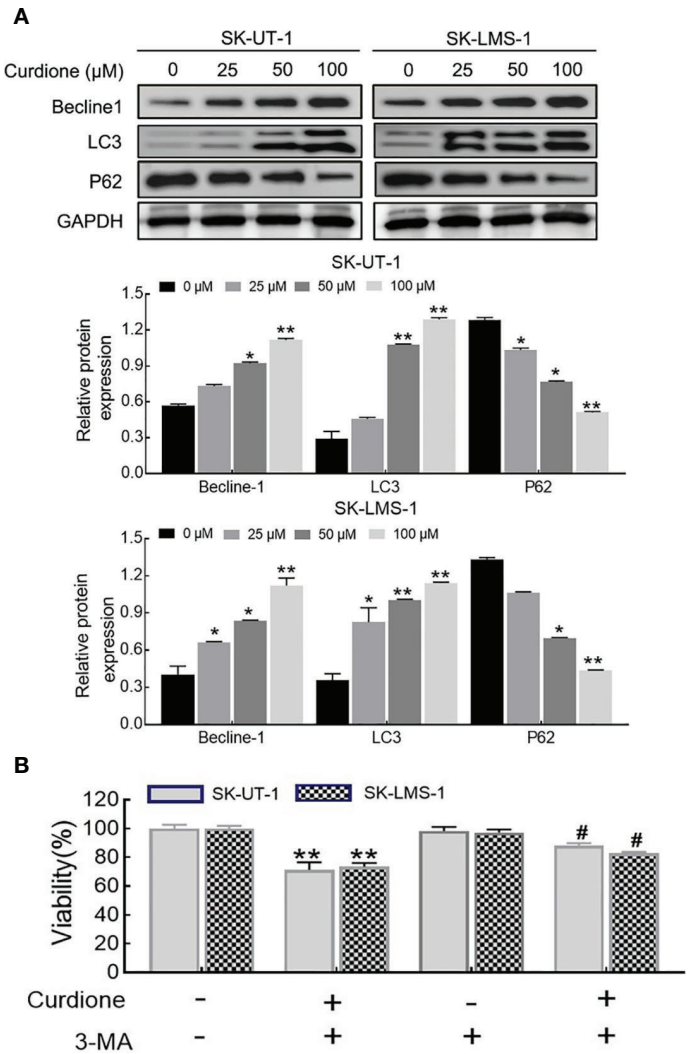

FIGURE 5 | Curdione induces autophagic death in uLMS cells. **(A)** Curdione induced autophagy. Beclin1, LC3, and P62 expression in SK-UT-1 and SK-LMS-1 cells treated with 0, 25, 50, and 100 μM curdione for 24 h were determined by Western blotting. **(B)** The autophagy induced by curdione was pro-death. The viability of SK-UT-1 and SK-LMS-1 cells treated with 3-MA (2 mM) for 2 h following with curdione (100 μM) for 24 h was detected by CCK8. Statistical analysis data were present with means ± SD, n = 3. $^{*}P < 0.05$, $^{**}P < 0.01$ compared with control; $^{\#}P < 0.05$; $^{\#\#}P < 0.01$ compared with curdione alone group.

curcumin and structurally similar to curcumin, which leads us to hypothesize that it might have an analogous effect on uLMS.

Based on the hypothesis, we first determined the effect of curdione on cell viability. Indeed, curdione inhibited the viability of SK-UT-1 and SK-LMS-1 cells in a dose and time-dependent manner. Accordingly, the IC50 was observed, and less than a third of IC50 was used in the subsequent experiment to ensure fidelity and reliability. The anti-proliferative effect of curdione was further confirmed by the decreased EdU and Ki67-positive fluorescence images in uLMS cells. In addition, curdione contributed to the alleviation of tumor load *in vivo* with few adverse effects. These data overwhelmingly illustrated that curdione has anti-tumor effect on uLMS. Cell proliferation is regulated by cell cycle checkpoints, thus, cell cycle progression is often used to evaluate the efficacy of anti-tumor drugs. In this study, curdione increased the cell population of the G2/M phase in a concentration-dependent manner, indicating that curdione suppressed the proliferative effect of uLMS cells by inducing cell cycle arrest at G2/M.

Apoptosis and autophagy are the two common death types induced in tumor cells by chemotherapeutic drugs and various plant-derived compounds (24). Apoptosis is crucial for maintaining the dynamic balance between cell survival and death (21). It is initiated through the intrinsic (mitochondrial) pathway or extrinsic (death receptor) pathways depending on the triggering factor, and then starts caspases mediated cascade reaction, and eventually leads to cell death (22). The cleaved caspases 3, 6, and 9 mainly participate in the intrinsic pathway. Curdione enhanced the apoptosis *in vitro* and *in vivo* in a dose-dependent manner, which was associated with

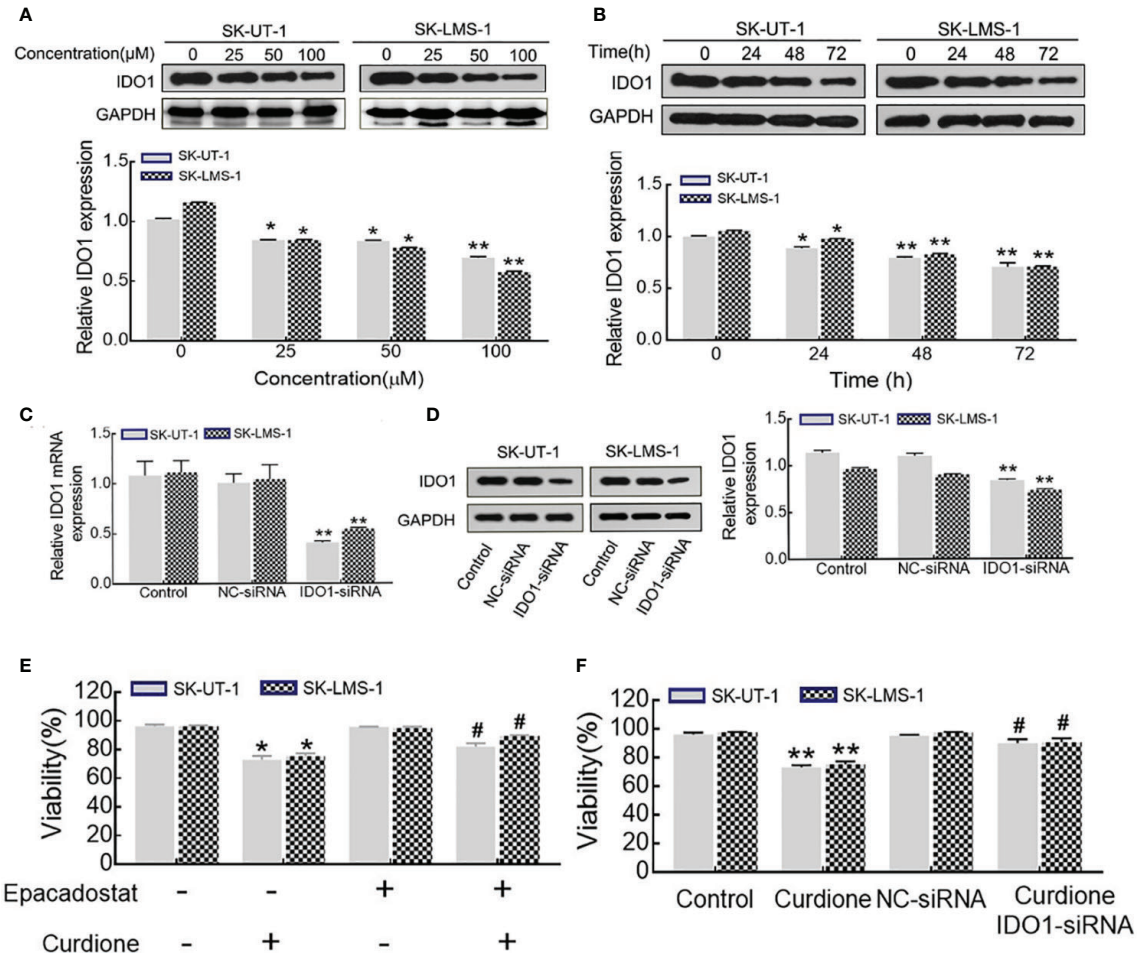

FIGURE 6 | IDO1 knockdown reversed the anti-proliferation effect of curdione in uLMS cells. **(A)** Curdione down-regulated IDO1 expression in a dose-dependent manner. IDO1 expression of SK-UT-1 and SK-LMS-1 cells treated with 0, 25, 50, 100 μM curdione for 24 h were analyzed by Western blotting. **(B)** Curdione down-regulated IDO1 expression in a time-dependent manner. IDO1 expression of uLMS cells treated with 100 μM curdione for 24, 48, 72 h was analyzed by Western blotting. **(C)** mRNA levels of IDO1 in uLMs cells after transfections with IDO1-siRNA was detected by RT-PCR, **(D)** Protein levels of IDO1 in uLMs cells after transfections with IDO1-siRNA was detected by Western blotting. **(E)** Epacadostat attenuated the suppressive effect on uLMS cells. The viability of uLMS cells pre-treated with IDO1 inhibitor epacadostat (25 nM) following with curdione was detected by CCK8. **(F)** IDO1-siRNA reversed the suppressive effect on uLMS cells. The viability of uLMS cells transfected with IDO1-siRNA was detected by CCK8. All data were present with means ± SD, n = 3. $^{*}P < 0.05$, $^{**}P < 0.01$ compared with control; $^{\#}P < 0.05$, $^{\#\#}P < 0.01$ compared with curdione group.

an increase in the levels of cleaved caspases 3, 6, and 9 but that of pro-and cleaved-caspase 8, which suggested that curdione induces caspase-mediated apoptosis through the intrinsic pathway. This is associated with Li's (34) reported that β-elemene induced caspase-mediated mitochondrial cell apoptosis. Autophagy is a self-digestion process that is activated in response to various stresses and ensures cell survival by recycling proteins and organelles, which play an important role in the growth and proliferation of various sarcoma as well (35), and autophagic death is the mechanistic basis of the action of several phytochemicals. We found that curdione increased the autophagic flux in uLMS by up-regulating LC3 and Beclin-1 and degrading p62. Interestingly, the suppressive effect of curdione on the uLMS cells was completely abrogated by the autophagy inhibitor 3-MA, indicating that curdione induced autophagic cell death in uLMS.

Tumor immunotherapy has been proved to be successful in clinical application, for instance, the immune checkpoint inhibitors have greatly improved the clinical prognosis of a subset of melanoma patients (36). The immune checkpoint IDO1 is highly expressed in many tumor types and is associated with poor overall survival and worse outcome (26, 37–39), indicating its potential as a therapeutic target (40). In the current study, curdione suppressed uLMS proliferation and down-regulated IDO1 expression. To further explore the correlation between them, the viability of uLMS cells pre-treated with IDO1 siRNA or IDO1 specific inhibitor epacadostat was detected. Surprisingly, the inhibitory

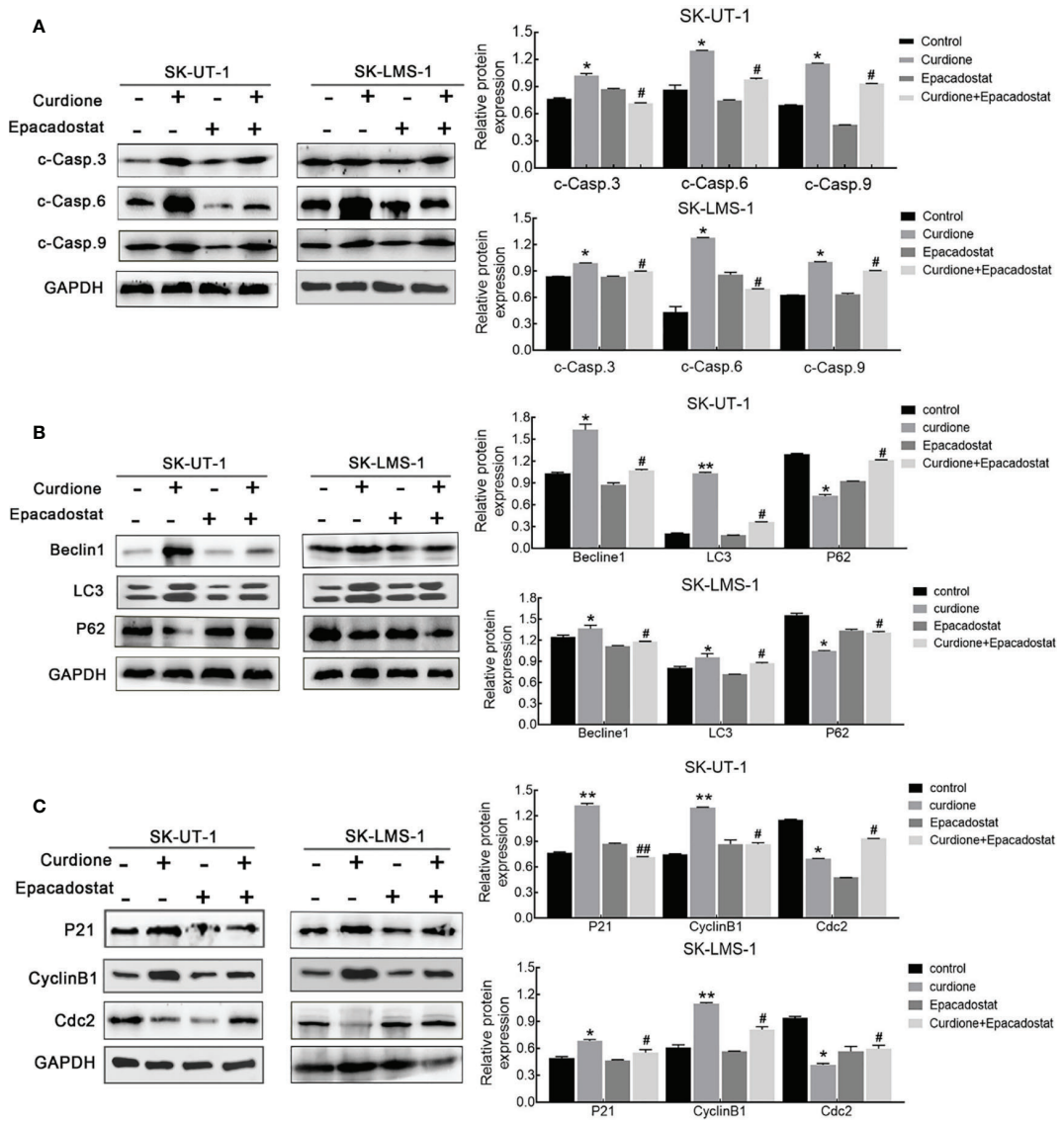

FIGURE 7 | IDO1 mediates apoptosis, autophagy, and G2/M phase arrest induced by curdione in uLMS cells. Western blotting detection of **(A)** cleaved caspase 3, 6, 9; **(B)** Beclin1, LC3, and P62; **(C)** P21, CylinB1, and Cdc2 expression in SK-UT-1 and SK-LMS-1 cells pre-treated with epacadostat (25 nM) for 2 h following with curdione for 24 h. All data were presened with mean ± SD, n = 3. $^{*}P < 0.05$; $^{**}P < 0.01$ compared with control; $^{\#}P < 0.05$, $^{\#\#}P < 0.01$ compared with curdione alone group.

effect of curdione on the uLMS cells was markedly weakened by blocking IDO1 through pharmacological or genetic means, which also reversed apoptosis, autophagy, and G2/M phase arrest induced by curdione. Thus, curdione exerts its anti-neoplastic effects on uLMS through targeting IDO1.

The limitation of this study should be addressed. Acting as a "brake" or "accelerator" in tumor immune regulation, IDO1 induces immunosuppressive tumor microenvironment and enables cancer cells to escape immune surveillance by catabolizing tryptophan into tryptophan (41). However, Thaker (29) reported that IDO1 promotes colon cancer growth directly independent of T cell-mediated immune regulation. We found that IDO1 mediated the anti-proliferative effect of curdione on uLMS, further research is needed to evaluate whether the immunomodulatory effects of IDO1 play a role in inhibiting uLMS growth. Analyzing the tryptophan and kynurenine levels, as well as the immune landscape of tumors can provide more insights.

Furthermore, the focus of this study is to investigate the efficacy of curdione on uterine leiomyosarcoma and analyze its mechanism. Therefore, a series of experiments of uLMS cell lines were performed to detect the anti-tumor effect of curdione, two cell lines mutual authentication, which strongly illustrates the anti-uLMS effect of curdione. In this work, we preliminarily explore the efficiency of curdione on uLMS, it does not involve the influence

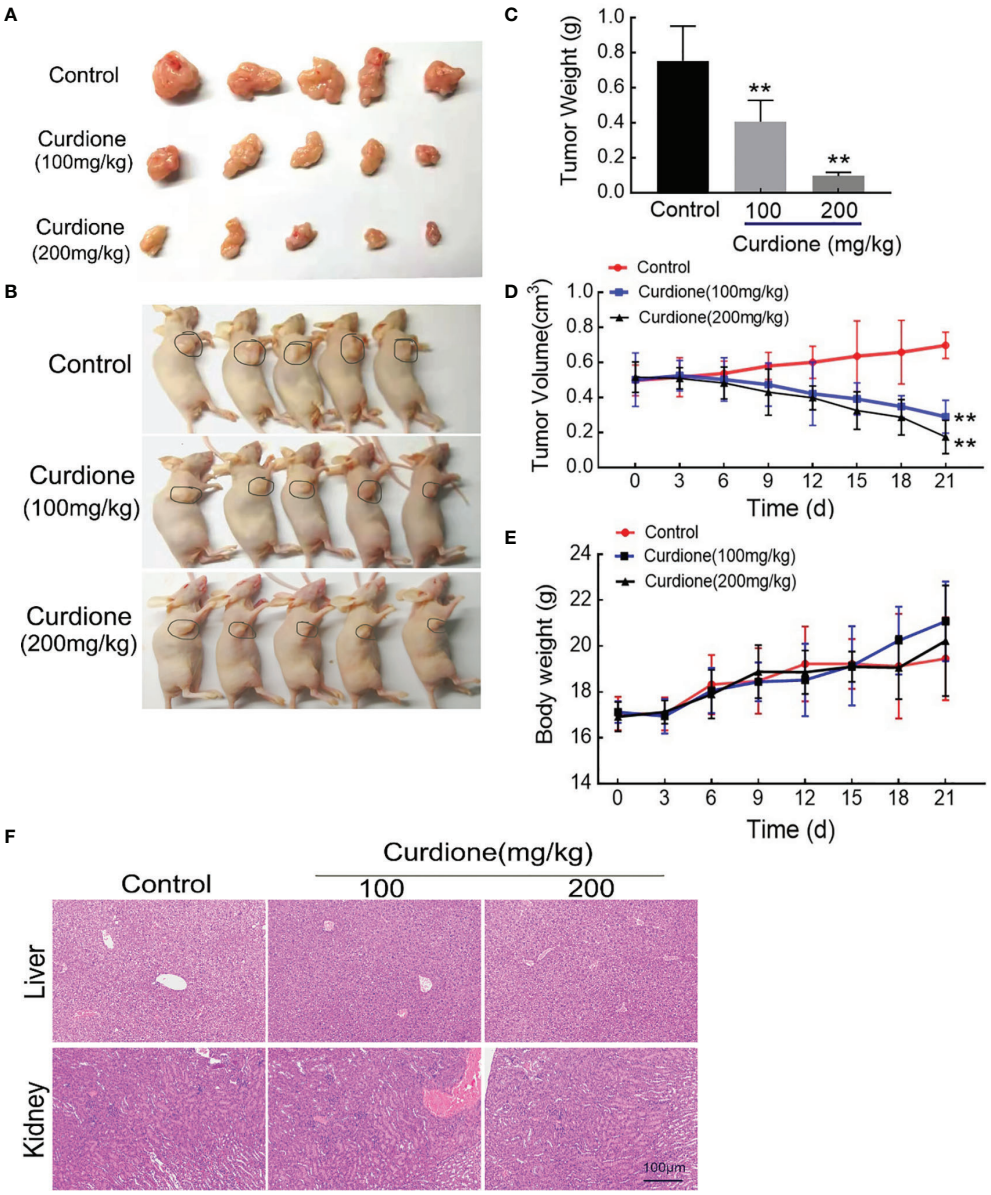

FIGURE 8 | Anti-growth effect of curdione in the SK-UT-1 xenograft tumor model. SK-UT-1 xenograft tumor models were established, and randomly divided into three groups (n = 5), and then injected intraperitoneally (i.p.) with 100 or 200 mg/kg/d curdione, or same volume saline. Tumor volume and body weight were measured every three days. 21 days later, all mice were sacrificed. Representative images of **(A)** tumor-bearing nude mice and **(B)** subcutaneous dissection of tumor tissue were photographed, **(C)** tumor weight, **(D)** tumor volume, and **(E)** body weight was determined and recorded. **(F)** The pathological injury of liver and kidney tissues was assessed by the H&E staining (×200 magnification). Scale bars = 100 μm. All data were presented with mean ± SD, n = 3. $^{*}P < 0.05$, $^{**}P < 0.01$ compared with control.

on normal cells. It is indisputable that including the normal cells would be more convincing to investigate the adverse effect of curdione *in vitro*. A great majority of experiments will be needed to further verify its effectiveness and safety, in the subsequent experimental research on the toxicity and safety evaluation of curdione, including the non-cancerous cell study will be necessary.

To summarize, we have demonstrated the anti-uLMS effect of curdione *in vitro* and *in vivo*, and elucidated the underlying mechanisms. *In vitro*, curdione suppressed uLMS cell proliferation by inducing G2/M phase arrest, apoptosis, and autophagy *via* targeting IDO1. *In vivo*, it markedly reduced the tumor growth in subcutaneous xenograft tumor models by down-

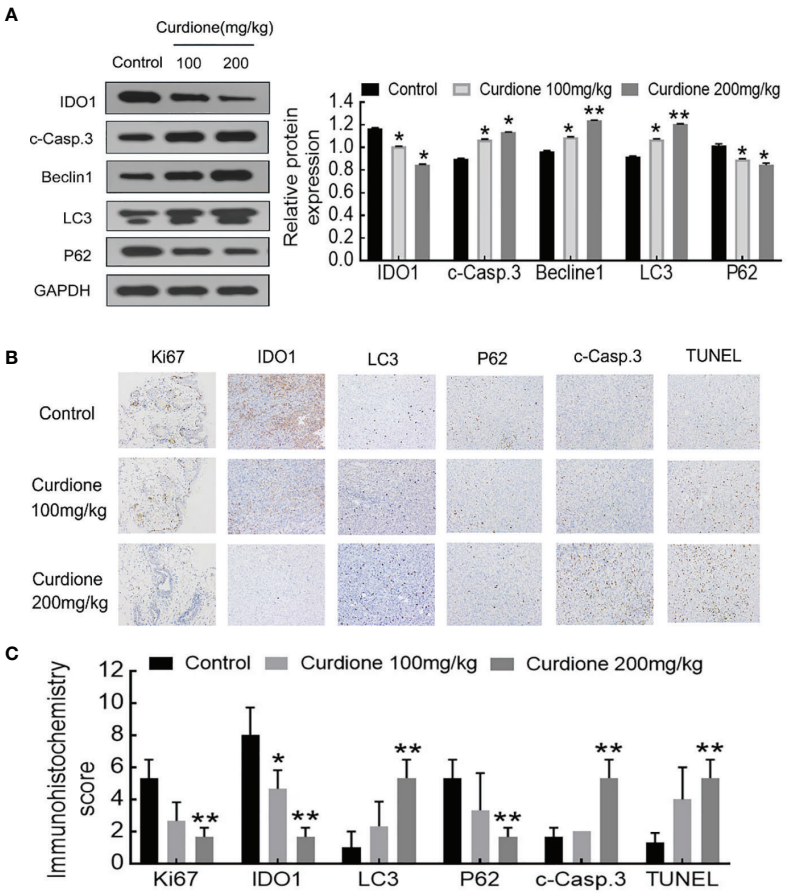

FIGURE 9 | IDO1 mediates the suppressive effect of curdione in the SK-UT-1 xenograft tumor model. **(A)** Western blotting detection of protein expression of IDO1, cleaved caspase-3, Beclin1, LC3, p62 in tumor tissue. **(B)** Immunohistochemistry staining of Ki67, IDO1, LC3, p62, cleaved caspase-3, and TUNEL in tumor tissue (×200 magnification), Scale bars = 100 μm. **(C)** Expression scores of Ki67, IDO1, LC3, p62, cleaved caspase-3, and TUNEL was calculated according to immunostaining intensity and positive expression rate. All statistical analysis data were present with mean ± SD, n = 3. $^{*}P < 0.05$, $^{**}P < 0.01$ compared with control.

regulating IDO1 and activating apoptosis and autophagy. Briefly, curdione inhibited uLMS through IDO1 mediated apoptosis, autophagy, and G2/M phase arrest, it is a promising drug for treating uLMS that warrants clinical investigation.

DATA AVAILABILITY STATEMENT

The original contributions presented in the study are included in the article/supplementary material. Further inquiries can be directed to the corresponding author.

ETHICS STATEMENT

The animal study was reviewed and approved by the Ethics Committee of Capital Medical University.

AUTHOR CONTRIBUTIONS

CW and DL conceived and designed the experiments. CW performed the experiments and wrote the manuscript. YL, WW, and TQ contributed to the experimental study design, preparation, and review of this manuscript. DL was responsible for manuscript revision and financial support. All authors contributed to the article and approved the submitted version.

FUNDING

This work was supported by the National Natural Science Foundation of China (no. 81774072, 81373812, 81073096), the Natural Science Foundation of Beijing Municipality (no. 7202015).

REFERENCES

1. Ricci S, Stone RL, Fader AN. Uterine leiomyosarcoma: Epidemiology, contemporary treatment strategies and the impact of uterine morcellation. *Gynecol Oncol* (2017) 145:208–16. doi: 10.1016/j.ygyno.2017.02.019
2. Roberts ME, Aynardi JT, Chu CS. Uterine leiomyosarcoma: A review of the literature and update on management options. *Gynecol Oncol* (2018) 151:562–72. doi: 10.1016/j.ygyno.2018.09.010
3. Bogani G, Fuca G, Maltese G, Ditto A, Martinelli F, Signorelli M, et al. Efficacy of adjuvant chemotherapy in early stage uterine leiomyosarcoma: A systematic review and meta-analysis. *Gynecol Oncol* (2016) 143:443–47. doi: 10.1016/j.ygyno.2016.07.110
4. Bogani G, Cliby WA, Aletti GD. Impact of morcellation on survival outcomes of patients with unexpected uterine leiomyosarcoma: a systematic review and meta-analysis. *Gynecol Oncol* (2015) 137:167–72. doi: 10.1016/j.ygyno.2014.11.011
5. Cantrell LA, Blank SV, Duska LR. Uterine carcinosarcoma: A review of the literature. *Gynecol Oncol* (2015) 137:581–8. doi: 10.1016/j.ygyno.2015.03.041
6. Pritts EA, Parker WH, Brown J, Olive DL. Outcome of occult uterine leiomyosarcoma after surgery for presumed uterine fibroids: a systematic review. *J Minim Invasive Gynecol* (2015) 22:26–33. doi: 10.1016/j.jmig.2014.08.781
7. Lin KH, Torng PL, Tsai KH, Shih HJ, Chen CL. Clinical outcome affected by tumor morcellation in unexpected early uterine leiomyosarcoma. *Taiwan J Obstet Gyne* (2015) 54:172–77. doi: 10.1016/j.tjog.2015.03.001
8. Zhong Z, Chen X, Tan W, Xu Z, Zhou K, Wu T, et al. Germacrone inhibits the proliferation of breast cancer cell lines by inducing cell cycle arrest and promoting apoptosis. *Eur J Pharmacol* (2011) 667:50–5. doi: 10.1016/j.ejphar.2011.03.041
9. Lu JJ, Dang YY, Huang M, Xu WS, Chen XP, Wang YT. Anti-cancer properties of terpenoids isolated from Rhizoma Curcumae - A review. *J Ethnopharmacol* (2012) 143:406–11. doi: 10.1016/j.jep.2012.07.009
10. Zhou Y, Xie M, Song Y, Wang WP, Zhao HR, Tian YX, et al. Two Traditional Chinese Medicines Curcumae Radix and Curcumae Rhizoma: An Ethnopharmacology, Phytochemistry, and Pharmacology Review. *Evid-Based Compl Alt* (2016) 2016:4973128. doi: 10.1155/2016/497312
11. Zheng J, Zhou Y, Li Y, Xu DP, Li S, Li HB. Spices for Prevention and Treatment of Cancers. *Nutrients* (2016) 8:495. doi: 10.3390/nu8080495
12. Xia Q, Wang X, Xu DJ, Chen XH, Chen FH. Inhibition of platelet aggregation by curdione from Curcuma wenyujin essential Oil. *Thromb Res* (2012) 130:409–14. doi: 10.1016/j.thromres.2012.04.005
13. Fang H, Gao B, Zhao Y, Fang X, Bian M, Xia Q. Curdione inhibits thrombin-induced platelet aggregation via regulating the AMP-activated protein kinase-vinculin/talin-integrin alphaIIbbeta3 sign pathway. *Phytomedicine* (2019) 61:152859. doi: 10.1016/j.phymed.2019.152859
14. Oh OJ, Min HY, Lee SK. Inhibition of inducible prostaglandin E2 production and cyclooxygenase-2 expression by curdione from Curcuma zedoaria. *Arch Pharm Res* (2007) 30:1236–9. doi: 10.1007/BF02980264
15. Song Z, Wei D, Chen Y, Chen L, Bian Y, Shen Y, et al. Association of astragaloside IV-inhibited autophagy and mineralization in vascular smooth muscle cells with lncRNA H19 and DUSP5-mediated ERK signaling. *Toxicol Appl Pharmacol* (2018) 364:45–54. doi: 10.1016/j.taap.2018.12.002
16. Li XJ, Liang L, Shi HX, Sun XP, Wang J, Zhang LS. Neuroprotective effects of curdione against focal cerebral ischemia reperfusion injury in rats. *Neuropsychiatr Dis Treat* (2017) 13:1733–40. doi: 10.2147/NDT.S139362
17. Wu Z, Zai W, Chen W, Han Y, Jin X, Liu H. Curdione Ameliorated Doxorubicin-Induced Cardiotoxicity Through Suppressing Oxidative Stress and Activating Nrf2/HO-1 Pathway. *J Cardiovasc Pharmacol* (2019) 74:118–27. doi: 10.1097/FJC.0000000000000692
18. Hashem S, Nisar S, Sageena G, Macha MA, Yadav SK, Krishnankutty R, et al. Therapeutic Effects of Curcumol in Several Diseases; An Overview. *Nutr Cancer* (2020) 73:1–15. doi: 10.1080/01635581.2020.1749676
19. Li J, Bian WH, Wan J, Zhou J, Lin Y, Wang JR, et al. Curdione inhibits proliferation of MCF-7 cells by inducing apoptosis. *Asian Pac J Cancer Prev* (2014) 15:9997–10001. doi: 10.7314/apjcp.2014.15.22.9997
20. Elmore S. Apoptosis: a review of programmed cell death. *Toxicol Pathol* (2007) 35:495–516. doi: 10.1080/01926230701320337
21. Knight T, Luedtke D, Edwards H, Taub JW, Ge Y. A delicate balance - The BCL-2 family and its role in apoptosis, oncogenesis, and cancer therapeutics. *Biochem Pharmacol* (2019) 162:250–61. doi: 10.1016/j.bcp.2019.01.015
22. Van Opdenbosch N, Lamkanfi M. Caspases in Cell Death, Inflammation, and Disease. *Immunity* (2019) 50:1352–64. doi: 10.1016/j.immuni.2019.05.020
23. Vidoni C, Ferraresi A, Secomandi E, Vallino L, Dhanasekaran DN, Isidoro C. Epigenetic targeting of autophagy for cancer prevention and treatment by natural compounds. *Semin Cancer Biol* (2020) 66:34–44. doi: 10.1016/j.semcancer.2019.04.006
24. Braicu C, Zanoaga O, Zimta AA, Tigu AB, Kilpatrick KL, Bishayee A, et al. Natural compounds modulate the crosstalk between apoptosis- and autophagy-regulated signaling pathways: Controlling the uncontrolled expansion of tumor cells. *Semin Cancer Biol* (2020) S1044-579X(20):30111–5. doi: 10.1016/j.semcancer.2020.05.015
25. Singh SS, Vats S, Chia AY, Tan TZ, Deng S, Ong MS, et al. Dual role of autophagy in hallmarks of cancer. *Oncogene* (2018) 37:1142–58. doi: 10.1038/s41388-017-0046-6
26. Schafer CC, Wang Y, Hough KP, Sawant A, Grant SC, Thannickal VJ, et al. Indoleamine 2,3-dioxygenase regulates anti-tumor immunity in lung cancer by metabolic reprogramming of immune cells in the tumor microenvironment. *Oncotarget* (2016) 7:75407–24. doi: 10.18632/oncotarget.12249
27. Liu M, Wang X, Wang L, Ma X, Gong Z, Zhang S, et al. Targeting the IDO1 pathway in cancer: from bench to bedside. *J Hematol Oncol* (2018) 11:100. doi: 10.1186/s13045-018-0644-y
28. Li F, Zhang R, Li S, Liu J. IDO1: An important immunotherapy target in cancer treatment. *Int Immunopharmacol* (2017) 47:70–7. doi: 10.1016/j.intimp.2017.03.024
29. Thaker AI, Rao MS, Bishnupuri KS, Kerr TA, Foster L, Marinshaw JM, et al. IDO1 metabolites activate beta-catenin signaling to promote cancer cell proliferation and colon tumorigenesis in mice. *Gastroenterology* (2013) 145:416–25 e1-4. doi: 10.1053/j.gastro.2013.05.002
30. Afrin S, Giampieri F, Gasparrini M, Forbes-Hernandez TY, Cianciosi D, Reboredo-Rodriguez P, et al. Dietary phytochemicals in colorectal cancer prevention and treatment: A focus on the molecular mechanisms involved. *Biotechnol Adv* (2020) 38:107322. doi: 10.1016/j.biotechadv.2018.11.011
31. Ning L, Ma H, Jiang Z, Chen L, Li L, Chen Q, et al. Curcumol Suppresses Breast Cancer Cell Metastasis by Inhibiting MMP-9 Via JNK1/2 and Akt-Dependent NF-kappaB Signaling Pathways. *Integr Cancer Ther* (2016) 15:216–25. doi: 10.1177/1534735416642865
32. Wong TF, Takeda T, Li B, Tsuiji K, Yaegashi N. Curcumin targets the AKT–mTOR pathway for uterine leiomyosarcoma tumor growth suppression. *Int J Clin Oncol* (2014) 19:354–63. doi: 10.1007/s10147-013-0563-4
33. Wong TF, Takeda T, Li B, Tsuiji K, Kitamura M, Kondo A, et al. Curcumin disrupts uterine leiomyosarcoma cells through AKT-mTOR pathway inhibition. *Gynecologic Oncol* (2011) 122:141–48. doi: 10.1016/j.ygyno.2011.03.001
34. Li QQ, Wang G, Huang F, Banda M, Reed E. Antineoplastic effect of beta-elemene on prostate cancer cells and other types of solid tumour cells. *J Pharm Pharmacol* (2010) 62:1018–27. doi: 10.1111/j.2042-7158.2010.01135.x
35. Min L, Choy E, Pollock RE, Tu C, Hornicek F, Duan Z. Autophagy as a potential target for sarcoma treatment. *Biochim Biophys Acta* (2017) 1868:40–50. doi: 10.1016/j.bbcan.2017.02.004
36. Qu J, Jiang M, Wang L, Zhao D, Qin K, Wang Y, et al. Mechanism and potential predictive biomarkers of immune checkpoint inhibitors in NSCLC. *BioMed Pharmacother* (2020) 127:109996. doi: 10.1016/j.biopha.2020.109996
37. Kolijn K, Verhoef EI, Smid M, Bottcher R, Jenster GW, Debets R, et al. Epithelial-Mesenchymal Transition in Human Prostate Cancer Demonstrates Enhanced Immune Evasion Marked by IDO1 Expression. *Cancer Res* (2018) 78:4671–79. doi: 10.1158/0008-5472.CAN-17-3752
38. Lindstrom V, Aittoniemi J, Jylhava J, Eklund C, Hurme M, Paavonen T, et al. Indoleamine 2,3-dioxygenase activity and expression in patients with chronic lymphocytic leukemia. *Clin Lymphoma Myeloma Leuk* (2012) 12:363–5. doi: 10.1016/j.clml.2012.06.001

39. Cheong JE, Sun L. Targeting the IDO1/TDO2-KYN-AhR Pathway for Cancer Immunotherapy - Challenges and Opportunities. *Trends Pharmacol Sci* (2018) 39:307–25. doi: 10.1016/j.tips.2017.11.007
40. Ricciuti B, Leonardi GC, Puccetti P, Fallarino F, Bianconi V, Sahebkar A, et al. Targeting indoleamine-2,3-dioxygenase in cancer: Scientific rationale and clinical evidence. *Pharmacol Ther* (2019) 196:105–16. doi: 10.1016/j.pharmthera.2018.12.004
41. Sharma P, Hu-Lieskovan S, Wargo JA, Ribas A. Primary, Adaptive, and Acquired Resistance to Cancer Immunotherapy. *Cell* (2017) 168:707–23. doi: 10.1016/j.cell.2017.01.017

Conflict of Interest: The authors declare that the research was conducted in the absence of any commercial or financial relationships that could be construed as a potential conflict of interest.

frontiers in Pharmacology

SYSTEMATIC REVIEW
published: 18 March 2021
doi: 10.3389/fphar.2020.630825

The Efficacy of Ginsenoside Rg3 Combined with First-line Chemotherapy in the Treatment of Advanced Non-Small Cell Lung Cancer in China: A Systematic Review and Meta-Analysis of Randomized Clinical Trials

Ze Peng[1†], *Wen Wen Wu*[2†] *and Ping Yi*[3*]

[1]*Institute of Integrated Traditional Chinese and Western Medicine, Tongji Hospital, Tongji Medical College, Huazhong University of Science and Technology, Wuhan, China,* [2]*West China School of Medicine, Sichuan University, Chengdu, China,* [3]*Department of Integrated Traditional Chinese and Western Medicine, Tongji Hospital, Tongji Medical College, Huazhong University of Science and Technology, Wuhan, China*

OPEN ACCESS

Edited by:
Raghuram Kandimalla, James Graham Brown Cancer Center, United States

Reviewed by:
Ashish Tyagi, University of Louisville, United States
Sanjeeb Kalita, Institute of Advanced Study in Science and Technology, India

***Correspondence:**
Ping Yi
pyi219@163.com

[†]*These authors have contributed equally to this work*

Specialty section:
This article was submitted to Pharmacology of Anti-Cancer Drugs, a section of the journal Frontiers in Pharmacology

Received: *18 November 2020*
Accepted: *31 December 2020*
Published: *18 March 2021*

Citation:
Peng Z, Wu WW and Yi P (2021) The Efficacy of Ginsenoside Rg3 Combined with First-line Chemotherapy in the Treatment of Advanced Non-Small Cell Lung Cancer in China: A Systematic Review and Meta-Analysis of Randomized Clinical Trials. Front. Pharmacol. 11:630825. doi: 10.3389/fphar.2020.630825

Background: For advanced non-small cell lung cancer (NSCLC) patients, first-line chemotherapy is the main treatment in the clinic despite its efficacy is limited and adverse effects are always inescapable. Ginsenoside Rg3, an anti-cancer active ingredient by suppressing angiogenesis, has been increasingly widely used as an adjuvant in first-line chemotherapy for advanced NSCLC to optimize treatment in China. However, no comprehensive meta-analyses have been conducted to estimate the efficacy and safety of the therapy combining ginsenoside Rg3 and first-line chemotherapy in advanced NSCLC patients.

Methods: Randomized controlled trails using a combination of first-line chemotherapy and ginsenoside Rg3 for advanced NSCLC patients were searched and selected from six databases. The Cochrane Risk of Bias tool was used to assessed the quality of these selected original researches. And we used Review Manager 5.3 and STATA to analyze the data.

Results: Twenty-two RCTs that matched our selection criteria with a number of 2202 patients were included in our review. The results showed that compared with first-line chemotherapy alone, the combination of ginsenoside Rg3 and first-line chemotherapy could better improve the objective response rate (ORR) (RR [95% CI], 1.44 [1.27, 1.63], $p < 0.00001$), the disease control rate (DCR) (RR [95% CI], 1.24 [1.12, 1.38], $p < 0.0001$), karnofsky performance status (KPS) (RR [95% CI], 1.62 [1.42, 1.84], $p < 0.00001$), one-year survival rate (RR [95% CI], 1.49 [1.08, 2.06], $p = 0.01$), two-year survival rate (RR [95% CI], 6.22 [1.68, 22.95], $p = 0.006$), weight change (RR [95% CI], 1.31 [1.04, 1.66], $p = 0.02$), and higher reduce the VEGF levels (RR [95% CI], -2.21 [-4.03, -0.38], $p = 0.02$), the

incidence of gastrointestinal reactions (RR [95% CI], 0.66 [0.47, 0.93], $p = 0.02$) and bone marrow suppression (RR [95% CI], 0.43 [0.30, 0.61], $p < 0.00001$).

Conclusion: Ginsenoside Rg3 can enhance drug efficacy and reduce drug-induced toxicity from chemotherapy. These findings provide helpful information for clinicians indicating that a therapy combined of ginsenoside Rg3 and first-line chemotherapy may be used to optimal the treatment of advanced NSCLC.

Keywords: Ginsenoside Rg3, advanced non-small cell lung cancer, first-line chemotherapy, meta-analysis, systematic review

INTRODUCTION

As a serious health issue all over the world, lung cancer has the highest morbidity and mortality in all cancers (Siegel et al., 2020). Approximately 85% of patients with lung cancer have a group of histological subtypes that are collectively known as non-small cell lung cancer (NSCLC) (Herbst et al.,2018). Since the majority of patients with NSCLC are diagnosed at an advanced stage (III or IV) when the cancer cells have usually metastasized (Du and Morgensztern 2015), most of them unfortunately lose the opportunity for surgical treatment. Only 18% of patients with advanced NSCLC undergo surgery, and nearly 62% advanced patients with NSCLC are treated with radiation treatment and systemic treatment including chemotherapy, targeted therapy and immunotherapy to improve long-term survival rate (Miller et al., 2019). Although in the past several years, great progress has been significantly made in molecularly targeted therapy and immunotherapy, first-line chemotherapy remains a mainstay in the therapeutic management of NSCLC (Rossi and Di, 2016; Nasim et al., 2019). Particularly, platinum-based regimens are the most active combinations in clinical practice and show a meaningful clinical benefit for advanced NSCLC patients (Watanabe et al., 2017; Herbst et al.,2018).

However, although platinum-based regimens show several benefits for patients with advanced NSCLC, only a minority of patients indeed achieve an objective treatment response and the 5-year survival rate is still less than 20% (Rose et al., 2014). Moreover, it cannot be ignored that chemotherapy drugs often lead to severe side effects, such as bone marrow suppression, serious gastrointestinal reaction and liver abnormalities (Islam et al.,2019; von Plessen, 2011). And another limitation of first-line chemotherapy is the increasing ineffectiveness of chemotherapy caused by drug resistance. It's reported that the drug resistance induced by platinum-based chemotherapies can be as high as 70% in advanced NSCLC patients (Rossi and Di Maio, 2016; Zhao and Chen, 2020). Therefore, looking for optimal therapy which can improve the efficacy of chemotherapy and reduce the incidence of side effects is of great necessity.

In recent years, traditional Chinese medicine (TCM) has played an increasingly important role in anti-cancer for its efficacy and security (Xiang et al., 2019). The combination of Chinese and Western therapy in anti-cancer treatment has become a hot trend all over the world (Liao et al., 2017; So et al., 2019). Ginseng, as a famous Chinese herbal medicine, has a medicinal history of four thousand years in China and is well known as 'the king of herbs' (Wang and Jin, 2018). Ginsenoside Rg3, a naturally active ingredient extracted from ginseng leachate, has been showed to possess anti-cancer in various tumors, especially in advanced NSCLC (Li Y et al., 2016). The therapeutic effects of ginsenoside Rg3 include inducing tumor apoptosis, inhibiting tumor metastasis, suppressing tumor angiogenesis and reversing drug resistance (Luo et al., 2019; Nakhjavani et al., 2020). In addition, there is a synergistic effect when ginsenoside Rg3 is used in combination with chemotherapy drugs (Sun et al., 2017; Wang and Jin, 2018; Zhao and Chen, 2020). Nowadays, an increasing number of studies have indicated that ginsenoside Rg3 may be a widely applied natural medicine in the treatment of NSCLC (Gao and Liu, 2019) and its combination with first-line chemotherapy drugs may brings great promise to the management of advanced NSCLC.

At present, some clinical trials of ginsenoside Rg3 combined with first-line chemotherapy on NSCLC have been conducted in China. However, no comprehensive meta-analyses have been conducted to estimate the efficacy and safety of this combination therapy. The purpose of this systematic review and meta-analysis is to evaluate the efficacy and safety of the therapy combining ginsenoside Rg3 and first-line chemotherapy in advanced NSCLC.

MATERIALS AND METHODS

Search Strategy

A systematic literature search for RCTs testing the combination of ginsenoside Rg3 and first-line chemotherapy in advanced NSCLC published from the inception of each database to October 2020 was conducted without language restrictions in six databases, including PubMed, Web of Science, the Cochrane Library, Wan Fang Database, Chinese VIP Information (VIP) and China National Knowledge Infrastructure (CNKI).

A free term strategy was used, for Chinese databases, the following terms were used in combined ways: "Renshen zao gan Rg3 or Shenyi jiaonang" and "feixiao xibao feiai"; for English databases, we used text terms including "ginsenoside Rg3 or Shenyi capsule" and "NSCLC".

Selection Criteria

The inclusion criteria were as follows: 1) patients: age of ≥18 years, histological or cytological confirmation of

advanced NSCLC. 2) interventions: the control group were treated with first-line chemotherapy and the combination of ginsenoside Rg3 and first-line chemotherapy was conducted in the experiment group relatively. 3) the outcome should include at least one of the following indicators: objective response rate, disease control rate, Karnofsky`s performance score (KPS) and adverse effects. 4) study design: randomized clinical trials (RCTs).

The exclusion criteria were as follows: 1) non-RCTs including case reports, reviews, animal or cell studies and studies without a control group. 2) patients treated with other therapies, expect for ginsenoside Rg3 and chemotherapy. 3) patients with small cell lung cancer (SCLC) or other serious diseases. 4) early NSCLC.

Data Extraction

Two independent reviewers (Ze Peng and Wen Wen Wu) extracted the data according to the inclusion criteria. The characteristics of the data consisted of the author, publication year, the number and sex of participants, interventions, treatment cycles, the stage of NSCLC and outcomes. Where outcomes were ambiguous or missing in an article, the decision to retrieve from that article was resolved by consensus.

Methodological Quality

The Cochrane Risk of Bias tool was used to assessed the quality of the literature by two reviewers (Ze Peng and Wen Wen Wu) separately. The assessed items included: 1) random sequence and allocation concealment; 2) blinding of participants and personnel; 3) blinding of outcome assessment; 4) incomplete outcome data; 5) selective reporting; 6) other bias. For any disagreement, the risk of bias was discussed by consensus.

Data Synthesis and Analysis

We performed the analysis by using Review Manager (ver. 5.3) and STATA (ver.14) software. For binary variables, the risk ratio (RR) with 95% confidence interval (CI) was used to evaluate the pool effects. p value <0.05 was considered statistically significant. We used Chi-squared and I^2 tests to evaluate the heterogeneity of all studies included. The fixed-effect model was selected for analysis with $p > 0.05$ or $I^2 < 50\%$; otherwise, we choose the random-effect model. And we assessed the sensitivity analysis to state the effect of changing the study model on the pooled analysis results. Begg's tests were carried out to determine the publication biases and p value >0.05 was considered as no publication bias.

RESULTS

Study Inclusions

A total of 360 studies were identified through systematic search, which included 190 repeated records (**Figure 1**). After a first screening, 36 were included by browsing the titles and abstracts of the remaining 170 studies. Then the remaining studies were further carefully scrutinized, and 134 articles were eliminated due to animals or cell experiments (n = 19), review (n = 16) and other therapies consisting of radiotherapy, postoperative lung cancer, and maintenance therapy (n = 99). Finally, excluding the studies with no control group or non-first-line chemotherapy regimens, 22 articles were included in this systematic analysis (Chen and Li 2012; Chen et al., 2014; Du 2014; Li and Bai 2017; Li et al., 2012; Liang and Han 2016; Lin et al., 2014; Liu et al., 2007; Liu et al. 2009; Liu et al. 2015; Pan and Wu, 2016; Pan et al., 2019; Pang, 2012; Qi and Zhang 2011; Shen et al., 2018; Sun et al., 2006; Tu,

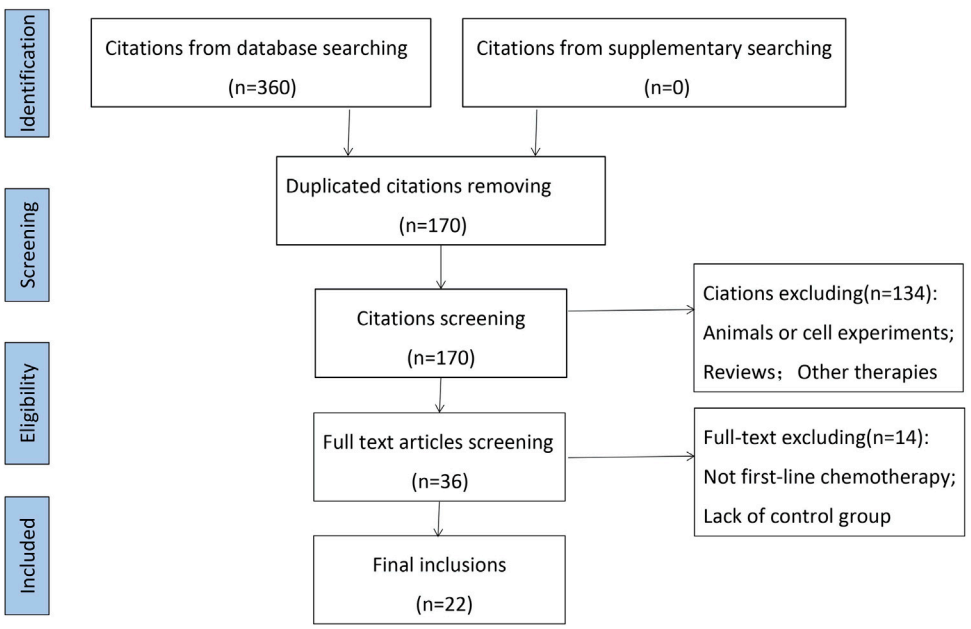

FIGURE 1 | Flow chart of study selection process.

TABLE 1 | Characteristics of RCTs included in the study.

Study	Sample size(E/C)	Age	Sex(Man/Feman)	Clinical stage	Pathological type	Experiment Group(E)	Control Group(C)	Treatment Cycle	First Treatment	Outcome
Chen and Li (2012)	35/35	55.5/60.5	24/11; 22/13	III 14,IV 21; III 13,IV 22	S20,A15; S18,A17	Rg3 20 mg po.bid +C	GP	6-9 weeks	NO	Efficac (RECIST) ; Adverse reactions ; KPS
Chen et al. (2014)	34/34	4 1 ~ 7 3	39/29	IIIB-IV	A26,S21,AC18,B3	Rg3 20 mg po.bid +C	TP	12 weeks	No	Efficacy(RECIST) ; Adverse reactions ; Immune index
Du (2014)	30/30	40.2 ± 3.6	31/29	advanced	NSCLC	Rg3 20 mg po.bid +C	TP	6 weeks	No	Efficacy(RECIST) ; KPS
Li and Bai (2017)	90/90	57 ± 1. 3/58 ± 1. 0	49/41; 49/41	advanced	NSCLC	Rg3 20 mg po.bid +C	GP	9 weeks	No	Efficacy(RECIST) ; PFS,OS; Adverse reactions
Li et al. (2012)	39/38	-	-	advanced	A23,S14,B2; A20,S16,B2	Rg3 20 mg po.bid +C	GP	6 weeks	No	Efficacy(RECIST) ; KPS;Adverse reactions PFS ; one-year survival rate
Liang and Han (2016)	47/46	67.47 ± 7.74/ 66. 32 ± 6. 21	34/13; 31/15	IIIA-IV	NSCLC	Rg3 20 mg po.bid +C	GP	12 weeks	No	KPS;Adverse reactions
Lin et al. (2014)	33/25	65-85	32/26	IIIA6,IIIB6,IV46	A44,S8,P6	Rg3 20 mg po.bid +C	PC	6 weeks	No	Efficacy(RECIST) ; KPS;Adverse reactions
Liu et al. (2007)	35/35	35-70	43/27	IIIB-IV	S26,A40,B4	Rg3 20 mg po.bid +C	NP	6 weeks	Yes	Efficacy(WHO) ; KPS;Adverse reactions;Immune index
Liu et al. (2009)	34/30	43-75/31-66	26/8;19/11	IIIB22,IV12/IIIB26,IV4	A21,S9,AC4/ A21,S6,AC2,B1	Rg3 20 mg po.bid +C	NP	6 weeks	No	Efficacy(WHO) ; Adverse reactions ; one-year survival rate
Liu et al. (2015)	60/60	52.5 ± 2.0/ 54.6 ± 2.1	46/14;35/25	III37,IV23/III29,IV31	A19,S41/A13,S46	Rg3 20 mg po.bid +C	NP	-	No	Efficacy(unclear) ; Adverse reactions
Pan and Wu (2016)	24/24	71.5/71	16/8;15/9	advanced	unclear	Rg3 20 mg po.bid +C	TP	6 weeks	No	Efficacy(RECIST) ; KPS;Adverse reactions
Pan et al. (2019)	103/104	60.6 ± 10.4/ 62.5 ± 11.9	53/50;51/53	III-IV	unclear	Rg3 20 mg po.bid +C	TP	9 weeks	Yes	Efficacy(RECIST) ; KPS;Immune index
Pang (2012)	22/21	63.95	26/17	IIIB13,IV30	A26,S18	Rg3 20 mg po.bid +C	GP/PC/TP	6 weeks	Yes	Efficacy(RECIST) ; KPS;Adverse reactions
Qi and Zhang (2011)	35/35	37-70	48/22	advanced	A40,S26,B4	Rg3 20 mg po.bid +C	GP	6 weeks	Yes	Efficacy(unclear) ; KPS;Adverse reactions
Shen et al. (2018)	25/27	66-78/66-77	14/11;17/10	IIIB-IV	A15,S10/A19,S8	Rg3 20 mg po.bid +C	GP/PC	6 weeks	Yes	Efficacy(WHO); Adverse reactions ; one-year survival rate
Sun et al. (2006)	51/50	59.54/57.44	40/14;39/22	III21,IV33/III24,IV37	S16,A27,AC6,05; S13,A44,AC2,O2	Rg3 20 mg po.bid +C	NP	6 weeks	No	Efficacy(WHO); Adverse reactions; PFS
Tu (2018)	21/20	-	13/8;11/9	III7,IV14;III8,IV12	A10,S7,04;A9,S9,02	Rg3 20 mg po.bid +C	TP	6 weeks	Yes	Efficacy(RECIST) ; KPS;VEGF
Wang et al. (2020)	39/39	54.9 ± 8.1/ 55.6 ± 7.8	21/18;22/17	IIIB18,IV21;IIIB19,IV20	A20,S19;A21,S18	Rg3 20 mg po.bid +C	GP/PC	6 weeks	No	Efficacy(WHO); Adverse reactions
Wang et al. (2011)	59/58	53	74/43	IIIB-IV	A31,S28/A37,S21	Rg3 20 mg po.bid +C	GP/NP	-	Yes	VEGF;KPS;Adverse reactions
Wang et al. (2017)	45/44	58. 95	52/37	IIIb41,IV48	A58,S31	Rg3 20 mg po.bid +C	TP/PC/ GP/NP	6 weeks	No	Efficacy(unclear);KPS;Adverse reactions
Zhang et al. (2020)	41/41	71. 34 ± 4. 25/ 71. 52 ± 3. 65	27/14;26/15	IIIb18,IV23/IIIb17,IV24	UNCLEAR	Rg3 20 mg po.bid +C	GP	12 weeks	No	Efficacy(WHO);KPS;Immune index; Adverse reactions
Zhang et al. (2018)	199/215	61.16 ± 10.41/ 60.76 ± 10.39	128/71; 161,64	IIIA25,IIIB74,IV100/ IIIA20,IIIB73,IV122	A114,S65,B3,017/ A121,S72,B3,O19	Rg3 20 mg po.bid +C	NP/TP	≥6 weeks	Yes	Adverse reactions

S, squamous cell carcinoma; A, adenocarcinoma; AC, adenosquamous carcinoma; B, large cell carcinoma; O, poorly differentiated carcinoma; GP, gemcitabine; TP, PTX; PC, pemetrexeddisodium; NP, navelbine.

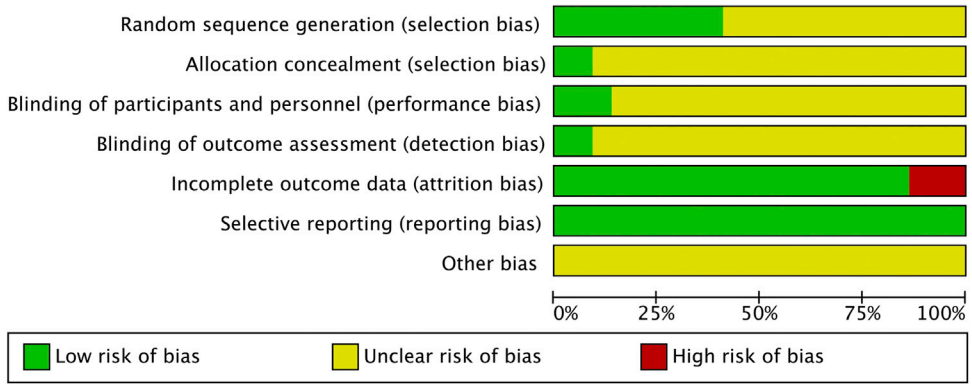

FIGURE 2 | Risk of bias.

2008; Wang et al., 2020; Wang et al., 2011; Wang et al., 2017; Zhang et al., 2020; Zhang et al., 2018).

Characteristics of the Studies

Twenty-two studies with 2202 patients were included in our review. All RCTs originated from China and were published in Chinese journals. The year of publication was between 2006 and 2020, with 19 studies from the last decade. The patients' characteristics of included studies included age, gender, clinical stage, chemotherapy regimen, and treatment indicators and were summarized in **Table 1**.

Quality Assessment

Figure 2 showed our assessment of the bias risk of the included studies by Review Manger 5. All included studies described the process of random sequence generation. However, only 9 of the 22 studies described the detailed process of avoiding selection bias and just two studies reported the allocation concealment and blinding of outcome assessment in detail. As for the performance bias, only three studies mentioned and the rest were not. Among the included studies, three articles were identified as high risk of reporting bias for outcome because the disease control rate was not reported. Nevertheless, they included other important indicators to evaluate the efficacy and safety of ginsenoside Rg3 in combination with first-line chemotherapy in advanced NSCLC, such as KPS, weight change, and side effects. Therefore, after our discussion, we decided to include these three studies in this analysis. The results of each study were reported faithfully, therefore we considered all studies to be free of reporting bias (**Figures 2**, **3**).

Tumor Response

Nineteen studies with 1470 advanced NSCLC participants recorded the short-term treatment efficiency of ginsenoside Rg3 combined with first-line chemotherapy. The overall heterogeneity of the meta-analysis showed that the included studies had clinical and statistical homogeneity, so a fixed-effect model was chosen. As illustrated in **Figure 4**, the experimental group had a higher objective response rate (ORR) than the control group (RR [95% CI], 1.44 [1.27, 1.63], $p < 0.00001$). For disease control rate (DCR), heterogeneity test ($I^2 = 77\%$) suggested that there was considerable heterogeneity, so we turned to a random effect model. Compared with chemotherapy alone, the combine of ginsenoside Rg3 and chemotherapy had a better effect on DCR (RR [95% CI], 1.24 [1.12, 1.38], $p < 0.0001$) (**Figure 5**). Subsequently, we performed regression analysis and subgroup analysis, suggesting that there was no difference in year of publication, evaluation criteria, chemotherapy drugs and first treatment (**Supplementary Figures S1**, **S2**).

Quality of Life

Karnofsky performance status (KPS) score was used to evaluate quality of life. Fourteen of the twenty-two studies evaluated the effect of ginsenoside Rg3 combined with chemotherapy on quality of life in patients with advanced NSCLC (**Figure 6**). An increased of 10 or more in KPS score after treatment was considered as a significant improvement in quality of life, otherwise, it was considered as a stable or even deteriorating quality of life. There was no clinically and statistically significant heterogeneity in these trials. For KPS increase rate, the experimental group was significantly higher than the control group (RR [95% CI], 1.62 [1.42, 1.84], $p < 0.00001$). As for KPS stability rate, the experimental group was higher when compared with the control group (RR [95% CI], 1.21 [1.08, 1.36], $p = 0.001$) (**Supplementary Figure S3**).

Year Survival Rate

For patients with advanced NSCLC, survival rate is an important parameter to evaluate the therapeutic effect. A fixed-effect model was chosen because of the low heterogeneity. Three articles reported one-year survival rate, the results showed that ginsenoside Rg3 combined with chemotherapy had a higher one-year survival rate than chemotherapy alone (RR [95% CI], 1.49 [1.08, 2.06], $p = 0.01$) (**Figure 7**). Two studies reported two-year survival rate, the results showed that ginsenoside Rg3 combined with chemotherapy group had a higher two-year survival rate than chemotherapy alone group (RR [95% CI], 6.22 [1.68, 22.95], $p = 0.006$) (**Figure 8**).

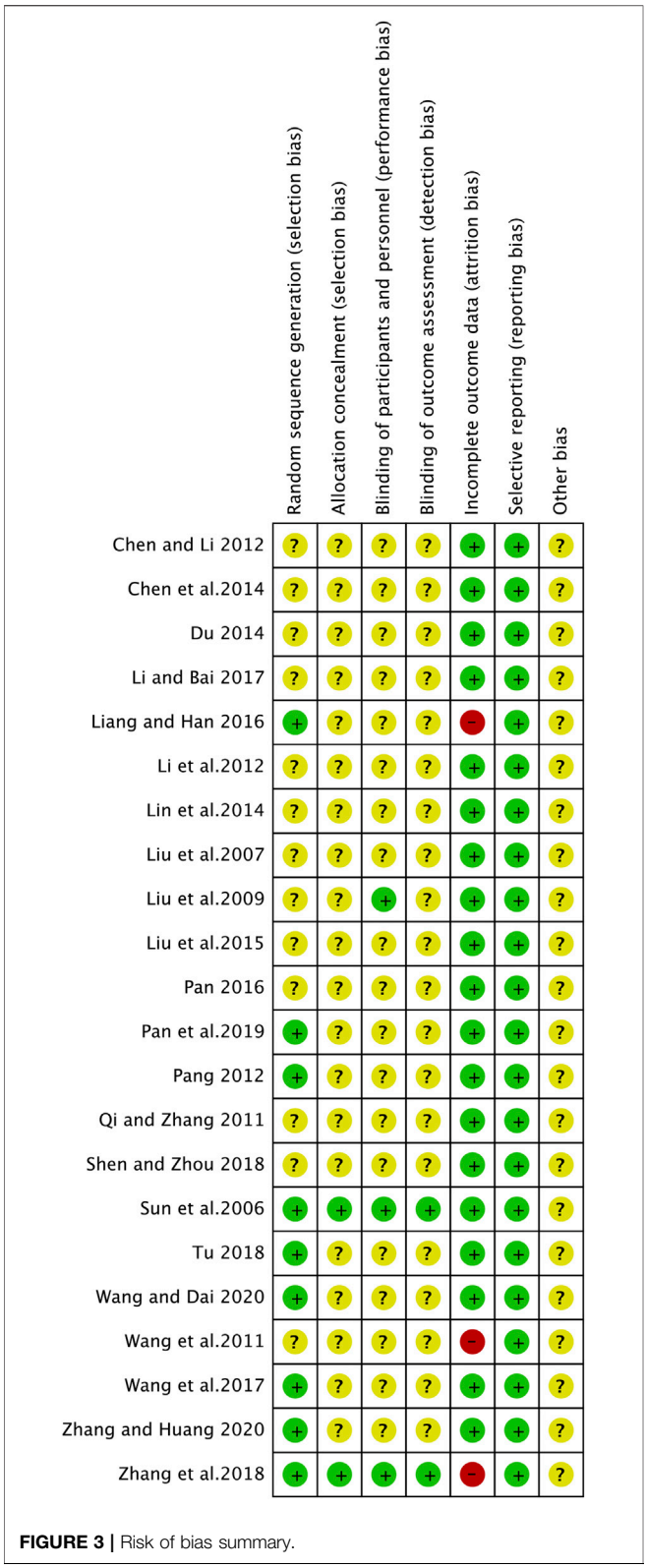

FIGURE 3 | Risk of bias summary.

Weight Change

A total number of five studies reported changes in body weight before and after treatment, and weight gain of ≥1 kg was defined as weight improvement. Compared with the control group, the experimental group had a higher rate of weight improvement. (RR [95% CI], 1.31 [1.04, 1.66], $p = 0.02$) (**Supplementary Figure S4**).

VEGF Leaves

Four articles reported the changes in serum VEGF levels before and after chemotherapy. Because of the high heterogeneity, we chose the random effect model. The experimental group could reduce the level of VEGF more effectively after treatment compared to the control group (RR [95% CI], −2.21 [−4.03, −0.38], $p = 0.02$) (**Supplementary Figure S5**).

Side Effects

The side effects of chemotherapy mainly include gastrointestinal reactions, liver and kidney injury, bone marrow suppression, and hematological toxicity. The incidence of liver and kidney dysfunction (RR [95% CI], 0.72 [0.52, 1.00], $p = 0.05$) and hematotoxicity (thrombocytopenia: RR [95% CI], 0.64 [0.33, 1.22], $p = 0.17$; leukopenia: RR [95% CI], 0.82 [0.66, 1.02], $p = 0.07$; hemoglobin reduction: RR [95% CI], 0.84 [0.60, 1.17], $p = 0.29$) in the experimental group was not statistically different compared with the control group (**Supplementary Figures S6–S9**). The experimental group had a lower incidence of gastrointestinal reactions compared to the control group (RR [95% CI], 0.66 [0.47, 0.93], $p = 0.02$) (**Figure 9**). Although some studies influenced the overall heterogeneity of this metric ($I^2 = 92\%$; $p < 0.00001$), the overall effects remained largely significant. In addition, six studies reported the occurrence of myelosuppression and showed that the experimental group had a lower incidence of myelosuppression than the control group (RR [95% CI], 0.43 [0.30, 0.61], $p < 0.00001$) , with no heterogeneity ($I^2 = 0\%$; $p = 0.57$) (**Supplementary Figure S10**).

According to WHO toxicity classification criteria, grade III-IV was defined as serious adverse reactions. The incidence of leukopenia in the experimental group was lower than that in the control group among the serious adverse reactions (RR [95% CI], 0.48 [0.34, 0.67], $p < 0.001$) (**Supplementary Figure S11**), and the remaining serious adverse reactions were not statistically different.

Publication Bias and Sensitivity Analysis

We performed publication bias analysis on the main parameters and the results showed that publication bias may have an impact on disease control rate and KPS (ORR: $p = 0.555$; DCR: $p = 0.008$; KPS: $p = 0.015$) (**Figure 10**). We conducted sensitivity analyses of the key effect indicators, including objective response rate, disease control rate, and KPS, and the results showed all to be authentic, verifiable, and of good stability (**Figure 11**).

DISCUSSION

In recent years, the combination of ginsenoside Rg3 and chemotherapy has been increasingly proposed and conducted in advanced NSCLC. This systematic review and meta-analysis is the latest to evaluate the efficacy and safety of the therapy combining ginsenoside Rg3 and first-line chemotherapy in

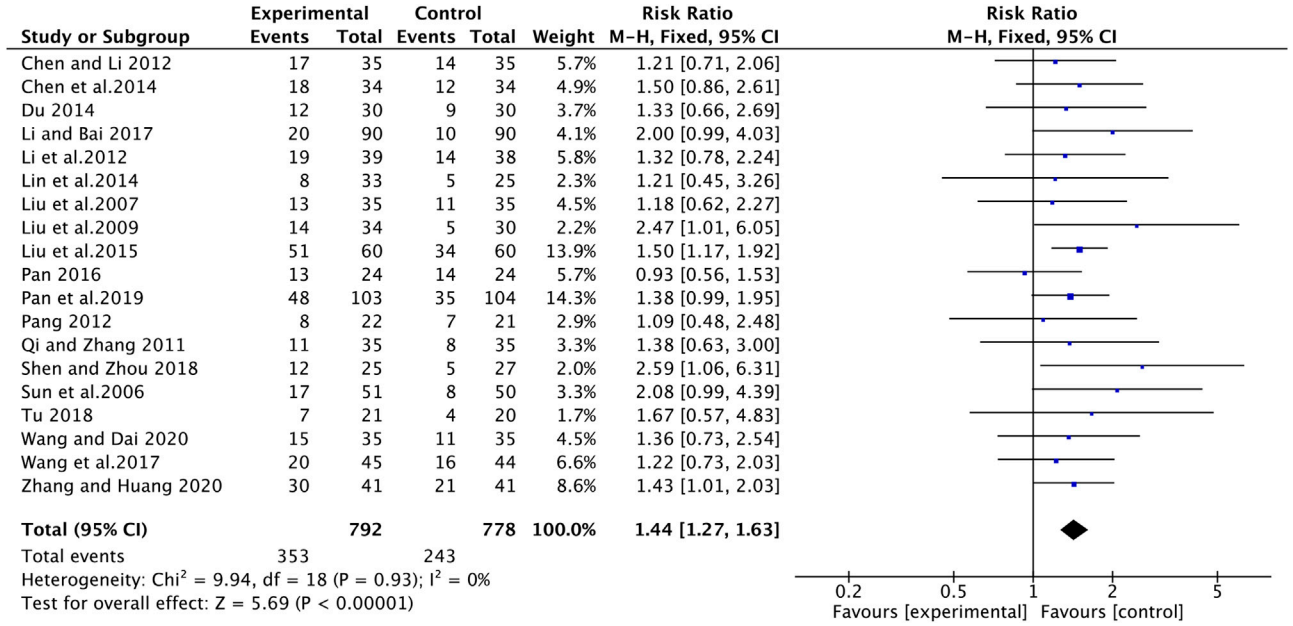

FIGURE 4 | The pooled effects of ginsenosides Rg3-containing chemotherapy on objective response rate.

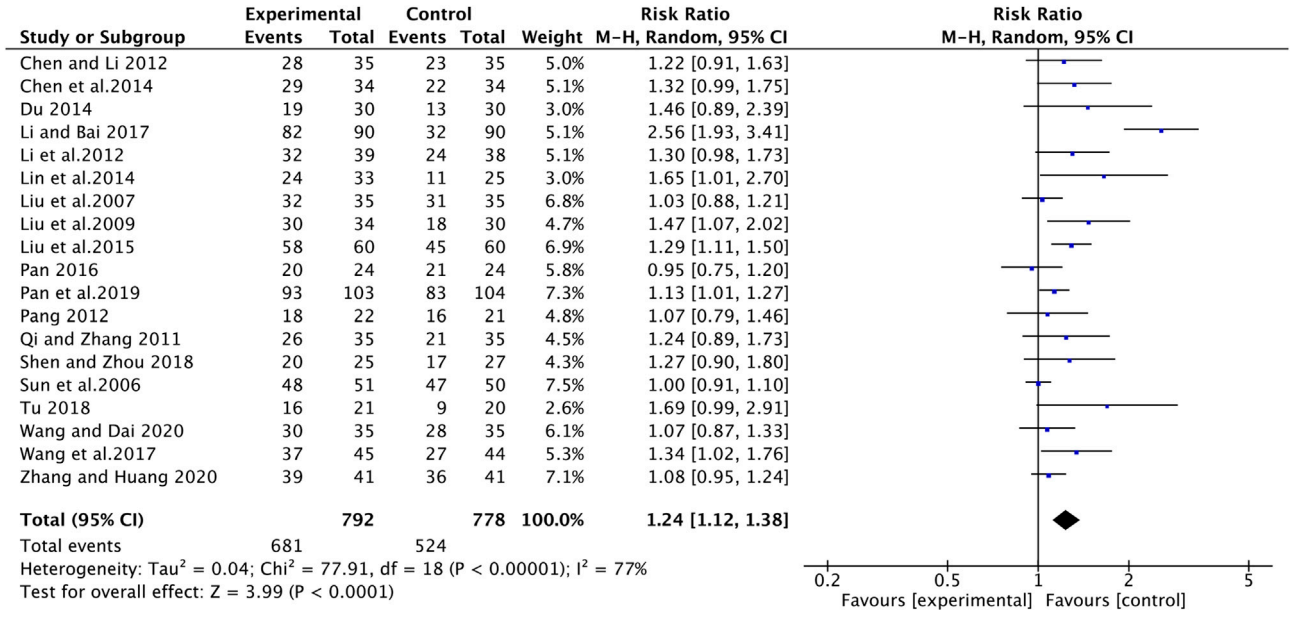

FIGURE 5 | The pooled effects of ginsenosides Rg3-containing chemotherapy on disease control rate.

advanced NSCLC. The results showed that ginsenoside Rg3 in combination with first-line chemotherapy resulted in better objective response rate, disease control rate, KPS score and one-/two-year survival rate, higher increases in patients weight, and higher reduction in VEGF levels and side effects compared with chemotherapy alone.

According to the Response Evaluation Criteria in Solid Tumors (RECIST), assessment of the change in tumour burden is an important feature of the clinical evaluation of cancer therapeutics: both tumour shrinkage (objective response) and disease progression are useful endpoints in clinical trials (Eisenhauer et al., 2009). ORR was defined as

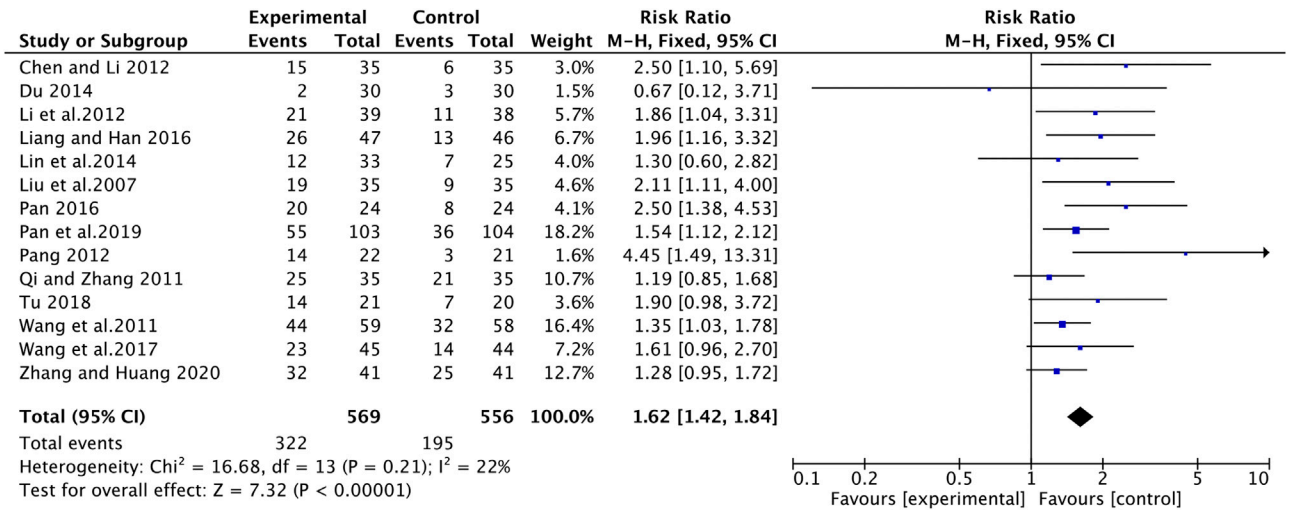

FIGURE 6 | The pooled effects of ginsenosides Rg3-containing chemotherapy on KPS.

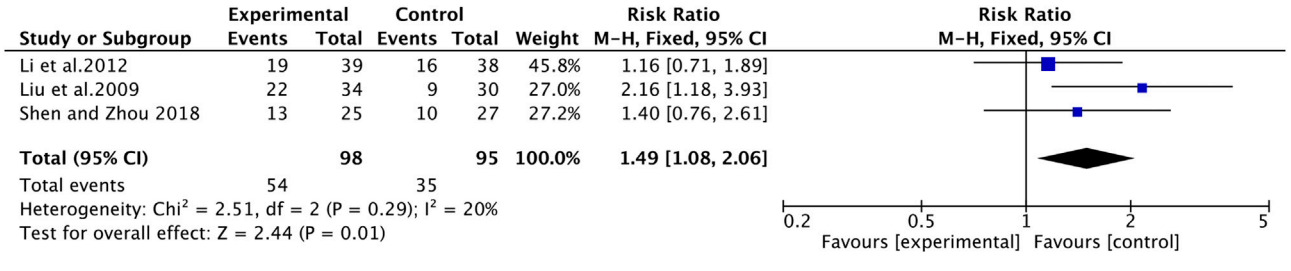

FIGURE 7 | The pooled effects of ginsenosides Rg3-containing chemotherapy on one-year survival rate.

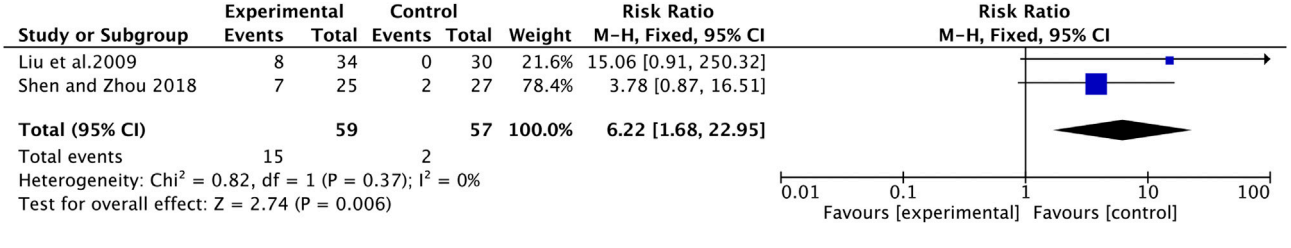

FIGURE 8 | The pooled effects of ginsenosides Rg3-containing chemotherapy on two-year survival rate.

complete response (CR) or partial response (PR). Disease control rate (DCR)was defined as CR or PR in all patients or stable disease (SD) in patients with progressive disease (PD) at the treatment of chemotherapy. At the current time ORR carries with it a body of evidence greater than for any other biomarker supporting its utility as a measure of promising treatment effect in clinical trails.

In our study, 19 studies reported ORR and DCR. Consistent with previous meta-analysis, the results suggested that ginsenoside Rg3 in combination with chemotherapy had a significant advantage in improving ORR (RR 1.44) and DCR (RR 1.23). Subsequently, we classified the patients included in the study as whether they were receiving antineoplastic therapy for the first time. Subgroup analysis showed no statistical difference between the two groups, indicating that chemotherapy containing ginsenosides was significantly beneficial in improving ORR, regardless of whether the patient had received prior anticancer treatment. In addition, there are four main first-line chemotherapy drugs in clinical

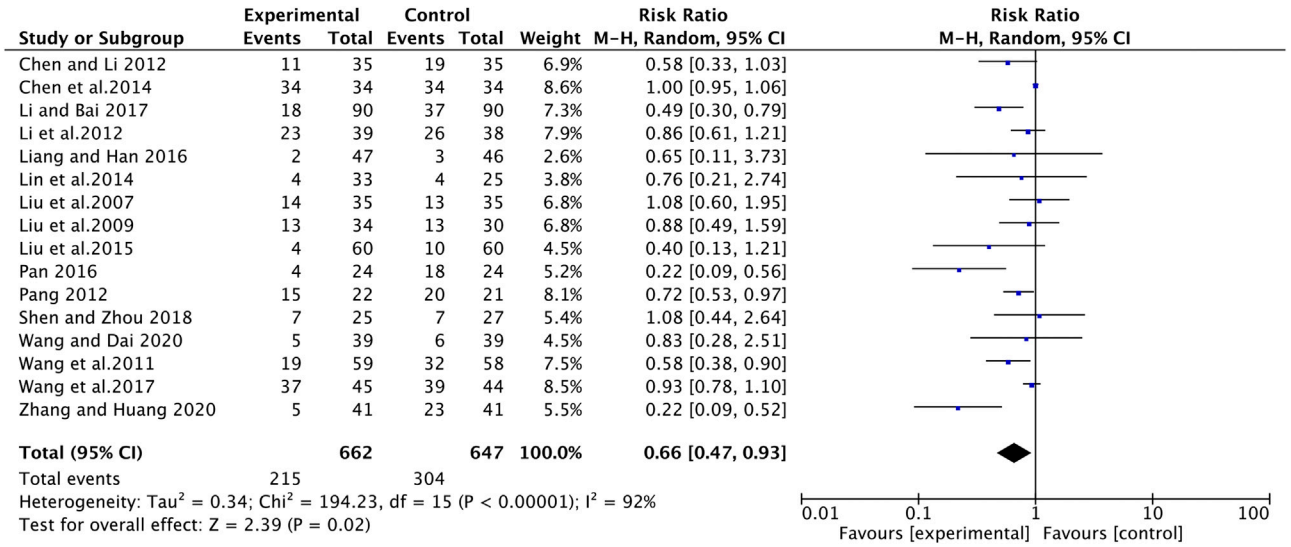

FIGURE 9 | The pooled effects of ginsenosides Rg3-containing chemotherapy on gastrointestinal reactions.

practice, namely gemcitabine (GP), paclitaxel (TP), norvinblastine (NP), and pemetrexide (PC). The results of subgroup analysis showed that ginsenoside combination chemotherapy improved ORR independent of the type of chemotherapeutic agent. The above results suggested us that ginsenoside Rg3 a broad application prospect in the clinical field.

KPS is the Karnofsky performance status scoring standard. The higher the score, the better you are and the more you can tolerate the side effects of treatment, therefore, NSCLC patients are likely to receive complete chemotherapy (Terret et al., 2011). Adding ginsenoside Rg3 to chemotherapy could effectively improve the quality of life of patients with advanced NSCLC and reduce the suffering caused by the disease and chemotherapy (Lu et al., 2008). Previous meta-analysis had demonstrated that ginsenoside combined with chemotherapy could significantly increase KPS in patients with NSCLC (Xu et al., 2016). In our analysis, summary estimates of 14 trials also showed a significant improvement of KPS in the treatment group compared with control group, the improvement was statistically significant. In addition, for the first time, we included weight change as an indicator, which is also important for assessing quality of life. Our results showed that ginsenoside Rg3 combined with chemotherapy was effective in increasing the weight of NSCLC patients ($p = 0.02$).

Annual survival rate is an important parameter to evaluate the prognosis of patients with advanced cancer. Ginseng itself has anti-cancer properties and health benefits, which has been used for centuries in Oriental medicine as a panacea to promote longevity (Kiefer and Pantuso, 2003; Wang et al., 2016). In our analysis, one-year survival and two-year survival rates were reported for the first time. The results showed that ginsenoside Rg3 combined with chemotherapy significantly improved survival time in patients with advanced NSCLC compared with chemotherapy alone. Unfortunately, the credibility of the evidence was relatively low due to the paucity of literature, and more data were needed to support this conclusion.

The vascular endothelial growth factor A (usually referred to as VEGF) play a central role in angiogenesis, promoting endothelial cell proliferation, migration and invasion. Recent evidence shows that VEGF directly targets tumor cells contributing to cancer growth and metastasis. High VEGF expression has been described in lung cancer (Frezzetti et al., 2017). Ginsenoside Rg3 has anti-angiogenic effects, which may be related to the fact that ginsenoside Rg3 reduces the expression of genes related to vascular genetics (Tang et al., 2018). In agreement with the previous meta-analysis, ginsenoside Rg3 combined with chemotherapy could effectively reduce VEGF levels in serum of advanced NSCLC patients ($p = 0.02$).

Systemic chemotherapy typically has very limited efficacy, along with severe systemic adverse effects, such as gastrointestinal reactions, hematological toxicity, liver and kidney injury and so on, which severely affect NSCLC patients' quality of life (Mangal et al., 2017; Islam et al., 2019). Patients with advanced NSCLC are usually forced to interrupt treatment because they can not tolerate the severe side effects, which greatly reduces the treatment outcome. Compared to the previous study (Xu et al., 2016), our article provided a comprehensive analysis of the side effects, and the results suggested that ginsenoside Rg3 combined with chemotherapy was effective in reducing the incidence of gastrointestinal reactions and also played a certain role in reducing other side effects, although there was no statistical difference. In conclusion, ginsenoside Rg3 was safe and effective as an adjuvant for chemotherapy.

Recently, many researchers had conducted *in vitro* experiments on the anti-NSCLC effects of ginsenoside Rg3. Liu et al. (2019) Reported that ginsenoside Rg3 could upregulate VRK1 expression and P53BP1 foci formation in response to DNA damage, thereby inhibiting the tumorigenesis and viability of cancer cells. Futhermore, ginsenoside Rg3 could enhance the anticancer activity of Gefitinib through increasing apoptosis and decreasing migration in NSCLC cell lines (Dai et al., 2019). Therefore,

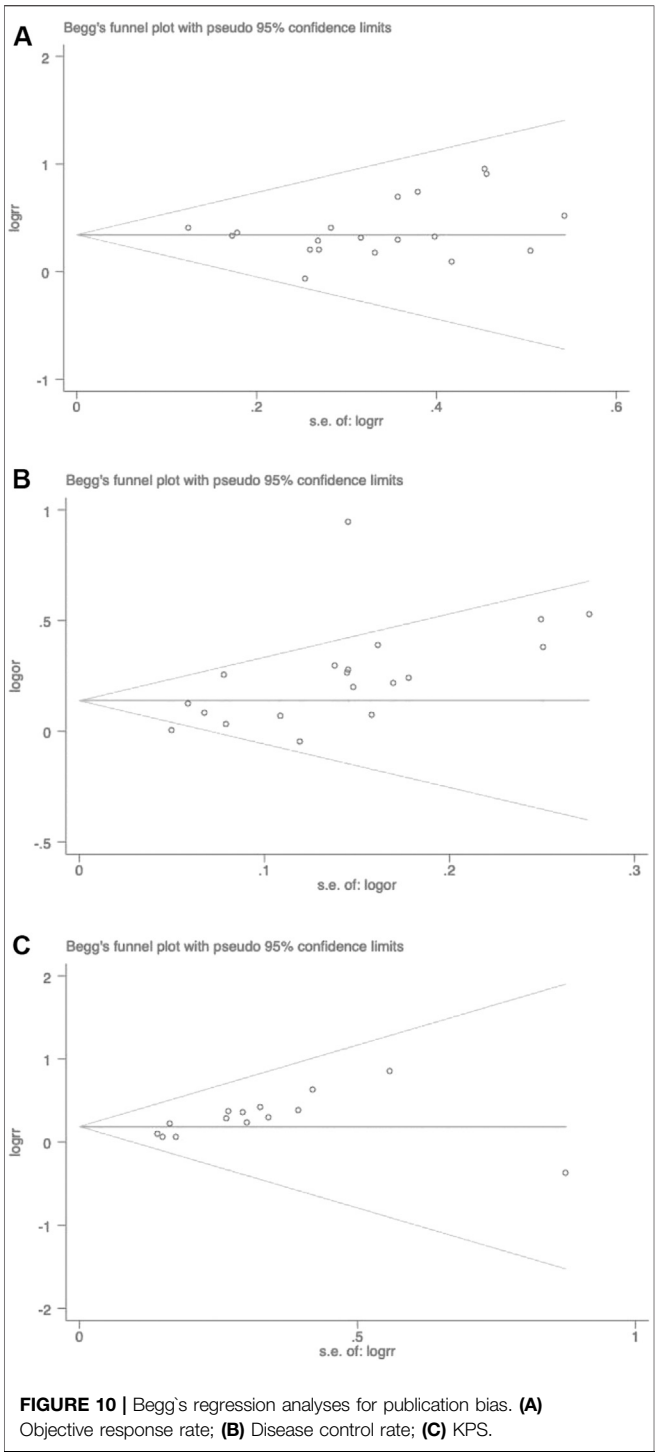

FIGURE 10 | Begg`s regression analyses for publication bias. **(A)** Objective response rate; **(B)** Disease control rate; **(C)** KPS.

ginsenoside Rg3 can effectively improve the efficacy and reverse drug resistance, suggesting that it can be used as an adjuvant in clinical treatment to benefit NSCLC patients.

Limitations

Several limitations are worthy of discussion; firstly, the participants in the selected researches were all Chinese which may not be sufficiently representative. More studies with diverse populations are looking forward to validate the generalizability of our findings. Secondly, the blinded presentation of some studies is too simple or even missing, thus affecting the overall quality of the literature. Therefore, we may need more rigorous clinical experimental design to evaluate the efficacy and safety of ginsenoside Rg3 combined with chemotherapy for advanced NSCLC patients in the future. Thirdly, as an important parameter for evaluating the prognosis of patients with advanced NSCLC, the 5-year survival rate was missing in the original studies we analyzed. However, these studies reported 1-year and 2-year survival rate, both of which are important prognostic evaluation indicators for patients with advanced NSCLC as well. Finally, the sample size of articles screened in this study was not large enough due to the limited number of studies on the combination of chemotherapy and ginsenoside Rg3. More studies with high quality are expected to further validate the efficacy and safety of ginsenoside Rg3 in combination with first-line chemotherapy in advanced NSCLC.

CONCLUSION

Ginsenoside Rg3 can enhance drug efficacy and reduce drug-induced toxicity from chemotherapy. The efficacy and safety of ginsenoside Rg3 in combination with first-line chemotherapy was superior to that of single chemotherapy in patients with advanced NSCLC. These findings provide helpful information for clinicians, indicating that ginsenoside Rg3 can be used as an adjuvant to optimize the treatment of advanced NSCLC.

DATA AVAILABILITY STATEMENT

The raw data supporting the conclusions of this article will be made available by the authors, without undue reservation.

AUTHOR CONTRIBUTIONS

PY designed the study. ZP and WW conducted the experiments and wrote the manuscript.

FUNDING

This article was supported by the National Natural Science Foundation of China (No.81673757).

SUPPLEMENTARY MATERIAL

The Supplementary Material for this article can be found online at: https://www.frontiersin.org/articles/10.3389/fphar.2020.630825/full#supplementary-material.

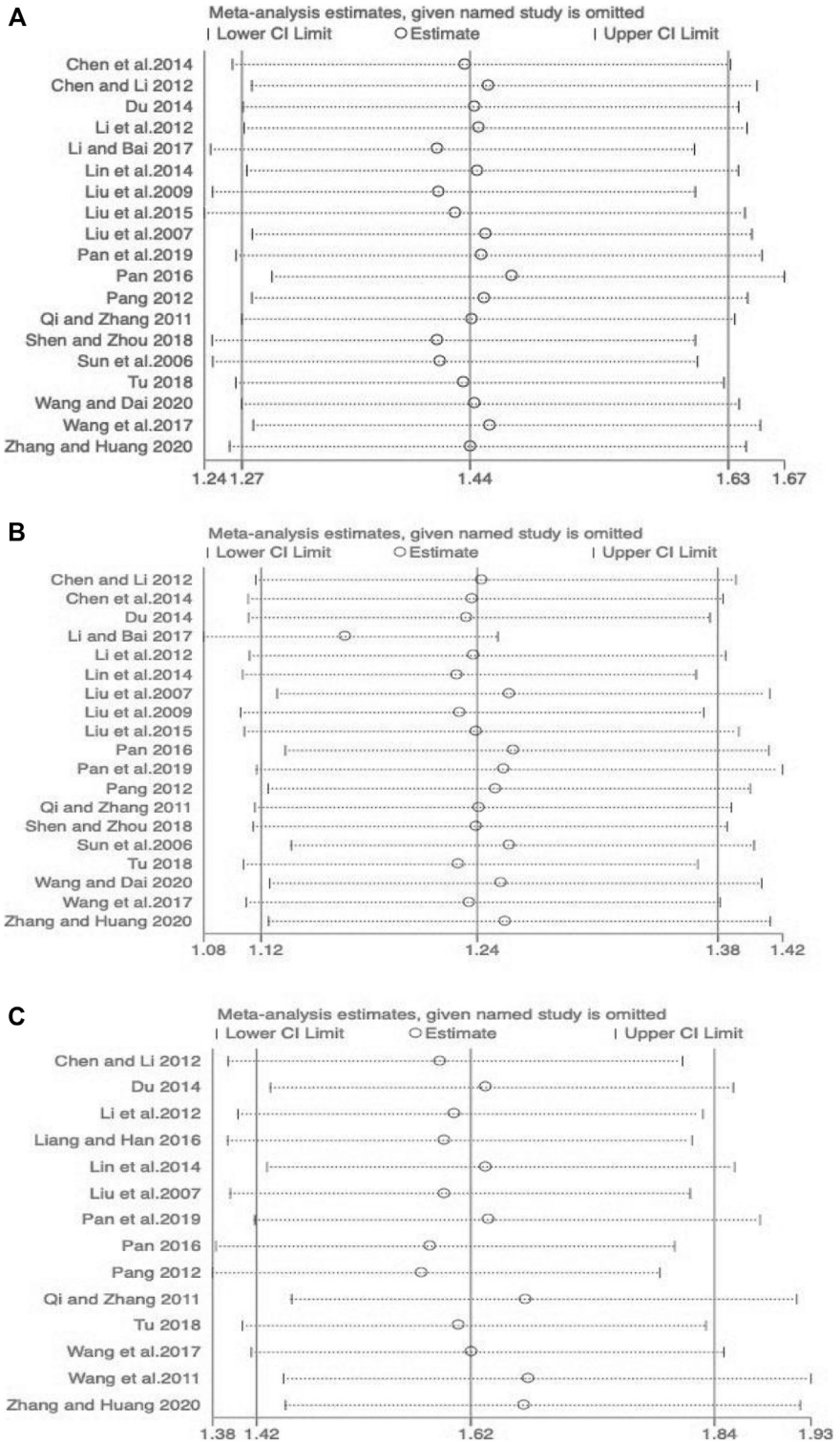

FIGURE 11 | Sensitivity analysis plots. **(A)** Objective response rate; **(B)** Disease control rate; **(C)** KPS.

REFERENCES

Ando, K., Kishino, Y., Homma, T., Kusumoto, S., Yamaoka, T., Tanaka, A., et al. (2020). Nivolumab plus ipilimumab versus existing immunotherapies in patients with PD-L1-positive advanced non-small cell lung cancer: a systematic review and network meta-analysis. *Cancers* 12, 1905. doi:10.3390/cancers12071905

Chen, S., and Li, R. (2012). Clinical observation of Shenyi capsule combined with GP regimen in the treatment of advanced non-small cell lung cancer. *Contemp. Med.* 31, 1. doi:10.3969/j.issn.1009-4393.2012

Chen, W., Tian, Yi, and Shi, Y. (2014). Observation on the efficacy of integrated traditional Chinese and western medicine in the treatment of advanced non-small cell lung cancer. *Mod. J. Integrated Tradit. Chin. West. Med.* 23 (8), 880–881. doi:10.3969/j.issn.1008-8849.2014.08.037

Chinese Medical Association (2020). Chinese medical association guidelines for clinical diagnosis and treatment of lung cancer (2019 edition). *Zhonghua Zhong Liu Za Zhi* 42 (4), 257–287. doi:10.3760/cma.j.cn112152-20200120-00049

Dai, Y., Wang, W., Sun, Q., and Tuohayi, J. (2019). Ginsenoside Rg3 promotes the antitumor activity of gefitinib in lung cancer cell lines. *Exp. Ther. Med.* 17 (1), 953–959. doi:10.3892/etm.2018.7001

Du, L. (2014). Clinical observation of Shenyi capsule in adjuvant treatment of advanced non-small cell lung cancer. *J. Inner Mongolia Tradit. Chin. Med.* 33 (34), 7. doi:10.3969/j.issn.1006-0979.2014.34.007

Du, L., and Morgensztern, D. (2015). Chemotherapy for advanced-stage non-small cell lung cancer. *Cancer J.* 21 (5), 366–370. doi:10.1097/PPO.0000000000000141

Eisenhauer, E. A., Therasse, P., Bogaerts, J., Schwartz, L. H., Sargent, D., Ford, R., and et al. (2009). New response evaluation criteria in solid tumours: revised RECIST guideline (version 1.1). *Eur. J. Cancer* 45 (2), 228–247. doi:10.1016/j.ejca.2008.10.026

Ettinger, D. S., Wood, D. E., Aggarwal, C., Aisner, D. L., Akerley, W., Bauman, J. R., et al. (2019). NCCN guidelines insights: non-small cell lung cancer, version 1.2020. *J. Natl. Compr. Cancer Netw.* 17 (12), 1464–1472. doi:10.6004/jnccn.2019.0059.PMID:31805526

Frezzetti, D., Gallo, M., Maiello, M. R., D'Alessio, A., Esposito, C., Chicchinelli, N., et al. (2017). VEGF as a potential target in lung cancer. *Expert Opin. Ther. Targets* 21, 959–966. doi:10.1080/14728222.2017.1371137

Gao, P. X., and Liu, Y. (2019). A brief discussion on the anticancer research results of ginsenosides Rg3 and Rh2. *Contemp. Med.* 25 (26), 193–194. doi:10.3969/j.issn.1009-4393.2019.26.084

Herbst, R. S., Morgensztern, D., and Boshoff, C. (2018). The biology and management of non-small cell lung cancer. *Nature* 553, 446–454. doi:10.1038/nature25183

Islam, K. M., Anggondowati, T., Deviany, P. E., Ryan, J. E., Fetrick, A., Bagenda, D., et al. (2019). Patient preferences of chemotherapy treatment options and tolerance of chemotherapy side effects in advanced stage lung cancer. *BMC Cancer* 19 (1), 835. doi:10.1186/s12885-019-6054-x

Kiefer, D., and Pantuso, T (2003). Panax ginseng. *Am. Fam. Physician* 68 (8), 1539–1542.

Li, C., Li, Q., and Xu, J. (2012). Clinical observation of Shenyi capsule combined with GP regimen in the treatment of advanced non-small cell lung cancer. *Cancer Res. Prev. Treat.* 39 (9), 1125–1127. doi:10.3971/j.issn.1000-8578.2012.09.017

Li, Y., and Bai, W. (2017). Efficacy analysis of Shenyi capsule combined with GP chemotherapy regimen in the treatment of non-small cell lung cancer. *Liaoning J. Tradit. Chin. Med.* 44 (3), 553–555. doi:10.13192/j.issn.1000-1719.2017.03.037

Li, Y., Wang, Y., Niu, K., Chen, X., Xia, L., Lu, D., et al. (2016). Clinical benefit from EGFR-TKI plus ginsenoside Rg3 in patients with advanced non-small cell lung cancer harboring EGFR active mutation. *Oncotarget* 7 (43), 70535–70545. doi:10.18632/oncotarget.12059

Liang, J., and Han, X. (2016). The effect of ginsenoside Rg3 combined with chemotherapy on serum TGF-α, TGF-β1 and VEGF in patients with advanced non-small cell lung cancer. *J. Clin. Pulm. Med.* 21 (9), 1675–1678. doi:10.3969/j.issn.1009-6663.2016.09.035

Liao, Y. H., Li, C. I., Lin, C. C., Lin, J. G., Chiang, J. H., and Li, T. C. (2017). Traditional Chinese medicine as adjunctive therapy improves the long-term survival of lung cancer patients. *J. Cancer Res. Clin. Oncol.* 143 (12), 2425–2435. doi:10.1007/s00432-017-2491-6

Lin, Q., Shen, D., and Lu, C. (2014). Clinical observation of pemetrexed combined with shenyi capsule in the treatment of NSCLC. *Med. Inf.* 27 (24), 167–168. doi:10.3969/j.issn.1006-1959.2014.24.183

Liu, S., Sun, L., and Ban, L. (2007). Clinical observation of Shenyi capsule combined with NP regimen in the treatment of advanced non-small cell lung cancer. *J. Clin. Oncol.* 12 (11), 847–849. doi:10.3969/j.issn.1009-0460.2007.11.014

Liu, X., Yang, H., and Li, L. (2009). Observation on the efficacy of Shenyi capsule combined with chemotherapy in the treatment of advanced non-small cell lung cancer. *Jilin Med.* 30 (19), 2319–2320. doi:10.3969/j.issn.1004-0412.2009.19.064

Liu, S., Zheng, R., and Cui, J. (2015). Clinical study of Shenyi capsule combined with first-line chemotherapy in the treatment of advanced non-small cell lung cancer. *Electron. J. Clin. Med. Lit.* (24), 5040–5041. doi:10.16281/j.cnki.jocml.2015.24.073

Liu, T., Zuo, L., Guo, D., Chai, X., Xu, J., Cui, Z., and et al. (2019). Ginsenoside Rg3 regulates DNA damage in non-small cell lung cancer cells by activating VRK1/P53BP1 pathway. *Biomed. Pharmacother.* 120, 109483. doi:10.1016/j.biopha.2019.109483

Lu, P., Su, W., Miao, Z. H., Niu, H. R., Liu, J., and Hua, Q. L. (2008). Effect and mechanism of ginsenoside Rg3 on postoperative life span of patients with non-small cell lung cancer. *Chin. J. Integr. Med.* 14, 33–36. doi:10.1007/s11655-007-9002

Luo, H., Vong, C. T., Chen, H., Gao, Y., Lyu, P., Qiu, L., et al. (2019). Naturally occurring anti-cancer compounds: shining from Chinese herbal medicine. *Chin. Med.* 14, 48. doi:10.1186/s13020-019-0270-9

Mangal, S, Gao, W, Li, T, and Zhou, Q. T (2017). Pulmonary delivery of nanoparticle chemotherapy for the treatment of lung cancers: challenges and opportunities. *Acta Pharmacol. Sin.* 38 (6), 782–797. doi:10.1038/aps.2017.34.Epub2017May1

Miller, K. D., Nogueira, L., Mariotto, A. B., Rowland, J. H., Yabroff, K. R., Alfano, C. M., et al. (2019). Cancer treatment and survivorship statistics, *CA Cancer J. Clin.* 69 (5), 363–385. doi:10.3322/caac.21565

Nakhjavani, M., Smith, E., Townsend, A. R., Price, T. J., and Hardingham, J. E. (2020). Anti-angiogenic properties of ginsenoside Rg3. *Molecules* 25 (21), E4905. doi:10.3390/molecules25214905

Nasim, F., Sabath, B. F., and Eapen, G. A. Lung cancer (2019). *Med. Clin. North Am.* 103, 463–473. doi:10.1016/j.mcna.2018.12.006

Pan, Y., Sun, M., and Liu, X. (2019). The effect of Shenyi capsule on the chemotherapy effect of patients with advanced non-small cell lung cancer. *Med. Clin. Res.* 36 (10), 2043–2044. doi:10.3969/j.issn.1671-7171.2019.10.063

Pan, Y., and Wu, X. (2016). Docetaxel and Shenyi capsule combined with cisplatin in the treatment of elderly non-small cell lung cancer. *J. Pract. Med.* 33 (8), 699–700. doi:10.14172/j.issn1671-4008.2016.08.012

Pang, M. (2012). *Study on the correlation between the short-term efficacy of Shenyi capsule combined with chemotherapy in the treatment of advanced non-small cell lung cancer and the changes of serum VEGF and bFGF levels*: Jinan: University of Jinan.

Qi, C., and Zhang, H. (2011). Clinical observation of traditional Chinese medicine vascular inhibitor ginsenoside Rg3 combined with GP regimen in the treatment of non-small cell lung cancer. *J. Pract. Clin. Med.* 15 (11), 121–122. doi:10.3969/j.issn.1672-2353.2011.11.043

Rose, M. C, Kostyanovskaya, E, and Huang, R. S. (2014). Pharmacogenomics of cisplatin sensitivity in non-small cell lung cancer. *Dev. Reprod. Biol.* 12, 198–209. doi:10.1016/j.gpb.2014.10.003

Rossi, A., and Di Maio, M. (2016). Platinum-based chemotherapy in advanced non-small-cell lung cancer: optimal number of treatment cycles. *Expert Rev. Anticancer Ther.* 16, 653–660. doi:10.1586/14737140.2016.1170596

Shen, K., Zhou, W., and Ye, Z. (2018). Efficacy observation of Shenyi capsule combined with chemotherapy regimen in the treatment of elderly advanced non-small cell lung cancer. *J. Pract. Clin. Med.* 22 (23), 123–124. doi:10.7619/jcmp.201823037

Siegel, R. L., Miller, K. D., and Jemal, A (2020). Cancer statistics. *CA Cancer J. Clin.* 70, 7–30. doi:10.3322/caac.21590

So, T. H., Chan, S. K., Lee, V. H., Chen, B. Z., Kong, F. M., and Lao, L. X. (2019). Chinese medicine in cancer treatment–how is it practised in the east and the west?. *Clin. Oncol.* 31 (8), 578–588. doi:10.1016/j.clon.2019.05.016

Sun, Y., Lin, H., and Zhu, Y. (2006). A multicenter double-blind randomized clinical study report of vinorelbine combined with cisplatin (NP) plus Shenyi

capsule or placebo in the treatment of advanced non-small cell lung cancer. *Chin. J. Lung Cancer* 9 (3), 254–258.

Sun, M., Ye, Y., Xiao, L., Duan, X., Zhang, Y., and Zhang, H. (2017). Anticancer effects of ginsenoside Rg3 (review). *Int. J. Mol. Med.* 39, 507–518. doi:10.3892/ijmm.2017.2857

Tang, Y. C., Zhang, Y., Zhou, J., Zhi, Q., Wu, M. Y., Gong, F. R., et al. (2018). Ginsenoside Rg3 targets cancer stem cells and tumor angiogenesis to inhibit colorectal cancer progression *in vivo*. *Int. J. Oncol.* 52 (1), 127–138. doi:10.3892/ijo.2017.4183.Epub2017Nov1

Terret, C., Albrand, G., Moncenix, G., and Droz, J. P. (2011). Karnofsky performance scale (KPS) or physical performance test (PPT)? That is the question. *Crit. Rev. Oncol. Hematol.* 77, 142–147. doi:10.1016/j.critrevonc.2010.01.015

Tu, H. (2008). *Effect of ginsenoside Rg3 combined with chemotherapy on serum vascular endothelial growth factor in patients with non-small cell lung cancer and observation of its efficacy*: Fuzhou: Fujian University of Traditional Chinese Medicine.

von Plessen, C. (2011). Improving chemotherapy for patients with advanced non-small cell lung cancer. *Clin. Respir. J.* 5 (1), 60–61. doi:10.1111/j.1752-699X.2010.00199.x

Wang, Y., Liu, J., and Zhao, H. (2011). The efficacy of ginsenoside Rg3 capsule combined with chemotherapy in the treatment of advanced non-small cell lung cancer. *J. Pract. Oncol.* 25 (1), 33–35. doi:10.3969/j.issn.1002-3070.2011.01.010

Wang, C. Z., Anderson, S., DU, W., He, T. C., and Yuan, C. S., (2016). Red ginseng and cancer treatment. *Chin. J. Nat. Med.* 14 (1), 7–16. doi:10.3724/SP.J.1009.2016.00007.PMID:26850342

Wang, G., Liu, F., and Zhang, Z. (2017). Observation on the efficacy of Shenyi capsule combined with chemotherapy in the treatment of advanced non-small cell lung cancer and changes in serum MMP-9 and TIMP-1. *Mod. Oncol.* 25 (6), 896–901. doi:10.3969/j.issn.1672-4992.2017.06.015

Wang, F., Dai, L., and Shan, S. (2020). Application of Shenyi capsule combined with chemotherapy in the treatment of advanced non-small cell lung cancer. *China Healthcare Nutr.* 30 (20), 319–320.

Wang, H. Y., and Jin, H. (2018). Research progress on anti-tumor effects of ginsenoside Rg3. *Digest World Latest Med. Inf.* 18 (68), 50–51. doi:10.19613/j.cnki.1671-3141.2018.68.022

Watanabe, S. I., Nakagawa, K., Suzuki, K., Takamochi, K., Ito, H., Okami, J., et al.Group Lung Cancer Surgical Study, Group of the Japan Clinical Oncology (2017). Neoadjuvant and adjuvant therapy for Stage III non-small cell lung cancer. *Jpn. J. Clin. Oncol.* 47 (12), 1112–1118. doi:10.1093/jjco/hyx147

Xiang, Y., Guo, Z., Zhu, P., Chen, J., and Huang, Y. (2019). Traditional Chinese medicine as a cancer treatment: modern perspectives of ancient but advanced science. *Cancer Med.* 8 (5), 1958–1975. doi:10.1002/cam4.2108

Xu, T., Jin, Z., Yuan, Y., Wei, H., Xu, X., He, S., et al. (2016). Ginsenoside Rg3 serves as an adjuvant chemotherapeutic agent and VEGF inhibitor in the treatment of non-small cell lung cancer: a meta-analysis and systematic review. *Evid. Based Compl. Alternat. Med.* 2016, 7826753. doi:10.1155/2016/7826753

Zhang, Y., Wang, X., and Liu, H. (2018). A multi-center large-sample randomized clinical study of Shenyi capsule combined with chemotherapy to improve the prognosis of patients with advanced non-small cell lung cancer. *Chin. J. Oncol.* 40 (4), 295–299. doi:10.3760/cma.j.issn.0253-3766.2018.04.011

Zhang, L., Huang, L., and Huang, K. (2020). Shenyi capsule combined with chemotherapy on the short-term curative effect of patients with advanced non-small cell lung cancer and the effect of serum NKG2D, IFN-γ, IL-2 levels and T lymphocyte subsets. *Chin. J. Gerontol.* 40 (11), 2296–2299. doi:10.3969/j.issn.1005-9202.2020.11.017

Zhao, H., and Chen, J. H. (2020). Research progress in maintenance treatment of advanced non-small cell lung cancer. *Oncol. Pharmacy.* 10 (03), 269–274. doi:10.3969/j.issn.2095-1264.2020.03.03

Conflict of Interest: The authors declare that the research was conducted in the absence of any commercial or financial relationships that could be construed as a potential conflict of interest.

frontiers in Pharmacology

ORIGINAL RESEARCH
published: 25 March 2021
doi: 10.3389/fphar.2021.637098

The Tubulin Inhibitor VERU-111 in Combination With Vemurafenib Provides an Effective Treatment of Vemurafenib-Resistant A375 Melanoma

Hongmei Cui[1,2], *Qinghui Wang*[1], *Duane D. Miller*[1] *and Wei Li*[1]*

[1]*Department of Pharmaceutical Sciences, University of Tennessee Health Science Center, Memphis, TN, United States,* [2]*Institute of Toxicology, School of Public Health, Lanzhou University, Lanzhou, China*

Melanoma is one of the deadliest skin cancers having a five-year survival rate around 15–20%. An overactivated MAPK/AKT pathway is well-established in BRAF mutant melanoma. Vemurafenib (Vem) was the first FDA-approved BRAF inhibitor and gained great clinical success in treating late-stage melanoma. However, most patients develop acquired resistance to Vem within 6–9 months. Therefore, developing a new treatment strategy to overcome Vem-resistance is highly significant. Our previous study reported that the combination of a tubulin inhibitor ABI-274 with Vem showed a significant synergistic effect to sensitize Vem-resistant melanoma both *in vitro* and *in vivo*. In the present study, we unveiled that VERU-111, an orally bioavailable inhibitor of α and β tubulin that is under clinical development, is highly potent against Vem-resistant melanoma cells. The combination of Vem and VERU-111 resulted in a dramatically enhanced inhibitory effect on cancer cells *in vitro* and Vem-resistant melanoma tumor growth *in vivo* compared with single-agent treatment. Further molecular signaling analyses demonstrated that in addition to ERK/AKT pathway, Skp2 E3 ligase also plays a critical role in Vem-resistant mechanisms. Knockout of Skp2 diminished oncogene AKT expression and contributed to the synergistic inhibitory effect of Vem and VERU-111. Our results indicate a treatment combination of VERU-111 and Vem holds a great promise to overcome Vem-resistance for melanoma patients harboring BRAF (V600E) mutation.

Keywords: VERU-111, vemurafenib-resistance, melanoma, ERK, akt, skp2

OPEN ACCESS

Edited by:
Farrukh Aqil,
University of Louisville, United States

Reviewed by:
Mohammad Sherwani,
University of Alabama at Birmingham, United States
Maqsood Ahmed Siddiqui,
King Saud University, Saudi Arabia

***Correspondence:**
Wei Li
wli@uthsc.edu

Specialty section:
This article was submitted to Pharmacology of Anti-Cancer Drugs, a section of the journal Frontiers in Pharmacology

Received: *02 December 2020*
Accepted: *08 February 2021*
Published: *25 March 2021*

Citation:
Cui H, Wang Q, Miller DD and Li W (2021) The Tubulin Inhibitor VERU-111 in Combination With Vemurafenib Provides an Effective Treatment of Vemurafenib-Resistant A375 Melanoma. Front. Pharmacol. 12:637098. doi: 10.3389/fphar.2021.637098

INTRODUCTION

Melanoma is one of the most common skin cancers, and the five-year survival rate for metastatic melanoma is 15–20% (Patel et al., 2020). Exposure to UV radiation increases the risk of DNA damage and genetic changes, thus confers susceptibility to melanoma.

It is well-established that the mitogen-activated protein kinase (MAPK) and phosphatidylinositol 3-kinase (PI3K)/protein kinase B (AKT) signaling pathways are overactivated in melanoma since BRAF mutation leads to uncontrollable cell growth and ultimately develops into cancer (Lim et al., 2017; Faghfuri et al., 2018). BRAF mutant melanoma accounts for nearly 50% of metastatic

melanoma cases, among which V600E mutant represents 84.6% of the BRAF mutations (Patel et al., 2020). Currently, targeted therapies for metastatic melanoma mainly include BRAF and MEK inhibitors, such as Vemurafenib (the first FDA-approved BRAF inhibitor), dabrafenib, encorafenib, trametinib (the first FDA-approved MEK inhibitor), cobimetinib, and binimetinib (Shirley 2018). However, although ATP-competitive BRAF (V600E) kinase inhibitor such as Vem or its combination with a MEK inhibitor has dramatically improved the treatment outcome for patients with metastatic melanoma (Spain et al., 2016; Simeone et al., 2017; Trojaniello et al., 2019), over 50% of patients develop acquired drug resistance and began to show signs of tumor recurrence within 6–9 months of treatment (Torres-Collado et al., 2018).

Several mechanisms have been documented to mediate Vem-resistance, for example, overexpression of P-glycoprotein (P-gp), BRAF mutation, aberrant expression of miRNA, translocation of E3 ligase, or PI3K/AKT pathway (Johnson et al., 2014; Duggan et al., 2017; Lim et al., 2017; Thang et al., 2017; Diaz-Martinez et al., 2018). Such mechanistic understandings have led to a number of exciting synergistic combinations to re-sensitize Vem against metastatic melanoma. For example, JQ1, a bromodomain inhibitor, was found to re-sensitize the Vem-resistant melanoma cells to undergo apoptosis *in vitro* by decreasing the expressions of P-gp and acetylated histone H3 (Zhao et al., 2018). Since checkpoint kinase 1 (Chk1) plays a pivotal role in controlling cell cycle progression, Hwang et al. reported that PF477736 (a potent and specific inhibitor of Chk1) effectively promotes Vem-resistant melanoma cells to regain sensitivity to Vem by lowering the total level of Chk1 and modifying its phosphorylation (Hwang et al., 2018). Recently, PRIMA-1^{Met}, also known as APR-246, propels both Vem-sensitive and Vem-resistant melanoma cells to apoptotic cell death via directly activating p53 and indirectly inhibiting PI3K/AKT pathway (Krayem et al., 2016).

Although combinations of BRAF inhibitor with MEK or ERK inhibitors benefit Vem-resistant patients (Atefi et al., 2011; Gadiot et al., 2013; Pulkkinen et al., 2020), half of the patients still gain resistance after 6–8 months. Intriguingly, some tubulin destabilizing agents reported previously by us targeting the colchicine-binding site showed promise to overcome Vem-resistance, paclitaxel-resistance in melanoma, breast cancer, lung cancer, prostate cancer, cervical cancer et al. (Wang et al., 2014; Guan et al., 2017; Arnst et al., 2018; Deng et al., 2020; Kashyap et al., 2020; Mahmud et al., 2020). In our previous studies, we have demonstrated that a tool tubulin inhibitor, ABI-274, showed strong synergistic efficacy in a Vem-resistant xenograft mouse model (Wang et al., 2014). Besides, the combination of Vem with ABI-274 arrested both A375 and A375 Vem-resistant cells at both G0-G1 and G2-M phase, which arrested the tumor cells at G2-M phase and captured resistant cells escaping from G0-G1 Phase. ABI-274 is a tool compound developed in our lab as a potent tubulin inhibitor that binds to the colchicine binding site (Chen et al., 2010; Wang et al., 2018). Further structural optimization from ABI-274 led to VERU-111 (**Figure 1A**), which is orally available and much more potent and less toxic in several types of tumor models, including prostate cancer, melanoma, breast cancer, lung cancer, and pancreatic cancer (Chen et al., 2012; Deng et al., 2020; Kashyap et al., 2020; Mahmud et al., 2020). As literature reported, the IC_{50} of ABI-274 was 25.3 nM while IC_{50} of VERU-111 was 8.2 nM in MDA-MB-231 breast cancer cell, and the IC_{50} of ABI-274 was 18.7 nM while IC_{50} of VERU-111 was 10.4 nM in A375 melanoma cell (Chen et al., 2020). VERU-111 has now been under Phase 1b/2 clinical trials for men with metastatic castration and androgen-blocking agent resistant prostate cancer (ClinicalTrials.gov Identifier: NCT03752099) and holds great promise to become an oral tubulin inhibitor targeting the colchicine binding site. In the present study, we investigated the ability of VERU-111 to re-sensitize Vem and thus effectively overcome Vem-resistance in BRAF^{V600E} melanoma tumor models.

MATERIALS AND METHODS

Reagents and Cell Lines

Vemurafenib was purchased from LC Laboratories (Woburn, MA), and VERU-111 was synthesized as described previously (**Figure 1A**). The human melanoma A375 cell line was acquired from ATCC (ATCC® CRL-1619) and maintained in DMEM with 10% FBS. Vemurafenib-resistant melanoma cells were built according to literature (Su et al., 2012). Briefly, cells were chronically selected by culturing A375 cells in increasing concentrations of Vem for at least 3 months and named VR1 cells. The isolated resistant VR1 cell line steadily increased IC_{50} values for Vem above 10 μm and maintained in full growth medium containing 5 μm Vem. VR1-SgSkp2 cells generated from VR1 cells and Skp2 was knocked out with guide RNA sequence: 5′-atgcacaggaagcacctcc-3′, screened with puromycin and maintained in full growth medium containing 5 μm Vem.

Cell Proliferation and IC_{50} Measurement

Cell proliferation was determined using the MTS [3-(4,5-dimethylthiazol-2-yl)-5(3-carboxymethoxyphenyl)-2-(4-sulfopheny)-2H-tetrazolium, inner salt] reagents (Promega, Madison, WI) following manual instruction. Briefly, cells were seeded at a concentration of 5,000 cells/well in 96-well plate, on next day, the cell culture medium contains the vemurafenib or VERU-111 at different concentrations was added into the well with four duplications. After 72 h later, 20 ul MTS solution was added and measured at 490 nm absorbance. IC_{50} was calculated using Graphpad Prism software with transformed drug concentration in Log10. Compound concentrations used *in vivo* animal study was based on previous publication (Wang et al., 2014).

Cell-Cycle and Apoptosis Analysis

To determine apoptosis and cell-cycle distributions, treated cells (24 h) were harvested with trypsin and fixed in 70% cold ethanol for overnight, then stained with PI (50 μg/ml)/RNase (100 μg/ml) solution for 60 min at room temperature in the dark according to the manufacturer's instructions (Sigma Aldrich, St. Louis, MO).

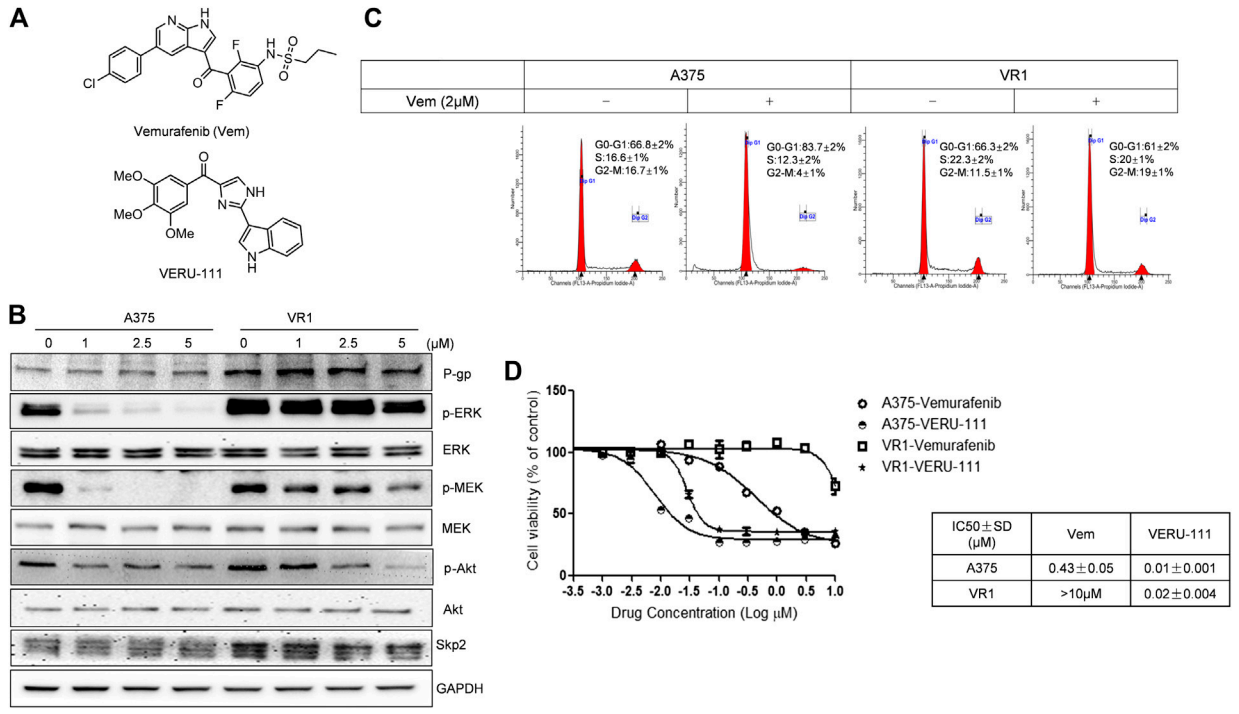

FIGURE 1 | VERU-111 is efficient in both A375 and A375-Vem resistant (VR1) cells **(A)** Structure of compound Vemurafenib (Vem) and VERU-111 **(B)** p-ERK/p-MEK is persistantly expressed in VR1 cells **(C)** Vem treatment leads to G0-G1 arrest in both parental A375 and Vem-resistant VR1 cell **(D)** MTS assay to test IC_{50} in parental A375 melanoma and VR1 cells.

Cell apoptosis was monitored by using the Annexin V-FITC Apoptosis Detection Kit (Abcam) following manufacturer's instructions, and the data was processed using the Modfit 2.0 software and analyzed by a BD LSR-II cytometer (BD Biosciences).

Colony Formation Assays

For colony formation assays, 1,000 cells were plated in 6-well plates with triplicates, compound with indicated concentration was added in the next day, and surviving colonies were stained with crystal violet 10 days later and counted.

Western Blot Analysis

At the indicated time (24 h), treated A375, VR1, VR1-SgSkp2 cells were collected to investigate levels of relevant cascade protein or apoptotic markers by Western blot analysis. The following antibodies from Cell Signaling were used: p-ERK1/2 (#9101), p44/42 MAPK (ERK1/2; #9102), p- AKT (Ser473; #9271), AKT (#9272), cleaved PARP (#9185), or GAPDH (#3683). Skp2 antibody was purchased from Santa Cruz (sc-74477).

Endogenous Co-Immunoprecipitation Assay

For the co-immunoprecipitation assay, A375 cells and VR1 cells were treated with 5 μm Vem for 24 h, the cell lysates were incubated with A/G beads (Millipore) with corresponding equal amount of antibody in RIPA buffer (50 mM Tris-HCl, pH 7.4, 100 mM NaCl, 1% NP-40, 0.1% SDS, 0.5% sodium deoxycholate and 1 mM EDTA) at 4°C overnight. After extensive washes, precipitated proteins on beads were boiled and loaded onto SDS-PAGE gel and further performed Western blotting.

Vemurafenib-Resistant Tumor Xenograft and Treatment

6–8-weeks NSG male mice were provided by Dr Seagrous lab. VR1 cells were suspended in PBS and mixed with high concentration Matrigel (BD Biosciences) at a ratio of 2:1 right before use. 100 μl of this mixture containing 2×10^6 cells were injected subcutaneously to the right-side dorsal flank of each mouse. The regimen formulation and treatment refer to (Wang et al., 2014). Briefly, VERU-111 or Vem was diluted in PEG300 (Sigma Aldrich) and administered through intraperitoneal injection once per day, 5 days per week for three continuous weeks. Tumor volume and body weight of each mouse were measured three times per week. At the end of the experiments, mice were euthanized and tumor tissues were isolated and prepared for pathogen analysis. One-way ANOVA was used to compare tumor size and body weight for *in vivo* xenograft study. Tumor growth inhibition (TGI) was calculated as $100 - 100 \times [(T - T0)/(C - C0)]$, and tumor regression was calculated as $(T - T0)/T0 \times 100$, where T, T0, C, and C0 are the mean tumor volume for the specific group on the last day of treatment, mean tumor volume of the same group on the first day of treatment, mean tumor volume for the vehicle control group on the last day of treatment, and mean tumor

volume for the vehicle control group on the first day of treatment, respectively (Wang et al., 2014).

Pathology and Immunohistochemistry Analysis

Tumor tissues fixed in formalin buffer for more than 1 week were stained with hematoxylin and eosin (H&E). For immunohistochemistry (IHC) analysis, the excised tumor tissues were collected in 10% formalin and embedded in paraffin. The following primary antibodies were used with rabbit anti-Ki67 (#9027, Cell Signaling Technology), rabbit anti-cleaved-caspase 3 (#9664, Cell Signaling Technology), rabbit anti-phospho-ERK1/2 (#4376, Cell Signaling Technology), rabbit anti-AKT (#4691, Cell Signaling Technology), p-AKT (#4060) following HRP-DAB-methods with signal boost reagents (#8114, Cell Signaling Technology). Slides were imaged with BZ-X700 microscope and analyzed by image J.

Statistical Analysis

Data were analyzed using Prism Software 5.0 (GraphPad Software, Inc.). The statistical significance ($p < 0.05$) was evaluated by student t test, and one-way ANOVA.

RESULTS

Development of Vem-Resistant VR1 Cells From Vem-Sensitive A375 Cells

A375 cells are one of the most widely used and representative V600E mutant melanoma cells, and we have previously reported the anti-tumor efficiency of VERU-111 in many cancer types (Kashyap et al., 2019; Deng et al., 2020; Kashyap et al., 2020; Mahmud et al., 2020) as well as the synergy of Vem in combination with ABI-274 in A375 Vem-resistant melanoma cells (Wang et al., 2014). Herein, we investigate whether the combination of VERU-111 (ABI-274 derivative) with Vem can also overcome Vem-resistance in A375. A375 cells are one of the most widely used and representative V600E mutant melanoma cells. We first developed Vem-resistant cells (VR1) from the $BRAF^{V600E}$ mutant A375 melanoma cells by increasing the concentration of Vem as reported previously (Su et al., 2012). As expected, the persistent expressions of p-ERK, p-MEK and overexpression of P-gp were detected in VR1-Vem treatment cells (**Figure 1B**), the hallmarks of acquired Vem-resistance (Boussemart et al., 2014). AKT has no significant change in VR1 cells, accompanied with decreased AKT activation (p-AKT) in a Vem-dependent manner. Notably, when treated with Vem at 2 μm, A375 cells but not resistant VR1 cells were effectively arrested at G0-G1 phase (**Figure 1C**). Furthermore, the IC_{50} value of Vem in VR1 cells (>10 μm) increased more than 25-fold compared with that in the parental A375 cells (0.43 μm, **Figure 1D**). All these together strongly support the Vem-resistant property of VR1 cells. In contrast, the IC_{50} value of VERU-111 in VR1 cells only marginally increased from 0.01 to 0.02 μm, which is in line with our previous result, indicating the ability of VERU-111 to overcome Vem-resistance as a single agent (Wang et al., 2014).

Combination of VEM with VERU-111 Inhibits Cell Proliferation and Increases Apoptosis in Both A375 and VR1 cells by Inhibiting AKT Expression

Next, we investigated whether VERU-111 has any synergistic interaction with Vem on melanoma cell lines, by comparing the single-agent treatment efficacy with their combination in both A375 and VR1 cells. Colony formation assays unveiled that proliferation of both parental A375 cells and Vem-resistant VR1 cells were inhibited following the entire regimen (**Figures 2A,B**). Moreover, Vem did not change cell cycle distribution of both cell lines, while addition of tubulin inhibitor bypassed G0-G1 cell cycle phase and arrested cell cycle at G2-M phase in both A375 and VR1 cells (**Figure 2C**). As **Figure 2C** showed that in VR1 cells, there is 61.3, 27.8, 10.9% of cells distributing in the G0-G1, S or G2-M phase, respectively. Vem single treatment produced similar cell - cycle phase distribution. In VERU-111 single treatment group, the percentage of cells distributed in the G2-M phase had accumulated up to 88.6%. The combination of Vem and VERU-111 strongly arrested VR1 cells in both G0-G1 (3.7%) and G2-M (78.6%) phases while the combination regimen arrested parental A375 cells in both G0-G1 (47.9%) and G2-M (35.6%) phases, which indicated VERU-111 could capture Vem-resistant cells leaking from G0-G1 arrest, and thus produce a strong synergistic effect with Vem. Correspondingly, there are 0.8, 0.7, 10.5, 18.5% of apoptotic cells were detected in DMSO, Vem, VERU-111, combination treatment groups in VR1 cells respectively, and 0, 5.5, 8.9, 10.6% of apoptotic cells were observed in the indicated treatment groups in A375 cells. All these data suggested combination regimen has stronger efficiency in arresting the cell cycle and inducing apoptosis than a single treatment.

VR1 has sustained expressions of p-ERK upon single-agent Vem treatment (**Figure 2D**), similarly, sustained p-MEK expression was noted in VR1 cells after Vem treatment, consistent with the cross-resistance to MEK inhibitors in these Vem-resistant VR1 cells compared with the parental A375 cells (**Figure 2D**). In contrast, when treated with the combination of Vem and VERU-111, both A375 and VR1 cells had significantly more apoptosis (cleaved-PARP, **Figure 2D**), together with additional decreased expression of AKT expression and p-AKT activation (**Figure 2D**). In VR1 cells, the combination of VERU-111 and Vem reduced the level of AKT to 67 and 75% (0.6/0.9 × 100%, 0.6/0.8 × 100%) compared with single treatment, whereas the p-AKT expression level inhibited to 75 and 60% (0.3/0.4 × 100%, 0.3/0.5 × 100%) compared with a single treatment (**Figure 2D**). AKT is a serine/threonine kinase activated downstream of PI3K, which is a receptor for various pro-proliferation and bioactive substances. To our knowledge, the activation of AKT often contributes to tumorigenesis and plays a role in regulating cell motility, local invasion, and metastasis. Furthermore, our previously published outcomes proved that the synergistic anti-proliferation might be mediated by simultaneously targeting both ERK and AKT pathways (Wang et al., 2014).

Recently, F-box protein S-phase kinase-associated protein 2 (Skp2) was reported to be involved in drug resistance, including paclitaxel resistance(Kajiyama et al., 2007; Yang et al., 2014; Yang

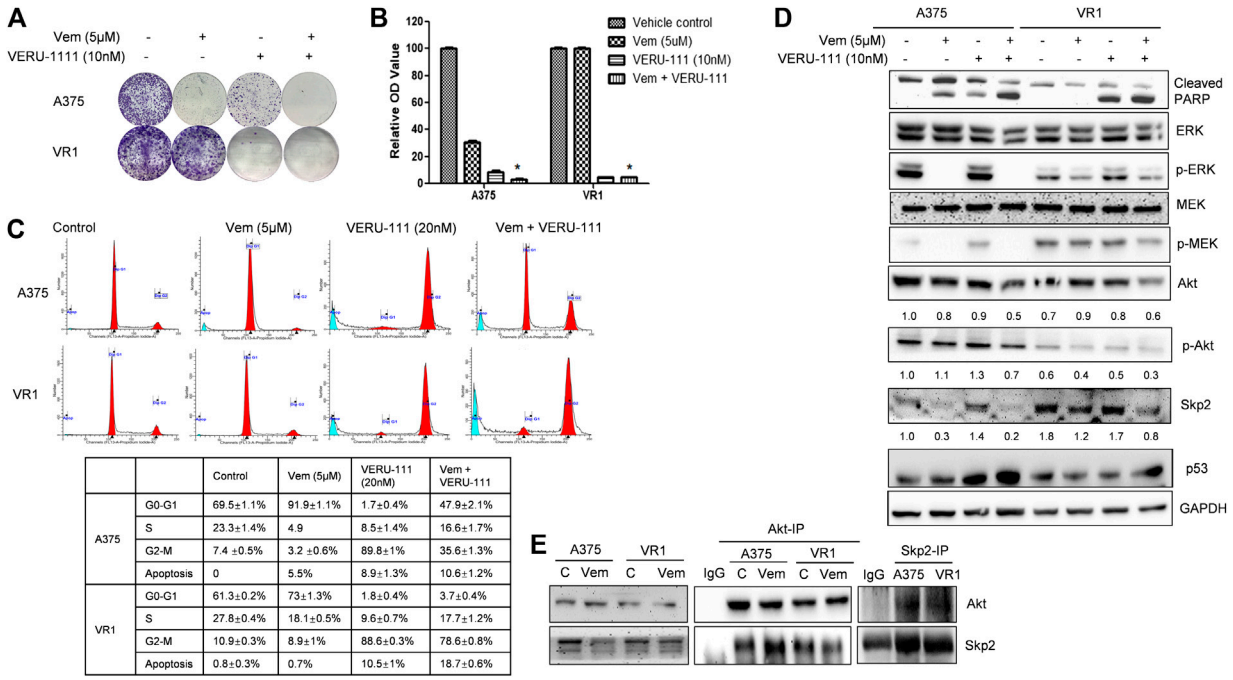

		Control	Vem (5μM)	VERU-111 (20nM)	Vem + VERU-111
A375	G0-G1	69.5±1.1%	91.9±1.1%	1.7±0.4%	47.9±2.1%
	S	23.3±1.4%	4.9	8.5±1.4%	16.6±1.7%
	G2-M	7.4 ±0.5%	3.2 ±0.6%	89.8±1%	35.6±1.3%
	Apoptosis	0	5.5%	8.9±1.3%	10.6±1.2%
VR1	G0-G1	61.3±0.2%	73±1.3%	1.8±0.4%	3.7±0.4%
	S	27.8±0.4%	18.1±0.5%	9.6±0.7%	17.7±1.2%
	G2-M	10.9±0.3%	8.9±1%	88.6±0.3%	78.6±0.8%
	Apoptosis	0.8±0.3%	0.7%	10.5±1%	18.7±0.6%

FIGURE 2 | Combination treatment of Vem and VERU-111 sensitizes both A375 and VR1 cells **(A)** Colony formation assay. 1,000 Cells were seeded in the 12-well plates and treated with indicated concentration of drugs, after 8 days, stained with crystal violet **(B)** Quantification of clone formation assay. Colonies were lyzed in buffer with SDS, then read the absorbance at 490 nm *, $p < 0.05$, compared with single-agent treatment groups **(C)** Cell cycle distribution and apoptosis of combination of vemurafenib and VERU-111 in A375 and VR1 cells. Data was analyzed with Modfit 2.0 software, and apoptosis cells were counted automatically **(D)** Signaling pathway in both A375 and VR1 cells after corresponding treatment **(E)** Both A375 and VR1 cell were treated with DMSO and 5uM Vem, and then performed endogenous Co-IP between AKT and Skp2.

et al., 2016; Huang et al., 2017; Byun et al., 2018; Cui et al., 2020), PI3K inhibitor resistance (Liu et al., 2013; Jia et al., 2014; Clement et al., 2018; Tian et al., 2018; Wang et al., 2018), and vemurafenib resistance (Feng et al., 2020), et al.

Interestingly, we also observed the overexpressed S-phase kinase-associated protein 2 (Skp2) in VR1 cells when treated with different concentrations of Vem compared with parental A375 cells (**Figure 1B**). However, the mRNA level of Skp2 did not increase in VR1 cells (Data not shown). Additionally, in the Vem-resistant cells, the expression of Skp2 dramatically reduced to 67 and 47% after the combination treatment compared with vem treatment (lane density normalized with GAPDH, 0.8/1.2 × 100%) and VERU-111 treatment (0.8/1.7 × 100%) (**Figure 2D**), indicating that Skp2 plays a role in the Vem-resistance. In our experiment, we also noticed Skp2 inhibition induced by Vem (**Figures 2D,E**) in parental A375 cells, which might be dependent on c-Myc transcriptional regulation (Feng et al., 2020). In malignant melanoma, Skp2 is highly expressed and correlates with tumor malignancy. It is noteworthy that Skp2 E3 ligase binds to AKT and is responsible for AKT degradation, and Skp2 is also required for AKT activation and membrane recruitment (Chan et al., 2012). Conversely, phosphorylation of Skp2 on Ser72 by AKT promotes its stabilization (Song et al., 2015). In line with these studies, a dramatic reduction of AKT levels and p-AKT expression was also seen in the combination treatment group (**Figure 2D**). Skp2 binds with AKT (**Figure 2E**), and the interaction was increased in parental A375 cells while decreased in VR1 cells after Vem treatment. Collectively, the result highlighted that Skp2 is involved in Vem-resistance, and it may contribute to the synergistic effect of Vem and VERU-111. It is worthy to note that p53 expression increased upon combination treatment, which is consistent with our recent finding that VERU-111 could inhibit tumor growth and migration in cervical cancer cells by promoting DNA damage response mediated by p53 (Kashyap et al., 2020).

Skp2 involved in mechanisms of Vem-resistance and contributes to the effect of combination treatment

To further clarify the role of Skp2 in the indicated treatment, we knocked out Skp2 in VR1 cells using CRISPR-Cas9 technique. Expectedly, IC_{50} of Vem and VERU-111 improved approximately 2- and 5-fold (Vem from 33.92 to 16.74 μm and VERU-111 from 0.056 to 0.01 μm) respectively, which indicated that knockout of Skp2 not only restored compound sensitivity of VR1 cells to Vem, but also increased drug sensitivity to VERU-111 (**Figure 3A**). Interestingly, increased apoptosis was observed in VR1-SgSkp2 (**Figure 3B**). Indeed, Skp2 may inhibit apoptosis and contribute to drug resistance (Schüler et al., 2011; Wang et al., 2011). In line with these observations, we also found highly expressed Skp2 in Vem-resistant melanoma cells (**Figures 1B, 2D**), and decreased AKT

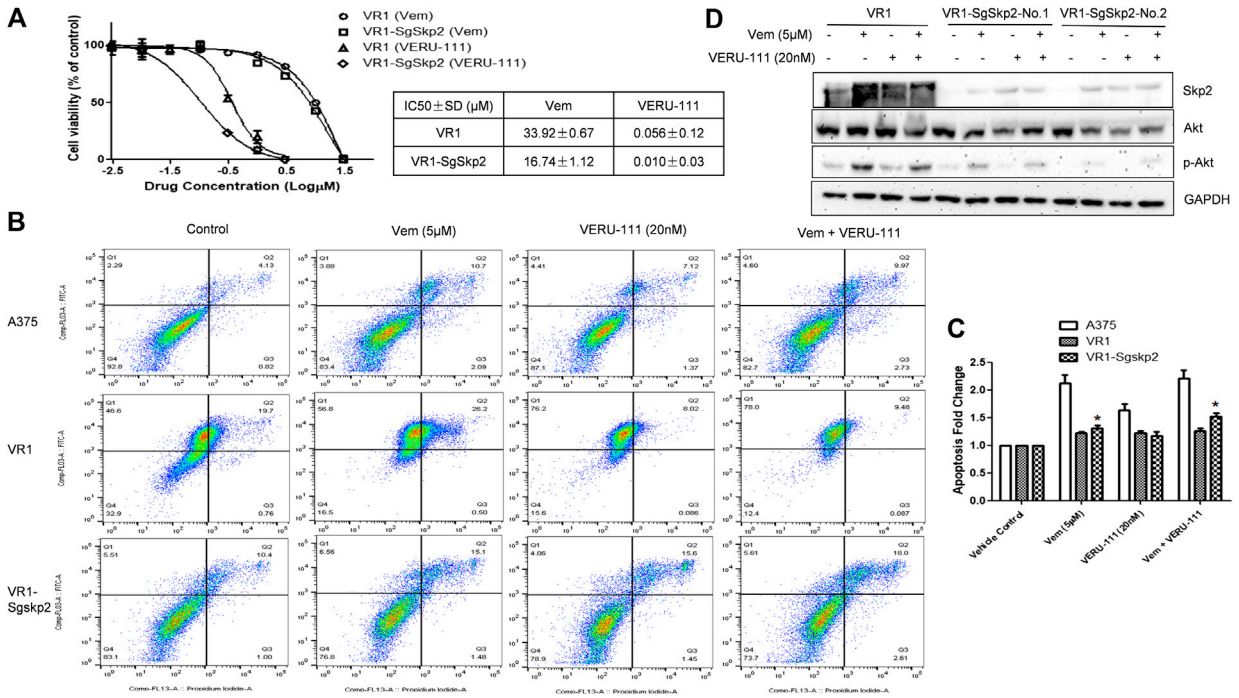

FIGURE 3 | Knockout of Skp2 restore drug sensitivity of Vem-resistant cell to Vem and VERU-111 **(A)** Skp2 guide RNA (SgSkp2) was introducced to VR1 cells to make stable Skp2 knockout clones (VR1-SgSkp2). IC_{50} was measured upon indicated treatment using MTS assay **(B)** Apoptosis of VR1 and Skp2 knockout VR1 cells upon treatment. Data was analyzed by Flowjo 10.4 software. In order to compare apoptosis, we fixed gate in three cell lines, as quantified in **(C)** *, $p < 0.05$, compared with VR1 cells **(D)** Deficient of Skp2 eliminating AKT expression, which paralled with decreased p-AKT.

expression and AKT phosphorylation in two single clones of VR1-SgSkp2 cells (VR1-SgSkp2-No.1 and No.2), which might be the reason to increased cell apoptosis and cell growth arrest caused by the combination regimen (**Figures 2, 3C**). Of note, in order to keep the resistant feature, VR1-SgSkp2 cells were still cultured in the medium with Vem, which explains minor alteration about of IC_{50} of Vem. Further analysis demonstrated that knockout of Skp2 compromised AKT activation, as indicated by decreased phosphorylation of AKT (**Figure 3C**).

Combination of VEM and VERU-111 Synergistically Suppress Vemurafenib-resistant Tumor Growth *in vivo*

The combination of dabrafenib (BRAF inhibitor) and trametinib (MEK inhibitor) is approved to treat Braf V600E mutant melanoma patients (Robert et al., 2015; Long et al., 2017; Hauschild et al., 2018). To evaluate our *in vivo* xenograft mouse model, we compared the inhibitory effect of dabrafebnib and its combination with trametinib. Based on previous research, the doses of 30 mg/kg dabrafenib and 0.3 mg/kg trametinib were selected (Kawaguchi et al., 2017; Yanagihara et al., 2018). **Figure 4A** showed no significant toxic effect in all three groups as no much change of body weight was observed. Importantly, dabrafenib plus trametinib regimen has a stronger tumor inhibitory effect (TGI at 28.6%) with statistical significance ($p < 0.05$, compared with vehicle control and dabrafenib alone) (**Figures 4B,C** and **Table 1**), demonstating the efficacy of our *in vivo* animal model.

Next, we evaluated whether there was a strong synergistic interaction between Vem and VERU-111 to counteract Vem-resistance *in vivo*. We inoculated VR1 cells in the right flank of NSG mice and treated them either with a single compound or the combination treatment strategy to assess the inhibitory effect on tumors. Based on our previous research on ABI-274, the dose of 10 mg/kg VERU-111 was selected in the current (Wang et al., 2014). As depicted in **Figure 5A**, no significant change was noted in body weight in all the groups. At the end of the experiment, we euthanized all the mice and examined their major organs, and no injure was found. This indicated that no general toxicity was induced by VERU-111 *in vivo*. Notably, the combination treatment strategy dramatically inhibited tumor growth compared with a single treatment or control group (**Figures 5B,C**), in which the tumor size in the combination group was within 100 mm^3, while it reached 1,000 mm^3 in vehicle group after 4 weeks of treatment. As shown in **Figures 5B,C** and **Table 2**, Vem (30 mg/kg) single treatment achieved minimal (40.6%) TGI and VERU-111 (10 mg/kg) resulted in slightly better TGI at 76.6%, whereas combination treatment significantly enhanced tumor inhibition to 96.1% after 4 weeks treatment to Vem-resistant xenograft model. Hematoxylin and eosin (H&E) staining of the tumor tissue showed that the tumor cell lost intact shape, nuclei shrank, and even some cells lost membranes, highlighting the

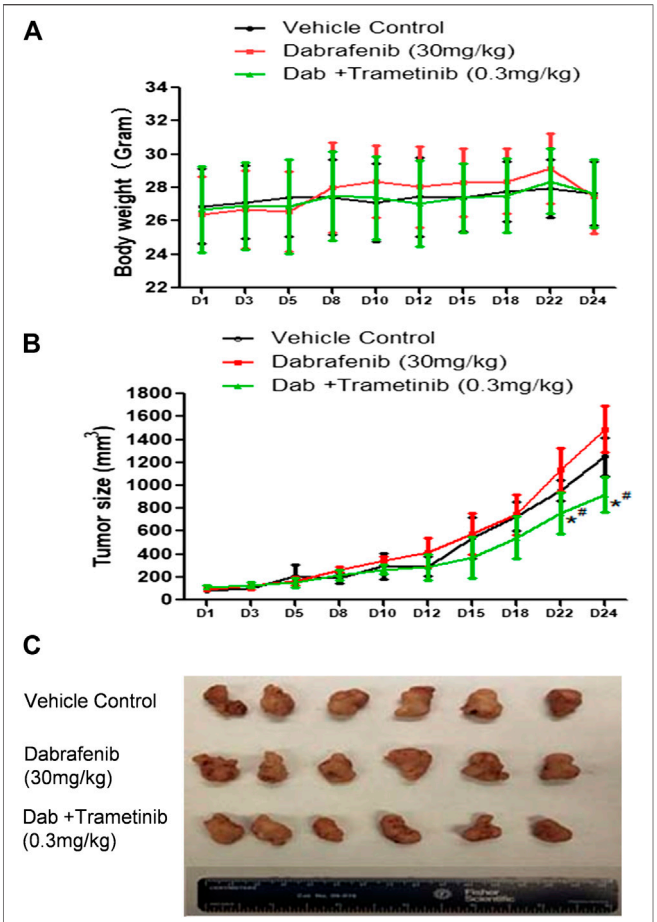

FIGURE 4 | Synergistic effect of BRAF inhibitor dabrafenib and MEK inhibitor trametinib **(A)** Mice body weight curves during the administration time period **(B)** Tumor growth curve. *, $p < 0.05$, compared with Vehicle treatment groups. #, $p < 0.05$, compared with Dab treatment group. **(C)** Pictures of isolated tumor tissue.

antitumor effect of tubulin inhibitor (**Figure 5D**). Immunohistochemistry (IHC) staining revealed that decreased proliferation (Ki67 staining), increased cell apoptosis (cleaved-caspase three staining), and remarkably reduced expressions of *p*-ERK, total AKT and *p*-AKT (**Figure 5D**). Overall, the above-mentioned findings demonstrated that the tubulin inhibitor had a strong inhibitory effect on Vem-resistant tumor growth either as a single candidate or combined regimen with Vem. Additionally, VERU-111 showed a giant potential to overcome Vem-resistance in melanoma cancer cells (**Figure 5D**), which may be advantageous for melanoma patients harboring BRAF(V600E) mutation.

DISCUSSION

Recently, the combination of BRAF inhibitor dabrafenib with MEK inhibitor trametinib was approved by FDA to treat patients harboring BRAF (V600E) mutation in NSCLC (non-small cell lung cancer) or melanoma. Although this regimen has exhibited great success in clinical therapy, patients may eventually acquire resistance after a couple of months (Robert et al., 2015; Long et al., 2017). We have developed a series of tubulin inhibitors that bind to the colchicine site in tubulin and have shown their anti-tumor effect and potential in overcoming Vem-resistance, paclitaxel-resistance in nude mice xenograft model (Lu et al., 2014; Wang et al., 2018; Wang et al., 2019; Chen et al., 2020). VERU-111 (ABI-231) is an orally available tubulin inhibitor that disrupts tubulin polymerization, promotes microtubule fragmentation, inhibits cancer cell migration, and is currently in phase 1b/2 clinical trials for men with metastatic castration and androgen-blocking agent resistant prostate cancer (ClinicalTrials.gov Identifier: NCT03752099). Tubulin inhibitor is less prone to develop resistance, therefore bearing potential to cure cancer and to sensitize drug-resistance cancer patience (Wang et al., 2014; Guan et al., 2017; Arnst et al., 2018; Deng et al., 2020; Kashyap et al., 2020; Mahmud et al., 2020).

In this study, we investigated whether the orally derivative of ABI-274, VERU-111, has synergistic effect with Vem. VERU-111 has been tested in many cancer cell lines and its IC_{50} is 5.6 nM in M14 cell, 7.2 nM in WM164 melanoma cell (Wang et al., 2019), 8.2 nM in MDA-MB-231 breast cancer cell (Chen et al., 2020), 55.6 nM in NSCLC A549 cell and 102.9 nM in A549-Paclitaxel resistant cells (Mahmud et al., 2020). In agreement with outcomes of previous research, it was confirmed that by synergisticly arresting cancer cells at G0-G1 and G2-M phases, the combined treatment regimen of Vem and VERU-111 could overcome the Vem-resistance through enhanced apoptosis and compromised Skp2-AKT signaling pathway. In a tumor xenograft model, the combined regimen displays a better inhibitory efficiency against tumor progression than either single treatment. Further IHC analysis of tissue sections confirmed decreased tumor proliferation and the diminished expression of AKT and *p*-AKT. Several studies reported an association between inhibition of AKT and tubulin polymerization (Zhang et al., 2009; Krishnegowda et al., 2011; Viola et al., 2012). Inhibition of AKT-mediated survival signaling pathway has been shown to increase sensitivity to microtubule-targeted tubulin-polymerizing agents (MTPAs)-induced apoptosis in cancer cells (Bhalla 2003). The results of the present research are consistent with findings of these studies, highlighting a close interaction between tubulin polymerization inhibitors and downregulation of AKT in melanoma.

Remarkably, Skp2 E3 ligase was also involved in the mechanisms of Vem-resistance and synergistic effect of combination regimen. Recent studies reported that overexpressed Skp2 was found in paclitaxel-resistant prostate cancer cells (Yang et al., 2016; Byun et al., 2018;

TABLE 1 | TGI comparison for combination of Braf inhibitor Dabrafenib and MEK inhibitor trametinib in Vem-resistant VR1 xenograft model.

Treatment group	TGI (100%)
Vehicle control	—
Dab (30 mg/kg)	121.3 ± 18.1
Dab + trametinib (0.3 mg/kg)	28.6 ± 21.2*

**, $p < 0.05$, Compared with either Dab treatment or Vehicle treatment group.*

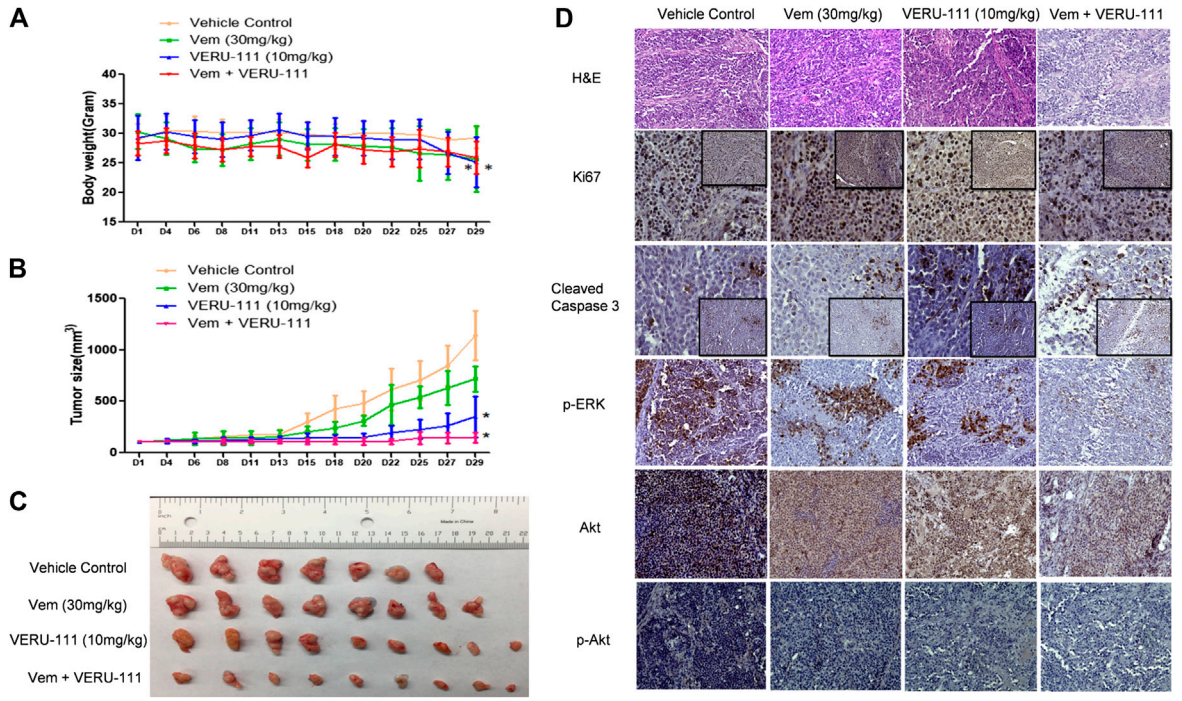

FIGURE 5 | VERU-111 sensitizes VR1 tumor growth *in vivo* **(A)** Mice body weight curve with time lapse **(B)** Tumor growth curve. *, $p < 0.05$, compared with Vehicle treatment group. **(C)** Pictures of isolated tumor tissue **(D)** Representative IHC images for H&E (10×), Ki67 (10× and 40×), cleaved-caspase 3 (10× and 40×), AKT (10×), p-AKT (10×), p-ERK (10×) staining of tumor tissue sections after 4 weeks of single-agent or combination treatment.

Gong et al., 2018), and knockdown of Skp2 restored the sensitivity of paclitaxel in prostate cancer cells (Byun et al., 2018). Skp2 also plays a pivotal role in mitosis and spindle checkpoint by triggering ubiquitination and activation of Aurora-B (Nakayama et al., 2004; Sugihara et al., 2006; Hu and Aplin, 2008; Wu et al., 2015). Skp2 depletion in melanoma cells resulted in a G2-M phase arrest (Hu and Aplin 2008), and suppression of both BRAF (V600E) and Skp2 inhibited cell growth and invasion in melanoma cell lines(Sumimoto et al., 2006). Since Skp2 was reported to interact with AKT (Chan et al., 2012), we also tested the interaction and found decreased AKT expression and AKT phosphorylation in VR1-SgSkp2 cells (**Figures 2E, 3D**), thereby leading to cell apoptosis and cell growth arrest caused by the combination treatment (**Figure 3**). Meanwhile, BRAF inhibitor dabrafenib combination with MEK inhibitor trametinib present a mild synergistic effect in inhibition of tumor growth, as shown in **Figure 4** and **Table 1**. By contrast, our *in vivo* xenograft tumor model demonstrated that combination regimen of Vem and VERU-111 has more potent tumor inhibitory effect than single administration (**Figure 5** and **Table 2**). When aministrtaed in combination with Vem, VERU-111 has a tumor growth inhibitory rate (TGI) of 96.1%, which was better than ABI-274 (TGI 88.6%) [**Table 2** and reference (Wang et al., 2014)].

Collectively, based on our study, VERU-111 overcome Vem-resistance through the following mechanisms: 1) As a tubulin destabilizing agent, disrupt tubulin polymerization, promote microtubule fragmentation, inhibit cancer cell migration; 2) Combined with Vem, arresting cell both in G0-G1 and G2-M phase; 3) Compromised Skp2-AKT signaling pathway. Our study showed that VERU-111bears inspiring potential in synergistically combination with BRAF inhibitor Vem to overcome drug resistance in melanoma. Furthermore, this synergistic effect might through regulating Skp2-AKT, as evidenced by increased apoptosis and drug sensitization when skp2 was knocked out, which suggested that silencing skp2 might be an effective way to overcome Vem-resistance.

TABLE 2 | TGI comparison for *in vivo* combination of vemurafenib (30 mg/kg) and VERU-111 (10 mg/kg) in the Vem-resistant VR1 xenograft model.

Treatment group	TGI (100%)
Vehicle control	—
Vem (30 mg/kg)	40.6 ± 11.6
VERU-111 (10 mg/kg)	76.6 ± 18.4
Vem + VERU-111	96.1 ± 4.8*

*, $p < 0.05$, *compared with single-agent treatment groups.*

CONCLUSION

In conclusion, our findings provide direct evidence and a reasonable explanation for giving a combination of a tubulin

inhibitor VERU-111 with a BRAF inhibitor to overcome Vem-resistance in melanoma pateints.

DATA AVAILABILITY STATEMENT

The original contributions presented in the study are included in the article/Supplementary Material, further inquiries can be directed to the corresponding author.

ETHICS STATEMENT

The animal study was reviewed and approved by the University of Tennessee HSC.

AUTHOR CONTRIBUTIONS

HC and WL designed the study, HC and QW performed the experiments; HC, QW, DM, and WL wrote the manuscript.

FUNDING

This work was supported by the National Institutes of Health grants R01CA148706, and the University of Tennessee College of Pharmacy Drug Discovery Center. The contents are solely the responsibility of the authors and do not necessarily represent the official views of the National Institutes of Health.

REFERENCES

Arnst, K. E., Wang, Y., Hwang, D. J., Xue, Y., Costello, T., Hamilton, D., et al. (2018). A potent, metabolically stable tubulin inhibitor targets the colchicine binding site and overcomes taxane resistance. *Cancer Res.* 78, 265–277. doi:10.1158/0008-5472.Can-17-0577

Atefi, M., von Euw, E., Attar, N., Ng, C., Chu, C., Guo, D., et al. (2011). Reversing melanoma cross-resistance to BRAF and MEK inhibitors by co-targeting the AKT/mTOR pathway. *PLoS.* 6, e28973. doi:10.1371/journal.pone.0028973

Bhalla, K. N. (2003). Microtubule-targeted anticancer agents and apoptosis. *Oncogene* 22, 9075–9086. doi:10.1038/sj.onc.1207233

Boussemart, L., Malka-Mahieu, H., Girault, I., Allard, D., Hemmingsson, O., Tomasic, G., et al. (2014). eIF4F is a nexus of resistance to anti-BRAF and anti-MEK cancer therapies. *Nature* 513, 105–109. doi:10.1038/nature13572

Byun, W. S., Jin, M., Yu, J., Kim, W. K., Song, J., Chung, H. J., et al. (2018). A novel selenonucleoside suppresses tumor growth by targeting Skp2 degradation in paclitaxel-resistant prostate cancer. *Biochem. Pharmacol.* 158, 84–94. doi:10.1016/j.bcp.2018.10.002

Chan, C. H., Li, C. F., Yang, W. L., Gao, Y., Lee, S. W., Feng, Z., et al. (2012). The Skp2-SCF E3 ligase regulates Akt ubiquitination, glycolysis, herceptin sensitivity, and tumorigenesis. *Cell* 151, 913–914. doi:10.1016/j.cell.2012.10.025

Chen, J., Wang, Z., Li, C. M., Lu, Y., Vaddady, P. K., Meibohm, B., et al. (2010). Discovery of novel 2-aryl-4-benzoyl-imidazoles targeting the colchicines binding site in tubulin as potential anticancer agents. *J. Med. Chem.* 53, 7414–7427. doi:10.1021/jm100884b

Chen, J., Ahn, S., Wang, J., Lu, Y., Dalton, J. T., Miller, D. D., et al. (2012). Discovery of novel 2-aryl-4-benzoyl-imidazole (ABI-III) analogues targeting tubulin polymerization as antiproliferative agents. *J. Med. Chem.* 55, 7285–7289. doi:10.1021/jm300564b

Chen, H., Deng, S., Wang, Y., Albadari, N., Kumar, G., Ma, D., et al. (2020). Structure-activity relationship study of novel 6-Aryl-2-benzoyl-pyridines as tubulin polymerization inhibitors with potent antiproliferative properties. *J. Med. Chem.* 63, 827–846. doi:10.1021/acs.jmedchem.9b01815

Clement, E., Inuzuka, H., Nihira, N. T., and Toker, W. A. (2018). Skp2-dependent reactivation of AKT drives resistance to PI3K inhibitors. *Sci. Signal.* 11, eaao3810. doi:10.1126/scisignal.aao3810

Cui, H., Arnst, K., Miller, D. D., and Li, W. (2020). Recent Advances in Elucidating Paclitaxel Resistance Mechanisms in Non-small Cell Lung Cancer and Strategies to Overcome Drug Resistance. *Curr. Med. Chem.* 27, 6573–6595. doi:10.2174/0929867326666191016113631

Deng, S., Krutilina, R. I., Wang, Q., Lin, Z., Parke, D. N., Playa, H. C., et al. (2020). An orally available tubulin inhibitor, Veru-111, suppresses triple-negative breast cancer tumor growth and metastasis and bypasses taxane resistance. *Mol. Cancer Ther.* 19, 348–363. doi:10.1158/1535-7163.Mct-19-0536

Díaz-Martínez, M., Benito-Jardón, L., Alonso, L., Koetz-Ploch, L., and Teixidó, E. J. (2018). miR-204-5p and miR-211-5p contribute to BRAF inhibitor resistance in melanoma. *Cancer Res.* 78, 1017–1030. doi:10.1158/0008-5472.Can-17-1318

Duggan, M. C., Stiff, A. R., Bainazar, M., Regan, K., Olaverria Salavaggione, G. N., Maharry, S., et al. (2017). Identification of NRAS isoform 2 overexpression as a mechanism facilitating BRAF inhibitor resistance in malignant melanoma. *Proc. Natl. Acad. Sci. U S A* 114, 9629–9634. doi:10.1073/pnas.1704371114

Faghfuri, E., Nikfar, S., Niaz, K., and Abdollahi, M. A. M. (2018). Mitogen-activated protein kinase (MEK) inhibitors to treat melanoma alone or in combination with other kinase inhibitors. *Expert Opin. Drug Metab. Toxicol.* 14, 317–330. doi:10.1080/17425255.2018.1432593

Feng, L., Li, J., Bu, X., Zuo, Y., and Qu, L. X. (2020). BRAFV600E dictates cell survival via c-Myc-dependent induction of Skp2 in human melanoma. *Biochem. Biophys. Res. Commun.* 524, 28–35. doi:10.1016/j.bbrc.2019.12.085

Gadiot, J., Hooijkaas, A. I., Deken, M. A., and Blank, C. U. (2013). Multiobjective optimization identifies cancer-selective combination therapies. *Onco Targets Ther.* 6, 1649–1658. doi:10.2147/ott.S52552

Gong, J., Zhou, Y., Liu, D., and Huo, J. (2018). F—box proteins involved in cancer—associated drug resistance (Review). *Oncol. Lett.* 15, 8891–8900. doi:10.3892/ol.2018.8500

Guan, F., Ding, R., Zhang, Q., Chen, W., Li, F., Long, L., et al. (2017). WX-132-18B, a novel microtubule inhibitor, exhibits promising anti-tumor effects. *Oncotarget* 8, 71782–71796. doi:10.18632/oncotarget.17710

Hauschild, A., Dummer, R., Schadendorf, D., Santinami, M., Atkinson, V., Mandalà, M., et al. (2018). Longer follow-up confirms relapse-free survival benefit with adjuvant dabrafenib plus trametinib in patients with resected BRAF V600-mutant stage III melanoma. *J. Clin. Oncol.* 36, 3441–3449. doi:10.1200/jco.18.01219

Hu, R., and Aplin, A. E. (2008). Skp2 regulates G2/M progression in a p53-dependent manner. *Mol. Biol.Cell* 19, 4602–4610. doi:10.1091/mbc.E07-11-1137

Huang, T., Yang, L., Wang, G., Ding, G., Peng, B., Wen, Y., et al. (2017). Inhibition of Skp2 sensitizes lung cancer cells to paclitaxel. *Onco. Targets Ther.* 10, 439–446. doi:10.2147/ott.s125789

Hwang, B.-J., Adhikary, G., Eckert, R. L., and Lu, A.-L. (2018). Chk1 inhibition as a novel therapeutic strategy in melanoma. *Oncotarget* 9, 30450–30464. doi:10.18632/oncotarget.25765

Jia, T., Zhang, L., Duan, Y., Zhang, M., Wang, G., Zhang, J., et al. (2014). The differential susceptibilities of MCF-7 and MDA-MB-231 cells to the cytotoxic effects of curcumin are associated with the PI3K/Akt-SKP2-Cip/Kips pathway. *Cancer Cell Int.* 14, 126. doi:10.1186/s12935-014-0126-4

Johnson, G. L., Stuhlmiller, T. J., Angus, S. P., Zawistowski, J. S., and Graves, L. M. (2014). Molecular pathways: adaptive kinome reprogramming in response to targeted inhibition of the BRAF-MEK-ERK pathway in cancer. *Clin. Cancer Res.* 20, 2516–2522. doi:10.1158/1078-0432.Ccr-13-1081

Kajiyama, H., Shibata, K., Terauchi, M., Yamashita, M., Ino, M., Nawa, A., et al. (2007). Chemoresistance to paclitaxel induces epithelial-mesenchymal transition and enhances metastatic potential for epithelial ovarian carcinoma cells. *Int. J. Oncol.* 31, 277–283. doi:10.3892/ijo.31.2.277

Kashyap, V. K., Wang, Q., Setua, S., Nagesh, P. K. B., Chauhan, N., Kumari, S., et al. (2019). Therapeutic efficacy of a novel βIII/βIV-tubulin inhibitor (VERU-111) in pancreatic cancer. *J. Exp. Clin. Cancer Res.* 38, 29. doi:10.1186/s13046-018-1009-7

Kashyap, V. K., Dan, N., Chauhan, N., Wang, Q., Setua, S., Nagesh, P. K. B., et al. (2020). VERU-111 suppresses tumor growth and metastatic phenotypes of

cervical cancer cells through the activation of p53 signaling pathway. *Cancer Lett.* 470, 64–74. doi:10.1016/j.canlet.2019.11.035

Kawaguchi, K., Igarashi, K., Murakami, T., Kiyuna, T., Lwin, T. M., Hwang, H. K., et al. (2017). MEK inhibitors cobimetinib and trametinib, regressed a gemcitabine-resistant pancreatic-cancer patient-derived orthotopic xenograft (PDOX). *Oncotarget* 8, 47490–47496. doi:10.18632/oncotarget.17667

Krayem, M., Journe, F., Wiedig, M., Morandini, R., Najem, S., Sales, F., et al. (2016). p53 Reactivation by PRIMA-1(Met) (APR-246) sensitises (V600E/K)BRAF melanoma to vemurafenib. *Eur. J. Cancer.* 55, 98–110. doi:10.1016/j.ejca.2015.12.002

Krishnegowda, G., Prakasha Gowda, A. S., Tagaram, H. R., Carroll, K. F., Irby, R. B., Sharma, A. K., et al. (2011). Synthesis and biological evaluation of a novel class of isatin analogs as dual inhibitors of tubulin polymerization and Akt pathway. *Bioorg. Med. Chem.* 19, 6006–6014. doi:10.1016/j.bmc.2011.08.044

Lim, S. Y., Menzies, A. M., and Rizos, H. (2017). Mechanisms and strategies to overcome resistance to molecularly targeted therapy for melanoma. *Cancer* 123, 2118–2129. doi:10.1002/cncr.30435

Liu, X., Wang, H., Ma, J., Xu, J., Sheng, C., Yang, S., et al. (2013). The expression and prognosis of Emi1 and Skp2 in breast carcinoma: associated with PI3K/Akt pathway and cell proliferation. *Med. Oncol.* 30, 735. doi:10.1007/s12032-013-0735-0

Long, G. V., Flaherty, K. T., Stroyakovskiy, D., Gogas, H., Levchenko, E, de Braud, F., et al. (2017). Dabrafenib plus trametinib versus dabrafenib monotherapy in patients with metastatic BRAF V600E/K-mutant melanoma: long-term survival and safety analysis of a phase 3 study. *Ann. Oncol.* 28, 1631–1639. doi:10.1093/annonc/mdx176

Lu, Y., Chen, J., Wang, J., Li, C. M., Ahn, S., Barrett, C. M., et al. (2014). Design, synthesis, and biological evaluation of stable colchicine binding site tubulin inhibitors as potential anticancer agents. *J. Med. Chem.* 57, 7355–7366. doi:10.1021/jm500764v

Mahmud, F., Deng, S., Chen, H., Miller, D. D., and Li, W. (2020). Orally available tubulin inhibitor VERU-111 enhances antitumor efficacy in paclitaxel-resistant lung cancer. *Cancer Lett.* 495, 76–88. doi:10.1016/j.canlet.2020.09.004

Nakayama, K., Nagahama, H., Minamishima, Y. A., Miyake, S., Ishida, N., Hatakeyama, S., et al. (2004). Skp2-mediated degradation of p27 regulates progression into mitosis. *Dev. Cell.* 6, 661–672. doi:10.1016/s1534-5807(04)00131-5

Patel, H., Yacoub, N., Mishra, R., White, A., Long, Y., Alanazi, S., et al. (2020). Current advances in the treatment of BRAF-mutant melanoma. *Cancers* 12, 482. doi:10.3390/cancers12020482

Pulkkinen, O. I., Gautam, P., Mustonen, V., and Aittokallio, T. (2020). Multiobjective optimization identifies cancer-selective combination therapies. *PLoS Comput. Biol.* 16, e1008538. doi:10.1371/journal.pcbi.1008538

Robert, C., Karaszewska, B., Schachter, J., Rutkowski, P., Mackiewicz, A., Stroiakovski, D., et al. (2015). Improved overall survival in melanoma with combined dabrafenib and trametinib. *N. Engl. J. Med.* 372, 30-39. doi:10.1056/NEJMoa1412690

Schüler, S., Diersch, S., Hamacher, R., Schmid, R. M., Saur, G., and Schneider, D. (2011). SKP2 confers resistance of pancreatic cancer cells towards TRAIL-induced apoptosis. *Int. J. Oncol.* 38, 219–(225)

Shirley, M. (2018). Encorafenib and binimetinib: first global approvals. *Drugs* 78, 1277–1284. doi:10.1007/s40265-018-0963-x

Simeone, E., Grimaldi, A. M., Festino, L., Vanella, V., Palla, M., and Ascierto, P. A. (2017). Combination treatment of patients with BRAF-mutant melanoma: a new standard of care. *BioDrugs* 31, 51–61. doi:10.1007/s40259-016-0208-z

Song, G. J., Leslie, K. L., Barrick, S., Mamonova, T., Fitzpatrick, J. M., Drombosky, K. W., et al. (2015). Phosphorylation of ezrin-radixin-moesin-binding phosphoprotein 50 (EBP50) by Akt promotes stability and mitogenic function of S-phase kinase-associated protein-2 (Skp2). *J. Biol. Chem.* 290, 2879–2887. doi:10.1074/jbc.M114.609768

Spain, L., Julve, M., and Larkin, J. (2016). Combination dabrafenib and trametinib in the management of advanced melanoma with BRAFV600 mutations. *Expert Opin. Pharmacother.* 17, 1031–1038. doi:10.1517/14656566.2016.1168805

Su, F., Bradley, W. D., Wang, Q., Yang, H., Xu, L., Higgins, B., et al. (2012). Resistance to selective BRAF inhibition can be mediated by modest upstream pathway activation. *Cancer Res.* 72, 969–978. doi:10.1158/0008-5472.Can-11-1875

Sugihara, E., Kanai, M., Saito, S., Nitta, T., Toyoshima, H., Nakayama, K., et al. (2006). Suppression of centrosome amplification after DNA damage depends on p27 accumulation. *Cancer Res.* 66, 4020–4029. doi:10.1158/0008-5472.Can-05-3250

Sumimoto, H., Hirata, K., Yamagata, S., Miyoshi, H., Miyagishi, M., Taira, K., et al. (2006). Effective inhibition of cell growth and invasion of melanoma by combined suppression of BRAF (V599E) and Skp2 with lentiviral RNAi. *Int. J. Cancer* 118, 472–476. doi:10.1002/ijc.21286

Thang, N. D., Van Minh, N., and Huong, P. T. (2017). Translocation of BBAP from the cytoplasm to the nucleus reduces the metastatic ability of vemurafenib-resistant SKMEL28 cells. *Mol. Med. Rep.* 15, 317–322. doi:10.3892/mmr.2016.5976

Tian, Y. F., Wang, H. C., Luo, C. W., Hung, W. C., Lin, Y. H., Chen, T. Y., et al. (2018). Preprogramming therapeutic response of PI3K/mTOR dual inhibitor via the regulation of EHMT2 and p27 in pancreatic cancer. *Am. J. Cancer Res.* 8, 1812–1822.

Torres-Collado, A., Knott, J., and Jazirehi, A. (2018). Reversal of resistance in targeted therapy of metastatic melanoma: lessons learned from vemurafenib (BRAFV600E-specific inhibitor). *Cancers* 10, 157. doi:10.3390/cancers10060157

Trojaniello, C., Festino, L., Vanella, V., and Ascierto, P. A. (2019). Encorafenib in combination with binimetinib for unresectable or metastatic melanoma with BRAF mutations. *Expert Rev. Clin. Pharmacol.* 12, 259–266. doi:10.1080/17512433.2019.1570847

Viola, G., Bortolozzi, ., Hamel, E., Moro, S., Brun, P., Castagliuolo, I., et al. (2012). MG-2477, a new tubulin inhibitor, induces autophagy through inhibition of the Akt/mTOR pathway and delayed apoptosis in A549 cells. *Biochem. Pharmacol.* 83, 16-26. doi:10.1016/j.bcp.2011.09.017

Wang, J., Han, F., Wu, J., Lee, S. W., Chan, C. H., Wu, C. H., et al. (2011). The role of Skp2 in hematopoietic stem cell quiescence, pool size, and self-renewal. *Blood* 118, 5429-5438. doi:10.1182/blood-2010-10-312785

Wang, J., Chen, J., and Li, D. D. W. (2014). Synergistic Combination of Novel Tubulin Inhibitor ABI-274 and Vemurafenib Overcomes Vemurafenib Acquired Resistance in BRAFV600E Melanoma. *Mol. Cancer Ther.* 13, 16–26. doi:10.1158/1535-7163.Mct-13-0212

Wang, Q., Arnst, K. E., Wang, Y., Kumar, G., Ma, D., Chen, H., et al. (2018). Structural modification of the 3,4,5-trimethoxyphenyl moiety in the tubulin inhibitor VERU-111 leads to improved antiproliferative activities. *J. Med. Chem.* 61, 7877–7891. doi:10.1021/acs.jmedchem.8b00827

Wang, Q., Arnst, K. E., Wang, Y., Kumar, G., Ma, D., White, S. W., et al. (2019). Structure-guided design, synthesis, and biological evaluation of (2-(1H-Indol-3-yl)-1H-imidazol-4-yl)(3,4,5-trimethoxyphenyl) methanone (ABI-231) analogues targeting the colchicine binding site in tubulin. *J. Med. Chem.* 62, 6734–6750. doi:10.1021/acs.jmedchem.9b00706

Wu, J., Huang, Y. F., Zhou, X. K., Zhang, W., Lian, Y. F., Lv, X. B., et al. (2015). Skp2 is required for Aurora B activation in cell mitosis and spindle checkpoint. *Cell Cycle* 14, 3877–3884. doi:10.1080/15384101.2015.1120916

Yanagihara, K., Kubo, T., Mihara, K., Kuwata, T., Ochiai, A., Seyama, T., et al. (2018). Establishment of a novel cell line from a rare human duodenal poorly differentiated neuroendocrine carcinoma. *Oncotarget* 9, 36503–36514. doi:10.18632/oncotarget.26367

Yang, Q., Huang, Q., Wu, Q., Cai, Y., Zhu, L., Lu, X., et al. (2014). Acquisition of epithelial-mesenchymal transition is associated with Skp2 expression in paclitaxel-resistant breast cancer cells. *Br. J. Cancer* 110, 1958–1967. doi:10.1038/bjc.2014.136

Yang, Y., Lu, Y., Wang, L., Mizokami, A., Keller, E. T., Zhang, J., et al. (2016). Skp2 is associated with paclitaxel resistance in prostate cancer cells. *Oncol. Rep.* 36, 559–566. doi:10.3892/or.2016.4809

Zhang, C., Yang, N., Yang, J., Ding, H., Luo, C., Zhang, Y., et al. (2009). S9, a novel anticancer agent, exerts its anti-proliferative activity by interfering with both PI3K-Akt-mTOR signaling and microtubule cytoskeleton. *PLoS One* 4, e4881. doi:10.1371/journal.pone.0004881

Zhao, B., Cheng, X., and Zhou, X. (2018). The BET-bromodomain inhibitor JQ1 mitigates vemurafenib drug resistance in melanoma. *Melanoma Res.* 28, 521–526. doi:10.1097/cmr.0000000000000497

Conflict of Interest: WL is a scientific consultant for Veru, Inc. who licensed VERU-111 for commercial development. WL and DM also report receiving sponsored research agreement grants from Veru, Inc.

The remaining authors declare that the research was conducted in the absence of any commercial or financial relationships that could be construed as a potential conflict of interest.

frontiers in Pharmacology

MINI REVIEW
published: 11 June 2021
doi: 10.3389/fphar.2021.673209

Nanotechnology-Based Celastrol Formulations and Their Therapeutic Applications

Pushkaraj Rajendra Wagh[†], *Preshita Desai*[†], *Sunil Prabhu and Jeffrey Wang**

Department of Pharmaceutical Sciences, College of Pharmacy, Western University of Health Sciences, Pomona, CA, United States

Celastrol (also called tripterine) is a quinone methide triterpene isolated from the root extract of *Tripterygium wilfordii* (thunder god vine in traditional Chinese medicine). Over the past two decades, celastrol has gained wide attention as a potent anti-inflammatory, anti-autoimmune, anti-cancer, anti-oxidant, and neuroprotective agent. However, its clinical translation is very challenging due to its lower aqueous solubility, poor oral bioavailability, and high organ toxicity. To deal with these issues, various formulation strategies have been investigated to augment the overall celastrol efficacy *in vivo* by attempting to increase the bioavailability and/or reduce the toxicity. Among these, nanotechnology-based celastrol formulations are most widely explored by pharmaceutical scientists worldwide. Based on the survey of literature over the past 15 years, this mini-review is aimed at summarizing a multitude of celastrol nanoformulations that have been developed and tested for various therapeutic applications. In addition, the review highlights the unmet need in the clinical translation of celastrol nanoformulations and the path forward.

Keywords: celastrol, nanoformulations, targeting, bioavailability, anti-inflammatory, anti-autoimmune, anti-cancer, anti-oxidant

OPEN ACCESS

Edited by:
Jamal Arif,
Shaqra University, Saudi Arabia

Reviewed by:
Wei Gao,
Capital Medical University, China
Mohammed Kuddus,
University of Hail, Saudi Arabia
Syed Misbahul Hasan,
Integral University, India

****Correspondence:***
Jeffrey Wang
jwang@westernu.edu

[†]These authors have contributed equally to this work

Specialty section:
This article was submitted to Pharmacology of Anti-Cancer Drugs, a section of the journal Frontiers in Pharmacology

Received: *27 February 2021*
Accepted: *10 May 2021*
Published: *11 June 2021*

Citation:
Wagh PR, Desai P, Prabhu S and Wang J (2021) Nanotechnology-Based Celastrol Formulations and Their Therapeutic Applications. Front. Pharmacol. 12:673209. doi: 10.3389/fphar.2021.673209

INTRODUCTION

Clinical translation of bioactive compounds extracted from medicinal plants has gained substantial interest over the past several years due to their superior pharmacological activities especially as anti-inflammatory, anti-tumor, and neuroprotective agents. One such widely investigated medicinal plant is *Tripterygium wilfordii*, a perennial vine of the Celastraceae family, commonly known as "thunder god vine" or "lei gong teng." It is used traditionally in China to treat autoimmune disorders such as rheumatoid arthritis, Crohn's disease, and type 1 diabetes (Cascão et al., 2017). The plant is rich in phytochemicals that comprise triterpenoids and alkaloids, which are mainly extracted from the root pulp of the plant. Among these phytochemicals, the most abundant and promising bioactive compound is celastrol.

Celastrol, also known as tripterine, is a quinone methide triterpene (**Figure 1**). It has gained importance over the past two decades due to its potent anti-inflammatory (Pinna et al., 2004; Shaker et al., 2014; Ma et al., 2015), anti-cancer [gastric and ovarian cancers (Xu et al., 2019; Chen et al., 2020), cervical cancer (Zhou et al., 2017), and hepatocellular carcinoma (Wang et al., 2019; Chen et al., 2020; Du et al., 2020)], neuroprotective (Paris et al., 2010; Li et al., 2012; Jiang et al., 2018), and anti-oxidant (Cleren et al., 2005) activities. However, albeit potent, its clinical translation is impeded due to two main disadvantages that are poor water solubility of 0.044 mg/ml at 25°C (BCS class IV drug) (Yang et al., 2019), which limits its bioavailability, and high systemic toxicity resulting from its narrow therapeutic index (Zhang et al., 2014; Shi et al., 2020).

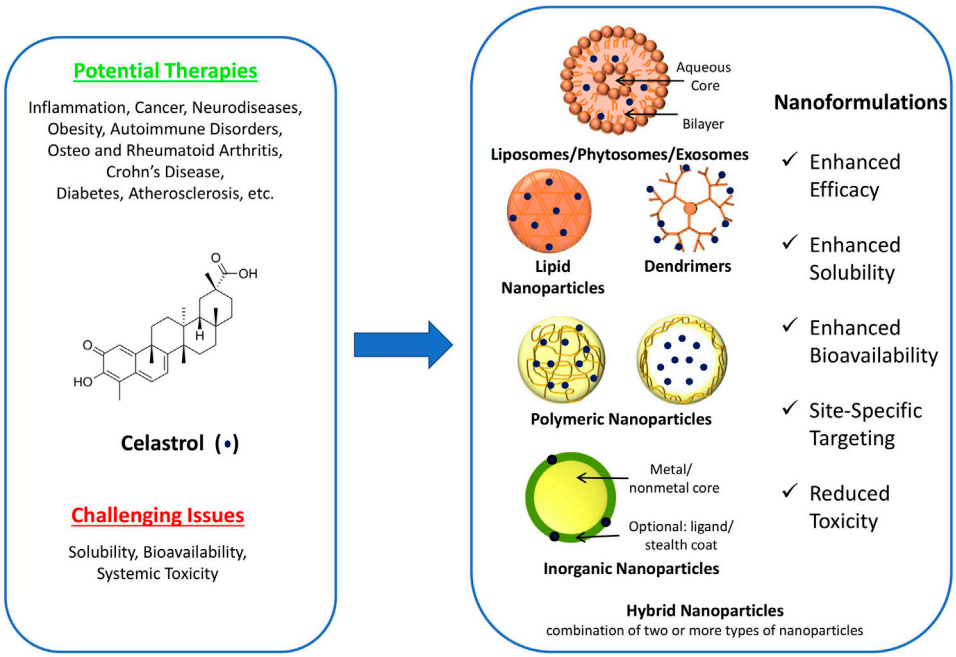

FIGURE 1 | Structure of celastrol, potential therapies, challenging issues, and schematic representation of various celastrol nanoformulations [modified from Desai et al. (2012)].

The reported therapeutic dose of celastrol against various mouse models is in the range of 3–5 mg/kg (Yang et al., 2006). At these doses, though effective, systemic toxicities including cardiotoxicity (Liu et al., 2019), hepatotoxicity (Jin et al., 2019), and nephrotoxicity (Wu et al., 2018) have been reported, whereas lower doses, though safe, show limited efficacy. To overcome the toxicity issues while achieving the desired therapeutic efficacy, various drug delivery approaches have been investigated that include combination with other chemotherapeutic agents such as afatinib, axitinib, and gefitinib (Zhang et al., 2014; Choi et al., 2016; Gao et al., 2019; Lee et al., 2019; Zhao et al., 2019; Dai et al., 2020), combination with traditional Chinese medicines such as betulinic and ellagic acids (An et al., 2015; Duan et al., 2019), overcoming multidrug resistance (Metselaar et al., 2019), nanoparticulate drug delivery systems (Qi et al., 2014; Hakala et al., 2020; Li et al., 2020), and combination with nucleic acid (Huang et al., 2017). Among these, nanoparticulate drug delivery systems/ nanoformulations of celastrol have been widely reported as a promising strategy to effectively deliver drug at the target site rendering enhanced efficacy and safety.

Furthermore, celastrol is classified as a BCS class IV molecule (exhibiting low solubility and permeability), and therefore, solubility and permeability enhancement strategies are the most effective in improving the bioavailability of the drug. In this context, nanoformulations, owing to its smaller size and targeting potential, offer advantages of enhanced solubility (high surface-to-volume ratio) and permeability, both of which are advantageous parameters in enhancing the bioavailability of celastrol. Thus, in view of a multitude of advantages offered by the nanotechnology, celastrol nanoformulations have been widely explored and reported in the literature. Specifically, celastrol nanoformulations have shown significant benefits in several therapeutic applications against prostate cancer, breast and pancreatic cancers, non-small-cell lung cancer, ovarian cancer, and human colon cancer and other applications in treating rheumatoid arthritis, polycystic kidney disease, inflammation, and Parkinson's disease (schematically depicted in **Figure 1**) (Abbas et al., 2007; Salminen et al., 2010; Yadav et al., 2010; Mou et al., 2011; Kim et al., 2013; Chang et al., 2018; Qi et al., 2018; Zha et al., 2018; Lin et al., 2019; Song et al., 2019; Wang et al., 2019; Yan et al., 2020). This review summarizes such state-of-the-art therapeutic applications of celastrol nanoformulations in the subsequent sections. For this, peer-reviewed publications over the past 15 years in the area of celastrol nanoformulations were searched, categorized based on the therapeutic application, and summarized to develop the comprehensive mini-review as presented.

CELASTROL NANOFORMULATIONS AND THEIR THERAPEUTIC APPLICATIONS

Cancer

NF-κB inhibition is the most commonly reported pharmacological mechanism of celastrol's anti-cancer activity

TABLE 1 | Literature overview of nanotechnology-based celastrol formulations.

Nanocarrier type	Indication	Key outcomes	Reference
Polymeric			
Silk fibroin nanoparticles	Cancer	Size: ~ 300 nm 2.4-fold bioavailability enhancement *in vivo*	Onyeabor et al. (2019)
Micelles	Macrophage-induced corneal neovascularization (CNV)	Size: ~ 48 nm Suppressed macrophage-induced CNV *in vitro* and *in vivo* Modulation of MAPK and NF-κB signaling pathways	Li et al. (2012), Li et al. (2016)
Micelles	Retinoblastoma	Size: ~ 48 nm Growth inhibition in the mouse xenograft model by inhibition of NF-κB Downregulation of expression of Bcl-2 leading to apoptosis	Li et al. (2012)
Micelles	Cancer	Size: 86.8 ± 7.6 nm Internalization of micelles in mitochondria *in vitro* and *in vivo* Modulation of mitochondria-mediated apoptotic pathway by increasing ROS levels	Tan et al. (2018)
Micelles	Rheumatoid arthritis	Regulation of the NF-κB and Notch1 pathways Relieved main rheumatoid arthritis symptoms (articular scores, ankle thickness, synovial inflammation, bone erosion, cartilage degradation)	An et al. (2020)
Micelles	Atherosclerosis, inflammation	Size: 14.8–17.9 nm (size increased with increase in drug loading) Reduced TNF-α secretion, number of neutrophils, and inflammatory monocytes within atherosclerotic plaques Inhibition of NF-κB signaling pathway	Allen et al. (2019)
Nanoconjugates	Cancer	Internalization of nanoparticles in MCF-7 and suppression of tumor growth *in vitro* and *in vivo* Inhibition of NF-κB, TNF-α, COX-2, and Ki-67	Abdelmoneem et al., (2021)
Nanoparticles	Prostate cancer	Size: 189.1 ± 2.9 nm Suppressed proliferation, angiogenesis, and cell cycle protein markers in PC3 cell line *in vitro* Significant decrease in the expression of Ki-67, PCNA, TNF-R1/2, and Fas, as well as induction of p21 and p27	Sanna et al. (2015)
Nanoparticles	Prostate cancer	Size: 75.4 nm Enhancement in anti-tumor effect *in vivo* Enhanced efficacy by pre-saturation of reticuloendothelial system by the blank nanoparticles	Yin et al. (2017)
Lipid			
Microemulsion	Ovarian cancer	Size: ~50 nm Combinational and tumor-targeted cancer therapy Active tumor targeting via transferrin and cell-penetrating peptide Reduced the toxicity of tripterine against the liver and kidney Enhanced antitumor efficacy *in vivo*	Zhao et al. (2020)
Microemulsion	Lung cancer	Size: 69.2 ± 3.3 nm Combination treatment of nano-*β*-elemene and celastrol showed synergistic anti-cancer efficacy *in vivo* No obvious systemic toxicity *in vivo*	Zhang et al. (2019)
Liposome	Lung cancer	Size: 89.61 ± 0.53 nm Enhanced permeability in four-site perfusion rat intestinal model due to cell membrane–mimicking liposome Enhanced anti-tumor activity *in vivo*	Song et al. (2011)
Nanostructured lipid carrier	Enhanced absorption	Size: 109.6 ± 5.8 nm Delayed drug release profile with enhanced absorption in rat intestinal perfusion model	Zhou et al. (2012)
Nanostructured lipid carrier gel	Arthritis and inflammation	Size: 26.92 ± 0.62 nm Combination of celastrol and indomethacin lipid nanocarriers showed significant reduction in paw edema model *in vivo* Inhibition of inflammation and pain by modulating IL-1β, TNF-*α*, *β*-endorphin, and substance *p*	Kang et al. (2018)
Inorganic			
Gold nanourchins	Glioblastoma	Significant reduction in the pro-survival signaling via the PI3 kinase–Akt pathway Significant inhibition of glioblastoma cells	Maysinger et al. (2018)

(Elhasany et al., 2020). Celastrol also inhibits M2-like polarized tumor-associated macrophages that are involved in tumor metastasis. In an *in vivo* study (Yang et al., 2018), the expression of M2-like genes by quantitative real-time PCR showed that genes including MRC1, Arg1, Fizz1, Mgl2, and CD11c were up-regulated by IL-13 administration, which was greatly reduced by celastrol co-administration. Other molecular targets include liver X receptor α and ATP-binding cassette

transporter A1 (Zhang et al., 2020), microRNA-21 (Yao et al., 2019), androgen receptor/microRNA-101 (Guo et al., 2015), lipoprotein receptor-1 (Gu et al., 2013), microRNA-33a-5p/E2F7 transcription factor (Liu et al., 2020), PI3K–Akt–mTOR signaling (Li et al., 2018), mitochondrial ubiquitination (Hu et al., 2017), CXC chemokine receptor type 4 (Yadav et al., 2010), peroxisome proliferator–activated receptor α signaling (Zhao et al., 2020), and transforming growth factor β1 (Kang et al., 2013). In spite of multi-target anti-cancer potency of celastrol, its clinical translation has not been realized due to poor bioavailability, inadequate tumor targeting, and high toxicity. The nanoformulations developed and investigated to overcome these challenges for various cancers are described below, and additional nanoformulations not discussed in detail are summarized in **Table 1**.

Cancer tumorigenesis and metastasis is induced by multiple mechanisms including migration, invasion, and angiogenesis. The tumor microenvironment (TME) plays a key role in these carcinogenic mechanisms, and multiple strategies have been investigated to alter the TME in order to treat cancers. Among various pharmacological responses, celastrol is reported to inhibit NLRP3 inflammasome, which in turn impedes the macrophage potency to promote migration and invasion of melanoma cells (Lee et al., 2019). To effectively deliver celastrol for treatment of melanoma, self-assembling amphiphilic polymer/celastrol prodrug nanoparticles were developed by chemically conjugating celastrol to the diblock polymer methoxy-poly(ethylene glycol)-*b*-poly(L-lysine) (Li et al., 2020). This celastrol prodrug underwent self-assembly to form stable micellar nanoparticles (103.1 ± 10.7 nm) due to hydrophobic and electrostatic interactions between the drug and the polymer. An *in vivo* study in the B16F10 mouse melanoma model showed significant uptake of the nanoparticle formulation due to the enhanced permeability and retention (EPR) effect that resulted in tumor growth reduction and lowered toxicity compared to that of celastrol alone, confirming the potential of functionalized nanoparticle-mediated drug targeting as a safe and effective tool (Li et al., 2020). In another investigation, a celastrol nanoemulsion was reported to downregulate programmed cell death-ligand 1, eliciting strong immunogenic cell death in a bilateral tumor model. This can be viewed as a promising avenue of chemotherapy-induced cancer immunotherapy (Qiu et al., 2021). Celastrol was also reported to have inhibitory effect on tumor-associated fibroblasts that play a critical role in desmoplastic melanoma. In view of the strong anti-fibroblast and immunomodulatory effects of celastrol, it has also been combined with potent anti-cancer drugs to achieve simultaneous chemo-immunotherapy in melanoma treatment. For instance, Liu et al. developed TME-responsive targeted aminoethylanisamide polymeric nanoparticles comprising a drug combination of the anti-cancer agent mitoxantrone and celastrol in a 5:1 ratio. The nanoparticles exhibited a size of 112 ± 6 nm with > 75% drug encapsulation for both drugs. *In vivo* melanoma tumor model studies confirmed inhibition of cancer progression/metastasis and TME immunosuppression, confirming the hypothesis synergistic anti-cancer efficacy with combination drug nanoparticles of mitoxantrone and celastrol (Liu et al., 2018). Similarly, bio-mimicking polyethylene glycol–poly(lactic-co-glycolic acid) (PEG–PLGA) nanoparticles coated with the neutrophil membrane showed higher internalization and apoptosis in the murine melanoma B16F10 cell line as compared to uncoated nanoparticles. This coating also helped to increase the biodistribution in the tumor xenograft model (Zhou et al., 2019).

Celastrol has also been reported to have potent activity against ovarian cancer via mechanisms that include intracellular accumulation of reactive oxygen species (ROS), apoptosis, cell cycle arrest (G2/M phase), and ultimately cell growth inhibition (Xu et al., 2019). For instance, an *in vitro* study with the ovarian cancer SKOV3 cell line showed proportional increase in intracellular ROS concentration with increased exposure to celastrol, confirming the ROS responsiveness of celastrol (Xu et al., 2019). To enhance the clinical efficacy with reduction in toxicity, various nanoformulations have been investigated. Furthermore, to enhance ovarian cancer targeting, Niu et al. prepared celastrol nanoparticles using the poly(lactic-*co*-glycolic acid)–poly(ethylene glycol) methyl ether (PLGA–mPEG) polymer and coated them with folic acid for active tumor targeting. Folate receptors upregulate in tumor tissue, and hence, the use of folic acid–coated nanoparticles enables enhanced uptake via active targeting. The prepared nanoparticles displayed the encapsulation efficiency of 95% with a particle size of 155 nm and showed significant enhancement in ROS levels' inhibitory potential against SKOV3 cells with prolonged treatment time (Niu et al., 2020). The folate receptor tumor targeting approach was also investigated by Law et al. wherein they developed folic acid–functionalized celastrol-conjugated gold–polymer nanoparticles to achieve active targeting against breast cancer. The developed nanoparticles showed significant enhancement in apoptosis in 2D and 3D breast tumor models compared to celastrol alone. The nanoparticles also exhibited higher cellular uptake efficiency and lower colony-forming assay units, confirming enhanced uptake of the nanoparticles leading to improved efficacy (Law et al., 2020). Celastrol nanosuspension with a size of 147.9 nm has also been developed and investigated for breast cancer treatment. Celastrol was stabilized in an amorphous form in the nanosuspension, hence enhancing its dissolution significantly to 69.2% in 48 h. Compared to intravenous injection of the anticancer drug paclitaxel, the oral and intravenous treatment with celastrol nanosuspension showed similar and higher tumor inhibition rates, respectively. Hence, the unique property of nanoformulations to enhance dissolution of poorly soluble drugs such as celastrol can be explored to enhance solubility and in turn the *in vivo* efficacy (Huang et al., 2020).

Non-small-cell lung cancer is the most predominant lung carcinoma, and tyrosine kinase inhibitors (TKIs) are classically used for chemotherapy. Celastrol has gained particular attention in treatment of this type of cancer due to its serine threonine protein kinase (Akt) inhibitory potential, which is proven to be very effective if combined with TKIs. Particularly, Xie et al. developed a nano-product comprising the TKI gefitinib and celastrol along with a fluorescent diagnostic probe. The combination nano-prodrug approach not only allowed fluorescence and optoacoustic tumor

imaging but was also proven to be superior, exhibiting significant tumor inhibition in an orthotopic mouse tumor model (Xie et al., 2020). In another study (Zhao et al., 2018), a nanoformulation comprising celastrol-loaded glucolipid-like conjugates tagged with avb3-ligand tetraiodothyroacetic acid was developed to inhibit the NF-kB signaling pathway in lung and breast metastatic cancer cells. The targeted nanoformulation was selectively taken up by the cells via the avb3 receptor–mediated interaction. The study showed reduction in the apoptotic marker MMP-9 *in vivo*, confirming that the prepared celastrol-loaded micelles suppressed breast tumor invasion and lung metastasis. In addition, self-assembled micelles containing covalently conjugated celastrol–PEG–ginsenoside Rh2 were developed for endosomal/lysosomal delivery. The formulation showed significant enhancement in the bioavailability due to introduction of PEG that imparted stealth (long circulation) properties to the nanoparticles and showed synergistic anti–lung cancer activity due to the combination approach (Li et al., 2017).

In addition to the use of folic acid for active tumor targeting, multiple other active targeting strategies have also been reported in this area. For instance, glucose was used as an affinity ligand to decorate mesoporous silica nanoparticles for the delivery of celastrol with high specificity to HeLa and A549 cancer cells. To further increase the specificity, poly(ethylene imine) was surface-branched on the nanoparticles that increased the overall positive charge and hence the cellular uptake (Niemelä et al., 2015). In another interesting study, theranostic (combining therapeutics with diagnostics) nanoparticles incorporated with a drug combination of celastrol and sulfasalazine were developed for targeted breast cancer management. Specifically, SPION-tagged amphiphilic zein–chondroitin sulfate micelles were used to achieve simultaneous CD44–tumor-targeted drug delivery of celastrol and sulfasalazine along with MRI. The combination nanoplatform showed highest efficacy compared to non-targeted and free drug treatment groups confirming its superiority (Elhasany et al., 2020). Furthermore, folate receptor–targeted liposomes carrying combination of celastrol and irinotecan have also been reported for lung and breast cancer treatment (Soe et al., 2018). The liposomes exhibited improved cellular uptake and apoptosis when tested in multiple cancer cell lines (MCF-7, MDA-MB-231, A549). The *in vivo* studies in MDA-MB-231 tumor-bearing female BALB/c nude mice confirmed highest suppression with the liposomal treatment group (Soe et al., 2018). Another vesicular nanoformulation investigated for lung cancer treatment was celastrol exosomes that showed efficacy against A549 and H1299 lung cancer cells. Additionally, when tested in a xenograft model, exosomal celastrol presented enhanced anti-tumor efficacy compared to free celastrol and was devoid of kidney and liver toxicity, confirming its promise in lung cancer treatment (Aqil et al., 2016).

Celastrol has also been proven to be effective against prostate cancer. For example, investigation of celastrol poly(ε-caprolactone) nanoparticles against prostate cancer cell lines (LNCaP, DU-145, and PC3) revealed significant inhibition (IC_{50} < 2 μM) with modulation of apoptotic proteins (Sanna et al., 2015). In another study, polycaprolactone polymeric tripterine nanoparticles were prepared with a size of about 75 nm. The nanoparticles were proven to elicit significant tumor reduction compared to the free drug in LNCaP cell BALB/c mice xenograft model (Yin et al., 2017). Lipid nanocarriers have also been investigated for this purpose. For example, Chen et al. developed nanostructured lipid carriers (NLCs) of celastrol and coated them with the cell-penetrating peptide to achieve active tumor targeting. The NLCs (size: 126.7 ± 9.2 nm) showed a controlled drug release profile with enhance absorption *in vivo* due to NLCs' colloidal form and nanosize. Specifically, the NLC formulation showed 484.75% enhancement in bioavailability compared to a plain drug (Chen et al., 2012). The similar group further investigated the efficacy of the targeted NLCs in the prostate cancer model *in vivo*. The studies confirmed enhanced anti-tumor effect and reduction in tumor markers (necrosis factor-alpha, interleukin-6 cytokine) compared to plain drug control in a dose-dependent manner (Yuan et al., 2013).

Celastrol has also been proven effective against pancreatic carcinoma (Cao et al., 2019). Celastrol-loaded neutrophil-mimicking nanoparticles were demonstrated to achieve pancreas-specific drug delivery by overcoming the blood–pancreas barrier *in vivo*. For this, the poly(ethylene glycol) methyl ether-block-poly(lactic-co-glycolic acid) polymer was used as a naive neutrophil membrane coating. The coating induced neutrophil-like properties to the nanoparticles that enhanced their uptake by the cells both *in vitro* and *in vivo*. *In vitro* evaluation of these nanoparticles in the lipopolysaccharide-stimulated RAW264.7 macrophages and L929 cells showed marked cellular uptake and internalization. Furthermore, the *in vivo* anti-tumor efficacy study in the female pancreatic cancer mice model proved enhanced and site-specific anti-tumor activity. Similarly, celastrol-loaded silk fibroin (SF) nanoparticles were synthesized and studied in human pancreatic cancer cells (MIA PaCa-2 and PANC-1). SF nanoparticles showed lower IC_{50} values in both the cell lines compared to free celastrol (Ding et al., 2017).

To target celastrol for solid tumor treatment, mesoporous silica nanoparticles capped with PEGylated polyaminoacid were prepared for mitochondria-targeted delivery of celastrol. The targeted nanoparticles were shown to have enhanced efficacy in the SCC-7 cancer cell–bearing xenograft tumor mice model (Choi et al., 2018). In a study to examine apoptotic effects of celastrol on cancer cells, SW620 colorectal cancer cells both *in vitro* and in nude mice were conducted along with biosafety studies in zebrafish and xenograft mice models. The prepared dendrimer bioconjugate of celastrol showed a particle size of 40 nm (spherical in shape) and induced apoptosis in the colorectal cancer cells *in vitro* and in mice with reduction in local and systemic toxicity (Ge et al., 2020). To summarize, a plethora of celastrol nanoformulations have shown their potential to enhance the efficacy and safety profile of celastrol in cancer treatment.

Osteoarthritis and Rheumatoid Arthritis

Celastrol is a potent therapeutic agent investigated for the treatment of osteoarthritis and rheumatoid arthritis. It elicits treatment benefit by regulating functions of Th1 and Th2 cells,

fibroblasts, macrophages, and endothelial cells that play critical roles in the etiology and pathogenesis of arthritis. In addition, celastrol inhibits numerous inflammatory chemokines that include mundane T cells expressed and secreted, monocyte chemoattractant protein 1, macrophage inflammatory proteins, and growth-regulated oncogene/keratinocyte chemoattractant. In addition to these molecular targets, celastrol also modulates the function of metalloprotein, JNK and MEK1 pathways (Song et al., 2019). Celastrol nanoformulations have been reported to further enhance the anti-inflammatory efficacy while offering promising safety profile. For example, celastrol-loaded palmitic acid–modified bovine serum albumin (PAB) nanoparticles and bovine serum albumin (BSA) nanoparticles were developed and tested for anti-inflammatory response in the AIA rats for scavenger receptor-A targeting via intravenous injection treatment (Gong et al., 2020). The celastrol PAB nanoparticles significantly improved rheumatoid arthritis symptoms at a lower dose with fewer toxic effects compared to the celastrol BSA nanoparticles. Furthermore, mechanistically, celastrol PAB nanoparticles were proven to enhance scavenger receptor-A targeting due to high electronegativity (excipients: BSA and palmitic acid) compared to celastrol BSA nanoparticles (excipient: BSA) (Gong et al., 2020). In another study, phytosomes with a combination of celastrol and selenium were administered via oral gavage to treat arthritis in male AIA rats. These phytosomes enhanced the transepithelial transport of drugs due to smaller phytosomal size (126 nm) and enhanced nanoparticle transmembrane diffusion. This enhanced uptake resulted in significant alleviation of the arthritis symptoms and also lowered the inflammatory factors (Zhu et al., 2020).

Miscellaneous

Celastrol nanoformulations have been studied to benefit in treatment of obesity (Liu et al., 2015), diabetes, lipid accumulation, psoriasis (Zhou et al., 2011), etc. For example, celastrol-loaded polyethylene glycol–polycaprolactone nanomicelles effectively ameliorated body weight, lipid accumulation, diabetes, and metabolic dysfunction in diet-induced obese mice. Furthermore, histopathological examination of the high-fat-diet–induced obese mice model confirmed that the treatment with celastrol nanoformulation did not result in any anal irritation or intestinal disturbance otherwise seen in control or plain celastrol–treated animals. Hence, celastrol nanomicelles can be deemed more effective and safer (Zhao et al., 2019). Celastrol has also been proven to be effective in treatment of renal diseases (Tang et al., 2018). But its severe systemic toxicity limits its use. Guo et al. prepared mesangial cell–targeting celastrol nanoparticles using human serum albumin for ameliorating the effects of mesangioproliferative glomerulonephritis (MsPGN). They confirmed the selective uptake of celastrol nanoparticles via *in vivo* fluorescence imaging and semiquantitative fluorescence intensity measurement of the kidneys (excised 5 min after tail vein injection of nanoparticles), and the nanoparticles with size 95 nm showed maximum uptake by the kidneys (Guo et al., 2017). The *in vivo* evaluation clearly showed that the formulation not only reduced the systemic toxicity but also minimized the off-targeting effects of celastrol. It also showed potent effects against proteinuria, inflammation, glomerular hypercellularity, and extracellular matrix (ECM) deposition in an anti-Thy1.1 nephritis rat model. This was attributed to the anti-inflammatory, anti-proliferative, and anti-fibrotic mechanisms, highlighting celastrol as a promising agent for the treatment of MsPGN such as IgA nephropathy (Guo et al., 2017). Multiple studies as described earlier have shown that nanoparticles enhance the bioavailability of celastrol. In one such specific study, Freag et al. encapsulated celastrol in a self-assembled phospholipid-based phytosomal nanocarrier system. The *in vivo* pharmacokinetic data in rabbits indicated that the phytosomes increased the bioavailability and C_{max} by fourfold and fivefold, respectively, compared to the celastrol suspension. The authors attributed the bioavailability enhancement to meticulous use of phospholipids that not only retain cell membrane fluidity but also potentially enhance the rate and extent of intestinal drug absorption and enhancement in the aqueous solubility of celastrol by incorporating it in a nanoformulation (Freag et al., 2018).

CONCLUSION AND FUTURE PROSPECTS

Medicinal plants containing bioactive constituents are a great resource for modern drug development, and *Tripterygium wilfordii* is one of them. Its major constituent celastrol has numerous pharmacological actions including anti-inflammatory, anti-obesity, anti-diabetic, and anti-cancer activities (Cascão et al., 2017; Chen et al., 2018; Hou et al., 2020; Yan et al., 2020; Lu et al., 2021). However, there are multiple challenges in translating traditional herbal medicines and their active constituents to modern drug therapies. In particular, celastrol presents issues of low solubility, bioavailability, and toxicity (Zha et al., 2018). For seven decades, numerous attempts have been made to overcome the problems of celastrol delivery, and recently, nanotechnology-based formulations have shown great promise in enhancing its overall pharmacological efficacy and safety. Celastrol nanoformulations (enhanced permeation, retention, tumor targeting, and controlled drug release) can be looked upon as a promising avenue toward successful clinical translation of this potent bioactive agent toward treatment of various human diseases (Fang and Tang, 2020). More importantly, the universal challenge of clinical translation of nanomedicine needs more attention, and as rightly pointed out by Sun et al. (2020), pharmaceutical scientists, engineers, chemists, and material scientists must work in synergy to develop stable, scalable, and effective nanoformulations. Furthermore, regulatory authorities worldwide are developing specific guidelines to streamline the approval of nanomedicine-based products that would help in successful clinical translation of these formulations in the near future (Paradise, 2019).

AUTHOR CONTRIBUTIONS

JW conceived and proposed the idea. PW and PD compiled the manuscript. SP and JW reviewed and revised the manuscript.

FUNDING

The funding was provided by the Western University of Health Sciences.

REFERENCES

Abbas, S., Bhoumik, A., Dahl, R., Vasile, S., Krajewski, S., Cosford, N. D. P., et al. (2007). Preclinical Studies of Celastrol and Acetyl Isogambogic Acid in Melanoma. *Clin. Cancer Res.* 13 (22 Pt 1), 6769–6778. doi:10.1158/1078-0432.Ccr-07-1536

Abdelmoneem, M. A., Abd Elwakil, M. M., Khattab, S. N., Helmy, M. W., Bekhit, A. A., Abdulkader, M. A., et al. (2021). Lactoferrin-dual Drug Nanoconjugate: Synergistic Anti-tumor Efficacy of Docetaxel and the NF-Kb Inhibitor Celastrol. *Mater. Sci. Eng. C* 118, 111422. doi:10.1016/j.msec.2020.111422

Allen, S. D., Liu, Y.-G., Kim, T., Bobbala, S., Yi, S., Zhang, X., et al. (2019). Celastrol-loaded PEG-B-PPS Nanocarriers as an Anti-inflammatory Treatment for Atherosclerosis. *Biomater. Sci.* 7 (2), 657–668. doi:10.1039/c8bm01224e

An, L., Li, Z., Shi, L., Wang, L., Wang, Y., Jin, L., et al. (2020). Inflammation-Targeted Celastrol Nanodrug Attenuates Collagen-Induced Arthritis through NF-Kb and Notch1 Pathways. *Nano Lett.* 20 (10), 7728–7736. doi:10.1021/acs.nanolett.0c03279

An, N., Li, H. Y., and Zhang, X. M. (2015). Growth Inhibitive Effect of Betulinic Acid Combined with Tripterine on MSB-1 Cells and its Mechanism. *Poult. Sci.* 94 (12), 2880–2886. doi:10.3382/ps/pev267

Aqil, F., Kausar, H., Agrawal, A. K., Jeyabalan, J., Kyakulaga, A.-H., Munagala, R., et al. (2016). Exosomal Formulation Enhances Therapeutic Response of Celastrol against Lung Cancer. *Exp. Mol. Pathol.* 101 (1), 12–21. doi:10.1016/j.yexmp.2016.05.013

Cao, X., Hu, Y., Luo, S., Wang, Y., Gong, T., Sun, X., et al. (2019). Neutrophil-mimicking Therapeutic Nanoparticles for Targeted Chemotherapy of Pancreatic Carcinoma. *Acta Pharmaceutica Sinica B* 9 (3), 575–589. doi:10.1016/j.apsb.2018.12.009

Cascão, R., Fonseca, J. E., and Moita, L. F. (2017). Celastrol: A Spectrum of Treatment Opportunities in Chronic Diseases. *Front. Med.* 4 (69), 4. doi:10.3389/fmed.2017.00069

Chang, M.-Y., Hsieh, C.-Y., Lin, C.-Y., Chen, T.-D., Yang, H.-Y., Chen, K.-H., et al. (2018). Effect of Celastrol on the Progression of Polycystic Kidney Disease in a Pkd1-Deficient Mouse Model. *Life Sci.* 212, 70–79. doi:10.1016/j.lfs.2018.09.047

Chen, S.-R., Dai, Y., Zhao, J., Lin, L., Wang, Y., and Wang, Y. (2018). A Mechanistic Overview of Triptolide and Celastrol, Natural Products from Tripterygium Wilfordii Hook F. *Front. Pharmacol.* 9 (104). doi:10.3389/fphar.2018.00104

Chen, X., Hu, X., Hu, J., Qiu, Z., Yuan, M., and Zheng, G. (2020). Celastrol-Loaded Galactosylated Liposomes Effectively Inhibit AKT/c-Met-Triggered Rapid Hepatocarcinogenesis in Mice. *Mol. Pharmaceutics* 17 (3), 738–747. doi:10.1021/acs.molpharmaceut.9b00428

Chen, X., Zhao, Y., Luo, W., Chen, S., Lin, F., Zhang, X., et al. (2020). Celastrol Induces ROS-Mediated Apoptosis via Directly Targeting Peroxiredoxin-2 in Gastric Cancer Cells. *Theranostics* 10 (22), 10290–10308. doi:10.7150/thno.46728

Chen, Y., Yuan, L., Zhou, L., Zhang, Z. H., Cao, W., and Wu, Q. (2012). Effect of Cell-Penetrating Peptide-Coated Nanostructured Lipid Carriers on the Oral Absorption of Tripterine. *Int. J. Nanomedicine* 7, 4581–4591. doi:10.2147/IJN.S34991

Choi, J. Y., Gupta, B., Ramasamy, T., Jeong, J.-H., Jin, S. G., Choi, H.-G., et al. (2018). PEGylated Polyaminoacid-Capped Mesoporous Silica Nanoparticles for Mitochondria-Targeted Delivery of Celastrol in Solid Tumors. *Colloids Surf. B: Biointerfaces* 165, 56–66. doi:10.1016/j.colsurfb.2018.02.015

Choi, J. Y., Ramasamy, T., Kim, S. Y., Kim, J., Ku, S. K., Youn, Y. S., et al. (2016). PEGylated Lipid Bilayer-Supported Mesoporous Silica Nanoparticle Composite for Synergistic Co-delivery of Axitinib and Celastrol in Multi-Targeted Cancer Therapy. *Acta Biomater.* 39, 94–105. doi:10.1016/j.actbio.2016.05.012

Cleren, C., Calingasan, N. Y., Chen, J., and Beal, M. F. (2005). Celastrol Protects against MPTP- and 3-nitropropionic Acid-Induced Neurotoxicity. *J. Neurochem.* 94 (4), 995–1004. doi:10.1111/j.1471-4159.2005.03253.x

Dai, C. H., Zhu, L. R., Wang, Y., Tang, X. P., Du, Y. J., Chen, Y. C., et al. (2020). Celastrol Acts Synergistically with Afatinib to Suppress Non-small Cell Lung Cancer Cell Proliferation by Inducing Paraptosis. *J. Cel. Physiol.* 236, 4538–4554. doi:10.1002/jcp.30172

Desai, P. P., Date, A. A., and Patravale, V. B. (2012). Overcoming Poor Oral Bioavailability Using Nanoparticle Formulations - Opportunities and Limitations. *Drug Discov. Today Tech.* 9 (2), e87–e95. doi:10.1016/j.ddtec.2011.12.001

Ding, B., Wahid, M. A., Wang, Z., Xie, C., Thakkar, A., Prabhu, S., et al. (2017). Triptolide and Celastrol Loaded Silk Fibroin Nanoparticles Show Synergistic Effect against Human Pancreatic Cancer Cells. *Nanoscale* 9 (32), 11739–11753. doi:10.1039/C7NR03016A

Du, S., Song, X., Li, Y., Cao, Y., Chu, F., Durojaye, O. A., et al. (2020). Celastrol Inhibits Ezrin-Mediated Migration of Hepatocellular Carcinoma Cells. *Sci. Rep.* 10 (1), 11273. doi:10.1038/s41598-020-68238-1

Duan, J., Zhan, J.-C., Wang, G.-Z., Zhao, X.-C., Huang, W.-D., and Zhou, G.-B. (2019). The Red Wine Component Ellagic Acid Induces Autophagy and Exhibits Anti-lung Cancer Activity *In Vitro* and *In Vivo*. *J. Cel. Mol. Med.* 23 (1), 143–154. doi:10.1111/jcmm.13899

Elhasany, K. A., Khattab, S. N., Bekhit, A. A., Ragab, D. M., Abdulkader, M. A., Zaky, A., et al. (2020). Combination of Magnetic Targeting with Synergistic Inhibition of NF-Kb and Glutathione via Micellar Drug Nanomedicine Enhances its Anti-tumor Efficacy. *Eur. J. Pharmaceutics Biopharmaceutics* 155, 162–176. doi:10.1016/j.ejpb.2020.08.004

Fang, G., and Tang, B. (2020). Current Advances in the Nano-Delivery of Celastrol for Treating Inflammation-Associated Diseases. *J. Mater. Chem. B* 8 (48), 10954–10965. doi:10.1039/D0TB01939A

Freag, M. S., Saleh, W. M., and Abdallah, O. Y. (2018). Self-assembled Phospholipid-Based Phytosomal Nanocarriers as Promising Platforms for Improving Oral Bioavailability of the Anticancer Celastrol. *Int. J. Pharmaceutics* 535 (1-2), 18–26. doi:10.1016/j.ijpharm.2017.10.053

Gao, Y., Zhou, S., Pang, L., Yang, J., Li, H. J., Huo, X., et al. (2019). Celastrol Suppresses Nitric Oxide Synthases and the Angiogenesis Pathway in Colorectal Cancer. *Free Radic. Res.* 53 (3), 324–334. doi:10.1080/10715762.2019.1575512

Ge, P., Niu, B., Wu, Y., Xu, W., Li, M., Sun, H., et al. (2020). Enhanced Cancer Therapy of Celastrol *In Vitro* and *In Vivo* by Smart Dendrimers Delivery with Specificity and Biosafety. *Chem. Eng. J.* 383, 123228. doi:10.1016/j.cej.2019.123228

Gong, T., Tan, T., Zhang, P., Li, H., Deng, C., Huang, Y., et al. (2020). Palmitic Acid-Modified Bovine Serum Albumin Nanoparticles Target Scavenger Receptor-A on Activated Macrophages to Treat Rheumatoid Arthritis. *Biomaterials* 258, 120296. doi:10.1016/j.biomaterials.2020.120296

Gu, L., Bai, W., Li, S., Zhang, Y., Han, Y., Gu, Y., et al. (2013). Celastrol Prevents Atherosclerosis via Inhibiting LOX-1 and Oxidative Stress. *PLoS One* 8 (6), e65477. doi:10.1371/journal.pone.0065477

Guo, J., Huang, X., Wang, H., and Yang, H. (2015). Celastrol Induces Autophagy by Targeting AR/miR-101 in Prostate Cancer Cells. *PLoS One* 10 (10), e0140745. doi:10.1371/journal.pone.0140745

Guo, L., Luo, S., Du, Z., Zhou, M., Li, P., Fu, Y., et al. (2017). Targeted Delivery of Celastrol to Mesangial Cells Is Effective against Mesangioproliferative Glomerulonephritis. *Nat. Commun.* 8 (1), 878. doi:10.1038/s41467-017-00834-8

Hakala, T. A., Davies, S., Toprakcioglu, Z., Bernardim, B., Bernardes, G. J. L., and Knowles, T. P. J. (2020). A Microfluidic Co-Flow Route for Human Serum Albumin-Drug-Nanoparticle Assembly. *Chem. Eur. J.* 26 (27), 5965–5969. doi:10.1002/chem.202001146

Hou, W., Liu, B., and Xu, H. (2020). Celastrol: Progresses in Structure-Modifications, Structure-Activity Relationships, Pharmacology and Toxicology. *Eur. J. Med. Chem.* 189, 112081. doi:10.1016/j.ejmech.2020.112081

Hu, M., Luo, Q., Alitongbieke, G., Chong, S., Xu, C., Xie, L., et al. (2017). Celastrol-Induced Nur77 Interaction with TRAF2 Alleviates Inflammation by Promoting Mitochondrial Ubiquitination and Autophagy. *Mol. Cel.* 66 (1), 141–153. doi:10.1016/j.molcel.2017.03.008

Huang, T., Wang, Y., Shen, Y., Ao, H., Guo, Y., Han, M., et al. (2020). Preparation of High Drug-Loading Celastrol Nanosuspensions and Their Anti-breast Cancer Activities *In Vitro* and *In Vivo*. *Sci. Rep.* 10 (1), 8851. doi:10.1038/s41598-020-65773-9

Huang, W., Chen, L., Kang, L., Jin, M., Sun, P., Xin, X., et al. (2017). Nanomedicine-based Combination Anticancer Therapy between Nucleic Acids and Small-Molecular Drugs. *Adv. Drug Deliv. Rev.* 115, 82–97. doi:10.1016/j.addr.2017.06.004

Jiang, M., Liu, X., Zhang, D., Wang, Y., Hu, X., Xu, F., et al. (2018). Celastrol Treatment Protects against Acute Ischemic Stroke-Induced Brain Injury

by Promoting an IL-33/ST2 axis-mediated Microglia/macrophage M2 Polarization. *J. Neuroinflammation* 15 (1), 78. doi:10.1186/s12974-018-1124-6

Jin, C., Wu, Z., Wang, L., Kanai, Y., and He, X. (2019). CYP450s-Activity Relations of Celastrol to Interact with Triptolide Reveal the Reasons of Hepatotoxicity of Tripterygium Wilfordii. *Molecules* 24 (11), 2162. doi:10.3390/molecules24112162

Kang, H., Lee, M., and Jang, S.-W. (2013). Celastrol Inhibits TGF-β1-Induced Epithelial-Mesenchymal Transition by Inhibiting Snail and Regulating E-Cadherin Expression. *Biochem. Biophysical Res. Commun.* 437 (4), 550–556. doi:10.1016/j.bbrc.2013.06.113

Kang, Q., Liu, J., Zhao, Y., Liu, X., Liu, X.-Y., Wang, Y.-J., et al. (2018). Transdermal Delivery System of Nanostructured Lipid Carriers Loaded with Celastrol and Indomethacin: Optimization, Characterization and Efficacy Evaluation for Rheumatoid Arthritis. *Artif. Cell Nanomedicine, Biotechnol.* 46 (Suppl. 3), S585–S597. doi:10.1080/21691401.2018.1503599

Kim, J. H., Lee, J. O., Lee, S. K., Kim, N., You, G. Y., Moon, J. W., et al. (2013). Celastrol Suppresses Breast Cancer MCF-7 Cell Viability via the AMP-Activated Protein Kinase (AMPK)-induced P53-polo like Kinase 2 (PLK-2) Pathway. *Cell Signal.* 25 (4), 805–813. doi:10.1016/j.cellsig.2012.12.005

Law, S., Leung, A. W., and Xu, C. (2020). Folic Acid-Modified Celastrol Nanoparticles: Synthesis, Characterization, Anticancer Activity in 2D and 3D Breast Cancer Models. *Artif. Cell Nanomedicine, Biotechnol.* 48 (1), 542–559. doi:10.1080/21691401.2020.1725025

Lee, H. E., Lee, J. Y., Yang, G., Kang, H. C., Cho, Y.-Y., Lee, H. S., et al. (2019). Inhibition of NLRP3 Inflammasome in Tumor Microenvironment Leads to Suppression of Metastatic Potential of Cancer Cells. *Sci. Rep.* 9 (1), 12277. doi:10.1038/s41598-019-48794-x

Lee, Y., Kim, S. Y., and Lee, C. (2019). Axl Is a Novel Target of Celastrol that Inhibits Cell Proliferation and Migration, and Increases the Cytotoxicity of Gefitinib in EGFR Mutant Non-small C-ell L-ung C-ancer C-ells. *Mol. Med. Rep.* 19 (4), 3230–3236. doi:10.3892/mmr.2019.9957

Li, J., Jia, Y., Zhang, P., Yang, H., Cong, X., An, L., et al. (2020). Celastrol Self-Stabilized Nanoparticles for Effective Treatment of Melanoma. *Ijn* 15, 1205–1214. doi:10.2147/IJN.S232603

Li, P., Zhou, X., Qu, D., Guo, M., Fan, C., Zhou, T., et al. (2017). Preliminary Study on Fabrication, Characterization and Synergistic Anti-lung Cancer Effects of Self-Assembled Micelles of Covalently Conjugated Celastrol-Polyethylene Glycol-Ginsenoside Rh2. *Drug Deliv.* 24 (1), 834–845. doi:10.1080/10717544.2017.1326540

Li, X., Zhu, G., Yao, X., Wang, N., Hu, R., Kong, Q., et al. (2018). Celastrol Induces Ubiquitin-dependent Degradation of mTOR in Breast Cancer Cells. *Ott* 11, 8977–8985. doi:10.2147/ott.S187315

Li, Y., He, D., Zhang, X., Liu, Z., Zhang, X., Dong, L., et al. (2012). Protective Effect of Celastrol in Rat Cerebral Ischemia Model: Down-Regulating P-JNK, P-C-Jun and NF-Kb. *Brain Res.* 1464, 8–13. doi:10.1016/j.brainres.2012.04.054

Li, Y., Li, Z., Wu, J., Li, J., Yao, L., Zhang, Y., et al. (2012). Antitumor Activity of Celastrol Nanoparticles in a Xenograft Retinoblastoma Tumor Model. *Ijn* 7, 2389–2398. doi:10.2147/IJN.S29945

Li, Z., Yao, L., Li, J., Zhang, W., Wu, X., Liu, Y., et al. (2012). Celastrol Nanoparticles Inhibit Corneal Neovascularization Induced by Suturing in Rats. *Int. J. Nanomedicine* 7, 1163–1173. doi:10.2147/IJN.S27860

Li, Z., Guo, Z., Chu, D., Feng, H., Zhang, J., Zhu, L., et al. (2020). Effectively Suppressed Angiogenesis-Mediated Retinoblastoma Growth Using Celastrol Nanomicelles. *Drug Deliv.* 27 (1), 358–366. doi:10.1080/10717544.2020.1730522

Li, Z., Li, J., Zhu, L., Zhang, Y., Zhang, J., Yao, L., et al. (2016). Celastrol Nanomicelles Attenuate Cytokine Secretion in Macrophages and Inhibit Macrophage-Induced Corneal Neovascularization in Rats. *Ijn* 11, 6135–6148. doi:10.2147/ijn.S117425

Lin, M.-W., Lin, C. C., Chen, Y.-H., Yang, H.-B., and Hung, S.-Y. (2019). Celastrol Inhibits Dopaminergic Neuronal Death of Parkinson's Disease through Activating Mitophagy. *Antioxidants* 9 (1), 37. doi:10.3390/antiox9010037

Liu, C., Zhang, C., Wang, W., Yuan, F., He, T., Chen, Y., et al. (2019). Integrated Metabolomics and Network Toxicology to Reveal Molecular Mechanism of Celastrol Induced Cardiotoxicity. *Toxicol. Appl. Pharmacol.* 383, 114785. doi:10.1016/j.taap.2019.114785

Liu, J., Lee, J., Salazar Hernandez, M. A., Mazitschek, R., and Ozcan, U. (2015). Treatment of Obesity with Celastrol. *Cell* 161 (5), 999–1011. doi:10.1016/j.cell.2015.05.011

Liu, P., Wang, M., Tang, W., Li, G., and Gong, N. (2020). Circ_SATB2 Attenuates the Anti-tumor Role of Celastrol in Non-small-cell Lung Carcinoma through Targeting miR-33a-5p/E2F7 Axis. *Ott* 13, 11899–11912. doi:10.2147/ott.S279434

Liu, Q., Chen, F., Hou, L., Shen, L., Zhang, X., Wang, D., et al. (2018). Nanocarrier-Mediated Chemo-Immunotherapy Arrested Cancer Progression and Induced Tumor Dormancy in Desmoplastic Melanoma. *ACS Nano* 12 (8), 7812–7825. doi:10.1021/acsnano.8b01890

Lu, Y., Liu, Y., Zhou, J., Li, D., and Gao, W. (2021). Biosynthesis, Total Synthesis, Structural Modifications, Bioactivity, and Mechanism of Action of the Quinone-methide Triterpenoid Celastrol. *Med. Res. Rev.* 41, 1022–1060. doi:10.1002/med.21751

Ma, X., Xu, L., Alberobello, A. T., Gavrilova, O., Bagattin, A., Skarulis, M., et al. (2015). Celastrol Protects against Obesity and Metabolic Dysfunction through Activation of a HSF1-Pgc1α Transcriptional Axis. *Cel. Metab.* 22 (4), 695–708. doi:10.1016/j.cmet.2015.08.005

Maysinger, D., Moquin, A., Choi, J., Kodiha, M., and Stochaj, U. (2018). Gold Nanourchins and Celastrol Reorganize the Nucleo- and Cytoskeleton of Glioblastoma Cells. *Nanoscale* 10 (4), 1716–1726. doi:10.1039/C7NR07833A

Metselaar, D. S., Meel, M. H., Benedict, B., Waranecki, P., Koster, J., Kaspers, G. J. L., et al. (2019). Celastrol-induced Degradation of FANCD2 Sensitizes Pediatric High-Grade Gliomas to the DNA-Crosslinking Agent Carboplatin. *EBioMedicine* 50, 81–92. doi:10.1016/j.ebiom.2019.10.062

Mou, H., Zheng, Y., Zhao, P., Bao, H., Fang, W., and Xu, N. (2011). Celastrol Induces Apoptosis in Non-small-cell Lung Cancer A549 Cells through Activation of Mitochondria- and Fas/FasL-Mediated Pathways. *Toxicol. Vitro* 25 (5), 1027–1032. doi:10.1016/j.tiv.2011.03.023

Niemelä, E., Desai, D., Nkizinkiko, Y., Eriksson, J. E., and Rosenholm, J. M. (2015). Sugar-decorated Mesoporous Silica Nanoparticles as Delivery Vehicles for the Poorly Soluble Drug Celastrol Enables Targeted Induction of Apoptosis in Cancer Cells. *Eur. J. Pharmaceutics Biopharmaceutics* 96, 11–21. doi:10.1016/j.ejpb.2015.07.009

Niu, W., Wang, J., Wang, Q., and Shen, J. (2020). Celastrol Loaded Nanoparticles with ROS-Response and ROS-Inducer for the Treatment of Ovarian Cancer. *Front. Chem.* 8, 8. doi:10.3389/fchem.2020.574614

Onyeabor, F., Paik, A., Kovvasu, S., Ding, B., Lin, J., Wahid, M. A., et al. (2019). Optimization of Preparation and Preclinical Pharmacokinetics of Celastrol-Encapsulated Silk Fibroin Nanoparticles in the Rat. *Molecules* 24 (18), 3271. doi:10.3390/molecules24183271

Paradise, J. (2019). Regulating Nanomedicine at the Food and Drug Administration. *AMA J. Ethics* 21 (4), E347–E355. doi:10.1001/amajethics.2019.347

Paris, D., Ganey, N. J., Laporte, V., Patel, N. S., Beaulieu-Abdelahad, D., Bachmeier, C., et al. (2010). Reduction of β-amyloid Pathology by Celastrol in a Transgenic Mouse Model of Alzheimer's Disease. *J. Neuroinflammation* 7, 17. doi:10.1186/1742-2094-7-17

Pinna, G. F., Fiorucci, M., Reimund, J.-M., Taquet, N., Arondel, Y., and Muller, C. D. Celastrol Inhibits Pro-inflammatory Cytokine Secretion in Crohn's Disease Biopsies. *Biochem. Biophysical Res. Commun.* (2004) 322(3):778–786. doi: doi:10.1016/j.bbrc.2004.07.186

Qi, X., Qin, J., Ma, N., Chou, X., and Wu, Z. (2014). Solid Self-Microemulsifying Dispersible Tablets of Celastrol: Formulation Development, Charaterization and Bioavailability Evaluation. *Int. J. Pharmaceutics* 472 (1-2), 40–47. doi:10.1016/j.ijpharm.2014.06.019

Qi, Y., Wang, R., Zhao, L., Lv, L., Zhou, F., Zhang, T., et al. (2018). Celastrol Suppresses Tryptophan Catabolism in Human Colon Cancer Cells as Revealed by Metabolic Profiling and Targeted Metabolite Analysis. *Biol. Pharm. Bull.* 41 (8), 1243–1250. doi:10.1248/bpb.b18-00171

Qiu, N., Liu, Y., Liu, Q., Chen, Y., Shen, L., Hu, M., et al. (2021). Celastrol Nanoemulsion Induces Immunogenicity and Downregulates PD-L1 to Boost Abscopal Effect in Melanoma Therapy. *Biomaterials* 269, 120604. doi:10.1016/j.biomaterials.2020.120604

Salminen, A., Lehtonen, M., Paimela, T., and Kaarniranta, K. (2010). Celastrol: Molecular Targets of Thunder God Vine. *Biochem. biophysical Res. Commun.* 394 (3), 439–442. doi:10.1016/j.bbrc.2010.03.050

Sanna, V., Chamcheu, J. C., Pala, N., Mukhtar, H., Sechi, M., and Siddiqui, I. A. (2015). Nanoencapsulation of Natural Triterpenoid Celastrol for Prostate Cancer Treatment. *Ijn* 10, 6835–6846. doi:10.2147/IJN.S93752

Shaker, M. E., Ashamallah, S. A., and Houssen, M. E. (2014). Celastrol Ameliorates Murine Colitis via Modulating Oxidative Stress, Inflammatory Cytokines and Intestinal Homeostasis. *Chemico-Biological Interactions* 210, 26–33. doi:10.1016/j.cbi.2013.12.007

Shi, J., Li, J., Xu, Z., Chen, L., Luo, R., Zhang, C., et al. (2020). Celastrol: A Review of Useful Strategies Overcoming its Limitation in Anticancer Application. *Front. Pharmacol.* 11, 11. doi:10.3389/fphar.2020.558741

Soe, Z. C., Thapa, R. K., Ou, W., Gautam, M., Nguyen, H. T., Jin, S. G., et al. (2018). Folate Receptor-Mediated Celastrol and Irinotecan Combination Delivery Using Liposomes for Effective Chemotherapy. *Colloids Surf. B: Biointerfaces* 170, 718–728. doi:10.1016/j.colsurfb.2018.07.013

Song, J., Shi, F., Zhang, Z., Zhu, F., Xue, J., Tan, X., et al. (2011). Formulation and Evaluation of Celastrol-Loaded Liposomes. *Molecules* 16 (9), 7880–7892. doi:10.3390/molecules16097880

Song, X., Zhang, Y., Dai, E., Du, H., and Wang, L. (2019). Mechanism of Action of Celastrol against Rheumatoid Arthritis: A Network Pharmacology Analysis. *Int. Immunopharmacology* 74, 105725. doi:10.1016/j.intimp.2019.105725

Sun, D., Zhou, S., and Gao, W. (2020). What Went Wrong with Anticancer Nanomedicine Design and How to Make it Right. *ACS Nano* 14 (10), 12281–12290. doi:10.1021/acsnano.9b09713

Tan, Y., Zhu, Y., Zhao, Y., Wen, L., Meng, T., Liu, X., et al. (2018). Mitochondrial Alkaline pH-Responsive Drug Release Mediated by Celastrol Loaded Glycolipid-like Micelles for Cancer Therapy. *Biomaterials* 154, 169–181. doi:10.1016/j.biomaterials.2017.07.036

Tang, M., Cao, X., Zhang, K., Li, Y., Zheng, Q-Y., Li, G-Q., et al. (2018). Celastrol Alleviates Renal Fibrosis by Upregulating Cannabinoid Receptor 2 Expression. *Cell Death Dis. [Internet]* 9 (6), 601. doi:10.1038/s41419-018-0666-y

Wang, G., Xiao, Q., Wu, Y., Wei, Y. j., Jing, Y., Cao, X. r., et al. (2019). Design and Synthesis of Novel Celastrol Derivative and its Antitumor Activity in Hepatoma Cells and Antiangiogenic Activity in Zebrafish. *J. Cel. Physiol.* 234 (9), 16431–16446. doi:10.1002/jcp.28312

Wang, S., Ma, K., Zhou, C., Wang, Y., Hu, G., Chen, L., et al. (2019). LKB1 and YAP Phosphorylation Play Important Roles in Celastrol-Induced β-catenin Degradation in Colorectal Cancer. *Ther. Adv. Med. Oncol.* 11, 175883591984373. doi:10.1177/1758835919843736

Wu, M., Chen, W., Yu, X., Ding, D., Zhang, W., Hua, H., et al. (2018). Celastrol Aggravates LPS-Induced Inflammation and Injuries of Liver and Kidney in Mice. *Am. J. Transl. Res.* 10 (7), 2078–2086.

Xie, X., Zhan, C., Wang, J., Zeng, F., and Wu, S. (2020). An Activatable Nano-Prodrug for Treating Tyrosine-Kinase-Inhibitor-Resistant Non-Small Cell Lung Cancer and for Optoacoustic and Fluorescent Imaging. *Small* 16 (38), 2003451. doi:10.1002/smll.202003451

Xu, L.-N., Zhao, N., Chen, J.-Y., Ye, P.-P., Nan, X.-W., Zhou, H.-H., et al. (2019). Celastrol Inhibits the Growth of Ovarian Cancer Cells *In Vitro* and *In Vivo*. *Front. Oncol.* 9, 2. doi:10.3389/fonc.2019.00002

Yadav, V. R., Sung, B., Prasad, S., Kannappan, R., Cho, S.-G., Liu, M., et al. (2010). Celastrol Suppresses Invasion of colon and Pancreatic Cancer Cells through the Downregulation of Expression of CXCR4 Chemokine Receptor. *J. Mol. Med.* 88 (12), 1243–1253. doi:10.1007/s00109-010-0669-3

Yan, F., Wu, Z., Li, Z., and Liu, L. (2020). Celastrol Inhibits Migration and Invasion of Triple-Negative Breast Cancer Cells by Suppressing Interleukin-6 via Downregulating Nuclear Factor-Kb (NF-Kb). *Med. Sci. Monit.* 26, e922814. doi:10.12659/MSM.922814

Yang, H., Chen, D., Cui, Q. C., Yuan, X., and Dou, Q. P. (2006). Celastrol, a Triterpene Extracted from the Chinese "Thunder of God Vine," Is a Potent Proteasome Inhibitor and Suppresses Human Prostate Cancer Growth in Nude Mice. *Cancer Res.* 66 (9), 4758–4765. doi:10.1158/0008-5472.CAN-05-4529

Yang, H., Pan, Z., Jin, W., Zhao, L., Xie, P., Chi, S., et al. (2019). Preparation, Characterization and Cytotoxic Evaluation of Inclusion Complexes between Celastrol with Polyamine-Modified β-cyclodextrins. *J. Incl. Phenom. Macrocycl. Chem.* 95 (1), 147–157. doi:10.1007/s10847-019-00933-7

Yang, Y., Cheng, S., Liang, G., Honggang, L., and Wu, H. (2018). Celastrol Inhibits Cancer Metastasis by Suppressing M2-like Polarization of Macrophages. *Biochem. Biophysical Res. Commun.* 503 (2), 414–419. doi:10.1016/j.bbrc.2018.03.224

Yao, S. S., Han, L., Tian, Z. B., Yu, Y. N., Zhang, Q., Li, X. Y., et al. (2019). Celastrol Inhibits Growth and Metastasis of Human Gastric Cancer Cell MKN45 by Down-regulating microRNA-21. *Phytotherapy Res.* 33 (6), 1706–1716. doi:10.1002/ptr.6359

Yin, J., Wang, P., Yin, Y., Hou, Y., and Song, X. (2017). Optimization on Biodistribution and Antitumor Activity of Tripterine Using Polymeric Nanoparticles through RES Saturation. *Drug Deliv.* 24 (1), 1891–1897. doi:10.1080/10717544.2017.1410260

Yuan, L., Liu, C., Chen, Y., Zhang, Z., Zhou, L., and Qu, D. (2013). Antitumor Activity of Tripterine via Cell-Penetrating Peptide-Coated Nanostructured Lipid Carriers in a Prostate Cancer Model. *Int. J. Nanomedicine* 8, 4339–4350. doi:10.2147/IJN.S51621

Zha, J., Zhang, Q., Li, M., Wang, J.-R., and Mei, X. (2018). Improving Dissolution Properties by Polymers and Surfactants: A Case Study of Celastrol. *J. Pharm. Sci.* 107 (11), 2860–2868. doi:10.1016/j.xphs.2018.07.008

Zhang, C.-j., Zhu, N., Long, J., Wu, H.-t., Wang, Y.-x., Liu, B.-y., et al. (2020). Celastrol Induces Lipophagy via the LXRα/ABCA1 Pathway in clear Cell Renal Cell Carcinoma. *Acta Pharmacol. Sin.* doi:10.1038/s41401-020-00572-6

Zhang, Q., Tian, X., and Cao, X. (2019). Transferrin-functionalised Microemulsion Co-delivery of β-elemene and Celastrol for Enhanced Anti-lung Cancer Treatment and Reduced Systemic Toxicity. *Drug Deliv. Transl. Res.* 9 (3), 667–678. doi:10.1007/s13346-019-00623-4

Zhang, X., Zhang, T., Zhou, X., Liu, H., Sun, H., Ma, Z., et al. (2014). Enhancement of Oral Bioavailability of Tripterine through Lipid Nanospheres: Preparation, Characterization, and Absorption Evaluation. *J. Pharm. Sci.* 103 (6), 1711–1719. doi:10.1002/jps.23967

Zhao, H., Chen, M., Zhao, Z., Zhu, L., and Yuan, S. (2020). A Multicomponent-Based Microemulsion for Boosting Ovarian Cancer Therapy through Dual Modification with Transferrin and SA-R6h4. *Drug Deliv. Transl. Res.* doi:10.1007/s13346-020-00859-5

Zhao, J., Luo, D., Zhang, Z., Fan, N., Wang, Y., Nie, H., et al. (2019). Celastrol-loaded PEG-PCL Nanomicelles Ameliorate Inflammation, Lipid Accumulation, Insulin Resistance and Gastrointestinal Injury in Diet-Induced Obese Mice. *J. Controlled Release* 310, 188–197. doi:10.1016/j.jconrel.2019.08.026

Zhao, Q., Tang, P., Zhang, T., Huang, J.-F., Xiao, X.-R., Zhu, W.-F., et al. (2020). Celastrol Ameliorates Acute Liver Injury through Modulation of PPARα. *Biochem. Pharmacol.* 178, 114058. doi:10.1016/j.bcp.2020.114058

Zhao, Y., Tan, Y., Meng, T., Liu, X., Zhu, Y., Hong, Y., et al. (2018). Simultaneous Targeting Therapy for Lung Metastasis and Breast Tumor by Blocking the NF-Kb Signaling Pathway Using Celastrol-Loaded Micelles. *Drug Deliv.* 25 (1), 341–352. doi:10.1080/10717544.2018.1425778

Zhou, L., Chen, Y., Zhang, Z., He, J., Du, M., and Wu, Q. (2012). Preparation of Tripterine Nanostructured Lipid Carriers and Their Absorption in Rat Intestine. *Pharmazie* 67 (4), 304–310.

Zhou, L.-L., Lin, Z.-X., Fung, K.-P., Cheng, C. H. K., Che, C.-T., Zhao, M., et al. (2011). Celastrol-induced Apoptosis in Human HaCaT Keratinocytes Involves the Inhibition of NF-Kb Activity. *Eur. J. Pharmacol.* 670 (2-3), 399–408. doi:10.1016/j.ejphar.2011.09.014

Zhou, X., Yu, R., Cao, X., Zhang, Z.-R., and Deng, L. (2019). Bio-Mimicking Nanoparticles for Targeted Therapy of Malignant Melanoma. *J. Biomed. Nanotechnol.* 15 (5), 993–1004. doi:10.1166/jbn.2019.2739

Zhou, Y., Li, W., Wang, M., Zhang, X., Zhang, H., Tong, X., et al. (2017). Competitive Profiling of Celastrol Targets in Human Cervical Cancer HeLa Cells via Quantitative Chemical Proteomics. *Mol. Biosyst.* 13 (1), 83–91. doi:10.1039/C6MB00691D

Zhu, S., Luo, C., Feng, W., Li, Y., Zhu, M., Sun, S., et al. (2020). Selenium-deposited Tripterine Phytosomes Ameliorate the Antiarthritic Efficacy of the Phytomedicine via a Synergistic Sensitization. *Int. J. Pharmaceutics* 578, 119104. doi:10.1016/j.ijpharm.2020.119104

Conflict of Interest: The authors declare that the research was conducted in the absence of any commercial or financial relationships that could be construed as a potential conflict of interest.

frontiers in Pharmacology

ORIGINAL RESEARCH
published: 01 July 2021
doi: 10.3389/fphar.2021.694562

Oxyresveratrol Modulates Genes Associated with Apoptosis, Cell Cycle Control and DNA Repair in MCF-7 Cells

Sarayut Radapong[1,2]*, *Kelvin Chan*[2], *Satyajit D. Sarker*[2] *and Kenneth J. Ritchie*[2]*

[1]*Toxicology Laboratory, Medicinal Plant Research Institute, Department of Medical Sciences, Ministry of Public Health, Nonthaburi, Thailand,* [2]*Centre for Natural Products Discovery, School of Pharmacy and Biomolecular Sciences, Liverpool John Moores University, Liverpool, United Kingdom*

Oxyresveratrol (OXY) is a small molecule phytochemical which has been reported to have important biological function. The aim of this study was to elucidate the gene expression and biological pathways altered in MCF-7, breast cancer cells following exposure to OXY. The cytotoxicity to different cancer cell lines was screened using MTT assay and then whole gene expression was elucidated using microarray. The pathways selected were also validated by quantitative PCR analysis, fluorometric and western blot assay. A total of 686 genes were found to have altered mRNA expression levels of two-fold or more in the 50 μM OXY-treated group, while 2,338 genes were differentially expressed in the 100 μM-treated group. The relevant visualized global expression patterns of genes and pathways were generated. Apoptosis was activated through mitochondria-lost membrane potential, caspase-3 expression and chromatin condensation without DNA damage. G0/G1 and S phases of the cell cycle control were inhibited dose-dependently by the compound. Rad51 gene (DNA repair pathway) was significantly down-regulated ($p < 0.0001$). These results indicate that OXY moderates key genes and pathways in MCF-7 cells and that it could be developed as a chemotherapy or chemo-sensitizing agent.

Keywords: oxyresveratrol, artocarpus lakoocha, anticancer, gene expression, microarray

OPEN ACCESS

Edited by:
Jamal Arif,
Shaqra University, Saudi Arabia

Reviewed by:
Kavindra Kumar Kesari,
Aalto University, Finland
Mohd Saeed,
University of Hail, Saudi Arabia
Yin Sim Tor,
Taylor's University, Malaysia
Melva Louisa,
University of Indonesia, Indonesia

***Correspondence:**
Sarayut Radapong
Sarayutradapong@gmail.com
Kenneth J. Ritchie
k.j.ritchie@ljmu.ac.uk

Specialty section:
This article was submitted to Pharmacology of Anti-Cancer Drugs, a section of the journal Frontiers in Pharmacology

Received: *13 April 2021*
Accepted: *22 June 2021*
Published: *01 July 2021*

Citation:
Radapong S, Chan K, Sarker SD and Ritchie KJ (2021) Oxyresveratrol Modulates Genes Associated with Apoptosis, Cell Cycle Control and DNA Repair in MCF-7 Cells. Front. Pharmacol. 12:694562. doi: 10.3389/fphar.2021.694562

INTRODUCTION

Oxyresveratrol (OXY) ($C_{14}H_{12}O_4$, M.W. 244.24 g/mol) is a naturally occurring polyphenol found to be particularly concentrated in the heartwood of *Artocarpus lakoocha* Wall. ex Roxb (family: Moraceae), an indigenous plant in Thailand (Radapong et al., 2020). The compound is in the group of small molecule hydroxystilbenoids such as resveratrol, pterostilbene, gnetol and piceatannol, which have been reported to possess various potent bioactivities such as cardioprotection, neuroprotection, anti-diabetic properties, depigmentation, anti-inflammation, cancer prevention and treatment (Akinwumi et al., 2018). However, several biological activities are unique to OXY (antivirus and antihelminthics) (Galindo et al., 2011; Preyavichyapugdee et al., 2016). In consideration of its chemical structure shown in **Figure 1**, which is similar to the well-known antioxidant, resveratrol, it was hypothesized that it may also share similar anticancer properties to resveratrol. Previously Chatsumpun et al. (2016) reported that OXY exhibited cytotoxicity to breast, cervical and lung cancer cell lines. However, the precise mechanism involved in the modulation of carcinogenesis remains to be elucidated.

The cancer hallmarks which identify cancer targets have been illustrated by Hanahan and Weinberg (2011). The hallmarks involve defects in the regulation of cell proliferation and

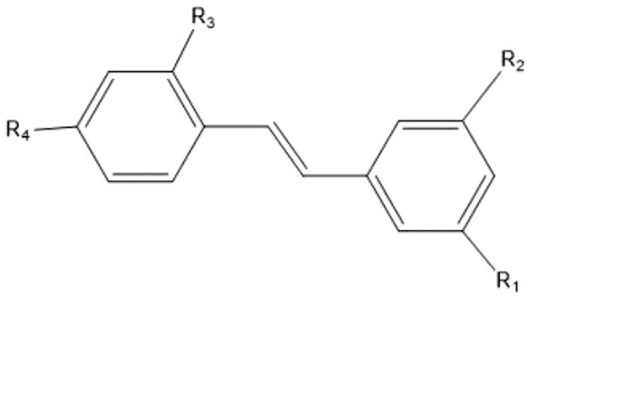

	R_1	R_2	R_3	R_4
Oxyresveratrol	OH	OH	OH	OH
Resveratrol	OH	OH	H	OH

FIGURE 1 | Chemical structure of OXY and resveratrol.

homeostasis, which include evading apoptosis, self–sufficiency in growth signals, evading growth suppressor, tissue invasion and metastasis, promoting inflammatory, autophagy, inducing angiogenesis and genomic instability. The potential molecular targets of an anticancer compound are illustrated in **Figure 2**. Pro-apoptotics and apoptosis inducers that target the apoptosis pathway are an effective way to treat to all types of cancer (Pfeffer and Singh, 2018). OXY has been reported to induce the intrinsic pathway of apoptosis in neuroblastoma cells (Rahman et al., 2017). Rahman et al. (2017) have provided supporting evidence of the apoptotic cell morphology changing and that OXY–treated cells shrank and became rounded with membrane blebbing and apoptotic vacuoles. The molecular targets of this pathway included BAX and BCL–2 proteins, which triggered the cascade proteins through mitochondrial apoptosis. Several phytochemicals inhibit cancer cell proliferation by modulating the genes that control several aspects of the cell cycle. Cyclin–dependent kinases (CDKs) and E3 ubiquitin ligases mainly play a crucial role throughout the process (Duronio and Xiong, 2013). Resveratrol is found to cause growth inhibition of human epidermoid carcinoma (A431) cells via cell cycle arrest. Treatment with resveratrol (1–50 μM for 24 h) causes an induction of WAF1/p21 that inhibits cyclin D1/D2–CDK6, cyclin D1/D2– CDK4, and cyclin E–CDK2 complexes, thereby imposing an artificial checkpoint at the G1→S transition of the cell cycle (Ahmad et al., 2001). OXY suppressed cell migration of Jurkat T cells in response to stromal cell-derived factor 1 (SDF–1). The mechanistic study indicated that OXY diminished CXCR4 –mediated T–cell migration via inhibition of the MEK/ERK signalling cascade (Chen et al., 2013). OXY has been reported to exhibit autophagy independently from apoptosis in neuroblastoma cells. The molecular targets were mostly *via* inhibition of PI3K/AKT/mTOR/pS6 signalling and activation of p38 MAPK pathway (Rahman et al., 2017). OXY also showed anti-inflammatory properties in murine macrophage cell line RAW 264.7 by inhibiting the nitric oxide synthase (iNOS) and cyclooxygenase-2 (COX-2) expression through down-regulation of NF-kB binding activity (Chung et al., 2003). Poly (ADP–ribose) polymerases (PARPs) are enzymes involved in DNA–damage repair. Recently, inhibition of PARP has emerged as a promising strategy for targeting cancers with defective DNA–damage repair, (Livraghi and Garber, 2015). The original concept of the activity of PARP inhibitors was that they acted through synthetic lethality by targeting the base excision repair pathway (BER) in BRCA–deficient tumours. Therefore, disruption of the two pathways led to cell death (Iglehart and Silver, 2009). Resveratrol has been reported to show cleavage induction of PARP1 (Demoulin et al., 2015). The compound also reduced the

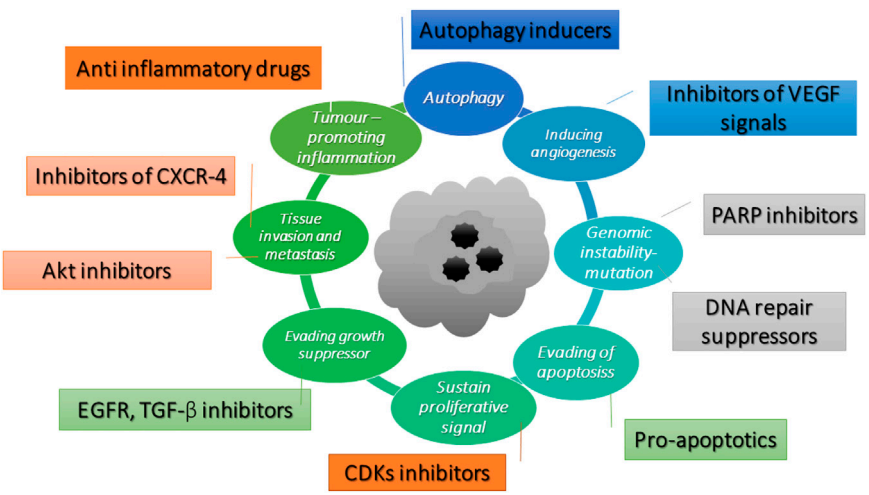

FIGURE 2 | Potential molecular targets of anti-cancer compounds adapted from Hanahan and Weinberg (2011).

expression of genes in homologous recombination (HR) of the DNA damage repair pathway including RAD recombinase 51 (RAD 51) in MCF-7 cells, enhancing the antiproliferative effect of cisplatin (Leon-Galicia et al., 2018). RAD51 is an important part of the mechanism and has been observed that the gene was overexpressed in chemoresistant cancers ((Slupianek et al., 2001; Hannay et al., 2007). Therefore, elucidation the of the mechanism of action of OXY using a high throughput tool such as microarray assay would allow greater understanding of how cells respond to OXY.

This study aims to investigate the biological response to OXY in MCF-7 cells focusing on cytotoxic and anti-cancer effects by elucidating key genes and biological pathways involved.

MATERIALS AND METHODS

Cell Lines and Reagents

Human caucasian lung carcinoma cells (A–549), human colorectal cancer cells (CACO–2), human caucasian hepatocyte carcinoma cells (HepG2), human breast cancer cells (MCF-7), Caucasian prostate adenocarcinoma cells (PC–3), Mouse macrophage cells (RAW 264.7) and the two non-transformed cell lines including Human foetal lung cells (MRC–5) and normal human breast cells (MCF10A) were from the European collection of authenticated cell cultures (ECACC) (Salisbury, United Kingdom). A–549, CACO–2, HepG2, MCF-7, and MRC–5 cells were maintained in Eagle's minimum essential medium (EMEM); RAW 264.7 cells were cultured in Dulbecco's modified eagle's medium (DMEM); PC–3 were in RPMI 1640 medium from Thermo Fisher Scientific (New York, NY, United States) supplemented with 10% fetal bovine serum in a 5% CO_2 incubator at 37°C, while MCF10A cells were maintained in DMEM/F12 medium supplemented with 5% horse serum, 20 ng/ml epidermal growth factor, 0.5 mg/ml hydrocortisone, 100 ng/ml cholera toxin, 10 μg/ml insulin and 1x pen/strep. OXY (>97%) was obtained from Sigma-Aldrich (Buchs, Switzerland). The stock solution was freshly prepared by dissolving in dimethyl sulfoxide (DMSO) and diluted in the culture medium.

MTT Proliferation Assay

The cells were plated at a density of 7×10^3 cells per well in a 96-well plate to determine the cytotoxic effect of OXY. Cells were incubated for 24 h and then treated with 1.56–200 μM OXY for 48 h. After incubation, 0.5 mg/ml MTT [3-(4,5-Dimethylthiazol-2-yl)-2,5-Diphenyltetrazolium Bromide] was added to each well and incubated for 4 h followed by 200 μL DMSO. Absorbance was measured at 570 nm using Clariostar microplate reader (MBG Labtech GmBH, Ortenberg, Germany). The data were normalized to the untreated (control) cells at 100% viability. The 50% inhibitory concentration (IC_{50}) was calculated using non-linear regression (curve fit) analysis, GraphPad software and Doxorubicin was used as a standard drug.

Gene Expression Profiling

MCF-7 cells were seeded at 2.5×10^5 cells/well in 6-well plates for 24 h, then they were treated with OXY at the concentrations of 0, 50, and 100 μM for 24 h. Total RNA of each sample was extracted using the RNeasy Mini Kit (Qiagen, Hilden, Germany) pre-treated with on-column DNA digestion with an RNase-free DNase kit (Qiagen, Hilden, Germany). According to the manufacturer's protocol, RNA was re-suspended in 30 μL of nuclease-free water and stored at −80°C until further analysis. The amount and quality of the RNA samples were analyzed by NanoDrop 2000 (Thermo Fisher Scientific, New York, NY, United States). The samples were run on an Agilent RNA 6,000 Pico chip to assess RNA integrity using the 2,100 Expert Software RNA 6,000 Pico kit through 2,100 Bioanalyzer instrument, which was proceeded by the 2,100 Expert Software (Agilent Technologies, Palo Alto, CA, United States).

Total RNA was processed using GeneChipTM WT PLUS Reagents (Thermo Fisher Scientific, Palo Alto, CA, United States) containing WT amplification kit module1, WT amplification kit module2, Poly-A RNA Control Kit, WT Terminal Labeling Kit and Hybridization Control Kit. The samples were hybridized in biological triplicate to the Human Clariom S arrays (a 400 format array) (Affymetrix Inc., Santa Clara, CA, United States), following the manufacturer's recommendations.

Briefly, 100 ng of the pooled RNA was converted into the first-strand cDNA. Second-strand cDNA synthesis was followed by an *in-vitro* transcription to generate cRNA. The cRNA products were used as templates for the second cycle of cDNA synthesis, where deoxyuridine triphosphates were incorporated into the new strand. The cDNA was then fragmented using a uracil-DNA glycosylase and apurinic/apirymidinic endonuclease. The fragments (50–70 mers) were then labelled by means of a biotin-labelled deoxynucleotide terminal addition reaction. The labelled cDNA product was heated to 99°C and hybridized to each array for 16 h at 45°C. Samples were washed with stain cocktail and the array-holding buffer on the GeneChipTM Fluidics Station 450 (Thermo Fisher Scientific, Palo Alto, CA, United States).

A GeneChip 3000G scanner (Affymetrix Inc.) and the Expression Console software (Affymetrix Inc.) were used to obtain fluorescent signals and quality control data of the scanned arrays. Signal intensities from each array were analyzed using Partek Genomic Suite version 6.4 (Partek, St Louis, MO, United States).

The microarray data were deposited at the NCBI GEO database (GSE151139). The Transcriptome Analysis Console (TAC) Software (Thermo Fisher Scientific, Palo Alto, CA, United States) was used for the visualization of the expression data in the biological pathways context. The data set was analyzed using this tool and a gene expression fold change > 2 or < −2. Ebayes Anova was used for statistical analysis with a p-value < 0.05.

Real-Time Reverse-Transcription Polymerase Chain Reaction

cDNA was synthesed using QuantiTect Rev. Transcription Kit (Qiagen, Valencia, CA, United States) following the manufacturer's protocol. Briefly, 2-μg template RNA was added to the reverse-transcription master mix and then the samples tubes were incubated at 42°C for 15 min. The cDNA samples were tested in triplicate with quantitative PCR using a QuantiTect SYBR Green PCR Reagents kit (Qiagen, Valencia, CA, United States). Total 2 μL of each sample was mixed with SYBR Green PCR Master Mix and 10x QuantiTect Primers (Qiagen, Valencia, CA, United States). Real-time (RT-PCR) was then performed following the manufacturer's protocol in a Rotor-Gene Q (Qiagen, Valencia, CA, United States). mRNA ratios relative to the Glyceraldehyde 3-phosphate dehydrogenase (GAPDH) housekeeping gene were calculated for the standardization of gene expression levels. A melting curve analysis was also performed to verify the specificity and identity of PCR products. Finally, the products were run on agarose gels to check the specificity of the PCR.

For selected genes, the data were analyzed using the equation described by Livak and Schmittgen (Livak and Schmittgen, 2001) as follows: the amount of target = $2^{-\Delta\Delta Ct}$. The average Δ_{Ct} from OXY untreated MCF-7 cells as a calibrator for each gene tested. Data were presented as mean ± SD.

Quantification of Apoptotic Cells

Apoptosis was detected with the PE Annexin V apoptosis detection kit I (BD Biosciences Inc, San Jose, CA, United States). MCF-7 cells were seeded in 6–well plates and then treated with OXY at different concentrations of 0, 25, 50 and 100 μM for 0, 3, 6, and 24 h. The cells were trypsinized and washed twice with ice–cold phosphate-buffered saline (PBS), and then cells were re–suspended at a concentration of 1×10^6/ml cells in binding buffer. A total of 100 μL of the cell suspension was transferred into a 2 ml micro centrifuge tube to which 5 μL PE annexin V and 5 μL 7–amino–actinomycin D (a vital nucleic acid dye) were added. The cells were gently mixed and incubated in the dark for 15 min at room temperature. Finally, a 400 μL of binding buffer was then added to each tube and the apoptotic cells were quantified using the flow cytometer (BD Biosciences, San Jose, CA) within 1 h. Cells that stained positive for PE annexin V and negative for 7–amino–actinomycin D were undergoing apoptosis; cells that stain positive for both PE annexin V and 7–amino–actinomycin D were either in the end stage of apoptosis, undergoing necrosis, or were already dead; and cells that stain negative for both PE annexin V and 7–amino–actinomycin D were alive and not undergoing measurable apoptosis.

Determination of Caspase–3 Expression Induced by Oxyresveratrol

Active caspase–3 staining protocol was performed following manufacturer's instructions (PE active caspase–3 apoptosis kit, BD biosciences, San diego, CA, United States). Total 5×10^5 cells of MCF-7 treated with different concentrations of OXY were harvested and transferred into 15 ml centrifuge tubes and then the suspension was centrifuged at 300 × g for 5 min at 4°C. Cells were washed twice with 1 ml ice–cold PBS and then re–suspended in 0.50 ml BD Cytofix/Cytoperm™ solution. The cells were incubated on ice for 20 min. After that the buffer was removed, the cells were washed twice with 0.50 ml BD Perm/Wash™ buffer at room temperature. Then, the cells were re–suspended with 100 μL BD Perm/Wash™ buffer plus antibody and incubated for 30 min at room temperature. Finally, the cells were washed with 1 ml washing buffer and re–suspended in 0.50 ml washing buffer. The cells were maintained at 4°C until analysed by flow cytometer.

Mitochondrial Membrane Potential (ΔΨm) Analysis by JC–1 Fluorescence

Cellular mitochondrial dysfunction can be reflected by the loss of the mitochondrial membrane potential, which can be indirectly measured by the fluorescent probe JC–1 using BD™ MitoScreen Kit (BD Biosciences, Sandiego, CA, United States). The protocol was followed according to the manufacturer's instruction. Briefly, MCF-7 cells treated with different concentrations of OXY were harvested and transferred into 15 ml centrifuge tubes and then the suspension was centrifuged at 300 × g for 5 min at 4°C. Then the cells were re–suspended with 0.50 ml JC–1 working solution and incubated at 37°C in a cell's incubator for 15 min. The cell pellet was washed twice with 1X assay buffer (2 and 1 ml, respectively). Finally, the cells were re–suspended with 0.50 ml 1X assay buffer, then analysed by flow cytometry.

Nuclear Morphological Detection Using Hoechst 33,342 Staining

The nuclear morphological changes of chromatin condensation and chromosome fragmentation induced by OXY were examined using hoechst 33,342 the staining was carried-out according to the manufacture's instructions. Briefly, the cells were treated with different concentrations of OXY in 6–well plates for 24 h. The 10 mg/ml Hoechst stock solution was prepared and diluted with PBS (1:2000). The medium was removed from each well and then 500 μL of the dye working solution was added. The plate was incubated in the cell incubator for 10 min. Afterwards, the cells were washed with 1 ml PBS for three times. The cells were viewed under fluorescence microscope (Olympus, Hamburg, Germany). The mode of cell death was then determined in terms of distinct morphological changes, including membrane blebbing, nuclear and cytosolic condensation and nuclear fragmentation in the treated group compared to the untreated cells which served as the control.

Measurement of DNA Damage by Comet Assay

The comet assay was performed under alkaline conditions. Cells were seeded in 6–well tissue–culture plates. They were treated with 50 and 100 μM OXY. After 24 h of exposure with OXY or

100 μM H_2O_2 for 4 h as the positive control, cells were collected by trypsinization, washed with PBS and resuspended in ice–cold PBS. 10 μL of the resuspended cells was mixed with 100 μL of low melting point agarose at 37°C and spread the suspension over the well with the pipette tip. The slides were placed at 4°C in the dark until gelling occurred and then immersed in pre–chilled lysis buffer at 4°C. After 60 min incubation, the buffer was aspirated and replaced with pre–chilled alkaline solution for 30 min at 4°C. After lysis and unwinding, the slides were placed in a horizontal electrophoresis tank filled with freshly prepared alkaline electrophoresis buffer. The electrophoresis was run for 25 min at 15 V and 300 mA. After electrophoresis, the slides were transferred to pre–chilled distilled water and immersed for 2 min, aspirated and repeated twice. The final water rinse was aspirated and replaced with cold 70% ethanol for 5 min. Thereafter, the slides were allowed to air dry and 100 μL/well of diluted Vista Green DNA dye was added to each slide for 15 min in the dark at room temperature for DNA staining. DNA migration was observed using fluorescence microscope at a magnification of 10X (Leica Microsystems CMS GmbH, Germany).

Cell Cycle Analysis Using Flow Cytometry

Cell cycle analysis was conducted by BD Cycletest™ Plus kit (BD biosciences, San Diego, CA, United States) using propidium iodide as a DNA stain to determine DNA content in the cells. The effect of OXY treatment on the cell cycle was determined by flow cytometry as described by the manufacturer's instruction. Briefly, MCF-7 cells were seeded at 2.5×10^5 cells/well in 6–well plates. MCF-7 cells were treated with OXY at the concentration of 25, 50, and 100 μM for 3, 6 and 24 h. Cells were trypsinized with 300 μL of 0.25% trypsin solution for 3 min in the cell incubator. Total 200 μL of fetal bovine serum was added and then all of the cell suspension was transferred into a 15 ml centrifuge tube. The suspension was centrifuged at 300 rcf for 5 min. The supernatant was discarded, the cell pellet was re–suspended with 1 ml buffer solution (contains sodium citrate, sucrose, and DMSO). The cells were centrifuged and re–suspended one more time and then counted using a hemacytometer for 5×10^5 cells. Cells were frozen in the freezer (–80°C) for PI staining. The cell suspensions were thawed in water bath, centrifuged at 400 g for 5 min at room temperature (20–25°C). All the supernatant was carefully decanted. A 250 μL of solution A (trypsin buffer) was added to each tube and gently mixed by tapping the tube, incubated for 10 min at room temperature. Afterwards, a 200 μL of solution B (trypsin inhibitor and RNase buffer) was added to each tube and gently mixed by tapping the tube by hand, and incubating for 10 min at room temperature. Finally, a 200 μL solution C (PI stain solution) was added to each tube and incubated for 10 min in the dark on ice or in the refrigerator (2–8 °C) until analyzed by flow cytometer. A total number of 1×10^4 cells was subjected to cell cycle analysis using the flow cytometer.

Western Blot

Cells were seeded at 2.5×10^5 cells/well on 6-well dishes and allowed to adhere overnight. Cells were then treated with OXY at the concentrations of 50 and 100 μM for 24 h and then washed twice with ice-cold PBS. The cells were then lyzed in lysis buffer (protease inhibitor cocktail) left on ice for 5 min then, transferred to centrifuge tubes, sonicated for 30 s with 50% pulse and then centrifuged at ~14,000 ×g for 15 min to pellet the cell debris. The supernatants were then collected, and protein concentrations determined by Bradford assay (Bio-Rad, Richmond CA, United States). An equal amount of protein sample (20 μg) was resolved by a volume of 2x Laemmli sample buffer, then boiled for 5 min 7.5% Mini-PROTEAN® TGX Stain-Free™ protein gels (Bio-Rad, Richmond, CA, United States) were used and run at 180 V for 1 h. Protein transfer was achieved using Trans-Blot® Turbo™ mini PVDF transfer packs (Bio-Rad, Richmond, CA, United States). Proteins were transferred onto PVDF membrane at 1.3 A for 7 min. Membranes were then blocked with 5% skim milk/TBST for 1 h and then probed with the indicated primary antibody overnight at 4°C and then blotted with appropriate horseradish peroxidase-conjugated secondary anti-rabbit antibody. Visualization was performed using an enhanced chemiluminescence kit (BioRad Inc., Hercules, CA, United States) with Clarity™ Western ECL Substrate. Protein level was normalized to the matching densitometric value of the internal control β-actin.

TABLE 1 | Inhibitory concentration (IC_{50}, μM) of OXY to the cells.

	Oxyresveratrol (μM)	Doxorubicin (μg/ml)
A–549	148.63 ± 4.48	0.54 ± 0.02
CACO–2	>200	3.27 ± 1.06
HepG2	104.47 ± 0.82	0.84 ± 0.08
MCF–7	30.64 ± 4.79	0.21 ± 0.07
PC–3	106.90 ± 8.63	3.08 ± 0.48
RAW 264.7	115.95 ± 11.28	0.21 ± 0.07
MRC–5	>200	0.37 ± 0.01
MCF10A	>200	NA

Statistical Analysis

Results of MTT assays were expressed as mean ± standard error. Significant differences in genes in WikiPathways were detected using Fisher's Exact Test. Statistical significance was assessed by One-way analysis of variance followed by Dunnett's test or the unpaired *t*-test using GraphPad Prism 9 (GraphPad Software, La Jolla, CA, United States).

RESULTS

MTT Cytotoxicity

MTT assay was used to analyze the viability of the cells treated with different concentrations of the compound for 48 h. The total DMSO concentration in the cell culture medium did not exceed 0.5% which was found not to affect the cell growth or viability of the cells. After 48 h of treatment, OXY significantly inhibited cell growth and viability in a dose-dependent manner to MCF-7, HepG2, PC–3, RAW 264.7 and A–549 cells with the IC_{50} values of 30.64 ± 4.79, 104.47 ± 0.82, 109.35 ± 9.63, 115.95 ± 11.28, and 148.63 ± 4.48 μM, respectively. Whereas,

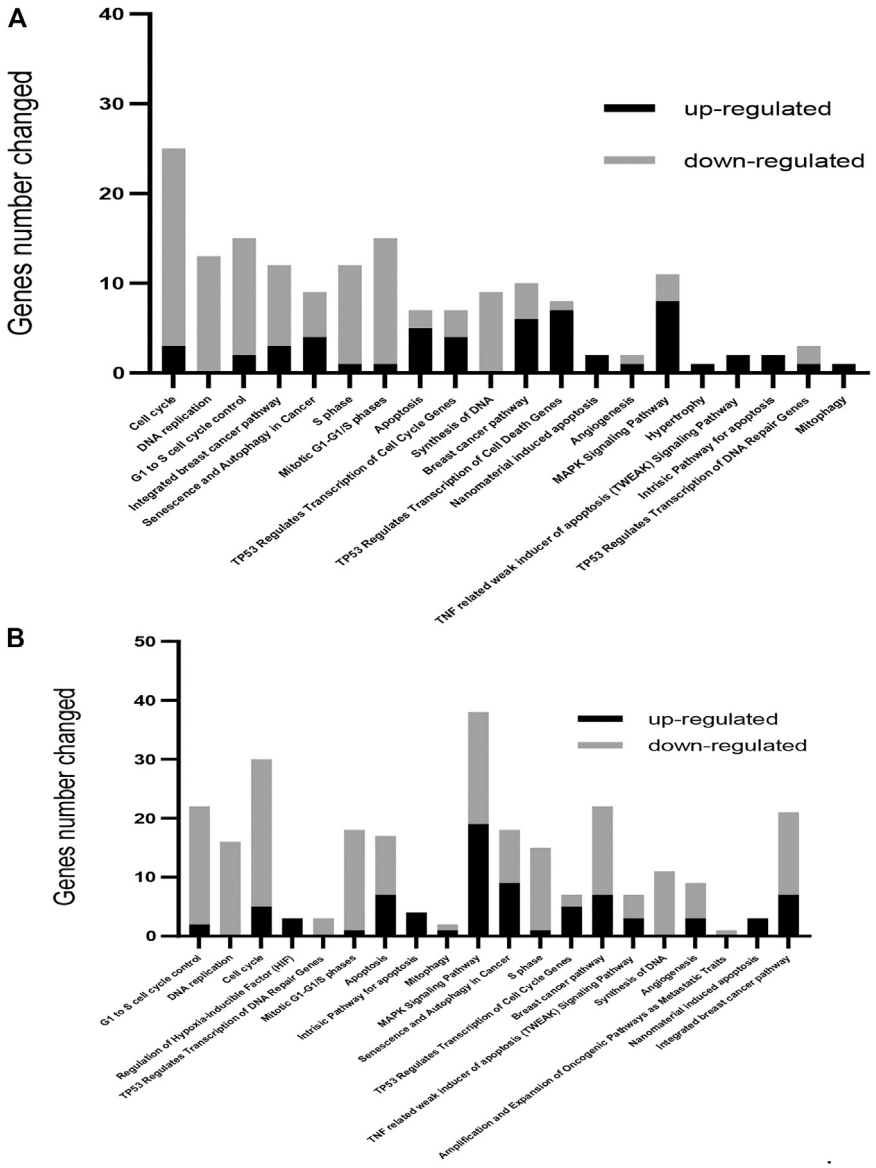

FIGURE 3 | Gene ontology-based biological process pathways altered by OXY in MCF-7 breast cancer cells. Differentially expressed genes in MCF-7 cells treated with 50 μM **(A)** or 100 μM **(B)** of OXY for 24 h. To determine the biological process and pathways involved, the list of significantly upregulated and downregulated genes was analyzed using Fisher's Exact Test, and then analyzed using WikiPathways.org.

the compound showed no toxicity to CACO–2, MCF10A and MRC–5 (IC_{50} > 200 μM). IC_{50} values of OXY and doxorubicin are shown in **Table 1**.

Effect of Oxyresveratrol on the Human Breast Cancer Cells Gene Expression Profiles

Global expression patterns of genes and pathways were obtained using microarray technology and data analysis software. Gene expression changes occurring as a consequence of the exposure of MCF-7 cells to 50 or 100 μM OXY for 24 h was performed as described in the materials and methods section. The number of differentially expressed genes under both conditions compared to the control group were observed. The cellular pathways in which these differentially expressed are found were shown in **Figure 3**.

A total of 686 genes were differentially expressed in the 50 μM-treatment group; with 262 genes being upregulated and 424 downregulated. Total 2,338 genes were differentially expressed in the 100 μM-treated groups; among these, 907 were upregulated and 1,431 were downregulated (showed in the Supplementary Materials). WikiPathways (wikipathways.org), a biology community maintained website that displays biological

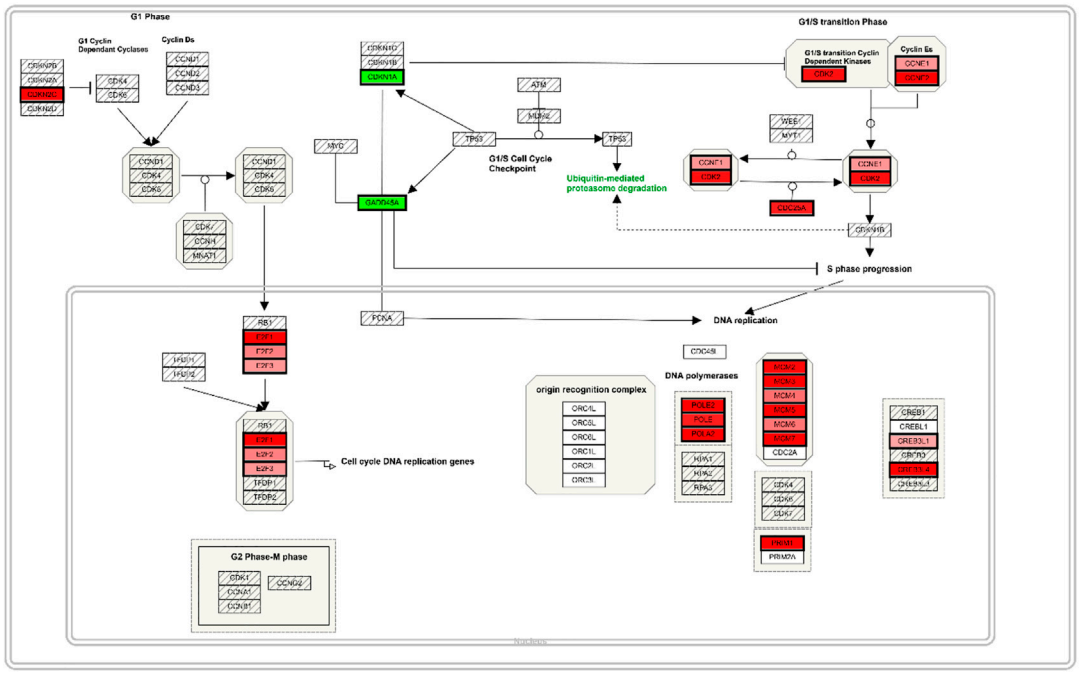

FIGURE 4 | Cell cycle control pathway integrating expression data for MCF-7 cells treated with 100μM OXY for 24 h. Genes labelled in green are up regulated and in red are down regulated.

pathways, was utilized to identify pathways and the functions of genes altered by OXY treatment in MCF-7 cells.

From this analysis, it was found that the first 20 most affected pathways (arranged from significant values in the 100 μM-OXY treatment) following OXY treatment were associated with cell cycle control, apoptosis and DNA repair, as well as the senescence and autophagy processes. It was also noted that the majority of the genes in cell cycle control and DNA repair were down regulated, while those in apoptosis and autophagy were up regulated.

Among these, the most dramatically affected pathways were that of cell cycle control. At both 50 and 100 μM OXY, the expression of DNA-damage-inducible, alpha (*GADD45A*) and cyclin-dependent kinase inhibitor 1A (*p21*, *CDKN1A*) were up regulated. Whereas, cyclin-dependent kinase 2 (*CDK2*), E2F transcription factor one (*E2F1*) were down regulated (**Figure 4**).

Validation of Differentially Expressed Genes

To validate the microarray results, the mRNA expression of selected genes involved in the regulation of cell cycle, apoptosis, DNA repair and autophagy (*CDK2*, *CDK4*, *BCL-2*, *E2F1*, *BAX*, *CDKN1A*, *GADD45A*, *CASP8*, *DIABLO*, *FAS*, *JUNB*, *MAPK8*, *TNFRSF10B*, *PARP1*, *BRCA1*, *RAD51*, *AKT1*, *ESR1*,

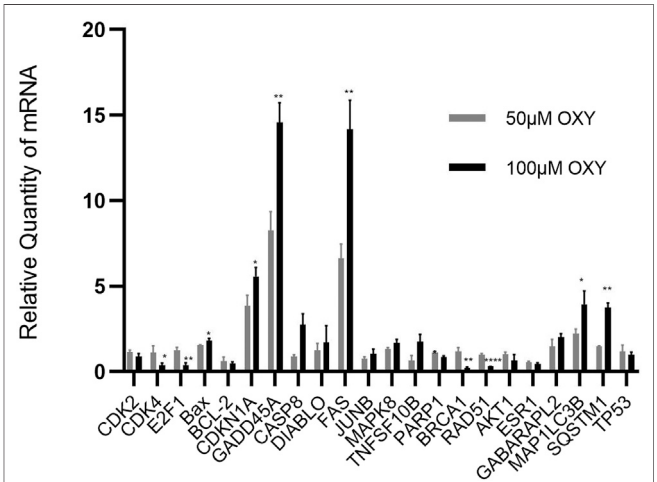

FIGURE 5 | Relative quantity of mRNA expression from MCF-7 cells treated with OXY. Validation of selected genes differentially expressed in MCF-7 cells treated for 24 h with 50 or 100 μM of OXY vs. control data set. Statistical analysis was carried out using unpaired *t* test (*$p < 0.5$, **$p < 0.05$ and ****$p < 0.0001$).

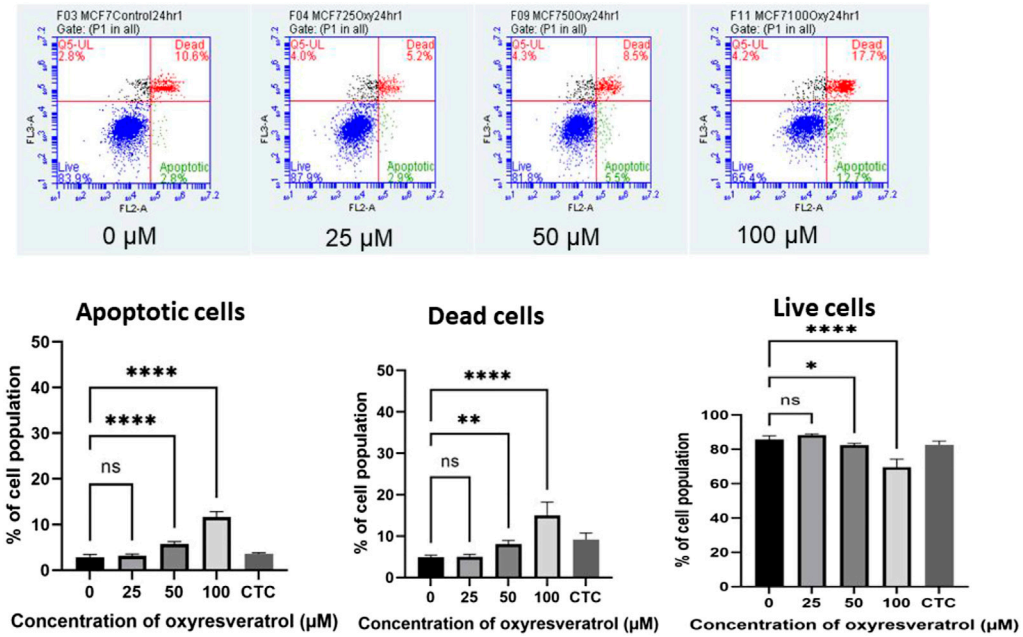

FIGURE 6 | Induction of apoptosis by OXY in MCF-7 cells determined using flow cytometry. Bar graphs showing the percentage of MCF-7 cells in apoptosis, live cells and dead cells when treated with 0, 25, 50 and 100 µM OXY for 24 h and camptothecin (CTC) for 4 h and then subject to flow cytometric analysis. Data are the mean ± SEM of three independent experiments. Statistical analysis was carried out using One-way ANOVA analysis of variance followed by Dunnett's test. The significant difference was compared relatively to control (*p = 0.037, **p = 0.003 and ****p < 0.0001).

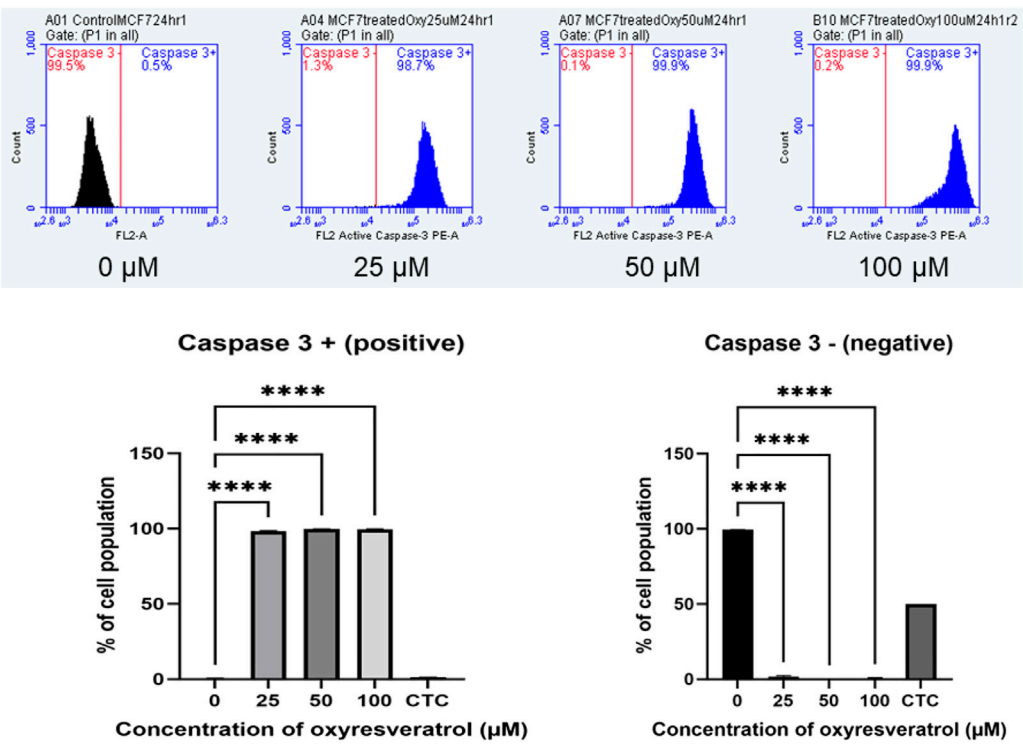

FIGURE 7 | Caspase–3 expression in MCF-7 cells following exposure to various concentrations of OXY for 24 h and camptothecin (CTC) for 4 h. The cells were stained with anti–active caspase–3 and analyzed by flow cytometry. Data are the mean ± SD of three experiments. Statistical analysis was carried out using One-way ANOVA analysis of variance followed by Dunnett's test. The significant difference was compared relatively to the control (****p < 0.0001).

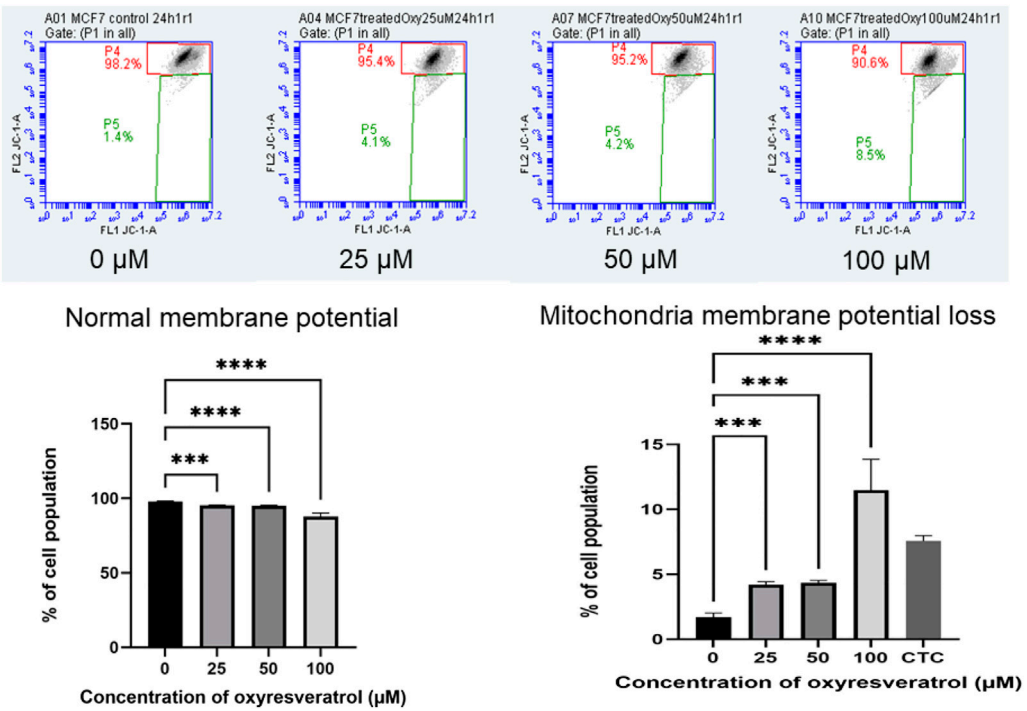

FIGURE 8 | Mitochondrial membrane potential of MCF-7 cells following exposure to various concentrations of OXY for 24 h and camptothecin (CTC) for 4 h. The cells were stained with JC–1 and analyzed by flow cytometry. Data are the mean ± SD of three experiments. Statistical analysis was carried out using One-way ANOVA analysis of variance followed by Dunnett's test. The significant difference was compared relatively to control (***$p < 0.001$ and ****$p < 0.0001$).

GABARAPL2, *MAP1LC3B*, *SQSTM*, and *TP53*) was confirmed using RT-qPCR. Triplicates were performed for each gene. In all cases, the RT-qPCR data confirmed those obtained by 50 and 100 µM-OXY treated array analyses (**Figure 5**). The genes involving cell cycle control, DNA replication, apoptosis, senescence and autophagy in cancer pathways including *CDK4*, *E2F1*, *Bax*, *CDKN1A*, *GADD45A*, *FAS*, *GABARAPL2*, and *SQSTM* were significantly upregulated. Whereas, the genes in DNA repair pathway including *PARP1*, *BRCA1*, and *RAD51* were significantly downregulated compared between the two doses treated.

Quantification of Apoptosis

Apoptosis induction by OXY in the cells was determined. The apoptotic cells expressing PS on their cell membranes were detected using Annexin V conjugated with PE. OXY induced apoptosis in MCF-7 cells dose–dependently at the concentrations tested of 25, 50 and 100 µM compared to the untreated control (0 µM) exhibiting the PE Annexin V fluorescence percentage of 3.14 ± 0.37, 5.74 ± 0.53 and 11.69 ± 1.15%, respectively. Following 24 hours of treatment; the cells treated with OXY 25 µM became apoptotic, while those treated with OXY 50 and 100 µM were significantly different from the controls. These results illustrate that most of the cells treated with 50 and 100 µM OXY within 24 h underwent apoptosis and as a consequence died (**Figure 6**).

Caspase–3 Expression

The apoptotic executioner protein, caspase 3, which made the cells cytomorphological charateristic change was also determined using anti-active caspase–3 conjugated with PE. MCF-7 cells treated with different concentrations of OXY at doses of 25, 50 and 100 µM for 24 h showed a dramatically changed amount of caspase–3 expression on cell membranes compared to the control; more than 98% of the population was caspase–3 positive in all doses treated, while the cell population of the caspase–3 negative decreased proportionally. All treatments were significantly different compared with the control (**Figure 7**).

Mitochondrial Membrane Potential (ΔΨm)

Mitochondrial dysfunction is associated with changes in ΔΨm. Mitochondrial membrane depolarization was measured by JC-1. At high ΔΨm, JC-1 the cationic lipophilic probe spontaneously formed J-aggregates with red fluorescence. On the other hand, at low ΔΨm, depolarized mitochondria, JC-1 stayed monomeric resulting in low or no fluorescence signal. As the concentration of OXY increased, the mean values of FL2 FL1–1A gating P4 decreased (normal membrane potential). These results indicate that the mitochondrial membrane was depolarized in a dose-dependent manner. MCF-7 cells lost mitochondria membrane potential dose–dependently following exposure to several concentrations of OXY, which caused the cells to undergo apoptosis. 24–h treatment was found to cause membrane potential loss to a significant degree compared to the untreated control; 4.15 ± 0.08, 4.77 ± 2.56 and 11.47 ± 2.75% for 25, 50 and 100 µM–OXY, respectively (**Figure 8**).

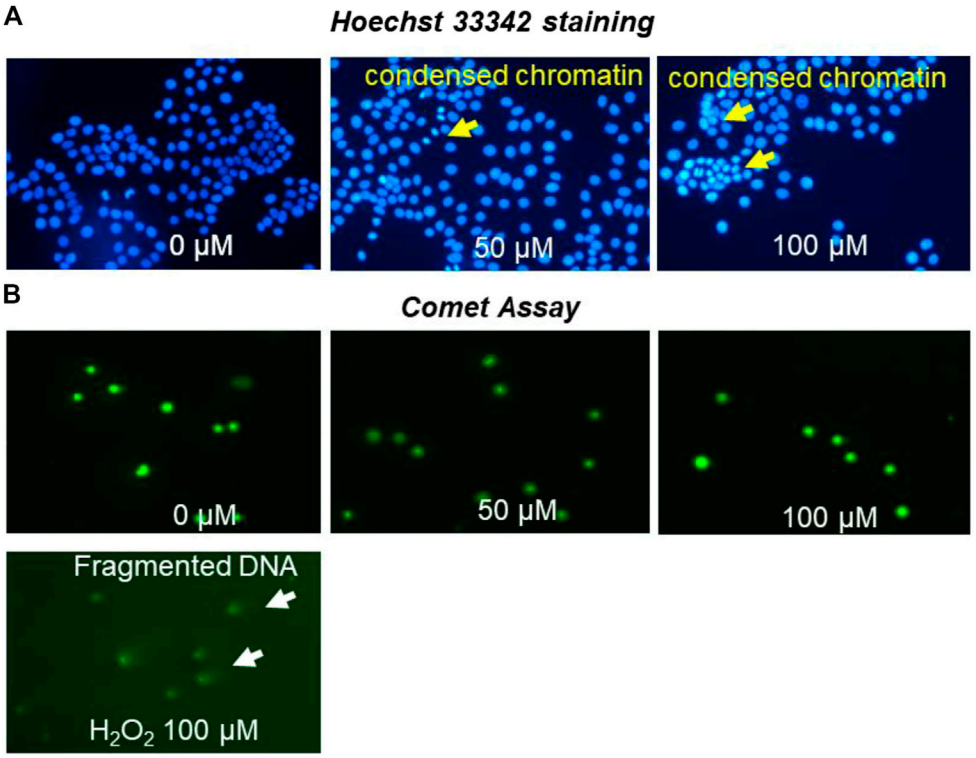

FIGURE 9 | MCF-7 nuclei staining by Hoechst 33,342 **(A)** photomicrographs of stained DNA of MCF-7 cells (alkaline comet assay) **(B)** apoptosis detection following treatment with different concentrations of OXY for 24 h and 100 μM H_2O_2 for 4 h.

Nuclear Morphological Detection

MCF-7 cells were investigated for nuclear and chromatin changes following treatment with OXY. The pictures of chromatin changed are shown in **Figure 9A**. MCF-7 cells were observed to have undergone chromatin condensation at all doses used.

DNA Damage by Comet Assay

MCF-7 cells treated with OXY were investigated for DNA damage as shown in **Figure 9B**. The cells treated with 50 and 100 μM of OXY for 24 h did not display DNA damage. OXY at the effective doses did not cause damage to DNA in MCF-7 cells.

Cell Cycle Analysis

The cell cycle arrest was also analyzed by treating the cells with different doses of OXY. The results in **Figure 10** show that the compound decreased DNA content dose-dependently in G0/G1 phase of the cell cycle at 24 h. Compared with the untreated control (0 μM), 25, 50 and 100 μM OXY decreased the percentage of the cell population from 85.43 ± 0.34 to 75.39 ± 0.75, 72.34 ± 0.82, and 62.27 ± 0.68%, respectively. S phase also significantly decreased from 19.37 ± 0.09 to 19.35 ± 0.48, 16.47 ± 0.63, and 14.66 ± 0.57%, respectively. whereas G2/M phase was induced from 3.52 ± 0.11 to 4.50 ± 0.46, 3.68 ± 0.17, and 7.40 ± 0.38%, respectively during the time incubated. These results indicate that OXY arrested G0/G1 and S phases of the cell cycle.

Western Blot Analysis

Protein bands of the expected size corresponding to RAD51, PARP1 and BRCA1 in the whole-cell extracts treated with different doses of 50 and 100 μM OXY were observed compared to untreated controls (**Figure 11**). The protein expression of RAD51 (ratio to ACTB) was significantly different relative to control (0.54 ± 0.15 to 0.33 ± 0.06, and 0.25 ± 0.02), respectively. While PARP1 and BRCA1 expression decreased slightly, but not significantly compared to the control. These proteins were also evaluated for changes in expression in MCF10A cells following treatment with OXY, but expression levels of the proteins of interest were not found to be significantly different from the controls (data not shown).

DISCUSSION

Microarray-based techniques including GeneChip™ are high-throughput technologies for genetic exploration. These technologies have been developed as a single platform which provides extensive information on gene networks and functions on drug efficacy and toxicity (Taylor et al., 2005). Over the years, this kind of platform has been extensively implemented to evaluate the effect of OXY and derivatives, especially resveratrol on several cancerous cells such as multiple myeloma and colorectal cancer cells (Geng et al., 2018; Lee et al., 2018). However, OXY, in this study is also reported to

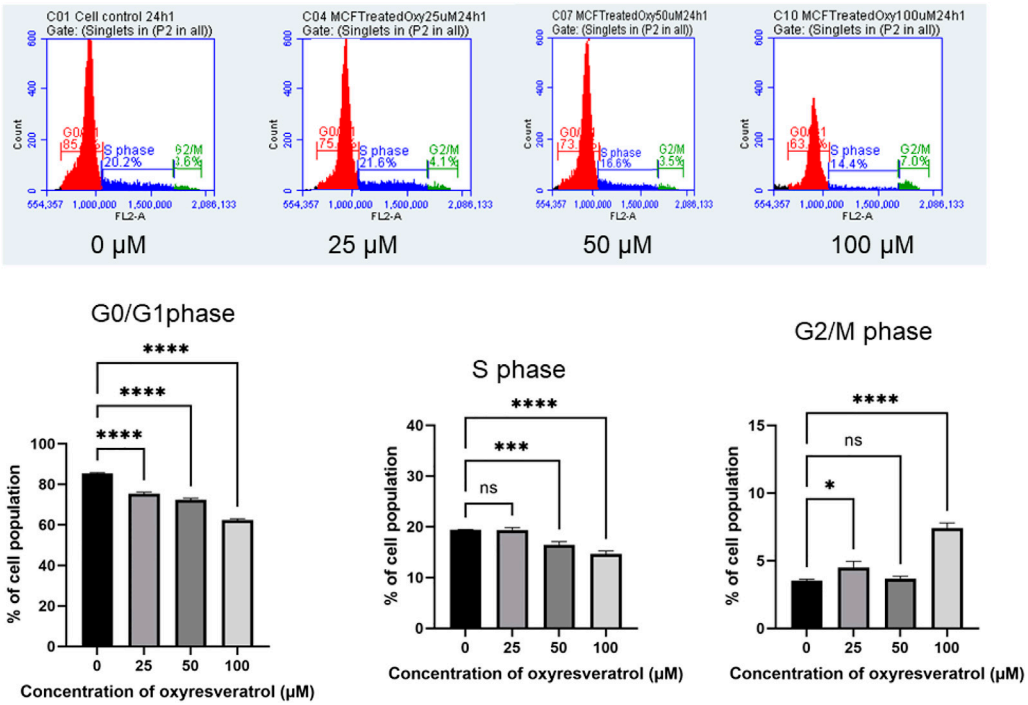

FIGURE 10 | Effect of OXY on cell cycle distribution in MCF-7 cells determined using flow cytometry. The histograms showing the numbers of cells in different phases after MCF-7 cells were treated with 25–100 μM OXY for 3–24 h and then subjected to flow cytometric analysis. Data are the mean ± SD of three experiments. Statistical analysis was carried out using One-way ANOVA analysis of variance followed by Dunnett's test. The significant difference was compared relatively to control (*p = 0.0134, ***p = 0.002 and ****p < 0.0001).

demonstrate selective toxicity towards MCF-7 cells compared to MCF10A cells and others. The exposure time between the cells and OXY was reduced to 24 h (IC_{50} for MCF-7 cells = 368.37 μM) in microarray and qPCR analysis because the experiment was designed to analyze the gene expression of the main molecular effects at the early stage (Li and Sarkar, 2002). Amongst the OXY-modulated genes observed in MCF-7 cells, the genes that were significantly changed (mostly downregulated) were involved in cell cycle control, DNA replication and DNA synthesis.

Apoptosis is a vital component of cellular processes moderating life and death of cells and therefore is of great therapeutic potential (Kruidering and Evan, 2000). Moreover, Apoptosis, which can cause damage to DNA, is the central mechanism of chemotherapeutics and most plant–derived anticancer drugs (Cragg and Pezzuto, 2016). OXY induced apoptosis through both intrinsic and extrinsic pathways. It is possible in consideration of the results reported here that OXY decreased the expression of anti-apoptotic proteins such as B-cell lymphoma 2 (BCL-2) and increased pro-apoptotic proteins like BAX and BCL-2 -antagonist/killer-1 (BAK). It is then possible that DIABLO and cytochrome c released, activated apoptotic peptidase activating factor 1 (APAF1) forming apoptosomes, which led to the loss of mitochondrial membrane potential. On the other hand, the results reported here suggest that the extrinsic apoptotic pathway may have been initiated by OXY through Fas cell surface death ligand/receptor (FASL/FASR) and tumour necrosis factor-alpha/receptor (TNF-α/TNFR1), activating CASP8, with the subsequent activation of CASP3. Notably, OXY has been previously reported to induce the intrinsic pathway of apoptosis in neuroblastoma cells (Rahman et al., 2017).

CDK2, CDK4 expression plays an important role in G1-S phase checkpoint control normally working together with cyclin E as a complex protein. This complex increases the synthesis of histone proteins and DNA replication (Caruso et al., 2018). Therefore, the G0/G1 and S phases of cell cycle were arrested. CDK2 is also inhibited by CDKN1A, which represents a major target of p53 activity. Interestingly, TP53 remained unchanged in response to the treatment, which was consistent to the previous study reported that OXY moderated p53-independent S phase arrest, ROS–independent apoptosis in neuroblastoma cells (Rahman et al., 2017). The results here illustrate that OXY induced apoptosis in the cells but did not activate TP53, which was responsible for the DNA damage. However, p53-independent upregulation of CDKN1A may be induced by some genes in cell cycle, apoptosis or senescence and autophagy in cancer pathways (Aliouat-Denis et al., 2005). Recently, CDK inhibitors have been investigated as a possible chemotherapeutic (Wood et al., 2019). OXY significantly decreased the expression of CDK4 and E2F1, which subsequently conducted cell cycle arrest.

OXY-treated MCF-7 cells induced the expression of autophagic genes including microtubule-associated protein one light chain 3 beta (*MAP1LC3B*), sequestosome 1 (*SQSTM1*) and

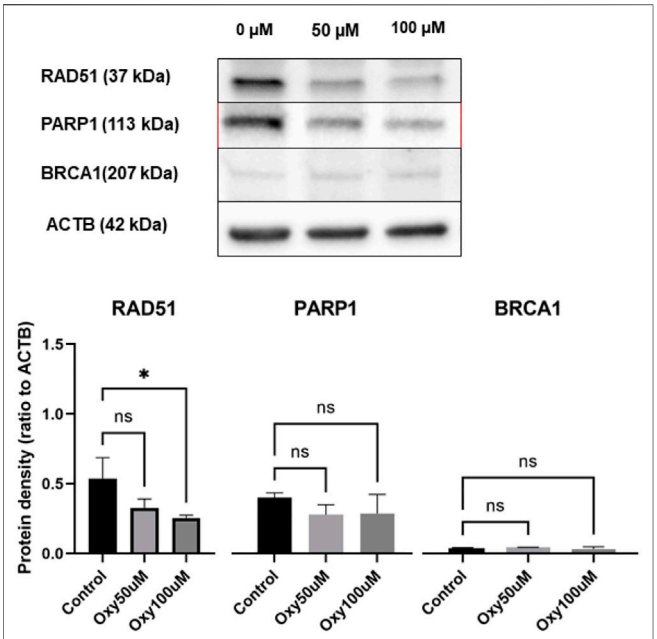

FIGURE 11 | Expression of DNA repair proteins in MCF-7 breast cancer cells treated for 24 h with 50 and 100 μM of OXY compared with untreated control. Total cell lysates were blotted and identified as described in the materials and methods section. Statistical analysis was carried out using One-way ANOVA analysis of variance followed by Dunnett's test. The significant difference was compared relatively to control (*p = 0.0191).

GABA(A) receptor-associated protein like 2 (*GABARAPL2*). Autophagy or self-eating is an evolutionarily conserved catabolic pathway in eukaryotes playing a significant role in the recycling of cellular components as part of a housekeeping function with Beclin1 and Atg5 reported to play important roles (Bilir et al., 2002). Autophagy-mediated cell death can be the starting process of apoptosis, and blocking caspase activity can cause a cell to enter autophagy cell death instead of apoptosis (Lockshin and Zakeri, 2004). OXY has been previously reported to be capable of inducing neuroblastoma cell death by autophagy *via* the PI3K/AKT/mTOR pathway (Rahman et al., 2017).

OXY dose-dependently mediated down regulation of DNA repair gene expression (PARP1, RAD51 and BRCA1) in MCF-7 cells. The significantly down-regulated expression of RAD51 by OXY may be the key mechanism by which OXY mediates its anticancer effect in consideration of RAD51 being overexpressed in a variety of cancer cells (Raderschall et al., 2002; Hannay et al., 2007; Klein, 2008). The principle of inhibiting DNA repair genes has been proposed for cells that carry mutations in the breast cancer susceptibility genes *BRCA1* or *BRCA2* as a possible cancer drug target (Farmer et al., 2005). Previously Walsh (2015) reported that a deficiency in *PARP* or *BRCA* alone had no impact on cancer cell viability, but a deficiency in both leads to a lethal effect on cancer cells. The western blot analysis presented here demonstrates that OXY inhibited the protein expression of RAD51 and slightly decreased the expression of PARP1 and BRCA1. Moreover, the inhibition of RAD51 also enhanced cytotoxicity and apoptosis induction in cancer stem cells (Ruiz et al., 2018) Oxyresveratrol's property of apoptosis activation, cell cycle arrest, cell senescence and autophagy including the implication of inhibiting RAD51 may be able to facilitate an increase in the efficacy of commonly used chemotherapeutics.

CONCLUSION

In this research report, we clearly demonstrate that OXY regulates the expression of various genes, which have important roles in carcinogenesis-associated pathways. OXY enhanced the apoptosis cascade through both extrinsic and intrinsic pathways. OXY also decreased the expression of *CDK2*, *CDK4* and *E2F1*, affecting the initial stage of the cell cycle (G1-S phase). More interestingly, the compound induced a down-regulation of genes and protein activities involved in DNA repair, including RAD51 and PARP1. These results indicate that OXY may be utilized to overcome drug resistance and enhance the efficacy of chemotherapy drugs.

DATA AVAILABILITY STATEMENT

The original contributions presented in the study are publicly available. This data can be found here: https://www.ncbi.nlm.nih.gov/, GSE151139.

AUTHOR CONTRIBUTIONS

The following statements should be used Conceptualization, SR, KC, SS, and KR; methodology, SR and KR; software, KR; validation, SR, SS and KR; formal analysis, SR; investigation, SR and KR; resources, SR, SS and KR; data curation, SR; writing—original draft preparation, SR; writing—review and editing, KC, SS and KR; visualization, SR; supervision, SS and KR; project administration, KR; funding acquisition, SS and KR.

FUNDING

This research was funded by The Royal Thai government, Thailand; in the PhD project no. R253184.

ACKNOWLEDGMENTS

The author would like to express profound gratitude to Centre for Genomic Research, University of Liverpool, United Kingdom for using the microarray platform and the excellent support from Liverpool John Moores University for the laboratory facilities. Partial gene expression data (about 10%) of MCF-7 cells treated with OXY has been shared in the poster presentation in the Phytochemical Society of Europe (PSE): Trends in Natural Product Research-PSE Young Scientists' Meeting on Biochemistry, Molecular Aspects and Pharmacology of Bioactive Natural Products, 19–22 June 2019, Budapest, Hungary.

REFERENCES

Ahmad, N., Adhami, V. M., Afaq, F., Feyes, D. K., and Mukhtar, H. (2001). Resveratrol Causes WAF-1/p21-Mediated G1-phase Arrest of Cell Cycle and Induction of Apoptosis in Human Epidermoid Carcinoma A431 Cells. *Clin. Cancer Res.* 7 (5), 1466–1473.

Akinwumi, B., Bordun, K.-A., and Anderson, H. (2018). Biological Activities of Stilbenoids. *Int. J. Mol. Sci.* 19 (3), 792. doi:10.3390/ijms19030792

Aliouat-Denis, C.-M., Dendouga, N., Van den Wyngaert, I., Goehlmann, H., Steller, U., van de Weyer, I., et al. (2005). p53-Independent Regulation of p21Waf1/Cip1 Expression and Senescence by Chk2. *Mol. Cancer Res.* 3 (11), 627–634. doi:10.1158/1541-7786.mcr-05-0121

Bilir, A., Altinoz, M. A., Erkan, M., Ozmen, V., and Aydiner, A. (2002). Autophagy and Nuclear Changes in FM3A Breast Tumor Cells after Epirubicin, Medroxyprogesterone and Tamoxifen Treatment *In Vitro*. *Pathobiology* 69 (3), 120–126. doi:10.1159/000048766

Caruso, J. A., Duong, M. T., Carey, J. P. W., Hunt, K. K., and Keyomarsi, K. (2018). Low-molecular-weight Cyclin E in Human Cancer: Cellular Consequences and Opportunities for Targeted Therapies. *Cancer Res.* 78 (19), 5481–5491. doi:10.1158/0008-5472.can-18-1235

Chatsumpun, N., Chuanasa, T., Sritularak, B., Lipipun, V., Jongbunprasert, V., Ruchirawat, S., et al. (2016). Oxyresveratrol: Structural Modification and Evaluation of Biological Activities. *Molecules* 21 (4), 489–481. doi:10.3390/molecules21040489

Chen, Y.-C., Tien, Y.-J., Chen, C.-H., Beltran, F. N., Amor, E. C., Wang, R.-J., et al. (2013). Morus alba and Active Compound Oxyresveratrol Exert Anti-inflammatory Activity via Inhibition of Leukocyte Migration Involving MEK/ERK Signaling. *BMC Complement. Altern. Med.* 13, 45. doi:10.1186/1472-6882-13-45

Chung, K. O., Kim, B. Y., Lee, M. H., Kim, Y. R., Chung, H. Y., Park, J. H., et al. (2003). *In-vitro* and *In-Vivo* Anti-inflammatory Effect of Oxyresveratrol from Morus alba L. *J. Pharm. Pharmacol.* 55 (12), 1695–1700. doi:10.1211/0022357022313

Cragg, G. M., and Pezzuto, J. M. (2016). Natural Products as a Vital Source for the Discovery of Cancer Chemotherapeutic and Chemopreventive Agents. *Med. Princ Pract.* 25 (Suppl. 2), 41–59. doi:10.1159/000443404

Demoulin, B., Hermant, M., Castrogiovanni, C., Staudt, C., and Dumont, P. (2015). Resveratrol Induces DNA Damage in colon Cancer Cells by Poisoning Topoisomerase II and Activates the ATM Kinase to Trigger P53-dependent Apoptosis. *Toxicol. Vitro* 29 (5), 1156–1165. doi:10.1016/j.tiv.2015.04.015

Duronio, R. J., and Xiong, Y. (2013). Signaling Pathways that Control Cell Proliferation. *Cold Spring Harbor Perspect. Biol.* 5 (3), a008904–a008904a008904/008912. doi:10.1101/cshperspect.a008904

Farmer, H., McCabe, N., Lord, C. J., Tutt, A. N. J., Johnson, D. A., Richardson, T. B., et al. (2005). Targeting the DNA Repair Defect in BRCA Mutant Cells as a Therapeutic Strategy. *Nature* 434 (7035), 917–921. doi:10.1038/nature03445

Galindo, I., Hernáez, B., Berná, J., Fenoll, J., Cenis, J. L., Escribano, J. M., et al. (2011). Comparative Inhibitory Activity of the Stilbenes Resveratrol and Oxyresveratrol on African Swine Fever Virus Replication. *Antiviral Res.* 91 (1), 57–63. doi:10.1016/j.antiviral.2011.04.013

Geng, W., Guo, X., Zhang, L., Ma, Y., Wang, L., Liu, Z., et al. (2018). Resveratrol Inhibits Proliferation, Migration and Invasion of Multiple Myeloma Cells via NEAT1-Mediated Wnt/β-Catenin Signaling Pathway. *Biomed. Pharmacother.* 107, 484–494. doi:10.1016/j.biopha.2018.08.003

Hanahan, D., and Weinberg, R. A. (2011). Hallmarks of Cancer: the Next Generation. *Cell* 144 (5), 646–674. doi:10.1016/j.cell.2011.02.013

Hannay, J. A. F., Liu, J., Zhu, Q.-S., Bolshakov, S. V., Li, L., Pisters, P. W. T., et al. (2007). Rad51 Overexpression Contributes to Chemoresistance in Human Soft Tissue Sarcoma Cells: a Role for P53/activator Protein 2 Transcriptional Regulation. *Mol. Cancer Ther.* 6 (5), 1650–1660. doi:10.1158/1535-7163.mct-06-0636

Iglehart, J. D., and Silver, D. P. (2009). Synthetic Lethality - a New Direction in Cancer-Drug Development. *N. Engl. J. Med.* 361 (2), 189–191. doi:10.1056/nejme0903044

Klein, H. L. (2008). The Consequences of Rad51 Overexpression for normal and Tumor Cells. *DNA Repair* 7 (5), 686–693. doi:10.1016/j.dnarep.2007.12.008

Kruidering, M., and Evan, G. I. (2000). Caspase-8 in Apoptosis: the Beginning of "the End"? *IUBMB Life* 50 (2), 85–90. doi:10.1080/15216540050212088

Lee, S. R., Jin, H., Kim, W. T., Kim, W. J., Kim, S. Z., Leem, S. H., et al. (2018). Tristetraprolin Activation by Resveratrol Inhibits the Proliferation and Metastasis of Colorectal Cancer Cells. *Int. J. Oncol.* 53 (3), 1269–1278. doi:10.3892/ijo.2018.4453

Li, Y., and Sarkar, F. H. (2002). Gene Expression Profiles of Genistein-Treated PC3 Prostate Cancer Cells. *J. Nutr.* 132 (12), 3623–3631. doi:10.1093/jn/132.12.3623

Livak, K. J., and Schmittgen, T. D. (2001). Analysis of Relative Gene Expression Data Using Real-Time Quantitative PCR and the 2−ΔΔCT Method. *Methods* 25 (4), 402–408. doi:10.1006/meth.2001.1262

Livraghi, L., and Garber, J. E. (2015). PARP Inhibitors in the Management of Breast Cancer: Current Data and Future Prospects. *BMC Med.* 13, 1–16. doi:10.1186/s12916-015-0425-1

Lockshin, R. A., and Zakeri, Z. (2004). Apoptosis, Autophagy, and More. *Int. J. Biochem. Cel Biol.* 36 (12), 2405–2419. doi:10.1016/j.biocel.2004.04.011

Pfeffer, C. M., and Singh, A. T. K. (2018). Apoptosis: a Target for Anticancer Therapy. *Int. J. Mol. Sci.* 19 (2), 448–441. doi:10.3390/ijms19020448

Preyavichyapugdee, N., Sangfuang, M., Chaiyapum, S., Sriburin, S., Pootaeng-on, Y., Chusongsang, P., et al. (2016). schistosomicidal activity of the crude extract of artocarpus lakoocha. *Southeast. Asian J. Trop. Med. Public Health* 47 (1), 1–15.

Radapong, S., Radapong, S., Sarker, S. D., and Ritchie, K. J. (2020). Oxyresveratrol Possesses DNA Damaging Activity. *Molecules* 25 (11). doi:10.3390/molecules25112577

Raderschall, E., Stout, K., Freier, S., Suckow, V., Schweiger, S., and Haaf, T. (2002). Elevated Levels of Rad51 Recombination Protein in Tumor Cells. *Cancer Res.* 62 (1), 219–225.

Rahman, M. A., Bishayee, K., Sadra, A., and Huh, S.-O. (2017). Oxyresveratrol Activates Parallel Apoptotic and Autophagic Cell Death Pathways in Neuroblastoma Cells. *Biochim. Biophys. Acta (Bba) - Gen. Subjects* 1861 (2), 23–36. doi:10.1016/j.bbagen.2016.10.025

Ruíz, G., Valencia-González, H. A., León-Galicia, I., García-Villa, E., García-Carrancá, A., and Gariglio, P. (2018). Inhibition of RAD51 by siRNA and Resveratrol Sensitizes Cancer Stem Cells Derived from HeLa Cell Cultures to Apoptosis. *Stem Cell Int* 2018, 2493869. doi:10.1155/2018/2493869

Slupianek, A., Schmutte, C., Tombline, G., Nieborowska-Skorska, M., Hoser, G., Nowicki, M. O., et al. (2001). BCR/ABL Regulates Mammalian RecA Homologs, Resulting in Drug Resistance. *Mol. Cel.* 8 (4), 795–806. doi:10.1016/s1097-2765(01)00357-4

Taylor, I., Pauloski, N. R., and Bigwood, D. (2005). *Gene Expression Profiles and Microarrays for Use in Diagnosis and Drug Screening for Lung Cancer*. USA: Bayer Pharmaceuticals Corp., 60.

Walsh, C. S. (2015). Two Decades beyond BRCA1/2: Homologous Recombination, Hereditary Cancer Risk and a Target for Ovarian Cancer Therapy. *Gynecol. Oncol.* 137 (2), 343–350. doi:10.1016/j.ygyno.2015.02.017

Wood, D. J., Korolchuk, S., Tatum, N. J., Wang, L.-Z., Endicott, J. A., Noble, M. E. M., et al. (2019). Differences in the Conformational Energy Landscape of CDK1 and CDK2 Suggest a Mechanism for Achieving Selective CDK Inhibition. *Cel. Chem. Biol.* 26 (1), 121–130.e5. doi:10.1016/j.chembiol.2018.10.015

Conflict of Interest: The authors declare that the research was conducted in the absence of any commercial or financial relationships that could be construed as a potential conflict of interest.

frontiers in Oncology

SYSTEMATIC REVIEW
published: 07 July 2021
doi: 10.3389/fonc.2021.697143

Cancer Preventive and Therapeutic Potential of Banana and Its Bioactive Constituents: A Systematic, Comprehensive, and Mechanistic Review

Arijit Mondal[1], Sabyasachi Banerjee[2], Sankhadip Bose[3], Partha Pratim Das[3], Elise N. Sandberg[4], Atanas G. Atanasov[5,6,7] and Anupam Bishayee[4]**

[1] Department of Pharmaceutical Chemistry, Bengal College of Pharmaceutical Technology, Dubrajpur, India, [2] Department of Pharmaceutical Chemistry, Gupta College of Technological Sciences, Asansol, India, [3] Department of Pharmacognosy, Bengal School of Technology, Chuchura, India, [4] Lake Erie College of Osteopathic Medicine, Bradenton, FL, United States, [5] Ludwig Boltzmann Institute for Digital Health and Patient Safety, Medical University of Vienna, Vienna, Austria, [6] Institute of Genetics and Animal Biotechnology of the Polish Academy of Sciences, Magdalenka, Poland, [7] Department of Pharmacognosy, University of Vienna, Vienna, Austria

OPEN ACCESS

Edited by:
Raghuram Kandimalla,
James Graham Brown Cancer Center,
United States

Reviewed by:
Saif Khan,
University of Ha'il, Saudi Arabia
Suman Kumar Samanta,
Ministry of Science and Technology,
India

***Correspondence:**
Anupam Bishayee
abishayee@lecom.edu;
abishayee@gmail.com
Arijit Mondal
juarijitmondal@gmail.com

Specialty section:
This article was submitted to Pharmacology of Anti-Cancer Drugs, a section of the journal Frontiers in Oncology

Received: 19 April 2021
Accepted: 24 May 2021
Published: 07 July 2021

Citation:
Mondal A, Banerjee S, Bose S, Das PP, Sandberg EN, Atanasov AG and Bishayee A (2021) Cancer Preventive and Therapeutic Potential of Banana and Its Bioactive Constituents: A Systematic, Comprehensive, and Mechanistic Review. Front. Oncol. 11:697143. doi: 10.3389/fonc.2021.697143

Background: The banana (*Musa* spp.) plant produces elongated and edible fruit. The two main parthenocarpic species of banana are *Musa accuminata* Colla and *Musa balbisiana* Colla. There are several health-promoting and disease-preventing effects of *Musa accuminata* Colla, which are attributed to its important bioactive compounds, including phenolics, carotenoids, biogenic amines, phytosterols, and volatile oils, found in the stem, fruit, pseudostem, leaf, flower, sap, inner trunk, root, and inner core. Banana possesses numerous pharmacological activities, such as antioxidant, immunomodulatory, antimicrobial, antiulcerogenic, hypolipidemic, hypoglycemic, leishmanicidal, anthelmintic, and anticancer properties. Various individual studies have reported anticancer effects of different components of the banana plant. However, according to our understanding, an up-to-date, systematic, and critical analysis of existing scientific results has not yet been carried out.

Objectives: This review aims to include a thorough assessment of banana and its phytochemicals for cancer prevention and therapy with a focus on cellular and molecular mechanisms of action.

Methods: The available research studies on anticancer activities of banana extracts, fractions and pure compounds were collected using various scholarly databases, such as PubMed, ScienceDirect, and Scopus, based on predetermined selection criteria.

Results: Various banana extracts, fractions, and phytoconstituents, including ferulic acid, protocatechualdehyde, 2-pentanone, 4-epicyclomusalenone, cycloeucalenol acetate, and chlorogenic acid, have been shown to exhibit cancer preventative and anticancer activities in breast, cervical, colorectal, esophageal, hepatic, oral, prostate, and skin cancers. Bioactive components present in bananas have exhibited antiproliferative, cell

cycle arrest-inducing, apoptotic, anti-adhesive, anti-invasive, and antiangiogenic effects through modulation of diverse, dysregulated oncogenic signaling pathways.

Conclusion: Based on the critical analysis of available literature, banana products and phytoconstituents show enormous potential for future development of drugs for cancer prevention and therapy. However, more mechanistic studies and well-designed clinical trials should be performed to establish its efficacy.

Keywords: cancer, banana, *Musa accuminata* Colla, *Musa balbisiana* Colla, *Musa* spp., prevention, therapy, molecular mechanisms

INTRODUCTION

Cancer, the second most frequent cause of mortality, is a hyper-proliferative disorder that involves cellular transformation, deregulation of apoptosis, and excessive proliferation, invasion, angiogenesis, and metastasis (1). Despite innovative therapeutic approaches and newer technological developments, cancer continues to be amongst the most fatal disorders (2, 3). According to the 2020 Global Cancer Observatory report provided by the International Agency for Research on Cancer (World Health Organization), there were 18.1 million new cases of cancer and 9.5 million cancer-related deaths that occurred globally in 2018. They also stated that the number of newly diagnosed cancer cases is projected to increase to 29.5 million per year, and projected cancer-related deaths are expected to increase to16.4 million per year by 2040 (www.cancer.gov). While the precise cause for cancer initiation is still unclear, the most important contributing variables for this condition are toxins, pollution, radioactive substances, oncogenic viruses (4, 5), and epigenetic abnormalities (6). Many anticancer medications currently in use not only destroy cancer cells, but also healthy cells too. The major obstacles involved with cancer chemotherapy are non-specific targeting and the evolution of drug resistance. The need for more effective anticancer medications with improved safety profiles has become an urgent need to defeat this dreaded disease, despite significant advances in cancer screening, diagnosis, and treatment.

For most of the world, modern medicine has replaced traditional medicine as means of therapy for human illnesses (7). Nevertheless, the use of medicinal plants for health promotion and disease prevention has increased in recent decades (8). Phytochemicals are being extensively investigated, and they have demonstrated promising anticarcinogenic properties by interfering with cancer initiation and modulating various pathways, including cell proliferation, differentiation, apoptosis, angiogenesis, invasion, and metastasis (9–12).

The term "banana" refers to the cultivated varieties of the genus *Musa*, which are made up of two subgroups: sweet bananas and plantains (13). *Musa*, *Ensete*, and *Musella* are the three genera of the Musaceae family (14), with the *Musa* genus comprising of 65 species of wild and cultivated bananas and plantains. Banana has been described in ancient Indian treatises, including the Ramayana (2000 BC), Arthsastra (250 BC), and Chilappthikaram (500 AD), suggesting the fruit's importance and demonstrating its ancient use in India. The genus name *Musa* was chosen to commemorate Roman physician and botanist Antonius Musa (63 BC-14 AD) (15). Historically, *Musa acuminata* has been discovered in the native habitats of India (15). At present, banana is cultivated around the world, and the significant producers of banana fruits are India (29 million tonnes/year), China (11 million tonnes/year), Philippines (7.5 million tonnes/year), and Brazil, as well as Ecuador, which produces 7 million tonnes/year on average (16).

The banana is a perennial herb that looks like a tree (**Figure 1A**). It forms shoots that emerge from the rhizome's lateral buds, which then grow into fruit-bearing stems. A pseudostem (**Figure 1B**) begins to appear like a trunk, however it is actually is a compact assembly of wrapping, spirally arranged leaf sheaths. The banana plant's flowers (**Figure 1C**) produce a big spike, which subsequently opens by turning downward towards the soil. A single plant produces both male and female flowers. The fruits (**Figure 1D**) are green or yellow in color, have a long shape, and are produced in bunches and clusters. Each leaf (**Figure 1E**) arises from the pseudostem's center. The elongating leaf sheath's distal end expands into a petiole. The midrib, which splits the blade into two lamina halves, is formed by the petiole (17).

Nearly every portion of the banana plant has its essential use and is beneficial in many respects to mankind. Traditionally, *M. acuminate* plants have been used to treat non-communicable as well as transmissible diseases, especially in Asia and Africa. It has been extensively used by indigenous people as both food and medicine (18, 19). Various parts of the plant, such as the stem, fruit, pseudostem, leaf, vine, sap, inner trunk, root, and inner core, have been used in the management of various diseases, including the regulation of blood pressure (20), diabetes (18), hypertension (21), anemia (22), allergic reaction, microbial infections, and chronic bronchitis disorders. *M. acuminate* has also been used for the treatment of fever, cough, tuberculosis, and dysentery by many tribes and communities (23, 24). The root extract has been utilized to prevent conception (25), stimulate labor (26), and cure infections of sexually transmitted diseases, such as human immunodeficiency virus-related infections, internal and external sores of the genitalia, vaginitis and leucorrhoea (27, 28). Some common uses recorded in the literature include its usefulness as an anthelmintic, as dressing for cuts and blistered skin, and as a liqueur to reduce joint inflammation and promote blood circulation (15). Aside from the conventional uses mentioned earlier, the *Musa* species has

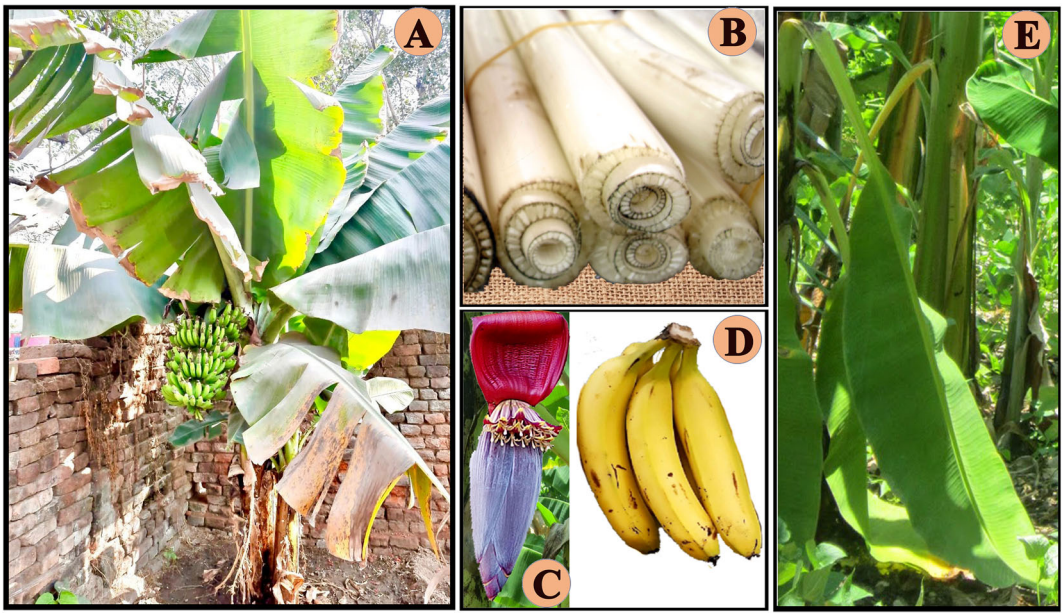

FIGURE 1 | Various photographs of banana showing a whole plant **(A)**, pseudostem **(B)**, flowers **(C)**, fruits **(D)** and leaves **(E)**.

also been documented to possess pharmacological activities, demonstrating antioxidant, immunomodulatory, antimicrobial, anticancer, antiulcerogenic, hypolipidemic, hypoglycemic, leishmanicidal, and anthelmintic properties (29).

Many bioactive phytoconstituents of bananas have been isolated, characterized, and analyzed for their anticancer properties; however, no previous reviews offer a systematic analysis of published anticancer studies of *Musa* species. There are only a limited number of prior publications that provide a brief overview of the nutritional values of banana and its overall pharmacological activities (29, 30). There are no articles focusing on the antineoplastic properties of *Musa* species, their phytoconstituents in different kind of cancers and related signaling pathways. While there are numerous and emerging information on anticancer properties of banana and its constituents based on laboratory and clinical findings, a comprehensive assessment of cancer preventive and therapeutic characteristics of banana, banana products, extracts, fractions, and isolated phytochemicals has yet to be performed. In view of this limitation, our current work elucidates cancer preventive and therapeutic potential of banana and its bioactive phytoconstituents observed in several types of cancers and highlights underlying mechanisms of action, which involve targeting various cell signaling pathways and molecules.

PHYTOCHEMICAL PROFILES OF *MUSA* SPECIES

The phytochemical analysis of different anatomical parts of banana plant, such as the leaves, fruits, peels, flowers, pseudostems, and rhizomes, has shown that there are numerous secondary plant metabolites, including polyphenols, terpenoids, alkaloids, steroids, anthocyanins, tannins, and fatty acids (**Table 1**). Banana fruit has been recorded as a significant source of phenolic compounds, including phenolic acids, flavonoids, and glycosides. The pulps and peels of banana and plantain have demonstrated potential to be utilized by the pharmaceutical and food industries for their catechin and rutin content (60, 61). Plantain pulps and peels are also a good resource of phenolic compounds. Recent examinations of plantains have revealed that hydroxycinnamic acids represent the majority of phenolic compounds in the fruit pulp, while flavonoids are mostly found in higher concentrations in the peel (62).

Borges et al. (60) proposed that parental combinations of banana genotypes of *M. acuminata* and *M. balbisiana* may be chosen for hybrid production. The biofortification of *Musa* spp. produced diploid, triploid, and tetraploid hybrids which contained higher amounts of bioactive compounds than non-hybrid plants. Several studies have reported catechin, epicatechin, and gallocatechin as major compounds in the triploids cultivars Highgate (AAA) genotype of *M. acuminata* and *M. balbisiana* which have an epicatechin content of 114.44 mg/100 g dry weight basis and gallocatechin content of 591.41 mg/100 g dry weight basis. In addition to catechin compounds, protocatechuic acid, gallic acid, 7-*O*-neohesperoside naringenin, and hydroxycinnamic acids have additionally been identified in banana pulp (41, 60, 62, 63).

The content of phenolic compounds varies in the raw and ripe fruits. Thermal treatments of the banana fruits weakened the cell wall and facilitated the release of phenolic component,

TABLE 1 | Phytochemicals identified in various parts of *Musa* spp.

Plant parts	Category	Phytochemicals from various banana cultivars	Quantitative values	Extract	References
Ripe fruit	Phenolic acids	Octadeca-9,12,15 trienoic acid (**1**)	36-405 mg/kg of dry material	Dichloromethane	(31)
		Octadeca-9,12-dienoicacid (**2**)	12-198 mg/kg of dry material		
		Vanillic acid (**3**)	8.54 mg/100g of acetone extract	Acetone	(32)
		Caffeic acid (**4**)	1.36 mg/100g of acetone extract		
		Ellagic acid (**5**)	68.82 mg/100g of acetone extract		
Peel		13-octadecanoic acid (**6**)	5.59%	Methanol, oil	(29, 33–35)
		Palmitic acid (**7**)	30%		
		Oleic acid (**8**)	7%		
		Linoleic acid (**9**)	8%		
		Methyl palmitate (**10**)	–		
		Methyl oleate (**11**)	–		
		Methyl linoleate (**12**)	–		
		Stearic acid (**13**)	2%		
		Carvacrol (**14**)	–		
		Pentadecanoic acid (**15**)	18.81% of extract		
		Palmitoleic acid (**16**)	–		
		Benzoic acid (**17**)	16.04% of extract		
Leaves		Tannic acid (**18**)	7.04-12.19 mg/ml	Ethanol, acetone, petroleum ether	(36)
		Cinnamic acid (**19**)	43-80 ng/g dry weight	Leaf powder	(37)
		Ferulic acid (**20**)	2680-5900 ng/g dry weight		
Bract		Delphinidin-3-rutinoside (**21**)	0.00-66.70 mg/100 g	Methanol	(38–40)
		Cyanidin-3-rutinoside (**22**)	0.00-37.52 mg/100 g		
		Petunidin-3-rutinoside (**23**)	0.00-11.91 mg/100 g		
		Peonidin-3-rutinoside (**24**)	0.00-36.92 mg/100 g		
		Malvidin-3-rutinoside (**25**)	0.00-70.27 mg/100 g		
Seeds		Leucoanthocyanidin (**26**)	–	Acetone	(29)
Pulp of banana fruit		Gallic acid (**27**)	–	Not specified	(41)
Over ripe fruit		Protocatechualdehyde (**28**)	–	Not specified	(42)
Sap		Hydroxycinnamic acid (**29**)	24-45% of sap	Ethanol	(43)
		Caffeoylquinic acid (**30**)	24-45% of sap		
Ripe fruit	Flavonoids	Quercetin (**31**)	6.5-18.9 µg/100 g of dry weight pulp	Pulp	(41, 44)
		Proanthocyanidin (**32**)	–		
		Catechin (**33**)	33.3-143.2 µg/100 g of dry weight pulp		
		Gallocatechin (**34**)	37.3-542 µg/100 g of dry weight pulp	Methanol	(41, 45)
		Epicatechin (**35**)	17.9-459.8 µg/100 g of dry weight pulp		
		Procyanidin (**36**)	1.6-124.7 µg/100 g of dry weight pulp		
		(+) Catechin hydrate (**37**)	23.34 mg/100 g of acetone extract	Acetone	(32)
Sap		Apigenin (**38**)	5.50-23.81% of sap	Ethanol	(43)
		Myricetin (**39**)	1-45% of sap		
		Kaempferol (**40**)	2.89-23.50% of sap		
Ripe fruits	Glycosides	Endo-β-1,3-glucanase (Ban-Glu) (**41**)	208 and 237 amino acids are present in two varieties	Pulp	(46)
		α-tocopherol (**42**)	2-7 mg/kg of dry material	Dichloromethane	(31)
	Triterpenoids	Cycloartenol (**43**)	1-4 mg/kg of dry material	Dichloromethane	
	Sterols	Campesterol (**44**)	18-59 mg/kg of dry material	Dichloromethane	
		Stigmasterol (**45**)	23-49 mg/kg of dry material		
		β-sitosterol (**46**)	105-226 mg/kg of dry material		
Peels		Pyrogallol (**47**)	22.24%	Methanol	(33)
Ripe banana		Sitosteryl glucoside (Sitogluside) (**48**)	–	Not specified	(47)

(Continued)

TABLE 1 | Continued

Plant parts	Category	Phytochemicals from various banana cultivars	Quantitative values	Extract	References
Peel	Lignan	Sesamin (**49**)	–	Methanol, oil	(48)
Peel		Epi-sesamin (**50**)	–		
Ripe fruit	Carotenoids	Ascorbic acid (**51**)	–	Pulp, Peel	(29)
		Retinol (**52**)	–		(49)
		α-carotene (**53**)	–		(50, 51)
		β-carotene (**54**)	–		
		Zeaxanthin (**55**)	–		
Unripe fruit	Miscellaneous	2-(4-hydroxyphenyl)-naphthalic anhydride (**56**)	–	Pulp	(52)
		methyl 2-benzimidazole carbamate (**57**)	–		
Peel		Dopamine (**58**)	3.9-381 mg/100 dry weight banana peel extract	Acetone:water	(53)
Ripe fruit		Serotonin (**59**)	1-2 mg/100 g	Not specified	(54, 55)
		Histamine (**60**)	0.04 mg/100 g		
		Tryptamine (**61**)	0.06 mg/100 g		
		2-phenylethylamine (**62**)	0.04 mg/100 g		
		Putrescine (**63**)	0.04 mg/100 g		
		Cadaverine (**64**)	0.04 mg/100 g		
		Tyramine (**65**)	0.06 mg/100 g		
Peels		2,3-dihydro-3,5-dihydroxy-6-methyl-4H-pyran-4-one (**66**)	–	Methanol, oil	(29, 33, 48)
		5-(hydroxymethyl)-2-Furancarboxyaldehyde (**67**)	–		
		cis-9-hexadecenal (**68**)	21.20%		
Rhizome		(S)(+)-naproxene (**69**)	–		(56–58)
		2-methoxy-9-phenyl-phenalen-1-one (**70**)	0.3 mg/478 mg of peel extract		
Rhizome, Root		Anigorufone (**71**)	–	Methanol	(29)
Fruit		2-pentanone (**72**)	4.8-6.0 mg/kg	Not specified	(59)
Sap		N-acetylserotonin (**73**)	17-34.76% of sap	Ethanol	(43)

such as ferulic acid (62). Boiled plantain pulps with or without peel demonstrated an increased number of phenols in pulps (62). Additionally, protocatechualdehyde, a naturally occurring polyphenol, was isolated, purified, and characterized in green cavendish bananas (42). The phenolic compounds collectively present in the banana are octadeca-9,12,15 trienoic acid (**1**) (**Figure 2**), octadeca-9,12-dienoicacid (**2**), vanillic acid (**3**), caffeic acid (**4**), ellagic acid (**5**), 13-octadecanoic acid (**6**), palmitic acid (**7**), oleic acid (**8**), linoleic acid (**9**), methyl palmitate (**10**), methyl oleate (**11**), methyl linoleate (**12**), stearic acid (**13**), carvacrol (**14**), pentadecanoic acid (**15**), palmitoleic acid (**16**), benzoic acid (**17**), tannic acid (**18**), cinnamic acid (**19**), ferulic acid (**20**), delphinidin-3-rutinoside (**21**), cyanidin-3-rutinoside (**22**), petunidin-3-rutinoside (**23**), peonidin-3-rutinoside (**24**), malvidin-3-rutinoside (**25**) (**Figure 3**), leucoanthocyanidin (**26**), gallic acid (**27**), protocatechualdehyde (**28**), hydroxycinnamic acid (**29**), caffeoylquinic acid (**30**), quercetin (**31**), proanthocyanidin (**32**), catechin (**33**), gallocatechin (**34**), epicatechin (**35**), procyanidin (**36**), (+) catechin hydrate (**37**), apigenin (**38**), myricetin (**39**), kaempferol (**40**), endo-β-1,3-glucanase (Ban-Glu) (**41**), and α-tocopherol (**42**).A triterpenoid, namely cycloartenol (**43**), was extracted from the dichloromethane extract of ripe pulp of various banana cultivars (29, 31–41, 43–46).

Banana fruits have substantial phytosterol concentrations (64). Several sterol components are present in the *Musa* spp., namely, campesterol (**44**), stigmasterol (**45**), β-sitosterol (**46**) (**Figure 4**), which exist in the dichloromethane extract (31). The methanol extract of banana peel contains pyrogallol/benzene-1,2,3-triol (**47**) (33). In addition to these phytochemicals, sitosteryl glucoside (sitogluside) (**48**) is present in ripe banana fruits (47). Two kinds of lignan, namely sesamin (**49**) and epi-sesamin (**50**), have also been isolated and identified in the methanol extract of banana peel (48).

Carotenoids, vitamin C (ascorbic acid) (**51**), and vitamin A (retinol) (**52**) are the most abundant antioxidants present in the banana pulp and peel (49). Significant quantities of bioactive carotenoids have been extracted and identified in *Musa* spp. biomasses as well (50, 51). Various banana genotypes may even produce higher amounts (approx. 90%) of vitamin A precursors, such as α- and β-carotene (**53** and **54**) (65). Zeaxanthin (**55**) has additionally been found in bananas. Several additional novel compounds, such as 2-(4-hydroxyphenyl)-naphthalic anhydride (**56**), and methyl 2-benzimidazolecarbamate (**57**), were reported to be present in banana (52).

According to Xiao et al. (66), the consumption of banana, which is considered relatively rich in serotonin, leads to a rapid elevation of the hormone level within the blood. The quantity and specific type of biogenic amines formed are affected by the composition of the plant's nutritional intake, microbial flora, storage (e.g., degree of ripeness and temperature), and processing to which they are subjected (54, 67, 68). The most common amine compounds are spermidine and spermine. Diamines, such as putrescina and agmatina, are precursors of these polyamines (69). Dopamine (**58**), serotonin (**59**) and histamine (**60**) have all been detected in bananas and their by-products (54). Serotonin has been extracted in higher amounts in the fruits of *Musa* spp., particularly when compared with other fruits and vegetables (32). Additionally, several biogenic amines, tryptamine (**61**), 2-phenylethylamine (**62**), putrescine (**63**), cadaverine (**64**), and tyramine (**65**), are also present in banana (55). Interestingly, a ketone compound, namely 2-pentanone, has been isolated from bananas as well (59). Several other miscellaneous components are reported to exist in *Musa* spp., including 2,3-dihydro-3,5-dihydroxy-6-methyl-4H-pyran-4-one (**66**), 5-(hydroxymethyl)-2-furancarboxyaldehyde (**67**), cis-9-hexadecenal (**68**), (S) (+)-naproxene (**69**) (**Figure 5**), 2-methoxy-9-phenyl-phenalen-1-one (**70**), Anigorufone (**71**), 2-pentanone (**72**), and N-acetylserotonin (**73**) (33, 43, 48, 56–59). The phytoconstituent compositions of different banana species (**Table 1**) differ quantitatively due to soil, temperature, banana type, maturation stage, processing site, and other factors (70).

SAFETY PROFILE OF BANANA

Local and tribal communities have discovered that the use of banana fruit and other parts of the banana plant is non-toxic. Banana fruits and other plant parts are consumed by indigenous populations throughout the world. The banana (*M. acuminata*) flower is used to prepare a popular Sri Lankan dish as a curry, boiled or deep-fried salad (71). There were no adverse consequences upon the administration of banana (*M. acuminata*) extracts in preclinical trials (22, 72–74). The flowering stalk of *M. acuminata* was documented to be non-toxic against the murine monocytic macrophages cell line (75). A toxicity examination in brine shrimp (administered in *Artemia salina*) revealed that *M. acuminata* flower extract was safe as well (76). Likewise, the utilization of *M. acuminata* peel as an ingredient in food products suggests that it's considered safe for consumption (77–79). Furthermore, banana peel exhibited no toxicity towards normal human cells (80). According to acute and subacute toxicity analysis, aqueous fermented extract of *M. paradisiaca* plantain was reported to be non-toxic and considered safe when administered to rats at a dose of 800 mg/kg body weight, which revealed no significant changes in the hematological and serum biochemical parameters or histopathological studies of the liver and kidney (81). According to Abbas et al. (82), the methanol extract of *M. paradisiaca* (bract and flowering stalk) showed potent nephroprotective activity in gentamicin-induced nephrotoxicity in mice. Cellulose nanofibers isolated from the banana peel (*M. paradisiaca*) exhibited no cytotoxicity against Caco-2 cell line (83). The methanol extract of *M. paradisiaca* root exhibited no signs of toxicity or mortality in broiler chickens with doses up to 4000 mg/kg body weight (84). Similarly, the hydro-ethanol extract of pseudostem of *M. paradisiaca* did not demonstrate any signs of toxicity or mortality in male Wistar rats when administered doses of up to 3000 mg/kg body weight (85). Additionally, the hydro-methanolic extract of *M. balbisiana* flower exhibited its non-toxic effects in streptozotocin-induced diabetic male albino Wistar rats (86). Aqueous extract of fresh ripe peel (*M. sapientum* Linn.) also did not induce any cytotoxicity in RAW 264.7 murine macrophage cell lines, which was evident from the presence of 70% viable cells (87).

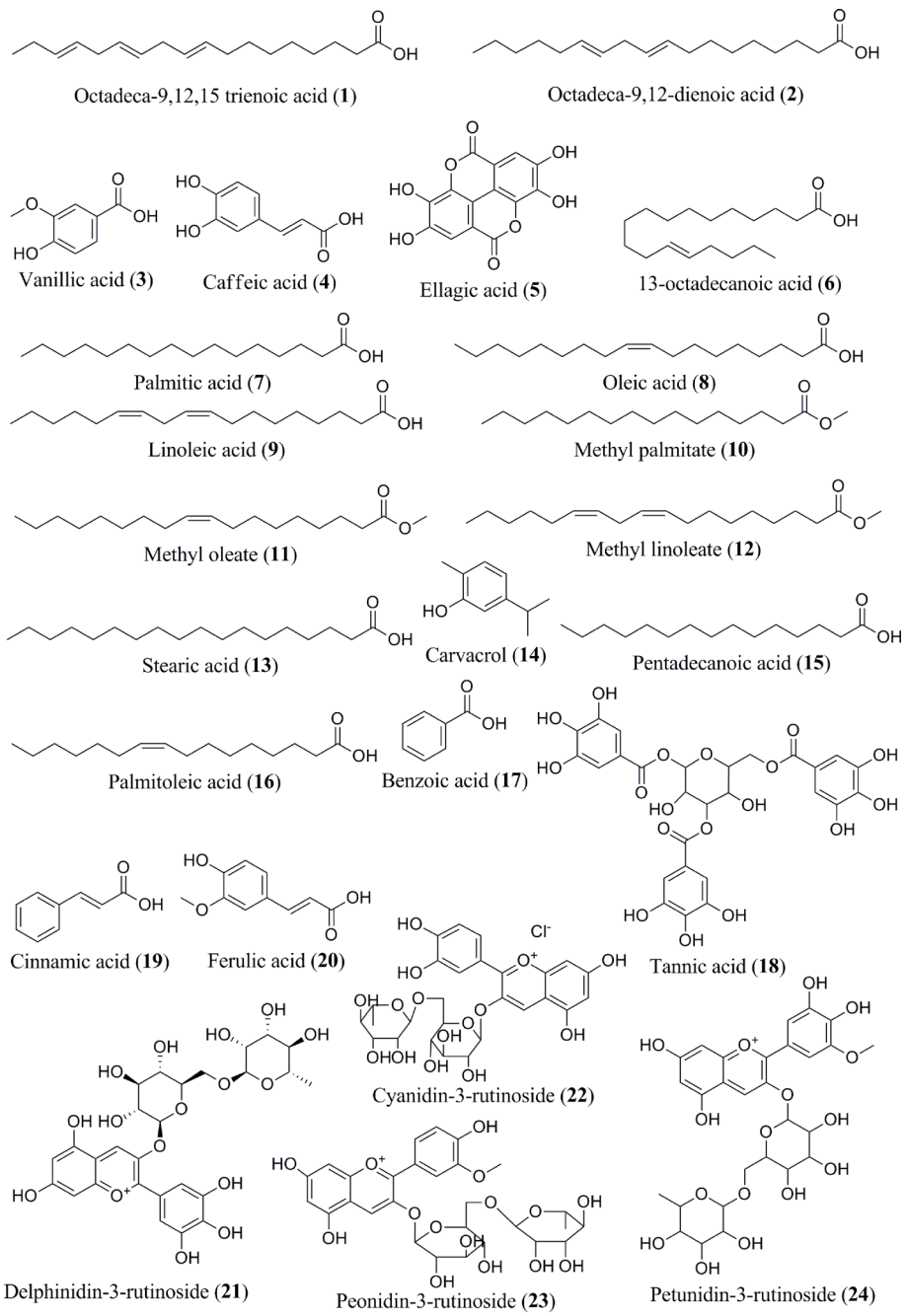

FIGURE 2 | Isolated phytoconstituents (**1–24**) present in *Musa* spp.

CANCER PREVENTIVE AND ANTICANCER THERAPEUTIC POTENTIAL OF *MUSA SPP*.

Literature Search Methodology

We have followed the guidelines of Preferred Reporting Items for Systemic Reviews and Meta-Analysis (PRISMA) (88) which is a credible process utilized for systematic analysis compilation (**Figure 6**). The major databases used to find primary literature were PubMed, ScienceDirect, and Scopus. Additionally, clinical trials were searched using clinicaltrials.gov. There were no time restraints on research articles that were published. The last search was performed in March 2021. Various combinations of keywords that were used included: *Musa* species; banana; chemopreventive, chemotherapeutic, *in vivo*, *in vitro*, cancer,

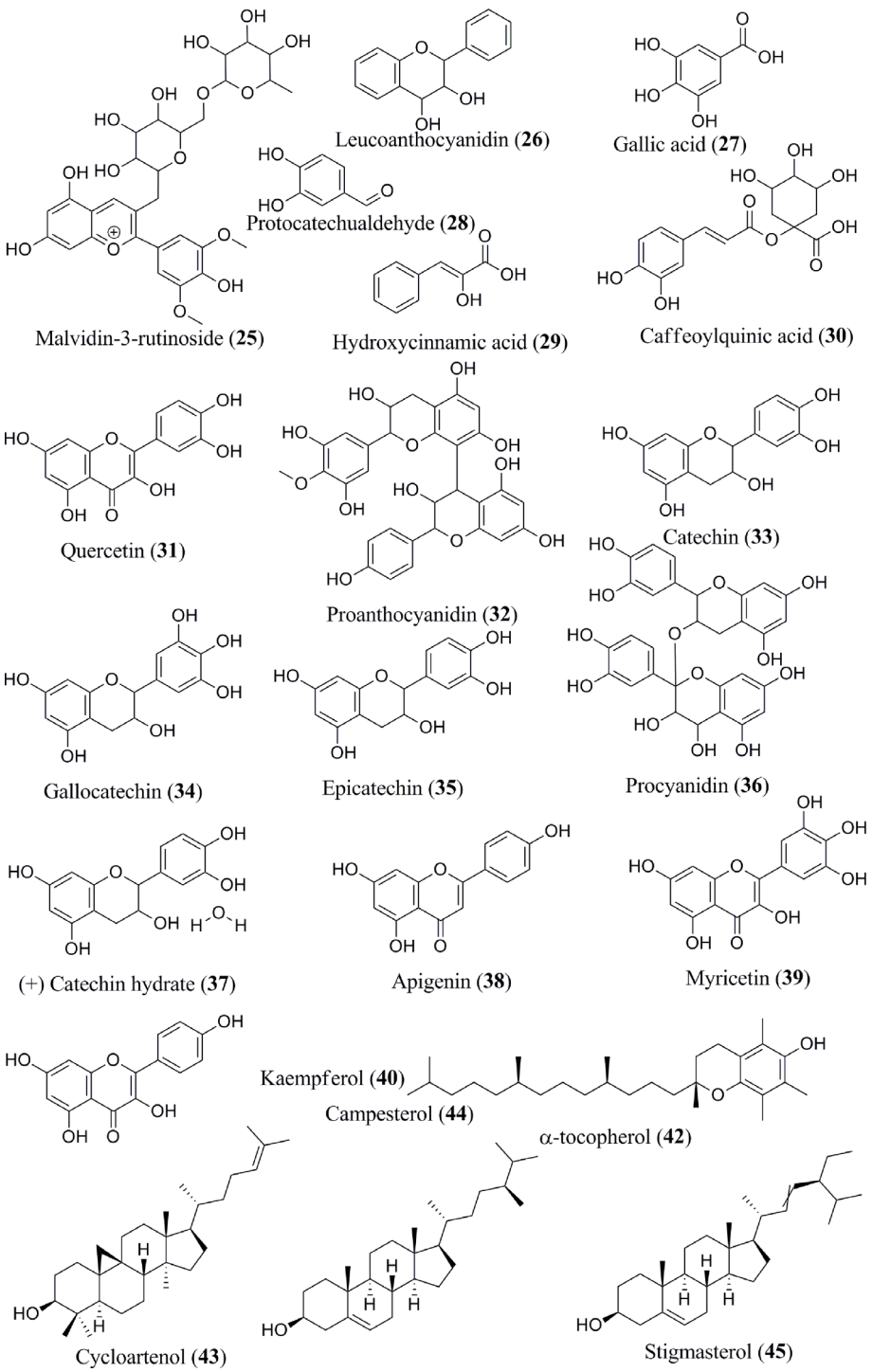

FIGURE 3 | Isolated phytoconstituents (**25–45**) present in *Musa* spp.

tumor, prevention, treatment, proliferation, apoptosis, and clinical studies. We only considered studies that investigated anticancer effects on banana extracts or constituents against cancer cell lines and/or animal tumor models. Initially, the abstracts of all publications were reviewed to determine the next step, i.e., the collection of full-length articles. Once a full article was reviewed, a decision was made regarding its incorporation for further analysis. Only reports published in

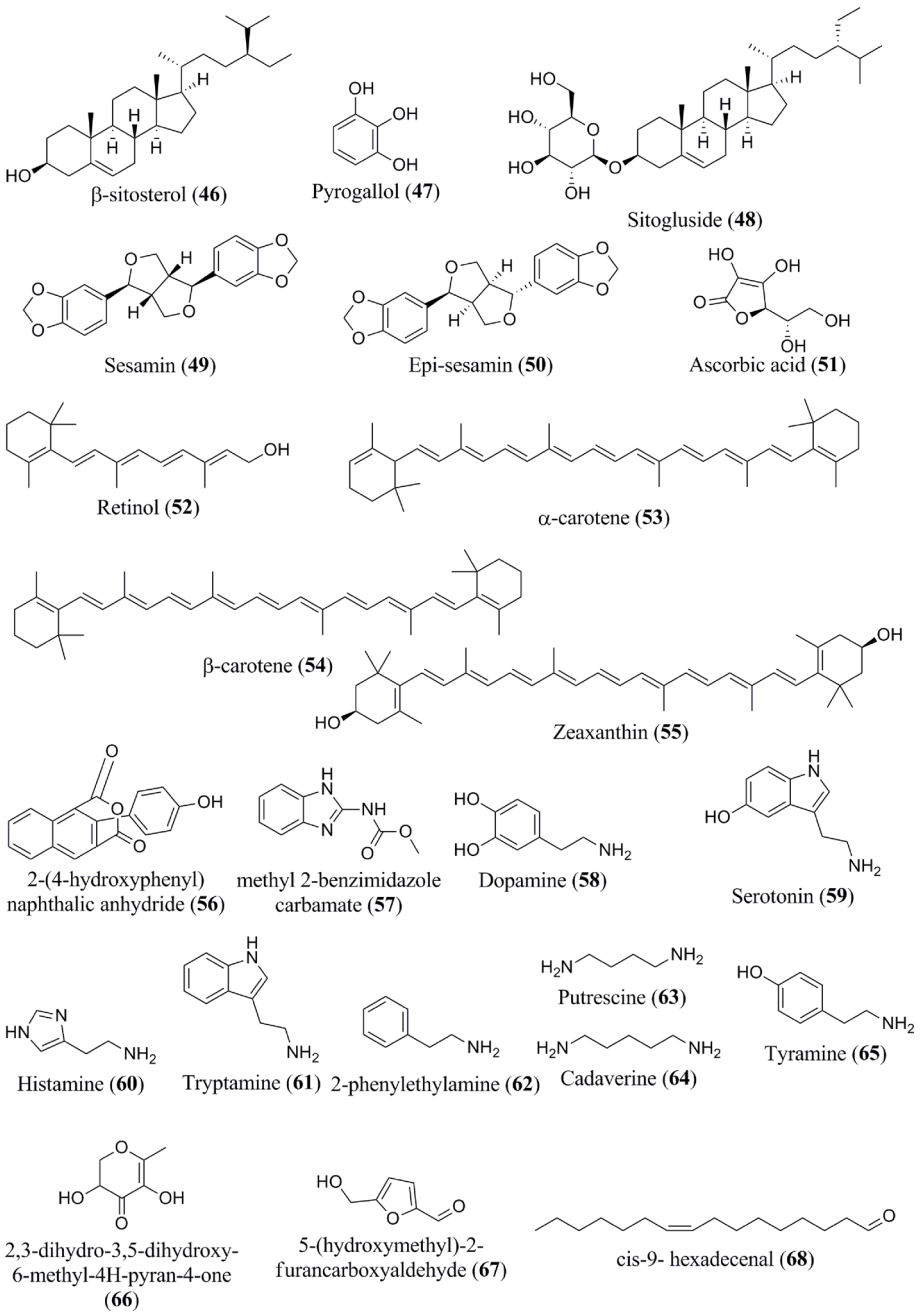

FIGURE 4 | Isolated phytoconstituents (**46–68**) present in *Musa* spp.

the English language were included. Reviews, systemic reviews, meta-analyses, letters to editors, book chapters, and conference abstracts were excluded. These searches were also performed by reviewing the bibliography sections of published papers.

Preclinical Studies

Bananas showed a predominance of flavonoids, cinnamic acids, and polyphenolic compounds, which exhibit chemopreventive potential through various pathways analysed through *in vitro* (**Table 2**) and *in vivo* (**Table 3**) studies. Banana, as well their bioactive compounds, which exhibited anticancer, cytotoxic, and antiproliferative activity against various cancer types, are discussed below.

Breast Cancer

Regarding *in vitro* studies, aqueous methanol extract of *Nendran* banana peel exhibited significant antitumor activity against the MCF-7 breast cancer cell line by inducing concentration-

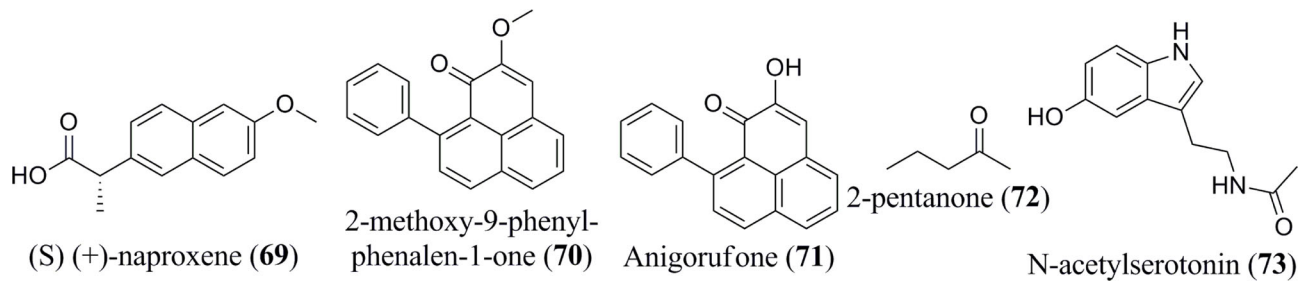

FIGURE 5 | Isolated phytoconstituents (**69-73**) present in *Musa* spp.

dependent apoptosis (89). Another *in vitro* experimental study showed that the anthocyanin extracted from methanol extracts of *M. acuminata* bract suppressed the proliferation of MCF-7 cells through induction of apoptosis (90). Additionally, *M. cavendish* green peel hydroalcoholic extract exhibited antiproliferative activity against the MCF-7 cell line at a concentration of 100 µg/mL (91). Additionally, hexane extract of banana (*M. sapientum*) peel and pulp was observed to be cytotoxic and blocked the proliferation of MCF-7 cells (92).

Aqueous fruit extract of ripe banana was utilized for evaluating its anticancer activity in Swiss albino mice bearing Erhlich ascites carcinoma cells. In comparison to the positive control, in which 100% of the animals died due to the carcinogenic effect, regular feeding of 2 g banana/day/mouse resulted in the growth suppression of malignant ascites leading to survival of 30% of the animals with Erhlich carcinoma which survived more than 35 days (104). Mannose-specific *M. acuminate* lectin (MAL) from the phloem exudates of *M. acuminate* pseudostem also demonstrated antitumor activity in Swiss albino mice bearing Erhlich carcinoma cells. Mechanistic studies showed initiation of apoptosis through the arrest of cell cycle progression at G2/M phase *via* stimulation of caspase-3, caspase-8 and caspase-9 with increased poly (ADP-ribose) polymerase (PARP) cleavage. It further triggered apoptosis through the phosphoinositide 3-kinase (PI3K)/Akt (also known as protein kinase B) signaling pathway, which inhibited the expression level of phosphorylated Akt (pAkt). MAL also blocked the phosphorylation of extracellular signal-regulated kinase 1 and 2 (ERK1/2) and c-Jun N-terminal kinase (JNK) (94).

Cervical Cancer

Ethanol extract of banana flower (*M. paradisiaca*) exhibited anticancer activity against HeLa cervical cancer cell line. The extract inhibited cellular proliferation and induced apoptosis, which was evident by the appearance of breaking up of the nuclei associated with significantly increased caspase-9 activity. The extract also blocked the cell cycle progression at the G_0/G_1 phase as well (93). Interestingly, the extract did not induce any toxicity on normal human peripheral lymphocytes. In a separate study, MAL exhibited similar cytotoxicity and antiproliferative activity against HeLa cells by initiating apoptosis and arresting cell cycle progression at the G2/M stage through activation of caspase-3, caspase-8 and caspase-9 associated with elevated PARP cleavage. It also induced apoptosis through the PI3K/Akt signaling pathway, in which it blocked the expression level of phosphorylated Akt (pAkt). It further inhibited the phosphorylation of ERK1/2 and JNK (94). Ferulic acid was isolated from banana peel using *Staphylococcus aureus*, and it exhibited antiproliferative and cytotoxic activities against HeLa cervical cancer cells by inducing DNA fragmentation (95). Additionally, the methanol extract of *M. acuminate* flower showed antiproliferative and cytotoxic potential against HeLa cells (96). An ethyl acetate fraction of *M. x paradisiaca* L. leaves also showed strong cytotoxic and anticancer activity against HeLa and A375 cervical cancer cell lines (97).

Colon Cancer

The hexane fraction of banana (*M. sapientum*) peel and pulp exhibited *in vitro* anticancer activity against HCT-116 colon carcinoma cell line. It was observed that the peel and pulp extract arrested cell growth by inducing cytotoxicity and blocked the proliferation of HCT-116 cells (92). In a separate study, *M. cavendish* green peel hydroalcoholic extract suppressed the proliferation of Caco-2 human colorectal adenocarcinoma cells (91). Protocatechualdehyde (PCA, 3,4-dihydroxybenzaldehyde), a polyphenol, was isolated from green cavendish bananas (106). It exhibited antiproliferative activity by triggering apoptosis in human colorectal carcinoma cells (HCT116 and SW480) in a concentration-dependent manner *via* histone deacetylase 2 (HDAC2)-initiated cyclin D1 suppression. It also downregulated the transcriptional level of the cyclin D1 gene and reduced the expression level of cyclin-dependent kinase 4 (CDK4). Additionally, PCA attenuated the enzymatic activity of HDAC and reduced the expression of HDAC2, but not HDAC1, thereby inducing cell cycle arrest at the G_1 to S phase in both the cell lines tested (42). PCA increased the expression level of activating transcription factor 3 (ATF3) and ATF3-mediated apoptosis in human colorectal carcinoma (HCT116 and SW480 cell lines). PCA decreased the cell viability in a concentration-dependent manner by increasing the expression of ATF3 protein and mRNA ATF3 levels *via* phosphorylation of extracellular

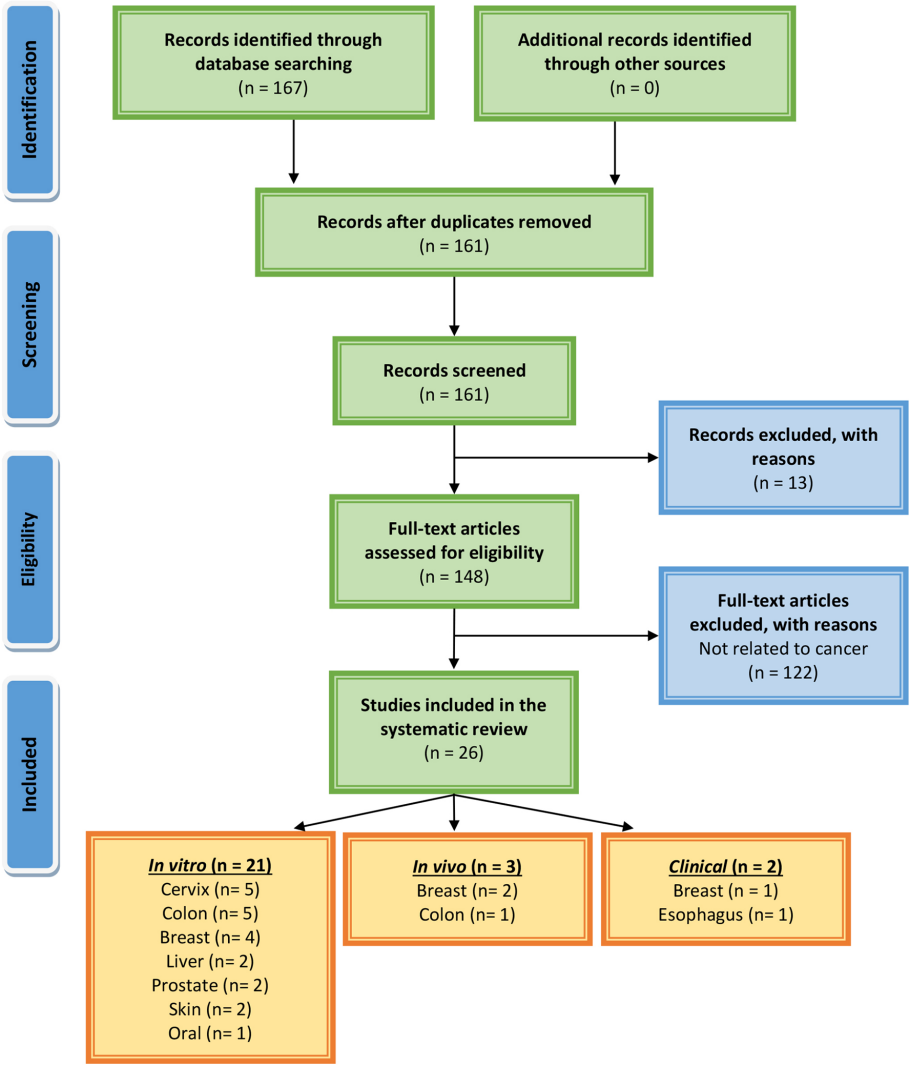

FIGURE 6 | PRISMA flow chart describing the process of literature search and study selection related to banana in cancer research.

signal-regulated protein kinase 1 and 2 (ERK1/2) and p38 mitogen-activated protein kinase (MAPK) proteins and cleavage of PARP (98). Pettersson et al. (59) reported that 2-pentanone, a methyl propyl ketone present in banana, exhibited antiproliferative action by inhibiting the prostaglandin (PGE_2) production and cyclooxygenase-2 (COX-2) protein expression in tumor necrosis factor-α (TNF-α)-stimulated colon cancer cells (HT29).

In an *in vivo* study, green banana flour (10%) was used as a dietary supplement to evaluate its anticancer potency in 1,2-dimethylhydrazine (DMH)-induced colon carcinogenesis in male Swiss mice over a 12-week experimental period. In all treated groups, it reduced the number of aberrant crypt foci (a colon cancer biomarker) in the colorectal mucosa, suggesting anticarcinogenic efficacy although the detail mechanism of action was not reported (105).

Liver Cancer

An anticancer study on *M. cavendish* green peel hydroalcoholic extract reported antiproliferative activity against HepG2 human hepatocellular carcinoma cell lines. The extract initiated both apoptosis and necrosis in a concentration-dependant manner, associated with alteration in cell morphology. It was also observed that it decreased the level of mitochondrial membrane potential (MMP) and increased reactive oxygen species (ROS) level (91). Another study has reported that various extracts of banana (*Musa* AAB var. Nanjanagudu Rasabale) pseudostem and rhizome demonstrated cytotoxicity against HepG2 cell lines. Crude chloroform and acetone extracts of the banana pseudostem and rhizome exhibited substantial cytotoxicity against the cell line tested (99). Bioactive compounds, such as 4-epicyclomusalenone and cycloeucalenol acetate, were isolated from chloroform extract, and chlorogenic

TABLE 2 | *In vitro* anticancer activities of *Musa* sp., extract and its phytoconstituents.

Materials tested	Cell line used	Effects and mechanisms	EC_{50}/IC_{50}	References
Breast cancer				
Aqueous methanol extract of *Nendran* banana peel	MCF-7 breast cancer	↓Cell viability; ↑apoptosis	120.6 μg/mL	(89)
Methanol extracts from *Musa acuminata* bract		⊥Proliferation; ↑apoptosis	12.24% inhibition at 1000 μg/mL	(90)
Musa cavendish green peel hydroaloholic extract		⊥Proliferation	100 μg/mL	(91)
Hexane extract of banana (*Musa sapientum*) peel and pulp		↑Cytotoxicity; ⊥proliferation	48.22% inhibition at 50 μg/mL (peel) and 61.21% inhibition at 50 μg/mL (pulp)	(92)
Cervical cancer				
Ethanol extract of banana flower	HeLa cells	↑Cytotoxicity; ⊥proliferation; ↑apoptosis; ⊥cell cycle at G_0/G_1 phase; ↑caspase-9 activity	20 μg/mL	(93)
Mannose specific *Musa acuminata* Lectin (MAL) from the phloem exudates of *M. acuminata* pseudostem	HeLa cells	↑Cytotoxicity; ⊥proliferation; ↑apoptosis; ↑DNA fragmentation; ⊥cell cycle at G_2/M phase; ↓Bcl-2; ↑Bax; activation of caspase-3, caspase-8 and caspase-9; ↑cleaved PARP; ⊥pAkt; ⊥p-ERK1/2; ⊥p-JNK	13.25 μg/mL	(94)
Ferulic acid from banana peel using *Staphylococcus aureus*	HeLa cells	↓Cell viability; ↑cytotoxicity; ↑DNA fragmentation	125μg/mL	(95)
Methanolic flower extract of *Musa acuminata*	HeLa cells	↑Cytotoxicity; ⊥proliferation	71.9% cytotoxicity at 100 μL	(96)
Musa Paradisiaca L. leaves ethyl extract	HeLa and A375 cell lines	↑Cytotoxicity	249.1 and 224.4 μg/mL	(97)
Colon cancer				
Hexane extract of banana (*Musa sapientum*) peel and pulp	HCT-116	↑Cytotoxicity	62.04% inhibition at 50 μg/mL (peel) and 32.76% inhibition at 50 μg/mL (pulp)	(92)
M. cavendish green peel hydroaloholic extract	Human colorectal adenocarcinoma Caco-2 cells	⊥Proliferation	29.7 ± 0.007% inhibition at 1000 μg/mL	(91)
Protocatechualdehyde	HCT116 and SW480	⊥Proliferation; ↑apoptosis; ↓ (HDAC2)-initiated cyclin D1; ↓CDK4; ↓enzymatic activity of HDAC; ↓HDAC2; cell cycle arrest from G_1 to S phase; ↑ATF3; ↑mRNA ATF3; ↑p-ERK1/2; ↑MAPK; ↑ PARP cleavage	71% inhibition at 200 μM and 58% inhibition at 200 μM 43% reduced cell viability at 200 μM and 56% reduced cell viability at 200 μM	(42, 98)
2-pentanone	HT29	⊥ PGE_2; ⊥COX-2	400 μM	(59)
Liver cancer				
Musa cavendish green peel hydroaloholic extract	Hepatocellular carcinoma HepG2 cells	↑Cytotoxicity; ⊥proliferation; ↑apoptosis; ↑necrosis; ↓MMP; ↑ROS	100 μg/mL; 100-400 μg/mL (apoptosis); 100, 200 and 400 μg/mL	(91)
Crude extracts (BPS and BR) of chloroform and acetone	HepG2 cells	↑Cytotoxicity	25 μg/mL (chloroform); 300 μg/mL (acetone)	(99)
4-epicyclomusalenone	HepG2 cells	↑Cytotoxicity	108 ± 1.8 μg/mL	
Cycloeucalenol acetate	HepG2 cells	↑Cytotoxicity	93 ± 1.5 μg/mL	
Chlorogenic acid	HepG2 cells	↑Cytotoxicity	382 ± 3.6μg/mL	
Oral cancer				
Ethyl acetate fraction of ethanol extract of banana soft piths (BSPs)	Human oral squamous cell carcinoma (OSCC) cell lines (HSC-4)	↑Cytotoxicity	26.95 μg/mL	(100)
Prostate cancer				
Aqueous banana flower extract	Epithelial cell line BPH-1 cells	⊥Proliferation; cell cycle arrest at G_1 phase; ↓cyclin D1; ↓cyclin dependent kinase (Cdk) 6; ↑p53; ↑p27; ⊥ PGE_2; ⊥COX-2	2 mg/mL	(101)
Banana peel methanolic extract	LNCaP human prostate cancer cell line	⊥Testosterone induced cell growth; ⊥5α-reductase activity	25 μg/mL	(102)
Skin cancer				
Musa cavendish green peel hydroaloholic extract	Malignant melanoma A-375 cells	⊥Proliferation; ↓MMP	100 μg/mL	(91)
Sucrier banana peel methanolic extracts	B16F10 mouse melanoma cells	↓MITF; ↑p-p38; ↑MITF protein degradation	100-500 μg/mL	(103)

Various symbols (↑, ↓ and ⊥) indicate increase, decrease and inhibition in the obtained variables, respectively.

TABLE 3 | *In vivo* anticancer activities of *Musa* spp. extracts.

Materials tested	Animal models	Effects and mechanisms	Dose	References
Breast cancer				
Aqueous extract of ripe banana	Erhlich's ascites carcinoma cells in Swiss albino mice	Prolonged survival and reduced tumor development	2 g banana/day/ mouse	(104)
MAL from the phloem exudates of *M. acuminate* pseudostem	Erhlich's ascites carcinoma cells in Swiss albino mice	⊥Tumor development; ↓neoangiogenesis; ↑survival	10mg/kg	(94)
Colon cancer				
Green banana flour (10%) as supplement	DMH-induced colon carcinogenesis in male Swiss mice	↓Number of aberrant crypt foci	Not specified	(105)

Various symbols (↑, ↓ and ⊥) indicate increase, decrease and inhibition in the obtained variables, respectively.

acid was extracted and purified from the acetone extract of the banana rhizome. These compounds also exhibited potent cytotoxicity against HepG2 cell lines.

Oral Cancer

Ethyl acetate sub-fraction of the ethanol extract of banana (*M. paradisiaca*) soft piths (BSPs) exhibited potent cytotoxic and antiproliferative activity against the human oral squamous cell carcinoma (OSCC) cell line (HSC-4) (100).

Prostate Cancer

Aqueous banana flower extract exhibited anticancer activity against benign prostatic hyperplasia (BPH) *in vitro*. The banana flower extract at a concentration of 2 mg/mL reduced the viability of BPH-1 cells through cell-cycle arrest at the G_1 phase. Moreover, it reduced the expression level of cyclin D1 and cyclin-dependentkinase6 (Cdk6) and elevated the expression level of p53 and p27 (101). It further reduced PGE_2 production by inhibition of COX-2 enzymes during inflammation, which has shown to be the key factor in BPH-1 cell growth and proliferation. In another study, the methanol fraction of the banana peel inhibited testosterone-induced cell growth in a concentration-dependant manner against the androgen-responsive LNCaP human prostate carcinoma cell line by inhibiting 5α-reductase activity (102).

Skin Cancer

M. cavendish green peel hydroalcoholic extract demonstrated antiproliferative and cytotoxic activity against A-375 human malignant melanoma cells at a concentration of 100 μg/mL (91). Another study demonstrated that Sucrier banana peel methanolic extract induced inhibition of melanogenesis in B16F10 mouse melanoma cells by down-regulating microphthalmia-associated transcription factor (MITF) expression and p38 signaling pathway and up-regulating the phosphorylation of p38, which activated the MITF protein degradation at concentrations of 100-500 μg/mL (103).

Clinical Studies

According to a hospital-based case-control analysis of Singapore Chinese esophageal cancer patients, esophageal cancer occurs at a higher incidence in male patients who eat fewer or no bananas in their diet and weekly consumption of banana reduces the risk of esophageal cancer (107). Moreover, based on a population-based case-control study, frequent consumption of bananas (8.9 g/day) lowers the risk of breast cancers (108). Clinical evidence from randomized controlled trials has been lacking. Hence, additional clinical trials are needed to understand the therapeutic effectiveness of banana constituents. Banana is a very acceptable food for all types of communities. So, banana should be a part of regular diet to reduce the incidence of esophageal cancer and breast cancer; however other similar clinical studies should be performed to analyze the therapeutic activity of banana on other cancer types.

CONCLUSION AND FUTURE PERSPECTIVES

Banana is a magnificent plant that has been cultivated for food and medicinal purposes for thousands of years. We have summarized various secondary metabolites from different banana plant belonging to *Musa* species in this review. In this article, we analyzed the *in vitro* and *in vivo* chemopreventive and chemotherapeutic effects of banana and its phytochemicals and also the toxicity of specific active components. The phytoconstituents were isolated from different varieties of banana belonging to *Musa* species, such as *M. accuminata, M. balbisiana*, and other varieties; among which majority of the phytoconstituents belonging to *M. accuminata* which exhibited chemopreventive and anticancer activities. There are variations in the phytochemical compositions of different varieties of banana due to soil, temperature, banana variety, maturation stage, processing location, and other variables. While the banana fruit (including the pulp and peel) has gained a lot of interest, other parts of the banana plant, such as the leaf, flower, and stem, have also been investigated for anticancer purposes. In addition to banana extracts and fractions, some phytoconstituents, including ferulic acid, protocatechualdehyde, 2-pentanone, 4-epicyclomusalenone, cycloeucalenol acetate, and chlorogenic acid, have been shown to exhibit cancer preventative and anticancer therapeutic abilities. Cancer preventive studies are limited, although two such study is reported where consumption of banana can reduce the incidence of esophageal cancer (107) and breast cancers (108); however other similar studies should be performed to analyze the cancer preventive activity of banana on other cancer types. We have

also addressed the various mechanisms by which numerous extracts of banana and their active constituents carry out their biological functions in cancer. Bioactive components present in bananas have exhibited momentous cancer preventive and anticancer activities utilizing various mechanisms, which include cytotoxicity, cell cycle arrest, apoptosis of cancer cells, antioxidant, and anti-inflammatory effects. The cell cycle is a sequence of events in a cell that split it into two cells. Cell cycle check points are control mechanisms that ensure the proper progression. Banana and its phytoconstituents induced cell cycle arrest at these check points to halt the progression through the cell cycle of neoplastic cells (**Figure 7**). Banana phytoconstituents also demonstrate various mechanisms in the modulation of diverse, dysregulated signaling pathways in order to prohibit cancer progression (**Figure 8**). Banana and its phytochemicals are able to induce changes in expression level of some commonly known genes to regulate well-known signaling networks, such as MAPK signaling pathways, the ERK signaling pathway, the ERK1/2 signaling pathway, and HDAC2 signaling pathway, in addition to inhibiting pro-inflammatory mediators, such as COX-2. By modulating these pathways, phytoconstituents from banana restraint cell proliferation, adhesion, invasion, and angiogenesis in breast, cervical, colorectal, esophageal, hepatic, oral, prostate, and skin cancers (**Figure 9**).

Poor bioavailability and bioaccessibility of various phytochemical constituents of banana are barriers to their therapeutic use. The weak bioavailability as well as bioaccessibility were due to the initial hepatic first pass effect, poor absorption of the intestines, and low solubility (Sidhu and Zafar, 2018). Different aspects, such as banana processing and variety, often affect bioavailability and accessibility.

Despite the vast amount of research that has been performed and documented over the last few decades, the bulk of the findings cited in this review are focused on *in vitro* experiments. Breast, cervical, colorectal, esophageal, hepatic, oral, prostate, and skin cancers are only a few of the cancer types affected by banana and its phytochemicals. The reviewed literature reveals the promise that banana and its phytochemicals can be used in chemotherapy for different forms of cancer. The role of banana and its phytoconstituents on breast cancer and colon cancer have been studied extensively in both *in vitro* and *in vivo* research. Findings from *in vivo* studies on other cancer types and clinical situations are sparse. With encouraging preclinical data, mechanistic investigations on anticancer actions of the components of banana are warranted. The translation impact of available research findings is restricted by the lack of well-designed, prospective clinical studies and safety evaluation of banana extracts and constituents in humans. The potential pharmacokinetic constraints of banana phytochemicals highlight the need to establish efficient and well-regulated delivery mechanisms for optimized delivery systems against various malignancies. More experiments on novel molecular targets and signaling pathways of banana bioactive materials, in addition to well-controlled clinical trials, will increase the therapeutic potential of this popular and medicinal fruit for cancer prevention and treatment. According to the selective toxicity tests, bananas and their main components are safe. However, more research is to be carried out to see whether the same favourable safety profile occurs in human subjects, and to determine which banana secondary metabolites may be cytotoxic, if any. Moreover, banana-derived products may be utilized as an adjuvant to various chemotherapeutic drugs (which have many adverse side effects) for a variety of cancer subtypes.

Our systematic study and review of limitations also identify various future research paths. Although numerous bioactive banana compounds have been identified, further research into the anticancer ability of these phytochemicals found in bananas is required. Furthermore, since the bulk of research is limited to *in vitro* studies, more *in vivo* mechanistic experiments should

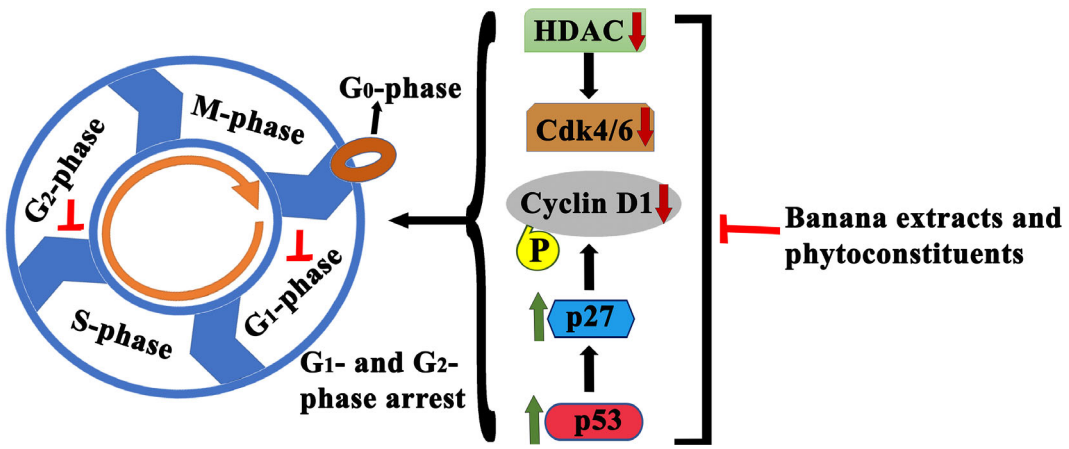

FIGURE 7 | Schematic illustration of anticancer effects of banana extracts and its phytoconstituents through cell cycle arrest. Multiple studies found cell cycle arrest effects of banana extracts and its phytoconstituents at various check points which lead to the proliferation inhibition.

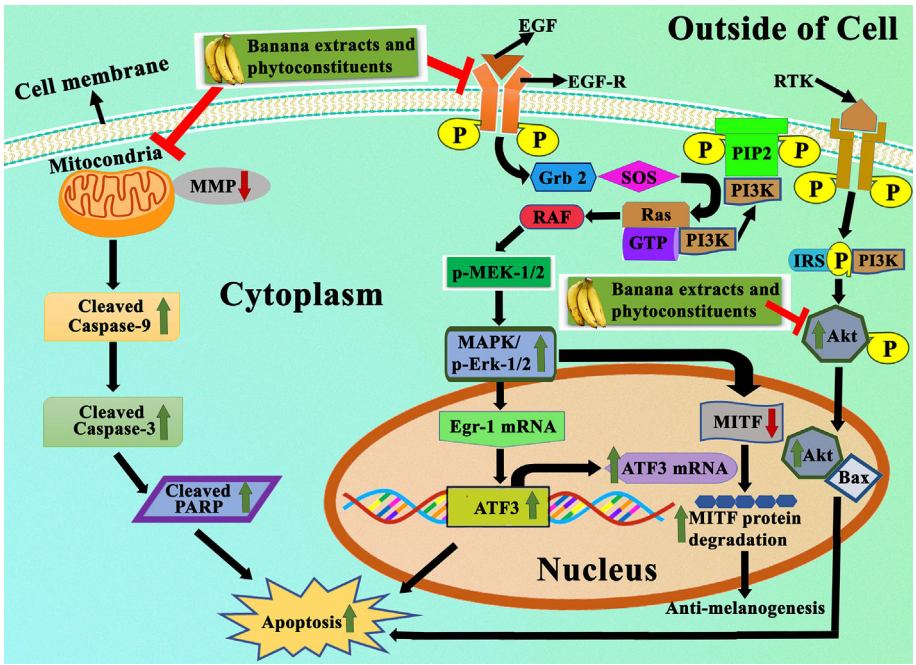

FIGURE 8 | Representation of apoptotic effects of banana extracts and its bioactive phytoconstituents. Under the apoptotic effects, banana extracts and its bioactive phytoconstituent can induce the expression of Bax, caspase-3, caspase-9, cleaved PARP and block the expression of Bcl-2. It also regulates the MAPK/ERK1/2 signaling pathway, PI3K-Aktsignaling pathway, in which the expressional levels of p-ERK1/2, ATF3, and ATF3 are modulated.

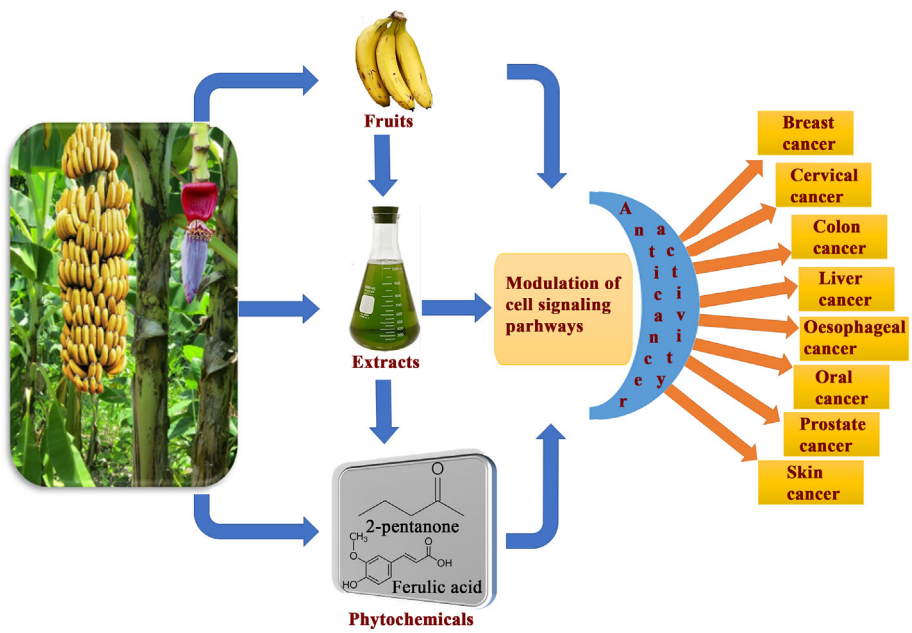

FIGURE 9 | Overview of consumption banana fruits, extracts and its phytoconstituents exhibiting cancer preventive and anticancer activity against various cancer types through modulation of diverse cell signaling pathways.

be performed. Provided the positive anticancer findings presented in this study, randomized clinical trials involving banana phytochemicals should be carried out. However, further research into the anticancer ability of other important phytochemicals found in bananas is warranted. Characterization of different phytochemicals found in bananas that function alone or synergistically with other compounds or established drugs to have cancer ameliorative or protective effects is also required. In conclusion, based on our in-depth analysis of the existing literature, banana extracts and the isolated phytoconstituents found in banana present as promising medicinal agents for cancer prevention and these agents could also be developed as multi-targeted drugs for cancer pharmacotherapy.

DATA AVAILABILITY STATEMENT

The original contributions presented in the study are included in the article/supplementary material. Further inquiries can be directed to the corresponding authors.

AUTHOR CONTRIBUTIONS

Conceptualization: AM. Literature search and collection: SBo, SBa, and PD. Writing—original draft preparation: AM, SBa, and ES. Writing—review and editing: AM, AA, and AB. Supervision: AM. Project administration: AB. All authors contributed to the article and approved the submitted version.

REFERENCES

1. Gupta SC, Kim JH, Prasad S, Aggarwal BB. Regulation of Survival, Proliferation, Invasion, Angiogenesis, and Metastasis of Tumor Cells Through Modulation of Inflammatory Pathways by Nutraceuticals. *Cancer Metastasis Rev* (2010) 29(3):405–34. doi: 10.1007/s10555-010-9235-2
2. de Mesquita ML, de Paula JE, Pessoa C, de Moraes MO, Costa-Lotufo LV, Grougnet R, et al. Cytotoxic Activity of Brazilian Cerrado Plants Used in Traditional Medicine Against Cancer Cell Lines. *J Ethnopharmacol* (2009) 123:439–45. doi: 10.1016/j.jep.2009.03.018
3. Mondal A, Bose S, Banerjee S, Patra JK, Malik J, Mandal SK, et al. Marine Cyanobacteria and Microalgae Metabolites-A Rich Source of Potential Anticancer Drugs. *Mar Drugs* (2020) 18:476. doi: 10.3390/md18090476
4. Clapp RW, Jacobs MM, Loechler EL. Environmental and Occupational Causes of Cancer New Evidence, 2005–2007. *Rev Environ Health* (2008) 23 (1):1. doi: 10.1515/reveh.2008.23.1.1
5. Bose S, Banerjee S, Mondal A, Chakraborty U, Pumarol J, Croley CR, et al. Targeting the JAK/STAT Signaling Pathway Using Phytocompounds for Cancer Prevention and Therapy. *Cells* (2020) 9(6):1451. doi: 10.3390/cells9061451
6. Laget S, Defossez PA. Master and Servant: Epigenetic Deregulations as a Cause and a Consequence of Cancer. *Med Sci (Paris)* (2008) 24(8–9):725–30. doi: 10.1051/medsci/20082489725
7. Tansaz M, Tajadini H. Comparison of Leiomyoma of Modern Medicine and Traditional Persian Medicine. *J Evid Based Complementary Altern Med* (2016) 21(2):160–3. doi: 10.1177/2156587215595299
8. Newman DJ, Cragg GM. Natural Products as Sources of New Drugs Over the Nearly Four Decades From 01/1981 to 09/2019. *J Nat Prod* (2020) 83 (3):770–803. doi: 10.1021/acs.jnatprod.9b01285
9. Bishayee A, Sethi G. Bioactive Natural Products in Cancer Prevention and Therapy: Progress and Promise. *Semin Cancer Biol* (2016) 40:1–3. doi: 10.1016/j.semcancer.2016.08.006
10. Block KI, Gyllenhaal C, Lowe L, Amedei A, Amin AR, Amin A, et al. Designing a Broad-Spectrum Integrative Approach for Cancer Prevention and Treatment. *Semin Cancer Biol* (2015) 35:S276–304. doi: 10.1016/j.semcancer.2015.09.007
11. Kotecha R, Takami A, Espinoza JL. Dietary Phytochemicals and Cancer Chemoprevention: A Review of the Clinical Evidence. *Oncotarget* (2016) 7 (32):52517. doi: 10.18632/oncotarget.9593
12. Lefranc F, Tabanca N, Kiss R. Assessing the Anticancer Effects Associated With Food Products and/or Nutraceuticals Using *In Vitro* and *In Vivo* Preclinical Development-Related Pharmacological Tests. *Semin Cancer Biol* (2017) 46:14–32. doi: 10.1016/j.semcancer.2017.06.004
13. Karadi RV, Shah A, Parekh P, Azmi P. Antimicrobial Activities of *Musa Paradisiaca* and *Cocos Nucifera*. *Int J Res Pharm Biomed Sci* (2011) 2(1):264–7.
14. Constantine D, Rossel G. *The Musaceae. An Annotated List of the Species of Ensete, Musa & Musella* (2001). Available at: http://www.users.globalnet.co.uk/~drc/musaceae.htm.
15. Subbaraya U. *Farmers Knowledge of Wild Musa in India*. Rome: Food and Agriculture Organization of the United States (2006).
16. Ploetz RC, Evans EA. The Future of Global Banana Production. *Hortic Rev* (2015) 43:311–52. doi: 10.1002/9781119107781.ch06
17. Karamura D, Karamura EB, Guy B. General Plant Morphology of Musa. In: M Pillay and A Tenkouano, editors. *Banana Breeding*. Boca Raton, FL, USA: CRC Press (2011). p. 1–20. doi: 10.1201/b10514-2
18. Chintamunnee V, Mahomoodally MF. Herbal Medicine Commonly Used Against Non-Communicable Diseases in the Tropical Island of Mauritius. *J Herb Med* (2012) 2(4):113–25. doi: 10.1016/j.hermed.2012.06.001
19. Ghorbani A, Langenberger G, Liu JX, Wehner S, Sauerborn J. Diversity of Medicinal and Food Plants as Non-Timber Forest Products in Naban River Watershed National Nature Reserve (China): Implications for Livelihood Improvement and Biodiversity Conservation. *Econ Bot* (2012) 66(2):178–91. doi: 10.1007/s12231-012-9188-1
20. Muthee JK, Gakuya DW, Mbaria JM, Kareru PG, Mulei CM, Njonge FK. Ethnobotanical Study of Anthelmintic and Other Medicinal Plants Traditionally Used in Loitoktok District of Kenya. *J Ethnopharmacol* (2011) 135(1):15–21. doi: 10.1016/j.jep.2011.02.005
21. De Wet H, Ramulondi M, Ngcobo ZN. The Use of Indigenous Medicine for the Treatment of Hypertension by a Rural Community in Northern Maputaland, South Africa. *South Afr J Bot* (2016) 103:78–88. doi: 10.1016/j.sajb.2015.08.011
22. Okon JE, Esenowo GJ, Afaha IP, Umoh NS. Haematopoietic Properties of Ethanolic Fruit Extract of *Musa Acuminata* on Albino Rats. *Bull Env Pharmacol Life Sci* (2013) 2:22–6.
23. Di Stasi LC, Oliveira GP, Carvalhaes MA, Queiroz-Junior M, Tien OS, Kakinami SH, et al. Medicinal Plants Popularly Used in the Brazilian Tropical Atlantic Forest. *Fitoterapia* (2002) 73(1):69–91. doi: 10.1016/s0367-326x(01)00362-8
24. Camacho-Corona MD, Ramírez-Cabrera MA, Santiago OG, Garza-González E, Palacios ID, Luna-Herrera J. Activity Against Drug Resistant-Tuberculosis Strains of Plants Used in Mexican Traditional Medicine to Treat Tuberculosis and Other Respiratory Diseases. *Phytother Res* (2008) 22 (1):82–5. doi: 10.1002/ptr.2269
25. Ticktin T, Dalle SP. Medicinal Plant Use in the Practice of Midwifery in Rural Honduras. *J Ethnopharmacol* (2005) 96:233–48. doi: 10.1016/j.jep.2004.09.015
26. Kamatenesi-Mugisha M, Oryem-Origa H. Medicinal Plants Used to Induce Labour During Childbirth in Western Uganda. *J Ethnopharmacol* (2007) 109 (1):1–9. doi: 10.1016/j.jep.2006.06.011
27. De Wet H, Nzama VN, Van Vuuren SF. Medicinal Plants Used for the Treatment of Sexually Transmitted Infections by Lay People in Northern Maputaland, Kwazulu–Natal Province, South Africa. *South Afr J Bot* (2012) 78:12–20. doi: 10.1016/j.sajb.2011.04.002
28. Kambizi L, Afolayan AJ. An Ethnobotanical Study of Plants Used for the Treatment of Sexually Transmitted Diseases (Njovhere) in Guruve District, Zimbabwe. *J Ethnopharmacol* (2001) 77:5–9. doi: 10.1016/s0378-8741(01)00251-3

29. Mathew NS, Negi PS. Traditional Uses, Phytochemistry and Pharmacology of Wild Banana (*Musa Acuminate* Colla): A Review. *J Ethnopharmacol* (2017) 196:124–40. doi: 10.1016/j.jep.2016.12.009
30. Pereira A, Maraschin M. Banana (*Musaspp*) From Peel to Pulp: Ethnopharmacology, Source of Bioactive Compounds and Its Relevance for Human Health. *J Ethnopharmacol* (2015) 160:149–63. doi: 10.1016/j.jep.2014.11.008
31. Vilela C, Santos SA, Villaverde JJ, Oliveira L, Nunes A, Cordeiro N, et al. Lipophilic Phytochemicals From Banana Fruits of Several Musa Species. *Food Chem* (2014) 162:247–52. doi: 10.1016/j.foodchem.2014.04.050
32. Islam MR, Afrin S, Khan TA, Howlader ZH. Nutrient Content and Antioxidant Properties of Some Popular Fruits in Bangladesh. *Int J Pharm Sci Res* (2015) 6:1407–14. doi: 10.13040/IJPSR.0975-8232.6(4).1407-14
33. Niamah AK. Determination, Identification of Bioactive Compounds Extracts From Yellow Banana Peels and Used *In Vitro* as Antimicrobial. *Int J Phytomedicine* (2014) 6:625–32.
34. Lu Q, Liu T, Wang N, Dou Z, Wang K, Zuo Y. Nematicidal Effect of Methyl Palmitate and Methyl Stearate Against *Meloidogyne Incognita* in Bananas. *J Agric Food Chem* (2020) 68(24):6502–10. doi: 10.1021/acs.jafc.0c00218
35. Budirohmi A, Ahmad A, Taba P, Tahir D. Isolation and Characterization of Starch From the Hump of Kepok Banana (*Musa Balbisiana*. L) as a Precursor of Biodegradable Polyurethane Synthesis. *J Phys Conf Ser* (2019) 1341(3):32026. doi: 10.1088/1742-6596/1341/3/032026
36. Meenashree B, Vasanthi VJ, Mary RN. Evaluation of Total Phenolic Content and Antimicrobial Activities Exhibited by the Leaf Extracts of *Musa Acuminata* (Banana). *Int J Curr Microbiol Appl Sci* (2014) 3:136–41.
37. Mahouachi J, López-Climent MF, Gómez-Cadenas A. Hormonal and Hydroxycinnamic Acids Profiles in Banana Leaves in Response to Various Periods of Water Stress. *Sci World J* (2014) 2014:540962. doi: 10.1155/2014/540962
38. Gunavathy N, Padmavathy S, Murugavel SC. Phytochemical Evaluation of *Musa Acuminata* Bract Using Screening, FT-IR and Uv-Vis Spectroscopic Analysis. *J Int Acad Res Multidiscip* (2014) 2:212–21.
39. Kitdamrongsont K, Pothavorn P, Swangpol S, Wongniam S, Atawongsa K, Svasti J, et al. Anthocyanin Composition of Wild Bananas in Thailand. *J Agric Food Chem* (2008) 56:10853–7. doi: 10.1021/jf8018529
40. Roobha JJ, Saravanakumar M, Aravindhan KM, Suganyadevi P. *In Vitro* Evaluation of Anticancer Property of Anthocyanin Extract From *Musa Acuminata* Bract. *Res Pharm* (2011) 1:17–21.
41. Bennett RN, Shiga TM, Hassimotto NM, Rosa EA, Lajolo FM, Cordenunsi BR. Phenolics and Antioxidant Properties of Fruit Pulp and Cell Wall Fractions of Postharvest Banana (*Musa Acuminata* Juss.) Cultivars. *J Agric Food Chem* (2010) 58(13):7991–8003. doi: 10.1021/jf1008692
42. Jeong JB, Lee SH. Protocatechualdehyde Possesses Anti-Cancer Activity Through Downregulating Cyclin D1 and HDAC2 in Human Colorectal Cancer Cells. *Biochem Biophys Res Commun* (2013) 430:381–6. doi: 10.1016/j.bbrc.2012.11.018
43. Pothavorn P, Kitdamrongsont K, Swangpol S, Wongniam S, Atawongsa K, Svasti J, et al. Sap Phytochemical Compositions of Some Bananas in Thailand. *J Agric Food Chem* (2010) 58:8782–7. doi: 10.1021/jf101220k
44. Gu L, Kelm MA, Hammerstone JF, Beecher G, Holden J, Haytowitz D, et al. Screening of Foods Containing Proanthocyanidins and Their Structural Characterization Using LC-MS/MS and Thiolytic Degradation. *J Agric Food Chem* (2003) 51:7513–21. doi: 10.1021/jf034815d
45. Swanson MD, Winter HC, Goldstein IJ, Markovitz DM. A Lectin Isolated From Bananas Is a Potent Inhibitor of HIV Replication. *J Biol Chem* (2010) 285:8646–55. doi: 10.1074/jbc.M109.034926
46. Thulasy G, Nair AS. Comparative Analysis of β-1,3-glucanase Protein Sequences and Structure in Two Banana Cultivars From Kerala. *J Food Biochem* (2018) 42:e12559. doi: 10.1111/jfbc.12559
47. Menezes EW, Tadini CC, Tribess TB, Zuleta A, Binaghi J, Pak N, et al. Chemical Composition and Nutritional Value of Unripe Banana Flour (*Musa Acuminata* Var. Nanicão). *Plant Foods Hum Nutr* (2011) 66:231–7. doi: 10.1007/s11130-011-0238-0
48. Mordi RC, Fadiaro AE, Owoeye TF, Olanrewaju IO, Uzoamaka GC, Olorunshola SJ. Identification by GC-MS of the Components of Oils of Banana Peels Extract, Phytochemical and Antimicrobial Analyses. *Res J Phytochem* (2016) 10:39–44. doi: 10.3923/rjphyto.2016.39.44
49. Toh PY, Leong FS, Chang SK, Khoo HE, Yim HS. Optimization of Extraction Parameters on the Antioxidant Properties of Banana Waste. *Acta Sci Pol Technol Aliment* (2016) 15:65–78. doi: 10.17306/J.AFS.2016.1.7
50. Amorim EP, Cohen KDO, Amorim VBDO, Paes NS, Sousa HN, Santos-Serejo JAD, et al. Characterization of Banana Accessions Based on the Concentration of Functional Compounds. *Ciec Rural* (2011) 41:592–8. doi: 10.1590/S0103-84782011005000042
51. Borges CV, de Oliveira Amorim VB, Ramlov F, da Silva Ledo CA, Donato M, Maraschin M, et al. Characterisation of Metabolic Profile of Banana Genotypes, Aiming at Biofortified *Musa* Spp. Cultivars. *Food Chem* (2014) 145:496–504. doi: 10.1016/j.foodchem.2013.08.041
52. Hirai N, Ishida H, Koshimizu K. A Phenalenone-Type Phytoalexin From *Musa Acuminata*. *Phytochemistry* (1994) 37:383–5. doi: 10.1016/0031-9422(94)85064-x
53. Gonzalez-Montelongo R, Lobo MG, Gonzalez M. Antioxidant Activity in Banana Peel Extracts: Testing Extraction Conditions and Related Bioactive Compounds. *Food Chem* (2010) 119:1030–9. doi: 10.1016/j.foodchem.2009.08.012
54. Adão RC, Glória MBA. Bioactive Amines and Carbohydrate Changes During Ripening of 'Prata' Banana (*Musa Acuminata* × *M. Balbisiana*). *Food Chem* (2005) 90:705–11. doi: 10.1016/j.foodchem.2004.05.020
55. Tanasa V, Moise D, Stanca M. Separation and Quantification of Biogenic Amines in Bananas by High Performance Liquid Chromatography. *Food Environ Saf J* (2015) 14:245–9.
56. Kamo T, Kato N, Hirai N, Tsuda M, Fujioka D, Ohigashi H. Phenylphenalenone-Type Phytoalexins From Unripe Buñgulan Banana Fruit. *Biosci Biotechnol Biochem* (1998) 62:95–101. doi: 10.1271/bbb.62.95
57. Abad T, McNaughton-Smith G, Fletcher WQ, Echeverri F, Diaz-Peñate R, Tabraue C, et al. Isolation of (s)-(+)–Naproxene From *Musa Acuminata*. Inhibitory Effect of Naproxene and its 7-Methoxy Isomer on Constitutive COX-1 and Inducible COX-2. *Planta Med* (2000) 66:471–3. doi: 10.1055/s-2000-8581
58. Luque-Ortega JR, Martínez S, Saugar JM, Izquierdo LR, Abad T, Luis JG, et al. Fungal-Elicited Metabolites From Plants as an Enriched Source for New Leishmanicidal Agents. Antifungal Phenyl-Phenalenonephytoalexins From the Banana Plant (*Musa Acuminata*) Target Mitochondria of *Leishmania Donovani* Promastigotes. *Antimicrob Agents Chemother* (2004) 48:1534–40. doi: 10.1128/aac.48.5.1534-1540.2004
59. Pettersson J, Karlsson PC, Göransson U, Rafter JJ, Bohlin L. The Flavouring Phytochemical 2-Pentanone Reduces Prostaglandin Production and COX-2 Expression in Colon Cancer Cells. *Biol Pharm Bull* (2008) 31:534–7. doi: 10.1248/bpb.31.534
60. Borges CV, Maraschin M. Musa Spp.–Functional Properties, Biofortification, and Bioavailability. In: VA Pearson, editor. *Bananas: Cultivation, Consumption and Crop Diseases*. Hauppauge NY: Nova Science Publishers (2016). p. 1–26.
61. Tsamo CV, Herent MF, Tomekpe K, Emaga TH, Quetin-Leclercq J, Rogez H, et al. Phenolic Profiling in the Pulp and Peel of Nine Plantain Cultivars (*Musa* Sp.). *Food Chem* (2015) 167:197–204. doi: 10.1016/j.foodchem.2014.06.095
62. Tsamo CV, Herent MF, Tomekpe K, Emaga TH, Quetin-Leclercq J, Rogez H, et al. Effect of Boiling on Phenolic Profiles Determined Using HPLC/ESI-LTQ-Orbitrap-MS, Physico-Chemical Parameters of Six Plantain Banana Cultivars (*Musa* Sp). *J Food Compost Anal* (2015) 44:158–69. doi: 10.1016/j.jfca.2015.08.012
63. Aurore G, Parfait B, Fahrasmane L. Bananas, Raw Materials for Making Processed Food Products. *Trends Food Sci Technol* (2009) 20:78–91. doi: 10.1016/j.tifs.2008.10.003
64. Sheng Z, Dai H, Pan S, Ai B, Zheng L, Zheng X, et al. Phytosterols in Banana (Musa Spp.) Flower Inhibit α-Glucosidase and α-Amylasehydrolysations and Glycation Reaction. *Int J Food Sci Technol* (2017) 52:171–9. doi: 10.1111/ijfs.13263
65. Lopes S, Borges CV, de Sousa Cardoso SM, de Almeida Pereira da Rocha MF, Maraschin M. Banana (Musa Spp.) as a Source of Bioactive Compounds for Health Promotion. In: *Handbook of Banana Production, Postharvest Science, Processing Technology, and Nutrition*. Hoboken, NJ, USA: Wiley vol. 31. (2020). p. 227–44. doi: 10.1002/9781119528265.ch12

66. Xiao R, Beck O, Hjemdahl P. On the Accurate Measurement of Serotonin in Whole Blood. *Scand J Clin Lab Invest* (1998) 58:505–10. doi: 10.1080/00365519850186319
67. Bomtempo LL, Costa AM, Lima H, Engeseth N, Gloria MBA. Bioactive Amines in Passiflora Are Affected by Species and Fruit Development. *Food Res Int* (2016) 89:733–8. doi: 10.1016/j.foodres.2016.09.028
68. Plonka J, Michalski A. The Influence of Processing Technique on the Catecholamine and Indolamine Contents of Fruits. *J Food Compost Anal* (2017) 57:102–8. doi: 10.1016/j.jfca.2016.12.023
69. Moinard C, Cynober L, De Bandt JP. Polyamines: Metabolism and Implications in Human Diseases. *Clin Nutr* (2005) 24:184–97. doi: 10.1016/j.clnu.2004.11.001
70. Falcomer AL, Riquette RFR, de Lima BR, Ginani VC, Zandonadi RP. Health Benefits of Green Banana: A Systematic Review. *Nutrients* (2019) 11:1222. doi: 10.3390/nu11061222
71. Liyanage R, Rizliya V, Jayathilake C, Jayawardana BC, Vidanarachchi JK. (2015). Hypolipidemic Activity and Hypoglycemic Effects of Banana Blossom (*Musa Acuminate* Colla) Incorporated Experimental Diets in Wistar Rats. In: *Sri Lanka Association for the Advancement of Science Proceedings of the 71st Annual Sessions*, Part I Section E2 601/E2. Gangodawila, Nugegoda, Sri Lanka: University of Sri Jayewardenepura.
72. Giri SS, Jun JW, Sukumaran V, Park SC. Dietary Administration of Banana (*Musa Acuminata*) Peel Flour Affects the Growth, Antioxidant Status, Cytokine Responses, and Disease Susceptibility of Rohu, Labeorohita. *J Immunol Res* (2016) 2016:4086591. doi: 10.1155/2016/4086591
73. Benny P, Viswanathan G, Thomas S, Nair A. Investigation of Immunostimulatory Behaviour of *Musa Acuminat*a Peel Extract in *Clarias Batrachus*. *Inst Int Omics Appl Biotech J* (2010) 1:39–43.
74. Singhal M, Ratra P. Investigation of Immunomodulatory Potential of Methanolic and Hexane Extract of *Musa Acuminata* Peel (Plantain) Extracts. *Glob J Pharmacol* (2013) 7:69–74. doi: 10.5829/idosi.gjp.2013.7.1.71145
75. Lee KH, Padzil AM, Syahida A, Abdullah N, Zuhainis SW, Maziah M, et al. Evaluation of Anti-Inflammatory, Antioxidant and Antinociceptive Activities of Six Malaysian Medicinal Plants. *J Med Plants Res* (2011) 5:5555–63. doi: 10.5897/JMPR.9000612
76. Sumathy V, Lachumy SJ, Zakaria Z, Sasidharan S. *In Vitro* Bioactivity and Phytochemical Screening of *Musa Acuminata* Flower. *Pharmacologyonline* (2011) 2:118–27.
77. Ling SSC, Chang SK, Sia WCM, Yim HS. Antioxidant Efficacy of Unripe Banana (*Musa Acuminate* Colla) Peel Extracts in Sunflower Oil During Accelerated Storage. *Acta Sci Pol Technol Aliment* (2015) 14:343–56. doi: 10.17306/J.AFS.2015.4.34
78. Anal AK, Jaisanti S, Noomhorm A. Enhanced Yield of Phenolic Extracts From Banana Peels (*Musa Acuminate* Colla AAA) and Cinnamon Barks (*Cinnamomum Varum*) and Their Antioxidative Potentials in Fish Oil. *J Food Sci Technol* (2014) 51:2632–9. doi: 10.1007/s13197-012-0793-x
79. Rasidek NAM, Nordin MFM, Shameli K. Formulation and Evaluation of Semisolid Jelly Produced by *Musa Acuminate* Colla (AAA Group) Peels. *Asian Pac J Trop BioMed* (2016) 6:55–9. doi: 10.1016/j.apjtb.2015.09.025
80. Lee EH, Yeom HJ, Ha MS, Bae DH. Development of Banana Peel Jelly and its Antioxidant and Textural Properties. *Food Sci Biotechnol* (2010) 19:449–55. doi: 10.1007/s10068-010-0063-5
81. Ugbogu EA, Ude VC, Elekwa I, Arunsi UO, Uche-Ikonne C, Nwakanma C. Toxicological Profile of the Aqueous-Fermented Extract of *Musa Paradisiaca* in Rats. *Avicenna J Phytomedicine* (2018) 8:478–87.
82. Abbas K, Rizwani GH, Zahid H, Qadir MI. Evaluation of Nephroprotective Activity of *Musa Paradisiaca* L. @ in Gentamicin-Induced Nephrotoxicity. *Pak J Pharm Sci* (2017) 30:881–90.
83. Tibolla H, Pelissari FM, Martins JT, Lanzoni EM, Vicente AA, Menegalli FC, et al. Banana Starch Nanocomposite With Cellulose Nanofibers Isolated From Banana Peel by Enzymatic Treatment: *In Vitro* Cytotoxicity Assessment. *Carbohydr Polym* (2019) 207:169–79. doi: 10.1016/j.carbpol.2018.11.079
84. Anosa GN, Okoro OJ. Anticoccidial Activity of the Methanolic Extract of *Musa Paradisiaca* Root in Chickens. *Trop Anim Health Prod* (2011) 43:245–8. doi: 10.1007/s11250-010-9684-1
85. Panigrahi PN, Dey S, Sahoo M, Dan A. Antiurolithiatic and Antioxidant Efficacy of *Musa Paradisiaca* Pseudostem on Ethylene Glycol-Induced Nephrolithiasis in Rat. *Indian J Pharmacol* (2017) 49:77–83. doi: 10.4103/0253-7613.201026
86. Ara F, Tripathy A, Ghosh D. Possible Antidiabetic and Antioxidative Activity of Hydro-Methanolic Extract of *Musa Balbisiana* (Colla) Flower in Streptozotocin-Induced Diabetic Male Albino Wistar Strain Rat: A Genomic Approach. *Assay Drug Dev Technol* (2019) 17:68–76. doi: 10.1089/adt.2018.889
87. Phuaklee P, Ruangnoo S, Itharat A. Anti-Inflammatory and Antioxidant Activities of Extracts From *Musa Sapientum* Peel. *J Med Assoc Thai* (2012) 95(1):S142–6.
88. Liberati A, Altman DG, Tetzlaff J, Mulrow C, Gøtzsche PC, Ioannidis JP, et al. The PRISMA Statement for Reporting Systematic Reviews and Meta-Analyses of Studies That Evaluate Health Care Interventions: Explanation and Elaboration. *PloS Med* (2009) 6:e1000100. doi: 10.1371/journal.pmed.1000100
89. Durgadevi PKS, Saravanan A, Uma S. Antioxidant Potential and Antitumour Activities of Nendran Banana Peels in Breast Cancer Cell Line. *Indian J Pharm Sci* (2019) 81:464–73. doi: 10.36468/pharmaceutical-sciences.531
90. Jenshi Roobha J, Aravindhan MSK. *In Vitro* Evaluation of Anticancer Property of Anthocyanin Extract From *Musa Acuminate* Bract. *Res Pharm* (2011) 1:17–21.
91. Barroso WA, Abreu IC, Ribeiro LS, da Rocha CQ, de Souza HP, de Lima TM. Chemical Composition and Cytotoxic Screening of *Musa Cavendish* Green Peels Extract: Antiproliferative Activity by Activation of Different Cellular Death Types. *Toxicol In Vitro* (2019) 59:179–86. doi: 10.1016/j.tiv.2019.04.020
92. Dahham SS, Mohamad TA, Tabana YM, Majid AMSA. Antioxidant Activities and Anticancer Screening of Extracts From Banana Fruit (*Musa Sapientum*). *Acad J Cancer Res* (2015) 8:28–34. doi: 10.5829/idosi.ajcr.2015.8.2.95162
93. Nadumane VK, Timsina B. Anti-Cancer Potential of Banana Flower Extract: An *In Vitro* Study. *Bangladesh J Pharmacol* (2014) 9:628–35. doi: 10.3329/bjp.v9i4.20610
94. Srinivas BK, Shivamadhu MC, Jayarama S. *Musa Acuminata* Lectin Exerts Anti-Cancer Effects on HeLa and EAC Cells *Via* Activation of Caspase and Inhibitions of Akt, Erk, and Jnk Pathway Expression and Suppresses the Neoangiogenesis In *in-Vivo* Models. *Int J Biol Macromol* (2021) 166:1173–87. doi: 10.1016/j.ijbiomac.2020.10.272
95. Srinivasan S, Valarmathi S, Illanchezian S, Dhanalakshmi KG. Anticancer Activity and DNA Fragmentation of Ferulic Acid From Banana Peel Using HeLa Cell Line. *Int J Res Dev Technol* (2017) 7:631–5.
96. Das A, Bindhu J, Deepesh P, Priya GS, Soundariya S. *In Vitro* Anticancer Study of Bioactive Compound Isolated From Musa Extract (*Musa Acuminata*). *Indian J Public Health Res Dev* (2020) 11:340–6. doi: 10.37506/v11/i1/2020/ijphrd/193841
97. Deep A, Upadhyay ON, Nandal R, Kumar S, Sharma AK, Wadhwa D. Anticancer Potential of Musa× Paradisiaca as Cervical Carcinoma and Malignant Melanoma. *Res Square* (2021) 1–16. doi: 10.21203/rs.2.20790/v1
98. Lee JR, Lee MH, Eo HJ, Park GH, Song HM, Kim MK, et al. The Contribution of Activating Transcription Factor 3 to Apoptosis of Human Colorectal Cancer Cells by Protocatechualdehyde, A Naturally Occurring Phenolic Compound. *Arch Biochem Biophys* (2014) 564:203–10. doi: 10.1016/j.abb.2014.10.005
99. Kandasamy S, Ramu S, Aradhya SM. *In Vitro* Functional Properties of Crude Extracts and Isolated Compounds From Banana Pseudostem and Rhizome. *J Sci Food Agric* (2016) 96:1347–55. doi: 10.1002/jsfa.7229
100. Ghafar SAA, Fikri IHH, Eshak Z. Antioxidant Activity of *Musa Paradisiaca* (Banana) Soft Pith and its Cytotoxicity Against Oral Squamous Carcinoma Cell Lines. *Malaysian J Sci Health Technol* (2019) 3:1–11.
101. Liu LC, Lin YH, Lin YC, Ho CT, Hung CM, Way TD, et al. Banana Flower Extract Suppresses Benign Prostatic Hyperplasia by Regulating the Inflammatory Response and Inducing G_1 Cell-Cycle Arrest. *In Vivo* (2018) 32:1373–9. doi: 10.21873/invivo.11389
102. Akamine K, Koyama T, Yazawa K. Banana Peel Extract Suppressed Prostate Gland Enlargement in Testosterone-Treated Mice. *Biosci Biotechnol Biochem* (2009) 73:1911–4. doi: 10.1271/bbb.80770
103. Phacharapiyangkul N, Thirapanmethee K, Sa-Ngiamsuntorn K, Panich U, Lee CH, Chomnawang MT. Effect of Sucrier Banana Peel Extracts on

Inhibition of Melanogenesis Through the ERK Signaling Pathway. *Int J Med Sci* (2019) 16:602–6. doi: 10.7150/ijms.32137
104. Guha M, Basuray S, Sinha AK. Preventive Effect of Ripe Banana in the Diet on Ehrlich's Ascitic Carcinoma Cell Induced Malignant Ascites in Mice. *Nutr Res* (2003) 23:1081–8. doi: 10.1016/S0271-5317(03)00090-3
105. Navarro SD, Mauro MO, Pesarini JR, Ogo FM, Oliveira RJ. Resistant Starch: A Functional Food That Prevents DNA Damage and Chemical Carcinogenesis. *Genet Mol Res* (2015) 14:1679–91. doi: 10.4238/2015. March.6.14
106. Mulvena D, Webb EC, Zerner B. 3, 4-Dihydroxybenzaldehyde a Fungistatic Substance From Green Cavendish Bananas. *Phytochemistry* (1969) 8:393–5. doi: 10.1016/S0031-9422(00)85436-9
107. De Jong UW, Breslow N, Goh Hong JE, Sridharan M, Shanmugaratnam K. Aetiological Factors in Oesophageal Cancer in Singapore Chinese. *Int J Cancer* (1974) 13:291–303. doi: 10.1002/ijc.2910130304
108. Malin AS, Qi D, Shu XO, Gao YT, Friedmann JM, Jin F, et al. Intake of Fruits, Vegetables and Selected Micronutrients in Relation to the Risk of Breast Cancer. *Int J Cancer* (2003) 105:413–8. doi: 10.1002/ijc.11088

Conflict of Interest: The authors declare that the research was conducted in the absence of any commercial or financial relationships that could be construed as a potential conflict of interest.

frontiers in Oncology

ORIGINAL RESEARCH
published: 12 July 2021
doi: 10.3389/fonc.2021.706586

Biologically Active α-Amino Amide Analogs and γδ T Cells—A Unique Anticancer Approach for Leukemia

*Ahmed Al Otaibi[1], Subuhi Sherwani[2], Salma Ahmed Al-Zahrani[1], Eida Mohammed Alshammari[1], Wahid Ali Khan[3], Abdulmohsen Khalaf D. Alsukaibi[1], Shahper Nazeer Khan[4] and Mohd Wajid Ali Khan[1,5]**

[1] Department of Chemistry, College of Sciences, University of Ha'il, Ha'il, Saudi Arabia, [2] Department of Biology, College of Sciences, University of Ha'il, Ha'il, Saudi Arabia, [3] Department of Clinical Biochemistry, College of Medicine, King Khalid University, Abha, Saudi Arabia, [4] Interdisciplinary Nanotechnology Centre, Aligarh Muslim University, Aligarh, India, [5] Molecular Diagnostic and Personalised Therapeutics Unit, University of Ha'il, Ha'il, Saudi Arabia

OPEN ACCESS

Edited by:
Jamal Arif,
Shaqra University, Saudi Arabia

Reviewed by:
Barira Islam,
University of Birmingham, United Kingdom
Mohammad Azhar Aziz,
King Abdullah International Medical Research Center (KAIMRC), Saudi Arabia
Mohammed Amir,
Weill Cornell Medical Center, United States

***Correspondence:**
Mohd Wajid Ali Khan
mw.khan@uoh.edu.sa;
wajidkhan11@gmail.com

Specialty section:
This article was submitted to Pharmacology of Anti-Cancer Drugs, a section of the journal Frontiers in Oncology

Received: 07 May 2021
Accepted: 16 June 2021
Published: 12 July 2021

Citation:
Otaibi AA, Sherwani S, Al-Zahrani SA, Alshammari EM, Khan WA, Alsukaibi AKD, Khan SN and Khan MWA (2021) Biologically Active α-Amino Amide Analogs and γδ T Cells—A Unique Anticancer Approach for Leukemia. Front. Oncol. 11:706586. doi: 10.3389/fonc.2021.706586

Advanced stage cancers are aggressive and difficult to treat with mono-therapeutics, substantially decreasing patient survival rates. Hence, there is an urgent need to develop unique therapeutic approaches to treat cancer with superior potency and efficacy. This study investigates a new approach to develop a potent combinational therapy to treat advanced stage leukemia. Biologically active α-amino amide analogs (RS)-N-(2-(cyclohexylamino)-2-oxo-1-phenylethyl)-N-phenylpropiolamide (α-AAA-A) and (RS)-N-(2-(cyclohexylamino)-2-oxo-1-phenylethyl)-N-phenylbut2-enamide (α-AAA-B) were synthesized using linear Ugi multicomponent reaction. Cytotoxicities and IC_{50} values of α-AAA-A and α-AAA-B against leukemia cancer cell lines (HL-60 and K562) were analyzed though MTT assay. Cytotoxic assay analyzed percent killing of leukemia cell lines due to the effect of γδ T cells alone or in combination with α-AAA-A or α-AAA-B. Synthesized biologically active molecule α-AAA-A exhibited increased cytotoxicity of HL-60 (54%) and K562 (44%) compared with α-AAA-B (44% and 36% respectively). Similarly, α-AAA-A showed low IC_{50} values for HL-60 (1.61 ± 0.11 μM) and K562 (3.01 ± 0.14 μM) compared to α-AAA-B (3.12 ± 0.15 μM and 6.21 ± 0.17 μM respectively). Additive effect of amide analogs and γδ T cells showed significantly high leukemia cancer cell killing as compared to γδ T cells alone. A unique combinational therapy with γδ T cells and biologically active anti-cancer molecules (α-AAA-A/B), concomitantly may be a promising cancer therapy.

Keywords: cancer, biologically active molecules, γδ T cells, cytotoxicity, combinational therapy, leukemia

INTRODUCTION

Cancer is a disease characterized by uncontrolled growth of cells, causing mortality worldwide. In 2018, it was estimated that cancer was the second leading cause of death worldwide and was responsible for 9.6 million deaths (1). In 2020, an estimated 1.8 million new cancer cases were diagnosed, and 606,520 cancer related deaths occurred in the US (2). According to the World Health

Organization, the statistics for Saudi Arabia reported that, of the total deaths in the year of 2012, 10.2% deaths were due to cancer. A substantial number of cancer related deaths in the Saudi adult population were due to colorectal cancer (males; 19.3%) and breast cancer (females; 29%) [World Health Organization-Cancer Country Profiles, (3)]. According to statistics reported in 2018, the most common type of cancer among Saudi children of both sexes was leukemia (34.6%) (4). There are a number of conventional drugs available for the treatment of leukemia. However, severe toxicities (cardiotoxicity, neuropathy, hepatotoxicity, renal toxicity etc.) have been registered for almost all the drugs, which may also cause morbidity and mortality in patients (5–8). Best approach to reduce the burden of these toxicities is to strategize for better outcome for patients.

Cancer treatment options may include the use of various techniques ranging from surgery, radiation, medications and/or other therapies to cure, shrink or stop the progression of a cancer. Monotherapeutic treatments have limitations when it comes to advanced stage cancers, due to disease progression which makes the disease more complex (9). Scientists and clinicians are making concerted efforts to develop pharmacological and immunological interventions for multiple targets, which are efficient, cost effective and could potentially increase the life span of patients with advanced stage cancers. Some clinical studies on pediatric leukemia showed that the efficacy of monotherapies was remarkably enhanced when another drug was administered together during the treatment (10). Currently, biologically active molecules and adoptive cell therapies are considered to be the most advanced areas of research in the development of potential therapeutics for cancer treatments.

Some important molecules, such as Brentuximab Vedotin, Gemtuzumab Ozogamicin, Ado-trastuzumab emtansine, polatuzumab vedotin-piiq, and inotuzumab ozogamicin, are combined with monoclonal antibodies specific to surface antigens present on particular tumor cells and are used as combinational-targeted cancer therapies (11). There are a number of newly synthesized α-amino amide derivatives, which show potent anticancer and cytotoxic activities against a wide range of cancer cell lines (12). Derivatives of 3-cyano pyridine also exhibited cytotoxic activities against many human MCF-7, HCT-116, and HepG-2 cancer cell lines (13). However, the cytotoxic effects of these biologically active anticancer molecules vary depending on the type of cancer, as well as dosage. Adaptive cancer therapy is involved in the eradication of tumor cells.

Various immune cells (T cells, NK cells, dendritic cells etc.) work differently in immunotherapies for cancer. γδ T cells are one of the unconventional T cells, which can be distinguished from αβ T cells (major T cell subset). These cells express Vγ9Vδ2-TCR on their cell surface. Other than tumor killing, γδ T cells have numerous important functions in immunity, including cytokine production and mobilization of other types of immune cells (at least *in vitro*), which favor these cells as an anticancer therapy option (14–16). γδ T cells led clinical trials have used these as effector cells in the treatment of various cancers, including breast carcinoma (17), colorectal carcinoma (18) and renal cell carcinoma (19) and found them to be well tolerated. Even *in vivo* infusion of γδ T cells recognized tumor cells and showed cytotoxicity against them (20).

The aims of this study are to elucidate the role of α-amino amide analogs (α-AAA) (RS)-N-(2-(Cyclohexylamino)-2-oxo-1-phenylethyl)-N-phenylpropiolamide (α-AAA-A) and (RS)-N-(2-(Cyclohexylamino)-2-oxo-1-phenylethyl)-N-phenylbut2-enamide (α-AAA-B), as anticancer agents and investigate their anti-proliferative or anti-metastatic activities alone or in combination with γδ T cells against leukemia cancer cell lines HL-60 and K562.

MATERIALS AND METHODS

RPMI-1640 medium, lymphoprep™, 0.9% saline (NaCl), millipore filter (0.22 μM), fetus calf serum (FCS), L-glutamine (200 mM; 100×), pen/strep (10,000 unit/ml pen and 10,000 units/ml strep), MEM sodium pyruvate (100 mM), non-essential amino acids (10 mM; 100×). IL-2 (100 IU/ml) were from GIBCO Life Technologies, (USA). Human recombinant interleukin-2 and interleukin-15 were from Novartis (Switzerland) and Miltenyi Biotec (Germany), respectively. Mouse monoclonal antibodies specific for CD3 (UCHT1), TCR-Vγ9 (Immu360) were from Beckman Coulter (USA). Fixable aqua dead cell stain kit was from Invitrogen-Life Technologies (USA). Human IgG, methanol, aniline, benzaldehyde, propiolic acid, cyclohexyl isocyanide, dimethyl sulfoxide (DMSO) and 3-[4,5-dimethylthiazol-2-yl]-2,5-diphenyltratrazolium bromide were purchased from Sigma Aldrich (USA). Zoledronic acid injection (4 mg) were purchased from Cipla, (India). HL-60 and K562 cell lines were received from ATCC (USA).

Synthesis of Biologically Active Molecules

Biologically active α-amino amide analogs (RS)-N-(2-(Cyclohexylamino)-2-oxo-1-phenylethyl)-N-phenylpropiolamide (α-AAA-A) and (RS)-N-(2-(Cyclohexylamino)-2-oxo-1-phenylethyl)-N-phenylbut2-enamide (α-AAA-B) were synthesized using linear Ugi multicomponent reaction (batch reaction with methanol) as published previously (12). Briefly, for the synthesis of α-AAA-A, a solution was prepared using methanol (5 ml), aniline (0.09 ml; 1 mmol) and benzaldehyde (0.1 ml; 1 mmol). This solution was stirred at 25°C for half an hour. Then propiolic acid (0.06 ml; 1 mmol) was added to this solution, followed by the addition of cyclohexyl isocyanide (0.11 ml; 1 mmol). This reaction mixture was further stirred at 25°C for 24 h till a precipitate was formed, which was washed with diethyl ether and dried to obtain a white solid (0.2 gm).

For the synthesis of α-AAA-B, similar linear Ugi multicomponent reaction was used. A solution was prepared using methanol (5 ml), aniline (0.09 ml; 1 mmol) and benzaldehyde (0.1 ml; 1 mmol). This solution was stirred at

25°C for half an hour. Then 2-butyric acid (23 gm; 1 mmol) was added to this solution, followed by the addition of cyclohexyl isocyanide (0.11 ml; 1 mmol). This reaction mixture was stirred further at 25°C for 24 h till a precipitate formed, which was washed with diethyl ether and dried to obtain a white solid (0.21 gm).

Cancer Cell Lines

HL-60 and K562 were grown in complete RPMI 1640 medium which included nonessential amino acids and was supplemented with 10% FCS, 1 mM sodium pyruvate and 2 mM L-glutamate. All cells were grown at 37°C in 95% air with the addition of 5% CO_2.

MTT Assay

The 3-[4,5-dimethylthiazol-2-yl]-2,5-diphenyltratrazolium bromide (MTT) assay has been done as described previously (21, 22) with slight modifications. Briefly, the incubation of 1×10^5 cells/mL cancer cells (HL-60 or K562) in complete RPMI medium, with or without the addition of amide analogs (α-AAA-A or α-AAA-B), was followed by incubation for different durations (4–24 h) at 5% CO_2 and 37°C. Thereafter, the cells were treated with 100 µl of MTT (5 mg/ml). Four hours later, the entire medium, including MTT solution, was aspirated from the wells. The remaining formazan crystals were dissolved in DMSO (50 µl) and absorbance was measured at 570 nm using a 96 well microplate reader. The cytotoxicity index was determined using the untreated cells as negative control. The percentage of cytotoxicity was calculated using the background-corrected absorbance as follows:

$$\%\ \text{cytotoxicity} = \frac{(1\ -\ \text{absorbance of experimental well}) \times 100}{\text{absorbance of negative control well}}$$

γδ T Cell Lines

γδ T cell lines were prepared as described in our previous research publication (14). Briefly, γδ T cells which were present in freshly isolated PBMCs, were stimulated using 1 µM zoledronate and were cultured in complete RPMI 1640 medium at a density of 10^6 cells/ml in 24-well culture plate and kept in CO_2 (5%) incubator at 37°C for 2 weeks. The level of water in the incubator was checked often to prevent decrease in levels of medium. Cytokines IL-2 (100 IU/ml) and IL-15 (10 ng/ml) were added to the culture at day 3, 6, 8 and 11, and cells were split and fresh medium added. At day 14, the percent γδ T cells in culture were examined by flow cytometry. Fixable aqua dead cell stain kit was used to detect percent live γδ T cells. Total number of live cells was counted using trypan blue stain.

Cell Surface Staining

Approximately 100,000 to 500,000 PBMCs, before and after expansion, were plated in a total volume of up to 250 µl. These were centrifuged at 1100 rpm for 3 min at 4°C in a centrifuge. The cell pellets were then washed with 200 µl phosphate buffer saline (PBS). Three microliters of fixable aqua dead cell stain were added and incubated for 15 min in the dark, followed by the addition of 200 µl PBS containing 2% FCS (FACS buffer). After incubation, cells were centrifuged (1100 rpm for 3 mins) and the supernatant discarded. Cells were blocked with 100 µl of 1:1000 diluted human IgG for 15 min on ice. After incubation cells were centrifuged (1100 rpm for 3 mins) and pelleted. Again, the supernatant was discarded. Then cells were stained with 40 µl cocktails of antibodies & isotype by further incubating for 20 min on ice in the dark. Approximately 160 µl FACS buffer was added after incubation and then the mixture was centrifuged (1100 rpm for 3 min) again. Finally, cells were resuspended in 100 µl FACS buffer and were analyzed by flow cytometer (Beckman Coulter Flow cytometer, Navios A52101).

Cytotoxic Effect of γδ T Cells

Tumor cell-killing activity of expanded γδ T cell (14 days) was tested on the leukemia cancer cell lines (HL-60 and K562). Cancer cells were labeled with the membrane dye CellVue. Labeled cancer cells were incubated together with γδ T cells at increasing target cell (T) to effector (E) ratios (1:1; 1:5; 1:10; 1:25) for 12 h in CO_2 (5%) incubator at 37°C. Cancer cell-killing was determined by flow cytometry.

Combinational Cytotoxic Effect

Combinational cancer cell killing was determined by flow cytometry. Cancer cells were labeled with the membrane dye CellVue. Labeled cancer cells were incubated together with γδ T cells at increasing target cell (T)/effector (E) ratios (1:1; 1:5; 1:10; 1:25) for 12 h in CO_2 (5%) incubator at 37°C. Combinational cytotoxic effects of biologically active molecules (α-AAA-A and α-AAA-B) and expanded γδ T were analyzed for leukemia cancer cell lines (HL-60 and K562). α-AAA-A or α-AAA-B were added to the culture with different target (HL-60 or K652)/effector (γδ T cells) ratios. Cancer cells and γδ T cells alone served as controls (ctrl). For HL-60 cancer cell line, the concentrations used of α-AAA-A and α-AAA-B were 3.125 and 6.26 µM, respectively. For K-562 cancer cell line, concentrations used of α-AAA-A and α-AAA-B were 6.26 and 12.5 µM, respectively. Each assay is representative of three experiments.

Statistical Analysis

All results were expressed as the mean ± SD. Multiple comparisons between data were done using software OriginPro 8.5 followed by Student's t test. The p value for significance was set at < 0.05.

RESULTS

Most of the drugs used in the treatment of leukemia cause severe toxicities and, hence, it is important to synthesize and test novel biologically active molecules which can potentially be used as anti-cancer agents with low toxicities. Two biologically active compounds (**Figure 1**), α-AAA-A and α-AAA-B, were synthesized using linear Ugi multicomponent reaction (batch reaction with methanol). Both molecules were isolated without any further purification and were stable at room temperature.

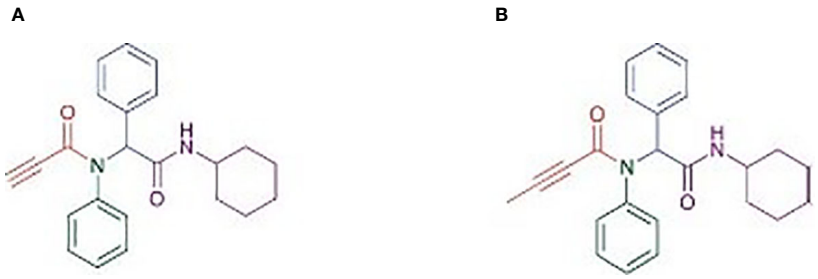

FIGURE 1 | Structure of α-amino amide analogs (RS)-N-(2-(Cyclohexylamino)-2-oxo-1-phenylethyl)-N-phenylpropiolamide **(A)** and (RS)-N-(2-(Cyclohexylamino)-2-oxo-1-phenylethyl)-N-phenylbut2-enamide **(B)**, synthesized using linear Ugi multicomponent reaction (batch reaction with methanol).

The cytotoxic effects of both biologically active molecules were analyzed for two different leukemia cancer cell lines (HL-60 and K562).

Cytotoxic Effect of Biologically Active Molecules

Cancer cell cytotoxicity was measured by MTT assay, and the absorbance was recorded at 570 nm. Comparably high cytotoxicity of HL-60 and K562 was recorded by α-AAA-A as compared to α-AAA-B. HL-60 cells visibly showed remarkably high inhibition at 3.125 μM after 12 h of incubation period, when co-cultured with α-AAA-A (**Figure 2A**). However, with α-AAA-B, increased inhibition was achieved at concentration of 6.25 μM after 12 h of incubation (**Figure 2B**). Highest percent of HL-60 cytotoxicity was 54% with α-AAA-A and 44% with α-AAA-B, respectively. No significant differences were observed in percent cell inhibition of HL-60 cells among α-AAA-A concentrations of 3.125, 6.25, and 12.5 μM for 12 and 24 h. However, significant differences ($p < 0.001$) were observed in percent cell inhibition of HL-60 cells between 1.56 and 3.125 μM concentrations after 12 and 24 h of incubations (**Figure 2A**). Similar patterns of cytotoxicity were observed with α-AAA-B, with exception of low percent inhibition at 3.125 μM (**Figure 2B**). Cancer cell cytotoxicities at 0.781 μM were significantly low for both molecules when compared with other concentrations.

Cancer cell line K562 cells showed high cytotoxicity at higher concentrations of 6.25 and 12.5 μM when incubated with α-AAA-A (**Figure 3A**) and α-AAA-B (**Figure 3B**), respectively post 12 h incubation periods. Highest percent of K562 cell cytotoxicities were 44% with α-AAA-A and 36% with α-AAA-B. Differences in percent cytotoxicity of K562 cells, using α-AAA-A at concentrations of 6.25 and 12.5 μM for 12 and 24 h, were not significant. However, observed percent cell cytotoxicity using α-AAA-A at concentrations of 0.781, 1.56, and 3.125 μM, were significantly lower ($p < 0.001$) when compared with concentrations 6.25 and 12.5 μM (**Figure 3A**).

For the molecule α-AAA-B, percent cytotoxicity of K562 cells at concentrations of 0.781, 1.56, 3.125, and 6.25 μM were significantly lower ($p < 0.001$) when compared with 12.5 μM (**Figure 3B**).

To determine the effect of solvent of molecules on the MTT assays, solvent in absence of molecules was also used as control,

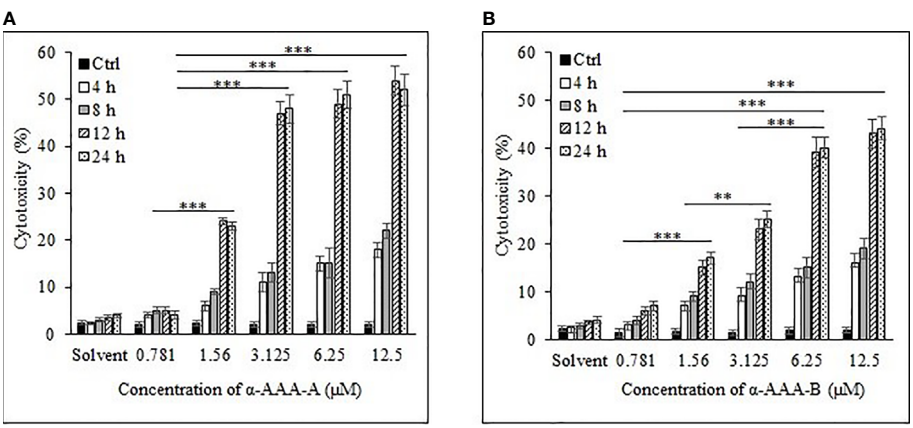

FIGURE 2 | Cancer cell line HL-60 cytotoxicity by α-AAA-A **(A)** and α-AAA-B **(B)** at different concentrations and durations of incubations. ***$P < 0.001$, when comparing cytotoxicity by α-AAA-A at 12.5, 6.25 and 3.125 μM with 1.56 μM after 12 and 24 h of incubations. ***$P < 0.001$, on comparing cytotoxicity by α-AAA-B at 12.5, 6.25 and 3.125 μM with 1.56 μM after 12 and 24 h of incubations. **$P < 0.01$, on comparing cytotoxicity by α-AAA-B at 1.56 with 3.125 μM. ***$P < 0.001$, on comparing cytotoxicity by α-AAA-A and α-AAA-B at 0.781 and 1.56 μM. Cancer cells without molecules served as control. Solvent was also used for different conditions.

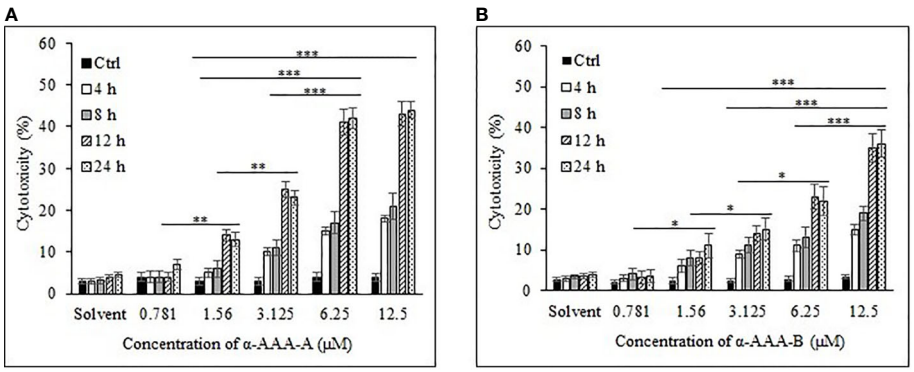

FIGURE 3 | Cancer cell line K562 cytotoxicity by α-AAA-A **(A)** and α-AAA-B **(B)** at different concentrations and time durations of incubations. ***$P < 0.001$, on comparing cytotoxicity by α-AAA-A at 12.5, 6.25 and 3.125 μM with 1.56 μM after 12 and 24 h of incubations. ***$P < 0.001$, on comparing cytotoxicity by α-AAA-B at 12.5 with 6.25 μM; 12.5 with 3.125 μM; 12.5 with 1.56 μM after 12 and 24 h of incubations. **$P < 0.01$, on comparing cytotoxicity by α-AAA-A at 3.125 with 1.56 μM; 1.56 with 0.781 μM. *$P < 0.05$, on comparing cytotoxicity by α-AAA-B at 6.25 with 3.125 μM; 3.125 with 1.56 μM; 1.56 with 0.781 μM.

and as expected, it did not show any appreciable cytotoxicity with different durations of incubation for both cancer cell lines (**Figures 2** and **3**).

These results show that α-AAA-A exhibited more cytotoxic effects on both leukemia cancer cell lines as compared to α-AAA-B. However, leukemia cancer cell line K562 showed more resistance against both molecules. Conventional FDA-approved drug methotrexate was also used to detect cytotoxicities against both leukemia cancer cell lines HL-60 and K562 (**Supplementary Figure 1**). Appreciable cytotoxicities were observed with higher concentrations of methotrexate.

Freshly isolated PBMCs were used as negative controls to test the cytotoxic effects of both analogs α-AAA-A (**Figure 4A**) and α-AAA-B (**Figure 4B**) using MTT assay. At varying concentrations (0.781–12.5 μM) of α-AAA-A and α-AAA-B, low cytotoxicities (4–7.6%) were observed with both the analogs. Similar findings were observed for another negative control used, i.e., normal breast cell line MCF10A, in which cytotoxicities were evaluated against both molecules α-AAA-A (**Figure 5A**) and α-AAA-B (**Figure 5B**). The cytotoxicity levels were found to be in the range of (3.3–7.1%) with the analogs.

IC_{50} Estimation

The half-maximal inhibitory concentration (IC_{50}) values were extrapolated from the concentration-response $\log_{10}$ graphs, using MTT assay. The IC_{50} values were calculated for HL-60 (**Figure 6A**) and were achieved at 1.61 ± 0.11 μM and 3.12 ± 0.15 μM for α-AAA-A and α-AAA-B, respectively. Cells of the leukemia cell line K562 (**Figure 6B**) exhibited the IC_{50} values at 3.01 ± 0.14 μM and 6.21 ± 0.17 μM for α-AAA-A and α-AAA-B, respectively. These results showed α-AAA-A showed greater cytotoxic effect as compared with α-AAA-B for both leukemia cancer cell lines HL-60 and K562.

Cytotoxic effect was demonstrated by both analogs in leukemia cancer cell lines HL-60 and K562, which varied with the concentrations of the molecules. Hence, both α-amino amide analogs can exhibit cytotoxicity toward both cancer cell lines in a dose- and time-dependent manner.

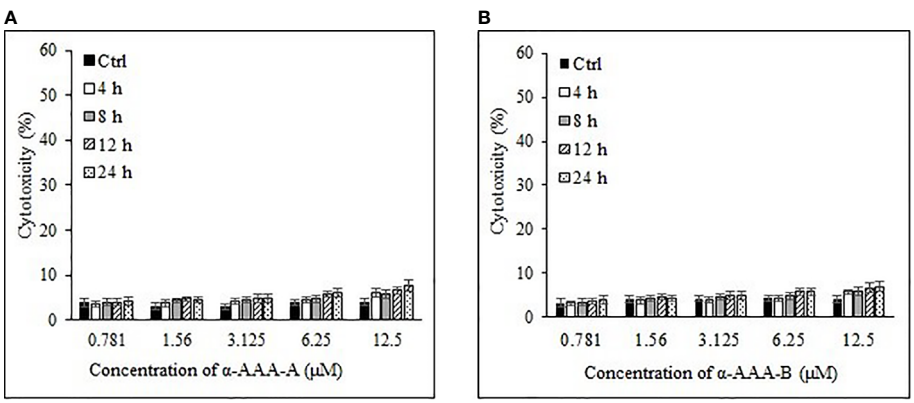

FIGURE 4 | Cytotoxicities of freshly isolated PBMCs cytotoxicities by α-AAA-A **(A)** and α-AAA-B **(B)** at different concentrations and time durations of incubation. PBMCs without molecules served as control.

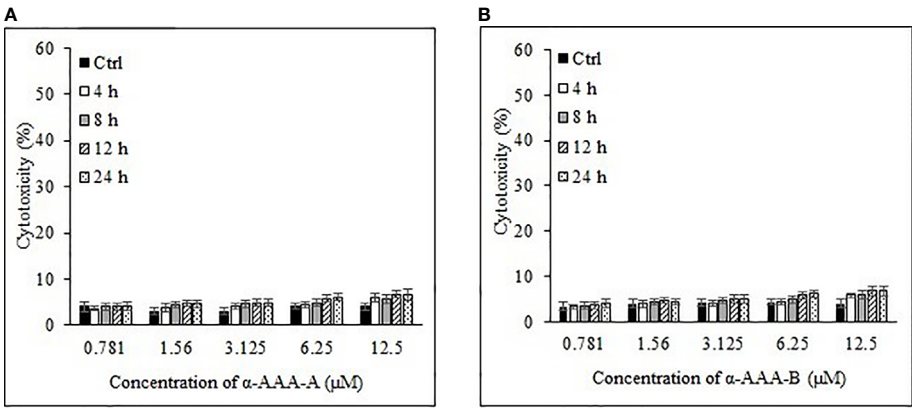

FIGURE 5 | Analysis of normal breast cell line MCF10A cytotoxicity by α-AAA-A **(A)** and α-AAA-B **(B)** at different concentrations and time durations of incubation. Control means MCF10A cells without molecules served as control.

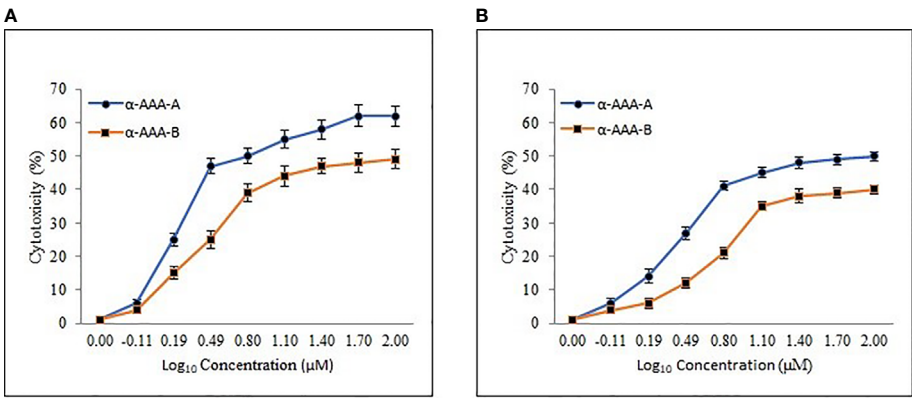

FIGURE 6 | Dose-response curve of α-AAA-A and α-AAA-B added to the HL-60 **(A)** and K562 **(B)** cancer cell culture. The incubation period for all the assays was 12 h. The IC_{50} was calculated from the curve generated. The lower the IC_{50}, the more cytotoxic the molecule is to specific the respective cancer cell line.

Expansion of Human γδ T Cells

Freshly isolated PBMCs (10^6 cells/ml) were stimulated using 1 μM zoledronate and were cultured in complete RPMI 1640 medium. Cytokines IL-2 (100 IU/ml) and IL-15 (10 ng/ml) were added to the culture according to the protocol using fresh medium. After fourteen days of culture, high yield (2279.2 ± 487) of pure γδ T (90.7 ± 4.6%) cells was recovered (**Table 1**). The purity and viability of expanded γδT cells were examined by flow cytometry.

These expanded γδ T cells were also analyzed for activation and costimulatory cell surface molecules (**Figure 7**). Expanded cells express high percent of activation molecule CD69 (86%), costimulatory molecules CD40, CD80, and CD86 (19%, 90% and 82% respectively). Moreover, high percent of major histocompatibility molecules HLA-DR and HLA-ABC were also expressed (97% and 99% respectively). CD25 a proliferation marker is expressed in an exceptionally small (5%) population of expanded cells.

Cytotoxic Effect of γδ T Cells

Freshly expanded γδ T cells showed cytotoxicity toward HL-60 (**Figure 8A**) and K562 (**Figure 8B**) cancer cells analyzed by flow cytometer. There was significant increase ($P < 0.001$) in killing of both HL-60 and K562 cells at the target (T) and effector (E) ratios of 1:10, 1:25 and 1:50 as compared to 1:1 T:E ratio. However, there are also significant differences ($P < 0.01$) between both cell lines in percent cell killing on comparison of T:E ratios of 1:10 and 1:25. Highest tumor cell killing for HL-60 cells was evident at a T:E ratio of 1:25 (41%). Similarly, highest killing for K562 cells was achieved at a T:E ratio of 1:25 (33%). It is evident that lesser numbers of γδ T cells (1:10, T:E ratio) are not able to successfully kill tumor cells. Also, γδ T cells kill HL-60 cells more effectively as compared with K562 cells. γδ T cells as well as both leukemia cancer cell lines (HL-60 and K562), when present alone, did not show substantial cell killing after 12 h of incubation under similar culture conditions.

TABLE 1 | *In vitro* expanded of γδ T cells from freshly isolated PBMCs in response to zoledronate (1 μM).

Donors	4
PBMC	1×10^6
γδ-T cells at day 0	$0.019 \pm 0.007 \times 10^6$
After 14 days expansion	
% Live Cells	85.9 ± 4.7
% $CD3^+$ cells	95.5 ± 2.8
% γδ-T cells (%)	90.7 ± 4.6
Total number of cells	$58.2 \pm 6.1 \times 10^6$
*Number of γδ-T cells	$43.3 \pm 8.5 \times 10^6$
#Expansion fold	2279.2 ± 487

Each donor PBMCs were cultured in triplicates.
Each value is the mean ± SD from 4 different donors.
**Total γδ-T cells (day 14) were calculated as: total cells × total live cells (%) × CD3+ cells (%) × γδ-T cells (%).*
#Expansion folds were calculated as: total γδ T cells (day 14)/γδ-T (day 0).

Combinational Cytotoxic Effect

The combinational effects of both synthesized analogs (α-AAA-A and α-AAA-B) and expanded γδ T cells were tested *in vitro* for their cytotoxic effects on leukemia cancer cell lines (HL-60 and K562) using flow cytometer. Significantly high percent of cancer cell killing was observed when these cell lines were co-cultured with molecule (α-AAA-A or α-AAA-B) and γδ T cells together. Highest percent of killings of HL-60 cells (72%) (**Figure 9A**) and K562 cells (59%) (**Figure 9B**) were observed in culture conditions which contained α-AAA-A and γδ T cells at 1:25 target to effector ratio. PBMCs alone, cancer cells alone and γδ T cells alone served as controls. These results suggested that α-AAA-A, in combination with γδ T cells, exhibited better leukemia cancer cell killing as compared to α-AAA-B and γδ T cells alone.

The control experiments were designed for co-culture of expanded γδ T cells with both molecules (α-AAA-A and α-AAA-B) at various concentrations to analyze the effect of α-amino amide analogs on 14 days expanded cells. Results showed no substantial cytotoxic effects (≤ 4%) on these cells (**Supplementary Figure 2**). One of the conventional drugs for leukemia, "methotrexate," when tested together with γδ T cells, showed appreciable cytotoxicity (**Supplementary Figure 3**).

DISCUSSION

For the development of potential cancer treatments, strategies need to focus on the inhibition of proliferative potential and migration of cancer cells, as well as destruction of tumors. Various available molecular drugs for the treatment of cancers can causes high toxicity and are often not well tolerated (23). In leukemia patients, toxicities such as cardiotoxicity, neuropathy, hepatotoxicity, renal toxicity, and so on, might be potential reasons for morbidity and mortality in these patients (5–8). Best approach to reduce the burden of these toxicities is to devise strategies for better patient outcomes.

In addition to palliative care, personalized cancer therapy options need to be investigated, especially in the case of advanced stage cancer patients, often characterized by a higher death rate. In such cases, it is challenging to treat cancers with monotherapies. To overcome these challenges and enhance efficacy, therapies directed at different signaling pathways or an amalgamation of different targeted therapies are needed. Hence combinational therapeutics may be a more effective route for a durable tumor response. Combinational therapies can act simultaneously, targeting different pathways to inhibit not only tumor cell proliferation potential, but also tumor cell killing (9, 24–26). Two of the most advanced research areas involved in the field of oncotherapeutics, i.e., medicinal chemistry and adoptive cell therapy, are currently involved in development of potential anti-cancer therapeutics. Hence, in this study, we have tested and evaluated two therapies and their additive effects *in vitro*.

Biologically active molecules have inherent advantages over adaptive immunotherapies, as these molecules can reach a wider spectrum of molecular targets, including intracellular targets and even those present deep in the tumor milieu (27). The anticancer

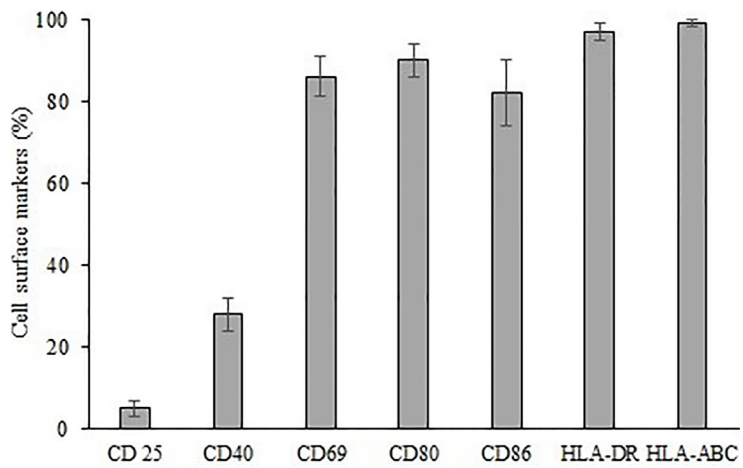

FIGURE 7 | Expression of cell surface markers CD 25, CD40, CD69, CD80, CD86, HLA-DR, HLA-ABC on expanded γδ T cells.

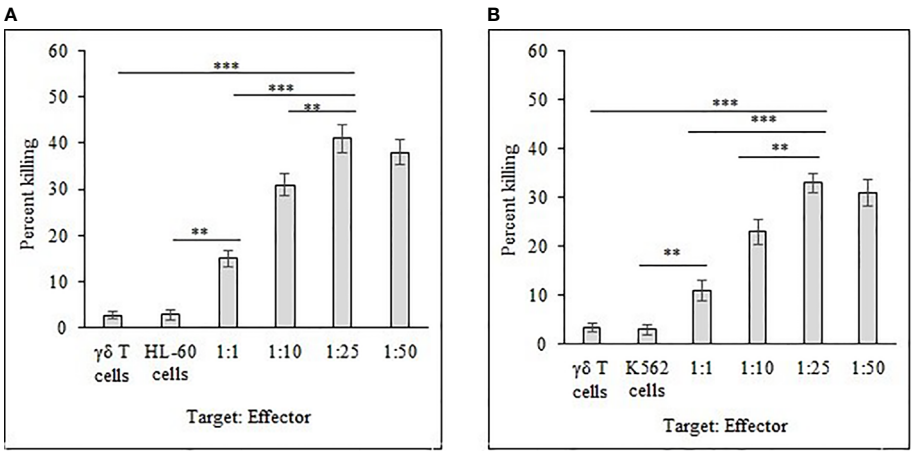

FIGURE 8 | Percent killing of HL-60 **(A)** and K562 **(B)** cancer cells by 14 day expanded γδ T cells. Different T:E ratios were incubated together for a duration of 12 h. γδ T cells and leukemia cancer cells (HL-60 and K562) alone served as controls. For both HL-60 and K562, $^{***}P < 0.001$ on comparison of percent cell killing at the T:E ratios of 1:25 to 1:1. $^{**}P < 0.01$ on comparison of percent cell killing at the T:E ratios of 1:25 to 1:10.

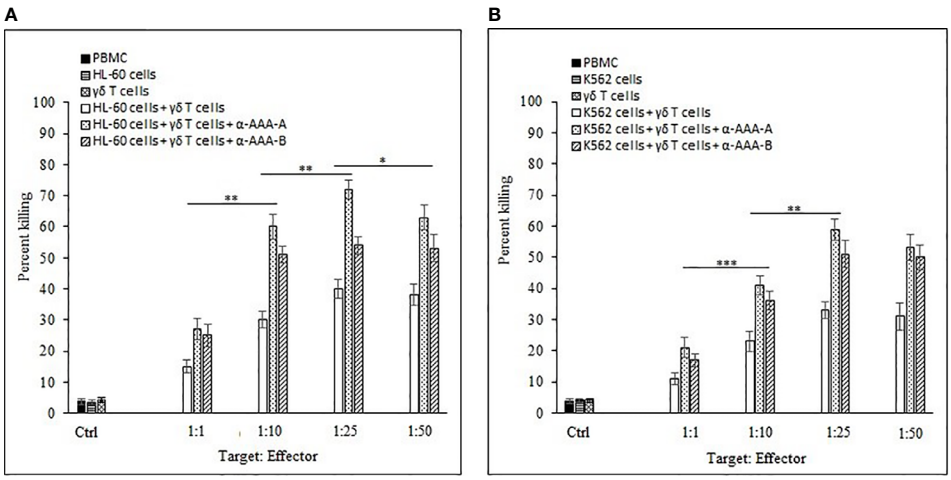

FIGURE 9 | Combinational effect of both amide analogs and expanded γδ T cells. Percent killing of HL-60 **(A)** and K562 **(B)** cancer cells by 14 days expanded γδ T cells in combination with α-AAA-A or α-AAA-B. Different T:E ratios were incubated together for a duration of 12 h. PBMCs alone, cancer cells alone and γδ T cells alone served as controls (ctrl). For HL-60 cancer cell line **(A)**, the concentrations of α-AAA-A and α-AAA-B used were 3.125 and 6.26 μM, respectively. For K-562 cancer cell line **(B)**, concentrations of α-AAA-A and α-AAA-B used were 6.26 and 12.5 μM, respectively. Significance represented as $^{***}P < 0.001$, $^{**}P < 0.01$ and $^{*}P < 0.05$.

potency of two α-amino amide analogs (RS)-N-(2-(cyclohexylamino)-2-oxo-1-phenylethyl)-N-phenylpropiolamide and (RS)-N-(2-(cyclohexylamino)-2-oxo-1-phenylethyl)-N-phenylbut2-enamide, which were synthesized using linear Ugi multicomponent reaction, was tested for leukemia cancer cell lines. These molecules are stable at room temperature and cost effective (12). It has been previously evaluated that amide derivatives exhibit effective anticancer properties against various cancer cell lines, such as breast cancer (MCF-7 and MDA-MB-231), lung cancer (A549), and prostate cancer (DU-145) (28). Similarly, our synthesized analogs (α-AAA-A and α-AAA-B) showed cytotoxic effects against HL-60 and K562 cancer cells, which varied depending on concentrations of the molecules used. Notably, the IC_{50} value of α-AAA-A is far less as compared with α-AAA-B for both cancer cell lines. In a previous study, it has been observed that analog A also showed low IC_{50} as compared to analog B, when tested for other cancer cell lines such as HT29, U87, A2780, H680, A431, Du145 etc., suggesting better efficiency of α-AAA-A as an anticancer molecule in comparison to α-AAA-B (12). Even when the concentration of α-AAA-A (3.125 μM) used was half of the concentration of α-AAA-B (6.26 μM), maximum cytotoxicity was exhibited for HL-60 cancer cell line. Moreover, at 6.26 μM concentration of α-AAA-A, which was half of the concentration of α-AAA-B (12.5 μM), maximum cytotoxicity was observed for K-562 cancer cell line. The reason behind higher toxicity of analog A as compared to the analog B is due to a minor structural difference.

The acetylenic moiety, which is present on α-AAA-A may have role in the higher potency of the molecule, as compared to the molecule α-AAA-B which retain argylic analog. Removal of the acetylene moiety from an amide derivative (RS)-N-(2-(Benzylamino)-2-oxo-1-phenylethyl)-N-phenylpropiolamide) results in more than 30-fold decrease in potency (12). However, the complete mechanisms behind the cytotoxicities associated with these molecules are still unknown and will be elucidated in future studies. A focused library of biologically active anticancer molecules, which are stable, efficient, cost effective and target various cancers, would be beneficial for efficient therapeutic screening purposes.

Enormous progress has been made recently in adoptive cell therapy treatments for advanced stage cancers. Immune cells have the ability to recognize and remove infected and cancerous cells. Many different types of immune cells, primarily T cells, NK cells and a specialized subset of T cells known as γδ T cells, are some of the candidates, which have been utilized (29–31). Consequently, various technologies focus on boosting function of immune cells by adding agents, aiming to improve their anti-tumor performance. These constitute personalized cancer immunotherapies. Immunotherapies use *in vitro* expanded immune effector cells, which on transference into cancer patients, target tumor cells or stimulate immune response to eliminate them (32). Currently, γδ T cells are an attractive candidate for cancer immunotherapy. We used these cells in this study as they are easy to manipulate *in vitro* and can grow to substantial numbers. These cells can recognize phosphoantigens, such as isopentenyl pyrophosphate produced by stressed cells, as well as bisphosphonates, such as zoledronic acid (14). In this study, expanded γδ T cells exhibited significant *in vitro* killing of both cancer cell lines (HL-60 and K562) at a target to effector ratio of 1:25. We did not further elucidate the differences in killing of two different cell lines. In our previous study, we have also shown the cytotoxic effects of these cells against another chronic myeloid leukemia cell line, i.e., KBM7 (14). Previously, it was observed that expanded γδ T cells retained tumor cell-killing activity without the need for prior activation. However, the myeloid KBM7 cells were much more efficiently killed following overnight incubation with HMBPP. This effect was reduced to the level of untreated KBM7 cells when γδ-TCR blocking Abs were included, demonstrating that the HMBPP pre-treatment of tumor cells directly promoted the γδ-TCR-mediated KBM7 killing. γδ-TCR-blocking Abs did not affect the killing of untreated KBM7 cells, whereas the addition of CD18 and/or NKG2D-blocking Abs reduced the killing of both untreated and HMBPP-pre-treated KBM7 cells.

Similarly, we expect that the mechanism which involve CD18 and/or NKG2D receptors on the expanded γδ T cells, possibly recognize and kill leukemia cancer cells (HL-60 and K562). However, direct blocking assays were not carried out in this study and would be included in future studies to elucidate the mechanism underlying cytotoxicity.

Other *in vitro* studies also showed that γδ T cells kill breast cancer cell lines MDA-MB231, MCF-7, and T47D (33–35). In one of the studies, γδ T cells, in the context of breast cancer, suggested that surface levels of MICA/B on breast cancer cells enhanced targeting and cytotoxicity by γδ T cells against these cell lines (35). Furthermore, the involvement of NKG2D on γδ T cells and MICA/B on MCF-7 and T47D was found in cytotoxicity of γδ T cell against breast tumor targets (36).

Furthermore, γδ T cells have the ability to kill many other tumors (lymphoma, myeloma, melanoma, colorectal, colon, breast, ovary, and prostate cancers) (37).

Pathways for cancer cells are difficult to understand, often due to the involvement of multiple complex molecules. Use of single drug or vaccine poses limitations in countering the complex pathogenesis of cancer. In light of these difficulties, combinational therapies present a unique approach and may provide effective outcomes for many different cancers (9, 24). Importantly, both γδ T cells and the biologically active molecules (α-AAA-A and α-AAA-B), used in this study, are easily produced under *in vitro* conditions and both can be generated in large numbers or amounts. Therefore, both biologically active α-amino amide analogs and γδ T cells are ideal candidates for their use in cancer therapy as combinational therapeutics.

Many studies conducted so far have successfully demonstrated the use of immune cells (T cells, CAR-T cells, NK cells, etc) with small biological molecules [anti-CTLA-4 Abs (Ipilimumab), anti-PD-1 Abs (Nivolumab)] which are immune check point inhibitors (38). Similarly, the combination of amide analogs (α-AAA-A or α-AAA-B) in combination with γδ T cells produced significant killing of two different leukemia cancer cell lines (HL-60 and K562). The killing of cancer cells was markedly substantial when the ratio of cancer cells to γδ T cell was 1:25 and the duration of incubation was 12 h for both molecules. We have discussed earlier the possible mechanisms behind the cytotoxicity of both leukemia cancer cell lines (HL-60 and K562) due to both amide analogs, as well as γδ T cells in combination therapy. Both amide derivative analogs contain acetylene moiety, which has an important role in anticancer activity. Moreover, argylic moiety, which is present on analog A leads to higher potency in combination with γδ T cells as compared with analog-B in combination with γδ T cells. Expanded γδ T cells may show tumor cell killing through the involvement of CD18 and/or NKG2D receptors, which mediate recognition and killing of leukemia cancer cells (HL-60 and K562). Moreover, this form of therapy will not be restricted to a particular type of cancer as most human cancers arouse T-cell responses.

Toxicity and increase of multidrug resistance in cancer patients is a major constraint in chemotherapy (9). Hence, combinational therapeutics have the potential to overcome molecular heterogeneity in patients diagnosed with various cancers. The effect of combinational therapeutics (γδ T cells in combination with biologically active anti-cancer molecules) is better as compared with monotherapies alone. However, it is important to check the toxicities of combinational therapeutics before administration. Preclinical studies are crucial and should be conducted in a regulated manner before clinical trials.

CONCLUSIONS

High yields of novel biologically active molecules (α-AAA-A and α-AAA-B) were achieved with simple reactions, minimum

efforts and without any purification. These molecules exhibited cytotoxic activities against leukemia cancer cell lines and remain stable at room temperature. Biologically active molecules can reach a wide spectrum of molecular targets, including intracellular targets or those present deep in the tumor microenvironment. Human γδ T cells exhibit tumor killing activity. The combination of α-AAA-A or α-AAA-B with γδ T cells effectively killed HL-60 and K562 cancer cells in *in vitro* conditions. Thus, biologically active molecule (α-AAA-A and α-AAA-B) and γδ T cells are potential agents for combinational therapy for leukemia. In the future, anticancer molecules may be engineered to perform dual function; first to exhibit cancer cell killing and second to activate *in vivo* γδ T cells.

DATA AVAILABILITY STATEMENT

The original contributions presented in the study are included in the article/**Supplementary Material**. Further inquiries can be directed to the corresponding author.

ETHICS STATEMENT

This study has been reviewed and approved by the Research Ethics Committee (REC) at the University of Hail dated: 27/11/2020 and approved by university president letter number Nr. 20455/5/42 dated 16/04/1442 H.

AUTHOR CONTRIBUTIONS

AO, SS, and MK designed the study. AO, SS, WK, SK, and MK performed the study. AO, SS, MK, SA, EA, and AA wrote the manuscript. All authors contributed to the article and approved the submitted version.

FUNDING

This research has been funded by Research Deanship of University of Ha'il, Saudi Arabia through project number RG-191332.

SUPPLEMENTARY MATERIAL

The Supplementary Material for this article can be found online at: https://www.frontiersin.org/articles/10.3389/fonc.2021.706586/full#supplementary-material

REFERENCES

1. Mathers C, Rebelo M, Parkin DM, Forman D, Bray F. Cancer Incidence and Mortality Worldwide: Sources, Methods and Major Patterns in GLOBOCAN 2012. *Int J Cancer* (2015) 1-136(5):359–86. doi: 10.1002/ijc.29210
2. American Cancer Society. *Cancer Facts and & Figures* (2021). Available at: https://www.cancer.org/research/cancer-facts-statistics/all-cancer-facts-figures/cancer-facts-figures-2021.html#:~:text=The%20Facts%20%26%20Figures%20annual%20report,deaths%20in%20the%20United%20States (Accessed May 6, 2021).
3. World Health Organization. *International Agency for Research on Cancer, Saudi Arabia, Globocon* (2020). Available at: https://gco.iarc.fr/today/data/factsheets/populations/682-saudi-arabia-fact-sheets.pdf (Accessed June 1, 2021).
4. International Childhood Cancer Day. *Health Days 2018 Ministry of Health, Kingdom of Saudi Arabia* (2018). Available at: https://www.moh.gov.sa/en/HealthAwareness/healthDay/2018/Pages/HealthDay-2018-02-15.aspx (Accessed June 1, 2021).
5. Neuendorff NR, Loh KP, Mims AS, Christofyllakis K, Soo WK, Bölükbasi B, et al. Anthracycline-related Cardiotoxicity in Older Patients With Acute Myeloid Leukemia: A Young SIOG Review Paper. *Blood Adv* (2020) 4(4):762–75. doi: 10.1182/bloodadvances.2019000955
6. George K, Erin LE, David S. Neurologic Complications of Chemotherapy Agents. *Curr Opin Neurol* (2007) 20:719–25. doi: 10.1097/WCO.0b013e3282f1a06e
7. Navarro VJ, Senior JR. Drug-Related Hepatotoxicity. *N Engl J Med* (2006) 354:731–9. doi: 10.1056/NEJMra052270
8. de Jonge MJA, Verweij J. Renal Toxicities of Chemotherapy. *Semin Oncol* (2006) 33:68–73. doi: 10.1053/j.seminoncol.2005.11.011
9. He B, Lu C, Zheng G, He X, Wang M, Chen G, et al. Combination Therapeutics in Complex Diseases. *J Cell Mol Med* (2016) 20(12):2231–40. doi: 10.1111/jcmm.12930
10. Liboiron BD, Tardi PG, Harasym TO, Mayer LD. Nanoscale Delivery System for Combination Chemotherapy. In: Kratz F, Senter PD, Steinhagen H, editors. *Drug Delivery in Oncology: From Basic Research to Cancer Therapy*. Weinheim, Germany: Wiley-VCH Verlag GmbH & Co. KGaA (2012). p. 1013–50.
11. Meegan MJ, O'Boyle NM. Anticancer Drugs. *Pharmaceuticals (Basel)* (2019) 3:134. doi: 10.3390/ph12030134
12. Al-Otaibi A, Deane FM, Russell CC, Hizartzidis L, McCluskey SN, Sakoff JA, et al. A Methanol and Protic Ionic Liquid Ugi Multicomponent Reaction Path to Cytotoxic Alpha-Phenylacetamido Amides. *RSC Adv* (2019) 9:7652–63. doi: 10.1039/C9RA00118B
13. Khaled AMA, Ghada HA, Abeer ME. Eco-Friendly Synthesis of Novel Cyanopyridine Derivatives and Their Anticancer and PIM-1 Kinase Inhibitory Activities. *Eur J Med Chem* (2017) 134:357–65. doi: 10.1016/j.ejmech.2017.04.024
14. Khan MWA, Curbishley SM, Chen HC, Thomas A, Steven N, Eberl M, et al. Expanded Human Blood-Derived γδt Cells Display Potent Antigen-Presentation Functions. *Front Immunol* (2014) 5:344. doi: 10.3389/fimmu.2014.00344
15. Davey MS, Lin C-Y, Roberts GW, Heuston S, Brown AC, Chess JA, et al. Human Neutrophil Clearance of Bacterial Pathogens Triggers Anti-Microbial γδ T Cell Responses in Early Infection. *PLoS Pathog* (2017) 5:e1002040. doi: 10.1371/journal.ppat.1002040
16. Khan MWA, Eberl M, Moser B. Potential Use of [Gammadelta] T Cell-Based Vaccines in Cancer Immunotherapy. *Front Immunol* (2014) 5:512. doi: 10.3389/fimmu.2014.00512
17. Dhar S, Chiplunkar SV. Lysis of Aminobisphosphonate-Sensitized MCF-7 Breast Tumor Cells by Vγ9vδ2 Cells. *Cancer Immun* (2010) 10:10.
18. Ferrarini M, Pupa SM, Zocchi MR, Rugarli C, Ménard S. Distinct Pattern of HSP72 and Monomeric Laminin Receptor Expression in Human Lung Cancers Infiltrated by Gamma/Delta T Lymphocytes. *Int J Cancer* (1994) 57:486–90. doi: 10.1002/ijc.2910570408
19. Choudhary A, Davodeau F, Moreau A, Peyrat MA, Bonneville M, Jotereau F. Selective Lysis of Autologous Tumor Cells by Recurrent Gamma Delta Tumor-Infiltrating Lymphocytes From Renal Carcinoma. *J Immunol* (1995) 154:3932–40.
20. Wada I, Matsushita H, Noji S, Mori K, Yamashita H, Nomura S, et al. Intraperitoneal Injection of *In Vitro* Expanded V9v2 T Cells Together With

Zoledronate for the Treatment of Malignant Ascites Due to Gastric Cancer. *Cancer Med* (2014) 3(2):362–75. doi: 10.1002/cam4.196
21. Carmichael J, DeGraff WG, Gazdar AF, Minna JD, Mitchell JB. Evaluation of a Tetrazolium Based Semiautomated Colorimetric Assay: Assessment of Chemosensitivity Testing. *Cancer Res* (1987) 47:936–42.
22. Hayon T, Dvilansky A, Sphilberg O, Nathan I. Appraisal of the MTT Based Assay as a Useful Tool for Predicting Drug Chemosensitivity in Leukemia. *Leuk Lymphoma* (2003) 44(11):1957–62. doi: 10.1080/1042819031000116607
23. Ismail M, Khan S, Khan F, Noor S, Sajid S, Yar S, et al. Prevalence and Significance of Potential Drug-Drug Interactions Among Cancer Patients Receiving Chemotherapy. *BMC Cancer* (2020) 20:335. doi: 10.1186/s12885-020-06855-9
24. Tolcher AW, Mayer LD. Improving Combination Cancer Therapy: The combiPlex® Development Platform. *Future Oncol* (2018) 14(13):1317–32. doi: 10.2217/fon-2017-0607
25. Chou TC. Theoretical Basis, Experimental Design, and Computerized Simulation of Synergism and Antagonism in Drug Combination Studies. *Pharmacol Rev* (2006) 58:621–81. doi: 10.1124/pr.58.3.10
26. Zimmermann GR, Lehar J, Keith CT. Multi-Target Therapeutics: When the Whole is Greater Than the Sum of the Parts. *Drug Discov Today* (2007) 12:34–42. doi: 10.1016/j.drudis.2006.11.008
27. Kerr WG, Chisholm JD. The Next Generation of Immunotherapy for Cancer: Small Molecules Could Make Big Waves. *J Immunol* (2019) 202(1):11–9. doi: 10.4049/jimmunol.1800991
28. Rani CS, Reddy AG, Susithra E, Mak KK, Pichika MR, Reddymasu S, et al. Synthesis and Anticancer Evaluation of Amide Derivatives of Imidazo-Pyridines. *Med Chem Res* (2021) 30:74–83. doi: 10.1007/s00044-020-02638-w
29. Todro M, Meraviglia S, Caccamo N, Stassi G, Dieli F. Combining Conventional Chemotherapy and Gammadelta T Cell-Based Immunotherapy to Target Cancer-Initiating Cells. *Oncoimmunology* (2013) 2(9):e25821. doi: 10.4161/onci.25821
30. Liu Z, Guo BL, Gehrs BC, Nan L, Lopez RD. *Ex Vivo* Expanded Human Vgamma9Vdelta2+ Gammadelta-T Cells Mediate Innate Antitumor Activity Against Human Prostate Cancer Cells *In Vitro*. *J Urol* (2005) 173(5):1552–6. doi: 10.1097/01.ju.0000154355.45816.0b
31. Caccamo N, Sireci G, Meraviglia S, Dieli F, Ivanyi J, Salerno A. Gammadelta T Cells Condition Dendritic Cells *In Vivo* for Priming Pulmonary CD8 T Cell Responses Against Mycobacterium Tuberculosis. *Eur J Immunol* (2006) 36 (10):2681–90. doi: 10.1002/eji.200636220
32. Zou C, Zhao P, Xiao Z, Han X, Fu F, Fu L. γδ T Cells in Cancer Immunotherapy. *Oncotarget* (2017) 8(5):8900–9. doi: 10.18632/oncotarget.13051
33. Guo BL, Liu Z, Aldrich WA, Lopez RD. Innate Anti-Breast Cancer Immunity of Apoptosis-Resistant Human Gammadelta-T Cells. *Breast Cancer Res Treat* (2005) 93:169–75. doi: 10.1007/s10549-005-4792-8
34. Dutta I, Postovit LM, Siegers GM. Apoptosis Induced *Via* Gamma Delta T Cell Antigen Receptor "Blocking" Antibodies: A Cautionary Tale. *Front Immunol* (2017) 8:776. doi: 10.3389/fimmu.2017.00776
35. Aggarwal R, Lu J, Kanji S, Das M, Joseph M, Lustberg MB, et al. Human Vgamma2vdelta2 T Cells Limit Breast Cancer Growth by Modulating Cell Survival-, Apoptosis-Related Molecules and Microenvironment in Tumors. *Int J Cancer* (2013) 133:2133–44. doi: 10.1002/ijc.28217
36. Siegers GM, Dutta I, Lai R, Postovit LM. Functional Plasticity of Gamma Delta T Cells and Breast Tumor Targets in Hypoxia. *Front Immunol* (2018) 9:1367. doi: 10.3389/fimmu.2018.01367
37. Lafont V, Sanchez F, Laprevotte E, Michaud H, Gros L, Eliaou J, et al. Plasticity of γδ T Cells: Impact on the Anti-Tumor Response. *Front Immunol* (2014) 5:622. doi: 10.3389/fimmu.2014.00622
38. Rotte A. Combination of CTLA-4 and PD-1 Blockers for Treatment of Cancer. *J Exp Clin Cancer Res* (2019) 38:255. doi: 10.1186/s13046-019-1259-z

Conflict of Interest: The authors declare that the research was conducted in the absence of any commercial or financial relationships that could be construed as a potential conflict of interest.

frontiers in Pharmacology

REVIEW
published: 19 July 2021
doi: 10.3389/fphar.2021.699629

Mcl-1 Inhibition: Managing Malignancy in Multiple Myeloma

*Omar S. Al-Odat[1,2], Max von Suskil[1,2], Robert J. Chitren[1,2], Weam O. Elbezanti[1,3], Sandeep K. Srivastava[4], Tulin Budak-Alpddogan[3], Subash C. Jonnalagadda[2], Bharat B. Aggarwal[5] and Manoj Pandey[1]**

[1]Department of Biomedical Sciences, Cooper Medical School of Rowan University, Camden, NJ, United States, [2]Department of Chemistry and Biochemistry, Rowan University, Glassboro, NJ, United States, [3]Department of Hematology, Cooper Health University, Camden, NJ, United States, [4]Department of Biosciences, Manipal University Jaipur, Jaipur, India, [5]Inflammation Research Center, San Diego, CA, United States

Multiple myeloma (MM) is a plasma cells neoplasm. The overexpression of Bcl-2 family proteins, particularly myeloid cell leukemia 1 (Mcl-1), plays a critical role in the pathogenesis of MM. The overexpression of Mcl-1 is associated with drug resistance and overall poor prognosis of MM. Thus, inhibition of the Mcl-1 protein considered as a therapeutic strategy to kill the myeloma cells. Over the last decade, the development of selective Mcl-1 inhibitors has seen remarkable advancement. This review presents the critical role of Mcl-1 in the progression of MM, the most prominent BH3 mimetic and semi-BH3 mimetic that selectively inhibit Mcl-1, and could be used as single agent or combined with existing therapies.

Keywords: multiple myeloma, drug resistant, Mcl-1, Bcl-2 homology 3 mimetics, apoptosis

OPEN ACCESS

Edited by:
Raghuram Kandimalla, James Graham Brown Cancer Center, United States

Reviewed by:
Chong Teik Tan, National University of Singapore, Singapore
Suman Kumar Samanta, Institute of Advanced Study in Science and Technology, India

****Correspondence:***
Manoj Pandey
pandey@rowan.edu

Specialty section:
This article was submitted to Pharmacology of Anti-Cancer Drugs, a section of the journal Frontiers in Pharmacology

Received: *23 April 2021*
Accepted: *24 June 2021*
Published: *19 July 2021*

Citation:
Al-Odat OS, von Suskil M, Chitren RJ, Elbezanti WO, Srivastava SK, Budak-Alpddogan T, Jonnalagadda SC, Aggarwal BB and Pandey M (2021) Mcl-1 Inhibition: Managing Malignancy in Multiple Myeloma. Front. Pharmacol. 12:699629. doi: 10.3389/fphar.2021.699629

INTRODUCTION

The innate and adaptive immune system comprises several different types of cells that elegantly work together to stave off infection and remove transformed or damaged cells. Lymphocytes including both T- and B-cells are among the most important cellular category within the immune system. The plasma cells are a type of unique B cells that reside in the bone marrow (BM) and secrete an antibody corresponding to the antigen. When these plasma cells begin proliferating out of control, they can build up within the BM and form numerous tumors across the body (**Figure 1**). This type of neoplasms is called Multiple Myeloma (MM) and considered the second most common hematologic malignancy, accounting around 12% of hematological malignancies (Kazandjian, 2016). MM is slightly more common among older men, with the median age of 65 years, and it is rarely diagnosed in younger people (Kumar et al., 2008; Gerecke et al., 2016; Naymagon and Abdul-Hay, 2016). Depending on the stage of disease, symptoms of MM begin with abnormalities in the bone and calcium homeostasis, low blood cell counts, renal insufficiency, and multiple infections. Because the symptoms are so generalized, MM is a challenging disease to diagnose. Furthermore, the protective role of the BM on the proliferating plasma cells make it even more challenging to treat.

In the last several decades the treatment options for MM have dramatically improved, unfortunately, the survival rate is marginal (Bergsagel and Kuehl, 2005). According to the American Cancer Society 2021 estimation, approximately 34,920 new MM cases will be diagnosed (19,320 men and 15,600 women), approximately 12,410 cancer deaths (6,840 men and 5,570 women) from MM alone in the United States (Siegel et al., 2021). **Table 1** illustrates the common drugs that have been used to treat MM patients. Most therapeutic approaches to date for MM patients, especially in relapsed/refractory (R/R) cases have been based on combined

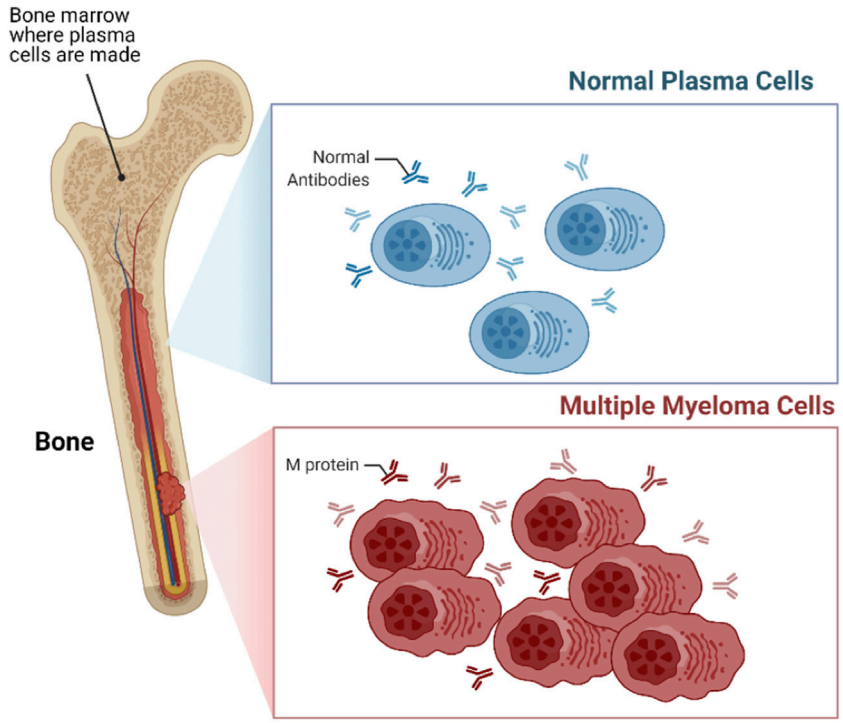

FIGURE 1 | Multiple myeloma (MM). MM is a type of blood cancer that initiates from the bone marrow (BM), arising from the aberrant proliferation of plasma cells.

formulations of available therapies. In spite of the efficacy and diversity of therapeutic approaches, drug resistance is a major challenge as MM continues to show high rates of relapse and quickly acquired resistance to therapies (Abdi et al., 2013). There are several unanswered questions regarding MM including: what are the causes of progression of MM from its precursor state? Why MM patients instigate to relapse? How MM clones resistant to drugs persist in the presence of effective therapies?

MCL-1 PROTEIN AS A POTENTIAL TARGET FOR MULTIPLE MYELOMA

Apoptosis is a vital procedure for regular development and maintaining the tissue homeostasis. Mammalian apoptosis occurs *via* one of two distinct pathways, either the intrinsic or extrinsic pathways (**Figure 2**). Both the intrinsic and extrinsic pathways end with the activation of a certain group of protease enzymes called Caspase proteins. The intrinsic pathway entails mitochondrial outer membrane permeabilization (MOMP) that regulates directly by interactions between B cell lymphoma 2 (Bcl-2) family proteins. The Bcl-2 family proteins are critical regulators of apoptosis. The members of this family proteins are divided into three groups according to function: anti-apoptotic proteins (Bcl-2, Mcl-1, Bcl-xL, Bcl-W, and Bfl-1); pro-apoptotic BH3-only proteins (Noxa, Puma, Bim, Bid, Bad, BMF, and Bik); and multi-domain pro-apoptotic proteins (Bax, Bak, and Bok). Intrinsic pathways like cytokine deprivation or DNA damage promote overexpression and activation of BH3-only proteins, which stimulate apoptosis in two different ways. First, the BH3-only proteins behave as inhibitors of anti-apoptotic proteins by competing for their binding with Bax and Bak proteins (Czabotar et al., 2014; **Figure 2**). This is accomplished *via* the amphipathic α-helix of the BH3 domain that contains four hydrophobic residues (h1-h4) that bind four hydrophobic pockets (P1–P4) within the anti-apoptotic proteins in their BH3 binding groove (Liang and Fesik, 1997; Czabotar et al., 2007; Stewart et al., 2010). For example, Noxa selectively inhibits Mcl-1 with high affinity binding thereby indirectly activating the Bax/Bak pathway (Smith et al., 2011; Kale et al., 2018). Simultaneously, BH3-only proteins can also result in the direct activation of multi-domain pro-apoptotic proteins Bax and Bak, which cause MOMP, leading to release of Cytochrome C and SMAC proteins into the cytosol resulting in downstream Caspase activation and ultimately activation of apoptosis (Dewson and Kluck, 2009).

The extrinsic pathway is promoted by death receptors activation. This leads to activation of initiator Caspases 8 and 10, which can directly induce the downstream executioner Caspase such as Caspase 3 and 7 to drive full commitment to apoptosis (Kaufmann et al., 2012). Moreover, Caspases 8 and Caspase 10 can activate Bid, which in turn activates Bak and Bax to induce MOMP, which is the connecting link between the extrinsic and intrinsic pathways (Kaufmann et al., 2012; **Figure 2**).

TABLE 1 | Mechanism of action and Side effects of Common Therapy in MM.

Drug	Mechanism of action	Side effects	Ref
Melphalan	Chemotherapy drug	Bone marrow damage and chemotherapy side effects	Bergsagel et al. (1962)
Thalidomide (Thalomid)	Immunomodulating agent	Drowsiness, fatigue, constipation, and painful nerve damage as well as severe birth defects when taken during pregnancy	Singhal et al. (1999)
Bortezomib (Velcade)	Proteasome inhibitor	Vomiting, tiredness, diarrhea, constipation, decreased appetite, fever, lowered blood counts and nerve damage	Richardson et al. (2003)
Lenalidomide (Revlimid)	Small molecule analogue of thalidomide	Drowsiness, fatigue, constipation, and painful nerve damage as well as severe birth defects when taken during pregnancy	Hideshima et al. (2000), Rajkumar et al. (2005), Richardson et al. (2002)
Carfilzomib (Kyprolis)	Proteasome inhibitor	Tiredness, nausea, vomiting, diarrhea, shortness of breath, fever and low blood counts and occasionally more serious problems such as pneumonia, heart problems, and kidney or liver failure	Herndon et al. (2013)
Pomalidomide (Pomalyst)	Small molecule analogue of thalidomide	Same thalidomide side effects with a less risk of nerve damage side effect	Lacy et al. (2009)
Panobinostat (Farydak)	Oral Histone deacetylase (HDAC) inhibitor	Feeling tired, weakness, nausea, diarrhea vomiting, loss of appetite, fever, swelling in the arms or legs, and occasionally altered blood cell counts and blood electrolytes. Rare cases of internal bleeding, liver damage, and changes in heart rhythm which can sometimes be life threatening	Laubach et al. (2015)
Ixazomib (Ninlaro)	Oral proteasome inhibitor	Nausea, vomiting, diarrhea, constipation, swelling in the hands or feet, back pain, lowered blood platelet count and nerve damage	Muz et al. (2016)
Daratumumab (Darzalex)	Intravenous monoclonal antibody	Coughing, wheezing, trouble breathing, throat tightness, runny nose, nasal congestion, feeling dizzy or lightheaded, headache, rash, nausea, fatigue, back pain, fever, and lower blood cell counts	Lokhorst et al. (2015)
Elotuzumab (Empliciti)	Intravenous monoclonal antibody	Chills, feeling dizzy or lightheaded, wheezing, trouble breathing, cough, tightness in the throat, runny nose, nasal congestion, upper respiratory tract infections and pneumonia, rash, fatigue, loss of appetite, diarrhea, constipation, fever, and nerve damage	Lonial et al. (2015)
Selinexor (Xpovio)	Oral Nuclear export inhibitor of XPO1	Diarrhea, nausea, vomiting, loss of appetite, weight loss, low blood sodium levels susceptibility to infection, low platelet counts, and low white blood cell counts	Vogl et al. (2018)

The mitochondrial membrane engages Mcl-1 with other Bcl-2 family partners for initiation of apoptosis. The interaction between the family members determine the outcome (Kale et al., 2018). Mcl-1 has a diverse localization within human cells. It is primarily found within the mitochondrial outer and inner membranes (Yang et al., 1995). However, studies have reported its localization in the nucleus and cytoplasm of polymorphonuclear leukocytes (PMNs) (Leuenroth et al., 2000). How different localization affects the function and its stability is not known.

The studies of Kozopas et al. first proved a high Mcl-1 expression in a differentiating human myeloid leukemia ML-1 cell line (Kozopas et al., 1993). Subsequently, it was shown to be expressed in several different cells as well. The MM cells exhibit imbalances in their anti-apoptotic proteins expression levels, especially Mcl-1 that leads to defects in the mitochondrial intrinsic pathway (Derenne et al., 2002; Zhang et al., 2002). In order to prevent apoptosis and allow continued cell growth, Mcl-1 forms a heterodimer protein-protein interaction with multi-domain pro-apoptotic proteins Bax and Bak (Sedlak et al., 1995; Willis and et al., 2005). Mcl-1 is known to be highly expressed in MM cells and plays a pivotal role in MM initiation, progression, and apoptosis resistance (Derenne et al., 2002; Zhang et al., 2002). Newly diagnosed cases of MM have continued to show increasing Mcl-1 protein expression, which predicts a higher relapse and poor patient survival rate (Wuillème-Toumi et al., 2005). Thus, Mcl-1 is an attractive therapeutic target for MM.

REGULATION OF MCL-1 PROTEIN

The interaction of myeloma cells to BM microenvironment (BMM) is the hall mark of MM (**Figure 3**). Additionally, MM cells receive crucial signals from the BMM that help them to evade apoptosis in order to maintain their long-term survival. The BM stromal cells (BMSCs) regulate the anti-apoptotic Bcl-2 family proteins by secreting a group of signaling cues. Mcl-1 is regulated through several extracellular signaling molecules including interleukins (IL-3, IL-5, and IL-6) (Wang et al., 1999; Huang et al., 2000; Jourdan et al., 2000); growth factors such as vascular endothelial growth factor (VEGF), epidermal growth factor (EGF) (Leu et al., 2000; Le Gouill et al., 2004); granulocyte macrophage colony stimulating factors (GM-CSF) (Chao et al., 1998); and interferon alpha (INF-α) (Jourdan et al., 2000). Combined, these stimuli trigger and modulate multiple signaling pathways including Janus kinase/signal transducer and activator of transcription (JAK/STAT), rat sarcoma/mitogen-activated protein kinase (Ras/MAPK), MEK/extracellular signal-related kinase (ERK) as well as phosphatidylinositol-3 kinase (PI3-K)/Akt (**Figure 3**).

The cytokine IL-6 is a main survival factor for MM cells (Klein et al., 1995). IL-6 triggers the upregulation of Mcl-1, Bcl-xL, and VEGF *via* stimulation of the JAK/STAT-3 signaling pathway (Puthier et al., 1999; Dankbar et al., 2000). In turn, VEGF promotes IL-6 induction in neighboring BM cells (BMCs) (Dankbar et al., 2000). Furthermore, IL-6 induces survival of

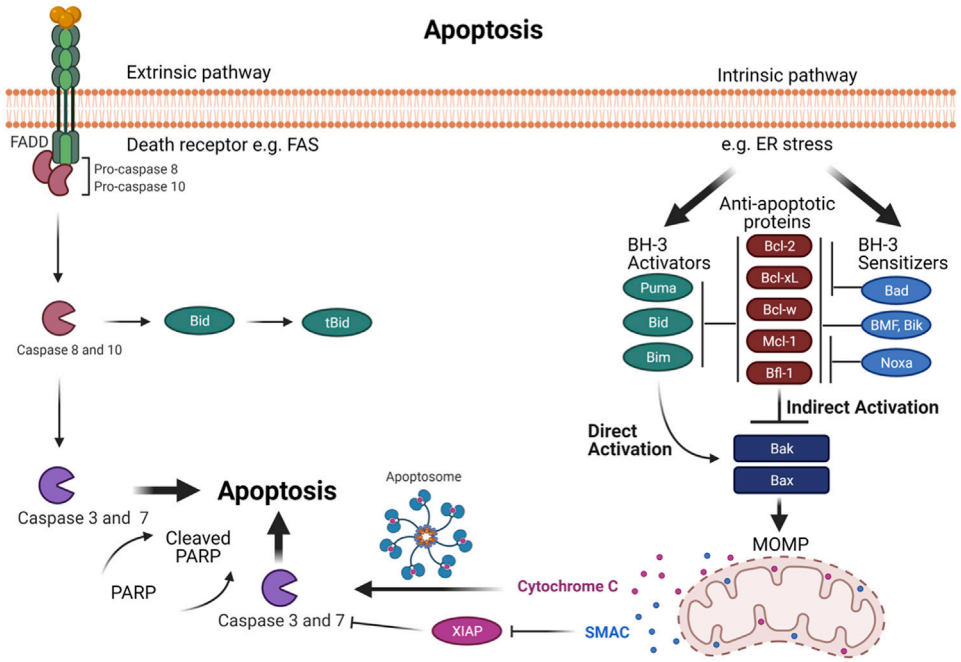

FIGURE 2 | The programmed cell death- *via* intrinsic and extrinsic pathways in normal mammalian cells. Intrinsic and extrinsic pathways result in the activation of a family of protease enzymes called Caspase proteins. The intrinsic pathway is promoted by cellular stresses that modulate Bcl-2 family proteins and activates Bak and Bax. In the indirect activation, upregulation of BH3-only proteins will act as inhibitors of anti-apoptotic proteins by competing for their binding with Bax and Bak proteins, leading Bax and Bak to oligomerize. In the direct activation, upregulation of BH3 activators proteins directly activates Bax and Bak. This activation leads to mitochondrial outer membrane permeabilization (MOMP), subsequently Cytochrome C and SMAC proteins release into the cytosol, causing the downstream of Caspase activation that ends with apoptosis. The extrinsic pathway is promoted by death receptors activation. This leads to activation of initiator Caspases 8 and 10, which can regulate the downstream executioner Caspase such as Caspase 3 and 7 to drive full commitment to apoptosis. Moreover, Caspases 8 and 10 can activate Bid, which in turn activates Bak and Bax to induce MOMP which establishes the link between the extrinsic and intrinsic pathways.

MM cells *via* stimulating the Ras/MAPK pathway, which engage in Mcl-1 overexpression (Ogata et al., 1997). Additionally, IFN-α induces Mcl-1 in a STAT-3 dependent manner (Jourdan et al., 2000). Furthermore, the tumor necrosis factor (TNF) family including B cell activating factor (BAFF), a proliferation-inducing ligand (APRIL) prevent apoptosis by inducing the expression of Mcl-1 and Bcl-2 (Moreaux et al., 2004). Insulin like growth factor 1 (IGF-1) affects the cell survival, by downregulating pro-apoptotic protein Bim (De Bruyne et al., 2010). The imbalance between Bim and Mcl-1 expression plays an important role in MM cell survival (Gomez-Bougie et al., 2004). The transcription factors such as B lymphocyte induced maturation protein 1 (Blimp-1), X-box binding protein 1 (XBP-1), and interferon regulatory factor 4 (IRF4) are critical for myeloma cells differentiation and development (Calame et al., 2003). The Blimp-1 downregulates the expression of pro-apoptotic protein Bim (Lin et al., 2007).

Mcl-1 and other anti-apoptotic proteins contain four Bcl-2 homology (BH) domains (BH1-3 domains interact to form a hydrophobic cleft termed "BH3-binding groove"), and a C-terminal tail of hydrophobic transmembrane domain (TM) that permeates into the mitochondrial membrane (Kozopas et al., 1993). Interestingly, compared to the other anti-apoptotic proteins, Mcl-1 has several unique properties including unique binding site, size, half-life, and localization. Mcl-1 has a shallow, relatively inflexible and more electropositive binding site abundant in lysine and histidine residues (Denis et al., 2020). Bcl-2 and Bcl-xL proteins contain 233 amino acids, whereas Mcl-1 protein contains 350 amino acids. This size difference is due to the presence of a large N-terminal domain of four PEST sequences [amino acids sequence extensive in proline (P), glutamic acid (E), serine (S), and threonine (T)] (Kozopas et al., 1993; Thomas et al., 2010), which can target Mcl-1 for degradation through the ubiquitin-proteasome system (UPS) and renders it short half-life (usually less than three hours depending on the cellular conditions) (Rogers et al., 1986; Kozopas et al., 1993; Yang et al., 1995).

In MM, the Mcl-1 gene is the most important and selective of the survival genes (Tiedemann et al., 2012). Gene coding of Mcl-1 is located on chromosome 1q21 region. Approximately 40% of MM cases have shown chromosomal amplification of 1q21, hence increased Mcl-1 expression (Shah et al., 2018; Slomp et al., 2019). Additionally, the gene coding of cytokine interleukin 6 receptor (IL-6R) is located on the same chromosome region (1q21) (Pawlyn and Morgan, 2017). The coding region of Mcl-1 contains three exons and two introns that undergoes alternative splicing to produce mature RNA (mRNA) isoforms. The Mcl-1L (Mcl-1 long) splice variant joins the three exons, has a full length of 350 amino acids and acts as an anti-apoptotic. On the other hand, Mcl-1S (Mcl-1 short) joins

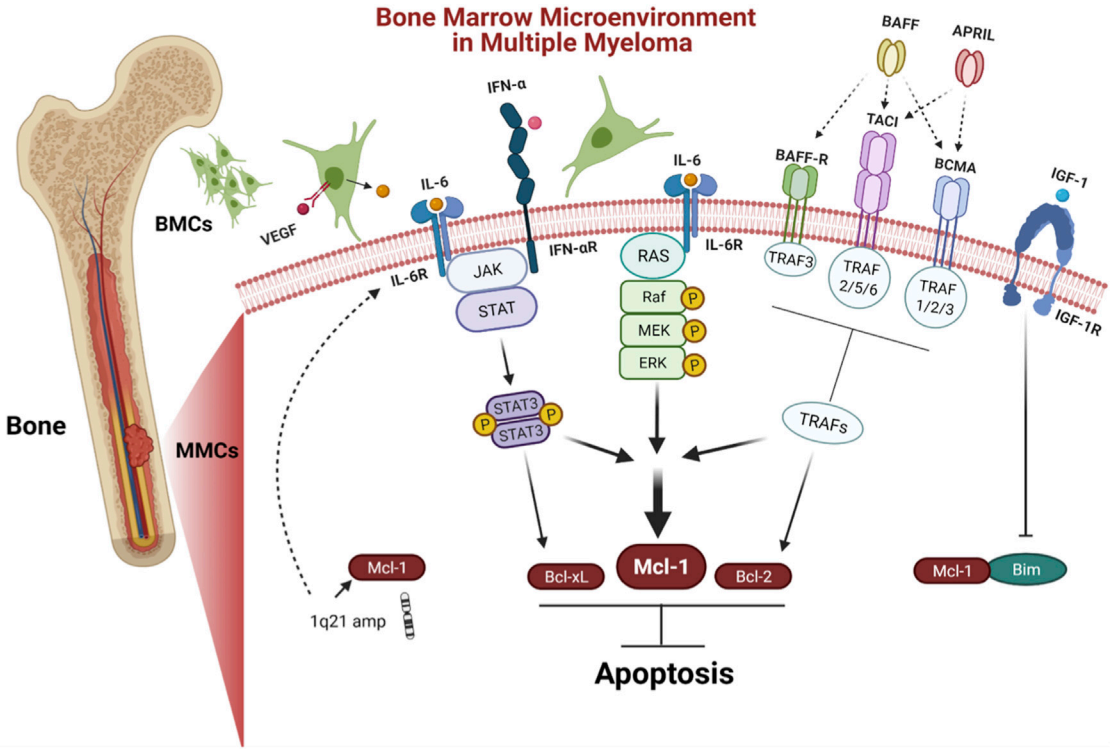

FIGURE 3 | Bone marrow microenvironment (BMM) in MM. BMM facilitates the long term survival of MM. Stromal cells in BM regulate anti-apoptotic proteins by secreting a variety of signaling molecules including IL-6 and IFN-α that trigger JAK/STAT pathway, leading to the upregulation of Mcl-1, Bcl-xL, and VEGF. VEGF promotes IL-6 induction in neighboring BMCs. Furthermore, IL-6 induces survival of MM cells *via* Ras/MAPK pathway, which modulates the expression of Mcl-1 The tumor necrosis factor (TNF) family including BAFF and APRIL are other stimuli from the BMM that induce expression of both Mcl-1 and Bcl-2 *via* tumor necrosis factor receptor-associated factors (TRAFs) including BAFF-R, BCMA, and TACI. IGF-1 is another stimulus that acts by downregulating Bim, leading to release Mcl-1. MM cases have shown chromosomal amplification of 1q21 region, where the gene coding for Mcl-1 and IL-6R are located.

only the first and the third exons without the central exon, with length of 271 amino acids, shows increased cytosolic localization and lacks the BH1, BH2 and TM domains but has the BH3 domain which plays a critical pro-apoptotic role (Bae et al., 2000; Bingle et al., 2000). Interestingly, Kim et al. (2009), found a new alternative splicing variant detected in the mitochondrion termed Mcl-1ES (Mcl-1 extra short) with a shorter length of 197 amino acids due to an absence of PEST sequences (Kim et al., 2009). Mcl-1ES forms an interaction with Mcl-1L in order to induce apoptosis (Kim et al., 2009).

The post transcriptional regulation of Mcl-1 is complex and controlled by multiple RNA binding proteins (RPBs) and microRNAs (miRNAs). For example, Mcl-1 has been shown to be downregulated in MM by miR-29b, miR-137, and miR-197 that leads to apoptosis (Zhang et al., 2011; Yang et al., 2015; Cui and Placzek, 2018). Additionally, at the post-translational level, the large N-terminal domain PEST allows for non-proteasomal degradation *via* cleavage (Herrant et al., 2004), proteasomal degradation *via* phosphorylation (Thomas et al., 2010), and ubiquitination (Mojsa et al., 2014), which further impact Mcl-1 expression, stability, localization, and function. Mcl-1 PEST undergoes Caspase cleavage at two different sites, located at Asp127 that produce Mcl-1^{1-127} associated with Mcl-$1^{128-350}$. At Asp158 that produce Mcl-1^{1-157} associated with Mcl-$1^{158-350}$ (Herrant et al., 2004). Interestingly, not all Mcl-1 cleavage fragments revoke anti-apoptotic function. Mcl-1Δ127 fragment has anti-apoptotic function same as Mcl-1 and exists mainly in the cytoplasm and sequester BH3-only or Bak in order to prevent apoptosis (Wang and et al., 2020).

The Mcl-1 phosphorylation plays a critical role in controlling Mcl-1 function as well. Mcl-1 phosphorylation occurs by several protein kinases including; c-Jun N-terminal kinase (JNK) (Inoshita et al., 2002), glycogen synthase kinase 3 (GSK-3) (Maurer et al., 2006; Ding et al., 2007), and extracellular signal-regulated kinase (ERK-1) (Domina et al., 2004; Ding et al., 2008). The phosphorylated Mcl-1 proteins have been reported to result in different functions according to phosphorylation sites (Thomas et al., 2010; Senichkin et al., 2020). Furthermore, a reversible form of post-translational ubiquitination controls several aspects of Mcl-1 including stability and proteasomal degradation and allow for rapid respond to environmental signals in order to change cell state from survival to apoptosis. The Mcl-1 ubiquitin-proteasome system is mediated by five different E3 ubiquitin-ligases including Mcl-1 ubiquitin ligase E3 (Mule) (Zhong et al., 2005), SCF beta-transducin repeats containing protein ($SCF^{\beta-TrCP}$) (Ding et al., 2007), SCF F-box and WD repeat domain containing 7 (SCF^{Fbw7}) (Inuzuka et al., 2011),

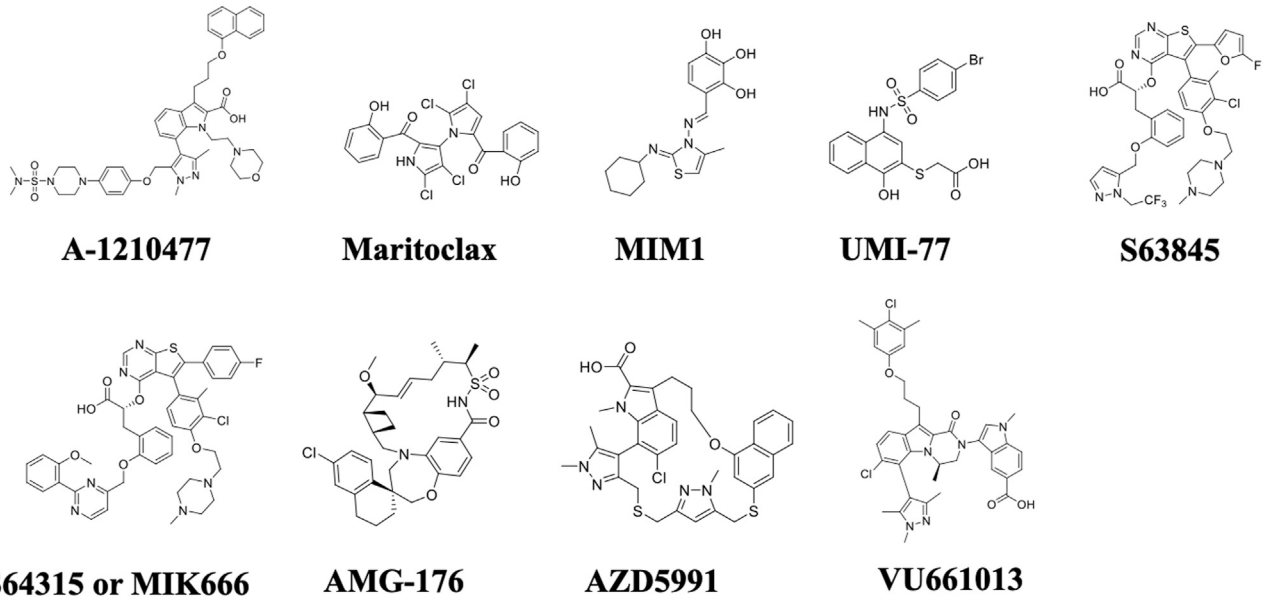

FIGURE 4 | Chemical structures of selective Mcl-1 inhibitors. The most prominent Mcl-1 inhibitors including A-1210477, Maritoclax, MIM1, UMI-77, S63845, S64315/MIK666, AMG-176, AZD5991, and VU661013.

anaphase-promoting complex/cyclosome (APC/CC^{dc20}) (Harley et al., 2010), and tripartite motif containing 17 (Trim17) (Magiera et al., 2013). Furthermore, the ubiquitin-proteasome system contains an additional deubiquitinase called ubiquitin specific peptidase 9, X-linked (USP9X) that removes poly-ubiquitin chains leading to stabilize Mcl-1 and prevent apoptosis (Schwickart et al., 2010). The degree of ubiquitination is also subject to variation based upon the variable phosphorylation of residues of Mcl-1 (Maurer et al., 2006; Ding et al., 2007). Our understanding of Mcl-1 regulations has been greatly expanded by the findings that have developed over the years and provide deep critical insights into exactly how Mcl-1 protein plays such a key role in cellular apoptosis as well as how it can be modulated to provide new options of potential therapeutic approach in MM and other Mcl-1 dependent cancers.

DEVELOPMENT OF SELECTIVE MCL-1 INHIBITORS

Studies have demonstrated that MM depends on Mcl-1 proteins for survival, prognosis, and chemo resistance. Thus, inhibition of Mcl-1 offers an attractive target and a promising strategy for myeloma treatment. Nonetheless, the targeting of Mcl-1 has been challenging because of its complex regulation. So far, two approaches have been adopted to inhibit Mcl-1, one is direct inhibition and second is indirect targeting. The indirect targeting is a less selective method inhibits other anti-apoptotic proteins, may have more serious side effects. Whereas, direct Mcl-1 inhibitors target the hydrophobic cleft BH3-binding groove of BH3-only proteins interactions domain. Therefore, these inhibitors are very specific to Mcl-1. Here we will review BH3-mimetic inhibitors that selectively bind Mcl-1. The structure of these inhibitors are shown in **Figure 4**. The current status of development of these agents are summarized in **Table 2**.

Indole-2-Carboxylic Acids Analog (A-1210477)

This was developed by AbbVie in 2008. A-1210477 induces intrinsic apoptosis pathway by selectively inhibiting Mcl-1 with high binding affinity (Ki = 0.454 nM) (Leverson and et al., 2015). Upon binding, BH3 mimetic A-1210477 results in an accumulation of Mcl-1 protein by preventing its degradation. A-1210477 disrupts the Mcl-1:Bim and Mcl-1: Noxa complexes in order to induce Bax/Bak- dependent MOMP, leading to Cytochrome C release and Caspase activation (Leverson and et al., 2015). The treatment of A-1210477 decreased the association of Mcl-1: Bak complex within an hour, however the complex was totally disrupted after three hours of treatment (Gomez-Bougie et al., 2018). Interestingly, the studies of Mallick et al. (2019) showed that A-1210477 induces rapid apoptosis within 0.5–1 h of treatment, without inducing Noxa (Mallick and et al., 2019). A-1210477 as a monotherapy or in a combination with Navitoclax resulted in death of different cell lines including MM, melanoma, and non-small cell lung cancer cell lines that were found to be Mcl-1 dependent by BH3 profiling or siRNA rescue experiments (Leverson and et al., 2015; Mukherjee and et al., 2018). This finding was reinforced by the efficacy of A-1210477 as a combination with Venetoclax against acute myeloid leukemia (AML) (Fiskus and et al., 2019). A-1210477 inhibited triple negative breast cancer cell line growth activity in vitro which

TABLE 2 | Direct Mcl-1 Inhibitors BH3 Mimetic and semi BH3 Mimetic drugs.

Mcl-1 inhibitor	Company	Affinity	Clinical trial status
A-1210477	Abbive	Ki = 0.45 nM	Preclinical
Maritoclax	Hong-Gang Wang's group at Pennsylvania State University	IC50 10 μM	Preclinical
MIM1	Cohen and coworkers	Only at very high concentration	Failed *in vivo*
UMI-77	Zaneta Nikolovska-Coleska's group at University of Michigan	Ki = 490 nM	Preclinical
S63845	Servier and Vernalis	Kd = 0.19 nM	Preclinical
S64315/ MIK666	Servier and Vernalis and Novartis	undisclosed	Phase I by Novartis, in R/R lymphoma or R/R MM patients (NCT02992483) Phase I by Servier, in AML and MDS patients (NCT02979366) Phase I by Servier as a combination of S64315/MIK666 plus Venetoclax in AML patients (NCT03672695)
AMG-176	Amgen	Ki = 0.06 nM	Phase I in R/R MM and R/R AML patients (NCT02675452) Phase I as a combination of AMG-176 plus Venetoclax in different R/R hematologic malignancies including AML, NHL, and DLBCL (NCT03797261)
AMG-397	Amgen	undisclosed	Phase I clinical trial is evaluating the safety, tolerability, pharmacokinetics, and efficacy of AMG 397 in MM, AML, DLBCL, and NHL patients (NCT03465540)
AZD5991	AstraZeneca	Ki = 0.2 nM	Phase I as a monotherapy in different R/R hematologic malignancies including NHL, ALL, RS, SLL, T-cell lymphoma, CTCL, CLL, AML/MDS, and MM patients (NCT03218683) Phase II is sequential, dose-escalation study of combination AZD5991 plus Venetoclax in R/R AML/MDS patients (NCT03218683)
VU661013	Stephen Fesik's group at Vanderbilt University	Ki = 0.097 nM	Have partnership with Boehringer Ingelheim Company for clinical trials but no plan disclosed yet. (https://www.boehringer-ingelheim.us/press-release/boehringeringelheim-and-vanderbilt-university-expand-partnership-develop-novel)

is also considered a Mcl-1 dependent cells type (Campbell and et al., 2018). However, a reference showing A-1210477 induced apoptosis in Bcl-2 dependent cells at higher concentration when compared with Mcl-1 inhibition concentration (Koss et al., 2016). Unfortunately, no in vivo activity was associated with A-1210477, even with the most sensitive cell lines. This was attributed to cell penetration issues and reduced bioavailability due to the high levels of serum protein binding.

Marinopyrrole A (Maritoclax)

This natural agent was first discovered by Hong-Gang Wang's group at Pennsylvania State University in 2012 (Doi et al., 2012). The BH3 mimetic drug Maritoclax induces degradation of Mcl-1 proteins and disrupt Mcl-1: Bim complex. Maritoclax effectively binds the site of the BH3-only proteins p4 binding site and leads to apoptosis. Further, it has been reported that this natural agent is effective against Mcl-1 overexpressing cancer cells (Doi et al., 2012). Blocking BH3 binding site is related with increasing amount of Mcl-1 protein, followed by its ubiquitination and degradation by the E3 ligase (ubiquitin ligase) (Kaleigh and Manabu, 2013). Moreover, the treatment of Maritoclax did not result in Noxa upregulation (Doi et al., 2012). We found that Maritoclax potentiates the apoptotic response of ABT-737 in human melanoma cells (Pandey and et al., 2013).

Mcl-1 Inhibitor Molecule 1 (MIM1)

Developed in 2012 by Cohen and co-workers, polyphenol compound MIM1 acts as a semi BH3 mimetic which induces Noxa (Cohen et al., 2012). MIM1 seems very similar to BH3 mimetic Mcl-1 inhibitors (Mallick and et al., 2019). This Mcl-1 inhibitor exhibited an ability to induce apoptosis in Mcl-1 dependent cells through upregulation of proapoptotic protein Noxa, which selectively inhibits Mcl-1 with high affinity binding (Smith et al., 2011; Kale et al., 2018; Mallick and et al., 2019). Also, induction of Noxa dissociates Mcl-1:Bim association complex. Unfortunately, MIM1 was only able to induce Bak dependent apoptosis at high concentrations (more than 10 μM). MIM1 failed to induce apoptosis in anti-apoptotic proteins dependent cell lines (Varadarajan et al., 2013).

UMI-77

Developed in 2013 by Zaneta Nikolovska-Coleska's group at University of Michigan, naphthol derivative UMI-77 is another semi BH3 mimetic Mcl-1 inhibitor with high binding affinity (Ki = 490 nM) (Azmi and et al., 2013; Abulwerdi et al., 2014). In order to induce apoptosis, UMI-77 was found to upregulate pro-apoptotic protein Noxa thereby selectively inhibit Mcl-1 (Mallick and et al., 2019). UMI-77 and Noxa competing for Mcl-1 binding with Bax and Bak proteins ultimately disrupt the Mcl-1: Bak and Mcl-1: Bak complexes, which results in Cytochrome C release and Caspase 3 activation (Abulwerdi et al., 2014). The *in vitro* and *in vivo* preclinical studies demonstrated that UMI-77 potently inhibits tumor growth and induces apoptosis in MM cells (Azmi and et al., 2013), and pancreatic cancer cells lines (Abulwerdi et al., 2014), both of which rely on the Mcl-1 protein as a survival factor (Miyamoto et al., 1999; Schniewind et al., 2004; Ren et al., 2009).

In addition to pancreatic cancer cell line BxPC-3 xenograft mouse model and MM animal xenografts, UMI-77 significantly delayed growth activity in breast cancer cell line MDA-MB-468 xenograft mouse model as well (Campbell and et al., 2018).

S63845

Developed in 2015 by a Servier and Vernalis partnership, atropisomers thienopyrimidine scaffold molecule S63845 is a selective BH3 mimetic Mcl-1 inhibitor that can activates the Bax/Bak dependent mitochondrial apoptotic pathway (Kotschy et al., 2016). S63845 is a selective and potent BH3 mimetic. It binds with high affinity to the BH3-binding groove of Mcl-1 (Kd = 0.19 nM) without any detectable binding to Bcl-2 or Bcl-xL proteins. S63845 showed effective anti-cancer activity in its *in vitro* and *in vivo* preclinical studies (Kotschy et al., 2016). The IV infusion of S63845 once daily for five consecutive days resulted in 100% tumor regression in MM subcutaneous tumor models and lymphoma disseminated mouse model Eμ-Myc (Kotschy et al., 2016; Brennan et al., 2018). The same tumor regression was related with AML as well (Kotschy et al., 2016). This inhibitor had a therapeutic effect without significant weight loss apparent side effects in normal mice tissues (Kotschy et al., 2016). Along with A-1210477 and UMI-77, S63845 also inhibited growth activity of TN breast cancer cell line (Campbell and et al., 2018).

After S63845 proved its eligibility as a selective Mcl-1 antagonist, impressive studies have continued coming up. Recently in 2019, S63845 showed activity both *in vitro* and *in vivo* by killing human T cell acute lymphoblastic leukemia cells (T-ALL) (Li et al., 2019). It was even more potent in inducing apoptosis as a combination therapy with Venetoclax without any appreciable toxicity (Li et al., 2019). In 2020, *in vitro*, *ex vivo,* and *in vivo* preclinical evaluations investigated the combination of S63845 plus Venetoclax. *In vitro* study tested the sensitivities of five MM cell lines to the drug while the *in vivo* study used an aggressive disseminated model of MM. The combined finding came clearly with increasing apoptotic cell death, reduced cell survival as well as delayed tumor growth *in vivo* (Algarín et al., 2020). Furthermore, S63845 was evaluated in a triple combination with Venetoclax plus dexamethasone. Clearly, *in vitro* and *in vivo* studies showed that dexamethasone increased the effectiveness of both S63845 and Venetoclax. Furthermore, *in vitro* studies illustrated that the triple therapy is a stronger synergism than the S63845 plus Venetoclax in resistant MM cell line (MM.1S) (Algarín et al., 2020). In addition, the combination of S63845 and Venetoclax, enhanced the Venetoclax sensitivity and overcome resistance to Venetoclax in human myeloma cell lines (HMCLs) (Wong and Chim, 2020).

Servier and Vernalis and Novartis have created another S-derivative called S64315 or MIK666. S64315/MIK666 is in clinical trial as a single agent in R/R lymphoma or R/R MM (NCT02992483). Furthermore, this molecule being tested in AML and myelodysplastic syndrome (MDS) patients (NCT02979366). Another clinical trial is undergoing by Servier and Vernalis in a combination with Venetoclax in AML patients (NCT03672695).

AMG-176

Developed in 2016 by Amgen, chirality macrocyclic acylsulfonamide (spiromacrocyclic) AMG-176 is an orally selective Mcl-1 inhibitor with high binding affinity (Ki = 0.06 nM), induces rapid apoptosis in different hematologic malignancies. The treatment of AMG-176 disrupts the interactions of the Mcl-1: Bak complex (Caenepeel et al., 2018; Caenepeel and et al., 2017). Preclinical studies have demonstrated that AMG-176 is non-toxic and efficacious in both MM subcutaneous xenograft models and disseminated models, inhibited 100% tumor growth (Caenepeel et al., 2018). In preclinical studies, AMG-176 has been shown to eradicate CLL cells as a single agent or in a combination with a low dose of Venetoclax (Yi and et al., 2020). Interestingly, AMG-176 was the first selective Mcl-1 inhibitor to be studied in humans. Currently, AMG-176 is in phase I clinical trials *via* IV administrations in patients with R/R MM and patients with R/R AML (NCT02675452). AMG-176 monotherapy has potent anti-myeloma and unique hematologic activity resulting in marked survival improvement. Furthermore, phase I clinical trials have also evaluated AMG-176 as a combination therapy with Venetoclax which presents as an interesting therapy for different R/R hematologic malignancies including AML, diffuse large B cell lymphoma (DLBCL), and Non-Hodgkin's lymphoma (NHL) (NCT03797261). Furthermore, as a combination with MEK inhibitor (Trametinib), AMG-176 increased the tumor regression effect in murine models of solid tumor cell lines (Nangia et al., 2018).

Amgen has developed another potent and selective analog AM-8621, nonetheless, this molecule has poor oral bioavailability and short half-life (Caenepeel et al., 2018). Interestingly, MM cells showed sensitivity to AM-8621 as a monotherapy and as a combination therapy with dexamethasone (Caenepeel et al., 2018). Caenepeel et al. (2019) investigated the activities of AMG 176 and AM-8621 in combination with Cytarabine, Doxorubicin, and Decitabine in a preclinical models of AML (Caenepeel and et al., 2019). The other analog AMG-397 is evaluated orally in the clinic. A phase I clinical trial evaluating its safety, tolerability, pharmacokinetics, and efficacy in MM, AML, DLBCL, and NHL patients by administrating AMG-397 in a weekly cycle consisting of two consecutive days of one oral dose followed by five days off at a weekly interval (NCT03465540).

AZD5991

Developed in 2017 by AstraZeneca, indole-2-carboxylic acids analog AZD5991, is a potent and selective macrocyclic Mcl-1 inhibitor that rapidly activates Caspase proteins, which leads to apoptosis in MM cell lines (GI_{50} = 10 nM) (Hird and et al., 2017; Tron et al., 2018). AZD5991 is a BH3 mimetic with high binding affinity (Ki = 0.2 nM) disrupts the Mcl-1: Bak complex (Hird and et al., 2017; Tron et al., 2018). Most notably, in a number of MM and AML mouse and rat xenograft models, AZD5991 exhibits a potent activity with the preclinical *in vivo* studies showing 100% tumor regression after a single IV dose in both monotherapy and in combination with Venetoclax or Bortezomib (Tron et al., 2018). The preclinical efficacy of AZD5991 is emphasized by the apoptosis and survival improvements in MM models resistant

to Venetoclax (Hird and et al., 2017). The remarkable *in vitro* and *in vivo* anti-tumor activities of AZD5991 in both MM and AML models support its consideration as a strong clinical candidate in different Mcl-1 dependent hematologic malignancies. The number of clinical trials are ongoing with AZD5991 as a single agent or in combinations. For example, phase 1 as a monotherapy dose escalation study in several R/R hematologic malignancies including NHL, ALL, Richter syndrome (RS), small lymphocytic lymphoma (SLL), T-cell lymphoma and cutaneous T-cell lymphoma (CTCL) (NCT03218683); phase 1 as a monotherapy in expansion groups of R/R CLL, AML/MDS, and MM patients; and Phase 2 sequential, dose escalation study in combination with Venetoclax in R/R AML/MDS patients (NCT03218683).

VU661013

Developed in 2017 by Stephen Fesik's group at Vanderbilt University, indole-2-carboxylic acids analog VU661013 is a potent and selective BH3 mimetic Mcl-1 inhibitor with high binding affinity (Ki = 0.097 nM) (Lee et al., 2017). VU661013 destabilizes the Mcl-1: Bim complex in order to initiate MOMP (Ramsey et al., 2018). VU661013 proved potency in Mcl-1 inhibition in both *in vitro* and *in vivo* studies through its induction of apoptosis in a variety of Mcl-1 dependent tumors. Furthermore, it demonstrated efficacy in combination with Venetoclax in Venetoclax resistant cells, patient derived xenografts, and murine models of AML (Ramsey et al., 2018). The further modifications of this molecule is being made to improve the efficacy and bioavailability. Another analog has been made (compound 42), which bound to Mcl-1 with picomolar affinity (Ki = 70–300 pM) in order to displace Bim (Lee et al., 2019). Compound 42 showed *in vivo* growth inhibition in xenograft models of MM and AML (Lee et al., 2019).

CONCLUSION AND FUTURE DIRECTION

The anti-apoptotic protein Mcl-1 is critical in survival and drug resistance of several malignancies including MM (Krajewska et al., 1996; Miyamoto et al., 1999; Andersen et al., 2005; Song et al., 2005; Ding et al., 2007; Boisvert-Adamo et al., 2009; Brotin et al., 2010). Last decade or so has seen tremendous development, various Mcl-1 inhibitors have been developed. These new inhibitors may help in overcoming drug resistance and improve treatment of MM and other hematological malignancies where Mcl-1 is an important survival factor. The numerous BH3 mimetic and semi BH3 mimetic drugs have proved their efficacy in preclinical studies. Hopefully, after clinical trial of one of these numerous drugs receive FDA approval. It may open up a new door in the targeted MM therapy that will help to improve medical approaches, and the outcome of MM patients. Although, Mcl-1 inhibitors have good anti-myeloma activity as a monotherapy in hematological cancer models, most development strategies are focused on combination, which can increase the potential of these molecules. These combinations are shown to be especially valuable if the drug consists of a selective Mcl-1 inhibitor plus an existing drug that inhibits other anti-apoptotic proteins including Bcl-2 and Bcl-xL, and/or drug that induce pro-apoptotic proteins expression. Combination therapies such as selective Bcl-2 proteins inhibitors or proteasome inhibitors (Venetoclax or Bortezomib) have been attempted to improve the therapeutic outcome (Caenepeel et al., 2018; Ramsey et al., 2018; Tron et al., 2018; Moujalled et al., 2019). Furthermore, the triple combination therapy plus dexamethasone has shown a good effect and presents as an effective strategy (Algarín et al., 2020). Interestingly, three of the recently developed BH3-mimetic are in clinical trials as a combination therapy with Venetoclax. These combination strategies allow patients to interrupt treatment for long periods of time and show a successful development for this new drug class. Based on this information, nowadays the small molecule BH3 mimetics and semi mimetics compounds represent the most promising approach for the selective inhibition of Mcl-1. This places the priority on the rational design of novel BH3 mimetic drugs that binds extremely tightly and selectively to Mcl-1 for the better outcome of the treatment.

AUTHOR CONTRIBUTIONS

OA-O, MS, RC, WE collected the literature, made figures, tables and wrote the draft. TB-A provided clinical insight and edited the draft. SJ and BA provided chemical and inflammatory insights and modified the draft, and MP conceived the idea, provided the instructions and finally edited the manuscript.

FUNDING

This work was supported by Camden Research Initiative fund (MP, TB-A, and SJ), New Jersey Health Foundation (SJ, MP.), and inter department fund from Cooper Medical School of Rowan University, Camden, NJ (MP).

ACKNOWLEDGMENTS

This work was supported by Camden Research Initiative fund (MP, TB-A, and SJ), New Jersey Health Foundation (SJ, MP), and inter department fund from Cooper Medical School of Rowan University, Camden, NJ (MP). The authors are thankful to Kishore Challagundla for helping in figures through Biorender.com. The authors are thankful to Rachel King, Cooper Medical School of Rowan University Library for careful proofreading and editing the manuscript.

REFERENCES

Abdi, J., Chen, G., and Chang, H. (2013). Drug Resistance in Multiple Myeloma: Latest Findings and New Concepts on Molecular Mechanisms. *Oncotarget* 4 (12), 2186–2207. doi:10.18632/oncotarget.1497

Abulwerdi, F., Liao, C., Liu, M., Azmi, A. S., Aboukameel, A., Mady, A. S. A., et al. (2014). A Novel Small-Molecule Inhibitor of Mcl-1 Blocks Pancreatic Cancer Growth *In Vitro* and *In Vivo*. *Mol. Cancer Ther.* 13 (3), 565–575. doi:10.1158/1535-7163.mct-12-0767

Algarín, E. M., Díaz-Tejedor, A., Mogollón, P., Hernández-García, S., Corchete, L. A., San-Segundo, L., et al. (2020). Preclinical Evaluation of the Simultaneous Inhibition of MCL-1 and BCL-2 with the Combination of S63845 and Venetoclax in Multiple Myeloma. *Haematologica* 105 (3), e116–e120. doi:10.3324/haematol.2018.212308

Andersen, M. H., Becker, J. C., and Thor Straten, P. (2005). The Antiapoptotic Member of the Bcl-2 Family Mcl-1 Is a CTL Target in Cancer Patients. *Leukemia* 19 (3), 484–485. doi:10.1038/sj.leu.2403621

Azmi, A. S., Nikolovka-Coleska, Z., Abidi, M., Marsack, K., Masood, A., Yano, H., et al. (2013). "Selective Inhibitors of Mcl-1 with Potent Activity against Multiple Myeloma Patient Cells and Animal Xenografts," in AACR 104th Annual Meeting 2013, April 6–10, 2013 (Washington, DC: AACR). doi:10.1158/1538-7445.am2013-3438

Bae, J., Leo, C. P., Hsu, S. Y., and Hsueh, A. J. W. (2000). MCL-1S, a Splicing Variant of the Antiapoptotic BCL-2 Family Member MCL-1, Encodes a Proapoptotic Protein Possessing Only the BH3 Domain. *J. Biol. Chem.* 275 (33), 25255–25261. doi:10.1074/jbc.m909826199

Bergsagel, D. E., Sprague, C. C., Austin, C., and Griffith, K. M. (1962). Evaluation of New Chemotherapeutic Agents in the Treatment of Multiple Myeloma. IV. L-Phenylalanine Mustard (NSC-8806). *Cancer Chemother. Rep.*, 21, 87–99.

Bergsagel, P. L., and Kuehl, W. M. (2005). Molecular Pathogenesis and a Consequent Classification of Multiple Myeloma. *J. Clin. Oncol.* 23 (26), 6333–6338. doi:10.1200/jco.2005.05.021

Bingle, C. D., Craig, R. W., Swales, B. M., Singleton, V., Zhou, P., and Whyte, M. K. B. (2000). Exon Skipping in Mcl-1 Results in a Bcl-2 Homology Domain 3 Only Gene Product that Promotes Cell Death. *J. Biol. Chem.* 275 (29), 22136–22146. doi:10.1074/jbc.m909572199

Boisvert-Adamo, K., Longmate, W., Abel, E. V., and Aplin, A. E. (2009). Mcl-1 Is Required for Melanoma Cell Resistance to Anoikis. *Mol. Cancer Res.* 7 (4), 549–556. doi:10.1158/1541-7786.mcr-08-0358

Brennan, M. S., Chang, C., Tai, L., Lessene, G., Strasser, A., Dewson, G., et al. (2018). Humanized Mcl-1 Mice Enable Accurate Preclinical Evaluation of MCL-1 Inhibitors Destined for Clinical Use. *Blood* 132 (15), 1573–1583. doi:10.1182/blood-2018-06-859405

Brotin, E., Meryet-Figuière, M., Simonin, K., Duval, R. E., Villedieu, M., Leroy-Dudal, J., et al. (2010). Bcl-XL and MCL-1 Constitute Pertinent Targets in Ovarian Carcinoma and Their Concomitant Inhibition Is Sufficient to Induce Apoptosis. *Int. J. Cancer* 126 (4), 885–895. doi:10.1002/ijc.24787

Caenepeel, S., Brown, S. P., Belmontes, B., Moody, G., Keegan, K. S., Chui, D., et al. (2018). AMG 176, a Selective MCL1 Inhibitor, Is Effective in Hematologic Cancer Models Alone and in Combination with Established Therapies. *Cancer Discov.* 8 (12), 1582–1597. doi:10.1158/2159-8290.CD-18-0387

Caenepeel, S., Belmontes, B., Osgood, T., Cajulis, E., Coxon, A., Canon, J., et al. (2019). "AMG 176 Exhibits Robust Antitumor Activity in Combination with Standard of Care Agents in Models of Acute Myeloid Leukemia," in AACR Annual Meeting 2019, March 29–April 3, 2019 (Atlanta, GA: AACR). doi:10.1158/1538-7445.am2019-2180

Caenepeel, S. R., Brown, S. P., Belmontes, B., Moody, G., Keegan, K. S., Chui, D., et al. (2017). "Preclinical Evaluation of AMG 176, a Novel, Potent and Selective Mcl-1 Inhibitor with Robust Anti-tumor Activity in Mcl-1 Dependent Cancer Models," in AACR Annual Meeting 2017, April 1–5, 2017 (Washington, DC: AACR). doi:10.1158/1538-7445.am2017-2027

Calame, K. L., Lin, K.-I., and Tunyaplin, C. (2003). Regulatorymechanisms Thatdetermine Thedevelopment Andfunction Ofplasmacells. *Annu. Rev. Immunol.* 21, 205–230. doi:10.1146/annurev.immunol.21.120601.141138

Campbell, K. J., Dhayade, S., Ferrari, N., Sims, A. H., Johnson, E., Mason, S. M., et al. (2018). MCL-1 Is a Prognostic Indicator and Drug Target in Breast Cancer. *Cell Death Dis* 9 (2), 19. doi:10.1038/s41419-017-0035-2

Chao, J.-R., Wang, J.-M., Lee, S.-F., Peng, H.-W., Lin, Y.-H., Chou, C.-H., et al. (1998). mcl-1 Is an Immediate-Early Gene Activated by the Granulocyte-Macrophage colony-stimulating Factor (GM-CSF) Signaling Pathway and Is One Component of the GM-CSF Viability Response. *Mol. Cel Biol* 18 (8), 4883–4898. doi:10.1128/mcb.18.8.4883

Cohen, N. A., Stewart, M. L., Gavathiotis, E., Tepper, J. L., Bruekner, S. R., Koss, B., et al. (2012). A Competitive Stapled Peptide Screen Identifies a Selective Small Molecule that Overcomes MCL-1-dependent Leukemia Cell Survival. *Chem. Biol.* 19 (9), 1175–1186. doi:10.1016/j.chembiol.2012.07.018

Cui, J., and Placzek, W. J. (2018). Post-transcriptional Regulation of Anti-apoptotic BCL2 Family Members. *Int. J. Mol. Sci.* 19 (1), 308. doi:10.3390/ijms19010308

Czabotar, P. E., Lee, E. F., van Delft, M. F., Day, C. L., Smith, B. J., Huang, D. C. S., et al. (2007). Structural Insights into the Degradation of Mcl-1 Induced by BH3 Domains. *Proc. Natl. Acad. Sci.* 104 (15), 6217–6222. doi:10.1073/pnas.0701297104

Czabotar, P. E., Lessene, G., Strasser, A., and Adams, J. M. (2014). Control of Apoptosis by the BCL-2 Protein Family: Implications for Physiology and Therapy. *Nat. Rev. Mol. Cel Biol* 15 (1), 49–63. doi:10.1038/nrm3722

Dankbar, B., Padró, T., Leo, R., Feldmann, B., Kropff, M., Mesters, R. M., et al. (2000). Vascular Endothelial Growth Factor and Interleukin-6 in Paracrine Tumor-Stromal Cell Interactions in Multiple Myeloma. *Blood* 95 (8), 2630–2636. doi:10.1182/blood.v95.8.2630.008k05_2630_2636

De Bruyne, E., Bos, T. J., Schuit, F., Van Valckenborgh, E., Menu, E., Thorrez, L., et al. (2010). IGF-1 Suppresses Bim Expression in Multiple Myeloma via Epigenetic and Posttranslational Mechanisms. *Blood* 115 (12), 2430–2440. doi:10.1182/blood-2009-07-232801

Denis, C., Sopková-de Oliveira Santos, J., Bureau, R., and Voisin-Chiret, A. S. (2020). Hot-Spots of Mcl-1 Protein. *J. Med. Chem.* 63 (3), 928–943. doi:10.1021/acs.jmedchem.9b00983

Derenne, S., Monia, B., Dean, N. M., Taylor, J. K., Rapp, M.-J., Harousseau, J.-L., et al. (2002). Antisense Strategy Shows that Mcl-1 rather Than Bcl-2 or Bcl-xL Is an Essential Survival Protein of Human Myeloma Cells. *Blood* 100 (1), 194–199. doi:10.1182/blood.v100.1.194

Dewson, G., and Kluck, R. M. (2009). Mechanisms by Which Bak and Bax Permeabilise Mitochondria during Apoptosis. *J. Cel Sci* 122 (Pt 16), 2801–2808. doi:10.1242/jcs.038166

Ding, Q., He, X., Hsu, J.-M., Xia, W., Chen, C.-T., Li, L.-Y., et al. (2007). Degradation of Mcl-1 by β-TrCP Mediates Glycogen Synthase Kinase 3-Induced Tumor Suppression and Chemosensitization. *Mol. Cel Biol* 27 (11), 4006–4017. doi:10.1128/mcb.00620-06

Ding, Q., He, X., Xia, W., Hsu, J.-M., Chen, C.-T., Li, L.-Y., et al. (2007). Myeloid Cell Leukemia-1 Inversely Correlates with Glycogen Synthase Kinase-3β Activity and Associates with Poor Prognosis in Human Breast Cancer. *Cancer Res.* 67 (10), 4564–4571. doi:10.1158/0008-5472.can-06-1788

Ding, Q., Huo, L., Yang, J.-Y., Xia, W., Wei, Y., Liao, Y., et al. (2008). Down-regulation of Myeloid Cell Leukemia-1 through Inhibiting Erk/Pin 1 Pathway by Sorafenib Facilitates Chemosensitization in Breast Cancer. *Cancer Res.* 68 (15), 6109–6117. doi:10.1158/0008-5472.can-08-0579

Doi, K., Li, R., Sung, S.-S., Wu, H., Liu, Y., Manieri, W., et al. (2012). Discovery of Marinopyrrole A (Maritoclax) as a Selective Mcl-1 Antagonist that Overcomes ABT-737 Resistance by Binding to and Targeting Mcl-1 for Proteasomal Degradation. *J. Biol. Chem.* 287 (13), 10224–10235. doi:10.1074/jbc.m111.334532

Domina, A. M., Vrana, J. A., Gregory, M. A., Hann, S. R., and Craig, R. W. (2004). MCL1 Is Phosphorylated in the PEST Region and Stabilized upon ERK Activation in Viable Cells, and at Additional Sites with Cytotoxic Okadaic Acid or Taxol. *Oncogene* 23 (31), 5301–5315. doi:10.1038/sj.onc.1207692

Fiskus, W., Cai, T., DiNardo, C. D., Kornblau, S. M., Borthakur, G., Kadia, T. M., et al. (2019). Superior Efficacy of Cotreatment with BET Protein Inhibitor and BCL2 or MCL1 Inhibitor against AML Blast Progenitor Cells. *Blood Cancer J.* 9 (2), 1–13. doi:10.1038/s41408-018-0165-5

Gerecke, C., Fuhrmann, S., Strifler, S., Schmidt-Hieber, M., Einsele, H., and Knop, S. (2016). The Diagnosis and Treatment of Multiple Myeloma. *Dtsch Arztebl Int.* 113 (27-28), 470–476. doi:10.3238/arztebl.2016.0470

Gomez-Bougie, P., Bataille, R. g., and Amiot, M. (2004). The Imbalance between Bim and Mcl-1 Expression Controls the Survival of Human Myeloma Cells. *Eur. J. Immunol.* 34 (11), 3156–3164. doi:10.1002/eji.200424981

Gomez-Bougie, P., Maiga, S., Tessoulin, B., Bourcier, J., Bonnet, A., Rodriguez, M. S., et al. (2018). BH3-mimetic Toolkit Guides the Respective Use of BCL2 and MCL1 BH3-Mimetics in Myeloma Treatment. *J. Am. Soc. Hematol.* 132 (25), 2656–2669. doi:10.1182/blood-2018-03-836718

Harley, M. E., Allan, L. A., Sanderson, H. S., and Clarke, P. R. (2010). Phosphorylation of Mcl-1 by CDK1-Cyclin B1 Initiates its Cdc20-dependent Destruction during Mitotic Arrest. *EMBO J.* 29 (14), 2407–2420. doi:10.1038/emboj.2010.112

Herndon, T. M., Deisseroth, A., Kaminskas, E., Kane, R. C., Koti, K. M., Rothmann, M. D., et al. (2013). US Food and Drug Administration Approval: Carfilzomib for the Treatment of Multiple Myeloma. *Clinical cancer research*, 19(17), 4559–4563.

Herrant, M., Jacquel, A., Marchetti, S., Belhacène, N., Colosetti, P., Luciano, F., et al. (2004). Cleavage of Mcl-1 by Caspases Impaired its Ability to Counteract Bim-Induced Apoptosis. *Oncogene* 23 (47), 7863–7873. doi:10.1038/sj.onc.1208069

Hideshima, T., Chauhan, D., Shima, Y., Raje, N., Davies, F. E., Tai, Y. T., et al. (2000). Thalidomide and its Analogs Overcome Drug Resistance of Human Multiple Myeloma Cells to Conventional Therapy. *Blood*, 96(9), 2943–2950.

Hird, A. W., Secrist, P. J., Adam, A., Belmonte, M. A., Gangl, E., Gibbons, F., et al. (2017). "Abstract DDT01-02: AZD5991: A Potent and Selective Macrocyclic Inhibitor of Mcl-1 for Treatment of Hematologic Cancers," in AACR Annual Meeting 2017, April 1–5, 2017 (Washington, DC: AACR). doi:10.1158/1538-7445.am2017-ddt01-02

Huang, H.-M., Huang, C.-J., and Yen, J. J.-Y. (2000). Mcl-1 Is a Common Target of Stem Cell Factor and Interleukin-5 for Apoptosis Prevention Activity via MEK/MAPK and PI-3K/Akt Pathways. *Blood* 96 (5), 1764–1771. doi:10.1182/blood.v96.5.1764

Inoshita, S., Takeda, K., Hatai, T., Terada, Y., Sano, M., Hata, J., et al. (2002). Phosphorylation and Inactivation of Myeloid Cell Leukemia 1 by JNK in Response to Oxidative Stress. *J. Biol. Chem.* 277 (46), 43730–43734. doi:10.1074/jbc.m207951200

Inuzuka, H., Shaik, S., Onoyama, I., Gao, D., Tseng, A., Maser, R. S., et al. (2011). SCFFBW7 Regulates Cellular Apoptosis by Targeting MCL1 for Ubiquitylation and Destruction. *Nature* 471 (7336), 104–109. doi:10.1038/nature09732

Jourdan, M., De Vos, J., Mechti, N., and Klein, B. (2000). Regulation of Bcl-2-Family Proteins in Myeloma Cells by Three Myeloma Survival Factors: Interleukin-6, Interferon-Alpha and Insulin-like Growth Factor 1. *Cell Death Differ* 7 (12), 1244–1252. doi:10.1038/sj.cdd.4400758

Kale, J., Osterlund, E. J., and Andrews, D. W. (2018). BCL-2 Family Proteins: Changing Partners in the Dance towards Death. *Cel Death Differ* 25 (1), 65–80. doi:10.1038/cdd.2017.186

Kaleigh, F., and Manabu, K. (2013). Evading Apoptosis in Cancer. *Trends Cel Biol* 23, 620–633. doi:10.1016/j.tcb.2013.07.006

Kaufmann, T., Strasser, A., and Jost, P. J. (2012). Fas Death Receptor Signalling: Roles of Bid and XIAP. *Cel Death Differ* 19 (1), 42–50. doi:10.1038/cdd.2011.121

Kazandjian, D. (2016). Multiple Myeloma Epidemiology and Survival: A Unique Malignancy. *Semin. Oncol.* 43 (6), 676–681. doi:10.1053/j.seminoncol.2016.11.004

Kim, J.-H., Sim, S.-H., Ha, H.-J., Ko, J.-J., Lee, K., and Bae, J. (2009). MCL-1ES, a Novel Variant of MCL-1, Associates with MCL-1L and Induces Mitochondrial Cell Death. *FEBS Lett.* 583 (17), 2758–2764. doi:10.1016/j.febslet.2009.08.006

Klein, B., Zhang, X., Lu, Z., and Bataille, R. (1995). Interleukin-6 in Human Multiple Myeloma. *Blood* 85 (4), 863–872. doi:10.1182/blood.v85.4.863.bloodjournal854863

Koss, B., Ryan, J., Budhraja, A., Szarama, K., Yang, X., Bathina, M., et al. (2016). Defining Specificity and On-Target Activity of BH3-Mimetics Using Engineered B-ALL Cell Lines. *Oncotarget* 7 (10), 11500–11511. doi:10.18632/oncotarget.7204

Kotschy, A., Szlavik, Z., Murray, J., Davidson, J., Maragno, A. L., Le Toumelin-Braizat, G., et al. (2016). The MCL1 Inhibitor S63845 Is Tolerable and Effective in Diverse Cancer Models. *Nature* 538 (7626), 477–482. doi:10.1038/nature19830

Kozopas, K. M., Yang, T., Buchan, H. L., Zhou, P., and Craig, R. W. (1993). MCL1, a Gene Expressed in Programmed Myeloid Cell Differentiation, Has Sequence Similarity to BCL2. *Proc. Natl. Acad. Sci.* 90 (8), 3516–3520. doi:10.1073/pnas.90.8.3516

Krajewska, M., Krajewski, S., Epstein, J. I., Shabaik, A., Sauvageot, J., Song, K., et al. (1996). Immunohistochemical Analysis of Bcl-2, Bax, Bcl-X, and Mcl-1 Expression in Prostate Cancers. *Am. J. Pathol.* 148 (5), 1567–1576.

Kumar, S. K., Rajkumar, S. V., Dispenzieri, A., Lacy, M. Q., Hayman, S. R., Buadi, F. K., et al. (2008). Improved Survival in Multiple Myeloma and the Impact of Novel Therapies. *Blood* 111 (5), 2516–2520. doi:10.1182/blood-2007-10-116129

Lacy, M. Q., Hayman, S. R., Gertz, M. A., Dispenzieri, A., Buadi, F., Kumar, S., et al. (2009). Pomalidomide (CC4047) Plus Low-Dose Dexamethasone as Therapy for Relapsed Multiple Myeloma. *J Clin Oncol*, 27(30), 5008–5014.

Laubach, J. P., Moreau, P., San-Miguel, J. F., and Richardson, P. G. (2015). Panobinostat for the Treatment of Multiple Myeloma. *Clin. Cancer Research*, 21(21), 4767-4773.

Le Gouill, S., Podar, K., Amiot, M., Hideshima, T., Chauhan, D., Ishitsuka, K., et al. (2004). VEGF Induces Mcl-1 Up-Regulation and Protects Multiple Myeloma Cells against Apoptosis. *Blood* 104 (9), 2886–2892. doi:10.1182/blood-2004-05-1760

Lee, T., Bian, Z., Zhao, B., Hogdal, L. J., Sensintaffar, J. L., Goodwin, C. M., et al. (2017). Discovery and Biological Characterization of Potent Myeloid Cell Leukemia-1 Inhibitors. *FEBS Lett.* 591 (1), 240–251. doi:10.1002/1873-3468.12497

Lee, T., Christov, P. P., Shaw, S., Tarr, J. C., Zhao, B., Veerasamy, N., et al. (2019). Discovery of Potent Myeloid Cell Leukemia-1 (Mcl-1) Inhibitors that Demonstrate *In Vivo* Activity in Mouse Xenograft Models of Human Cancer. *J. Med. Chem.* 62 (8), 3971–3988. doi:10.1021/acs.jmedchem.8b01991

Leu, C.-M., Chang, C., and Hu, C.-p. (2000). Epidermal Growth Factor (EGF) Suppresses Staurosporine-Induced Apoptosis by Inducing Mcl-1 via the Mitogen-Activated Protein Kinase Pathway. *Oncogene* 19 (13), 1665–1675. doi:10.1038/sj.onc.1203452

Leuenroth, S. J., Grutkoski, P. S., Ayala, A., and Simms, H. H. (2000). The Loss of Mcl-1 Expression in Human Polymorphonuclear Leukocytes Promotes Apoptosis. *J. Leukoc. Biol.* 68 (1), 158–166. doi:10.1189/jlb.68.1.158

Leverson, J. D., Zhang, H., Chen, J., Tahir, S. K., Phillips, D. C., Xue, J., et al. (2015). Potent and Selective Small-Molecule MCL-1 Inhibitors Demonstrate On-Target Cancer Cell Killing Activity as Single Agents and in Combination with ABT-263 (Navitoclax). *Cel Death Dis* 6, e1590. doi:10.1038/cddis.2014.561

Li, Z., He, S., and Look, A. T. (2019). The MCL1-specific Inhibitor S63845 Acts Synergistically with venetoclax/ABT-199 to Induce Apoptosis in T-Cell Acute Lymphoblastic Leukemia Cells. *Leukemia* 33 (1), 262–266. doi:10.1038/s41375-018-0201-2

Liang, H., and Fesik, S. W. (1997). Three-dimensional Structures of Proteins Involved in Programmed Cell Death. *J. Mol. Biol.* 274 (3), 291–302. doi:10.1006/jmbi.1997.1415

Lin, F.-R., Kuo, H.-K., Ying, H.-Y., Yang, F.-H., and Lin, K.-I. (2007). Induction of Apoptosis in Plasma Cells by B Lymphocyte Induced Maturation Protein-1 Knockdown. *Cancer Res.* 67 (24), 11914–11923. doi:10.1158/0008-5472.can-07-1868

Lokhorst, H. M., Plesner, T., Laubach, J. P., Nahi, H., Gimsing, P., Hansson, M., et al. (2015). Targeting CD38 with Daratumumab Monotherapy in Multiple Myeloma. *N. Engl. J. Med.*, 373(13), 1207–1219.

Lonial, S., Dimopoulos, M., Palumbo, A., White, D., Grosicki, S., Spicka, I., et al. (2015). Elotuzumab Therapy for Relapsed or Refractory Multiple Myeloma. *N. Engl. J. Med.*, 373(7), 621–631.

Magiera, M. M., Mora, S., Mojsa, B., Robbins, I., Lassot, I., and Desagher, S. (2013). Trim17-mediated Ubiquitination and Degradation of Mcl-1 Initiate Apoptosis in Neurons. *Cel Death Differ* 20 (2), 281–292. doi:10.1038/cdd.2012.124

Mallick, D. J., Soderquist, R. S., Bates, D., and Eastman, A. (2019). Confounding Off-Target Effects of BH3 Mimetics at Commonly Used Concentrations: MIM1, UMI-77, and A-1210477. *Cel Death Dis* 10 (3), 185. doi:10.1038/s41419-019-1426-3

Maurer, U., Charvet, C., Wagman, A. S., Dejardin, E., and Green, D. R. (2006). Glycogen Synthase Kinase-3 Regulates Mitochondrial Outer Membrane Permeabilization and Apoptosis by Destabilization of MCL-1. *Mol. Cel* 21 (6), 749–760. doi:10.1016/j.molcel.2006.02.009

Miyamoto, Y., Hosotani, R., Wada, M., Lee, J.-U., Koshiba, T., Fujimoto, K., et al. (1999). Immunohistochemical Analysis of Bcl-2, Bax, Bcl-X, and Mcl-1 Expression in Pancreatic Cancers. *Oncology* 56 (1), 73–82. doi:10.1159/000011933

Mojsa, B., Lassot, I., and Desagher, S. (2014). Mcl-1 Ubiquitination: Unique Regulation of an Essential Survival Protein. *Cells* 3 (2), 418–437. doi:10.3390/cells3020418

Moreaux, J., Legouffe, E., Jourdan, E., Quittet, P., Rème, T., Lugagne, C., et al. (2004). BAFF and APRIL Protect Myeloma Cells from Apoptosis Induced by Interleukin 6 Deprivation and Dexamethasone. *Blood* 103 (8), 3148–3157. doi:10.1182/blood-2003-06-1984

Moujalled, D. M., Pomilio, G., Ghiurau, C., Ivey, A., Salmon, J., Rijal, S., et al. (2019). Combining BH3-Mimetics to Target Both BCL-2 and MCL1 Has Potent Activity in Pre-clinical Models of Acute Myeloid Leukemia. *Leukemia* 33 (4), 905–917. doi:10.1038/s41375-018-0261-3

Mukherjee, N., Strosnider, A., Vagher, B., Lambert, K. A., Slaven, S., Robinson, W. A., et al. (2018). BH3 Mimetics Induce Apoptosis Independent of DRP-1 in Melanoma. *Cel Death Dis.* 9 (9), 1–12. doi:10.1038/s41419-018-0932-z

Muz, B., Ghazarian, R. N., Ou, M., Luderer, M. J., Kusdono, H. D., and Azab, A. K. (2016). Spotlight on Ixazomib: Potential in the Treatment of Multiple Myeloma. *Drug Des. Dev. Ther.*, 10, 217.

Nangia, V., Siddiqui, F. M., Caenepeel, S., Timonina, D., Bilton, S. J., Phan, N., et al. (2018). Exploiting MCL1 Dependency with Combination MEK + MCL1 Inhibitors Leads to Induction of Apoptosis and Tumor Regression in KRAS-Mutant Non-small Cell Lung Cancer. *Cancer Discov.* 8 (12), 1598–1613. doi:10.1158/2159-8290.cd-18-0277

Naymagon, L., and Abdul-Hay, M. (2016). Novel Agents in the Treatment of Multiple Myeloma: a Review about the Future. *J. Hematol. Oncol.* 9 (1), 52. doi:10.1186/s13045-016-0282-1

Ogata, A., Chauhan, D., Teoh, G., Treon, S. P., Urashima, M., Schlossman, R. L., et al. (1997). IL-6 Triggers Cell Growth via the Ras-dependent Mitogen-Activated Protein Kinase cascade. *J. Immunol.* 159 (5), 2212–2221.

Pandey, M. K., Gowda, K., Doi, K., Sharma, A. K., Wang, H. G., and Shantu, A. (2013). Proteasomal Degradation of Mcl-1 by Maritoclax Induces Apoptosis and Enhances the Efficacy of ABT-737 in Melanoma Cells. *PLoS One* 8 (11), e78570. doi:10.1371/journal.pone.0078570

Pawlyn, C., and Morgan, G. J. (2017). Evolutionary Biology of High-Risk Multiple Myeloma. *Nat. Rev. Cancer* 17 (9), 543–556. doi:10.1038/nrc.2017.63

Puthier, D., Bataille, R., and Amiot, M. (1999). IL-6 Up-Regulates Mcl-1 in Human Myeloma Cells through JAK/STAT rather Than Ras/MAP Kinase Pathway. *Eur. J. Immunol.* 29 (12), 3945–3950. doi:10.1002/(sici)1521-4141(199912)29:12<3945::aid-immu3945>3.0.co;2-o

Rajkumar, S. V., Hayman, S. R., Lacy, M. Q., Dispenzieri, A., Geyer, S. M., et al. (2005). Combination Therapy with Lenalidomide Plus Dexamethasone (Rev/Dex) for Newly Diagnosed Myeloma. *Blood*, 106(13), 4050–4053. doi:10.1182/blood-2005-07-2817

Ramsey, H. E., Fischer, M. A., Lee, T., Gorska, A. E., Arrate, M. P., Fuller, L., et al. (2018). A Novel MCL1 Inhibitor Combined with Venetoclax Rescues Venetoclax-Resistant Acute Myelogenous Leukemia. *Cancer Discov.* 8 (12), 1566–1581. doi:10.1158/2159-8290.cd-18-0140

Ren, L.-N., Li, Q.-F., Xiao, F.-J., Yan, J., Yang, Y.-F., Wang, L.-S., et al. (2009). Endocrine Glands-Derived Vascular Endothelial Growth Factor Protects Pancreatic Cancer Cells from Apoptosis via Upregulation of the Myeloid Cell Leukemia-1 Protein. *Biochem. Biophysical Res. Commun.* 386 (1), 35–39. doi:10.1016/j.bbrc.2009.05.149

Richardson, P. G., Barlogie, B., Berenson, J., Singhal, S., Jagannath, S., Irwin, D., et al. (2003). A Phase 2 Study of Bortezomib in Relapsed, Refractory Myeloma. *N. Engl. J. Med.*, 348(26), 2609–2617. doi:10.1056/NEJMoa030288

Richardson, P. G., Schlossman, R. L., Weller, E., Hideshima, T., Mitsiades, C., Davies, F., et al. (2002). Immunomodulatory Drug CC-5013 Overcomes Drug Resistance and is Well Tolerated in Patients with Relapsed Multiple Myeloma. *Blood*, 100(9), 3063–3067. doi:10.1182/blood-2002-03-0996

Rogers, S., Wells, R., and Rechsteiner, M. (1986). Amino Acid Sequences Common to Rapidly Degraded Proteins: the PEST Hypothesis. *Science* 234 (4774), 364–368. doi:10.1126/science.2876518

Schniewind, B., Christgen, M., Kurdow, R., Haye, S., Kremer, B., Kalthoff, H., et al. (2004). Resistance of Pancreatic Cancer to Gemcitabine Treatment Is Dependent on Mitochondria-Mediated Apoptosis. *Int. J. Cancer* 109 (2), 182–188. doi:10.1002/ijc.11679

Schwickart, M., Huang, X., Lill, J. R., Liu, J., Ferrando, R., French, D. M., et al. (2010). Deubiquitinase USP9X Stabilizes MCL1 and Promotes Tumour Cell Survival. *Nature* 463 (7277), 103–107. doi:10.1038/nature08646

Sedlak, T. W., Oltvai, Z. N., Yang, E., Wang, K., Boise, L. H., Thompson, C. B., et al. (1995). Multiple Bcl-2 Family Members Demonstrate Selective Dimerizations with Bax. *Proc. Natl. Acad. Sci.* 92 (17), 7834–7838. doi:10.1073/pnas.92.17.7834

Senichkin, V. V., Streletskaia, A. Y., Gorbunova, A. S., Zhivotovsky, B., and Kopeina, G. S. (2020). Saga of Mcl-1: Regulation from Transcription to Degradation. *Cel Death Differ* 27 (2), 405–419. doi:10.1038/s41418-019-0486-3

Shah, V., Sherborne, A. L., Walker, B. A., Johnson, D. C., Boyle, E. M., Ellis, S., et al. (2018). Prediction of Outcome in Newly Diagnosed Myeloma: a Meta-Analysis of the Molecular Profiles of 1905 Trial Patients. *Leukemia* 32 (1), 102–110. doi:10.1038/leu.2017.179

Siegel, R. L., Miller, K. D., Fuchs, H. E., and Jemal, A. (2021). Cancer Statistics, 2021. *CA A. Cancer J. Clin.* 71 (1), 7–33. doi:10.3322/caac.21654

Singhal, S., Mehta, J., Desikan, R., Ayers, D., Roberson, P., Eddlemon, P., et al. (1999). Antitumor Activity of Thalidomide in Refractory Multiple Myeloma. *N. Engl. J. Med.*, 341(21), 1565–1571. doi:10.1056/NEJM199911183412102

Slomp, A., Moesbergen, L. M., Gong, J.-n., Cuenca, M., von dem Borne, P. A., Sonneveld, P., et al. (2019). Multiple Myeloma with 1q21 Amplification Is Highly Sensitive to MCL-1 Targeting. *Blood Adv.* 3 (24), 4202–4214. doi:10.1182/bloodadvances.2019000702

Smith, A. J., Dai, H., Correia, C., Takahashi, R., Lee, S.-H., Schmitz, I., et al. (2011). Noxa/Bcl-2 Protein Interactions Contribute to Bortezomib Resistance in Human Lymphoid Cells. *J. Biol. Chem.* 286 (20), 17682–17692. doi:10.1074/jbc.m110.189092

Song, L., Coppola, D., Livingston, S., Cress, W. D., and Haura, E. B. (2005). Mcl-1 Regulates Survival and Sensitivity to Diverse Apoptotic Stimuli in Human Non-small Cell Lung Cancer Cells. *Cancer Biol. Ther.* 4 (3), 267–276. doi:10.4161/cbt.4.3.1496

Stewart, M. L., Fire, E., Keating, A. E., and Walensky, L. D. (2010). The MCL-1 BH3 helix Is an Exclusive MCL-1 Inhibitor and Apoptosis Sensitizer. *Nat. Chem. Biol.* 6 (8), 595–601. doi:10.1038/nchembio.391

Thomas, L. W., Lam, C., and Edwards, S. W. (2010). Mcl-1; the Molecular Regulation of Protein Function. *FEBS Lett.* 584 (14), 2981–2989. doi:10.1016/j.febslet.2010.05.061

Tiedemann, R. E., Zhu, Y. X., Schmidt, J., Shi, C. X., Sereduk, C., Yin, H., et al. (2012). Identification of Molecular Vulnerabilities in Human Multiple Myeloma Cells by RNA Interference Lethality Screening of the Druggable Genome. *Cancer Res.* 72 (3), 757–768. doi:10.1158/0008-5472.can-11-2781

Tron, A. E., Belmonte, M. A., Adam, A., Aquila, B. M., Boise, L. H., Chiarparin, E., et al. (2018). Discovery of Mcl-1-specific Inhibitor AZD5991 and Preclinical Activity in Multiple Myeloma and Acute Myeloid Leukemia. *Nat. Commun.* 9 (1), 5341. doi:10.1038/s41467-018-07551-w

Varadarajan, S., Vogler, M., Butterworth, M., Dinsdale, D., Walensky, L. D., and Cohen, G. M. (2013). Evaluation and Critical Assessment of Putative MCL-1 Inhibitors. *Cel Death Differ* 20 (11), 1475–1484. doi:10.1038/cdd.2013.79

Vogl, D. T., Dingli, D., Cornell, R. F., Huff, C. A., Jagannath, S., Bhutani, D., et al. (2018). Selective Inhibition of Nuclear Export With Oral Selinexor for Treatment of Relapsed or Refractory Multiple Myeloma. *J. Clin. Oncol.*, 36(9), 859.

Wang, J.-M., Chao, J.-R., Chen, W., Kuo, M.-L., Yen, J. J.-Y., and Yang-Yen, H.-F. (1999). The Antiapoptotic Gene Mcl-1 Is Up-Regulated by the Phosphatidylinositol 3-kinase/Akt Signaling Pathway through a Transcription Factor Complex Containing CREB. *Mol. Cel Biol* 19 (9), 6195–6206. doi:10.1128/mcb.19.9.6195

Wang, Y., Chao, J. R., Chen, W., Kuo, M. L., Yen, J. J. Y., and Yang-Yen, H. (2020). Anti-apoptotic Capacity of Mcl-1Δ127. *Biochem. Biophysical Res. Commun.* 526 (4), 1042–1048. doi:10.1016/j.bbrc.2020.03.181

Willis, S. N., Chen, L., Dewson, G., Wei, A., Naik, E., Fletcher, J. I., et al. (2005). Proapoptotic Bak Is Sequestered by Mcl-1 and Bcl-xL, but Not Bcl-2, until Displaced by BH3-Only Proteins. *Genes Develop.* 19 (11), 1294–1305. doi:10.1101/gad.1304105

Wong, K. Y., and Chim, C. S. (2020). Venetoclax, Bortezomib and S63845, an MCL1 Inhibitor, in Multiple Myeloma. *J. Pharm. Pharmacol.* 72 (5), 728–737. doi:10.1111/jphp.13240

Wuillème-Toumi, S., Robillard, N., Gomez, P., Moreau, P., Le Gouill, S., Avet-Loiseau, H., et al. (2005). Mcl-1 Is Overexpressed in Multiple Myeloma and Associated with Relapse and Shorter Survival. *Leukemia* 19 (7), 1248–1252. doi:10.1038/sj.leu.2403784

Yang, T., Kozopas, K. M., and Craig, R. W. (1995). The Intracellular Distribution and Pattern of Expression of Mcl-1 Overlap with, but Are Not Identical to, Those of Bcl-2. *J. Cel Biol* 128 (6), 1173–1184. doi:10.1083/jcb.128.6.1173

Yang, Y., Li, F., Saha, M. N., Abdi, J., Qiu, L., and Chang, H. (2015). miR-137 and miR-197 Induce Apoptosis and Suppress Tumorigenicity by Targeting MCL-1 in Multiple Myeloma. *Clin. Cancer Res.* 21 (10), 2399–2411. doi:10.1158/1078-0432.ccr-14-1437

Yi, X., Sarkar, A., Kismali, G., Aslan, B., Ayres, M., Iles, L. R., et al. (2020). AMG-176, an Mcl-1 Antagonist, Shows Preclinical Efficacy in Chronic Lymphocytic Leukemia. *Clin. Cancer Res.* 26 (14), 3856–3867. doi:10.1158/1078-0432.CCR-19-1397

Zhang, B., Gojo, I., and Fenton, R. G. (2002). Myeloid Cell Factor-1 Is a Critical Survival Factor for Multiple Myeloma. *Blood* 99 (6), 1885–1893. doi:10.1182/blood.v99.6.1885

Zhang, Y.-K., Wang, H., Leng, Y., Li, Z.-L., Yang, Y.-F., Xiao, F.-J., et al. (2011). Overexpression of microRNA-29b Induces Apoptosis of Multiple Myeloma Cells through Down Regulating Mcl-1. *Biochem. biophysical Res. Commun.* 414 (1), 233–239. doi:10.1016/j.bbrc.2011.09.063

Zhong, Q., Gao, W., Du, F., and Wang, X. (2005). Mule/ARF-BP1, a BH3-Only E3 Ubiquitin Ligase, Catalyzes the Polyubiquitination of Mcl-1 and Regulates Apoptosis. *Cell* 121 (7), 1085–1095. doi:10.1016/j.cell.2005.06.009

Conflict of Interest: The authors declare that the research was conducted in the absence of any commercial or financial relationships that could be construed as a potential conflict of interest.

frontiers in Pharmacology

REVIEW
published: 20 July 2021
doi: 10.3389/fphar.2021.699044

Phytochemicals as Potential Chemopreventive and Chemotherapeutic Agents for Emerging Human Papillomavirus–Driven Head and Neck Cancer: Current Evidence and Future Prospects

*Nikita Aggarwal, Joni Yadav, Suhail Chhakara, Divya Janjua, Tanya Tripathi, Apoorva Chaudhary, Arun Chhokar, Kulbhushan Thakur, Tejveer Singh and Alok Chandra Bharti**

Molecular Oncology Laboratory, Department of Zoology, Faculty of Science, University of Delhi, Delhi, India

OPEN ACCESS

Edited by:
Farrukh Aqil, University of Louisville, United States

Reviewed by:
Lalit Batra, University of Louisville, United States
Carmela Spagnuolo, National Research Council (CNR), Italy

***Correspondence:**
Alok Chandra Bharti
alokchandrab@yahoo.com

Specialty section:
This article was submitted to Pharmacology of Anti-Cancer Drugs, a section of the journal Frontiers in Pharmacology

Received: *22 April 2021*
Accepted: *17 June 2021*
Published: *20 July 2021*

Citation:
Aggarwal N, Yadav J, Chhakara S, Janjua D, Tripathi T, Chaudhary A, Chhokar A, Thakur K, Singh T and Bharti AC (2021) Phytochemicals as Potential Chemopreventive and Chemotherapeutic Agents for Emerging Human Papillomavirus–Driven Head and Neck Cancer: Current Evidence and Future Prospects. Front. Pharmacol. 12:699044. doi: 10.3389/fphar.2021.699044

Head and neck cancer (HNC) usually arises from squamous cells of the upper aerodigestive tract that line the mucosal surface in the head and neck region. In India, HNC is common in males, and it is the sixth most common cancer globally. Conventionally, HNC attributes to the use of alcohol or chewing tobacco. Over the past four decades, portions of human papillomavirus (HPV)-positive HNC are increasing at an alarming rate. Identification based on the etiological factors and molecular signatures demonstrates that these neoplastic lesions belong to a distinct category that differs in pathological characteristics and therapeutic response. Slow development in HNC therapeutics has resulted in a low 5-year survival rate in the last two decades. Interestingly, HPV-positive HNC has shown better outcomes following conservative treatments and immunotherapies. This raises demand to have a pre-therapy assessment of HPV status to decide the treatment strategy. Moreover, there is no HPV-specific treatment for HPV-positive HNC patients. Accumulating evidence suggests that phytochemicals are promising leads against HNC and show potential as adjuvants to chemoradiotherapy in HNC. However, only a few of these phytochemicals target HPV. The aim of the present article was to collate data on various leading phytochemicals that have shown promising results in the prevention and treatment of HNC in general and HPV-driven HNC. The review explores the possibility of using these leads against HPV-positive tumors as some of the signaling pathways are common. The review also addresses various challenges in the field that prevent their use in clinical settings.

Keywords: head and neck cancer, human pappillomavirus, tobacco, smoking, phytochemicals, therapeutics, prevention

INTRODUCTION

Head and neck cancer (HNC) constitutes a large group of cancers arising in different anatomical sites of the head and neck (HN) region, comprising the lip and oral cavity, larynx, nasopharynx, hypopharynx, oropharynx, nasal cavity, paranasal sinuses, and salivary glands. Over 90% of these neoplastic tissues are squamous cell carcinomas (SCCs). According to WHO estimates for 2019, HNC was one of the leading forms of cancer with 931,931 new cases, representing 4.9% of all cancer cases (Globocan, 2020). Lip and oral cavity cancer made up nearly 40% of the total HNC cases followed by the cancer of the larynx region. Mortality statistics reported by GLOBOCAN estimate 467,125 deaths due to head and neck cancers, representing 4.7% of all cancer deaths. Prevalence data for 2020 point to India as carrying the highest burden of head and neck cancer, with 143,242 cases, followed by China (100,871), the United States of America (51,533), and the Russian Federation (23,772). These numbers are alarming and draw attention to immediate action against this highly preventable cancer as the etiological agents are well known.

Tobacco use, excessive alcohol consumption, and lately, infection of human papillomavirus (HPV) are the established risk factors for HNC (Marur and Forastiere, 2016). The risk of HNC is 10-fold higher in smokers than that of HNC in nonsmokers (IARC, 2004). Although excessive alcohol consumption is an independent risk factor, it also increases the risk for smokers (Smith et al., 2004; Chaturvedi et al., 2015). In the past decade, however, there has been a shift in the anatomic distribution of HNC with an increasing occurrence of neoplastic lesions in the oropharynx (Sturgis and Cinciripini, 2007). A concordant decrease in smoking prevalence and increase in HPV prevalence has been noted, especially in the younger age-group. The review of clinical manifestations of HNC based on their anatomical, histological, and etiological factors revealed a dichotomy in treatment response (Aggarwal et al., 2020). The data strongly point toward existence of two distinct types of HNC, namely, one that is caused by tobacco and alcohol abuse or occupational exposure to various carcinogens, and the other which is caused by biological agents like infection of HPV and possibly the EBV. The evidence presented in the present manuscript suggests discrete differences among the two disease groups, with each requiring separate clinical management.

Most patients with HNC seek clinical intervention at advanced stages of the disease (Haddad and Shin, 2008). This trend is quite common in individuals of low socioeconomic status, who cannot afford expensive medical/surgical treatments. Despite a well-standardized treatment regimen, current therapy has a very low success rate as 30–60% of patients diagnosed develop recurrent locoregional cancer or second primary cancers even after complete remission (Hashim et al., 2019). A major underlying factor is onset of chemo/radioresistance and treatment failure (Nikolaou et al., 2018). Thus, better therapeutic options are needed to mitigate this challenge. Moreover, prevention of HNC at an early precancer/cancer stage could be another window of opportunity by which disease burden and mortality due to HNC could be reduced. Currently, prevention focuses on risk behavior reduction like cessation of tobacco and early diagnosis of the disease. However, there is an unmet need for new therapeutics that could effectively eliminate HNC cells, reduce the onset of chemo/radioresistance, and could prevent the progression of the disease.

Recently, there has been a renewed interest in phytochemicals and herbal derivatives with therapeutic correlates from traditional medicine in the treatment and prevention of HNC due to their safety, availability, efficacy, and low cost. A number of studies carried out to investigate screening of phytochemicals using different HNC cell lines, animal models, and clinical evaluation in patients showed potent anticancer activities in a small set of phytochemicals. However, very limited number of studies addressed the impact of these herbal derivatives on HPV infection and HPV-positive HNC. In this article, we have systematically reviewed the existing data on various phytochemicals demonstrating chemotherapeutic and chemopreventive activities against HNC with a special emphasis on phytochemicals/herbal derivatives that showed anticancer effects against HPV-positive HNC. Further, major deficiencies and actionable leads in this field have been highlighted.

HEAD AND NECK CANCER SPECTRUM

HNC is a group of neoplastic diseases that can be broadly classified based on their anatomical site, histological origin, and etiological factors (**Figure 1A**).

Anatomical Site–Specific Classification

Figure 1B illustrates the anatomic sites of the HN region. Broadly, the HN area is classified into four regions, namely, the oral cavity, pharynx, nasal cavity, and larynx. The oral cavity consists of the vestibule (the area between the teeth and mucosa of the lips and cheeks) and the oral cavity proper. The oral cavity proper is the interior region of the mouth: the region between the two dental arches and majorly occupied by the tongue (Akintoye and Mupparapu, 2020). Soft palate and hard palate separates the oral cavity from the nasal cavity.

Oral SCC (OSCC) arises from mucosal areas of the lips, front 2/3rd of the tongue, gums, internal lining of cheeks and lips, floor of mouth below the tongue, hard palate, and the area behind the wisdom teeth (Gartner, 1994), and constitutes a major proportion of cancers of the HN region. Globally, lip and oral cavity cancer prevalence is 34.7% among the overall cases of HNC. Lip and oral cavity cancer has the highest incidence in South-Central Asia (Globocan, 2020). The prevalence of lip and oral cavity cancer in the past 5 years is the highest in India, with a total burden of 300,413 cases. In the oral cavity proper, the tongue accounts for 40% of intraoral carcinomas (Neville and Day, 2002).

The pharynx is a channel located in the region of the neck midline. The pharynx is majorly classified into three regions: the nasopharynx (located posterior to nasal cavity), oropharynx (posterior end of oral cavity), and hypopharynx (behind the opening of larynx) (Albahout and Lopez, 2021). Globally, among HNC, the prevalence of the nasopharynx is 15.8%,

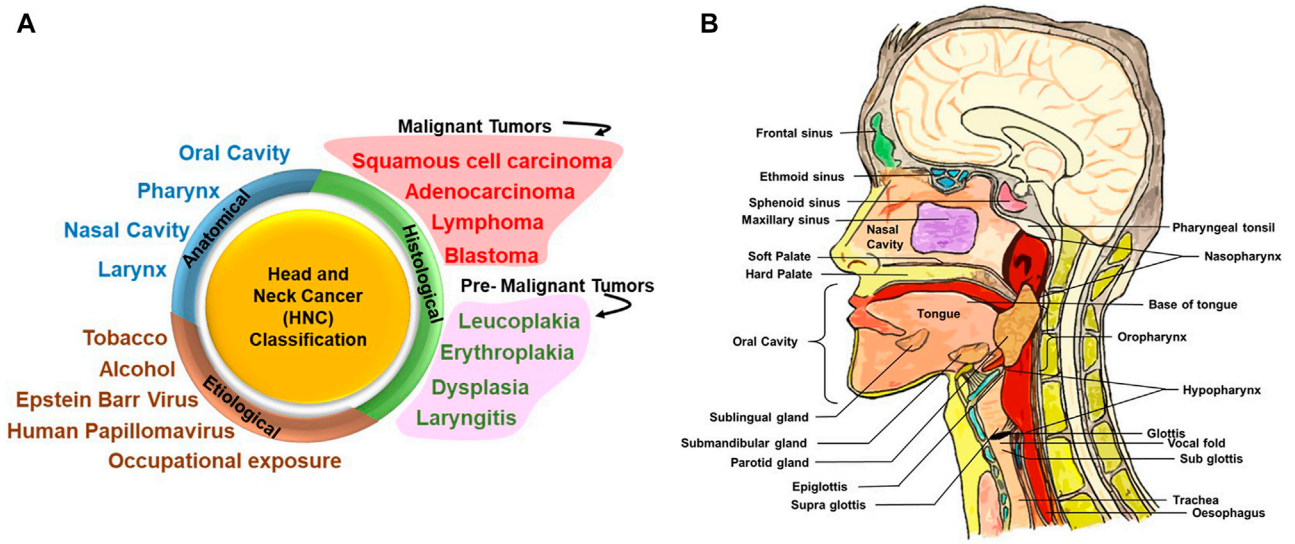

FIGURE 1 | Head and neck cancer (HNC) classification and different anatomical sites involved. **(A)** HNC can be broadly classified on the basis of its anatomical site, histological origin, and etiological factors. Upon histological evaluation, tumors in the head and neck region can be broadly classified into malignant and premalignant lesions. Premalignant lesions that have been indicated here are not cancer but are precursors of malignant lesions. **(B)** Detailed anatomical architecture of the head and neck region illustrating the location of the oral cavity, nasal cavity, tongue, salivary glands (sublingual gland, submaxillary gland, and parotid gland), larynx and pharynx (including oropharynx, nasopharynx, and hypopharynx), and site of primary tumors.

which is the highest among three regions, followed by oropharynx 10.7%, which is higher than hypopharynx 5.5%. The incidence rate of the nasopharynx is high in Southeastern Asia, whereas the incidence rate of the hypopharynx is high in Central and Eastern Europe (Globocan, 2020). Incidence rates for the oropharynx are high in Europe, which is linked with alcohol consumption, tobacco smoking, and HPV. Incidence of HPV infection in the oropharyngeal region is rising at an alarming rate (Wierzbicka et al., 2021).

The nasal cavity is the upper most part of the respiratory tract. The nasal cavity is surrounded by four types of paranasal sinuses: frontal sinuses, sphenoid sinuses, paired maxillary sinuses, and ethmoid sinuses. Paranasal sinus malignancies are rare, accounting for less than 3–5% of the total HNC (Patel, 2017). The nasal cavity and paranasal sinuses disease burden are not covered by (Globocan, 2020) under HNC.

The internal space of the larynx is a pyramid shaped about 5 cm long, connecting the pharynx to the trachea and is a part of the respiratory system. According to Globocan (2020), the incidence of larynx cancer is highest in Central and Eastern Europe. Laryngeal cancer constitutes around 21.4% among HNC (Globocan, 2020).

Exocrine glands and salivary glands function to secrete saliva in the oral cavity. Three type of salivary glands are present: parotid gland (situated front of both ears), submandibular gland (posterior of the mandible), and sublingual gland (floor of the oral cavity) (Ghannam and Singh, 2021). In the salivary gland, majority tumors are benign, whereas malignant tumors are generally mucoepidermoid carcinoma and adenocarcinoma. Primary SCC is rare and aggressive in salivary glands, specifically in the parotid gland (Flynn et al., 1999). The incidence of the salivary gland cancer has been reported to be the highest in Middle Africa. Salivary gland cancer constitutes 6.6% of total HNC.

Histological Classification

In the oral cavity, the mucosa is of masticatory, specialized, and mobile type. It covers around 25% of the oral cavity. In order to understand mechanical forces caused by mastication, it is covered by specialized, orthokeratinized, stratified squamous epithelium. Depending on the anatomic site, over 60% of the mucosa in the oral cavity is lined by the stratified squamous epithelium. The upper surface of the tongue is lined by specialized mucosa, with numerous lingual papillae (Winning and Townsend, 2000).

Histologically, the tumors of the HN region are classified as carcinoma, adenocarcinoma, lymphoma, and blastoma depending upon the tissue from where they are originating (Ologe et al., 2005). For instance, cancer originating in squamous cells in the HN region is collectively termed as HNSCC, and the one originating in salivary glands is of glandular origin and classified as an adenocarcinoma. The most common cancer affecting the HN region is epithelial carcinoma, which constitutes 80–90% of total cases, followed by lymphomas and blastomas accounting for the rest (Ologe et al., 2005; Gilyoma et al., 2015). Among carcinomas, squamous cell carcinoma constitutes 67.7% of total carcinoma cases, whereas other carcinomas like follicular carcinoma, adenocarcinoma, adenoid cystic carcinoma, clear cell carcinoma, mucoepidermoid carcinoma, and malignant melanoma cover the remaining carcinoma cases (Adeyemi et al., 2008).

Carcinomas mostly spread in the regions of the larynx, nasopharynx, and least in maxillofacial bones and oral cavity

regions, whereas predominant anatomical sites for lymphomas were lymph nodes, followed by the maxillofacial bones. In contrast, sarcomas occurred most frequently in the maxillofacial bones, face/scalp, and the nose area (Adisa et al., 2011). The distribution of these tumors varies among the age-group of the patients. Most of the carcinomas are detected in the age-group of 45–64 years in contrast to sarcomas frequently occurring in the age-group of 25–44 years (Adeyemi et al., 2008; Adisa et al., 2011).

In the oral cavity, leukoplakia (white plaque) and its variants, erythroplakia (fiery red patch) and submucous fibrosis (most prevalent in India), are three conditions that are highly associated with the development of oral epithelial dysplasia (OED) and oral squamous cell carcinoma (OSCC). Malignant transformation rates of leukoplakia range from 8.9 to 17.5 percent (Silverman et al., 1984; Lind, 1987). The buccal mucosa had the highest incidence of leukoplakia, with 18% of lesions, but had the lowest rate of malignant transformation (3%). The tongue accounted for 16% of lesions but had the highest rate of transformation at 24% (Warnakulasuriya and Ariyawardana, 2016). Erythroplakia occurs mainly in the middle aged and the elderly and has the prevalence ranging from 0.02 to 1%. Soft palate, floor of the mouth, and buccal mucosa have their highest rate of incidence. The reason for etiopathogenesis has not been determined, but chewing tobacco and consuming alcohol have been implicated as factors for the development erythroplakia. The malignant transformation rate in erythroplakia is very high (14–50%) (Reichart and Philipsen, 2005). Oral submucous fibrosis is another chronic and potentially malignant disorder characterized by juxtaepithelial fibrosis of the oral cavity. This lesion has been reported to have a malignant transformation rate of 7–30%. Its incidence is highly associated with the chewing of betel quid containing areca nut (Ranganathan et al., 2004).

Dysplasia can be categorized as mild (architectural disturbance and cytological atypia in lower third of the epithelium), moderate (architectural disturbance and cytological atypia in middle third of the epithelium), and severe (architectural disturbance and cytological atypia in greater than two-third of the epithelium). This classification of dysplasia by the WHO is referred to as the gold standard for histological diagnosis of oral potentially malignant disorders (OPMDs). The WHO defines OPMDs as "clinical presentation that carry a risk of cancer development in the oral cavity, whether in a clinically definable precursor lesion or in clinically normal mucosa" (Muller, 2018). Epithelial dysplasia, an important precursor of malignant transformation in the HN region, can be defined as a change in morphological characteristics of the epithelium, including architectural and cytotoxic changes and loss of differentiation of keratinocytes toward the surface. It involves replacement of a part or the entire epithelium by cells showing cellular atypia (Tilakaratne et al., 2019; Wils et al., 2020).

The stratified squamous epithelium lines the pharynx to protect it from mechanical stress. The pharynx and larynx both are lined with the ciliated pseudostratified columnar epithelium with goblet cells. A study suggests that lesions such as erythroplakia at high-risk sites in the oropharynx should be considered as invasive carcinoma or carcinoma *in situ* at high-risk sites unless a biopsy proves otherwise (Mashberg and Samit, 1995). However, the vocal cords are lined with the stratified squamous epithelium (Stiblar-Martincic, 1997). Although there is no consensus, premalignant lesions of the larynx are usually classified as chronic laryngitis, erythroplakia, leukoplakia, and erythroleukoplakia (Gale et al., 2009). In the premalignant and malignant lesions of the larynx, severe dysplasia and carcinoma *in situ* occur at the rate of 10–20% (Hellquist et al., 1982). The nasal mucous membrane is lined with the sensory epithelium with olfactory cells and the respiratory epithelium. The mucosa is rich in mucus-producing goblet cell. Nasal drainage is facilitated by the ciliated epithelium. Premalignant lesions of paranasal sinuses differ from other lesions of the HN region and are present as inverted papillomas. This cancer goes undiagnosed before the onset of symptoms. Malignant tumors of paranasal sinus are diagnosed at stages T3–T4 in two-thirds of cases. Additionally, in paranasal cancer, 10% of total SCCs and 4% of all adenocarcinomas have some degree of cervical lymph node involvement (Jegoux et al., 2013). Salivary glands constitute three cell types, namely, acinar cells, myoepithelial cells, and ductal cells (Brazen and Dyer, 2020). In the parotid gland, 70% of the tumors detected are benign. In the submandibular gland, adenoid cystic carcinoma is the common malignancy (16%). Sublingual gland tumors are rare but have the highest frequency of malignancy, ranging from 70 to 90% (Carlson and Schlieve, 2019).

Classification Based on Etiological Type

Tobacco-associated HNC: Association of tobacco and alcohol use with the onset of HNC is well established (IARC, 2004). Tobacco use is the leading cause of preventable death in the world. Tobacco smoking alone is the leading cause of cancer and cancer-related deaths worldwide. Nearly 85% of HNC are linked with tobacco use. Within the HN region, it has been conclusively shown to directly cause oral cavity, laryngeal, and pharyngeal cancer (Centers for Disease Control and Prevention, 2004). The International Agency for Research on *Cancer* (IARC) has classified carcinogens in groups, group 1: tobacco smoking, secondhand smoking, and smokeless tobacco for HNCs, which are sufficient for evident carcinogenicity in human (IARC, 2004). In developed countries, most inhaled or "mainstream" tobacco smoke comes from the use of manufactured cigarettes. Cigarettes burn at very high temperature and produce smoke that includes toxins and carcinogens. Similar drawbacks are with cigars, pipes, and water pipes (IARC, 2004).

Tobacco smoke contains a variety of group 1 carcinogens, namely, arsenic and benzene, but research is more focused on tobacco-specific N-nitrosamines, especially N-nitrosonornicotine and 4-(N-nitrosomethylamino)-1-(3-pyridyl)-1-butanone, as they are established carcinogens. In HNC of HNSCC type, the latter one is more associated with increasing the risk of cancer development (Oreggia et al., 1991). Tar is another compound which is linked with an increased risk of HNC (Franceschi et al., 1992).

Studies have shown that development of HNC is strongly related with dose-dependent tobacco smoking but can also occur with low daily usage (Berthiller et al., 2016). Moreover, the

TABLE 1 | Major historical milestone events in the description of HPV infection in the head and neck region (adapted from Syrjanen et al. (2017)).

Year	Milestones	References
1891, 1896	First speculation of contagious nature of cutaneous warts	Payne (1891), Jadassohn (1896)
1901	Contagious transmission of condyloma warts in the tongue after oral sex described	Heidingsfield (1901)
1907	Viral etiology of oral lesions	Ciuffo (1907)
1923	Association of human wart virus with laryngeal warts established	Ullman (1923)
1943	Oral papillomatosis as a viral disease was established in rabbits	Parsons and Kidd (1943)
1948, 1956	Reporting of koilocytotic atypia in laryngeal papilloma	Ayre and Ayre (1949), Ishiji et al. (1992)
1978	Epithelial atypia in laryngeal papilloma reported	Quick et al. (1978)
1973	Identification of HPV in laryngeal papilloma	Boyle et al. (1973)
1974–75	Detected virus-specific DNA in human tumors	zur Hausen et al. (1975)
1976–77	HPV association with koilocytotic atypia established as a sign of HPV infection	Meisels and Fortin (1976), Purola and Savia (1977)
1978	Development of noncommercial antiserum against HPVs	Pyrhonen and Neuvonen (1978)
1980	HPV 6 was isolated from condyloma acuminata	Gissmann and zur Hausen (1980)
1982	Expression of HPV structural proteins in laryngeal carcinoma	Syrjanen et al. (1992)
1982	HP 11 was detected in laryngeal papilloma	Gissmann et al. (1982)
1982	HPV detection in benign and malignant oral SCC	Jenson et al. (1982), Syrjanen et al. (1983a)
1983	An extensive squamous cell papilloma of the nasal cavity and also filling the entire left maxillary sinus is reported	Syrjanen et al. (1983b)
1983	Morphologic and immunohistochemically features indicate HPV infection in OSCC	Syrjanen et al. (1983a)
1987	HPV DNA in benign and malignant sinonasal lesions	Syrjanen et al. (1987)
1989	Detection of HPV DNA in human oral tissue biopsies and cultures	Maitland et al. (1989)
1989	HPV16 DNA detection in tonsillar carcinoma	Brandsma and Abramson (1989)
1992	Success in preparation of virus-like particles (VLPs), namely, BPV1 and HPV16, that established HPV serology and vaccination	Kirnbauer et al. (1992)
1992	First report showing the presence of transcriptionally active and integrated HPV infection with expression of E6/E7 mRNAs in tonsilar cancer	Snijders et al. (1992)
1992	HPV16/18 DNA in nasopharyngeal carcinoma	Dickens et al. (1992)
2004	Papillomaviruses recognized as a taxonomic family of their own	De Villiers et al. (2004)
2005	Differential expression and activity of transcription factors in HPV-positive oral cancers	Mishra et al. (2006)
2008	Halard zur Hausen was awarded with Nobel prize in physiology or medicine	—

duration of exposure also significantly affects the risk of HNC. The risk of daily smoking for more than 30 years was found to be more carcinogenic (Cohen et al., 2018).

Alcohol-associated HNC: HNC is also associated with alcohol abuse. Studies suggest that alcohol consumption and cigarette smoking are differentially associated with the risk of HNSCC subtypes (Bagnardi et al., 2001). A large prospective study has confirmed that alcohol consumption is strongly linked to HNSCC (Freedman et al., 2007). Among all, oropharyngeal SCC (OPSCC) is the most associated, while laryngeal SCC (LSCC) is the least associated with heavy alcohol consumption (Zeka et al., 2003; Lubin et al., 2009; Toporcov et al., 2015). Clinically, there is no distinction between alcohol- and tobacco-associated HNC.

Occupational exposure–associated HNC: Apart from smoking of tobacco products, occupational exposure to dusts from wood, textiles, leather industries, flour, nickel, chromium, fumes from rubbing alcohol (also called isopropyl alcohol), radium, glue, formaldehyde as well as solvent fumes used in furniture and shoe production, and asbestos are the main risk factors for sinonasal carcinomas. Hypopharygeal and laryngeal carcinoma are associated with the use of coal for heating or cooking (IARC, 2012). These tumors have an aggressive clinical behavior and resemble tobacco-associated tumors in progression and therapeutic response.

Epstein–Barr virus–associated HNC: The etiology and natural history of nasopharyngeal SCC (NPSCC) is closely linked to that of Epstein–Barr virus (EBV) infection. This neoplasm is an uncommon disease with very low prevalence in most countries (Wei and Sham, 2005). Although EBV infection is pervasive, NPSCC incidence differs considerably around the world (Chang and Adami, 2006). In most geographical regions where NPSCC is endemic, the onset of EBV infection occurs at an early age. The estimated latency period of this virus is around a decade, so other factors also contribute for NPSCC development. Evidences indicate that this cancer is predominant in individuals of Southeast Asian descent due to genetic differences (Chang and Adami, 2006; Bei et al., 2016; Liu et al., 2017).

HPV-associated HNC: HPV is a DNA virus with oncogenic potential associated with over a dozen genotypes referred to as high-risk HPV. Persistent HPV infection is chiefly associated with the development of anogenital and cervical carcinomas. HPV16 and HPV18 genotypes are the most prevalent carcinogenic types and act *via* action of two major oncogenes, E6 and E7. These oncogenes target cell cycle and promote tumor growth by targeting and downregulating p53 and pRb, respectively. Many molecular and epidemiological studies support association of HPV with HNC, especially with OPSCC (Franceschi et al., 1996). Over the last 125 years, observations

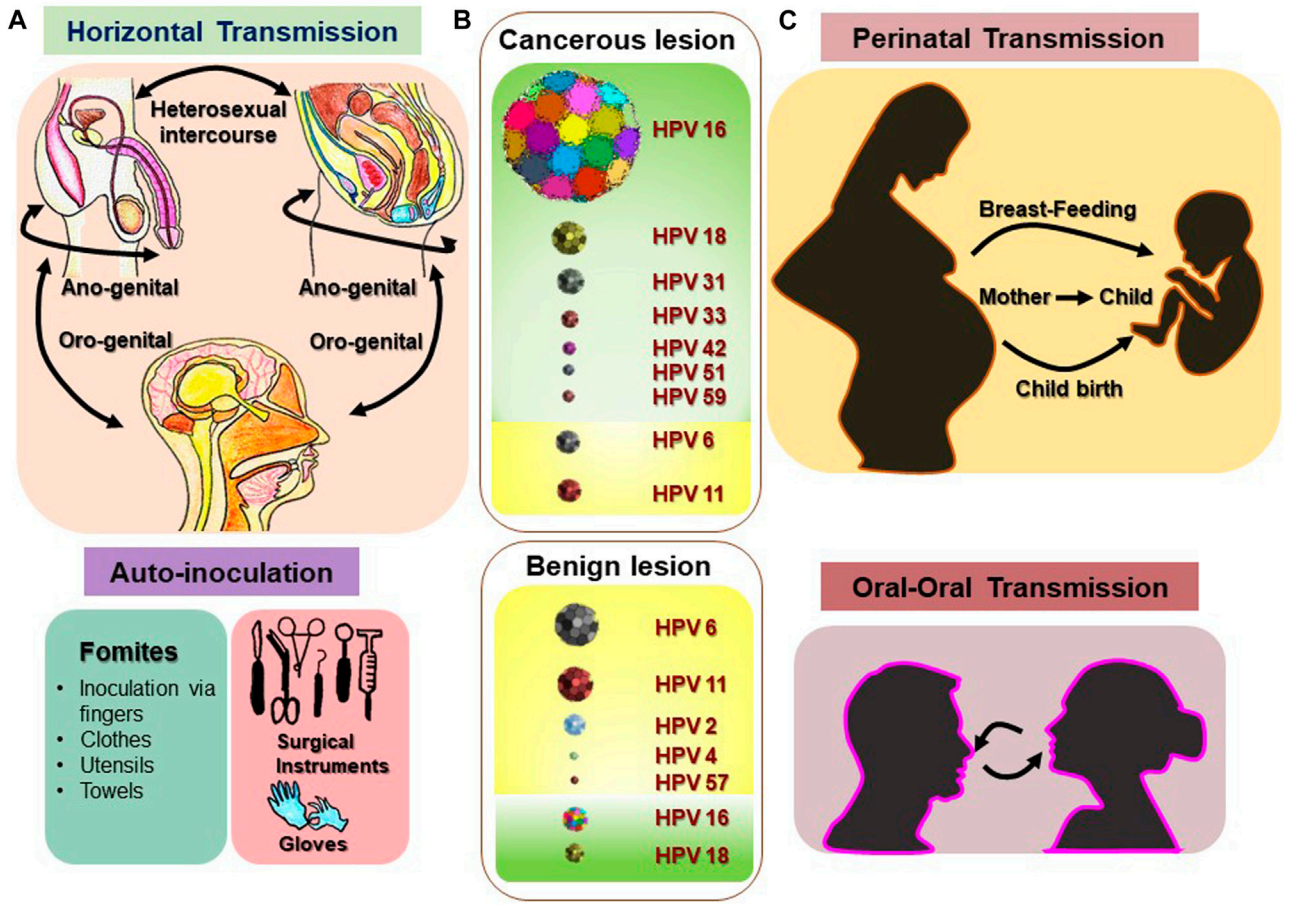

FIGURE 2 | Various routes and sites of HPV transmission. HPV is a sexually transmitted infection that can be received through horizontal transmission (heterosexual intercourse, anogenital, and oro-genital) and in some rare cases through various fomites, and inoculation *via* fingers, clothes, utensils, towels, and surgical instruments. **(A)** Vertical transmission (perinatal transmission: mother to baby) and oral–oral transmission of HPV could be the main source of nonsexual transmission of HPV in oral sites. **(C)** Most prevalent high-risk and low-risk HPV types reported in benign and malignant lesions of the HN region are depicted with representative figures where the relative frequency of the each type is indicated with corresponding sizes. **(B)** [Disclaimer: Pictures used to make composite diagram and to represent HPV types are derived from different internet sources and does not claim to be the original representation of the indicated HPV type] (Sarkola et al., 2008; Chaturvedi et al., 2015; Fu et al., 2015; Visalli et al., 2016; Louvanto et al., 2017; Sabeena et al., 2017; Syrjanen, 2018; Houlihan et al., 2019).

speculating the presence of a virus transmitting oral tumors have matured and led to the identification of a subset of HNC with distinct clinical presentation that show an early onset (**Table 1**). Approximately 35% of all HNC and 77% of tonsillar cancers harbor HPV, with greater than 60% of cases being the HPV16 subtype (McKaig et al., 1998). A significant variation in HPV prevalence in HNC types is recorded within different studies and from different geographical regions (Gillison et al., 2015).

Finding HPV in the HN region is paradoxical. However, a sexual mode of transmission has been suggested. Due to muco-epithelial tropicity of these viruses, if the virus gets access to these tissues *via* opportunistic contact with infected genital organs, it can result in the establishment of HPV infection in the HN region (**Figure 2**). Patients with other HPV-associated neoplasms or premalignant conditions are presumed to be at a higher risk of HNC development. Among spouses, women having a history of cervical dysplasia showed higher incidence of HPV-related oropharyngeal cancer (Hemminki et al., 2000). Patients with a history of anogenital cancer have shown a higher risk of tonsillar cancer (Frisch and Biggar, 1999). These HPV-positive cancers are primarily SCCs in their histological manifestations.

Recognition of Human Papillomavirus–Positive HNSCC as a Distinct Human Papillomavirus–Driven Subtype

Data emerged in last 2 decades strongly support the recognition of HPV-positive HNSCC as a distinct disease with a well-defined clinical and molecular pattern and unique risk factors (**Table 2**). These HPV-positive tumors were reported in early stage (Pintos et al., 1999; Smith et al., 2004; Hammarstedt et al., 2006), well differentiated histology (Pintos et al., 1999; Gupta et al., 2015), basaloid morphology (Gillison et al., 2000), larger tumors (Gletsou et al., 2018), and either no lymph node involvement (Pintos et al., 1999) or with cystic cervical lymph node positivity

TABLE 2 | Representative studies demonstrating the existence of HPV-positive HNC as a distinct disease group.

Study (year)	Sample size and HPV positivity	Study design	Anatomical sites examined	HPV-positive HNSCC	HPV-negative HNSCC
Pintos et al. (1999)	Archival specimens of UADT (*n* = 101), HPV positivity: 16.8%	Cross-sectional study	Pharynx, buccal, larynx	Gender bias [M:F::14:3 (4.7)] Younger age [<60: >60 years::12:8 (1.5)] Higher proportion of WDSCC [6/17 (0.35)] Early stage [T1-2:T3-4::11: 6 (1.8)] Without lymph node metastasis [2/17 (0.12)]	Gender [M:F::66:18 (3.7)] Age [<60:>60 years::30: 54 (0.55)] WDSCC [14/84 (0.17)] Stage [T1-2: T3-4::41: 43 (0.95)] Lymph node metastasis [29/84 (0.35)]
Gillison et al. (2000)	Fresh tissues (*n* = 253), HPV positivity: 22%	Prospective analysis of tissues with patient follow-up and association with history	All sites of the HN region	HPV16 associated, viral integration, poor tumor grade (OR-2.4) Over-representation in oropharynx Basaloid morphology (OR- 18.7) Better DFS (HR- 0.26) Better prognosis (59% risk reduction)	Moderate-to-heavy drinkers (OR- 5.88) Smokers (OR- 6.25) TP53 mutations detected (OR- 16.7) Age at diagnosis >60 years
Van Houten et al. (2001)	Fresh specimens of UADT (*n* = 84) HPV positivity: 23.8%	Prospective analysis	All sites of the HN region	p53 wild type, non-mutated in E6 positive tumor (9/9) p53 mutations only in HPV E6RNA negative tumors [4/11 (36.4%)]	Frequent p53 mutations [40/64 (62.5%)]
Mork et al. (2001)	Serum from cohort studies (cases = 292; controls = 1,568) HPV positivity: 12%	Case–control retrospective study	All sites of the HN region	Seropositivity for HPV16–35/292 (12%) against control group—102/1,568 (7%)	Reference
Smith et al. (2004)	Patient biopsy (*n* = 193) HPV positivity: 20%	Prospective analysis	All sites of the HN region	Younger age (<55: >55 years; OR-3.4) More lifetime sex partners (OR-3.8), practiced oral-genital sex (OR-4.3), or oral–anal sex (OR-19.5)	Reference
Mishra, et al. (2006) Mishra et al. (2006)	Patient biopsy (*n* = 66) HPV positivity: 27%	Prospective analysis	All sites of the HN region	Selective participation of p65 subunit in the NF-κB complex	Constitutively active NF-κB complex with p50 homodimer
Hammarstedt et al. (2006)	Archival specimens (*n* = 203) HPV positivity: 49%	Retrospective study of cases b/w 1970–2002	Tonsils	Younger patients [<60: >60 years::58:41 (1.41)]	Age [<60:>60 years::30: 74 (0.41)]
Ragin and Taioli (2007)	Pooled analysis (*n* = 1747) HPV positivity: 27.7%	Meta-analysis	Oral cavity, oropharynx	Lower risk of dying (HR-0.85) Lower risk of recurrence (HR-0.62)DFS (HR: 0.51)	Reference
Fakhry et al. (2008)	Fresh tissues (*n* = 96 patients) —	Prospective clinical trial controlled for known factors of prognostic values	Oropharynx, larynx	Higher response after induction chemotherapy (82%) and chemoradiation (84%) Increased 2-years survival (95%) with lower risk of progression and death Lower risk of dying (HR-0.36) Lower risk of progression (HR-0.27)	Moderate response after induction chemotherapy (55%) and chemoradiation (57%) —
Chaturvedi et al. (2008)	SEER (1973–2004) (*n* = 45,769) HPV positivity: 38.5%	Cohort analysis for investigation of survival of OSCC patients	Oral cavity	Mean ages at diagnosis-61.0 years APC in incidence (1973–2004) - 0.80 Showed increased 2-year survival from 9.9 to 18.6%	Mean ages at diagnosis-63.8 years APC in incidence (1973–2004)–(–)1.85 Showed 2-year survival from 5.6 to 9.9%

(Continued on following page)

TABLE 2 | (*Continued*) Representative studies demonstrating the existence of HPV-positive HNC as a distinct disease group.

Study (year)	Sample size and HPV positivity	Study design	Anatomical sites examined	HPV-positive HNSCC	HPV-negative HNSCC
Gillison et al. (2008)	Newly diagnosed HNSCC patient (*n* = 240) and 322 controls [HPV(16) positivity: 38.3%]	Case–control study to compare risk factors in HPV-positive vs HPV-negative tumors	Oral cavity, paranasal sinus, pharynx, larynx	Gender bias [M:F::78:14 (5.6)] association increased with the increasing number of oral sex partners, with increasing intensity (joints per month), duration (in years), and cumulative joint-years of marijuana use	Gender bias [M:F::111: 37 (3.0)] Associated with tobacco smoking, alcohol drinking, and poor oral hygiene Not associated with sexual behavior or marijuana use
Golderberg et al. (2008)	FFPE (*n* = 84) [HPV(16) positivity: 87%]	Retrospective review of patients undergoing neck dissection between 2002 and 2004	Oropharynx, oral cavity, larynx, hypopharynx	Related with cystic cervical lymph node	Associated with solid nodal metastasis
Ang et al. (2010)	Patients (*n* = 323)	Retrospective analysis for tumor HPV status and survival among patients	Oropharynx	3-year rate of survival (82.4%) 3-year rates of PFS (73.7%) Reduction in the risk of death (58%) Reduction in the risk of relapse or death (51%)	3-year rate of survival (57.1%) —
Rischin et al. (2010)	Stage III and IV patients (*n* = 172) HPV positivity: 53.5%; p16 positivity[a]–59.3%	Retrospective study	Oropharynx	Lower T and higher N categories and better ECOG performance status in p16 positive. 2-year overall survival [91% (HR-0.36)]. 2-year failure-free survival in p16 positive [87% (HR-0.39)]	2-year overall survival (74%). 2-year failure-free survival (72%)
Chaturvedi et al. (2011)	Archival tissue from year 1988 to 2004 (*n* = 271)	Retrospective time period study	Oropharynx	Median survival (131 months) Increased prevalence from 1984 to 1989 (16.3%) to 2000 to 2004 (71.7%) Population-level incidence increased (225%; from 0.8 per 100,000 to 2.6 per 100,000)	Median survival (20 months). Population-level incidence declined (50%; 2.0–1.0 per 100,000)
Posner et al. (2011)	Patients (*n* = 111) —	Retrospective study to evaluate OS, PFS, and HPV	Oropharynx	Median age: 54 years T1/T2 primary: 49% 5-year PFS: 78% 5-year OS: 82%	Median age: 58 years T1/T2 primary: 20% 5-year PFS: 28% 5-year OS: 35%
De Martel et al. (2012)	GLOBOCAN data 2008 (sample size not described)	Synthetic analysis of HPV PCR positivity in tumor tissue with HPV E6 or E7 expression	Oropharynx	Geographical variations (north America: 56%, northern and western Europe: 39%, eastern Europe: 38%; southern Europe: 17%, Australia–45%, Japan: 52%, rest of world: 13%	Not assessed
Ndiaye et al. (2014)	Patients (*n* = 12,163) [overall HPV positivity: 31.54%; for oropharynx: 45.8%, for larynx (including hypopharynx): 22·1%, and for oral cavity: 24·2%]	Meta-analysis of 148 studies	Oropharynx, larynx, oral cavity	p16INK4a positivity in HPV-positive oropharyngeal cancer cases: 86·7% and E6/E7 mRNA positivity: 86·9% HPV attributable fraction in oropharyngeal cancer defined by expression of positive cases of E6/E7 mRNA was estimated as 39·8% and of p16INK4a was 39·7%	Reference

(Continued on following page)

TABLE 2 | (*Continued*) Representative studies demonstrating the existence of HPV-positive HNC as a distinct disease group.

Study (year)	Sample size and HPV positivity	Study design	Anatomical sites examined	HPV-positive HNSCC	HPV-negative HNSCC
Fakhry et al. (2014)	Patients (*n* = 181) p16 positivity[a]-58%	Retrospective evaluation of OS	Oropharynx	Improved 2-year OS in p16 positive patients (54.6%; median: 2.6 years)	OS in p16-negative patients (27.6%; median: 0.8 years)
Vermorken et al. (2014)	Patient samples-FFPE (*n* = 416) HPV positivity: 6%	Retrospective analysis of R/M HNSCC	All sites of the HN region	Better OS for HPV+/p16+. CT + cetuximab (median month-12.6). CT (median month-7.1)	OS for HPV-/p16-CT + cetuximab (median month-9.6). CT (median month-6.7)
The Cancer Genome Atlas Network (2015)	Tumor tissues (*n* = 279) HPV positivity: 12.9%	Cohort study	Oral cavity oropharynx, larynx	Helicase domain mutations of the oncogene PIK3CA. Novel alterations involving loss of TRAF3. Amplification of the cell cycle gene E2F1	Near universal loss-of-function TP53 mutations and CDKN2A with frequent copy number alterations including a novel amplification of 11q22
Gupta et al. (2015), Gupta et al. (2018)	Fresh biopsies (*n* = 50) [HPV(16) positivity: 28%]	Prospective study	Tongue	Well differentiated tongue carcinomas (78.5%) Higher expression and DNA binding activity of AP-1 and NF-κB with c-fos and Fra-2; and p50 and c-rel as the major binding partners forming the functional AP-1 and NF-κB complex, and selective participation of p65 Induced expression of p65 and p27 leading to well differentiation and better prognosis	Poorly differentiated carcinomas (72.2%) Low expression and DNA binding activity of AP-1 with c-Jun as the major binding partners forming the functional AP-1 complex Participation of c-Rel with p50 that in crosstalk with AP-1/Fra-2 leading to poor differentiation and aggressive tumorigenesis
Gaykalova et al. (2015)	Tissues from HNSCC patients (*n* = 195) and noncancer-affected patients (*n* = 63) [discovery- HPV(16) positivity: 29.5%]	Cohort study	All sites of the HN region	Described 5 top-scoring pair biomarkers from STATs, NF-κB and AP1 pathways that distinguished HPV + HNSCC based on TF activity	High expression of CCND1, CEBPD, ICAM1, IRF1, JAG1, JAK3, and NOS3
Verma et al. (2017)	Fresh biopsies and FFPE tissues (*n* = 135) [HPV(16) positivity: 23%]	Prospective and archival study	Oral cavity oropharynx	Direct correlation with tissue immunopositivity for JunB and p65, whereas pSTAT3 were inversely correlated	Presence of STAT3/pSTAT3 with NF-κB irrespective immunopositivity for AP-1 members
Gletsou et al. (2018)	Patient samples-FFPE (*n* = 28) HPV positivity: 10.7%	Analytical study	Oropharynx	Low $pEGFR^{Y1092}$ status Bigger Tumor diameter of 3.7 ± 1.5 cm, volume of 9.5 ± 5.8 cm^3	High $pEGFR^{Y1092}$ status Comparatively smaller Tumor diameter of 2.7 ± 0.6 cm, volume of 5.4 ± 2.7 cm^3
Adjei Boakya et al. (2018)	Patient samples (*n* = 109,512) from SEER HPV positivity: 38.1%	Cohort study	All sites of the HN region	Low risk of second primary malignant neoplasms	High risk of second primary malignant neoplasms
Abdel-Rahman (2020), (Abdel-Rahman, 2020)	Patient records (*n* = 1,157) from SEER HPV positivity: 24%	Cohort analysis for investigation of survival of hypopharyngeal carcinoma patients	Hypopharynx	OS (HR: 1.76) Better OS with regional and distance disease Head and neck cancer–specific survival (HR: 1.54)	Reference

[a]*p16 positivity was taken as surrogate marker for (transcriptionally active) HPV positivity.*

Abbreviations: AP1, activator protein 1; APC, annual percentage change; CT, chemotherapy; DFS, disease-free survival; DNA, deoxyribose nucleic acid; ECOG, Eastern Cooperative Oncology Group; EGFR, epidermal growth factor receptor; FFPE, formalin fixed paraffin embedded; HPV, human papillomavirus; HR, hazard ratio; HN, head and neck; HNSCC, head and neck squamous cell carcinoma; NF-κB, nuclear factor-kappa B; OS, overall survival; OR, odds ratio; OSCC, oral squamous cell carcinoma; OPSCC, oropharyngeal squamous cell carcinoma; PIK3CA, phosphatidylinositol-4,5-bisphosphate 3-kinase catalytic subunit alpha; PCR, polymerase chain reaction; PFS, progression-free survival; R/M, recurrent and/or metastatic; STAT3, signal transducer and activator of transcription 3; SEER, surveillance, epidemiology, and end result program registries; TRAF3, TNF receptor-associated factor 3; UADT, upper aerodigestive tract; WDSCC, well-differentiated squamous cell carcinoma.

TABLE 3 | Representative studies showing specific molecular differences in HPV negative vs HPV positive HNC.

Study (Year)	Sample size and HPV positivity	Study design	Anatomical sites examined	HPV-positive HNSCC	HPV-negative HNSCC
Van Houtenet al. (2001)	Fresh specimens of UADT (*n* = 84) (HPV positivity- 23.8%)	Prospective analysis	All sites of H&N region	p53 wild type, non-mutated in E6 positive tumor p53 mutations only in HPV E6RNA negative tumors (36.45%)	Frequent p53 mutations (62.5%)
Licitra et al. (2006)	Patient samples (*n* = 90). HPV positivity- 55.6%	Retrospective study	Oropharynx	p16 expression as surrogate marker Normal $p16^{INK4a}$ gene-100% P16 immunophenotype-100% Integration of HPV16 DNA-17% TP53 mutation-39%	Homozygous deletion in $p16^{INK4a}$–47% Normal p16INK4a gene-52.5% P^{16} immunophenotype-21% TP53 mutation-48%
Zhang et al. (2013)	Patient samples (*n* = 325) HPV positivity- (OPC-46.27%) HPV positivity- (OCC-9.5%)	Case control study	Oropharynx, oral cavity	Short telomere length in PBLs—increased risk of OPC. No association was observed between telomere length in PBLs and risk of OCC. —	Reference
Chung et al. (2015)	Data from TCGA cohort Patients FFPE tissue (*n* = 252)	Observational study	All sites of H&N region	Genomic alterations of PIK3CA and PTEN genes Altered pathways- PI3K pathway	Genomic alterations of CDKN2A/B and TP53 genes Altered pathways- DNA repair p53 and cell cycle pathways
Seiwert et al. (2015)	Patients (*n* = 120) (HPV positivity-42.5%)	Cohort study	All sites of H&N region	Unique mutational spectrum-mutation in DDX3X, FGFR2/3 and aberrations in PIK3CA, KRAS, MLL2/3, and NOTCH1 genes Somatic aberrations in DNA-repair genes (BRCA1/2, fanconi anemia genes, and ATM)	Mutational spectrum- mutation in TP53, CDKN2A, MLL2, CUL3, NSD1, PIK3CA, and NOTCH genes
Pollock et al. (2015) (Pollock et al., 2015)	FFPE pretreatment tissue samples of HNSCC (n = 88)	Retrospective cohort based study	All sites of H&N region	Elevated expression of total HER2, total HER3, HER2:HER3 heterodimers, and the HER3:PI3K complex	Elevated expression of total EGFR (HER1)
Masterson et al. (2015)	Prospective cohort (*n* = 24) Retrospective cohort (*n* = 27) (HPV positivity-80.4%)	Cohort based study	Oropharynx	Retrospective cohort- increased expression of CDKN2A transcript Prospective cohort- increased expression of SYCP2 transcript —	Reference
Partlova et al. (2015) (Partlova et al., 2015)	Prospective study (*n* = 54) (HPV positivity-54.5%)	Prospective study	All sites of H&N region	High infiltration rate of $CD8^+$ $IFN\gamma^+$ T lymphocytes, Tc17 lymphocytes, naïve $CD4^+$ T lymphocytes and myeloid DCs. Production of high level of chemokines CXCL9, CXCL10, CXCL12, CXCL17 and CXCL21. Lower expression of Cox-2 mRNA. Higher expression of PD1 mRNA	Reference
Verma et al. (2017)	Fresh biopsies and FFPE tissues (*n* = 135) (HPV positivity- 23%) —	Prospective and archival study	Oral cavity, oropharynx	Low expression of STAT3 and pSTAT3 Strong or moderate expression of NF-κB and p65 Marked expression of AP-1 family members	Moderate or strong expression of STAT3 and pSTAT3 No expression of NF-κB Low expression of p65 irrespective of presence or absence family member AP-1
Hajek et al. (2017)	TCGA (*n* = 279) (HPV-positivity 12.9%)	Cohort study	All sites of H&N region	Mutations in TRAF3 or CYLD genes activate NF-κB signaling	Gene alterations in TRAF3 (2%)
Koneva et al. (2018)	HPV^+ UM tumors (*n* = 18) HPV^+ TCGA tumors (*n* = 66)	Prospective and archival study	Oropharynx, oral cavity, larynx, hypopharynx	Recurrent integration of CD274, FLJ37453, KLF12, RAD51B, and TTC6 genes Integrated genes interact with Tp63, ETS, and/or FOX1A	Reference
Ren et al. (2018)	Discovery cohort (*n* = 75) (HPV positivity-66.675) Validation cohort (*n* = 46) (HPV positivity-52.17%)	Cohort study	Oropharynx	Hypermethylation of ATP5EP2, OR6S1, ZNF439, VSTM2B, ZNF137P, ZNF773 DMRs — —	Hypomethylation of ATP5EP2, OR6S1, ZNF439, VSTM2B, ZNF137P, ZNF773 DMRs

(Continued on following page)

TABLE 3 | (*Continued*) Representative studies showing specific molecular differences in HPV negative vs HPV positive HNC.

Study (Year)	Sample size and HPV positivity	Study design	Anatomical sites examined	HPV-positive HNSCC	HPV-negative HNSCC
Gerle et al. (2018)	HPV positive cell line (UDSCC-2)	*In-vitro* study	Hypopharynx and tongue	Significant increase in asmase activity after irradiation and more sensitive to cisplatin treatment	Not significant increase in asmase activity after irradiation
Brand et al. (2018)	HPV positive cell lines (93-vu-147T, UPCI-SCC152, UPCI-SCC90, UM-SCC47, UM-SCC104 and UD-SCC2	*In-vitro* study	Oral cavity, hypopharynx and tongue	Cross-talk between HER3 and HPV oncoproteins E6 and E7 maintains AKT signaling	Reference
Salazar -Ruales et al. (2018)	Patient samples (*n* = 108) Controls (*n* = 108) HPV positivity (12.7%)	Case control study	All sites of H&N region	Upregulation of miR-205-5p, miR-122-5p, miR-124-3p, and miR-146a-5p	Downregulation of miR-205-5p, miR-122-5p, miR-124-3p, and miR-146a-5p
Chen et al. (2018)	TCGA (*n* = 516)	Cohort study	Oropharynx, larynx	Genes associated with immune-associated processes were upregulated	Reference
	HPV positivity (8.7%)			Greater numbers of infiltrating B and T cells and fewer neutrophils	
	Independent HNSCC datasets (*n* = 78) HPV positivity (30.8%)			Predominated cytotoxic T cell subtypes Higher ratio of M1/M2 macrophages	
Xiao et al. (2018)	Patient samples (*n* = 94) HPV positivity (53.19%)	Prospective study	Oral cavity, oropharynx, larynx	HPV-related tumors exhibited lower fatigue and inflammation	HPV-unrelated tumors experienced persistently high levels of fatigue and inflammation
Beaty et al. (2019)	Patient samples (*n* = 77)	Clinical trial prospective cohort study	Oropharynx	PIK3CA mutation was significantly associated with disease recurrence and worse DFS.	Reference
Fleming et al. (2019)	Patient samples (*n* = 35) HPV positivity (31.4%)	Cohort study meta analysis	All sites of H&N region	Reference	Elevated expression of genes associated with glycolysis and oxidative phosphorylation

Abbreviations: ASNase- Acid sphingomyelinase activity, CYLD-Cylindromatosis Lysine 63 deubiquitinase, DFS-Disease Free Survival, DMRs-Differentially Methylated Regions, FFPE-Formalin Fixed Paraffin Embedded, HNSCC-Head And Neck Squamous Cell Carcinoma, OCC-Oral Cavity Carcinoma, OPC-Oropharyngeal Carcinoma, OPSCC- Oropharyngeal Squamous Cell Carcinoma, PBLs-Peripheral Blood Lymphocytes, TRAF3-Tumornecrosis Factor Receptor-Associated Factor 3, UADT- Upper Aero Digestive Tract.

(Goldenberg et al., 2008). These tumors showed low risk of second primary malignant neoplasm (Adjei Boakye et al., 2018) with a better overall and disease-free survival (Ragin and Taioli, 2007; Fakhry et al., 2008; Ang et al., 2010; Rischin et al., 2010; Posner et al., 2011; Fakhry et al., 2014). Irrespective of the tissue subtype involved, HPV positivity in HNSCC emerged as a strong biomarker associated with better prognosis (Gillison et al., 2000; Wookey et al., 2019).

HNSCC is overrepresented in males (Pintos et al., 1999; Gillison et al., 2008). The gender bias increases further in HPV-positive tumors (Pintos et al., 1999). Gender-specific data derived from HPV-positive oropharyngeal cancer (OPC) patients showed a higher risk of premalignant lesions in men (Ryerson et al., 2008). These observations are indicative of a tumor-promoting role of either male-specific hormones leading to differences in clearance of HPV infections due to the endocrine-immune interactions (Klein, 2000), or a distinct cellular environment in oral mucosal cells of men that promote transcriptional activation of viral oncogenes and HPV-mediated HNC. An increased anal HPV16/18 prevalence has been noticed, which correlated with high free testosterone levels in men having sex with men (Hsu et al., 2015).

Time trend studies carried out in different cohorts and registries particularly in North America and Europe revealed an interesting disease dynamics among all the HN sites (Chaturvedi et al., 2008; Chaturvedi et al., 2011). OPC showed a characteristic change in incidence (Hammarstedt et al., 2006; Mehanna et al., 2013). During the 30 year period, HPV-negative OPC declined steeply with a simultaneous and more prominent emergence of HPV-positive OPC (Chaturvedi et al., 2011). HPV-negative OPC and non-OPC that included all other HN sites are HPV-unrelated and traditionally linked to smoking and alcohol abuse. On the contrary, the studies showed a definitive and strong link of HPV-positive tumors with the oral–genital sexual contact (Gillison et al., 2008). The HPV-positive HNSCC shows large variations in prevalence among different geographical regions (De Martel et al., 2019) and may be associated with prevailing sociocultural and sexual practices, whereas genetic predispositions that may also play a sizable role in this phenomenon cannot be ruled out. In line with these observations, a higher incidence of HPV-positive tumors in Hispanic population has been reported (Gillison et al., 2008).

Early studies repeatedly pointed to a lower median age of HPV-positive HNSCC (Chaturvedi et al., 2008; Posner et al., 2011). However, a recent study demonstrated increased HPV positivity even in older age-group (Windon et al., 2018), thus indicating that early onset of HNSCC was merely circumstantial. Reviewing the factors contributing to the changing pattern of HNSCC over last 50 years revealed a major shift in societal practices with respect to depiction of sexuality (Syrjanen et al.,

1982). Surprisingly, in 1969, Denmark legitimized display of explicit content, which was followed by the Netherlands and Sweden, and by 1972, the United States observed a peak in the films displaying oral sexual acts. Therefore, the shift in the HNSCC from HPV-negative to HPV-positive tumors observed in the western population is possibly associated with two independent phenomena that occurred simultaneously. First, establishment of tobacco's carcinogenic potential (Vizcaino et al., 2015) and consequent implementation of anti-tobacco policies; and second, display of oral sex on motion pictures that promoted indulgence in high-risk behavior leading to increased exposure of oral mucosa to genital HPV infections. Treatment efficacy can be maintained by evaluating the HPV-positivity in OPSCC; as they have better prognosis, they can be treated with less aggressive treatment to avoid serious side effects to reduce treatment-associated toxicities in relatively younger patients (Boscolo-Rizzo et al., 2016).

Molecular Signatures of Human Papillomavirus–Positive Head and Neck Cancer

During first 2 decades, research was emphasized on the detection of HPV and its distribution in the HN region. Subsequent studies revealed a series of distinctive molecular features in HPV-positive HNC (**Table 3**). In HPV-positive tumors, wild-type p53 was functionally active and was downregulated by E6 oncoprotein. Reduced p53 transcript was associated with the activation of many oncongenic pathway genes, which contributes to genetic instability in the development of cancer (van Houten et al., 2001; Licitra et al., 2006). HPV-positive HNC lesions show characteristically high expression of $p16^{INK4a}$, which serves as a surrogate marker for HPV (Licitra et al., 2006). In contrast, HPV-negative tumors showed inactivating p53 and $p16^{INK4a}$ mutation in HNSCC.

In the proliferative cell signaling pathway, HPV-positive HNC showed elevated expression of HER2, HER3, and HER2:HER3, and HER3:PI3K complex. In contrast, HPV-negative HNC showed higher expression of EGFR (HER1), which is responsible for resistance to EGFR inhibitors (Pollock et al., 2015). HPV-positive HNC was PI3K inhibitor resistant due to abundance of E6 and E7 oncoproteins. A crosstalk among PI3K, HER3, and E6/E7 oncogenes was reported (Brand et al., 2018). Differential regulation of several microRNAs was observed in HNC, miR-205-5p, miR-122-5p, miR-124-3p, and miR-146a-5p that were upregulated in HPV-positive HNC. In contrast, these miRNAs were downregulated in HPV-negative HNC (Salazar-Ruales et al., 2018).

Based on transcription milieu, HNC showed constitutively active nuclear factor-κB (NF-κB) irrespective of their HPV status. However, a detailed molecular dissection of the constitutively active NF-κB complex showed the presence of p50:p65 heterodimer in HPV-positive tumors, whereas homodimer of p50:p50 was found in HPV-negative tumors (Mishra et al., 2006; Gupta et al., 2018). Similarly, in HNC tumors for constitutively active AP-1, JunB and JunD were involved with c-Fos and Fra-2 in HPV-positive HNC, whereas in HPV-negative HNC, c-Jun was the major binding partner (Gupta et al., 2015).

STAT3, another transcription factor that is linked with carcinogenic outcome, was strongly associated with HPV-negative HNC and was characteristically low in HPV-positive tumors (Gaykalova et al., 2015; Verma et al., 2017). SOX2 amplification was observed in HPV-negative HNC, while there was no amplification in HPV-positive HNC (Schrock et al., 2014). HPV-positive HNCs were immunologically more active with high infiltration of T and B lymphocytes and myeloid dendritic cells, and had higher M1-type macrophages along with high chemokine production and PD1 expression (Partlova et al., 2015; Chen et al., 2018). A detailed discussion of various differentially expressed carcinogenically relevent genes in HPV-positive and HPV-negative HNC that contribute to better prognosis was described earlier (Aggarwal et al., 2020).

Current Treatment Strategies Against Head and Neck Cancer

Treatment of HNC requires a multi-modality approach depending on the stage and site of the tumor (Marur and Forastiere, 2008). Early tumors are treated with surgery or radiation, whereas intermediate- and late-stage tumors benefit from a combined modality approach. Due to essential requirement of clear margins in surgery, it is an option only for early tumors; still it carries a risk of cosmetic deformity and impaired function (Kofler et al., 2014). A study on the quality of life after oropharyngeal surgery reports high incidence of fatigue, reduced sexuality, difficulty in swallowing and other teeth, salivary gland, and mouth-opening–related problems (Bozec et al., 2018). Surgery also requires additional treatment to reduce the risk of locoregional and distant failure in advanced-stage HNC (Porceddu et al., 2004). Platinum-based chemotherapy has been central in treating HNC. Combinatorial therapies with or without platinum drugs have been proven superior in terms of the response rate and the ability to tackle drug resistance than platinum-based chemotherapy treatment. Targeted therapies using monoclonal antibodies such as cetuximab, against epidermal growth factor receptor (EGFR) either in combination with a standard chemotherapy regimen or as a single agent, have also proven effective to some extent to treat HNC. But these approaches also bear side effects apart from the development of chemoresistance in a short period of time (Price and Cohen, 2012). These therapies have a myriad of debilitating toxic effects such as nephrotoxicity, hepatotoxicity, and cardiotoxicity. Also, various cardiac events have been reported, like arrhythmias, myocarditis, and cardiomyopathy, to congestive heart failure (Hartmann and Lipp, 2003).

Radiation therapy (RT) is often performed as an adjunct to surgery or in concurrence with chemotherapy (Marur and Forastiere, 2016). Wendt et al. reported a 3-year overall survival rate of 24% in RT arm vs. 48% in RT plus CT arm in stage III/IV HNC, whereas the 3-year locoregional control rate was 17% in RT arm and 36% in RT plus CT arm (Wendt et al., 1998). However, a long-term toxicity risk to the salivary glands, pharyngeal constrictor muscles, and thyroid gland, leading to

xerostomia, dysphagia, percutaneous endoscopic gastrostomy tube dependence, chronic aspiration, and hypothyroidism, had been observed (Langendijk et al., 2008).

Despite a clear prognostic advantage and better response to therapy, therapeutic management for HPV-positive HNC is almost the same as that of any HPV-negative HNC. Considering the younger age of the patients, there have been efforts to reduce the long-term toxicity of anticancer treatment without risking the survival benefits (Kofler et al., 2014). Reduction in dose of radiotherapy, use of cetuximab (Marur et al., 2017) instead of cisplatin for chemoradiation, and transoral robotic surgery (TORS) are a few efforts to mention that are specifically directed to HPV-positive HNC. Considering HPV-positive tumors to be immunologically active, in recent past, attempts have been made to design PD1-PDL1 immunotherapeutic strategies (Qiao et al., 2020). New cancer immune-prevention treatments include FDA-approved inhibitory antibodies such as pembrolizumab (anti-PD1 mAb), nivolumab (anti-PD1), and ipilimumab (anti–CTLA-4 mAb) (Bauman and Ferris, 2014; Ferris et al., 2018; Mehra et al., 2018; Havel et al., 2019); co-stimulation and co-inhibition pathways (Kuss et al., 2003; Tsukishiro et al., 2003; Baruah et al., 2012; Pardoll, 2012); and check-point blockade therapy (Davis et al., 2016; Muzaffar et al., 2021). A systematic assessment of the cost effectiveness of ICIs showed nivolumab was not cost-effective over chemotherapy for HNC (Verma et al., 2018). Moreover, none of these approaches target HPV. A study attempted to develop Trojan vaccine against HPV could not show significant benefit of therapeutic vaccines against HPV in HNC (Voskens et al., 2012). A recent study showed a chimeric HPV16 E7 DNA vaccine induced prophylactic and therapeutic efficacy in a cervical cancer mouse model, but its effect on HPV-positive HNC remains to be examined (Garza-Morales et al., 2019).

Therapeutic Challenges in Head and Neck Cancer Management

Despite aggressive treatment and organ preservation with current clinically administered curative therapies, the overall 5-year survival is less than 50% (Forastiere et al., 2013). With existing heterogeneity in the origin, poor response rates and substantial systemic toxicity associated with current standard-of-care treatment of advanced HNC remain a significant challenge (De Lartigue, 2015). As molecular targeted therapies come into clinical use, the great interindividual variability in the efficacy of these compounds highlights the absolute need to determine predictive factors of tumor and toxic responses to these new therapeutic agents (Bozec et al., 2009). Further, patients with locally advanced or recurrent HNC present a separate therapeutic challenge. Treatment options are limited, and morbidity can be substantial. Surgical intervention has debilitating effect on normal daily routine and patient psychology. Recurrent HNC is difficult to treat for multiple reasons, including the effects of prior treatment on tumor cells and normal tissues, as well as the infiltrative and multifocal nature that typically characterizes recurrent disease in this area (Ho et al., 2014).

Limitations of these therapies have prompted clinical and translational research for better chemotherapeutics with less treatment-associated toxicities. Many studies are focusing on biologically active compounds from herbal origin to develop chemotherapeutic agents with fewer side effects and higher efficacy (Seo et al., 2015; Kunnumakkara et al., 2017). Many of these phytochemicals can serve as alternatives for chemotherapy sensitizers (Bharti and Aggarwal, 2017; Huang and Yu, 2017).

Emerging Chemotherapeutic Phytochemicals/Herbal Derivatives Against Head and Neck Cancer

Phytochemicals have found relevance in HNC therapy because natural compounds provide a cost-effective, safe, and less toxic alternative to synthetic drugs currently in wide use. Effectiveness of various phytochemicals as therapeutic agents has been well documented in the literature, and they are now widely being studied as potential agents to treat and prevent HNC. Many preclinical studies have successfully demonstrated the anticancer activity of pure and well-characterized phytochemicals and herbal derivatives on cells obtained from different HN regions using *in vitro* and *in vivo* experimental systems (**Table 4**). However, a majority of these studies employed cell lines derived from the oral cavity, so the data may be slightly skewed.

A range of phytochemicals showed anticancer activity against different HNC cells over 2 decades (**Figure 3**). Phytochemicals like thymol, oridonin, shikonin, and moscatilin with potent dose-dependent antiproliferative activity showed IC50 values lower than 10 μM over a wide range of HNC cell types. A detailed investigation of molecular mechanisms revealed targeting of key cellular carcinogenic pathways, namely, MAPK/JNK/p38 (role of ROS), NF-κB, EGFR/JAK2/STAT3, P13K/Akt, mTOR/P70S6K, c-Raf/ERK, GSK3β, FOXO1, FOXO3a, and p53, that concurrently operate in HNC and contribute to cancer progression and treatment resistance.

NF-κB is a family of transcription factors (TFs) comprising c-Rel, RelA (p65), RelB, NF-κB1 (p50 and p105), and NF-κB2 (p52), which plays important roles in immunity, inflammation, cell proliferation, survival, and differentiation (Oeckinghaus and Ghosh, 2009). Many basic and clinical studies demonstrated aberrantly expressed and constitutively expressed NF-κB in HNC with its contribution to cancer cell survival and proliferation, and poor survival of patients (Mishra et al., 2006; Monisha et al., 2017; Verma et al., 2017). Cigarette smoke phosphorylates IκBα, which in turn activates NF-κB (Anto et al., 2002). Early evidence of phytochemicals like curcumin showing anticancer action on HNC came from abrogated IκBα kinase (IKK) which inhibited NF-κB activation and cell survival/proliferation genes such as cyclin D1, Bcl-2, IL-6, COX-2, and MMP-9 (Aggarwal et al., 2004). Based on a similar approach, blocking activity of NF-κB, or its downstream molecules, therapies were designed to downregulate cell growth and metastasis. Caffeic acid phenethyl ester (CAPE) and goniothalamin inhibited NF-κB-p65 activity in a potential primary and metastatic OSCC (Kuo et al., 2013; Li et al., 2016).

STAT3, a central transcription factor and known oncogene, works downstream of EGFR, and TGFα signaling also plays a key

TABLE 4 | Preclinical studies showing therapeutic phytochemicals/herbal derivatives against tobacco/alcohol-associated HNC.

Bioactive compound/ Herbal derivative PubChem CID (Class) Source	Cell type/Model	Test and oosage	Anti-tumour outcome	Molecular outcome	References
Curcumin CID- 969516 (Phenolics) *Curcuma Longa*	*In vitro*: **MDA 1986** (OSCC), **Tu 686** (LSCC), **Tu 167**, **JMAR C42** (Floor of mouth OSCC), **MDA 686LN** (OPSCC)	**Cell proliferation:** 10 μM, 50 μM	• Proliferation↓ • Apoptosis↑ • Arrests cell cycle in G1/S phase	• NF-κB activation↓ • Bcl-2↓, cyclin D1↓, IL-6↓, COX-2↓, MMP-9↓	Aggarwal et al. (2004)
Gossypol CID- 3503 Phenolic *Gossypium arboreum L.*	*In vitro:* **UMSCC-1**, **UMSCC-17B** (Floor of mouth OSCC), Human oral keratinocytes and Normal keratinocytes *In vivo*: NCr-nu/nu mice	**Cell proliferation:** UMSCC-1, UMSCC-17B, Human oral keratinocytes and Normal keratinocytes IC50- 3, 6,2, 12.5 μM respectively	• Proliferation↓ • Growth of tumour↓ • Mitotic rate↓ • Apoptosis↑	NA	Wolter et al. (2006)
Berberine CID: 2353 (Alkaloid) *Rhizoma coptidis*	*In vitro:* **HSC-3** (Tongue OSCC)	**Cell viability:** 10 μM	• Cell viability↓ • G0/G1-phase arrest • ROS↑,Ca^{2+}↑, MMP↓, Apoptosis↑	• Bcl-2↓, BAX↑, p53↑ • Cyt C release	Lin et al. (2007)
	In-vitro study: **FADU** (Hypopharyngeal SCC)	**Cell cytotoxicity:** 12 or 25 μM for 24 h	• Cytotoxicity ↑ • Apoptosis ↑ • Cell viability ↓ • Cell migration ↓	• FasL ↑, TRAIL ↑ • Cleaved caspase-8 ↑, cleaved • caspase-7 ↑ • Bcl-2 ↓, Bcl-xL ↓, Bax ↑, Bad ↑, Apaf-1↑, cleaved caspase-9 ↑, cleaved caspase-3 ↑, PARP ↑ • MMP-2 ↓, MMP-9 ↓ • ERK, JNK and p38 phosphorylation ↓	Seo et al. (2015)
Physalis angulate (Crude extract)	*In-vitro* study: **HSC-3** (OSCC)	**Cell viability:** IC50: 10 μg/ml	• Mitochondrial reductase activity ↓ • Apoptosis ↑ • Oxidative stress ↑ • Loss of cell function ↑ • S- and G2/M-phase arrest • Mitochondrial function impaired	• ROS ↑ • Bcl2 ↓, Bax ↓, AIF ↓, cytochrome c ↓, proform caspase-3 protein levels ↓, caspase-9 ↑, proform caspace-4 protein levels ↑, MMP attenuated • ORP150 ↓, HSP70 ↑ • HO-1 ↑, SOD ↑	Lee et al. (2009)
Guggulsterone CID- 6450278 (3-hydroxy steroid) *Commiphora mukul*	*In vitro:* **SCC-4** (Tongue OSCC), **HSC-2** (OSCC)	**Protein expression:** 50 μM	NA	• Phosphorylation of p65, IkBα & STAT3, NF-κB↓ • IL-6↓ , COX-2↓ • Expression VEGF↓	
Proanthocyanidins CID- 108065 (Phenolic) *Vitis vinifera*	*In vitro:* **UMSCC-1**, **UMSCC-5** (Floor of mouth OSCC), **FaDu** (Hypopharyngeal OSCC), **OSC-19** (Tongue OSCC), **Beas-2B** (Bronchial Epithelium transformed with Ad12-SV40 2B) *In vivo:* athymic nude mice	*In vitro:* IC50- 101 nM, 67 nM for 24 and 48 hrs, respectively *In vivo:* 0.5%, w/w	• Cell viability↓ • Apoptosis↑ • G1 phase arrest • 61% less tumor volume (p<0.001)	• Cyclin D1↓ and Cyclin D2↓ • cdk2↓, cdk4↓, cdk6↓ • Cip1/p21↑ and Kip1/p27↑ • Bax↑, Bcl-2↓, caspase 3↑ and poly(ADP-ribose)polymerase↑.	Prasad and Katiyar, (2012)
Wogonin CID- 5281703 (Phenolic) *Scutellaria baicalensis*	*In vitro:* **NPC-TW076, NPCTW039** (NPSCC)	**Autophagy:** 50 μM	• Autophagy↑ • Apoptosis↑	• P13K/Akt↓, mTOR/P70S6K↓, c-Raf/ERK↓	Chow et al. (2012)
Caffeic Acid Phenethyl Ester CID- 5281703 (Phenolic) *Populus nigra L.*	*In vitro:* **TW2.6** (OSCC)	**Cell proliferation:** IC50- 83.8, 46.6, and 18.8 μM for 24, 48, and 96 h treatment, respectively	• Cell proliferation↓, colony formation↓ • Apoptosis↑ • G1 phase↓, G2/M phase↑ cell population	• Akt↓, GSK3β↓, FOXO1↓, FOXO3a↓, NF-κB↓, Rb↓, Skp2↓, cyclin D1↓, p27Kip↑	Kuo et al. (2013)
Ellagic acid CID- 5281855 (Phenolic) *Rubus occidentalis*	*In vitro:* **HSC-2** (OSCC), **HF-1** (Normal fibroblasts)	**Cytotoxicity:** (IC50- 260 & 142 μM on 2nd and 3rd day of exposure, respectively)	• Apoptosis↑	• Caspase 3/7 ↑ • Cleavage of poly ADP ribose polymerase	Weisburg et al. (2013)
Cucurbitacin CID- 5281316 (Terpene) *Cucumic melo L*	*In vitro:* **SAS** (Tongue OSCC)	**Cytotoxicity:** IC50- 3.7 μM	• Sub G0/G1 phase arrest • Apoptosis↑	• Caspase 3 Activation • MMP↓	Hung et al. (2013)
BME (crude extract) *Momordica charantia*	*In vitro:* **Cal-27** (Tongue OSCC), **JHU-22**, **JHU-29** (Laryngeal SCC) *In vivo:* BALB/c athymic nude mice	*In vitro*: 1% BME *In vivo:* 100 μl BME (0.1 g/ml) for 5 days	• Cell proliferation↓ • Tumor growth and volume↓ • Keratinocyte formation↓, mitosis↓	• c-Met signaling pathway↓ • Mcl-1, pSTAT3, cMyc expression↓ • cyclinD1↓, survivin↓, cell arrest • MCM2↓	Rajamoorthi et al. (2013)
Honokiol CID-72303 (Phenolic)	*In vitro:* **SCC-1, SCC- 5** (Floor of mouth OSCC), **OSC-19** (Tongue OSCC), **FaDu** (Hypopharyngeal SCC)	*In vitro*: ~60 μM for 24, 48 and 72 hrs *In vivo:* 100 mg/kg body weight (mw-266.3)	• Cell viability↓ • Apoptosis↑	• Expression levels of Cyclins: D1, D2, and Cdks: 4 and 6↓ • EGFR↓, mTOR and their downstream signalling molecules↓	Singh et al. (2015)

(Continued on following page)

TABLE 4 | (*Continued*) Preclinical studies showing therapeutic phytochemicals/herbal derivatives against tobacco/alcohol-associated HNC.

Bioactive compound/ Herbal derivative PubChem CID (Class) Source	Cell type/Model	Test and oosage	Anti-tumour outcome	Molecular outcome	References
Magnolia officinalis Cepharanthine CID- 10206 (Alkaloid) *Stephania cepharantha*	*In vitro:* **CNE-1, CNE-2** (NPSCC)	**Cell proliferation:** IC50 for CNE-1 and CNE-2: 20 and 32 nM after 48 hrs, respectively	• Cell proliferation↓ • G1 phase arrest	• DNA repair genes ↓	Liu et al. (2015)
MEAG (Crude extract) (Terpenes) *Withania somnifera*	*In vitro:* **MC3** (Chronic myelogenous leukemia), **HN22** (OSCC)	**Cytotoxic effect:** IC50 for MC3 and HN22: 6.5 and 4.6 μg/ml, respectively	• Mitochondria mediated apoptosis↑ • Nuclear condensation and fragmentation	• MMP↓, Cyt C release, caspase 9 ↑, t-Bid↑, cleaved caspase-8↑, DR5↑.	Lee et al. (2016)
Goniothalamin CID- 6440856 (Phenolic) *Goniothalamus marcrophyllus*	*In vitro:* **H400** (OSCC)	**Cytotoxic effect:** IC50: 8.9 nM after 72 h	• Cell viability↓ • Cell proliferation↓ • Apoptotic-like morphology (cell shrinkage, dense cytoplasm, blebbing of cell surface) • S phase arrest.	• MMP↓, Cyt C release • NF-κB activation↓	Li et al. (2016)
Lupeol CID- 259846 (Terpene) *Camellia japonica*	*In vitro:* **HEp-2** (Human papillomavirus-related endocervical adenocarcinoma), **UPCI:SCC131** (Floor OSCC) *Ex vivo:* Fresh HNSCC tumor tissues	**Cell viability:** IC50 for Hep-2 and SCC131: 53.5 and 52.4 μM after 24 hrs, respectively	• G1 phase arrest • Apoptosis↑ via intrinsic pathway • Cell viability↓	• Expression p53↑, Bax↑, CDKN2A↑, CyclinD1↓, Ki67↓ • Caspase 3 activation	Bhattacharyya et al. (2017)
Icaritin CID- 5318980 (Phenolic) *Epimedium grandiflorum*	*In vitro:* **KB** (Human papillomavirus-related endocervical adenocarcinoma), **SCC9** (Tongue OSCC)	**Cell viability:** ~20 μM for 24 and 48 h	• Mitochondria mediated apoptosis↑	• MMP↓, Cyt c release • miR-124↑ • Sp1/DNMT1 signaling↓	Jin et al. (2017)
Osmuda regalis root (crude extract) *Osmuda regalis*	*In vitro:* **FaDu** (Hypopharyngeal SCC), **HLaC78, HLaC79, HLaC79-tax** (LSCC)	**Cytotoxicity:** IC50 for HLaC79, FaDu, HLaC79-Tax and HLaC79: 21.4, 8.5, 20.6 and 9.9 μg/ml, respectively	• Cell growth↓ • Apoptosis↑ • Invasion↓	• CLEC3B↓, KAL1↓, MMP 11↓, MMP 15↓, MMP2↓ • Integrin such as ITGB3↑, ITGA1↑, ITGAM↑ • metastasis genes such as CTFG↑, PPIA↑, SELP↑, VCAN↑	Schmidt et al. (2017)
Piperine CID- 638024 (Alkaloid) *Piper nigrum*	*In vitro:* **KB** (Human papillomavirus-related endocervical adenocarcinoma)	**Cell proliferation:** IC50: 124 μM for 24 h	• Apoptosis↑ • Cell viability↓ • Cell growth↓ • Cellular morphological changes • G2/M phase arrest	• ROS↑, MMP↓ • Caspase 3 activation	Siddiqui et al. (2017)
Embelin CID- 32798 (Phenolic) *Embelia ribes*	*In vitro:* **SCC25**, **Cas9-22**, **YD10B** (Tongue squamous cell carcinoma)	**Cytotoxicity:** 0–300 μM for 24 h; cell specific effect	• Cell viability↓ • Condensed fragmented nuclei • Autophagic vacuoles appears	• MMP↓, caspase 9 & 3↓ • p62/SQSTM1↓ • Conversion↑ LC3-I to LC3-II	Lee et al. (2017)
Dihydroartemisinin CID- 3000518 (Sesquiterpene lactone) *Artemisia annua*	*In vitro:* **Cal-27** (Tongue OSCC)	**Cell proliferation:** IC50: 24.4 μM for 24 h	• Autophagosomes↑ • Oxidative stress↑ • DNA double-strand break • Weight and volume of Xenograft tumor↓ by 56.58%	• LC3-II ↑, Bevlin-1↑, γH2AX foci↑ • STAT3 activation↓ and disrupted p-STAT3 nuclear translocation	Shi et al. (2017)
β-Elemene CID- 6918391 (Terpene) *Curcuma wenyujin*	*In vitro:* **YD-38** (Gingival OSCC) *In vivo*: BALB/c nude mice	**Colony formation and Apoptosis:** 195 nM β-Elemene	• Cell proliferation↓ • Apoptosis↑	• Expressions of STAT3↓, p-STAT3↓, p-JAK2↓, and Bcl-2↓, Bax↑ and caspase-3↑ • Block JAK2-STAT3 pathway	Huang and Yu, (2017)
Thymol CID- 6989 (Terpene) *Thymus vulgaris*	*In vitro:* **Cal27, SCC-4, SCC-9** (Tongue OSCC) *In vivo:* Athymic nu/nu mice	**Cytotoxicity:** 2.3 μM	• Cell viability↓ • No colony formation • *In vivo* tumor growth↓ • Apoptosis↑	• c-PARP↑, MMP dysfunction	De La Chapa et al. (2018)
Tanshinone CID- 114917 (Abietane diterpenoid) *Salvia miltiorrhiza*	*In vitro:* **SCC-9** (Tongue OSCC) *In vivo:* BALB/c-nu	**Cell viability:** IC50: 17.5 μM.	• Apoptosis↑ • Autophagy↑ • Growth of solid tumors in vivo	• LC3-I↑ • Beclin-1/Atg7/Atg12-Atg5 pathway↑ • PI3K/Akt/mTOR pathway↓	Qiu et al. (2018)
Oridonin CID- 5321010 (Terpene) *Rabdosia rubescens*	*In vitro:* **UM1, SCC25** (Tongue OSCC)	**Cell proliferation:** IC50 for SCC25, UM1, UM2, HSC3 and Ca127: 9.1, 8.2, 10.6, 15.4 and 9.6 μM, respectively.	• G2/M phase arrest • Apoptosis↑	• Bax/Bcl-2↑ • Cyclin B1↓, pCDK1↑, cyclin D1↑, cyclin D3↑, p21↑ and cyclin A2↑ • Activates caspase-3, caspase-9 and PARP-1 • P13K/Akt/mTOR pathway↓	Yang et al. (2018b)

(Continued on following page)

TABLE 4 | (*Continued*) Preclinical studies showing therapeutic phytochemicals/herbal derivatives against tobacco/alcohol-associated HNC.

Bioactive compound/ Herbal derivative PubChem CID (Class) Source	Cell type/Model	Test and oosage	Anti-tumour outcome	Molecular outcome	References
Epigallocatechin-3-gallate CID- 65064 (Phenolic) *Camellia sinensis*	*In vitro:* **HSC** (Tongue OSCC) *In vivo:* BALB/c nude (nu/nu) mice	**Cell proliferation:** IC50 value at 24, 48 and 72 h were >100, 43.2 and 39.3 μM, respectively	• Cell viability↓ • G1 phase arrest • Apoptosis↑ • Tumor size↓ 45.2%	• Caspase-3 and -7↑ • miR-22↑	Yoshimura et al. (2019)
Quercetin (Phenolic) CID: 5280343 *Allium cepa L.*	*In vitro:* **hNOK** (Human normal oral keratinocytes), **Tc8113, SAS** (Tongue OSCC) *In vivo*: BALB/c nu/nu mice	**Cell viability:** CC_{50} for hNOK, Tc8113 & SAS: 298.6, 48.7 & 44.3 mM, respectively	• Cell viability↓ • Tumor volume and weight↓	• miR-22/WNT1/Beta-catenin pathway↓	Zhang et al. (2019)
Ursolic Acid CID- 64945 (Terpene) *Salvia rosmarinus*	*In vitro:* **Ca9-22** (Tongue OSCC), **SCC2095** (OSCC)	**Cell proliferation:** IC50 for UA, Ca9-22: 11.5 and 13.8 μM, respectively	• Caspase-dependent apoptosis • Autophagy↑, autophagosomes↑ • Migration↓, Invasion↓	• Akt/mTOR/NF-κB signaling↓, ERK↓, and p38↓ • LC3B-II conversion, p62↑ • Proteolytic activity of MMP-2↓	Lin et al. (2019)
Shikonin CID- 479503 (Hydroxy-1,4-naphthoquinone) *Lithospermum erythrorhizon*	*In vitro:* **5-8F** (NPSCC) *In vivo:* BALB/c nude mice	**Cell proliferation:** IC50: 7.5 μM after 6 h	• Necroptosis↑ • *In vivo* tumor growth↓	• Necrostatin-1↑ • RIPK1↑, RIPK3↑, MLKL↑ • Caspase-8 and -3↑ • ROS↑	Liu et al. (2019)
Chrysophanol CID- 10208 (Phenolic) *Rheum rhabarbarum*	*In vitro:* **FaDu** (Hypopharyngeal SCC), **SAS** (Tongue OSCC)	**Cell viability:** IC50 for FaDu and SAS: 9.6 ± 1.3 and 12.6 ± 2.1 μm at 24 h, respectively	• Cell viability↓ • G1 phase arrest • Metastasis↓, EMT↓	• ROS↑ • Expression of procaspase 3↓, cyclin D1↓, CDK4↓, CDK2↓, cdc2↓	Hsu et al. (2020)
Moscatilin CID- 176096 (Phenolic) *Dendrobium sp.*	*In vitro:* **FaDu** (Hypopharyngeal SCC)	**Cell cytotoxicity:** IC50: 1.4 μM at 72 h	• Cell viability↓ • Cell proliferation↓ • Apoptosis via intrinsic as well as extrinsic pathway	• Activation of caspases-3,-8,-9,-7↑ • MMP↓, Cyt C release • JNK pathway↓	Lee et al. (2020)
Demethoxycurcumin CID- 5469424 (Phenolic) *Curcuma Longa*	*In vitro:* **SCC-9, HSC-3** (Tongue SCC)	**Cell proliferation:** IC50: 50 μM	• Cell viability↓ • Cell proliferation↓ • G2/M phase arrest • Morphological changes	• cIAP1/XIAP↓, heme oxygenase-1↑ • Caspase-3↑, -9↑, -8↑, p38-MAPK-HO-1 signaling↑, MAPK↑, JNK1/2↑	Chien et al. (2020)

Abbreviations: Akt- Protein kinase B; Apaf-1- Apoptotic protease activating factor 1; Atg7- Autophagy related 7; Bad- BCL2-associated Agonist of cell Death; Bcl-2- B-cell lymphoma 2; BME- Bitter Melon Extract; Cdc2- Cell division control 2; Cdk2- Cyclin-dependent kinase 2; CDKN2A- Cyclin-dependent kinase inhibitor 2A; cIAP- Calf Intestinal Alkaline phosphatase; Cip1- CDK interacting protein 1; CLEC3B- C- type lectin domain family three member B; c-Met- tyrosine-protein kinase Met; COX-2- Cyclooxygenase-2; c-PARP- Cleaved Poly (ADP-ribose) polymerase; c-Raf-c- Rapidly Accelerated Fibrosarcoma; CTGF- Connective tissue growth factor; Cyt C- Cytochrome complex; DNMT1- DNA (cytosine-5)-methyltransferase 1; DR5- Death receptor five; ERK- Extracellular-signal-regulated kinase; FasL- Fast ligand or cell death receptor; FOXO1- Forkhead box protein O1; GSK3β- Glycogen synthase kinase three beta; H&N- Head and neck; HO-1- Heme oxygenase 1; HSP70–70 kilodalton heat shock proteins; IkBα- I-kappa-B-alpha; ITGA1- Integrin alpha-1; ITGAM- Integrin alpha M; ITGB3- Integrin beta three; JNK- c-Jun N-terminal kinase; Kip1- kinase inhibitor 1; LC3- Microtubule-associated protein 1A/1B-light chain three; MAPK- Mitogen-activated protein kinase; Mcl-1- Myeloid leukemia cell differentiation protein 1; MCM2- Minichromosome maintenance protein complex 2; MLKL- Mixed lineage kinase domain-like pseudokinase; MMP- Matrix metallopeptidase; mTOR-mammalian target of rapamycin; NF-κB- Nuclear factor kappa light chain enhancer of activated B cells; ORP150–150-kDa oxygen-regulated protein; P13K- Phosphatidylinositol 3-kinase; P70S6K- 70-kDa ribosomal protein S6 kinase; PARP- Poly-ADP ribose polymerase; JAK- Janus kinase; PPIA- Peptidylprolyl isomerase A; Rb- Retinoblastoma protein; RIPK1- Receptor-interacting serine/threonine-protein kinase 1; ROS- Reactive oxygen species; SOD- Superoxide dismutases; Sp1- Specificity protein 1; SQSTM1- Sequestosome-1; STAT3- Signal transducer and activator of transcription three; t-Bid-truncated BH3 interacting-domain death agonist; TRAIL- TNF-related apoptosis-inducing ligand; VEGF- Vascular endothelial growth factor; WNT1- Wingless-related integration site 1; XIAP- X-linked inhibitor of apoptosis protein; γH2AX- Phosphorylated X-linked inhibitor of apoptosis protein.

carcinogenic role in HNC (Song and Grandis, 2000). Guggulsterone, a biosafe nutraceutical, phosphorylated p65 and inhibited tobacco smoke and nicotine-induced NF-κB and pSTAT3 proteins and their downstream targets COX-2 and VEGF (Macha et al., 2011). Dihydroartemisinin is a known phytochemical, which is effective as an antimalarial agent, induces DNA double-strand break and promoted oxidative stress, and decreases pSTAT3 nuclear localization which successively increases autophagic cell death (Shi et al., 2017).

In 90% HNC, the PI3K/AKT/mTOR pathway is upregulated (Marquard and Jucker, 2020). Whenever ligand-like growth factors bind with RTKs, they dimerize and lead to the activation of intercellular tyrosine kinase. PI3K partially activates Akt through PIP3 and PIP2. Then to stimulate full activity of Akt, mTORC2 phosphorylates its carboxy-terminal. Akt functions by phosphorylation that leads to the activation or suppression of many proteins involved in cell proliferation, growth, and cell motility (Brazil and Hemmings, 2001; Chaisuparat et al., 2016). Wogonin, a flavonoid compound, has anticancer activity which induces autophagy by LC3 I/II cleavage and inhibits mTOR/P70S6K and Raf/ERK, which in turn inactivates PI3K/Akt and induces apoptosis in NPC cells (Chow et al., 2012). Urosolic acid downregulated Akt/mTOR signaling and expression of NF-κB, which further downregulates ERK and MMP-2 in OSCC cells (Lin et al., 2019).

Loss of carcinogenic signaling was associated with reduced cell survival mechanisms. Honokiol, a phytochemical from *Magnolia* plant, reduced the level of Bcl-xL protein, while Bax expression in xenograft HNC tumors increased. It also reduces the expression of mTOR and its downstream p70S6K (Singh et al., 2015). Similarly, (-)-gossypol, a polyphenol, was reported to bind to Bcl-xL that inhibited HNC proliferation (Wolter et al., 2006).

Antiproliferative activity of phytochemicals was associated with various degrees of cell cycle arrest in most of these studies. Cell cycle–regulating molecules such as cyclins and cdks were downregulated by oridonin, chrysophanol, lupeol, honokiol, and proanthocyadins. Piperine, a nitrogenous pungent substance, induced cell cycle arrest in the G2/M phase and induced apoptosis by changing mitochondrial membrane potential and by activating caspase-3 (Siddiqui et al., 2017). Chrysophanol, a secondary metabolite, downregulated the expression of cyclinD1, CDK4, cdc2, and CDK2, and arrested cell cycle at the G1 phase. It also induced cell death by ROS production (Hsu et al., 2020). Similarly, lupeol induced cell cycle arrest in the G1 phase by increasing the expression of p53, Bax, and CDKN2A, and downregulating cyclin D1 (Bhattacharyya et al., 2017). Oridonin, a bioactive diterpenoid, induced apoptosis by regulating Bax/Bcl-2 and activating caspases. It also decreased cell proliferation by downregulating PI3K/Akt/mTOR pathways. By regulating cyclins, it arrested cells in the G2/M phase (Yang et al., 2018b). Even though the end effect was antiproliferative, the mechanism of action of these phytochemicals differed significantly.

A family of cysteine proteases known as caspases regulates apoptosis. Targeting these caspases can induce apoptosis in OSCC. Demethoxycurcumin, a curcumin analog, induced apoptosis in tongue SCCs by upregulating caspase-3, -9, and -8. It also regulated p38-MAPK-HO1 signaling, MAPK, and JNK1/2 (Chien et al., 2020). Shikonin induced necroptosis in NPC *via* upregulating the expression of RIPK1/RIPK3/MLKL, caspase-3, and -8, and increasing ROS production (Liu et al., 2019). Ellagic acid induced apoptosis by upregulating caspase-3 and -7 (Weisburg et al., 2013). Curcurbitacin, embelin, and proanthacyadins induced apoptosis by attenuating mitochondrial membrane potential and by regulating the activity of Bcl-2, Bcl-xL, and Bax in cells (Prasad and Katiyar, 2012; Hung et al., 2013; Lee et al., 2017).

In *in vivo* studies, the phytochemicals were tested in murine models, where nude mice were implanted with OSCC cell lines. These mice were used to measure the effect of phytochemical on tumor growth. Tumors from euthanized mice were examined for their size and volume. ECGC (Yoshimura et al., 2019), gossypol (Wolter et al., 2006), quercentin (Zhang et al., 2019), proanthocyadins (Prasad and Katiyar, 2012), tanshinomes (Qiu et al., 2018), shikonin (Liu et al., 2019), β elemene (Huang and Yu, 2017), and bitter melon extract (Rajamoorthi et al., 2013) depicted reduction in size and volume of tumor xenografts, and inhibition of xenograft growth. Inhibition of growth was also observed in the *ex vivo* study with lupeol.

Some of the phytochemicals were also tested in clinical trials; however, these studies are very limited (**Table 5**) and emphasize an urgent unmet need in this area to harness the translational potential of emerging phytochemicals. Lippman et al., 1988 conducted a phase II randomized study with 13-cis-retinoic acid (isotretinoin) (3 mg/kg/day) and methotrexate (15 mg/m^2 on the first three days in a 3-week cycle) among 40 patients with advanced SCCs. They achieved a response rate of 16% with isotretinoin, which included a complete response, a partial response, and a minor response. In the methotrexate-treated group, however, the response rate was 5%. The median survival rate from the start of treatment was also lower in the methotrexate group (4 months) than that in the isotretinoin group (4.5 months) (Lippman et al., 1988). Another phase I study with isotretinoin by Weisman et al., 1998 reported its strong synergetic relationship with cisplatin. The maximum tolerated dosage as determined by the study (20 mg/day) was able to attain a complete response at the primary site in all of the 10 evaluable patients (Weisman et al., 1998). There are very few clinical trials on therapeutic potential of phytochemicals in HNC because of lack of interest from pharma industry due to low cost of the molecules, and clinical trial requires a lot of investments. Also, HNC patients with advance stage tumor do not participate in therapeutic clinical trials as it may risk the available therapeutic benefits of existing therapies; however, use of phytochemicals as adjunct therapies may prove beneficial in long run as they will not compromise the benefits of participating patients. Nevertheless, more *in vivo* studies are needed to screen promising leads into clinical trials.

Emerging Chemopreventive Phytochemicals/Herbal Derivatives Against Head and Neck Cancer

Cancer chemoprevention refers to the use of agents to retard the progression of carcinogenesis, reverse, or inhibit it. The aim of chemoprevention is to lower the risk of developing invasive or

clinically significant disease. Chemopreventive phytochemicals thus seek to occasion a chemopreventive response when the primary tumors have not reached a critical size, or seek to block and reverse development of a diagnosed premalignant tumor, or prevent metastasis and growth of metastatic tumors (Tosetti et al., 2002). Angiogenesis, which refers to the biological process of vessel formation, also plays a crucial role in cancer progression. Angiogenesis is also responsible for transition of a dormant tumor to a malignant state (Sogno et al., 2009). An early intervention could possibly prevent cancer formation by regulating "angiogenic switch," the point at which the tumor induces angiogenesis. Thus, angiogenesis is a critical target for chemoprevention (Tosetti et al., 2002).

A battery of phytochemicals reportedly possess cell invasion, migration, angiogenesis, and metastasis inhibitory activities (**Table 6**). These phytochemicals exhibit these antitumor activities by regulating the expression of various molecules such as metalloproteinases (MMPs), especially MMP-2 and MMP-9, which affect cancer migration and invasion. Some MMPs also exhibit proangiogenic properties as they can activate proangiogenic factors such as VEGF, and angiopoietin (Folgueras et al., 2004). These phytochemicals were also observed to regulate the MAPK/ERK pathway, which plays a crucial role in cell proliferation (Chen et al., 2019).

In vitro studies conducted with epigallocatechin-3-gallate, berberine, gypenosides, phenethyl isothiocyanate, resveratrol, tricetin, nobiletin, evodiamine, salvianolic acid A, gallic acid, pimosylvin, and extracts of *Eclipta prostrata*, *Physalis angulata*, *Selaginella tamariscina*, *Leucaena leucocephala*, *Duchesnea indica*, rasberries (*Rubus idaeus*), and *Galium verum* downregulated the expression of MMPs (Thomas et al., 1999; Ho et al., 2007; Ho et al., 2009; Hseu et al., 2011; Lu et al., 2011; Chen et al., 2013; Chien et al., 2015; Lin et al., 2015; Peng et al., 2015; Chung HH. et al., 2017; Chung TT. et al., 2017; Huang et al., 2017; Pang et al., 2017; Fang et al., 2018; Liao et al., 2018; Chen et al., 2019; Yang et al., 2019). The increase in MMPs is generally associated with invasive and metastatic phenotype of oral carcinoma (Thomas et al., 1999). Tissue inhibitor of metalloproteinases (TIMPs) are endogenous inhibitors of MMPs, and play a role in cell migration and wound healing. TIMPs were found to be up-regulated in phenethyl isothiocyanate, nobiletin, gallic acid, *Physalis angulata*, *Selaginella tamariscina*, and *Galium verum* (Chen et al., 2013; Hsin et al., 2013; Chien et al., 2015; Yu et al., 2016; Pang et al., 2017).

Berberine, phenethyl isothiocyanate, resveratrol, gypenosides, lycopene, evodiamine, gallic acid, nobiletin, tricetin salvianolic acid A, pinosylvin, and extracts of *Eclipta prostrata*, *Selaginella tamariscina*, *Leucaena leucocephala*, *Duchesnea indica*, and *Rubus idaeus* inhibited the MAPK/ERK pathway (Ho et al., 2009; Hseu et al., 2011; Chen et al., 2013; Hsin et al., 2013; Schmidt et al., 2014; Chien et al., 2015; Ye et al., 2016; Yu et al., 2016; Chung HH. et al., 2017; Huang et al., 2017; Pang et al., 2017; Fang et al., 2018; Yang et al., 2019). Additionally, genistein, triptolide, and *Physalis angulata* extract downregulated VEGF expression (Myoung et al., 2003; Hseu et al., 2011; Zhang et al., 2016).

In vivo studies with nobiletin on male BALB/c nude mice suppressed tumor formation and metastasis by downregulating NF-κB translocation, MMP-2, and TIMP-2 proteins, and decreased phosphorylation of ERK1/2 (Chien et al., 2015). *Toona sinensis* crude extract decreased the incidences of SCCs, tumor number, tumor volume, and tumor burden in male Syrian golden hamsters by downregulating protein levels of survivin, XIAP, PCNA, iNOS, and COX-2 (Wang et al., 2016). Delayed tumor initiation incidence was reported in bitter melon extract–fed mice (Sur et al., 2018). Oral lesion incidence decreased in 4NQO exposed mice after being fed a black raspberry diet by downregulating PKA-AMPK pathway genes, which regulates mitochondrial functions (Knobloch et al., 2019).

Most of the reported clinical trials focusing on chemoprevention in HNC have been conducted on oral premalignant lesions (**Table 7**). Historically, clinical studies conducted on HNC chemoprevention with natural agents have centered on the use of retinoid. Bichler et al. (1983) reported that serum levels of retinol, RBP, and PACB were significantly lower in patients with carcinomas of the HN region (Bichler et al., 1983). This was considered to be of significance in tumor development studies, and since then, it has been corroborated by various research groups such as by Kapil et al. (2003). One of the initial studies conducted with retinoids was by Hong et al., 1986. The double-blind study demonstrated the effectiveness of 13-cRA in reducing the size of oral premalignant lesions in 44 patients. In a study conducted by Stich et al. (1988a) on 65 patients having well-developed oral leukoplakia, a complete remission in the lesions was observed in 57.1% of patients in the vitamin A group as compared to 3% of patients in the placebo group (Stich et al., 1988a). An interesting study was also conducted by Mathew et al., (1995) using lyophilized *Spirulina fusiformis*, an effective source of dietary vitamin A and other micronutrients (Mathew et al., 1995). A 1 g/day dose of oral *Spirulina fusiformis* powder demonstrated an effective chemoprevention activity by producing a complete response in 20/44 subjects in the treatment group as compared to 3/43 subjects in the placebo group. A partial response was observed in five patients in the *Spirulina fusiformis* treatment group as compared to zero in the placebo group.

A study by Stich et al. (1988b) reported on the combined effect of beta-carotene and vitamin A on betel quid chewers in India with well-established leukoplakias. Remission in the group receiving combined treatment was 27.5% as compared to 14.8 and 3% in groups receiving just beta-carotene and the placebo, respectively. The rate of new leukoplakia occurrence was also found to be higher in the beta-carotene (14.8%) and placebo groups (21.2%) that that of new leukoplakia occurrence in the group treated with both beta-carotene and vitamin A (7.8%) (Stich et al., 1988a). The effectiveness of beta-carotene as a chemopreventive agent was also established by Garewal et al., (1990), who in study with 25 patients achieved a response rate of 71% in the group treated with 30 mg/day beta-carotene (Garewal et al., 1990). A comparative study conducted in two phases with beta-carotene and isotretinoin by Lippman et al. (1993) reported that low-dose isotretinoin therapy was significantly more active against leukoplakia than beta carotene when preceded

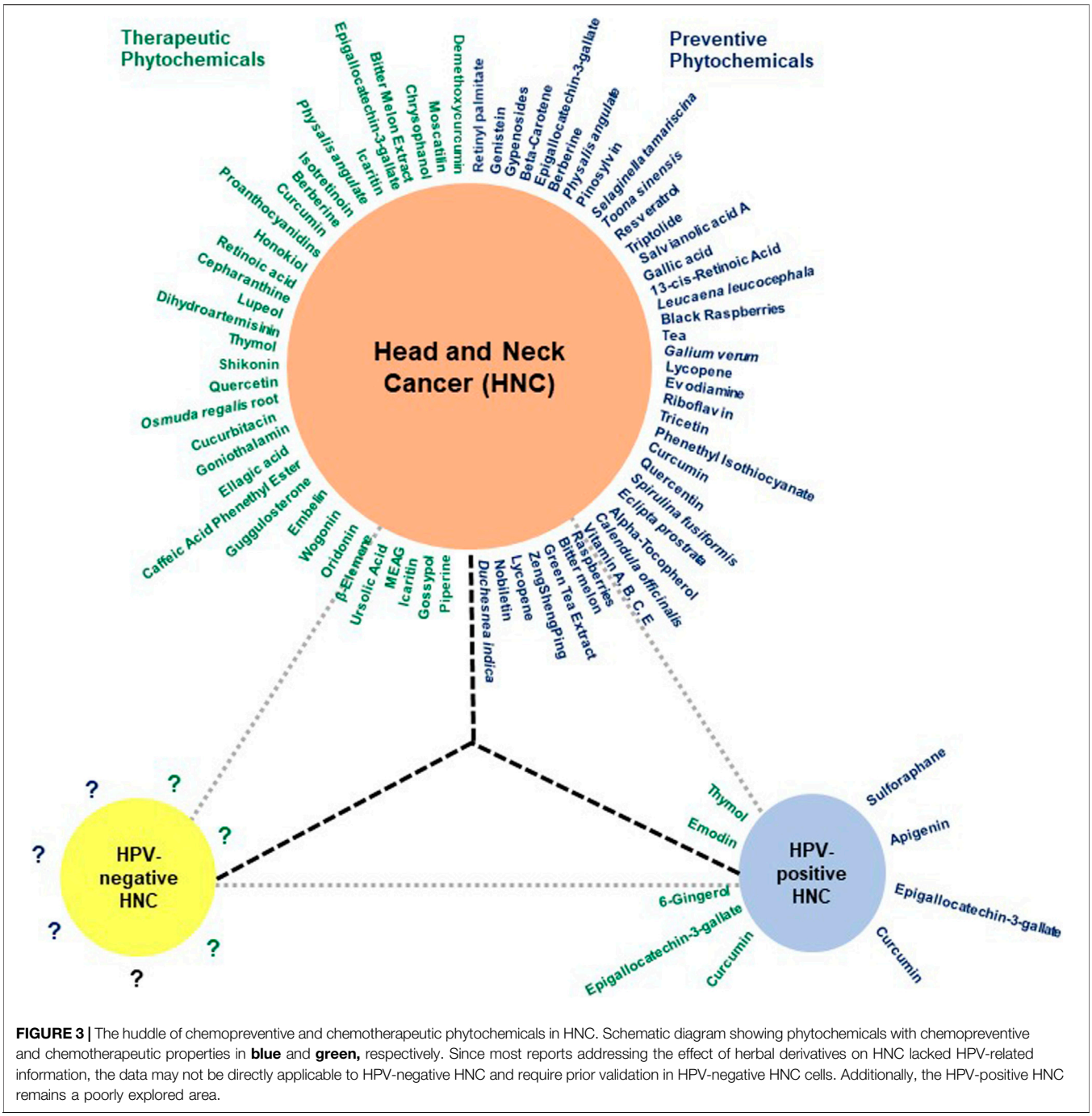

FIGURE 3 | The huddle of chemopreventive and chemotherapeutic phytochemicals in HNC. Schematic diagram showing phytochemicals with chemopreventive and chemotherapeutic properties in **blue** and **green,** respectively. Since most reports addressing the effect of herbal derivatives on HNC lacked HPV-related information, the data may not be directly applicable to HPV-negative HNC and require prior validation in HPV-negative HNC cells. Additionally, the HPV-positive HNC remains a poorly explored area.

by high-dose induction therapy (Lippman et al., 1993). In another three-arm double-blind study conducted with 160 patients by Sankaranarayana et al. (1997), the vitamin A and beta-carotene arms attained a complete regression of leukoplakia lesions in 52 and 32% of the subjects, respectively, as compared to just 10% in the placebo arm (Sankaranarayanan et al., 1997).

Two clinical studies conducted with retinyl palmitate by Jyothimayi et al. (1996) and Issing et al. (1996) reported a complete inhibition of the formation of secondary primary tumors (SPTs) and a complete remission of leukoplakia lesions in 75% of participants in drug-receiving arms, respectively (Issing et al., 1996; Jyothirmayi et al., 1996). Significant decrease in the prevalence odds ratio of oral leukoplakia was observed by Zaridze et al. (1993) in a double-blind trial conducted among 532 subjects with various combinations of riboflavin, retinol, vitamin E, and beta-carotene (Zaridze et al., 1993). Another combinatorial study with beta-carotene, ascorbic acid, and alpha-tocopherol by Kaugars et al. (1994) noted a clinical improvement in 55.7% of the participants; 48.8% of people who continued their pre-study levels of risk factor exposure showed improvement (Kaugars et al., 1994).

TABLE 5 | Clinical studies in therapeutic phytochemicals/herbal derivatives against HNC.

Phytochemical/ Herbal extract	Type of study	Study subject	Dosage, treatment duration (follow up)	Criteria (I: Inclusion/E: Exclusion)	Outcomes	Adverse effects	References
Isotretinoin	Phase II randomized trial	*n* = 40	Isotretinoin: 3 mg/kg/day	**Inclusion**	• Complete response: 1	• Moderate, consisting primarily of mucocutaneous toxicity with no life-threatening problems	Lippman et al. (1988)
		Evaluable: 38	Methotrexate: 15 mg/m^2 on days 1,2,3 of a 3 weeks cycle	• Measurable histologically confirmed locally advanced or metastatic SCCA of the head and neck	• Partial response: 1		
		Isotretinon: Methotrexate:: 19:19	For atleast 6 weeks. Evaluation: Every 3 weeks	• Karnofsky performance score of >50%	• Minor response: 1		
		Age- 42–76 years		• Life expectancy of at least 8 weeks	• Total response rate: 16%		
		Gender bias-M: F::33:5		• Adequate renal and liver function (creatinine <2.0 mg/dl and bilirubin <2.0 mg/dl)	• Median survival rate from start of treatment with isotretinoin: 4.5 months		
				• Must not have received			
				• Radiation therapy within six weeks prior to starting this trial			
				Exclusion			
				• Women with reproductive capacity			
				• Persons taking large doses of vitamin a (>25,000 IU per day)			
Retinoic acid	Phase I open trial	*n* = 15	Starting dose of 20 mg/day. Increased in increments of 20 mg 20 mg/day, 40 mg/day, 60 mg/day	**Inclusion**	• The maximum tolerated dosage in this setting for CRA was 20 mg/day	• Dose limiting toxicity: Neutropenia only; observed in 1/6 patients treated at 20 mg dose and 3/20 patients treated with 40 mg dose and 1 patient treated at 60 mg dose	Weisman et al. (1998)
		RA20:RA40: RA60::6:8:1	All 7 days prior to chemoradiation therapy with high dose cos-platinum (150 mg/m^2)	• Older than age 18	• Of 10 patients with fully evaluable data, all achieved a complete response at the primary site and 9 had a complete response in the neck	• Grade III and one had grade IV stomatitis in 6 and 1 patients respectively	

(Continued on following page)

TABLE 5 | (*Continued*) Clinical studies in therapeutic phytochemicals/herbal derivatives against HNC.

Phytochemical/ Herbal extract	Type of study	Study subject	Dosage, treatment duration (follow up)	Criteria (I: Inclusion/E: Exclusion)	Outcomes	Adverse effects	References
		Age- 40–74 years No. of patients with stage IV disease: 15 No. of patients with neck disease (N3/ N4): 12 Types of tumor- T3:T4::3:12 Fully evaluable and completed treatment: 10	Tumor responses were determined every 2 weeks and drug toxicities evaluated weekly	• Untreated, biopsyproven, squamous cell carcinoma of the upper digestive tract • No evidence of distant metastases **Exclusion** Patients with another malignancy diagnosed within 5 years of the head and neck malignancy	• Pretreatment with retinoic acid results in stronger synergy than concurrent drug exposure alone	• Thrombocytopeniamild dry mouth and mild dry skin	

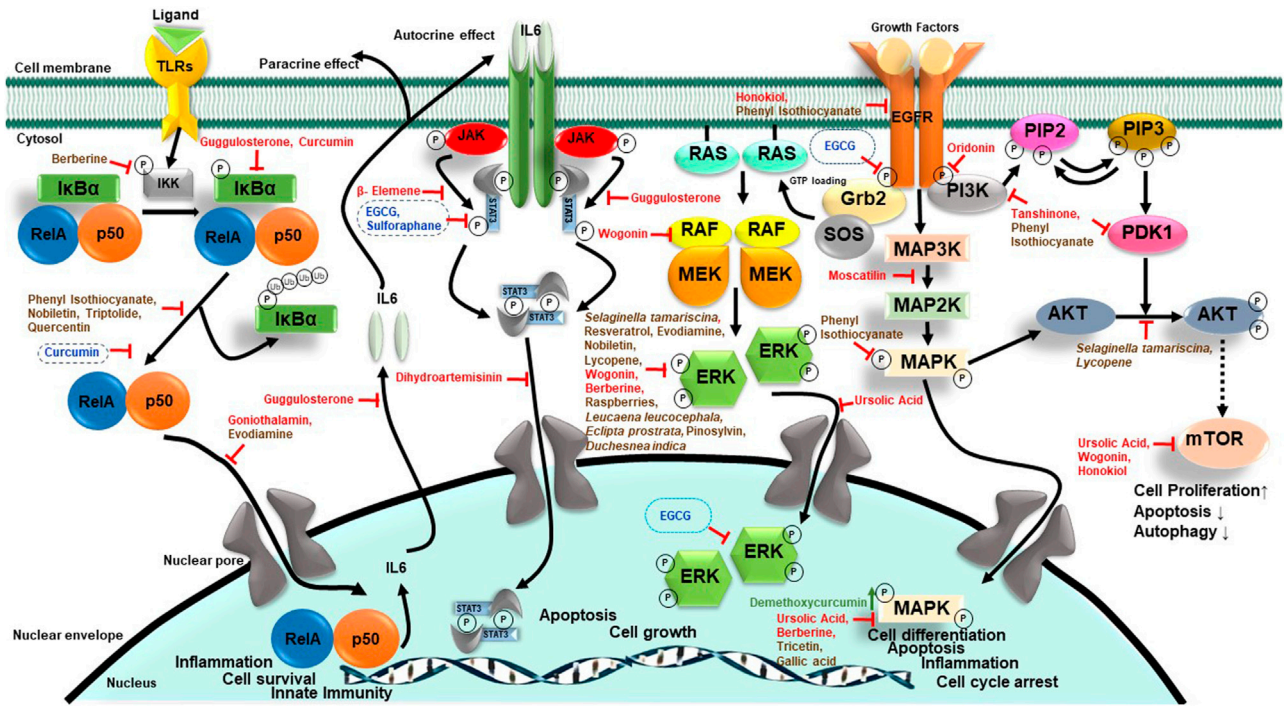

FIGURE 4 | Effect of phytochemicals on different oncogenic signaling pathways of HNC. Summarized here are chemotherapeutic (**red**) and chemopreventive (**brown**) phytochemicals that target different signaling pathways along with specific phytochemicals (**blue**) demonstrating anti-HPV activity in HPV-positive HNC.

TABLE 6 | Pre-clinical studies in emerging chemopreventive phytochemicals/herbal derivatives against HNC.

Bioactive compound/Herbal derivative PubChem CID (class) source	Cell type/Model	Test and dosage	Anti-tumor outcome	Molecular outcome	References
Genistein CID-5280961 (Phenolic)	*In vitro study:*HSC-3 OSCC) *In vivo* study: Female BALB/c nude mice	*In vitro* invasion assay: 27.3 μg/ml for 24 h *In vivo* assay: 0.5 mg/kg daily	• Invasion↓ • Gelatinolytic activity↓	• VEGF mRNA↓	Myoung et al. (2003)
Epigallocatechin-3-gallate CID-65064 (Phenolic) *Camellia sinensis*	*In vitro:* OC2 (OSCC)	Invasion and migration assays: >40 μM	• No cytotoxic effect • Migration↓	• MMP-2↓, MMP-9↓, and uPA↓	Ho et al. (2007)
Berberine CID-2,353 (Phenolic) *Berberis vulgaris*	*In vitro:* SCC-4 (tongue OSCC)	Wound-healing assay: 125 μM for 48 h	• Cell migration and invasiveness ↓	• MMP-2↓, MMP-9↓, u-PA↓, FAK↓, p-p38↓, *p*-JNK↓, *p*-ERK↓, IKK↓, NF-κB↓	Ho et al. (2009)
Gypenosides (Terpene) Gynostemma pentaphyllum Makino	*In vitro:* SAS (tongue OSCC)	Wound-healing assay: 180 μM for 48 h	• Cell migration and invasiveness ↓	• NF-κB↓, COX-2↓, ERK1/2↓, MMP-9↓, MMP-2↓, SOS↓, Ras↓, uPA↓, FAK↓, Akt↓ • mRNA levels of MMP-2↓, MMP-7↓, MMP-9↓	Lu et al. (2011)
Physalis angulate (crude extract)	*In vitro:* HSC-3 (OSCC), huvec (human umbilical vein endothelial cells) *In vivo:* Fertilized chick embryos	Wound-healing assay and Trans well assay: ~5, 10 μg/ml for 12, 24 h respectively CAM assay: 10–20 μg/ml for 48 h	• Cell migration and invasiveness ↓ • *In-vivo* angiogenesis ↓	• MMP-9 ↓, MMP-2 ↓ and u-PA ↓ • TIMP-1 ↑, TIMP-2↑, PAI-1 ↑ and PAI-2 ↑ • VEGF ↓	Hseu et al. (2011)
Selaginella tamariscina (crude extract)	*In vitro* study:HSC-3 (tongue OSCC)	Scratch-wound assay: ~75, 50 μg/ml for 12 and 24 h, respectively	• Cell motility ↓ • Cell migration and invasiveness ↓	• MMP-2 ↓, MMP-9 ↓ • TIMP-1 ↑, TIMP-2 ↑ • MMP-9 promoter activity ↓ • Binding of CREB, SP-1 and AP-1 to the MMP-2 promoter ↓ • Akt phosphorylation ↓	Yang et al. (2013)
Selaginella tamariscina (crude extract)	*In vitro:* HONE-1 (NPSCC)	Scratch-wound assay: >25*μg/mL for 24 h	• Cell motility ↓ • Cell migration and invasiveness ↓	• MMP-9 ↓ • FAK-src phosphorylation ↓ • ERK1/2 phosphorylation ↓	Hsin et al. (2013)
Phenethyl isothiocyanate CID-16741 (Alkaloid) *Brassica oleracea var. italica*	*In vitro:* SAS (tongue OSCC)	Matrigel invasion assay: 0.5, 1, 2 μM for 48 h	• EGF-stimulated invasion↓ • No effect on cell viability	• MMP-2↓, MMP-9↓ • TIMP-1↑, TIMP-2↑ • Activation of EGFR↓ • PDK1↓, P13K (P85) ↓, AKT↓, NF-κB↓, MMP-1↓, MMP-2↓ • Phosphorylation of p38↑, JNK↑, ERk↑, MAPK signaling pathway↑	Chen et al. (2013)
Galium verum (crude extract)	*In vitro:* FADU (hypopharyngeal SCC), HLaC78 (LSCC), MK (mucosal keratinocytes)	*In vitro* motility assays: Sub-lethal doses of 33.3 μL/ml	• Cell growth ↓ • Cell migration and invasiveness ↓	• MMP-9 ↑, TIMP-1 ↑	Schmidt et al. (2014)
Resveratrol CID-445154 (Phenolic) *Arachis hypogaea*	*In vitro* study*:* SCC-9 (tongue OSCC)	Wound-healing assay: >25 μM for 24 h	• No cytotoxicity • Cell motility↓ • Cell migration and invasiveness ↓	• MMP9↓ • Phosphorylation of ERK and JNK↓ • MAPK activation↓	Lin et al. (2015)
Evodiamine CID-442088 (Alkaloid) *Tetradium* spp.	*In vitro:* HONE1, CNE1 (NPSCC)	Wound-healing assay: ~25 μM for 24 h	• Cell migration and invasiveness ↓	• mRNA and protein of MMP-2↓ • Translocation of NF-κB (p65)↓ • MMP-2↓ • Phosphorylation ERK1/2↓	Peng et al. (2015)
Nobiletin CID-72344 (Phenolic) *Citrus reticulata*	*In vitro:* HONE-1, NPC-BM (NPSCC) *In vivo:* Male BALB/c nude mice	*In vitro* wound closure: 40 μM for 24 and 48 h	• Cell migration and invasiveness ↓ • *In vivo* tumor formation and metastasis↓	• MMP-2↓, TIMP-2↑ • NF-κB and AP-1 signaling pathways↓ • Phosphorylation of ERK1/2↓—	Chien et al. (2015)
Lycopene CID-394156 (Terpenes) *Daucus carota subsp. Sativus*	*In vitro:* FaDu (hypopharyngeal SCC), Cal-27 (tongue OSCC)	Colony formation: 25 μM for 24, 48 and 72 h	• Cell proliferation↓, colony formation↓ • Cell invasion↓	• Bcl-2↓, Bax↓, caspase-3↓, cleaved caspase-9↓ • Phosphorylation of AKT↓, ERK↓ • PI3K/AKT, MAPK pathways↓	Ye et al. (2016)
Toona sinensis (crude extract) *Toona sinensis*	*In vivo:* Male syrian golden hamsters	***In vivo*** treatment: 1 g/kg body weight for 4 weeks	• Incidence of SCC↓, epithelial dysplasia↓ • Tumor number↓, tumor volume↓, tumor burden↓, severe dysplastic lesions↓ • Apoptosis↑	• Proteins of survivin↓, XIAP↓, PCNA↓, iNOS↓, and COX-2 ↓	Wang et al. (2016)
Triptolide CID-107985 (Terpene) *Tripterygium wilfordii*	*In vitro:* CNEn (NPSCC) *In vivo:* BalB/C nude mice female	Cell clonogenicity: 4 ng/ml with IR at 0, 2, 4 and 8 Gy *In vivo* treatment: 0.075 mg/kg per day	• Cell growth↓, colony number↓ • ionizing radiation↑ induces apoptosis • Anti-angiogenesis effects	• Bax↑ • Proteins phosph-NF-κb p65↓, Bcl-2↓ and VEGF↓	Zhang et al. (2016)
Raspberries (crude extract) *Rubus idaeus*	*In-vitro* study*:* SCC-9, SAS (tongue OSCC)	Scratch-wound assay: ~100 μg/ml for 48 h	• No cell viability effect • Cell migration and invasiveness ↓ • Metastasis ↓	• MMP-2 mRNA↓, protein level ↓ and enzyme activity↓ • FAK-src phosphorylation ↓ • ERK1/2 phosphorylation ↓	Huang et al. (2017)
Tricetin CID-5281701 (Phenolic) *Eucalyptus globulus*	*In vitro:* SCC-9, HSC-3 (tongue OSCC), OECM-1 (OSCC)	Boyden chamber assays: >20 μM in 24 h	• Cell migration and invasiveness ↓	• MMP9 enzyme activity↓, MMP9 mRNA expression↓ • Regulated MAPK signaling pathway by *p*-JNK1/2↓ and p-p38↓ • p38/jnk-MMP9 axis signaling ↓	Chung et al. (2017b)
Raspberries (crude extract) *Rubus idaeus*	*In-vitro* study: HONE-1, NPC-39 and NPC-BM (NPSCC)	Wound-healing assay: 100 μg/ml for 12 and 24 h	• Tumor cell migration ↓ • Invasive ability ↓	• MMP-2 mRNA↓, protein level ↓ and enzyme activity↓ • ERK1/2 phosphorylation ↓ • Inhibits MAPK signaling pathway	Hsin et al. (2017)

(Continued on following page)

TABLE 6 | (*Continued*) Pre-clinical studies in emerging chemopreventive phytochemicals/herbal derivatives against HNC.

Bioactive compound/Herbal derivative PubChem CID (class) source	Cell type/Model	Test and dosage	Anti-tumor outcome	Molecular outcome	References
Quercentin CID-4444051 (Phenolic) *Allium cepa*	*In vivo:* Male syrian hamsters	*In vivo* treatment: 50 mg/kg for 14 weeks	• DMBA induced carcinogenesis and apoptosis↓ • Tumor incidence↓	• NF-Kb p50↓, p65↓ • DBMA induced Bcl-2↓, Bax↓	Zhang et al. (2017)
Leucaena leucocephala (crude extract)	*In-vitro* study: SCC-9, SAS (tongue OSCC)	Scratch-wound assay: ~20 µg/ml for 6–48 h	• Cell motility ↓ • Cell migration and invasiveness ↓ • Anti-metastatic activity	• MMP-2 ↓ • ERK and p38 phosphorylation ↓	Chung et al. (2017a)
Gallic acid CID-370 *Hamamelidaceae* spp.	*In vitro:* NPC-BM1 (NPSCC)	*In Vitro* matrix invasion: 25 µM in 24 h	• Invasion↓	• mRNA expression and transcription of MMP-1↓ • MMP-1 promoter↓, AP-1↓ and ETS-1↓, TIMP-1↓ • p38 MAPK pathway ↓	Pang et al. (2017)
Salvianolic acid A CID-5281793 (Phenolic) *Salvia miltiorrhiza*	*In vitro:* SCC-9, SCC-25 (tongue OSCC)	Wound healing migration assay: 50 µM for 24, 48 h	• Cell migration and invasiveness ↓ • Anti-metastatic	• MMP-2↓, p-c-Raf↓, *p*-MEK1/2↓, *p*-ERK1/2↓ protein	Fang et al. (2018)
Bitter melon (crude extract) *Momordica charantia*	*In vivo:* C57BL/6 mice	*In vivo* treatment: 4-NQO- 50 µg/ml; BME- 30% v/v, 600 mg/mouse	• No histological abnormality • Delayed tumor initiation • Incidence of tongue tumor↓	• PCNA↓ • GO categories "Keratin filament"↓,"extracellular region"↓, "GTP binding"↓, "extracellular space"↑, "cytokine activity"↑, "immune response"↑, "positive apoptotic process"↑	Sur et al. (2018)
Eclipta prostrata (crude extract) *Eclipta prostrata*	*In vitro:* SCC-9, HSC-3, (tongue OSCC) TW2.6 (OSCC)	Boyden chamber assay: ~100 µg/ml for 24 h	• Cell migration and invasiveness ↓ • Oral cancer metastasis↓	• MMP-2↓ • Phosphorylated ERK1/2↓	Liao et al. (2018)
Black raspberries (crude extract) *Rubus occidentalis*	*In vivo:* Male F344 mice	*In vivo* treatment: 4-NQO- 20 µg/ml BRB- 5 and 10% w/w for 6 weeks	• Oral lesion incidence and multiplicity↓	• Aldoa↓, Hk2↓, Tpi1↓, Pgam2↓, Pfkl↓, Pkm2↓ • PKA-AMPK pathway genes↓	Knobloch et al. (2019)
Pinosylvin CID-5280457 (Phenolic) *Gnetum cleistostachyum*	*In vitro:* SAS, SCC-9, HSC-3 (tongue OSCC)	*In vitro* wound closure: ~20 µM for 2 h	• Cell migration↓	• Enzymatic activity and protein level of MMP-2↓ • TIMP-2↑, phosphorylation of ERK1/2↓	Chen et al. (2019)
Duchesnea indica (crude extract)	*In vitro* study: SCC-9, SCC-14 (tongue OSCC) and TW2.6 (OSCC)	Wound-healing assay: ~20, 40 µg/ml for 24, 48 h, respectively	• Cell motility ↓ • Cell migration and invasiveness ↓ • MAPK/ERK signaling pathway ↓	• MMP-2 ↓ • ERK1/2 phosphorylation ↓ • FAK Y397, src, c-raf, and MEK1/2 phosphorylation ↓	Yang et al. (2019)

Abbreviations: 4-NQO: 4-Nitroquinoline 1-oxide; Akt: Protein kinase B; AMPK: AMP-activated protein kinase; AP-1: Activator protein 1; Bax: Bcl-2-associated X protein; Bcl-2: B-cell lymphoma 2; COX-2: Cyclooxygenase-2; c-Raf: c- Rapidly Accelerated Fibrosarcoma; CREB: cAMP response element-binding protein; DMBA: 7,12-dimethylbenz(a)anthracene; ERK: Extracellular-signal-regulated kinase; FAK-Src: Focal adhesion kinase-Steroid receptor coactivator; GO: Gene ontology; HK2: hexokinase 2; IKK: Inhibitor of nuclear factor-κB (IκB) kinase; iNOS: Inducible nitric oxide synthase; JNK: c-Jun N-terminal kinase; LC3: Microtubule-associated protein 1A/1B-light chain three; LSCC: Laryngeal squamous cell carcinoma; MAPK: Mitogen-activated protein kinase; MMP: Matrix metallopeptidase; mTOR: mammalian target of rapamycin; NF-κB: Nuclear factor kappa light chain enhancer of activated B cells; NPSCC: Nasopharyngeal squamous cell carcinoma; OSCC: Oral squamous cell carcinoma; PI3K: Phosphatidylinositol 3-kinase; PAI-1: Plasminogen activator inhibitor-1; PCNA: Proliferating cell nuclear antigen; PDK1: 3-Phosphoinositide-dependent kinase 1; PFK1: Phosphofructokinase-1; PGAM2: Phosphoglycerate mutase 2; PKA: Adiponectin activates protein kinase A; PKM2: Pyruvate kinase M2; MEK: Mitogen-activated protein kinase; SCC: Squamous cell carcinoma; SP-1: Specificity protein 1; TIMP-1: Tissue inhibitor of metallopeptidase inhibitor 1; Tpi1: Triosephosphate isomerase; u-PA: urokinase-type plasminogen activator; XIAP: X-linked inhibitor of apoptosis protein.

A 24-week study by Benner et al. (1993) using alpha-tocopherol as a single agent to treat patients with oral leukoplakia attained a clinical response in 20 patients from the 43 patients who had signed up for it (Benner et al., 1993). Alpha-tocopherol was part of yet another study by Shin et al. (2001), when delivered with IFN-α and 13-cis-retinoic acid; among 44 patients evaluable at a median 24-month follow-up, 9% had locoregional recurrence, 5% had both locoregional recurrence and distant metastases, and 2% developed an SPT. The overall survival rate at the 24-month follow-up was noted to be 91% (Shin et al., 2001).

Green tea, a widely consumed beverage, has been previously reported to exhibit chemopreventive properties against cancer (Imai et al., 1997). Since it inhibits tumor development, is nontoxic, and is easily available to the general population, it has been a subject of interest in cancer studies. Two clinical studies where green tea was used as an agent to treat precancerous lesions like leukoplakia were included. Li et al. (1999) reported a decrease in lesions in 37.9% patients in the tea-receiving arm as compared to improvement in lesions of only 10% patients in the placebo arm (Li et al., 1999). Tsao et al. (2009) reported a dose-dependent clinical response by randomizing 41 patients in three green tea extract–receiving arms (dosage: 500 mg/m^2, 750 mg/m^2, 1,000 mg/m^2) and 1 placebo arm, with a clinical response in 50% of patients in the three combined arms and a 58% clinical response rate in the two combined higher dose arms (Tsao et al., 2009). They also reported a histological improvement in lesions after treatment.

Lycopene is a carotenoid that is abundant in a human diet and has been associated with a reduced risk of cancer of the upper digestive tract (De Stefani et al., 2000). Singh et al. (2004) reported a dose-dependent response of oral leukoplakia for administration of lycopene, with clinical improvement observed in 80% of patients receiving 8 mg/day lycopene; 66.3% patients receiving 4 mg/day dose showed a clinical response (Singh et al., 2004). A clinical study with lycopene and *Calendula officinalis* by Singh and Bagewadi (2017) reported a reduction in the average size of lesions posttreatment. The mean difference in the reduction in size before and after treatment for Group I was 2% ± 1.0 cm, while for the Group II, it was 1.6% ± 0.9 cm (Singh and Bagewadi, 2017).

Curcumin, a flavonoid derived from *Curcuma longa*, has been extensively investigated for its pharmacological properties. It is known to have antioxidant, anti-inflammatory, and anticancer properties, and thus is a promising phytochemical for HN region chemoprevention. A randomized double-blind phase IIB study by Kuriakose et al. (2016) on 223 patients with oral leukoplakia reported a clinical response in 67.5% of patients in the curcumin arm (dosage: 3.6 g/day for 6 months) and a histological response in 22.5% of patients (Kuriakose et al., 2016).

Sun et al. (2010) conducted a randomized placebo-controlled study with ZengShengPing; a mixture of six medicinal herbs was known to have pharmacological effects. 3.6 g of ZSP administered daily for 8–12 months was observed to produce a positive response in 67.8% of patients in the treatment arm as compared to 17% in the placebo group (Sun et al., 2010).

Mallery et al. (2014) conducted a placebo-controlled clinical trial using topically applied 10% w/w black raspberry (BRB) gel among 40 patients with oral premalignant lesions. The study reported an average decrease of 26% in the size of BRB-treated lesions as compared to an increase in size by 18% in the placebo gel–applied lesions. Two patients in the BRB arm exhibited a complete lesional resolution as compared to zero in the placebo gel group (Mallery et al., 2014).

Although a large volume of data reflects targeting of key pro-carcinogenic signaling pathways by various phytochemicals, none of them directly address their possible impact on HPV infection or in HPV-positive HNC lesions. Therefore, we specifically looked for evidences where phytochemicals have been tested against HNC cells with HPV-positive background.

Chemotherapeutic and Chemopreventive Phytochemicals/Herbal Derivative With Anti-Cancer and/or Anti-Human Papillomavirus Activity in Head and Neck Cancer

Most of the studies described earlier lack specificity against HPV infection. The natural derivatives having both anti-HPV and anti-HNC activity hold great potential as chemotherapeutic and chemopreventive agents for HNC caused by HPV. However, there are only limited resources in terms of HPV-related HNC model systems. Unlike many other infections, HPV cannot be propagated in *in vitro* cultures or in animal models. Unfortunately, suitable animal models that mimic HPV-driven HNC do not exist. In such a scenario, HPV-positive HNSCC cell lines serve as a suitable *in vitro* system. There are currently only a limited set of HPV-driven HN cancer cell lines developed by different investigators (**Table 8**). As of now, we could identify only 11 cell lines that have been described as HPV positive, and their HPV genotype has been confirmed. A majority of them have HPV16 positivity, and the genome was found to be integrated (Steenbergen et al., 1995; Ballo et al., 1999; White et al., 2007; Brenner et al., 2010; Ye et al., 2011; Tang et al., 2012; Kalu et al., 2017). Similarly, one cell line each of HPV18 and HPV33 has been reported (Owen et al., 2016; Kalu et al., 2017). Although there are various HNSCC cell lines described so far, their HPV status must be ascertained. These cells lines proved to be useful model systems as they showed p16 positivity and demonstrated higher radiosensitivity (Rieckmann et al., 2013). In these cell line integration of HPV from E1, E2, L1, L2, and LCR have been observed which recapitulate observation in primary tumors by whole genome sequence which suggests various hotspots for HPV integration events in HPV-positive tumors and that may play varied role in the development of HNC (Gao et al., 2019). These cell lines and tumor tissues showed the presence of the viral infection by the presence of viral DNA and transcripts which emerged as valuable tools (Steenbergen et al., 1995; Ballo et al., 1999; White et al., 2007; Brenner et al., 2010; Ye et al., 2011; Tang et al., 2012; Kalu et al., 2017).

A limited set of studies have been conducted to examine anti-HPV and anticancer activities in HNC (**Table 9**). The evidence suggests that HPV-positive cells can serve as suitable tools for screening of anti-HPV and anti-HNC. Green tea polyphenol (-)-epigallocatechin-3-gallate (EGCG), a green tea derivative, exhibits various chemopreventive effects, including inhibition

TABLE 7 | Clinical studies in chemopreventive phytochemicals/herbal derivatives against HNC.

Phyto-chemical/herbal extract/	Type of study	Study participants	Dosage, treatment duration, and follow-up	Criteria (inclusion/exclusion)	Clinical outcome	Adverse effects reported	Ref
13-cis-Retinoic acid	Randomized double-blind trial	• *n* = 44 • Retinoic acid Placebo::24:20 • Age- <50: 6 50-69: 29 > 70: 6 • Gender M:F::31:13 Risk factors: o Alcohol and tobacco: 20/44 o Alcohol only: 11/44 o Tobacco only: 9/44 o Neither: 4/44	1–2 mg/(kg of body weight)/day (oral) 3 months (6 months) Evaluation: every 2–3 weeks (4–6 weeks)	Inclusion • Patients with histologically confirmed oral premalignant lesions Exclusion • Fertile women • People taking >25,000 USP/day units of vitamin A • People diagnosed with oral cancer 2 years before the study	• decrease in size of lesions in 67% of drug recipients as compared to 10% in placebo recipients Histologic response in 56% of drug recipients with clinical response • Dysplasia reversed in 54% of the drug recipients as compared to 10% of placebo recipients • Histological improvement in 50% of drug recipients	• Toxic effects acceptable except in 2 cases • Cheilitis, facial erythema, peeling of the skin in 79% drug recipients • Conjunctivitis in 54% • Hypertriglyceridemia in 71%	Hong et al. (1986)
Vitamin A	Randomized double-blind Trial	• *n* = 65 Vitamin A:Placebo::30:35 • Completed study = 54 Vitamin A: Placebo::21:33 Risk factors: o Betel quid chewing and alcohol drinking: 37% o Chewing, drinking and smoking of bidis:28% o Chewing and smoking of bidis: 2% • Betel quid chewing without any additional oral habit: 16%	200,000IU of vitamin A/week administered in the form of capsules administered twice weekly (0.14 mg/kg body weight per day) Duration of trial- 6 months Evaluation Every 3 months	Inclusion Betel quid chewers with well-established leukoplakias	• Complete remission in 57% in VitA as compared to 3% in placebo • No new leukoplakias in all chewers receiving vitamin A, as compared to 21% in the placebo • Number of layers of spinous cells decreased in 85% • Loss of polarity of basal cells was reduced from 72 to 22% • Subepidermal lymphocytic infiltration diminished from 66.7 to 5.5% • Nuclei with condensed chromatin disappeared from the epidermal layer (72.2% before to 0% at the trial end)	• No adverse effects	Stich et al. (1988a)
Beta-carotene and beta-carotene plus vitamin A	Randomized double-blind Trial	• *n* = 130 Three groups receiving: o Beta-carotene: Group I, 35 people o Beta-carotene and vitamin A: Group II, 60 people o Placebo-group III, 35 people • Completed study: Groups I, II, III are: 30, 54, 26 • Age: 48.8 ± 12.9 Risk factors: o Betel quid chewing and alcohol drinking: 37% o Chewing, drinking and smoking of bidis: 28% o Chewing and smoking of bidis: 2% • Betel quid chewing without any additional oral habit: 16%	Group I: 180 mg beta-carotene/week Group II: 180 mg beta-carotene + 100,000 IU vitamin A/week Group III: Placebo For 6 months	Inclusion Betel quid chewers with well-established leukoplakias	Frequency (%) of micronucleated cells was reduced in leukoplakia of betel quid chewers % micronucleated cells placebo, leukoplakia o Before: 3.69 ± 1.22 o After: 4.00 ± 1.32 • % micronucleated cells beta carotrene, leukoplakia o Before: 4.09 ± 1.10 o After: 1.18 ± 0.77 % micronucleated cells beta-carotene + vitamin A, leukoplakia o Before: 4.01 ± 1.05 o After: 1.16 ± 0.94 • Well-established leukoplakias regressed. Remission of leukoplakias in o Group I: 14.8% o Group II: 27.5% o Group III: 3% • The development of new leukoplakias was inhibited new leukoplakia occurrence: o Group I: 14.8% o Group II: 7.8% o Group III: 21.2%	• No adverse effects	Stich et al. (1988b)
Beta-carotene		• *n* = 25 • completed study = 24 • Gender Bias- M:F::21:3 • Age (years) o < 50: 9 o 50-69: 9 o > 70: 6 Risk factors o Alcohol and tobacco: 9	30 mg/day for 3 months Responding patients: 3 more months (rest were taken off the therapy) Evaluation: 2–3 months intervals	Inclusion • Adult patients diagnosed as having clinically measurable oral leukoplakia while undergoing routine dental examinations Exclusion Patients taking high daily doses of vitamin A	• 17 had major responses (two complete, 15 partial), a response rate of 71% • Relapses after discontinuation of treatment: 8/11 responders within 3 months of cessation of drug	• No significant toxicity attributable to beta-carotene was encountered in this trial	Garewal et al. (1990)

(Continued on following page)

TABLE 7 | (*Continued*) Clinical studies in chemopreventive phytochemicals/herbal derivatives against HNC.

Phyto-chemical/herbal extract/	Type of study	Study participants	Dosage, treatment duration, and follow-up	Criteria (inclusion/exclusion)	Clinical outcome	Adverse effects reported	Ref
		o Alcohol only: 7 o Tobacco only: 4					
Isotretinoin	Randomized placebo-controlled study	• *n* = 103 • Completed study = 100 • Drug:Placebo::49:51 • Gender bias: M:F::78:32 • Age- 31–73 years Risk factors – • Smoker: o Current:Former::33:57 • Alcohol o Yes:No::55:45	50–100 mg per square meter of body-surface area per day For 12 months and follow-up for 32 months Evaluation: Monthly during treatment and once in three months during follow-up	Inclusion • Clinically free of disease after having undergone surgery or radiation therapy (or both) for histologically confirmed primary OSCC, OPSCC, HPSCC, or LSCC Exclusion • Abnormal renal or hepatic function • Distant metastasis or a Karnofsky performance score <60% • Previous chemotherapy, within the 2 years • A diagnosis of any cancer except *in situ* or T1 HNSCC or skin cancer other than melanoma • Women of reproductive capacity • Patients taking large doses of vitamin a (>25,000 USP units per day)	• No significant differences between the two groups in the number of local, regional, or distant recurrences of the primary cancers • The isotretinoin group had significantly fewer second primary tumors • Only 2 patients (4 percent) in the isotretinoin group had second primary tumors, as compared with 12 (24%) in the placebo group • Multiple second primary tumors occurred in four patients, all of whom were in the placebo group	• Mild or moderate • Severe skin dryness, cheilitis, hypertriglyceridemia, and conjunctivitis, occurred in 12, 2, 6, and 8%, respectively, of isotretinoin recipients	Hong et al. (1990)
Alpha-tocopherol	A single-arm phase II study	• n = 43 • Gender bias- M:F::24:19 • Mean age: 55.6 years Tobacco use o Current: 48.8% o Past: 30.3% o Never 20.9% • Alcohol use o Current: 55.8% o Past: 18.6% • Never: 25.6%	400 IU twice daily for 24 weeks Evaluation: At 6, 12, and 24 weeks	Inclusion Patients with bi-dimensionally measurable symptomatic leukoplakia (i.e., lesions associated with discomfort such as burning or pain) or leukoplakia with dysplasia	• Clinical response (complete or partial) in 20/43 patients was observed • Histological response was observable in 9 patients	• No grade 3 or 4 toxic effects were reported • Observed side effects were grade 1: *Vertigo*, extremity aches, nausea, diarrhea, intestinal cramps, breast enlargement, fatigue, and fluid retention	Benner et al. (1993)
Isotretinoin Beta-carotene	Uncontrolled open trial conducted in two phases	**Phase I** (induction therapy with high dose isotretinoin) *n* = 70 Completed/evaluated: 66 **Phase II**: (Maintenance therapy with low dose isotretinoin OR beta-carotene with patients who responded to induction therapy) *n* = 59 Completed/evaluated: 53 • Beta- Carotene:isotretinoin::33:26	**Phase I**: isotretinoin: 1.5 mg/kg body weight/day **Phase II**: Low dose isotretinoin: 0.5 mg/kg body weight/day Beta-carotene: 30 mg/day **Phase I**: 3 months **Phase II**: 9 months Evaluation: Every 4 weeks	Inclusion • Oral lesions that were histologically confirmed as pre-malignant and could be measured in two dimensions • Normal hepatic and renal functions acceptable • Acceptable fasting triglyceride levels at entry Exclusion • High current vitamin A intake (>25,000 USP units per day) • High beta-carotene intake • History of oral cancer within two years before study	**Phase I** • Partial or complete response was observed in 55% of the patients and stable disease maintained in 35% of the patients **Phase II** • Positive outcome (improved/stable lesions) was observed in 92 percent (22) patients on low dose isotretinoin therapy • 45 percent (13) patients on beta carotene therapy showed a positive response	**Phase I**: Substantial side effects. 23 patients with grade 3 or 4 toxic reactions. Dry skin, cheilitis, conjunctivitis, Triglycerdemia **Phase II:** Relatively mild, favoring the beta-carotene group. Hypertriglycerdemia, mild and reversible skin yellowing, dry skin, cheilitis, conjunctivitis	Lippman et al. (1993)
Riboflavin, retinol vitamin E, and beta-carotene	Randomized double blind trial	• *n* = 532 • Completed study 487 at 6 months 471 at 20 months • Gender bias: All men • Age: 50–69 years • 191 with leukoplakia	Riboflavin (R): 80 mg/week Retinol (VA): 100,000 IU/week Beta-carotene (BC): 40 g/day Vitamin E (VE): 80 mg/week In 4 groups with placebo (*p*) 1: *p,p,p* 2: R,*p,p* 3: *p*,VA,VE,BC 4: R,VA,VE,BC For 20 Months Evaluation: At 6th and 20th month	**Inclusion:** Only men who had a diagnosis of chronic esophagitis and/or oral leukoplakia	• Significant decrease in the prevalence odds ratio (OR) of oral leukoplakia was observed after 6 months of treatment	Nausea, vomiting, and itching	Zaridze et al. (1993)

(Continued on following page)

TABLE 7 | (*Continued*) Clinical studies in chemopreventive phytochemicals/herbal derivatives against HNC.

Phyto-chemical/herbal extract/	Type of study	Study participants	Dosage, treatment duration, and follow-up	Criteria (inclusion/exclusion)	Clinical outcome	Adverse effects reported	Ref
Beta-carotene, ascorbic acid, and alpha-tocopherol	Open Trial	• *n* = 7 • Gender bias M:F::45:34 • Age 25–85 years • Risk factors (smoking, smokeless tobacco, alcohol): 65/79 • Risk factor reduction or cessation during the course of the study: 20/65	Beta-carotene: 30 mg/day Ascorbic acid: 1,000 mg/day Alpha-tocopherol: 800 IU/day For 9 months Evaluation: At 1st, 3rd, 6th, 9th month	Inclusion • Patients with clinically apparent oral leukoplakic lesions that had been histologically verified as either hyperkeratosis or epithelial dysplasia with hyperkeratosis Exclusion: Cases that were either consistent with lichen planus or were suggestive of lichenoid change	• Clinical improvement of the oral lesion was noted in 55.7% of patients • 22 (48.8%) of 45 patients who continued their pre-study levels of risk-factor exposure had clinical improvement • 4 out of 9 patients who had never used either tobacco or alcohol showed clinical improvement	No side effects were reported	Kaugars et al. (1994)
Spirulina fusiformis (lyophilized powder)	Blind Placebo Controlled trial	• n = 115 SF:Placebo::60:55 • Completed study = 87 SF: Placebo::44:43 • Mean age: 47.1 years • Smokers-Yes:No::28:59 • Alcohol-Yes::No::52:35 • Chewers-Yes:No::84:87	Lyophilized: *Spirulina fusiformis* 1 g/da for 12 months with a 2 years follow-up evaluation: Every 2 months during supplementation	**Inclusion**: Subjects with oral leukoplakia	• 20/44 subjects in the SF group showed a complete response as compared to 3/43 subjects in the placebo group • 5 subjects in SF group showed a partial response as compared to 0 in the placebo • The CR rates were 46% (17 of 37) for lesions 2 cm in diameter • After 1 year of stopping supplementation 9 of 20 (45%) subjects with CR in the SF arm reported with recurrence of lesions • 2 years follow-up: malignant transformations were observed in 10% of subjects in the placebo group and 5% of subjects in SF group	Headache, muscular pain	Mathew et al. (1995)
Retinyl palmitate	Randomized Blind Trial	• *n* = 106 • Drug:Placebo::56:50 • Gender bias: M:F::73:33 • Completed study = 93 • RP:Placebo::50:43 Risk factors o Chewing tobacco:65 o Smoking: 61	200,000 IU per week (administered orally) for 1 year with 2 years follow-up **Evaluation:** Every 2 months during supplementation	**Inclusion** • Patients with HNC with complete clinical regression of lesions on follow-up after therapy • Have had either radical radiotherapy or surgery or both **Exclusion** • Patients with clinical evidence of disease, abnormal kidney and liver function	• No second primaries were observed in subjects in the vitamin a group • 2 subjects developed primaries (1 case of tongue cancer and 1 of floor of mouth cancer) in the placebo group	No clinically obvious side effects (dryness of the tongue in two subjects)	Jyothirmayi et al. (1996)
Retinyl palmitate	Open trial conducted in two phases	• *n* = 20 • Gender bias-M:F::17:3 • Age range: 46-80 • Risk factors: o Alcohol and tobacco: 7 o Alcohol only: 8; tobacco only: 1 • Neither: 4	**Phase I** 300,000 IU/day to 1,500,000 IU/day in patients showing resistant lesions in the fifth week **Phase II** 150,000 IU/day for patients who responded to therapy Median duration of treatment and follow-up: 18 months **Evaluation:** Every 4 weeks during study and 3 months during follow-up	Inclusion • Presence of larynx leukoplakia which could be measured in two dimensions • Normal renal and hepatic function • Acceptable fasting triglyceride levels upon entry Exclusion • Possibility of pregnancy A current intake of large doses of vitamin a (>25,000 USP units per day) or betacarotene	• Complete remission rate observed in 75% (15 of 20 patients) Partial response was observed in 5 patients. Among the 5 patients with partial response, 3 relapsed.	None of the patients had more than grade 2 reactions; grade 3 and 4 reactions or a withdrawal because of intolerable toxic effects were not observed	Issing et al. (1996)
Vitamin a and beta-carotene	Randomized double blind trial	• *n* = 160 • Completed study = 131 • Vitamin A:Beta-Carotene: Placebo::50:55:55 • Completed study: vitamin A: Beta-carotene:: 42:46:43 • Gender bias-M:F::1.79:1 • Chewing tobacco-Yes:No::127:4 • Smokers-Yes:No::41:70 • Alcohol-Yes:No::72:59	Vitamin A: 300,000 IU/week Beta-carotene:360 mg/week For 12 months and 1 year follow-up **Evaluation:** Every 2 months during supplementation	NIL	• Vitamin a group: Complete regression in 22 of 42 (52%) subjects • Beta-carotene group: 15/46 (32%) of subjects showed complete regression • Homogeneous leukoplakias and smaller lesions responded better than non-homogeneous and larger lesions • 1 year after stopping treatment: o 64% complete responders with vitamin a and 53% complete responders with beta carotene developed recurrent lesions and • 10% subjects in the placebo group and 5% in the beta carotene group developed malignancy at the site of leukoplakia	Headache, muscular pain, dry mouth	Sankaranarayanan et al. (1997)
Tea	Double-blind intervention trial	*n* = 64 Tea:Placebo::32:32 Age-23–28 years	3 g, 4:1:1 mixture of green tea, green tea polyphenols and tea pigment administered orally and applied topically	Inclusion: Patients suffering from oral leukoplakia	• 37.9% showed decrease in the lesions among 29 treated patients; 3.4% showed an increase		Li et al. (1999)

(Continued on following page)

TABLE 7 | (*Continued*) Clinical studies in chemopreventive phytochemicals/herbal derivatives against HNC.

Phyto-chemical/herbal extract/	Type of study	Study participants	Dosage, treatment duration, and follow-up	Criteria (inclusion/exclusion)	Clinical outcome	Adverse effects reported	Ref
		Gender bias-M:F::40:24 Smokers Yes:No::46:18 Evaluated/completed trial: 59			• 10% of patients in the placebo group showed an decrease in lesions; 6.7% showed an increase • Micronucleated exfoliated oral mucosa cells in treated group was lower in placebo group		
Interferon-alfa, 13- cis -retinoic acid, and alpha-tocopherol	Phase II single-arm trial	• n = 45 • Gender bias-M:F::36:9 • Age o Median: 52 years o Range: 43–70 years • Initial stage o Stage III: 11 o Stage IV: 34 • Prior treatment o Surgery: 3 o Radiotherapy:15 • Surgery and radiotherapy: 27	Dose modifications based on monthly evaluated toleration of therapy Interferon-alfa: (1-3)X106 IU/m2 subcutaneous injection, three times a week 13-cRA: 20–50 mg/m2/day Alpha-tocopherol: 1,200 IU/day For 12 months **Evaluation:** Every 3 months (monthly check ups for dose modification) Follow up: median 24 months and median 49.4 months	Inclusion • Confirmed diagnosis of squamous cell carcinoma of the oral cavity, oropharynx, larynx, or hypopharynx • Locally advanced stage III or IV disease • Enrolled a minimum of 3 weeks and maximum of 24 weeks after definitive local therapy with surgery, radiotherapy, or both • Should not have received chemotherapy, immunotherapy, or hormonal therapy before entry onto the study • Must have recovered from the acute toxic effects of surgery, radiotherapy, or both • Must be able to swallow the pills without breaking them • Life expectancy of >12 weeks • Karnofsky performance status rating of >80% • Adequate bone marrow function and adequate renal and hepatic functions **Exclusion** • If taking megadoses of vitamin a (>25,000 IU) • If they were women of child-bearing potential who were not practicing adequate birth control If they had a baseline triglyceride level > twice the normal range	At median 24-months of follow-up, the clinical end point rates were Among 45 • 9% for local/regional recurrence (four patients) • 5% for local/regional recurrence and distant metastases (two patients) • 2% for SPT (one patient), which was acute promyelocytic leukemia • Median 1- and 2-years rates of overall survival were 98 and 91%, respectively, and of disease-free survival were 91 and 84%, respectively At median 49.4-months of follow-up • 9 (20%) of 44 patients experienced progressive disease, 3 since the last report • Two patients had local recurrences • 1 had local and distant relapse. The progression-free survival percentages at 1 year, 3 years, and 5 years were 88.9, 82.2 and 80% respectively • The overall survival percentages at 1 year, 3 years, and 5 years were 97.8, 88.9 and 81.3% respectively	Mild to moderate mucocutaneous side effects, flu-like symptoms, anorexia, and weight loss, fatigue, peripheral neuropath optic neuritis, mild to moderate hypertriglyceridemia	Shin et al. (2001), Seixas-Silva et al. (2005)
ZengShengPing (*Sophra tonkinensis, Polygonum bistorta, Prunella vulgaris, Sonchus brachyotus*, *Dictamnus dasycarpus*, and *Dioscorea bulbifer*)	Randomized placebo-controlled trial	*n* = 120 Completed/evaluated = 112 ZSP:Placebo::59:53 Mean age: (ZSP:Placebo)- 52.9:44.4 Gender bias-M:F::69:43 Risk factors- smokers Yes:No::53:59 Drinkers Yes:No::10:102	3.6 g per day for 8–12 months	Inclusion • 20 patients with oral leukoplakia i.e white patch or plaque that cannot be characterized clinically or pathologically as any other disease Exclusion • Those with a previous diagnosis of head and neck or oral cancer • Those currently treated by other drugs or having drug hypersensitivity • Those requiring extensive dental procedures Those with a history of social or psychiatric situations interfering with study compliance	Positive response was observed in 67.8% (40/59) patients of ZSP group, and in 17% (9/53) patients of placebo group		Sun et al. (2010)
Lycopene	Randomized placebo-controlled trial	*n* = 58 Gender bias-M:F::44:14 Age: 10–70 years (70% between 31 and 70 years)	Group B: 4 mg/day Group C: Placebo For 3 months Follow-up: 2 months Evaluation: Every 7–10 days during treatment and 15 days during follow-up	Inclusion • Patients suffering from oral leukoplakia	• Clinically the patients in groups A, B, C had a mean response of 80, 66.25 and 12.5% respectively • Group A: o Complete response-11 o Partial response-7 o Stable response-2		Singh et al. (2004)

(Continued on following page)

TABLE 7 | (*Continued*) Clinical studies in chemopreventive phytochemicals/herbal derivatives against HNC.

Phyto-chemical/herbal extract/	Type of study	Study participants	Dosage, treatment duration, and follow-up	Criteria (inclusion/exclusion)	Clinical outcome	Adverse effects reported	Ref
					• Group B: o Complete response -5 o Partial response-7 o Stable response-2 • Group C: o Complete response-0 o Partial response-3 o Stable response-15		
Green tea extract	Phase II, randomized double-blinded placebo-controlled trial	*n* = 41 Placebo:Group1:Group2:Group3::1:11:9:10 Gender bias-M:F::19:22 Smoker Never: 15 Former: 22 Current: 4 Cigar Former 1 Current 3 Smokeless tobacco Former: 1 Current: 0 Alcohol Never: 8 Former: 9 Current: 24	Group 1 GTE: 500 mg/m2 Group 2 GTE: 750 mg/m2 Group 3 GTE: 1,000 mg/m2 Group 4: Placebo For 12 weeks Follow up: 27.5 (median time) Evaluation: After 4 weeks	Inclusion • Presence of one or more histologically confirmed, bidimensionally measurable OPLs that could be sampled by biopsy and had at least one of the following high-risk features of malignant transformation • Harboring at least mild dysplasia • Located in a high-risk area (i.e., floor of mouth, ventrolateral tongue, and soft palate) • Significant extent of OPL tissue involvement • Presence of symptoms (pain or substantial discomfort) • Age between ≥18 and ≤75 years • Zubrod performance status of <2 • Adequate hematologic, liver, and renal function • Adequate cardiac function • Negative pregnancy test in females of childbearing potential within 7 days before first dose of study medication; use of effective contraceptive method while on the trial Exclusion • Known hypersensitivity to oral GTE or its analogs • Use of prior investigational agents within 30 days • Any serious intercurrent illness • History of prior malignancy with less than a 1-year disease-free interval before study entry • Lactating females patients who were not able to abstain from the consumption of methylxanthine-containing products (including coffee, tea, chocolate, caffeinated soft drinks, and theophylline) and decaffeinated tea	• The clinical response rate was higher in the three combined GTE arms (50%) vs. placebo (18.2%) • Histologic response rate 21.4% (GTE arms) vs. 9.1% (placebo) • The clinical response rate was dose dependent—58% in the combined higher-dose GTE arms (group 2 and 3) vs. 36.4% group 1 and 18.2% (placebo) • Dose dependency was not seen in histologic response • With a median follow-up time of 27.5 months, 15 patients subsequently developed oral cancer with a median time to oral cancer development of 46.4 months	Treatment-related adverse events reported by 28 of the 30 (93.3%) patients who received GTE There were only three grade 3 adverse events and no grade 4 or 5 adverse events Common grade 1 and 2 events: Headaches, insomnia, nausea, nervousness, flatulence, gastric reflux, back pain	Tsao et al. (2009)
Black raspberries		*n* = 40 BRB:Placebo::22:18 Gender Bias-M:F::14:24 Age-32–78 years Smoker Y:N::16:24	10% w/w For 12 weeks Follow-up: 3 months Long-term follow-up: 3–31 months	Inclusion criteria • Microscopically confirmed premalignant oral epithelial lesions • No use of tobacco products for six weeks prior and during the three-month study • No previous history of cancer Exclusion criteria • Previous or current history of non-basal cell cancer • Use of tobacco products Either a microscopic diagnosis of no premalignant change or oral squamous cell carcinoma (OSCC) in the pretrial biopsy	• 16 of the 21 BRB treated lesions decreased in size for an average overall size decrease of 26% • 17 of the 19 placebo gel treated lesions increased in clinical lesional size with an average increase of 18% • 2 BRB gel patients had 100% lesional resolution • Statistical decrease in histopathologic grade while placebo gel application did not significantly impact histopathologic grade • After 3 months 6 of 22 BRB and 7 of 17 placebo patients had visible evidence of lesional recurrence at the former treatment sites	No adverse effects	Mallery et al. (2014)
Curcumin	Randomized double blind phase IIB trial	• *n* = 223 Drug:Placebo::111:112 • Gender Bias-M:F::161:62 • Smoking- current(C)/Former(F)	Three 600 mg capsules taken twice daily; orally and after food (3.6 g/day) for six months 103 subjects for 6 more months. (Drug: Placebo::53:50)	Inclusion • The presence of clinical and histologically confirmed oral leukoplakia >15 mm^2 in area • 1 cm linearly • No previous biopsy or treatment for head and neck cancer prior to 3 months of accrual • No chemopreventive treatment prior to 3 months of accrual	• Statistically significant difference observed • Clinical response: 75 subjects (67.5%) in curcumin arm and in 62 subjects (55.3%) in placebo arm • Thirty (27%) subjects in curcumin arm and 46 (41.1%) subjects in placebo arm were non-responders • Histologic response was observed in 25 (22.5%) subjects in the curcumin arm and in 23 (20.5%) subjects in the placebo arm • Combined (clinical and histological) response was noticed in 65 (58.6%)	Moderate/severe AEs were recorded in 4 patients in the curcumin arm including anemia skin/ subcutaneous tissue disorders, and hypertension	Kuriakose et al. (2016)

(Continued on following page)

TABLE 7 | (*Continued*) Clinical studies in chemopreventive phytochemicals/herbal derivatives against HNC.

Phyto-chemical/herbal extract/	Type of study	Study participants	Dosage, treatment duration, and follow-up	Criteria (inclusion/exclusion)	Clinical outcome	Adverse effects reported	Ref
		Yes:No::112:111 (C/F::81:27) ● Alcohol- Daily/Non-Daily (D/ND Yes:No::93:130 (D:ND::16::51) ● Chewing Tobacco-Current(C)/ Former(F) Yes:No::156:63 (C:F::95:63)	**Evaluation:** Monthly during supplementation	● Zubrod performance of 0–2 ● Normal hematological and biochemical parameters Exclusion: The presence of oral submucous fibrosis	subjects in the curcumin arm and 50 (44.6%) subjects in the placebo arm ● Curcumin group: Of the 18 subjects available at follow-up, 16 (88.9%) continue to have CR at 12 months ● Placebo arm: 7 of 8 subjects (87.5%) demonstrating no relapse after 6 months follow-up		
Calendula officinalis and lycopene	Double-blinded comparative study	*n* = 60 COL-lycopene::30:30 Gender bias-M:F::50:10 Age 26–75 years (maximum in 56–65 years)	Calendula officinalis gel (group 1): 2 mg by weight/g Lycopene gel (group 2): 2 mg by weight/g Administered topically thrice a day For 1 month Follow-up: 3 months	Inclusion ● Patients with clinically and histopathologically confirmed cases of homogeneous leukoplakia	● Group 1 ᵃ Average size of leukoplakia before treatment: 4.14 cm2 (standard deviation [SD] = 2.07) o Average size treatment: 2.09 cm2 (SD = 2.59) Group 2 ᵃ The average size of leukoplakia before treatment: 4.46 cm2 (SD = 2.41) o Average size after treatment: 2.89 cm2 (SD = 3.07) ● The mean difference in the reduction in size before and after treatment for group I was 2.0 ± 1.0 cm while for the group II, it was 1.57 ± 0.87 cm		Singh and Bagewadi, (2017)

of growth factor–mediated proliferation (Liang et al., 1997; Liang et al., 1999a), induction of G1 arrest (Khafif et al., 1998; Liang et al., 1999b; Liberto and Cobrinik, 2000), and apoptosis (Ahmad et al., 1997; Paschka et al., 1998; Yang et al., 1998; Li et al., 2000). In this study, it induced apoptosis *via* the mitochondrial pathway through decreasing the expression level of Bcl2 and Bcl-xL and simultaneously increasing the Bax expression level that in turn activates caspase-9 in HNC cell lines YCU-N861 and HPV18 transformant YCU-H891 cell line. Treatment with EGCG inhibited the phosphorylation of EGFR, STAT3, and ERK proteins. It also inhibited the basal and transforming growth factor α-stimulated c-fos and cyclin D1 promoter activity. It decreased the level of cyclin D1 and pRB, accounting for the cellular arrest in the G1 phase (Masuda et al., 2001). The efficacy of the therapies used for the treatment of HNC can be enhanced by the incorporation of EGCG in current therapeutic regimens. Currently, anti-EGFR antibodies or specific tyrosine kinase inhibitors are being used in combination with radiation and certain chemotherapy agents in clinical trials for various types of cancer, as inhibition of the EGFR-related signal transduction pathway enhances the cytotoxic effects of radiation or various chemotherapy agents (Wu et al., 1995; Dent et al., 1999; Bonner et al., 2000). Hence, EGCG may have certain advantages over EGFR antibodies or selected tyrosine kinase inhibitors, as it is relatively inexpensive, natural, and nontoxic, and hence might be useful in administering for a longer period without any adverse effects. Clinical efficacy of EGCG still needs to be determined, and the direct correlation between chemopreventive effect of EGCG and HPV activity is yet to be established by further *in vitro* and *in vivo* studies. Also, the p53 status during EGCG administration needs to be determined as 50% of HNC carry mutations in the p53 gene, which in turn can modulate effects of EGCG (Wang et al., 2020).

Emodin, a natural trihydroxyanthraquinone, has lower oxidation–reduction potential than that of oxygen; hence, under hypoxic conditions, it can be reduced to cytotoxic agent, sensitizing the cells to irradiation (Zhu et al., 2005; Zou et al., 2010; Schwartz et al., 2011). It affected the NPC cell (CNE1, a HeLa contaminated cell line) promotion and progression by inducing oxidative damage by significantly increasing the expression level of ROS, which induces apoptosis and downregulates mRNA and protein levels of HIF-1α. It also reduces the promotion of survival of carcinoma cells and induces cell cycle arrest at the G2/M phase. Hence, exposure of NPC cells *in vitro* and xenografts *in vivo* to emodin enhanced their radiosensitivity (Hou et al., 2013). Therefore, incorporation of emodin, a bioreductive agent, represents a viable therapeutic strategy targeting HIF-1α, by enhancing cytotoxicity of chemotherapeutic drugs *via* modulation of redox status of cancer cells and multidrug resistance reversal (Yi et al., 2004; Brown et al., 2007; Cai et al., 2008; Huang et al., 2008). It may also serve as an effective radiosensor, thereby improving efficacy of radiation therapy in radiation-resistant cancer cells. Moreover, since emodin can effectively enhance the radiosensitivity *in vivo*, it holds a potential as a radiosensitizing drug for NPC patients in future. Still a direct correlation between emodin and HPV-activity needs to be established.

TABLE 8 | List of HPV positive Head and neck cancer cell lines developed and described with their key characteristics.

Cell lines	Anatomical site	HPV type	Key characteristics	Copy number	Developed by	References
93-VU-147T	Oral cavity	HPV16	Three integrated sites E1-17q21 E2-5p15.33 (promoter of TERT gene) L2-3p21 (Intergenic)	NA	VU University Medical Center, Amsterdam Netherlands	Steenbergen et al. (1995)
UD-SCC-2	Hypopharynx	HPV16	Two integrated sites E1-17q12 (Intergenic) E2-1p32.3 (Intron 14 of JAK1 gene)	14—23 copies	University of Dusseldorf, Dusseldorf, Germany	Ballo et al. (1999)
UPCI-SCC-90(SCC90)	Tongue	HPV16	Two integrated sites E1-12p13 (Intron 1 of ETV gene) E1-9q31.1 (Intergenic)	100—500 copies	University of Pittsburgh, Pittsburgh PA	White et al. (2007)
UPCI-SCC-154	Tongue	HPV16	Four integrated sites E1-21p11.1 (Intergenic) E1-11q22-23 (Intron 3 of PGR gene) E2-2q33.2 (exon 14 of TMEM237 gene) E2-7q36 (Intron 3 of PTPRN2 gene)	NA	University of Pittsburgh, Pittsburgh PA	White et al. (2007)
UPCI-SCC-152	Hypopharynx	HPV16	Four integrated sites E1-9q31.1 (Intergenic) E1-12p13 (Intron 1 of ETV gene) E2-9q22.33 (Intergenic) LCR-3q23 (Intron 36 of ATR gene)	NA	University of Pittsburgh, Pittsburgh PA	White et al. (2007)
UM-SCC-47	Oral cavity/ Tongue	HPV16	Two integrated sites E2-3q28 (Intron 10 of TP63 gene) E2-3q28 (exon 14 of TP63 gene)	21—47 copies	University of Michigan, Ann Arbor, MI	Brenner et al. (2010)
HB-2	Oral mucosa	HPV16	NA	NA	Tong University, Shanghai, China	Ye et al. (2011)
UM-SCC104	Oral cavity	HPV16	Three integrated sites E1-18q21.3 (Intron 1 of DCC gene) E2-17q22 (Intergenic) E2-17p11.2 (Intergenic)	NA	University of Michigan, Ann Arbor, MI	Tang et al. (2012)
UM-SCC-105	Larynx	HPV18	Two integrated sites L1-8q12.3/4p15.33 (Intergenic) L1-17q12 (Intergenic)	NA	University of Michigan, Ann Arbor, MIs	Owen et al. (2016)
HMS001	Oral cavity	HPV16	NA	NA	NA	Kalu et al. (2017)
UT-SCC-45	Floor of the mouth	HPV33	NA	NA	University of Turku, SF-20520 Turku, Finland	Kalu et al. (2017)

Abbreviation: NA, not available.

Curcumin (diferulolylmethane), an active component of turmeric and a perennial herb, has been shown to suppress the expression of HPV oncogenes mediated by downregulation and reduced transactivation of AP-1 and NF-kB superfamily members, representing a novel mechanism regulating HPV-induced oral carcinogenesis (Li et al., 1993; Prusty and Das, 2005). Its effect was also observed in HPV-positive 93VU147T cells. The cell viability is reduced significantly. It also induces apoptosis by decreasing the expression level of antiapoptotic factors such as Bcl-2 and cIAP2, and inducing proapoptotic factors like Bax. It downregulated the protein expression of AP-1 members: c-Jun, JunD, and JunB along with NF-kB members, p50 and p65. Curcumin also tends to show HPV-specific effects like reducing the mRNA levels of HPV16/E6, which in turn inhibits E6-mediated p53 degradation. Hence, curcumin exhibits therapeutic potential for HPV16-mediated oral oncogenesis suppression (Mishra et al., 2015). Similar result was observed in a later study on curcumin as phytochemical having both anti-HNSCC and anti-HPV activities, which was carried out on UD-SCC-2, UPCI: SCC131, and UPCI:SCC84 cell lines. It affected cancer promotion, cellular proliferation, and progression. Curcumin inhibited cancer cell growth and orosphere formation ability. Also, it induced cytotoxic effect along with HPV-specific effects like decreasing the expression level of HPV16 E6/E7 oncoproteins, and downregulated mi-RNA21 expression

TABLE 9 | Chemotherapeutic and Chemopreventive phytochemicals/Herbal derivative with anti-cancer and anti-HPV activity in HNC.

Phytochemicals/ Herbal Products; PubChem-CID (Class)	Cell type/Model/Clinical	Stage of Cancer	Anti-cancer activity in HPV positive cell	HPV specific effect	Ref.
EGCG (Green Tea Polyphenol (-)-Epigallocatechin-3-gallate) CID: 65064	*In vitro* study: **YCU-N861**[a] (NPSCC) and **YCU-H891#** (Hypopharyngeal SCC)	Promotion	• G1 phase Cells ↑; Cyclin D1 ↓, pRB ↓ • Apoptosis ↑; Bcl2 ↓, Bax ↑, Caspace 9↑: apoptosis↑. • Phosphorylation of EGFR, STAT3, ERK proteins ↓ • Basal and transforming growth factor α-stimulated C-fos and Cyclin D1 promoter activity ↓	NA	Masuda et al. (2001)
Emodin *(Polygonum multiflorum)* CID: 3220 (Trihydroxyanthraquinone)	*In vitro* study: **CNE-1#** (NPSCC epithelioid cell line)	Promotion and progression	• ROS ↑; Oxidative damage ↑ • Apoptosis ↑ • HIF-1α ↓ • Promotion of survival ↓	NA	Hou et al. (2013)
Curcumin CID: 969516 (Phytopolylphenol)	*In vitro* study: **93VU147T**[a] (OSCC)	Promotion and progression	• Cell viability ↓ • Bcl-2 ↓, cIAP2 ↓, Bax ↑ • AP-1 ↓, NF-KB ↓	• HPV16/E6 mRNA ↓ • E6-mediated p53↓	Mishra et al. (2015)
CIP-36 (Novel podophyllotoxin derivative)	*In-vitro* study: **KB**[a] (HeLa contaminant epidermal carcinoma of mouth)	Promotion and Progression	• Cell proliferation ↓ • Blocks cells in S/G2+M phase • Effects DNA cleavage mediated by Human Topo IIα	NA	Cao et al. (2015)
Sulforaphan CID: 5350 (Isothiocyanate	*In-vitro* study: **UM-SCC-22A** (Hypopharyngeal SCC), **UM-SCC-1** (OSCC), **CAL33** (Tongue OSCC), and **UPCI: SCC090**[a] (Tongue OSCC). *In-vivo* study: Female **C57BL/6 mice** (5–6 weeks; 18 mice/group). Clinical study: 10 human subjects	Initiation, promotion and progression	• NRF2 signaling ↑ • STAT3 phosphorylation ↓ • Promotes cell death • Consumption of BSE (Broccoli sprout extracts rich in sulforaphane) beverage demonstrated NRF2 pathway activation in oral mucosa.	NA	Bauman et al. (2016)
6-Gingerol CID: 442793 (Beta-hydroxy ketone)	*In-vitro* study: **KB**[a] (HeLa contaminant epidermal carcinoma of mouth), **SCC4** (Tongue SCC).	Promotion and progression	• Tumor cell proliferation ↓ • Cytotoxicity ↑ • Caspase-3 pro-apoptotic activity ↑ • Sub-G1 cells ↑; G2 and S phase arrest	NA	Kapoor et al. (2016)
Curcumin CID: 969516 (Phytopolylphenol)	*In-vitro* study: **UD-SCC-2**[a] (Hypopharyngeal SCC); **UPCI: SCC131** (OSCC), **UPCI:SCC84** (OSCC)	Promotion, Proliferation and progression	• Cell growth↓ • Orosphere formation ability↓ • Cytotoxic effect	• HPV 16 E6/E7 ↓ • miRNA21 ↓	Bano et al. (2018)
Thymol CID: 6989 (Monoterpene)	*In-vitro* study: **CAL27** (Tongue OSCC), **SCC4** (Tongue OOS), **SCC9** (Tongue OSCC) *In-vivo* study: athymic nude mice, **Cal27- and HeLa-derived**[a] mouse xenografts.	Initiation, promotion and progression	• Cellular proliferation↓; Apoptosis↑ • Long lasting cytotoxic effects • Long lasting cytotoxic effects • TRPA1 activation • Mitochondrial membrane potential↓ • Mitochondrial dysfunction • *In vivo* Tumor growth↓	NA	De La Chapa et al. (2018)
Apigenin (40 ,5,7, -trihydroxyflavone, AP)	*In-vitro* study: **SHEE**[a,b] (Human esophageal epithelial cell line)	Promotion and progression	• Migration Ability↓ • G1 phase arrest; CDK4↓, Cyclin-D1↓, pRB↓ • Apoptosis↑ activation of caspase-3. • DNA Alkylation↓	NA	Yin et al. (2020)

[a]*HPV16/18 positive cell lines* ***NA****: No HPV-specific effects have been reported.*

[b]*Some research papers have classified Human esophageal carcinoma under Head and neck squamous cell carcinoma but it should be classified under the broader category of digestive system carcinoma.*

Abbreviations: *AP-1: Activator protein 1; Bax: Bcl-2-associated X protein; Bcl2: B-cell lymphoma 2; BSE: Broccoli Sprot extracts; CDK: Cyclin-dependent kinases; cIAP: Calf Intestinal Alkaline phosphatase; EGFR: Epidermal growth factor receptor; ERK: Extracellular-signal-regulated kinase; HIF-1α: Hypoxia-inducible factor 1-alpha; HPV: Human papillomavirus; IFN-γ: Interferon gamma; NF-Kβ: Nuclear factor kappa light chain enhancer of activated B cells; NRF2: Nuclear factor erythroid 2-related factor 2; pRB: phosphorylated Retinoblastoma; STAT3: Signal transducer and activator of transcription 3; Topo IIα: topoisomerase II- alpha; TRPA1: Transient receptor potential cation channel, subfamily A, member 1.*

significantly in HPV-positive oral CSCs. Hence, curcumin can sensitize the HPV-positive oral CSCs, thus making the cancer treatment more effective when used in combination with standard anticancer drugs or radiation, depicting its potential as a therapeutic agent. Further studies are required for deciphering the therapeutic effects of curcumin by determining its solubility and bioavailability, mechanism(s) of action, and potential molecular targets (Bano et al., 2018).

Sulforaphane, an isothiocyanate, derived from broccoli sprout extracts; treatment of HPV-negative HNC cell lines–UM-SCC-22A, UM-SSC-1, and CAL33–and HPV-positive cell line SSC090 led to dose- and time-dependent stimulation of NRF2 signaling for carcinogen detoxication. It also dephosphorylated inhibitedSTAT3 and promoted cell death. Similar effects were also observed in *in vivo* and clinical study including female C57BL/6 mice (5–6 weeks; 18 mice/group) and 10 human subjects, respectively. The pilot clinical trial demonstrated consistent bioavailability of sulforaphane, promising sustainable chronic administration. Although it is a cost-effective and natural product, further studies planned with encapsulated broccoli extract are required to enhance the ease of acceptability and dispensing. Also, HPV-specific chemopreventive effects are yet to be determined (Bauman et al., 2016).

6-Gingerol, a β-hydroxy ketone, derived from ginger rhizome, inhibited tumor cell proliferation and induces cellular toxicity, cell cycle arrest, apoptosis, and caspase 3/7 activation, as observed in KB and SCC4 cells. Also, the caspase-3–dependent proapoptotic activity was stimulated. It also inhibited cell cycle progression arresting the cells in G2 and M phases. Hence, 6-gingerol can be considered as a safe and potent chemotherapeutic/chemopreventive compound acting *via* cell cycle arrest and induction of apoptosis (Kapoor et al., 2016). Further studies should be directed toward determination of the chemopreventive effects of 6-gingerol in *in vivo* conditions and clinical trials along with direct correlation with HPV activity.

Thymol, a monoterpene derivative phenol, is a TRPA1 agonist found in thyme and oregano. It inhibited cellular proliferation and exhibited long-lasting cytotoxic effects as observed in CAL27, SSC4, and SSC9 cell lines. It also inhibited tumor growth *in vivo* as observed in CAL27 and HeLa-derived mouse xenografts. It induces the activation of TRPA1 and apoptosis *via* the mitochondria-dependent pathway. It promoted mitochondrial dysfunction *via* reducing mitochondrial membrane potential significantly (De La Chapa et al., 2018). Its HPV-specific effects still need to be determined along with the determination of bioavailability and tolerability to understand its therapeutic effects for future incorporation into cancer treatment.

Apigenin, a flavonoid, found abundantly in flowers of plants, vegetables, and fruits, exerts anticarcinogenic effects *via* preventing malignant transformation of cells, regulating cell signal transduction pathways, increasing apoptosis, and modulating cell cycle (Fang et al., 2007; Zhao et al., 2011; Zhu et al., 2013; Salmani et al., 2017; Yang et al., 2018a). It inhibited cancerous cell migration ability and arrested them in the G1 phase as observed in SHEE cells induced by HPV-18 and 4-(methylnitrosamino)-1-(3-pyridyl)-1-butanone (NNK). It downregulated the expression of CDK4, cyclin D1, and pRB, affecting cell cycle. Apigenin also induced cellular apoptosis *via* caspase-3 activation and inhibits DNA alkylation. With low toxicity and various beneficial bioactivities, apigenin can be considered as a potential chemopreventive agent against cancers, particularly, in smokers with HR-HPV coinfection (Yin et al., 2020).

Hence, most of the phytochemicals mentioned above showed anticancer activity in HPV-positive cells, where only a limited studies focused on HPV-specific effects. Thus, considerable attention should be paid to analyze the correlation between anti-HNC and anti-HPV activity of the phytochemicals as a chemopreventive and chemotherapeutic measure to prevent HPV-HNC.

Critical Issues Associated With the Use of Phytochemicals

Despite their encouraging pharmacological activities, there are bottlenecks in the translation of phytochemical-based therapies applicable in clinical settings.

Low bioavailability: Many phytochemicals suffer from having poor aqueous solubility and low retention in blood circulation. Pharmacological concentration of these phytochemicals in blood and tumor tissues is low because of poor absorption, high rate of metabolism, chemical degradation, and speedy clearance. It has been reported that serum levels of curcumin were quite low, reaching a maximum of 0.06 ± 0.01 μg/ml after oral administration of 500 mg/kg in rats (Yang et al., 2007). Ravindranath and Chandrasekhara (1980) also demonstrated that 40% of curcumin gets excreted unchanged in feces when orally administered to rats (Ravindranath and Chandrasekhara, 1980). A pilot study conducted among 10 healthy patients also reported poor bioavailability of sulforaphane with a regimen of topical exposure to sulforaphane-rich broccoli sprout extracts (Bauman et al., 2016). Chen et al. (1997) investigated the plasma pharmacokinetics of EGCG in rats and found the oral bioavailability of only 1.6% after a 75 mg/kg oral dose and a 10 mg/kg intravenous dose (Chen et al., 1997). Similarly, circulation half-life of resveratrol when administered through i. v. was few minutes and showed rapid elimination (Marier et al., 2002), whereas EGCG and quercetin attain low concentrations in blood, which is inadequate for antitumor activity (Lagoa et al., 2017).

Obstacles associated with the use of phytochemicals for treating and preventing cancer can be overcome with advances in the field of nanotechnology. A 10-fold dose advantage was achieved without any loss of effectiveness by encapsulating ECGC in polylactic acid–polyethylene glycol nanoparticles (Siddiqui et al., 2009). Increased absorption was also reported by nanoparticle encapsulation of curcumin despite its low solubility in water. Additionally, curcumin loaded poly lactic-co-glycolic acid nanoparticles increased the oral bioavailability to nine times that of the native form, with piperine as absorption enhancer (Shaikh et al., 2009). Further advancements in this field should be encouraged.

Toxicity: Although phytochemicals may show toxicity when administered in high doses, they exhibit less adverse effects than conventional therapies. In a clinical trial with 50 oral leucoplakia

patients, significant toxicity, severe enough to cause withdrawal of 6 patients, was observed with the use of isoretinoin (Garewal et al., 1999). Additionally, not all phytochemicals are safe for consumption. It has been found that a few natural compounds such as capsaicin (chilli pepper), cycasin, and cycas seed are tumor-promoting and must be avoided (Bode and Dong, 2015). Moreover, unregulated use of phytochemicals may have a danger of contamination by potential carcinogens.

Pharmaceutical industry challenges: Pharma-research into phytochemicals and herbal derivatives has experienced a slow decline during the recent times (Koehn and Carter, 2005; Katiyar et al., 2012). This can be attributed to advancements in high-throughput screening technology against defined molecular targets, advances in genomics, molecular and cellular biology, development of combinatorial chemistry, and a declining importance among large pharma-companies on the commercial considerations of phytochemicals that are often associated with poor financial returns and nearly absent IPR protection. Unique features of natural compounds such as a greater number of chiral centers, higher number of oxygen atoms, and greater molecular rigidity pose further challenges for medicinal chemists as they develop analogs to reduce toxicity, improve absorption, or to improve the efficacy, which is often achieved by adding or deleting selected functional groups.

Poor independent agents: While phytochemicals may not be efficient as standalone chemotherapeutic agents, many groups have established their efficacy as adjuvants to traditional therapies. A study demonstrated the benefits of combining sulforaphane with cisplatin and 5-fluorouracil (Elkashty et al., 2018). Sulforaphane increased the cytotoxicity of cisplatin and 5-fluorouracil by two-fold and ten-fold, respectively. It did not alter the viability and functions of noncancerous stem cells. Sulforaphane combined treatments successfully inhibited cancer stem cell colony formation, sphere formation, and tumor progression *in vivo*. In an Italian study conducted among 23 patients undergoing treatment with 5-fluorouracil and cisplatin, prolonged responses were reported with the use of retinol palmitate in chemotherapy intervals. Toxicity levels were acceptable, and treatment did not interfere with the quality of life (Recchia et al., 1993). A study also observed significant growth inhibition and enhanced apoptosis in HNC cells with the use of curcumin along with 5-fluorouracil or doxorubicin. The study thus demonstrated the significant potential of combining curcumin with 5-fluorouracil or doxorubicin as a treatment modality for HNC management (Sivanantham et al., 2016).

Preclinical efficacy vs. clinical response: The cause for discrepancy in effectiveness of phytochemical agents in preclinical and human clinical trials has been conjectured to arise because of differences in dosage, metabolic differences, bioavailability, differences in circulating tissue levels of chemopreventive agents in humans and animals, exposure conditions to damaged tissue vs normal tissue, follow-up time, and the assessed ends. Second, high doses are often administered to animals in contrast to low doses admisible to humans in clinical trials. Although animal models have significantly helped in the identification of carcinogens, and chemopreventive and chemotherapeutic agents, they are not available for every HNC organ site. Furthermore, existing models cannot mimic human exposure complexities of carcinogens, metabolic competence, turnover of cells, and their repair capacity.

CONCLUSION AND FUTURE PROSPECTIVE

Phytochemicals show immense potential in the field of HNC chemotherapy and chemoprevention agents. In this evolving landscape, the success of employability of phytochemicals depends on our ability to decipher their molecular mechanics. Using phytochemicals in combination with another or in conjunction with existing chemotherapeutic practices or an alternate therapy is an area worth exploring.

We have also observed that there has not been much phytochemical-related research on HPV-induced HNC. However, numerous phytochemicals that are effective against HPV-induced cervical cancer have been reported in the literature (Bharti et al., 2018). In today's era, therapies to distinguish HPV-positive HNC from HPV-negative HNC are required. As HPV-positive HNC has better outcomes, the tumors can be treated with well-established phytochemicals targeting the HPV-mediated carcinogenic mechanisms. Thus, it might be valuable to study whether these phytochemicals can find application in HNC treatment and prevention. Activity of these phytochemicals can be checked on HNC cell lines or *in vivo* in laboratory conditions and can also be screened by using bioinformatic tools. There is a strong requirement to develop HPV-based concurrent therapies so that HNC can be treated more effectively. There are many associated challenges with the use of natural compounds. In pharmacological doses, the adverse effects of these natural compounds such as increased toxicity and low bioavailability are amplified. For chemoprevention to be feasible in treating premalignant lesions, the compound must be well tolerated and have long-lasting benefit. Moreover, the various signaling pathways contributing to HNC tumorigenesis mandate the use of compounds with multiple molecular targets. It is noteworthy that molecular targets of many such phytochemicals in active HNC are now well known (**Figure 4**). It is also worthy to note that not many clinical studies have been conducted despite discovery of numerous phytochemicals with multiple molecular targets. In order to determine the safety and efficacy of phytochemicals, it is imperative that more of such clinical studies, with different phytochemicals, are funded and conducted. Challenges associated with the use of phytochemicals such as low bioavailibilty, and toxicity can be possibly overcome with the use of chemical analogs, adjuvant therapies, and nanoparticle delivery mechanisms. Hence, a number of studies on phytochemicals against HPV-driven HNC are now accumulating; a comparative account on their relative efficacy is needed and should be addressed to harness the potential of phytochemicals in clinical studies. Research in these areas needs encouragement for effective management of HPV-positive HNC in future.

AUTHOR CONTRIBUTIONS

NA participated in study writing and manuscript preparation, JY, SC, DJ, TT, and A Chaudhary contributed to manuscript preparation. A Chhokar, KT, and TS: advisory in manuscript preparation. AB conceived the presented idea and designed the manuscript, and critically reviewed, drafted, and communicated the final manuscript. All authors have read and approved the final manuscript.

FUNDING

The study was supported by research funds to ACB from the Central Council for Research in Homeopathy, Department of AYUSH, Government of India (17-51/2016-17/CCRH/Tech/Coll./DU-Cervical Cancer.4850), the Department of Science and Technology-SERB, India (EMR/2017/004018/BBM), and the Indian Council of Medical Research (5/13/38/2014 NCDIII-Eoffice73143). Senior Research Fellowship to NA (09/045 (1,622)/2018-EMR-I), JY (09/045 (1,629)/2019-EMR-I), and Junior Research Fellowship to DJ (15/12/2019 (ii) EU-V) by the Council of Scientific and Industrial Research (CSIR); Senior Research Fellowship to A Chhokar (573/(CSIR-UGC NET JUNE 2017)); and Junior Research Fellowship to TT (764/(CSIR-UGC NET JUNE 2019)) by University Grants Commission (UGC). Senior Research Fellowship to KT (5/13/38/2014 NCDIII-Eoffice73143) by the ICMR, India. Senior Research Fellowship to TS, and Technical Assistantship to SC by CCRH, India (17-51/2016-17/CCRH/Tech/Coll./DU-Cervical Cancer.4850) Junior Research Fellowship to A Chaudhary by DST-SERB, India (EMR/2017/004018/BBM).

REFERENCES

Abdel-Rahman, O. (2020). Prognostic Value of HPV Status Among Patients with Hypopharyngeal Carcinoma: a Population-Based Study. *Clin. Transl Oncol.*

Adeyemi, B. F., Adekunle, L. V., Kolude, B. M., Akang, E. E., and Lawoyin, J. O. (2008). Head and Neck Cancer-Aa Clinicopathological Study in a Tertiary Care center. *J. Natl. Med. Assoc.* 100**,** 690–697. doi:10.1016/s0027-9684(15)31343-2

Adisa, A. O., Adeyemi, B. F., Oluwasola, A. O., Kolude, B., Akang, E. E., and Lawoyin, J. O. (2011). Clinico-pathological Profile of Head and Neck Malignancies at University College Hospital, Ibadan, Nigeria. *Head Face Med.* 7**,** 9. doi:10.1186/1746-160X-7-9

Adjei Boakye, E., Buchanan, P., Hinyard, L., Osazuwa-Peters, N., Schootman, M., and Piccirillo, J. F. (2018). Incidence and Risk of Second Primary Malignant Neoplasm after a First Head and Neck Squamous Cell Carcinoma. *JAMA Otolaryngol. Head Neck Surg.* 144**,** 727–737. doi:10.1001/jamaoto.2018.0993

Aggarwal, N., Yadav, J., Thakur, K., Bibban, R., Chhokar, A., Tripathi, T., et al. (2020). Human Papillomavirus Infection in Head and Neck Squamous Cell Carcinomas: Transcriptional Triggers and Changed Disease Patterns. *Front Cel Infect Microbiol* 10**,** 537650. doi:10.3389/fcimb.2020.537650

Aggarwal, S., Takada, Y., Singh, S., Myers, J. N., and Aggarwal, B. B. (2004). Inhibition of Growth and Survival of Human Head and Neck Squamous Cell Carcinoma Cells by Curcumin via Modulation of Nuclear Factor-kappaB Signaling. *Int. J. Cancer* 111**,** 679–692. doi:10.1002/ijc.20333

Ahmad, N., Feyes, D. K., Nieminen, A. L., Agarwal, R., and Mukhtar, H. (1997). Green tea Constituent Epigallocatechin-3-Gallate and Induction of Apoptosis and Cell Cycle Arrest in Human Carcinoma Cells. *J. Natl. Cancer Inst.* 89**,** 1881–1886. doi:10.1093/jnci/89.24.1881

Akintoye, S. O., and Mupparapu, M. (2020). Clinical Evaluation and Anatomic Variation of the Oral Cavity. *Dermatol. Clin.* 38**,** 399–411. doi:10.1016/j.det.2020.05.001

Albahout, K. S., and Lopez, R. A. (2021). "Anatomy, Head and Neck, Pharynx," in *StatPearls*. (Treasure Island (FL).

Ang, K. K., Harris, J., Wheeler, R., Weber, R., Rosenthal, D. I., Nguyen-Tân, P. F., et al. (2010). Human Papillomavirus and Survival of Patients with Oropharyngeal Cancer. *N. Engl. J. Med.* 363**,** 24–35. doi:10.1056/NEJMoa0912217

Anto, R. J., Mukhopadhyay, A., Shishodia, S., Gairola, C. G., and Aggarwal, B. B. (2002). Cigarette Smoke Condensate Activates Nuclear Transcription Factor-kappaB through Phosphorylation and Degradation of IkappaB(alpha): Correlation with Induction of Cyclooxygenase-2. *Carcinogenesis* 23**,** 1511–1518. doi:10.1093/carcin/23.9.1511

Ayre, J. E., and Ayre, W. B. (1949). Progression from "Precancer" Stage to Early Carcinoma of Cervix within One Year: Combined Cytologic and Histologic Study with Report of a Case. *Am. J. Clin. Pathol.* 19**,** 770–778. doi:10.1093/ajcp/19.8.770

Bagnardi, V., Blangiardo, M., La Vecchia, C., and Corrao, G. (2001). A Meta-Analysis of Alcohol Drinking and Cancer Risk. *Br. J. Cancer* 85**,** 1700–1705. doi:10.1054/bjoc.2001.2140

Ballo, H., Koldovsky, P., Hoffmann, T., Balz, V., Hildebrandt, B., Gerharz, C. D., et al. (1999). Establishment and Characterization of Four Cell Lines Derived from Human Head and Neck Squamous Cell Carcinomas for an Autologous Tumor-Fibroblast *In Vitro* Model. *Anticancer Res.* 19**,** 3827–3836.

Bano, N., Yadav, M., and Das, B. C. (2018). Differential Inhibitory Effects of Curcumin between HPV+ve and HPV-Ve Oral Cancer Stem Cells. *Front. Oncol.* 8**,** 412. doi:10.3389/fonc.2018.00412

Baruah, P., Lee, M., Odutoye, T., Williamson, P., Hyde, N., Kaski, J. C., et al. (2012). Decreased Levels of Alternative Co-stimulatory Receptors OX40 and 4-1BB Characterise T Cells from Head and Neck Cancer Patients. *Immunobiology* 217**,** 669–675. doi:10.1016/j.imbio.2011.11.005

Bauman, J. E., and Ferris, R. L. (2014). Integrating Novel Therapeutic Monoclonal Antibodies into the Management of Head and Neck Cancer. *Cancer* 120**,** 624–632. doi:10.1002/cncr.28380

Bauman, J. E., Zang, Y., Sen, M., Li, C., Wang, L., Egner, P. A., et al. (2016). Prevention of Carcinogen-Induced Oral Cancer by Sulforaphane. *Cancer Prev. Res. (Phila)* 9**,** 547–557. doi:10.1158/1940-6207.CAPR-15-0290

Beaty, B. T., Moon, D. H., Shen, C. J., Amdur, R. J., Weiss, J., Grilley-Olson, J., et al. (2019). PIK3CA Mutation in HPV-Associated OPSCC Patients Receiving Deintensified Chemoradiation. *J Natl Cancer Inst.*112(8):855-858. doi:10.1093/jnci/djz224

Bei, J. X., Su, W. H., Ng, C. C., Yu, K., Chin, Y. M., Lou, P. J., et al. (2016). A GWAS Meta-Analysis and Replication Study Identifies a Novel Locus within CLPTM1L/TERT Associated with Nasopharyngeal Carcinoma in Individuals of Chinese Ancestry. *Cancer Epidemiol. Biomarkers Prev.* 25**,** 188–192. doi:10.1158/1055-9965.EPI-15-0144

Benner, S. E., Winn, R. J., Lippman, S. M., Poland, J., Hansen, K. S., Luna, M. A., et al. (1993). Regression of Oral Leukoplakia with Alpha-Tocopherol: a Community Clinical Oncology Program Chemoprevention Study. *J. Natl. Cancer Inst.* 85**,** 44–47. doi:10.1093/jnci/85.1.44

Berthiller, J., Straif, K., Agudo, A., Ahrens, W., Bezerra Dos Santos, A., Boccia, S., et al. (2016). Low Frequency of Cigarette Smoking and the Risk of Head and Neck Cancer in the INHANCE Consortium Pooled Analysis. *Int. J. Epidemiol.* 45**,** 835–845. doi:10.1093/ije/dyv146

Bharti, A. C., Singh, T., Bhat, A., Pande, D., and Jadli, M. (2018). Therapeutic Startegies for Human Papillomavirus Infection and Associated Cancers. *Front. Biosci. (Elite Ed.* 10**,** 15–73. doi:10.2741/e808

Bharti, A. C., and Aggarwal, B. B. (2017). *Role of Nutraceuticals in Cancer Chemosensitization*. 1st Edn. Cambridge, MA: Academic Press.

Bhattacharyya, S., Sekar, V., Majumder, B., Mehrotra, D. G., Banerjee, S., Bhowmick, A. K., et al. (2017). CDKN2A-p53 Mediated Antitumor Effect of Lupeol in Head and Neck Cancer. *Cel Oncol (Dordr)* 40**,** 145–155. doi:10.1007/s13402-016-0311-7

Bichler, E., Daxenbichler, G., and Marth, C. (1983). Vitamin A Status and Retinoid-Binding Proteins in Carcinomas of the Head and Neck Region. *Oncology* 40**,** 336–339. doi:10.1159/000225757

Bode, A. M., and Dong, Z. (2015). Toxic Phytochemicals and Their Potential Risks for Human Cancer. *Cancer Prev. Res.* 8**,** 1–8. doi:10.1158/1940-6207.capr-14-0160

Bonner, J. A., Raisch, K. P., Trummell, H. Q., Robert, F., Meredith, R. F., Spencer, S. A., et al. (2000). Enhanced Apoptosis with Combination C225/radiation Treatment Serves as the Impetus for Clinical Investigation in Head and Neck Cancers. *J. Clin. Oncol.* 18, 47S–53S.

Boscolo-Rizzo, P., Pawlita, M., and Holzinger, D. (2016). From HPV-Positive towards HPV-Driven Oropharyngeal Squamous Cell Carcinomas. *Cancer Treat. Rev.* 42, 24–29. doi:10.1016/j.ctrv.2015.10.009

Boyle, W. F., Riggs, J. L., Oshiro, L. S., and Lennette, E. H. (1973). Electron Microscopic Identification of Papova Virus in Laryngeal Papilloma. *Laryngoscope* 83, 1102–1108. doi:10.1288/00005537-197307000-00013

Bozec, A., Demez, P., Gal, J., Chamorey, E., Louis, M. Y., Blanchard, D., et al. (2018). Long-term Quality of Life and Psycho-Social Outcomes after Oropharyngeal Cancer Surgery and Radial Forearm Free-Flap Reconstruction: A GETTEC Prospective Multicentric Study. *Surg. Oncol.* 27, 23–30. doi:10.1016/j.suronc.2017.11.005

Bozec, A., Peyrade, F., Fischel, J. L., and Milano, G. (2009). Emerging Molecular Targeted Therapies in the Treatment of Head and Neck Cancer. *Expert Opin. Emerg. Drugs* 14, 299–310. doi:10.1517/14728210902997947

Brand, T. M., Hartmann, S., Bhola, N. E., Li, H., Zeng, Y., O'keefe, R. A., et al. (2018). Cross-talk Signaling between HER3 and HPV16 E6 and E7 Mediates Resistance to PI3K Inhibitors in Head and Neck Cancer. *Cancer Res.* 78, 2383–2395. doi:10.1158/0008-5472.CAN-17-1672

Brandsma, J. L., and Abramson, A. L. (1989). Association of Papillomavirus with Cancers of the Head and Neck. *Arch. Otolaryngol. Head Neck Surg.* 115, 621–625. doi:10.1001/archotol.1989.01860290079018

Brazen, B., and Dyer, J. (2020). *Histology, Salivary Glands*. Davie, FL: StatPearls.

Brazil, D. P., and Hemmings, B. A. (2001). Ten Years of Protein Kinase B Signalling: a Hard Akt to Follow. *Trends Biochem. Sci.* 26, 657–664. doi:10.1016/s0968-0004(01)01958-2

Brenner, J. C., Graham, M. P., Kumar, B., Saunders, L. M., Kupfer, R., Lyons, R. H., et al. (2010). Genotyping of 73 UM-SCC Head and Neck Squamous Cell Carcinoma Cell Lines. *Head Neck* 32, 417–426. doi:10.1002/hed.21198

Brown, M., Bellon, M., and Nicot, C. (2007). Emodin and DHA Potently Increase Arsenic Trioxide Interferon-Alpha-Induced Cell Death of HTLV-I-Transformed Cells by Generation of Reactive Oxygen Species and Inhibition of Akt and AP-1. *Blood* 109, 1653–1659. doi:10.1182/blood-2006-04-015537

Cai, J., Niu, X., Chen, Y., Hu, Q., Shi, G., Wu, H., et al. (2008). Emodin-induced Generation of Reactive Oxygen Species Inhibits RhoA Activation to Sensitize Gastric Carcinoma Cells to Anoikis. *Neoplasia* 10, 41-IN19. doi:10.1593/neo.07754

Cancer Genome Atlas, N. (2015). Comprehensive Genomic Characterization of Head and Neck Squamous Cell Carcinomas. *Nature* 517, 576–582. doi:10.1038/nature14129

Cao, B., Chen, H., Gao, Y., Niu, C., Zhang, Y., and Li, L. (2015). CIP-36, a Novel Topoisomerase II-Targeting Agent, Induces the Apoptosis of Multidrug-Resistant Cancer Cells *In Vitro*. *Int. J. Mol. Med.* 35, 771–776. doi:10.3892/ijmm.2015.2068

Carlson, E. R., and Schlieve, T. (2019). Salivary Gland Malignancies. *Oral Maxillofac. Surg. Clin. North. Am.* 31, 125–144. doi:10.1016/j.coms.2018.08.007

Centers for Disease Control and Prevention, U. (2004). "The Health Consequences of Smoking: A Report of the Surgeon General," in *The Health Consequences of Smoking: A Report of the Surgeon General*. (Atlanta (GA)).

Chaisuparat, R., Limpiwatana, S., Kongpanitkul, S., Yodsanga, S., and Jham, B. C. (2016). The Akt/mTOR Pathway Is Activated in Verrucous Carcinoma of the Oral Cavity. *J. Oral Pathol. Med.* 45, 581–585. doi:10.1111/jop.12422

Chang, E. T., and Adami, H. O. (2006). The Enigmatic Epidemiology of Nasopharyngeal Carcinoma. *Cancer Epidemiol. Biomarkers Prev.* 15, 1765–1777. doi:10.1158/1055-9965.EPI-06-0353

Chaturvedi, A. K., Engels, E. A., Anderson, W. F., and Gillison, M. L. (2008). Incidence Trends for Human Papillomavirus-Related and -unrelated Oral Squamous Cell Carcinomas in the United States. *J. Clin. Oncol.* 26, 612–619. doi:10.1200/JCO.2007.14.1713

Chaturvedi, A. K., Engels, E. A., Pfeiffer, R. M., Hernandez, B. Y., Xiao, W., Kim, E., et al. (2011). Human Papillomavirus and Rising Oropharyngeal Cancer Incidence in the United States. *J. Clin. Oncol.* 29, 4294–4301. doi:10.1200/JCO.2011.36.4596

Chaturvedi, A. K., Graubard, B. I., Broutian, T., Pickard, R. K., Tong, Z. Y., Xiao, W., et al. (2015). NHANES 2009-2012 Findings: Association of Sexual Behaviors with Higher Prevalence of Oral Oncogenic Human Papillomavirus Infections in U.S. Men. *Cancer Res.* 75, 2468–2477. doi:10.1158/0008-5472.CAN-14-2843

Chen, H. J., Lin, C. M., Lee, C. Y., Shih, N. C., Amagaya, S., Lin, Y. C., et al. (2013). Phenethyl Isothiocyanate Suppresses EGF-Stimulated SAS Human Oral Squamous Carcinoma Cell Invasion by Targeting EGF Receptor Signaling. *Int. J. Oncol.* 43, 629–637. doi:10.3892/ijo.2013.1977

Chen, L., Lee, M. J., Li, H., and Yang, C. S. (1997). Absorption, Distribution, Elimination of tea Polyphenols in Rats. *Drug Metab. Dispos* 25, 1045–1050.

Chen, M. K., Liu, Y. T., Lin, J. T., Lin, C. C., Chuang, Y. C., Lo, Y. S., et al. (2019). Pinosylvin Reduced Migration and Invasion of Oral Cancer Carcinoma by Regulating Matrix Metalloproteinase-2 Expression and Extracellular Signal-Regulated Kinase Pathway. *Biomed. Pharmacother.* 117, 109160. doi:10.1016/j.biopha.2019.109160

Chen, X., Yan, B., Lou, H., Shen, Z., Tong, F., Zhai, A., et al. (2018). Immunological Network Analysis in HPV Associated Head and Neck Squamous Cancer and Implications for Disease Prognosis. *Mol. Immunol.* 96, 28–36. doi:10.1016/j.molimm.2018.02.005

Chien, M. H., Yang, W. E., Yang, Y. C., Ku, C. C., Lee, W. J., Tsai, M. Y., et al. (2020). Dual Targeting of the P38 MAPK-HO-1 Axis and cIAP1/XIAP by Demethoxycurcumin Triggers Caspase-Mediated Apoptotic Cell Death in Oral Squamous Cell Carcinoma Cells. *Cancers (Basel)* 12. doi:10.3390/cancers12030703

Chien, S.-Y., Hsieh, M.-J., Chen, C.-J., Yang, S.-F., and Chen, M.-K. (2015). Nobiletin Inhibits Invasion and Migration of Human Nasopharyngeal Carcinoma Cell Lines by Involving ERK1/2 and Transcriptional Inhibition of MMP-2. *Expert Opin. Ther. Targets* 19, 307–320. doi:10.1517/14728222.2014.992875

Chow, S. E., Chen, Y. W., Liang, C. A., Huang, Y. K., and Wang, J. S. (2012). Wogonin Induces Cross-Regulation between Autophagy and Apoptosis via a Variety of Akt Pathway in Human Nasopharyngeal Carcinoma Cells. *J. Cel Biochem* 113, 3476–3485. doi:10.1002/jcb.24224

Chung, C. H., Guthrie, V. B., Masica, D. L., Tokheim, C., Kang, H., Richmon, J., et al. (2015). Genomic Alterations in Head and Neck Squamous Cell Carcinoma Determined by Cancer Gene-Targeted Sequencing. *Ann. Oncol.* 26, 1216–1223. doi:10.1093/annonc/mdv109

Chung, H. H., Chen, M. K., Chang, Y. C., Yang, S. F., Lin, C. C., and Lin, C. W. (2017a). Inhibitory Effects of Leucaena Leucocephala on the Metastasis and Invasion of Human Oral Cancer Cells. *Environ. Toxicol.* 32, 1765–1774. doi:10.1002/tox.22399

Chung, T. T., Chuang, C. Y., Teng, Y. H., Hsieh, M. J., Lai, J. C., Chuang, Y. T., et al. (2017b). Tricetin Suppresses Human Oral Cancer Cell Migration by Reducing Matrix Metalloproteinase-9 Expression through the Mitogen-Activated Protein Kinase Signaling Pathway. *Environ. Toxicol.* 32, 2392–2399. doi:10.1002/tox.22452

Ciuffo, G. (1907). Innesto postiveo con filtrado di verrucae volgare. *Gior Ital. D Mal Ven* 48, 12–17.

Cohen, N., Fedewa, S., and Chen, A. Y. (2018). Epidemiology and Demographics of the Head and Neck Cancer Population. *Oral Maxillofac. Surg. Clin. North. Am.* 30, 381–395. doi:10.1016/j.coms.2018.06.001

Davis, R. J., Ferris, R. L., and Schmitt, N. C. (2016). Costimulatory and Coinhibitory Immune Checkpoint Receptors in Head and Neck Cancer: Unleashing Immune Responses through Therapeutic Combinations. *Cancers Head Neck* 1, 12. doi:10.1186/s41199-016-0013-x

De La Chapa, J. J., Singha, P. K., Lee, D. R., and Gonzales, C. B. (2018). Thymol Inhibits Oral Squamous Cell Carcinoma Growth via Mitochondria-Mediated Apoptosis. *J. Oral Pathol. Med.* 47, 674–682. doi:10.1111/jop.12735

De Lartigue, J. (2015). Rising to the Therapeutic challenge of Head and Neck Cancer. *J. Community Support. Oncol.* 13, 73–80. doi:10.12788/jcso.0111

De Martel, C., Ferlay, J., Franceschi, S., Vignat, J., Bray, F., Forman, D., et al. (2012). Global burden of Cancers Attributable to Infections in 2008: a Review and Synthetic Analysis. *Lancet Oncol.* 13, 607–615. doi:10.1016/S1470-2045(12)70137-7

De Martel, C., Georges, D., Bray, F., Ferlay, J., and Clifford, G. M. (2019). Global burden of Cancer Attributable to Infections in 2018: a Worldwide Incidence Analysis. *Lancet Glob. Health*.

De Stefani, E., Oreggia, F., Boffetta, P., Deneo-Pellegrini, H., Ronco, A., and Mendilaharsu, M. (2000). Tomatoes, Tomato-Rich Foods, Lycopene and

Cancer of the Upper Aerodigestive Tract: a Case-Control in Uruguay. *Oral Oncol.* 36, 47–53. doi:10.1016/s1368-8375(99)00050-0

De Villiers, E. M., Fauquet, C., Broker, T. R., Bernard, H. U., and Zur Hausen, H. (2004). Classification of Papillomaviruses. *Virology* 324, 17–27. doi:10.1016/j.virol.2004.03.033

Dent, P., Reardon, D. B., Park, J. S., Bowers, G., Logsdon, C., Valerie, K., et al. (1999). Radiation-induced Release of Transforming Growth Factor Alpha Activates the Epidermal Growth Factor Receptor and Mitogen-Activated Protein Kinase Pathway in Carcinoma Cells, Leading to Increased Proliferation and protection from Radiation-Induced Cell Death. *Mol. Biol. Cel* 10, 2493–2506. doi:10.1091/mbc.10.8.2493

Dickens, P., Srivastava, G., and Liu, Y. T. (1992). Human Papillomavirus 16/18 and Nasopharyngeal Carcinoma. *J. Clin. Pathol.* 45, 81–82. doi:10.1136/jcp.45.1.81

Elkashty, O. A., Ashry, R., Elghanam, G. A., Pham, H. M., Su, X., Stegen, C., et al. (2018). Broccoli Extract Improves Chemotherapeutic Drug Efficacy against Head-Neck Squamous Cell Carcinomas. *Med. Oncol.* 35, 124. doi:10.1007/s12032-018-1186-4

Fakhry, C., Westra, W. H., Li, S., Cmelak, A., Ridge, J. A., Pinto, H., et al. (2008). Improved Survival of Patients with Human Papillomavirus-Positive Head and Neck Squamous Cell Carcinoma in a Prospective Clinical Trial. *J. Natl. Cancer Inst.* 100, 261–269. doi:10.1093/jnci/djn011

Fakhry, C., Zhang, Q., Nguyen-Tan, P. F., Rosenthal, D., El-Naggar, A., Garden, A. S., et al. (2014). Human Papillomavirus and Overall Survival after Progression of Oropharyngeal Squamous Cell Carcinoma. *J. Clin. Oncol.* 32, 3365–3373. doi:10.1200/JCO.2014.55.1937

Fang, C. Y., Wu, C. Z., Chen, P. N., Chang, Y. C., Chuang, C. Y., Lai, C. T., et al. (2018). Antimetastatic Potentials of Salvianolic Acid A on Oral Squamous Cell Carcinoma by Targeting MMP-2 and the C-Raf/MEK/ERK Pathway. *Environ. Toxicol.* 33, 545–554. doi:10.1002/tox.22542

Fang, J., Zhou, Q., Liu, L. Z., Xia, C., Hu, X., Shi, X., et al. (2007). Apigenin Inhibits Tumor Angiogenesis through Decreasing HIF-1alpha and VEGF Expression. *Carcinogenesis* 28, 858–864. doi:10.1093/carcin/bgl205

Ferris, R. L., Blumenschein, G., Jr., Fayette, J., Guigay, J., Colevas, A. D., Licitra, L., et al. (2018). Nivolumab vs Investigator's Choice in Recurrent or Metastatic Squamous Cell Carcinoma of the Head and Neck: 2-year Long-Term Survival Update of CheckMate 141 with Analyses by Tumor PD-L1 Expression. *Oral Oncol.* 81, 45–51. doi:10.1016/j.oraloncology.2018.04.008

Fleming, J. C., Woo, J., Moutasim, K., Mellone, M., Frampton, S. J., Mead, A., et al. (2019). HPV, Tumour Metabolism and Novel Target Identification in Head and Neck Squamous Cell Carcinoma. *Br. J. Cancer* 120, 356–367. doi:10.1038/s41416-018-0364-7

Flynn, M. B., Maguire, S., Martinez, S., and Tesmer, T. (1999). Primary Squamous Cell Carcinoma of the Parotid Gland: the Importance of Correct Histological Diagnosis. *Ann. Surg. Oncol.* 6, 768–770. doi:10.1007/s10434-999-0768-y

Folgueras, A. R., Pendas, A. M., Sanchez, L. M., and Lopez-Otin, C. (2004). Matrix Metalloproteinases in Cancer: From New Functions to Improved Inhibition Strategies. *Int. J. Dev. Biol.* 48, 411–424.

Forastiere, A. A., Zhang, Q., Weber, R. S., Maor, M. H., Goepfert, H., Pajak, T. F., et al. (2013). Long-term Results of RTOG 91-11: a Comparison of Three Nonsurgical Treatment Strategies to Preserve the Larynx in Patients with Locally Advanced Larynx Cancer. *J. Clin. Oncol.* 31, 845–852. doi:10.1200/JCO.2012.43.6097

Franceschi, S., Barra, S., La Vecchia, C., Bidoli, E., Negri, E., and Talamini, R. (1992). Risk Factors for Cancer of the Tongue and the Mouth. A Case-Control Study from Northern Italy. *Cancer* 70, 2227–2233. doi:10.1002/1097-0142(19921101)70:9<2227::aid-cncr2820700902>3.0.co;2-z

Franceschi, S., Muñoz, N., Bosch, X. F., Snijders, P. J., and Walboomers, J. M. (1996). Human Papillomavirus and Cancers of the Upper Aerodigestive Tract: a Review of Epidemiological and Experimental Evidence. *Cancer Epidemiol. Biomarkers Prev.* 5, 567–575.

Freedman, N. D., Schatzkin, A., Leitzmann, M. F., Hollenbeck, A. R., and Abnet, C. C. (2007). Alcohol and Head and Neck Cancer Risk in a Prospective Study. *Br. J. Cancer* 96, 1469–1474. doi:10.1038/sj.bjc.6603713

Frisch, M., and Biggar, R. J. (1999). Aetiological Parallel between Tonsillar and Anogenital Squamous-Cell Carcinomas. *Lancet* 354, 1442–1443. doi:10.1016/S0140-6736(99)92824-6

Fu, T. C., Hughes, J. P., Feng, Q., Hulbert, A., Hawes, S. E., Xi, L. F., et al. (2015). Epidemiology of Human Papillomavirus Detected in the Oral Cavity and Fingernails of Mid-adult Women. *Sex. Transm. Dis.* 42, 677–685. doi:10.1097/OLQ.0000000000000362

Gale, N., Michaels, L., Luzar, B., Poljak, M., Zidar, N., Fischinger, J., et al. (2009). Current Review on Squamous Intraepithelial Lesions of the Larynx. *Histopathology* 54, 639–656. doi:10.1111/j.1365-2559.2008.03111.x

Gao, G., Wang, J., Kasperbauer, J. L., Tombers, N. M., Teng, F., Gou, H., et al. (2019). Whole Genome Sequencing Reveals Complexity in Both HPV Sequences Present and HPV Integrations in HPV-Positive Oropharyngeal Squamous Cell Carcinomas. *BMC Cancer* 19, 352. doi:10.1186/s12885-019-5536-1

Garewal, H. S., Katz, R. V., Meyskens, F., Pitcock, J., Morse, D., Friedman, S., et al. (1999). Beta-carotene Produces Sustained Remissions in Patients with Oral Leukoplakia: Results of a Multicenter Prospective Trial. *Arch. Otolaryngol. Head Neck Surg.* 125, 1305–1310. doi:10.1001/archotol.125.12.1305

Garewal, H. S., Meyskens, F. L., Jr., Killen, D., Reeves, D., Kiersch, T. A., Elletson, H., et al. (1990). Response of Oral Leukoplakia to Beta-Carotene. *J. Clin. Oncol.* 8, 1715–1720. doi:10.1200/JCO.1990.8.10.1715

Gartner, L. P. (1994). Oral Anatomy and Tissue Types. *Semin. Dermatol.* 13, 68–73.

Garza-Morales, R., Perez-Trujillo, J. J., Martinez-Jaramillo, E., Saucedo-Cardenas, O., Loera-Arias, M. J., Garcia-Garcia, A., et al. (2019). A DNA Vaccine Encoding SA-4-1BBL Fused to HPV-16 E7 Antigen Has Prophylactic and Therapeutic Efficacy in a Cervical Cancer Mouse Model. *Cancers (Basel)* 11. doi:10.3390/cancers11010096

Gaykalova, D. A., Manola, J. B., Ozawa, H., Zizkova, V., Morton, K., Bishop, J. A., et al. (2015). NF-κB and Stat3 Transcription Factor Signatures Differentiate HPV-Positive and HPV-Negative Head and Neck Squamous Cell Carcinoma. *Int. J. Cancer* 137, 1879–1889. doi:10.1002/ijc.29558

Gerle, M., Medina, T. P., Gülses, A., Chu, H., Naujokat, H., Wiltfang, J., et al. (2018). Acid Sphingomyelinase Activity as an Indicator of the Cell Stress in HPV-Positive and HPV-Negative Head and Neck Squamous Cell Carcinoma. *Med. Oncol.* 35, 58. doi:10.1007/s12032-018-1117-4

Ghannam, M. G., and Singh, P. (2021). "Anatomy, Head and Neck, Salivary Glands," in *StatPearls*. (Treasure Island (FL)).

Gillison, M. L., Chaturvedi, A. K., Anderson, W. F., and Fakhry, C. (2015). Epidemiology of Human Papillomavirus-Positive Head and Neck Squamous Cell Carcinoma. *J. Clin. Oncol.* 33, 3235–3242. doi:10.1200/JCO.2015.61.6995

Gillison, M. L., D'souza, G., Westra, W., Sugar, E., Xiao, W., Begum, S., et al. (2008). Distinct Risk Factor Profiles for Human Papillomavirus Type 16-positive and Human Papillomavirus Type 16-negative Head and Neck Cancers. *J. Natl. Cancer Inst.* 100, 407–420. doi:10.1093/jnci/djn025

Gillison, M. L., Koch, W. M., Capone, R. B., Spafford, M., Westra, W. H., Wu, L., et al. (2000). Evidence for a Causal Association between Human Papillomavirus and a Subset of Head and Neck Cancers. *J. Natl. Cancer Inst.* 92, 709–720. doi:10.1093/jnci/92.9.709

Gilyoma, J. M., Rambau, P. F., Masalu, N., Kayange, N. M., and Chalya, P. L. (2015). Head and Neck Cancers: a Clinico-Pathological Profile and Management Challenges in a Resource-Limited Setting. *BMC Res. Notes* 8, 772. doi:10.1186/s13104-015-1773-9

Gissmann, L., Diehl, V., Schultz-Coulon, H. J., and Zur Hausen, H. (1982). Molecular Cloning and Characterization of Human Papilloma Virus DNA Derived from a Laryngeal Papilloma. *J. Virol.* 44, 393–400. doi:10.1128/JVI.44.1.393-400.1982

Gissmann, L., and Zur Hausen, H. (1980). Partial Characterization of Viral DNA from Human Genital Warts (Condylomata Acuminata). *Int. J. Cancer* 25, 605–609. doi:10.1002/ijc.2910250509

Gletsou, E., Papadas, T. A., Baliou, E., Tsiambas, E., Ragos, V., Armata, I. E., et al. (2018). HPV Infection in Oropharyngeal Squamous Cell Carcinomas: Correlation with Tumor Size. *J. BUON* 23, 433–438.

Globocan (2020). "*Global Cancer Observatory*". Lyon, France: IARC.

Goldenberg, D., Begum, S., Westra, W. H., Khan, Z., Sciubba, J., Pai, S. I., et al. (2008). Cystic Lymph Node Metastasis in Patients with Head and Neck Cancer: An HPV-Associated Phenomenon. *Head Neck* 30, 898–903. doi:10.1002/hed.20796

Gupta, S., Kumar, P., Kaur, H., Sharma, N., Gupta, S., Saluja, D., et al. (2018). Constitutive Activation and Overexpression of NF-κB/c-Rel in Conjunction with P50 Contribute to Aggressive Tongue Tumorigenesis. *Oncotarget* 9, 33011–33029. doi:10.18632/oncotarget.26041

Gupta, S., Kumar, P., Kaur, H., Sharma, N., Saluja, D., Bharti, A. C., et al. (2015). Selective Participation of C-Jun with Fra-2/c-Fos Promotes Aggressive Tumor Phenotypes and Poor Prognosis in Tongue Cancer. *Sci. Rep.* 5, 16811. doi:10.1038/srep16811

Haddad, R. I., and Shin, D. M. (2008). Recent Advances in Head and Neck Cancer. *N. Engl. J. Med.* 359, 1143–1154. doi:10.1056/NEJMra0707975

Hajek, M., Sewell, A., Kaech, S., Burtness, B., Yarbrough, W. G., and Issaeva, N. (2017). TRAF3/CYLD Mutations Identify a Distinct Subset of Human Papillomavirus-Associated Head and Neck Squamous Cell Carcinoma. *Cancer* 123, 1778–1790. doi:10.1002/cncr.30570

Hammarstedt, L., Lindquist, D., Dahlstrand, H., Romanitan, M., Dahlgren, L. O., Joneberg, J., et al. (2006). Human Papillomavirus as a Risk Factor for the Increase in Incidence of Tonsillar Cancer. *Int. J. Cancer* 119, 2620–2623. doi:10.1002/ijc.22177

Hartmann, J. T., and Lipp, H. P. (2003). Toxicity of Platinum Compounds. *Expert Opin. Pharmacother.* 4, 889–901. doi:10.1517/14656566.4.6.889

Hashim, D., Genden, E., Posner, M., Hashibe, M., and Boffetta, P. (2019). Head and Neck Cancer Prevention: from Primary Prevention to Impact of Clinicians on Reducing burden. *Ann. Oncol.* 30, 744–756. doi:10.1093/annonc/mdz084

Havel, J. J., Chowell, D., and Chan, T. A. (2019). The Evolving Landscape of Biomarkers for Checkpoint Inhibitor Immunotherapy. *Nat. Rev. Cancer* 19, 133–150. doi:10.1038/s41568-019-0116-x

Heidingsfield, M. (1901). Condylomata Acuminata Linguata. *J. Cutan. Genitorium Dis.* 19, 226–234.

Hellquist, H., Lundgren, J., and Olofsson, J. (1982). Hyperplasia, Keratosis, Dysplasia and Carcinoma *In Situ* of the Vocal Cords-Aa Follow-Up Study. *Clin. Otolaryngol. Allied Sci.* 7, 11–27. doi:10.1111/j.1365-2273.1982.tb01557.x

Hemminki, K., Dong, C., and Frisch, M. (2000). Tonsillar and Other Upper Aerodigestive Tract Cancers Among Cervical Cancer Patients and Their Husbands. *Eur. J. Cancer Prev.* 9, 433–437. doi:10.1097/00008469-200012000-00010

Ho, A. S., Kraus, D. H., Ganly, I., Lee, N. Y., Shah, J. P., and Morris, L. G. (2014). Decision Making in the Management of Recurrent Head and Neck Cancer. *Head Neck* 36, 144–151. doi:10.1002/hed.23227

Ho, Y. C., Yang, S. F., Peng, C. Y., Chou, M. Y., and Chang, Y. C. (2007). Epigallocatechin-3-gallate Inhibits the Invasion of Human Oral Cancer Cells and Decreases the Productions of Matrix Metalloproteinases and Urokinase-Plasminogen Activator. *J. Oral Pathol. Med.* 36, 588–593. doi:10.1111/j.1600-0714.2007.00588.x

Ho, Y. T., Yang, J. S., Li, T. C., Lin, J. J., Lin, J. G., Lai, K. C., et al. (2009). Berberine Suppresses *In Vitro* Migration and Invasion of Human SCC-4 Tongue Squamous Cancer Cells through the Inhibitions of FAK, IKK, NF-kappaB, U-PA and MMP-2 and -9. *Cancer Lett.* 279, 155–162. doi:10.1016/j.canlet.2009.01.033

Hong, W. K., Endicott, J., Itri, L. M., Doos, W., Batsakis, J. G., Bell, R., et al. (1986). 13-cis-retinoic Acid in the Treatment of Oral Leukoplakia. *N. Engl. J. Med.* 315, 1501–1505. doi:10.1056/NEJM198612113152401

Hong, W. K., Lippman, S. M., Itri, L. M., Karp, D. D., Lee, J. S., Byers, R. M., et al. (1990). Prevention of Second Primary Tumors with Isotretinoin in Squamous-Cell Carcinoma of the Head and Neck. *N. Engl. J. Med.* 323, 795–801. doi:10.1056/NEJM199009203231205

Hou, H., Li, D., Cheng, D., Li, L., Liu, Y., and Zhou, Y. (2013). Cellular Redox Status Regulates Emodin-Induced Radiosensitization of Nasopharyngeal Carcinoma Cells *In Vitro* and *In Vivo*. *J. Pharm. (Cairo)* 2013, 218297.

Houlihan, C. F., Baisley, K., Bravo, I. G., Pavón, M. A., Changalucha, J., Kapiga, S., et al. (2019). Human Papillomavirus DNA Detected in Fingertip, Oral and Bathroom Samples from Unvaccinated Adolescent Girls in Tanzania. *Sex. Transm. Infect.* 95, 374–379. doi:10.1136/sextrans-2018-053756

Hseu, Y. C., Wu, C. R., Chang, H. W., Kumar, K. J., Lin, M. K., Chen, C. S., et al. (2011). Inhibitory Effects of Physalis Angulata on Tumor Metastasis and Angiogenesis. *J. Ethnopharmacol* 135, 762–771. doi:10.1016/j.jep.2011.04.016

Hsin, C. H., Huang, C. C., Chen, P. N., Hsieh, Y. S., Yang, S. F., Ho, Y. T., et al. (2017). Rubus Idaeus Inhibits Migration and Invasion of Human Nasopharyngeal Carcinoma Cells by Suppression of MMP-2 through Modulation of the ERK1/2 Pathway. *Am. J. Chin. Med.* 45, 1557–1572. doi:10.1142/S0192415X17500847

Hsin, C. H., Wu, B. C., Chuang, C. Y., Yang, S. F., Hsieh, Y. H., Ho, H. Y., et al. (2013). Selaginella Tamariscina Extract Suppresses TPA-Induced Invasion and Metastasis through Inhibition of MMP-9 in Human Nasopharyngeal Carcinoma HONE-1 Cells. *BMC Complement. Altern. Med.* 13, 234. doi:10.1186/1472-6882-13-234

Hsu, H. K., Brown, T. T., Li, X., Young, S., Cranston, R. D., D'souza, G., et al. (2015). Association between Free Testosterone Levels and Anal Human Papillomavirus Types 16/18 Infections in a Cohort of Men Who Have Sex with Men. *PLoS One* 10, e0119447. doi:10.1371/journal.pone.0119447

Hsu, P. C., Cheng, C. F., Hsieh, P. C., Chen, Y. H., Kuo, C. Y., and Sytwu, H. K. (2020). Chrysophanol Regulates Cell Death, Metastasis, and Reactive Oxygen Species Production in Oral Cancer Cell Lines. *Evid. Based Complement. Alternat Med.* 2020, 5867064. doi:10.1155/2020/5867064

Huang, C., and Yu, Y. (2017). Synergistic Cytotoxicity of β-Elemene and Cisplatin in Gingival Squamous Cell Carcinoma by Inhibition of STAT3 Signaling Pathway. *Med. Sci. Monit.* 23, 1507–1513. doi:10.12659/msm.903783

Huang, X. Z., Wang, J., Huang, C., Chen, Y. Y., Shi, G. Y., Hu, Q. S., et al. (2008). Emodin Enhances Cytotoxicity of Chemotherapeutic Drugs in Prostate Cancer Cells: the Mechanisms Involve ROS-Mediated Suppression of Multidrug Resistance and Hypoxia Inducible Factor-1. *Cancer Biol. Ther.* 7, 468–475. doi:10.4161/cbt.7.3.5457

Huang, Y. W., Chuang, C. Y., Hsieh, Y. S., Chen, P. N., Yang, S. F., Shih-Hsuan-Lin, L., et al. (2017). Rubus Idaeus Extract Suppresses Migration and Invasion of Human Oral Cancer by Inhibiting MMP-2 through Modulation of the Erk1/2 Signaling Pathway. *Environ. Toxicol.* 32, 1037–1046. doi:10.1002/tox.22302

Hung, C. M., Chang, C. C., Lin, C. W., Ko, S. Y., and Hsu, Y. C. (2013). Cucurbitacin E as Inducer of Cell Death and Apoptosis in Human Oral Squamous Cell Carcinoma Cell Line SAS. *Int. J. Mol. Sci.* 14, 17147–17156. doi:10.3390/ijms140817147

Iarc, W. G. O. T. E. O. C. R. T. H. (2012). Personal Habits and Indoor Combustions. Volume 100 E. A Review of Human Carcinogens. *IARC Monogr. Eval. Carcinog Risks Hum.* 100, 1–538.

Iarc, W. G. O. T. E. O. C. R. T. H. (2004). Tobacco Smoke and Involuntary Smoking. *IARC Monogr. Eval. Carcinog Risks Hum.* 83, 1–1438.

Imai, K., Suga, K., and Nakachi, K. (1997). Cancer-preventive Effects of Drinking green tea Among a Japanese Population. *Prev. Med.* 26, 769–775. doi:10.1006/pmed.1997.0242

Ishiji, T., Lace, M. J., Parkkinen, S., Anderson, R. D., Haugen, T. H., Cripe, T. P., et al. (1992). Transcriptional Enhancer Factor (TEF)-1 and its Cell-specific Co-activator Activate Human Papillomavirus-16 E6 and E7 Oncogene Transcription in Keratinocytes and Cervical Carcinoma Cells. *EMBO J.* 11, 2271–2281. doi:10.1002/j.1460-2075.1992.tb05286.x

Issing, W. J., Struck, R., and Naumann, A. (1996). Long-term Follow-Up of Larynx Leukoplakia under Treatment with Retinyl Palmitate. *Head Neck* 18, 560–565. doi:10.1002/(sici)1097-0347(199611/12)18:6<560::aid-hed11>3.0.co;2-c

Jadassohn (1896). Sind die verrucae vulgares ubertragbar? *Vehandel D Deutsch Dem Gesellsch* 5, 497–512.

Jégoux, F., Métreau, A., Louvel, G., and Bedfert, C. (2013). Paranasal Sinus Cancer. *Eur. Ann. Otorhinolaryngol. Head Neck Dis.* 130, 327–335. doi:10.1016/j.anorl.2012.07.007

Jenson, A. B., Sommer, S., Payling-Wright, C., Pass, F., Link, C. C., Jr., and Lancaster, W. D. (1982). Human Papillomavirus. Frequency and Distribution in Plantar and Common Warts. *Lab. Invest.* 47, 491–497.

Jin, L., Miao, J., Liu, Y., Li, X., Jie, Y., Niu, Q., et al. (2017). Icaritin Induces Mitochondrial Apoptosis by Up-Regulating miR-124 in Human Oral Squamous Cell Carcinoma Cells. *Biomed. Pharmacother.* 85, 287–295. doi:10.1016/j.biopha.2016.11.023

Jyothirmayi, R., Ramadas, K., Varghese, C., Jacob, R., Nair, M. K., and Sankaranarayanan, R. (1996). Efficacy of Vitamin A in the Prevention of Loco-Regional Recurrence and Second Primaries in Head and Neck Cancer. *Eur. J. Cancer B Oral Oncol.* 32B, 373–376. doi:10.1016/s0964-1955(96)00010-3

Kalu, N. N., Mazumdar, T., Peng, S., Shen, L., Sambandam, V., Rao, X., et al. (2017). Genomic Characterization of Human Papillomavirus-Positive and -negative Human Squamous Cell Cancer Cell Lines. *Oncotarget* 8, 86369–86383. doi:10.18632/oncotarget.21174

Kapil, U., Singh, P., Bahadur, S., Shukla, N. K., Dwivedi, S., Pathak, P., et al. (2003). Association of Vitamin A, Vitamin C and Zinc with Laryngeal Cancer. *Indian J. Cancer* 40, 67–70.

Kapoor, V., Aggarwal, S., and Das, S. N. (2016). 6-Gingerol Mediates its Anti Tumor Activities in Human Oral and Cervical Cancer Cell Lines through Apoptosis and Cell Cycle Arrest. *Phytother Res.* 30, 588–595. doi:10.1002/ptr.5561

Katiyar, C., Gupta, A., Kanjilal, S., and Katiyar, S. (2012). Drug Discovery from Plant Sources: An Integrated Approach. *Ayu* 33, 10–19. doi:10.4103/0974-8520.100295

Kaugars, G. E., Silverman, S., Jr., Lovas, J. G., Brandt, R. B., Riley, W. T., Dao, Q., et al. (1994). A Clinical Trial of Antioxidant Supplements in the Treatment of Oral Leukoplakia. *Oral Surg. Oral Med. Oral Pathol.* 78, 462–468. doi:10.1016/0030-4220(94)90039-6

Khafif, A., Schantz, S. P., Al-Rawi, M., Edelstein, D., and Sacks, P. G. (1998). Green tea Regulates Cell Cycle Progression in Oral Leukoplakia. *Head Neck* 20, 528–534. doi:10.1002/(sici)1097-0347(199809)20:6<528::aid-hed7>3.0.co;2-3

Kirnbauer, R., Booy, F., Cheng, N., Lowy, D. R., and Schiller, J. T. (1992). Papillomavirus L1 Major Capsid Protein Self-Assembles into Virus-like Particles that Are Highly Immunogenic. *Proc. Natl. Acad. Sci. U S A.* 89, 12180–12184. doi:10.1073/pnas.89.24.12180

Klein, S. L. (2000). The Effects of Hormones on Sex Differences in Infection: from Genes to Behavior. *Neurosci. Biobehav Rev.* 24, 627–638. doi:10.1016/s0149-7634(00)00027-0

Knobloch, T. J., Ryan, N. M., Bruschweiler-Li, L., Wang, C., Bernier, M. C., Somogyi, A., et al. (2019). Metabolic Regulation of Glycolysis and AMP Activated Protein Kinase Pathways during Black Raspberry-Mediated Oral Cancer Chemoprevention. *Metabolites* 9. doi:10.3390/metabo9070140

Koehn, F. E., and Carter, G. T. (2005). The Evolving Role of Natural Products in Drug Discovery. *Nat. Rev. Drug Discov.* 4, 206–220. doi:10.1038/nrd1657

Kofler, B., Laban, S., Busch, C. J., Lörincz, B., and Knecht, R. (2014). New Treatment Strategies for HPV-Positive Head and Neck Cancer. *Eur. Arch. Otorhinolaryngol.* 271, 1861–1867. doi:10.1007/s00405-013-2603-0

Koneva, L. A., Zhang, Y., Virani, S., Hall, P. B., Mchugh, J. B., Chepeha, D. B., et al. (2018). HPV Integration in HNSCC Correlates with Survival Outcomes, Immune Response Signatures, and Candidate Drivers. *Mol. Cancer Res.* 16, 90–102. doi:10.1158/1541-7786.MCR-17-0153

Kunnumakkara, A. B., Bordoloi, D., Harsha, C., Banik, K., Gupta, S. C., and Aggarwal, B. B. (2017). Curcumin Mediates Anticancer Effects by Modulating Multiple Cell Signaling Pathways. *Clin. Sci. (Lond)* 131, 1781–1799. doi:10.1042/CS20160935

Kuo, Y. Y., Lin, H. P., Huo, C., Su, L. C., Yang, J., Hsiao, P. H., et al. (2013). Caffeic Acid Phenethyl Ester Suppresses Proliferation and Survival of TW2.6 Human Oral Cancer Cells via Inhibition of Akt Signaling. *Int. J. Mol. Sci.* 14, 8801–8817. doi:10.3390/ijms14058801

Kuriakose, M. A., Ramdas, K., Dey, B., Iyer, S., Rajan, G., Elango, K. K., et al. (2016). A Randomized Double-Blind Placebo-Controlled Phase IIB Trial of Curcumin in Oral Leukoplakia. *Cancer Prev. Res. (Phila)* 9, 683–691. doi:10.1158/1940-6207.CAPR-15-0390

Kuss, I., Donnenberg, A. D., Gooding, W., and Whiteside, T. L. (2003). Effector CD8+CD45RO-CD27-T Cells Have Signalling Defects in Patients with Squamous Cell Carcinoma of the Head and Neck. *Br. J. Cancer* 88, 223–230. doi:10.1038/sj.bjc.6600694

Lagoa, R., Samhan-Arias, A. K., and Gutierrez-Merino, C. (2017). Correlation between the Potency of Flavonoids for Cytochrome C Reduction and Inhibition of Cardiolipin-Induced Peroxidase Activity. *Biofactors* 43, 451–468. doi:10.1002/biof.1357

Langendijk, J. A., Doornaert, P., Verdonck-De Leeuw, I. M., Leemans, C. R., Aaronson, N. K., and Slotman, B. J. (2008). Impact of Late Treatment-Related Toxicity on Quality of Life Among Patients with Head and Neck Cancer Treated with Radiotherapy. *J. Clin. Oncol.* 26, 3770–3776. doi:10.1200/JCO.2007.14.6647

Lee, E., Han, A. R., Nam, B., Kim, Y. R., Jin, C. H., Kim, J. B., et al. (2020). Moscatilin Induces Apoptosis in Human Head and Neck Squamous Cell Carcinoma Cells via JNK Signaling Pathway. *Molecules* 25. doi:10.3390/molecules25040901

Lee, H. E., Shin, J. A., Jeong, J. H., Jeon, J. G., Lee, M. H., and Cho, S. D. (2016). Anticancer Activity of Ashwagandha against Human Head and Neck Cancer Cell Lines. *J. Oral Pathol. Med.* 45, 193–201. doi:10.1111/jop.12353

Lee, H. Z., Liu, W. Z., Hsieh, W. T., Tang, F. Y., Chung, J. G., and Leung, H. W. (2009). Oxidative Stress Involvement in Physalis Angulata-Induced Apoptosis in Human Oral Cancer Cells. *Food Chem. Toxicol.* 47, 561–570. doi:10.1016/j.fct.2008.12.013

Lee, Y. J., Park, B. S., Park, H. R., Yu, S. B., Kang, H. M., and Kim, I. R. (2017). XIAP Inhibitor Embelin Induces Autophagic and Apoptotic Cell Death in Human Oral Squamous Cell Carcinoma Cells. *Environ. Toxicol.* 32, 2371–2378. doi:10.1002/tox.22450

Li, C. J., Zhang, L. J., Dezube, B. J., Crumpacker, C. S., and Pardee, A. B. (1993). Three Inhibitors of Type 1 Human Immunodeficiency Virus Long Terminal Repeat-Directed Gene Expression and Virus Replication. *Proc. Natl. Acad. Sci. U S A.* 90, 1839–1842. doi:10.1073/pnas.90.5.1839

Li, H. C., Yashiki, S., Sonoda, J., Lou, H., Ghosh, S. K., Byrnes, J. J., et al. (2000). Green tea Polyphenols Induce Apoptosis *In Vitro* in Peripheral Blood T Lymphocytes of Adult T-Cell Leukemia Patients. *Jpn. J. Cancer Res.* 91, 34–40. doi:10.1111/j.1349-7006.2000.tb00857.x

Li, L. K., Rola, A. S., Kaid, F. A., Ali, A. M., and Alabsi, A. M. (2016). Goniothalamin Induces Cell Cycle Arrest and Apoptosis in H400 Human Oral Squamous Cell Carcinoma: A Caspase-dependent Mitochondrial-Mediated Pathway with Downregulation of NF-Kβ. *Arch. Oral Biol.* 64, 28–38. doi:10.1016/j.archoralbio.2015.12.002

Li, N., Sun, Z., Han, C., and Chen, J. (1999). The Chemopreventive Effects of tea on Human Oral Precancerous Mucosa Lesions. *Proc. Soc. Exp. Biol. Med.* 220, 218–224. doi:10.1046/j.1525-1373.1999.d01-37.x

Liang, Y. C., Chen, Y. C., Lin, Y. L., Lin-Shiau, S. Y., Ho, C. T., and Lin, J. K. (1999a). Suppression of Extracellular Signals and Cell Proliferation by the Black tea Polyphenol, Theaflavin-3,3'-Digallate. *Carcinogenesis* 20, 733–736. doi:10.1093/carcin/20.4.733

Liang, Y. C., Lin-Shiau, S. Y., Chen, C. F., and Lin, J. K. (1999b). Inhibition of Cyclin-dependent Kinases 2 and 4 Activities as Well as Induction of Cdk Inhibitors P21 and P27 during Growth Arrest of Human Breast Carcinoma Cells by (-)-Epigallocatechin-3-Gallate. *J. Cel Biochem* 75, 1–12. doi:10.1002/(sici)1097-4644(19991001)75:1<1::aid-jcb1>3.0.co;2-n

Liang, Y. C., Lin-Shiau, S. Y., Chen, C. F., and Lin, J. K. (1997). Suppression of Extracellular Signals and Cell Proliferation through EGF Receptor Binding by (-)-epigallocatechin Gallate in Human A431 Epidermoid Carcinoma Cells. *J. Cel Biochem* 67, 55–65. doi:10.1002/(sici)1097-4644(19971001)67:1<55::aid-jcb6>3.0.co;2-v

Liao, M. Y., Chuang, C. Y., Hsieh, M. J., Chou, Y. E., Lin, C. W., Chen, W. R., et al. (2018). Antimetastatic Effects of Eclipta Prostrata Extract on Oral Cancer Cells. *Environ. Toxicol.* 33, 923–930. doi:10.1002/tox.22577

Liberto, M., and Cobrinik, D. (2000). Growth Factor-dependent Induction of p21(CIP1) by the green tea Polyphenol, Epigallocatechin Gallate. *Cancer Lett.* 154, 151–161. doi:10.1016/s0304-3835(00)00378-5

Licitra, L., Perrone, F., Bossi, P., Suardi, S., Mariani, L., Artusi, R., et al. (2006). High-risk Human Papillomavirus Affects Prognosis in Patients with Surgically Treated Oropharyngeal Squamous Cell Carcinoma. *J. Clin. Oncol.* 24, 5630–5636. doi:10.1200/JCO.2005.04.6136

Lin, C. C., Yang, J. S., Chen, J. T., Fan, S., Yu, F. S., Yang, J. L., et al. (2007). Berberine Induces Apoptosis in Human HSC-3 Oral Cancer Cells via Simultaneous Activation of the Death Receptor-Mediated and Mitochondrial Pathway. *Anticancer Res.* 27, 3371–3378.

Lin, C. W., Chin, H. K., Lee, S. L., Chiu, C. F., Chung, J. G., Lin, Z. Y., et al. (2019). Ursolic Acid Induces Apoptosis and Autophagy in Oral Cancer Cells. *Environ. Toxicol.* 34, 983–991. doi:10.1002/tox.22769

Lin, F. Y., Hsieh, Y. H., Yang, S. F., Chen, C. T., Tang, C. H., Chou, M. Y., et al. (2015). Resveratrol Suppresses TPA-Induced Matrix Metalloproteinase-9 Expression through the Inhibition of MAPK Pathways in Oral Cancer Cells. *J. Oral Pathol. Med.* 44, 699–706. doi:10.1111/jop.12288

Lind, P. O. (1987). Malignant Transformation in Oral Leukoplakia. *Scand. J. Dent Res.* 95, 449–455. doi:10.1111/j.1600-0722.1987.tb01959.x

Lippman, S. M., Batsakis, J. G., Toth, B. B., Weber, R. S., Lee, J. J., Martin, J. W., et al. (1993). Comparison of Low-Dose Isotretinoin with Beta Carotene to Prevent Oral Carcinogenesis. *N. Engl. J. Med.* 328, 15–20. doi:10.1056/NEJM199301073280103

Lippman, S. M., Kessler, J. F., Al-Sarraf, M., Alberts, D. S., Itri, L. M., Mattox, D., et al. (1988). Treatment of Advanced Squamous Cell Carcinoma of the Head and Neck with Isotretinoin: a Phase II Randomized Trial. *Invest. New Drugs* 6, 51–56. doi:10.1007/BF00170781

Liu, G., Wu, D., Liang, X., Yue, H., and Cui, Y. (2015). Mechanisms and *In Vitro* Effects of Cepharanthine Hydrochloride: Classification Analysis of the Drug-Induced Differentially-Expressed Genes of Human Nasopharyngeal Carcinoma Cells. *Oncol. Rep.* 34, 2002–2010. doi:10.3892/or.2015.4193

Liu, T., Sun, X., and Cao, Z. (2019). Shikonin-induced Necroptosis in Nasopharyngeal Carcinoma Cells via ROS Overproduction and

Upregulation of RIPK1/RIPK3/MLKL Expression. *Onco Targets Ther.* 12, 2605–2614. doi:10.2147/OTT.S200740

Liu, T. B., Zheng, Z. H., Pan, J., Pan, L. L., and Chen, L. H. (2017). Prognostic Role of Plasma Epstein-Barr Virus DNA Load for Nasopharyngeal Carcinoma: a Meta-Analysis. *Clin. Invest. Med.* 40, E1–E12. doi:10.25011/cim.v40i1.28049

Louvanto, K., Sarkola, M., Rintala, M., Syrjänen, K., Grenman, S., and Syrjänen, S. (2017). Breast Milk Is a Potential Vehicle for Human Papillomavirus Transmission to Oral Mucosa of the Spouse. *Pediatr. Infect. Dis. J.* 36, 627–630. doi:10.1097/INF.0000000000001546

Lu, K. W., Chen, J. C., Lai, T. Y., Yang, J. S., Weng, S. W., Ma, Y. S., et al. (2011). Gypenosides Inhibits Migration and Invasion of Human Oral Cancer SAS Cells through the Inhibition of Matrix Metalloproteinase-2 -9 and Urokinase-Plasminogen by ERK1/2 and NF-Kappa B Signaling Pathways. *Hum. Exp. Toxicol.* 30, 406–415. doi:10.1177/0960327110372405

Lubin, J. H., Purdue, M., Kelsey, K., Zhang, Z. F., Winn, D., Wei, Q., et al. (2009). Total Exposure and Exposure Rate Effects for Alcohol and Smoking and Risk of Head and Neck Cancer: a Pooled Analysis of Case-Control Studies. *Am. J. Epidemiol.* 170, 937–947. doi:10.1093/aje/kwp222

Macha, M. A., Matta, A., Chauhan, S. S., Siu, K. W., and Ralhan, R. (2011). Guggulsterone (GS) Inhibits Smokeless Tobacco and Nicotine-Induced NF-Kb and STAT3 Pathways in Head and Neck Cancer Cells. *Carcinogenesis* 32, 368–380. doi:10.1093/carcin/bgq278

Maitland, N. J., Bromidge, T., Cox, M. F., Crane, I. J., Prime, S. S., and Scully, C. (1989). Detection of Human Papillomavirus Genes in Human Oral Tissue Biopsies and Cultures by Polymerase Chain Reaction. *Br. J. Cancer* 59, 698–703. doi:10.1038/bjc.1989.146

Mallery, S. R., Tong, M., Shumway, B. S., Curran, A. E., Larsen, P. E., Ness, G. M., et al. (2014). Topical Application of a Mucoadhesive Freeze-Dried Black Raspberry Gel Induces Clinical and Histologic Regression and Reduces Loss of Heterozygosity Events in Premalignant Oral Intraepithelial Lesions: Results from a Multicentered, Placebo-Controlled Clinical Trial. *Clin. Cancer Res.* 20, 1910–1924. doi:10.1158/1078-0432.CCR-13-3159

Marier, J. F., Vachon, P., Gritsas, A., Zhang, J., Moreau, J. P., and Ducharme, M. P. (2002). Metabolism and Disposition of Resveratrol in Rats: Extent of Absorption, Glucuronidation, and Enterohepatic Recirculation Evidenced by a Linked-Rat Model. *J. Pharmacol. Exp. Ther.* 302, 369–373. doi:10.1124/jpet.102.033340

Marquard, F. E., and Jücker, M. (2020). PI3K/AKT/mTOR Signaling as a Molecular Target in Head and Neck Cancer. *Biochem. Pharmacol.* 172, 113729. doi:10.1016/j.bcp.2019.113729

Marur, S., and Forastiere, A. A. (2008). Head and Neck Cancer: Changing Epidemiology, Diagnosis, and Treatment. *Mayo Clin. Proc.* 83, 489–501. doi:10.4065/83.4.489

Marur, S., and Forastiere, A. A. (2016). Head and Neck Squamous Cell Carcinoma: Update on Epidemiology, Diagnosis, and Treatment. *Mayo Clin. Proc.* 91, 386–396. doi:10.1016/j.mayocp.2015.12.017

Marur, S., Li, S., Cmelak, A. J., Gillison, M. L., Zhao, W. J., Ferris, R. L., et al. (2017). E1308: Phase II Trial of Induction Chemotherapy Followed by Reduced-Dose Radiation and Weekly Cetuximab in Patients with HPV-Associated Resectable Squamous Cell Carcinoma of the Oropharynx- ECOG-ACRIN Cancer Research Group. *J. Clin. Oncol.* 35, 490–497. doi:10.1200/JCO.2016.68.3300

Mashberg, A., and Samit, A. (1995). Early Diagnosis of Asymptomatic Oral and Oropharyngeal Squamous Cancers. *CA Cancer J. Clin.* 45, 328–351. doi:10.3322/canjclin.45.6.328

Masterson, L., Sorgeloos, F., Winder, D., Lechner, M., Marker, A., Malhotra, S., et al. (2015). Deregulation of SYCP2 Predicts Early Stage Human Papillomavirus-Positive Oropharyngeal Carcinoma: A Prospective Whole Transcriptome Analysis. *Cancer Sci.* 106, 1568–1575. doi:10.1111/cas.12809

Masuda, M., Suzui, M., and Weinstein, I. B. (2001). Effects of Epigallocatechin-3-Gallate on Growth, Epidermal Growth Factor Receptor Signaling Pathways, Gene Expression, and Chemosensitivity in Human Head and Neck Squamous Cell Carcinoma Cell Lines. *Clin. Cancer Res.* 7, 4220–4229.

Mathew, B., Sankaranarayanan, R., Nair, P. P., Varghese, C., Somanathan, T., Amma, B. P., et al. (1995). Evaluation of Chemoprevention of Oral Cancer with Spirulina Fusiformis. *Nutr. Cancer* 24, 197–202. doi:10.1080/01635589509514407

Mckaig, R. G., Baric, R. S., and Olshan, A. F. (1998). Human Papillomavirus and Head and Neck Cancer: Epidemiology and Molecular Biology. *Head Neck* 20, 250–265. doi:10.1002/(sici)1097-0347(199805)20:3<250::aid-hed11>3.0.co;2-o

Mehanna, H., Beech, T., Nicholson, T., El-Hariry, I., Mcconkey, C., Paleri, V., et al. (2013). Prevalence of Human Papillomavirus in Oropharyngeal and Nonoropharyngeal Head and Neck Cancer-Ssystematic Review and Meta-Analysis of Trends by Time and Region. *Head Neck* 35, 747–755. doi:10.1002/hed.22015

Mehra, R., Seiwert, T. Y., Gupta, S., Weiss, J., Gluck, I., Eder, J. P., et al. (2018). Efficacy and Safety of Pembrolizumab in Recurrent/metastatic Head and Neck Squamous Cell Carcinoma: Pooled Analyses after Long-Term Follow-Up in KEYNOTE-012. *Br. J. Cancer* 119, 153–159. doi:10.1038/s41416-018-0131-9

Meisels, A., and Fortin, R. (1976). Condylomatous Lesions of the Cervix and Vagina. I. Cytologic Patterns. *Acta Cytol.* 20, 505–509.

Mishra, A., Bharti, A. C., Varghese, P., Saluja, D., and Das, B. C. (2006). Differential Expression and Activation of NF-kappaB Family Proteins during Oral Carcinogenesis: Role of High Risk Human Papillomavirus Infection. *Int. J. Cancer* 119, 2840–2850. doi:10.1002/ijc.22262

Mishra, A., Kumar, R., Tyagi, A., Kohaar, I., Hedau, S., Bharti, A. C., et al. (2015). Curcumin Modulates Cellular AP-1, NF-kB, and HPV16 E6 Proteins in Oral Cancer. *Ecancermedicalscience* 9, 525. doi:10.3332/ecancer.2015.525

Monisha, J., Roy, N. K., Bordoloi, D., Kumar, A., Golla, R., Kotoky, J., et al. (2017). Nuclear Factor Kappa B: A Potential Target to Persecute Head and Neck Cancer. *Curr. Drug Targets* 18, 232–253. doi:10.2174/1389450117666160201112330

Mork, J., Lie, A. K., Glattre, E., Hallmans, G., Jellum, E., Koskela, P., et al. (2001). Human Papillomavirus Infection as a Risk Factor for Squamous-Cell Carcinoma of the Head and Neck. *N. Engl. J. Med.* 344, 1125–1131. doi:10.1056/NEJM200104123441503

Müller, S. (2018). Oral Epithelial Dysplasia, Atypical Verrucous Lesions and Oral Potentially Malignant Disorders: Focus on Histopathology. *Oral Surg. Oral Med. Oral Pathol. Oral Radiol.* 125, 591–602. doi:10.1016/j.oooo.2018.02.012

Muzaffar, J., Bari, S., Kirtane, K., and Chung, C. H. (2021). Recent Advances and Future Directions in Clinical Management of Head and Neck Squamous Cell Carcinoma. *Cancers (Basel)* 13. doi:10.3390/cancers13020338

Myoung, H., Hong, S. P., Yun, P. Y., Lee, J. H., and Kim, M. J. (2003). Anti-cancer Effect of Genistein in Oral Squamous Cell Carcinoma with Respect to Angiogenesis and *In Vitro* Invasion. *Cancer Sci.* 94, 215–220. doi:10.1111/j.1349-7006.2003.tb01422.x

Ndiaye, C., Mena, M., Alemany, L., Arbyn, M., Castellsagué, X., Laporte, L., et al. (2014). HPV DNA, E6/E7 mRNA, and p16INK4a Detection in Head and Neck Cancers: a Systematic Review and Meta-Analysis. *Lancet Oncol.* 15, 1319–1331. doi:10.1016/S1470-2045(14)70471-1

Neville, B. W., and Day, T. A. (2002). Oral Cancer and Precancerous Lesions. *CA Cancer J. Clin.* 52, 195–215. doi:10.3322/canjclin.52.4.195

Nikolaou, M., Pavlopoulou, A., Georgakilas, A. G., and Kyrodimos, E. (2018). The challenge of Drug Resistance in Cancer Treatment: a Current Overview. *Clin. Exp. Metastasis* 35, 309–318. doi:10.1007/s10585-018-9903-0

Oeckinghaus, A., and Ghosh, S. (2009). The NF-kappaB Family of Transcription Factors and its Regulation. *Cold Spring Harb Perspect. Biol.* 1, a000034. doi:10.1101/cshperspect.a000034

Ologe, F. E., Adeniji, K. A., and Segun-Busari, S. (2005). Clinicopathological Study of Head and Neck Cancers in Ilorin, Nigeria. *Trop. Doct* 35, 2–4. doi:10.1258/0049475053001949

Oreggia, F., De Stefani, E., Correa, P., and Fierro, L. (1991). Risk Factors for Cancer of the Tongue in Uruguay. *Cancer* 67, 180–183. doi:10.1002/1097-0142(19910101)67:1<180::aid-cncr2820670130>3.0.co;2-r

Owen, J. H., Graham, M. P., Chinn, S. B., Darr, O. F., Chepeha, D. B., Wolf, G. T., et al. (2016). Novel Method of Cell Line Establishment Utilizing Fluorescence-Activated Cell Sorting Resulting in 6 New Head and Neck Squamous Cell Carcinoma Lines. *Head Neck* 38 Suppl 1 Suppl. 1, E459–E467. doi:10.1002/hed.24019

Pang, J. S., Yen, J. H., Wu, H. T., and Huang, S. T. (2017). Gallic Acid Inhibited Matrix Invasion and AP-1/ets-1-Mediated MMP-1 Transcription in Human Nasopharyngeal Carcinoma Cells. *Int. J. Mol. Sci.* 18. doi:10.3390/ijms18071354

Pardoll, D. M. (2012). The Blockade of Immune Checkpoints in Cancer Immunotherapy. *Nat. Rev. Cancer* 12, 252–264. doi:10.1038/nrc3239

Parsons, R. J., and Kidd, J. G. (1943). Oral Papillomatosis of Rabbits: A Virus Disease. *J. Exp. Med.* 77, 233–250. doi:10.1084/jem.77.3.233

Partlová, S., Bouček, J., Kloudová, K., Lukešová, E., Zábrodský, M., Grega, M., et al. (2015). Distinct Patterns of Intratumoral Immune Cell Infiltrates in Patients with HPV-Associated Compared to Non-virally Induced Head and Neck Squamous Cell Carcinoma. *Oncoimmunology* 4, e965570. doi:10.4161/21624011.2014.965570

Paschka, A. G., Butler, R., and Young, C. Y. (1998). Induction of Apoptosis in Prostate Cancer Cell Lines by the green tea Component, (-)-Epigallocatechin-3-Gallate. *Cancer Lett.* 130, 1–7. doi:10.1016/s0304-3835(98)00084-6

Patel, R. G. (2017). Nasal Anatomy and Function. *Facial Plast. Surg.* 33, 3–8. doi:10.1055/s-0036-1597950

Payne, A. (1891). On the Contagious Rise of Common Warts. *Br. J. Dermatol.* 3, 185. doi:10.1086/120258

Peng, X., Zhang, Q., Zeng, Y., Li, J., Wang, L., and Ai, P. (2015). Evodiamine Inhibits the Migration and Invasion of Nasopharyngeal Carcinoma Cells *In Vitro* via Repressing MMP-2 Expression. *Cancer Chemother. Pharmacol.* 76, 1173–1184. doi:10.1007/s00280-015-2902-9

Pintos, J., Franco, E. L., Black, M. J., Bergeron, J., and Arella, M. (1999). Human Papillomavirus and Prognoses of Patients with Cancers of the Upper Aerodigestive Tract. *Cancer* 85, 1903–1909. doi:10.1002/(sici)1097-0142(19990501)85:9<1903::aid-cncr4>3.0.co;2-6

Pollock, N. I., Wang, L., Wallweber, G., Gooding, W. E., Huang, W., Chenna, A., et al. (2015). Increased Expression of HER2, HER3, and HER2:HER3 Heterodimers in HPV-Positive HNSCC Using a Novel Proximity-Based Assay: Implications for Targeted Therapies. *Clin. Cancer Res.* 21, 4597–4606. doi:10.1158/1078-0432.CCR-14-3338

Porceddu, S. V., Campbell, B., Rischin, D., Corry, J., Weih, L., Guerrieri, M., et al. (2004). Postoperative Chemoradiotherapy for High-Risk Head-And-Neck Squamous Cell Carcinoma. *Int. J. Radiat. Oncol. Biol. Phys.* 60, 365–373. doi:10.1016/j.ijrobp.2004.03.011

Posner, M. R., Lorch, J. H., Goloubeva, O., Tan, M., Schumaker, L. M., Sarlis, N. J., et al. (2011). Survival and Human Papillomavirus in Oropharynx Cancer in TAX 324: a Subset Analysis from an International Phase III Trial. *Ann. Oncol.* 22, 1071–1077. doi:10.1093/annonc/mdr006

Prasad, R., and Katiyar, S. K. (2012). Bioactive Phytochemical Proanthocyanidins Inhibit Growth of Head and Neck Squamous Cell Carcinoma Cells by Targeting Multiple Signaling Molecules. *PLoS One* 7, e46404. doi:10.1371/journal.pone.0046404

Price, K. A., and Cohen, E. E. (2012). Current Treatment Options for Metastatic Head and Neck Cancer. *Curr. Treat. Options. Oncol.* 13, 35–46. doi:10.1007/s11864-011-0176-y

Prusty, B. K., and Das, B. C. (2005). Constitutive Activation of Transcription Factor AP-1 in Cervical Cancer and Suppression of Human Papillomavirus (HPV) Transcription and AP-1 Activity in HeLa Cells by Curcumin. *Int. J. Cancer* 113, 951–960. doi:10.1002/ijc.20668

Purola, E., and Savia, E. (1977). Cytology of Gynecologic Condyloma Acuminatum. *Acta Cytol.* 21, 26–31.

Pyrhönen, S., and Neuvonen, E. (1978). The Occurrence of Human Wart-Virus Antibodies in Dogs, Pigs and Cattle. *Arch. Virol.* 57, 297–305. doi:10.1007/BF01320069

Qiao, X. W., Jiang, J., Pang, X., Huang, M. C., Tang, Y. J., Liang, X. H., et al. (2020). The Evolving Landscape of PD-1/pd-L1 Pathway in Head and Neck Cancer. *Front. Immunol.* 11, 1721. doi:10.3389/fimmu.2020.01721

Qiu, Y., Li, C., Wang, Q., Zeng, X., and Ji, P. (2018). Tanshinone IIA Induces Cell Death via Beclin-1-dependent Autophagy in Oral Squamous Cell Carcinoma SCC-9 Cell Line. *Cancer Med.* 7, 397–407. doi:10.1002/cam4.1281

Quick, C. A., Faras, A., and Krzysek, R. (1978). The Etiology of Laryngeal Papillomatosis. *Laryngoscope* 88, 1789–1795. doi:10.1288/00005537-197811000-00009

Ragin, C. C., and Taioli, E. (2007). Survival of Squamous Cell Carcinoma of the Head and Neck in Relation to Human Papillomavirus Infection: Review and Meta-Analysis. *Int. J. Cancer* 121, 1813–1820. doi:10.1002/ijc.22851

Rajamoorthi, A., Shrivastava, S., Steele, R., Nerurkar, P., Gonzalez, J. G., Crawford, S., et al. (2013). Bitter Melon Reduces Head and Neck Squamous Cell Carcinoma Growth by Targeting C-Met Signaling. *PLoS One* 8, e78006. doi:10.1371/journal.pone.0078006

Ranganathan, K., Devi, M. U., Joshua, E., Kirankumar, K., and Saraswathi, T. R. (2004). Oral Submucous Fibrosis: a Case-Control Study in Chennai, South India. *J. Oral Pathol. Med.* 33, 274–277. doi:10.1111/j.0904-2512.2004.00116.x

Ravindranath, V., and Chandrasekhara, N. (1980). Absorption and Tissue Distribution of Curcumin in Rats. *Toxicology* 16, 259–265. doi:10.1016/0300-483x(80)90122-5

Recchia, F., Lelli, S., Di Matteo, G., Rea, S., and Frati, L. (1993). [5-fluorouracil, Cisplatin and Retinol Palmitate in the Management of Advanced Cancer of the Oral Cavity. Phase II Study]. *Clin. Ter* 142, 403–409.

Reichart, P. A., and Philipsen, H. P. (2005). Oral Erythroplakia-Aa Review. *Oral Oncol.* 41, 551–561. doi:10.1016/j.oraloncology.2004.12.003

Ren, S., Gaykalova, D., Wang, J., Guo, T., Danilova, L., Favorov, A., et al. (2018). Discovery and Development of Differentially Methylated Regions in Human Papillomavirus-Related Oropharyngeal Squamous Cell Carcinoma. *Int. J. Cancer* 143, 2425–2436. doi:10.1002/ijc.31778

Rieckmann, T., Tribius, S., Grob, T. J., Meyer, F., Busch, C. J., Petersen, C., et al. (2013). HNSCC Cell Lines Positive for HPV and P16 Possess Higher Cellular Radiosensitivity Due to an Impaired DSB Repair Capacity. *Radiother. Oncol.* 107, 242–246. doi:10.1016/j.radonc.2013.03.013

Rischin, D., Young, R. J., Fisher, R., Fox, S. B., Le, Q. T., Peters, L. J., et al. (2010). Prognostic Significance of p16INK4A and Human Papillomavirus in Patients with Oropharyngeal Cancer Treated on TROG 02.02 Phase III Trial. *J. Clin. Oncol.* 28, 4142–4148. doi:10.1200/JCO.2010.29.2904

Ryerson, A. B., Peters, E. S., Coughlin, S. S., Chen, V. W., Gillison, M. L., Reichman, M. E., et al. (2008). Burden of Potentially Human Papillomavirus-Associated Cancers of the Oropharynx and Oral Cavity in the US, *Cancer* 113, 2901–2909. doi:10.1002/cncr.23745

Sabeena, S., Bhat, P., Kamath, V., and Arunkumar, G. (2017). Possible Non-sexual Modes of Transmission of Human Papilloma Virus. *J. Obstet. Gynaecol. Res.* 43, 429–435. doi:10.1111/jog.13248

Salazar-Ruales, C., Arguello, J. V., López-Cortés, A., Cabrera-Andrade, A., García-Cárdenas, J. M., Guevara-Ramírez, P., et al. (2018). Salivary MicroRNAs for Early Detection of Head and Neck Squamous Cell Carcinoma: A Case-Control Study in the High Altitude Mestizo Ecuadorian Population. *Biomed. Res. Int.* 2018, 9792730. doi:10.1155/2018/9792730

Salmani, J. M. M., Zhang, X. P., Jacob, J. A., and Chen, B. A. (2017). Apigenin's Anticancer Properties and Molecular Mechanisms of Action: Recent Advances and Future Prospectives. *Chin. J. Nat. Med.* 15, 321–329. doi:10.1016/S1875-5364(17)30052-3

Sankaranarayanan, R., Mathew, B., Varghese, C., Sudhakaran, P. R., Menon, V., Jayadeep, A., et al. (1997). Chemoprevention of Oral Leukoplakia with Vitamin A and Beta Carotene: an Assessment. *Oral Oncol.* 33, 231–236. doi:10.1016/s0964-1955(97)00010-9

Sarkola, M. E., Grénman, S. E., Rintala, M. A., Syrjänen, K. J., and Syrjänen, S. M. (2008). Human Papillomavirus in the Placenta and Umbilical Cord Blood. *Acta Obstet. Gynecol. Scand.* 87, 1181–1188. doi:10.1080/00016340802468308

Schmidt, M., Polednik, C., Roller, J., and Hagen, R. (2014). Galium Verum Aqueous Extract Strongly Inhibits the Motility of Head and Neck Cancer Cell Lines and Protects Mucosal Keratinocytes against Toxic DNA Damage. *Oncol. Rep.* 32, 1296–1302. doi:10.3892/or.2014.3316

Schmidt, M., Skaf, J., Gavril, G., Polednik, C., Roller, J., Kessler, M., et al. (2017). The Influence of Osmunda Regalis Root Extract on Head and Neck Cancer Cell Proliferation, Invasion and Gene Expression. *BMC Complement. Altern. Med.* 17, 518. doi:10.1186/s12906-017-2009-4

Schröck, A., Bode, M., Göke, F. J., Bareiss, P. M., Schairer, R., Wang, H., et al. (2014). Expression and Role of the Embryonic Protein SOX2 in Head and Neck Squamous Cell Carcinoma. *Carcinogenesis* 35, 1636–1642. doi:10.1093/carcin/bgu094

Schwartz, D. L., Bankson, J., Bidaut, L., He, Y., Williams, R., Lemos, R., et al. (2011). HIF-1-dependent Stromal Adaptation to Ischemia Mediates *In Vivo* Tumor Radiation Resistance. *Mol. Cancer Res.* 9, 259–270. doi:10.1158/1541-7786.MCR-10-0469

Seiwert, T. Y., Zuo, Z., Keck, M. K., Khattri, A., Pedamallu, C. S., Stricker, T., et al. (2015). Integrative and Comparative Genomic Analysis of HPV-Positive and HPV-Negative Head and Neck Squamous Cell Carcinomas. *Clin. Cancer Res.* 21, 632–641. doi:10.1158/1078-0432.CCR-13-3310

Seixas-Silva, J. A., Jr., Richards, T., Khuri, F. R., Wieand, H. S., Kim, E., Murphy, B., et al. (2005). Phase 2 Bioadjuvant Study of Interferon Alfa-2a, Isotretinoin, and

Vitamin E in Locally Advanced Squamous Cell Carcinoma of the Head and Neck: Long-Term Follow-Up. *Arch. Otolaryngol. Head Neck Surg.* 131, 304–307. doi:10.1001/archotol.131.4.304

Seo, Y. S., Yim, M. J., Kim, B. H., Kang, K. R., Lee, S. Y., Oh, J. S., et al. (2015). Berberine-induced Anticancer Activities in FaDu Head and Neck Squamous Cell Carcinoma Cells. *Oncol. Rep.* 34, 3025–3034. doi:10.3892/or.2015.4312

Shaikh, J., Ankola, D. D., Beniwal, V., Singh, D., and Kumar, M. N. (2009). Nanoparticle Encapsulation Improves Oral Bioavailability of Curcumin by at Least 9-fold when Compared to Curcumin Administered with Piperine as Absorption Enhancer. *Eur. J. Pharm. Sci.* 37, 223–230. doi:10.1016/j.ejps.2009.02.019

Shi, X., Wang, L., Li, X., Bai, J., Li, J., Li, S., et al. (2017). Dihydroartemisinin Induces Autophagy-dependent Death in Human Tongue Squamous Cell Carcinoma Cells through DNA Double-Strand Break-Mediated Oxidative Stress. *Oncotarget* 8, 45981–45993. doi:10.18632/oncotarget.17520

Shin, D. M., Khuri, F. R., Murphy, B., Garden, A. S., Clayman, G., Francisco, M., et al. (2001). Combined Interferon-Alfa, 13-Cis-Retinoic Acid, and Alpha-Tocopherol in Locally Advanced Head and Neck Squamous Cell Carcinoma: Novel Bioadjuvant Phase II Trial. *Jco* 19, 3010–3017. doi:10.1200/jco.2001.19.12.3010

Siddiqui, I. A., Adhami, V. M., Bharali, D. J., Hafeez, B. B., Asim, M., Khwaja, S. I., et al. (2009). Introducing Nanochemoprevention as a Novel Approach for Cancer Control: Proof of Principle with green tea Polyphenol Epigallocatechin-3-Gallate. *Cancer Res.* 69, 1712–1716. doi:10.1158/0008-5472.CAN-08-3978

Siddiqui, S., Ahamad, M. S., Jafri, A., Afzal, M., and Arshad, M. (2017). Piperine Triggers Apoptosis of Human Oral Squamous Carcinoma through Cell Cycle Arrest and Mitochondrial Oxidative Stress. *Nutr. Cancer* 69, 791–799. doi:10.1080/01635581.2017.1310260

Silverman, S., Jr., Gorsky, M., and Lozada, F. (1984). Oral Leukoplakia and Malignant Transformation. A Follow-Up Study of 257 Patients. *Cancer* 53, 563–568. doi:10.1002/1097-0142(19840201)53:3<563::aid-cncr2820530332>3.0.co;2-f

Singh, M., and Bagewadi, A. (2017). Comparison of Effectiveness of Calendula officinalis Extract Gel with Lycopene Gel for Treatment of Tobacco-Induced Homogeneous Leukoplakia: A Randomized Clinical Trial. *Int. J. Pharm. Investig.* 7, 88–93. doi:10.4103/jphi.JPHI_19_17

Singh, M., Krishanappa, R., Bagewadi, A., and Keluskar, V. (2004). Efficacy of Oral Lycopene in the Treatment of Oral Leukoplakia. *Oral Oncol.* 40, 591–596. doi:10.1016/j.oraloncology.2003.12.011

Singh, T., Gupta, N. A., Xu, S., Prasad, R., Velu, S. E., and Katiyar, S. K. (2015). Honokiol Inhibits the Growth of Head and Neck Squamous Cell Carcinoma by Targeting Epidermal Growth Factor Receptor. *Oncotarget* 6, 21268–21282. doi:10.18632/oncotarget.4178

Sivanantham, B., Sethuraman, S., and Krishnan, U. M. (2016). Combinatorial Effects of Curcumin with an Anti-neoplastic Agent on Head and Neck Squamous Cell Carcinoma through the Regulation of EGFR-Erk1/2 and Apoptotic Signaling Pathways. *ACS Comb. Sci.* 18, 22–35. doi:10.1021/acscombsci.5b00043

Smith, E. M., Ritchie, J. M., Summersgill, K. F., Klussmann, J. P., Lee, J. H., Wang, D., et al. (2004). Age, Sexual Behavior and Human Papillomavirus Infection in Oral Cavity and Oropharyngeal Cancers. *Int. J. Cancer* 108, 766–772. doi:10.1002/ijc.11633

Snijders, P. J., Cromme, F. V., Van Den Brule, A. J., Schrijnemakers, H. F., Snow, G. B., Meijer, C. J., et al. (1992). Prevalence and Expression of Human Papillomavirus in Tonsillar Carcinomas, Indicating a Possible Viral Etiology. *Int. J. Cancer* 51, 845–850. doi:10.1002/ijc.2910510602

Sogno, I., Vannini, N., Lorusso, G., Cammarota, R., Noonan, D. M., Generoso, L., et al. (2009). Anti-Angiogenic Activity of a Novel Class of Chemopreventive Compounds: Oleanic Acid Terpenoids. *Recent Results Canc. Res.* 181, 209–212.

Song, J. I., and Grandis, J. R. (2000). STAT Signaling in Head and Neck Cancer. *Oncogene* 19, 2489–2495. doi:10.1038/sj.onc.1203483

Steenbergen, R. D., Hermsen, M. A., Walboomers, J. M., Joenje, H., Arwert, F., Meijer, C. J., et al. (1995). Integrated Human Papillomavirus Type 16 and Loss of Heterozygosity at 11q22 and 18q21 in an Oral Carcinoma and its Derivative Cell Line. *Cancer Res.* 55, 5465–5471.

Stiblar-Martincic, D. (1997). Histology of Laryngeal Mucosa. *Acta Otolaryngol. Suppl.* 527, 138–141.

Stich, H. F., Hornby, A. P., Mathew, B., Sankaranarayanan, R., and Nair, M. K. (1988a). Response of Oral Leukoplakias to the Administration of Vitamin A. *Cancer Lett.* 40, 93–101. doi:10.1016/0304-3835(88)90266-2

Stich, H. F., Rosin, M. P., Hornby, A. P., Mathew, B., Sankaranarayanan, R., and Nair, M. K. (1988b). Remission of Oral Leukoplakias and Micronuclei in Tobacco/betel Quid Chewers Treated with Beta-Carotene and with Beta-Carotene Plus Vitamin A. *Int. J. Cancer* 42, 195–199. doi:10.1002/ijc.2910420209

Sturgis, E. M., and Cinciripini, P. M. (2007). Trends in Head and Neck Cancer Incidence in Relation to Smoking Prevalence: an Emerging Epidemic of Human Papillomavirus-Associated Cancers? *Cancer* 110, 1429–1435. doi:10.1002/cncr.22963

Sun, Z., Guan, X., Li, N., Liu, X., and Chen, X. (2010). Chemoprevention of Oral Cancer in Animal Models, and Effect on Leukoplakias in Human Patients with ZengShengPing, a Mixture of Medicinal Herbs. *Oral Oncol.* 46, 105–110. doi:10.1016/j.oraloncology.2009.06.004

Sur, S., Steele, R., Aurora, R., Varvares, M., Schwetye, K. E., and Ray, R. B. (2018). Bitter Melon Prevents the Development of 4-NQO-Induced Oral Squamous Cell Carcinoma in an Immunocompetent Mouse Model by Modulating Immune Signaling. *Cancer Prev. Res. (Phila)* 11, 191–202. doi:10.1158/1940-6207.CAPR-17-0237

Syrjänen, K., Syrjänen, S., Lamberg, M., Pyrhönen, S., and Nuutinen, J. (1983a). Morphological and Immunohistochemical Evidence Suggesting Human Papillomavirus (HPV) Involvement in Oral Squamous Cell Carcinogenesis. *Int. J. Oral Surg.* 12, 418–424. doi:10.1016/s0300-9785(83)80033-7

Syrjänen, K., Syrjänen, S., and Pyrhönen, S. (1982). Human Papilloma Virus (HPV) Antigens in Lesions of Laryngeal Squamous Cell Carcinomas. *ORL J. Otorhinolaryngol. Relat. Spec.* 44, 323–334. doi:10.1159/000275612

Syrjänen, K. J., Pyrhönen, S., and Syrjänen, S. M. (1983b). Evidence Suggesting Human Papillomavirus (HPV) Etiology for the Squamous Cell Papilloma of the Paranasal Sinus. *Arch. Geschwulstforsch* 53, 77–82.

Syrjänen, S., Happonen, R. P., Virolainen, E., Siivonen, L., and Syrjänen, K. (1987). Detection of Human Papillomavirus (HPV) Structural Antigens and DNA Types in Inverted Papillomas and Squamous Cell Carcinomas of the Nasal Cavities and Paranasal Sinuses. *Acta Otolaryngol.* 104, 334–341. doi:10.3109/00016488709107337

Syrjänen, S. (2018). Oral Manifestations of Human Papillomavirus Infections. *Eur. J. Oral Sci.* 126 Suppl 1 Suppl. 1, 49–66. doi:10.1111/eos.12538

Syrjänen, S., Rautava, J., and Syrjänen, K. (2017). HPV in Head and Neck Cancer-30 Years of History. *Recent Results Cancer Res.* 206, 3–25. doi:10.1007/978-3-319-43580-0_1

Syrjanen, S., Andersson, B., Juntunen, L., and Syrjanen, K. (1992). Polymerase Chain Reaction for Producing Biotinylated Human Papillomavirus DNA Probes for *In Situ* Hybridization. *Sex. Transm. Dis.* 19, 140–145. doi:10.1097/00007435-199205000-00006

Tang, A. L., Hauff, S. J., Owen, J. H., Graham, M. P., Czerwinski, M. J., Park, J. J., et al. (2012). UM-SCC-104: a New Human Papillomavirus-16-Positive Cancer Stem Cell-Containing Head and Neck Squamous Cell Carcinoma Cell Line. *Head Neck* 34, 1480–1491. doi:10.1002/hed.21962

Thomas, G. T., Lewis, M. P., and Speight, P. M. (1999). Matrix Metalloproteinases and Oral Cancer. *Oral Oncol.* 35, 227–233. doi:10.1016/s1368-8375(99)00004-4

Tilakaratne, W. M., Jayasooriya, P. R., Jayasuriya, N. S., and De Silva, R. K. (2019). Oral Epithelial Dysplasia: Causes, Quantification, Prognosis, and Management Challenges. *Periodontol. 2000* 80, 126–147. doi:10.1111/prd.12259

Toporcov, T. N., Znaor, A., Zhang, Z. F., Yu, G. P., Winn, D. M., Wei, Q., et al. (2015). Risk Factors for Head and Neck Cancer in Young Adults: a Pooled Analysis in the INHANCE Consortium. *Int. J. Epidemiol.* 44, 169–185. doi:10.1093/ije/dyu255

Tosetti, F., Ferrari, N., De Flora, S., and Albini, A. (2002). Angioprevention': Angiogenesis Is a Common and Key Target for Cancer Chemopreventive Agents. *FASEB J.* 16, 2–14. doi:10.1096/fj.01-0300rev

Tsao, A. S., Liu, D., Martin, J., Tang, X. M., Lee, J. J., El-Naggar, A. K., et al. (2009). Phase II Randomized, Placebo-Controlled Trial of green tea Extract in Patients with High-Risk Oral Premalignant Lesions. *Cancer Prev. Res. (Phila)* 2, 931–941. doi:10.1158/1940-6207.CAPR-09-0121

Tsukishiro, T., Donnenberg, A. D., and Whiteside, T. L. (2003). Rapid Turnover of the CD8(+)CD28(-) T-Cell Subset of Effector Cells in the Circulation of

Patients with Head and Neck Cancer. *Cancer Immunol. Immunother.* 52, 599–607. doi:10.1007/s00262-003-0395-6

Ullman, E. V. (1923). On the Etiology of the Laryngeal Papilloma. *Acta Otolaryngol.* 5, 317–338.

Van Houten, V. M., Snijders, P. J., Van Den Brekel, M. W., Kummer, J. A., Meijer, C. J., Van Leeuwen, B., et al. (2001). Biological Evidence that Human Papillomaviruses Are Etiologically Involved in a Subgroup of Head and Neck Squamous Cell Carcinomas. *Int. J. Cancer* 93, 232–235. doi:10.1002/ijc.1313

Verma, G., Vishnoi, K., Tyagi, A., Jadli, M., Singh, T., Goel, A., et al. (2017). Characterization of Key Transcription Factors as Molecular Signatures of HPV-Positive and HPV-Negative Oral Cancers. *Cancer Med.* 6, 591–604. doi:10.1002/cam4.983

Verma, V., Sprave, T., Haque, W., Simone, C. B., 2nd, Chang, J. Y., Welsh, J. W., et al. (2018). A Systematic Review of the Cost and Cost-Effectiveness Studies of Immune Checkpoint Inhibitors. *J. Immunother. Cancer* 6, 128. doi:10.1186/s40425-018-0442-7

Vermorken, J. B., Psyrri, A., Mesía, R., Peyrade, F., Beier, F., De Blas, B., et al. (2014). Impact of Tumor HPV Status on Outcome in Patients with Recurrent And/or Metastatic Squamous Cell Carcinoma of the Head and Neck Receiving Chemotherapy with or without Cetuximab: Retrospective Analysis of the Phase III EXTREME Trial. *Ann. Oncol.* 25, 801–807. doi:10.1093/annonc/mdt574

Visalli, G., Currò, M., Facciolà, A., Riso, R., Mondello, P., Laganà, P., et al. (2016). Prevalence of Human Papillomavirus in Saliva of Women with HPV Genital Lesions. *Infect. Agent Cancer* 11, 48. doi:10.1186/s13027-016-0096-3

Vizcaíno, C., Mansilla, S., and Portugal, J. (2015). Sp1 Transcription Factor: A Long-Standing Target in Cancer Chemotherapy. *Pharmacol. Ther.* 152, 111–124. doi:10.1016/j.pharmthera.2015.05.008

Voskens, C. J., Sewell, D., Hertzano, R., Desanto, J., Rollins, S., Lee, M., et al. (2012). Induction of MAGE-A3 and HPV-16 Immunity by Trojan Vaccines in Patients with Head and Neck Carcinoma. *Head Neck* 34, 1734–1746. doi:10.1002/hed.22004

Wang, W. C., Chen, C. Y., Hsu, H. K., Lin, L. M., and Chen, Y. K. (2016). Chemopreventive Effect of Toona Sinensis Leaf Extract on 7,12-Dimethylbenz [a]anthracene-Induced Hamster Buccal Pouch Squamous Cell Carcinogenesis. *Arch. Oral Biol.* 70, 130–142. doi:10.1016/j.archoralbio.2016.06.015

Wang, Y., Hu, Y., Chen, L., Wu, J., Wu, K., Du, J., et al. (2020). Molecular Mechanisms and Prognostic Markers in Head and Neck Squamous Cell Carcinoma: a Bioinformatic Analysis. *Int. J. Clin. Exp. Pathol.* 13, 371–381.

Warnakulasuriya, S., and Ariyawardana, A. (2016). Malignant Transformation of Oral Leukoplakia: a Systematic Review of Observational Studies. *J. Oral Pathol. Med.* 45, 155–166. doi:10.1111/jop.12339

Wei, W. I., and Sham, J. S. (2000). Nasopharyngeal Carcinoma. *Lancet* 365, 2041–2054. doi:10.1016/S0140-6736(05)66698-6

Weisburg, J. H., Schuck, A. G., Reiss, S. E., Wolf, B. J., Fertel, S. R., Zuckerbraun, H. L., et al. (2013). Ellagic Acid, a Dietary Polyphenol, Selectively Cytotoxic to HSC-2 Oral Carcinoma Cells. *Anticancer Res.* 33, 1829–1836.

Weisman, R. A., Christen, R., Los, G., Jones, V., Kerber, C., Seagren, S., et al. (1998). Phase I Trial of Retinoic Acid and Cis-Platinum for Advanced Squamous Cell Cancer of the Head and Neck Based on Experimental Evidence of Drug Synergism. *Otolaryngol. Head Neck Surg.* 118, 597–602. doi:10.1177/019459989811800506

Wendt, T. G., Grabenbauer, G. G., Rödel, C. M., Thiel, H. J., Aydin, H., Rohloff, R., et al. (1998). Simultaneous Radiochemotherapy versus Radiotherapy Alone in Advanced Head and Neck Cancer: a Randomized Multicenter Study. *J. Clin. Oncol.* 16, 1318–1324. doi:10.1200/JCO.1998.16.4.1318

White, J. S., Weissfeld, J. L., Ragin, C. C., Rossie, K. M., Martin, C. L., Shuster, M., et al. (2007). The Influence of Clinical and Demographic Risk Factors on the Establishment of Head and Neck Squamous Cell Carcinoma Cell Lines. *Oral Oncol.* 43, 701–712. doi:10.1016/j.oraloncology.2006.09.001

Wierzbicka, M., Klussmann, J. P., San Giorgi, M. R., Wuerdemann, N., and Dikkers, F. G. (2021). Oral and Laryngeal HPV Infection: Incidence, Prevalence and Risk Factors, with Special Regard to Concurrent Infection in Head, Neck and Genitals. *Vaccine*.39(17), 2344-2350. doi:10.1016/j.vaccine.2021.03.047

Wils, L. J., Poell, J. B., Evren, I., Koopman, M. S., Brouns, E. R. E. A., De Visscher, J. G. A. M., et al. (2020). Incorporation of Differentiated Dysplasia Improves Prediction of Oral Leukoplakia at Increased Risk of Malignant Progression. *Mod. Pathol.* 33, 1033–1040. doi:10.1038/s41379-019-0444-0

Windon, M. J., D'souza, G., Rettig, E. M., Westra, W. H., Van Zante, A., Wang, S. J., et al. (2018). Increasing Prevalence of Human Papillomavirus-Positive Oropharyngeal Cancers Among Older Adults. *Cancer* 124, 2993–2999. doi:10.1002/cncr.31385

Winning, T. A., and Townsend, G. C. (2000). Oral Mucosal Embryology and Histology. *Clin. Dermatol.* 18, 499–511. doi:10.1016/s0738-081x(00)00140-1

Wolter, K. G., Wang, S. J., Henson, B. S., Wang, S., Griffith, K. A., Kumar, B., et al. (2006). (-)-gossypol Inhibits Growth and Promotes Apoptosis of Human Head and Neck Squamous Cell Carcinoma *In Vivo*. *Neoplasia* 8, 163–172. doi:10.1593/neo.05691

Wookey, V. B., Appiah, A. K., Kallam, A., Ernani, V., Smith, L. M., and Ganti, A. K. (2019). HPV Status and Survival in Non-oropharyngeal Squamous Cell Carcinoma of the Head and Neck. *Anticancer Res.* 39, 1907–1914. doi:10.21873/anticanres.13299

Wu, X., Fan, Z., Masui, H., Rosen, N., and Mendelsohn, J. (1995). Apoptosis Induced by an Anti-epidermal Growth Factor Receptor Monoclonal Antibody in a Human Colorectal Carcinoma Cell Line and its Delay by Insulin. *J. Clin. Invest.* 95, 1897–1905. doi:10.1172/JCI117871

Xiao, C., Beitler, J. J., Higgins, K. A., Glazer, T., Huynh, L. K., Paul, S., et al. (2018). Associations Among Human Papillomavirus, Inflammation, and Fatigue in Patients with Head and Neck Cancer. *Cancer* 124, 3163–3170. doi:10.1002/cncr.31537

Yang, G., Liao, J., Kim, K., Yurkow, E. J., and Yang, C. S. (1998). Inhibition of Growth and Induction of Apoptosis in Human Cancer Cell Lines by tea Polyphenols. *Carcinogenesis* 19, 611–616. doi:10.1093/carcin/19.4.611

Yang, J., Pi, C., and Wang, G. (2018a). Inhibition of PI3K/Akt/mTOR Pathway by Apigenin Induces Apoptosis and Autophagy in Hepatocellular Carcinoma Cells. *Biomed. Pharmacother.* 103, 699–707. doi:10.1016/j.biopha.2018.04.072

Yang, J., Ren, X., Zhang, L., Li, Y., Cheng, B., and Xia, J. (2018b). Oridonin Inhibits Oral Cancer Growth and PI3K/Akt Signaling Pathway. *Biomed. Pharmacother.* 100, 226–232. doi:10.1016/j.biopha.2018.02.011

Yang, J.-S., Lin, C.-W., Hsin, C.-H., Hsieh, M.-J., and Chang, Y.-C. (2013). Selaginella Tamariscina Attenuates Metastasis via Akt Pathways in Oral Cancer Cells. *PLoS One* 8, e68035. doi:10.1371/journal.pone.0068035

Yang, K. Y., Lin, L. C., Tseng, T. Y., Wang, S. C., and Tsai, T. H. (2007). Oral Bioavailability of Curcumin in Rat and the Herbal Analysis from Curcuma Longa by LC-MS/MS. *J. Chromatogr. B Analyt Technol. Biomed. Life Sci.* 853, 183–189. doi:10.1016/j.jchromb.2007.03.010

Yang, W. E., Ho, Y. C., Tang, C. M., Hsieh, Y. S., Chen, P. N., Lai, C. T., et al. (2019). Duchesnea Indica Extract Attenuates Oral Cancer Cells Metastatic Potential through the Inhibition of the Matrix Metalloproteinase-2 Activity by Down-Regulating the MEK/ERK Pathway. *Phytomedicine* 63, 152960. doi:10.1016/j.phymed.2019.152960

Ye, D., Zhou, X., Pan, H., Jiang, Q., Zhong, L., Chen, W., et al. (2011). Establishment and Characterization of an HPV16 E6/E7-Expressing Oral Squamous Cell Carcinoma Cell Line with Enhanced Tumorigenicity. *Med. Oncol.* 28, 1331–1337. doi:10.1007/s12032-010-9558-4

Ye, M., Wu, Q., Zhang, M., and Huang, J. (2016). Lycopene Inhibits the Cell Proliferation and Invasion of Human Head and Neck Squamous Cell Carcinoma. *Mol. Med. Rep.* 14, 2953–2958. doi:10.3892/mmr.2016.5597

Yi, J., Yang, J., He, R., Gao, F., Sang, H., Tang, X., et al. (2004). Emodin Enhances Arsenic Trioxide-Induced Apoptosis via Generation of Reactive Oxygen Species and Inhibition of Survival Signaling. *Cancer Res.* 64, 108–116. doi:10.1158/0008-5472.can-2820-2

Yin, F., Zhao, L., Zhang, L., Chen, Y., Sun, G., Li, J., et al. (2020). Chemopreventive Role of Apigenin against the Synergistic Carcinogenesis of Human Papillomavirus and 4-(Methylnitrosamino)-1-(3-Pyridyl)-1-Butanone. *Biomedicines* 8. doi:10.3390/biomedicines8110472

Yoshimura, H., Yoshida, H., Matsuda, S., Ryoke, T., Ohta, K., Ohmori, M., et al. (2019). The Therapeutic Potential of Epigallocatechin-3-gallate against Human Oral Squamous Cell Carcinoma through Inhibition of Cell Proliferation and Induction of Apoptosis: *In Vitro* and *In Vivo* Murine Xenograft Study. *Mol. Med. Rep.* 20, 1139–1148. doi:10.3892/mmr.2019.10331

Yu, X. D., Yang, J. L., Zhang, W. L., and Liu, D. X. (2016). Resveratrol Inhibits Oral Squamous Cell Carcinoma through Induction of Apoptosis and G2/M Phase Cell Cycle Arrest. *Tumour Biol.* 37, 2871–2877. doi:10.1007/s13277-015-3793-4

Zaridze, D., Evstifeeva, T., and Boyle, P. (1993). Chemoprevention of Oral Leukoplakia and Chronic Esophagitis in an Area of High Incidence of Oral

and Esophageal Cancer. *Ann. Epidemiol.* 3, 225–234. doi:10.1016/1047-2797(93)90023-w

Zeka, A., Gore, R., and Kriebel, D. (2003). Effects of Alcohol and Tobacco on Aerodigestive Cancer Risks: a Meta-Regression Analysis. *Cancer Causes Control* 14, 897–906. doi:10.1023/b:caco.0000003854.34221.a8

Zhang, C., Hao, Y., Sun, Y., and Liu, P. (2019). Quercetin Suppresses the Tumorigenesis of Oral Squamous Cell Carcinoma by Regulating microRNA-22/wnt1/β-Catenin axis. *J. Pharmacol. Sci.* 140, 128–136. doi:10.1016/j.jphs.2019.03.005

Zhang, W., Kang, M., Zhang, T., Li, B., Liao, X., and Wang, R. (2016). Triptolide Combined with Radiotherapy for the Treatment of Nasopharyngeal Carcinoma via NF-Kb-Related Mechanism. *Int. J. Mol. Sci.* 17. doi:10.3390/ijms17122139

Zhang, W., Yin, G., Dai, J., Sun, Y. U., Hoffman, R. M., Yang, Z., et al. (2017). Chemoprevention by Quercetin of Oral Squamous Cell Carcinoma by Suppression of the NF-Kb Signaling Pathway in DMBA-Treated Hamsters. *Anticancer Res.* 37, 4041–4049. doi:10.21873/anticanres.11789

Zhang, Y., Sturgis, E. M., Dahlstrom, K. R., Wen, J., Liu, H., Wei, Q., et al. (2013). Telomere Length in Peripheral Blood Lymphocytes Contributes to the Development of HPV-Associated Oropharyngeal Carcinoma. *Cancer Res.* 73, 5996–6003. doi:10.1158/0008-5472.CAN-13-0881

Zhao, M., Ma, J., Zhu, H. Y., Zhang, X. H., Du, Z. Y., Xu, Y. J., et al. (2011). Apigenin Inhibits Proliferation and Induces Apoptosis in Human Multiple Myeloma Cells through Targeting the trinity of CK2, Cdc37 and Hsp90. *Mol. Cancer* 10, 104. doi:10.1186/1476-4598-10-104

Zhu, X., Sui, M., and Fan, W. (2005). *In Vitro* and *In Vivo* Characterizations of Tetrandrine on the Reversal of P-Glycoprotein-Mediated Drug Resistance to Paclitaxel. *Anticancer Res.* 25, 1953–1962.

Zhu, Y., Mao, Y., Chen, H., Lin, Y., Hu, Z., Wu, J., et al. (2013). Apigenin Promotes Apoptosis, Inhibits Invasion and Induces Cell Cycle Arrest of T24 Human Bladder Cancer Cells. *Cancer Cel Int* 13, 54. doi:10.1186/1475-2867-13-54

Zou, Y., Cheng, C., Omura-Minamisawa, M., Kang, Y., Hara, T., Guan, X., et al. (2010). The Suppression of Hypoxia-Inducible Factor and Vascular Endothelial Growth Factor by siRNA Does Not Affect the Radiation Sensitivity of Multicellular Tumor Spheroids. *Jrr* 51, 47–55. doi:10.1269/jrr.09070

Zur Hausen, H., Gissmann, L., Steiner, W., Dippold, W., and Dreger, I. (1975). Human Papilloma Viruses and Cancer. *Bibl Haematol.*, 569–571. doi:10.1159/000399220

Conflict of Interest: The authors declare that the research was conducted in the absence of any commercial or financial relationships that could be construed as a potential conflict of interest.

GLOSSARY

4NQO 4-nitroquinoline 1-oxide
5-FU 5-fluorouracil
Akt protein kinase B
AP-1 activator protein 1
Bax Bcl-2–associated X protein
Bcl-2 B-cell lymphoma 2
Bcl-xL Bcl-2 homolog B-cell lymphoma-extra large
BH3 Bcl-2 homology 3
Bim Bcl-2–interacting mediator of cell death
BRB black raspberry
CAPE caffeic acid phenethyl ester
Cdc2 cell division control 2
CDK2/4 cyclin-dependent kinase 2/4
CDKN2A cyclin-dependent kinase inhibitor 2A
c-Fos cellular oncogene Fos
CIAP2 calf intestinal alkaline phosphatase
Cip1 CDK interacting protein 1
c-Jun cellular Jun
COX-2 cyclooxygenase-2
c-Raf c-Rapidly accelerated fibrosarcoma
CT concurrent chemotherapy
E6/7 Early protein 6/7
EBV Epstein–Barr virus
ECGC (-)-Epigallocatechin-3-gallate
EGFR epidermal growth factor receptor
ERK extracellular signal–regulated kinase
FOXO1 forkhead box protein O1
Fra-2 Fos-related antigen 2
GSK3 glycogen synthase kinase 3
SK3β glycogen synthase kinase 3 beta
HN head and neck
HER2 human epidermal growth factor receptor 2
HIF-1 α hypoxia-inducible factor-1 α
HNC head and neck cancer
HNSCC head and neck squamous cell carcinoma
HO1 heme oxygenase 1
HPV human papillomavirus
IARC international agency for research on cancer
IC50 half maximal inhibitory concentration
IgE immunoglobulin E
IKK inhibitor of nuclear factor-κB kinase
IL-6 interleukin 6
iNOS inducible nitric oxide synthase
IRS-1 insulin receptor substrate 1
IκB inhibitor of nuclear factor-κB
IκBα I-kappa-B-alpha
JAK2 janus kinase2
JNK c-Jun N-terminal kinase
Kip2 kinase inhibitor 1
LC3 microtubule-associated protein 1A/1B-light chain 3
LCN2 lipocalin-2
LSCC laryngeal squamous cell carcinoma
M1 type macrophages activated macrophages
MAPK mitogen-activated protein kinase
MDM2 mouse double minute 2 homolog
miR micro RNA
MLKL mixed lineage kinase domain-like pseudokinase
MMPs metalloproteinases
mTOR mammalian target of rapamycin
mTORC2 mTOR Complex 2
NF-κB nuclear factor kappa light chain enhancer of activated B cells
NPC nasopharyngeal carcinoma
NPSCC nasopharyngeal squamous cell carcinoma
OED oral epithelial dysplasia
OPC oropharyngeal carcinoma
OPMDs oral potentially malignant disorders
OPSCC oropharyngeal squamous cell carcinoma
OSCC oral squamous cell carcinoma
P70S6K 70-kDa ribosomal protein S6 kinase
PCNA proliferating cell nuclear antigen
PD1 programmed cell death protein 1
PI3K phosphatidylinositol 3-kinase
PIP2 phosphatidylinositol-4,5-bisphosphate
PIP3 phosphatidylinositol-3,4,5-bisphosphate
PKA-AMPK protein kinase A–AMP-activated protein kinase
PPARδ peroxisome proliferator–activated receptor delta
pRB phosphorylated retinoblastoma protein
PRR5 proline rich protein 5
pSTAT3 phosphorylated signal transducer and activator of transcription 3
PTEN phosphatase and tensin homolog
Raf rapidly accelerated fibrosarcoma
RBP RNA-binding protein
RICTOR rapamycin-insensitive companion of mammalian target of rapamycin
RIPK1 receptor-interacting serine/threonine-protein kinase 1
ROS reactive oxygen species

RT radiation therapy
RTK receptor tyrosine kinase
S6K1 ribosomal protein S6 kinase beta-1
SCC squamous cell carcinoma
Sin1 stress-activated protein kinase-interacting protein
SLT smokeless tobacco
SOX2 SRY (sex determining region Y)-box 2
STAT3 signal transducer and activator of transcription 3
TFs transcription factors
TIMPs tissue inhibitor of metalloproteinases
TNFα tumor necrosis factor alpha
Topo IIα topoisomerase II- alpha
TRPA1 transient receptor potential ankyrin 1
VEGF vascular endothelial growth factor
WHO World Health Organization
XIAP X-linked inhibitor of apoptosis protein
ZSP ZengShengPing

frontiers in Pharmacology

ORIGINAL RESEARCH
published: 29 July 2021
doi: 10.3389/fphar.2021.673103

Phenethyl Isothiocyanate Induces Apoptosis Through ROS Generation and Caspase-3 Activation in Cervical Cancer Cells

*Shoaib Shoaib [1], Saba Tufail [1], Mohammad Asif Sherwani [2], Nabiha Yusuf [2] and Najmul Islam [1]**

[1]Department of Biochemistry, J.N.M.C, Aligarh Muslim University, Aligarh, India, [2]Department of Dermatology, University of Alabama at Birmingham, Birmingham, AL, United States

The latest research shows that current chemotherapeutics are ineffective because of the development of resistance in cervical cancer cells, and hence, their scope of use is limited. The main concern of researchers at the moment is the discovery of safe and effective antiproliferative plant chemicals that can aid in the battle against cervical cancer. Previous studies have shown the possible anticancer potential of phenethyl isothiocyanate obtained from cruciferous plants for many cancers, which targets various signaling pathways to exercise chemopreventive and therapeutic effects. This provides the basis for studying phenethyl isothiocyanate's therapeutic potential against cervical cancer. In the present study, cervical cancer cells were treated with various doses of phenethyl isothiocyanate, alone and in combination with cisplatin. Phenethyl isothiocyanate alone was sufficient to cause nucleus condensation and fragmentation and induce apoptosis in cervical cancer cells, but evident synergistic effects were observed in combination with cisplatin. In addition, phenethyl isothiocyanate treatment increased the production of intracellular ROS in a dose-dependent manner in cervical cancer cells. Furthermore, investigation of phenethyl isothiocyanate induced mitochondrial reactive oxygen species production, and activation of caspases showed that phenethyl isothiocyanate significantly activated caspase-3.

Keywords: cervical cancer, HPV16+, ROS, apoptosis, DNA fragmentation

OPEN ACCESS

Edited by:
Farrukh Aqil,
University of Louisville, United States

Reviewed by:
Hamidullah Khan,
University of Wisconsin–Madison, United States
Irfan Ansari,
Integral University, India
Farrukh Afaq,
University of Alabama at Birmingham, United States

****Correspondence:***
Najmul Islam
najmulamu@gmail.com

Specialty section:
This article was submitted to Pharmacology of Anti-Cancer Drugs, a section of the journal Frontiers in Pharmacology

Received: *26 February 2021*
Accepted: *14 June 2021*
Published: *29 July 2021*

Citation:
Shoaib S, Tufail S, Sherwani MA, Yusuf N and Islam N (2021) Phenethyl Isothiocyanate Induces Apoptosis Through ROS Generation and Caspase-3 Activation in Cervical Cancer Cells. Front. Pharmacol. 12:673103. doi: 10.3389/fphar.2021.673103

INTRODUCTION

Being one of the critical and major public health problems, cervical cancer stands fourth in women and seventh among all the cancers in the world (Ferlay et al., 2015). Epidemiological studies have indicated its high incidence and mortality, accounting for 0.57 million cases and 0.311 million deaths in 2018 (Cohen et al., 2019). In most cervical cancer malignancies, human papilloma virus (HPV) infection was found to be related to HPV16 and HPV18 at higher risk (Moody and Laimins, 2010). Although medical facilities have progressed, cervical cancer is still rising in terms of incidence and deaths worldwide due to the lack of cost-effective diagnosis and therapies (Arbyn et al., 2011).

The most common cervical cancer treatment strategies are hysterectomy, radiotherapy, chemotherapy, and chemoradiotherapy. The surgery is successful if cervical cancer is diagnosed early, but largely, metastasized cervical cancer is diagnosed at the late stage (Sak, K., 2014). Radiation

therapy of patients with cervical cancer or any other cancer has been reported for adverse side effects on the gastrointestinal, gynecological, and urological systems (Klee et al., 2000). The concurrent use of chemotherapy combined with radiotherapy has also been reported to give rise to hematologic and gastrointestinal side effects in cervical cancer (Eifel, 2006). The standard first-line medicaments (chemotherapeutics) for the treatment of cervical cancer are cisplatin and 5-fluorouracil–based chemotherapy; however, it is accompanied by drug resistance. Reckoning with these conditions, the development of a safe treatment plan, which is more precise and effective, with the least side effects is urgently required.

In recent decades, cervical cancer has been targeted by a variety of herbal compounds for their anticancer potential, creating opportunities to discover new anticancer medicines to address the problems of drug resistance and adverse side effects caused by traditional therapies. Multiple herbal compounds have been shown to have important effects on various signaling pathways of the cervical cancer cell (Chauhan et al., 2009; Moga et al., 2016). Phenethyl isothiocyanate (PEITC), most commonly seen in watercress and cruciferous vegetables, exhibits various beneficial behaviors. In cancer cells, PEITC has been shown to have antioxidant, anti-inflammatory, and antiproliferative activity and induces apoptosis (Xu et al., 2005; Satyan et al., 2006; Hong et al., 2015; Sarkar et al., 2016; Ramirez et al., 2018). In the current study, we tried to investigate the effects of PEITC on the HPV16+ and HPV18+ cervical cancer cell lines (CaSki and HeLa).

MATERIALS AND METHODS

Reagents

All the reagents used in this study were of molecular grade. PEITC, cisplatin, propidium iodide (PI), 4,6-diamidino-2-phenylindole (DAPI), 2,7-dichlorofluorescein diacetate(DCF-DA), dihydrorhodamine 123, N-acetylcysteine (NAS), 3-(4,5-dimethylthiazol-2-yl)-2,5-diphenyl tetrazolium bromide (MTT), dimethyl sulfoxide, and caspase-3, -8, and -9 inhibitors were procured from Sigma Aldrich Chemical Co. (United States). Caspase activity kits were purchased from BioVision, United States, and an FITC Annexin V Apoptosis kit was obtained from BD Biosciences (United States). Fetal bovine serum (FBS), Dulbecco's modified Eagle's medium (DMEM), and other chemicals were purchased from Thermo Fisher Scientific.

Cell Culture

Human cervical cancer cell lines (CaSki and HeLa) and a normal human keratinocyte cell line (HaCaT) were purchased from the National Center for Cell Sciences (NCCS), Pune, India and ATCC, respectively. The cells were grown in DMEM supplemented with 10% FBS and 1% antibiotic–antimycotic solution containing penicillin and streptomycin. The cells were maintained in a humidified atmosphere containing 5% CO_2 at 37°C in a CO_2 incubator.

Determination of Cell Viability Using MTT Assay

To determine the effect of phenethyl isothiocyanate on normal human keratinocyte, HaCaT cells and cervical cancer cells (CaSki and HeLa) were analyzed using MTT assay. Briefly, the cells were seeded into a 96-well plate at a density of 5×10^3 cells per well in triplicate and incubated at 37°C for 24 h. The cells were treated with different concentrations of PEITC (0, 2, 5, 10, 15, 20, and 25 μM) for 24 and 48 h. Control group cells were treated with 0.01% DMSO in media. Subsequently, cell survival was determined by adding 10 μL of 5 mg/ml MTT reagent in each well, followed by incubation for 4 h at 37°C, and then 100 μL of dimethyl sulfoxide was added to dissolve formazan by gentle shaking. The absorbance of each well was measured at 570 nm, and cell survival was calculated as percentage over the control. Additionally, cisplatin was also used to determine and compare cytotoxicity on the cell lines, either alone or in combination with the tested compound. The purpose of including HaCaT cells (normal keratinocyte cell line) is to compare the cytotoxic effect of phenethyl isothiocyanate.

Analysis of Morphological Changes by Phase Contrast Microscopy

The morphological changes in PEITC-treated normal and cervical cancer cells were analyzed by phase contrast microscopy as described previously (Kim et al., 2015). 5×10^3 cells were seeded per well in a 96-well plate in triplicate and incubated for 24 h in a 5% CO_2 incubator at 37°C. Thereafter, the cell lines were re-supplemented with increasing concentrations of PEITC for 24 h, and then cellular morphological changes were observed under a phase contrast microscope and compared with the control untreated cell group.

Determination of DNA Fragmentation by DAPI Staining

The nuclear morphology of the apoptotic cells was observed by fluorescence microscopy after DAPI staining (Al-Otaibi et al., 2018). Briefly, 5×10^3/ml CaSki and HeLa cells were seeded into a 6-well plate, followed by incubation for 24 h, and then treated with various concentrations of PEITC for 24 h. Thereafter, the cells were washed with cold phosphate-buffered saline (PBS) and fixed in ice-cold 70% methanol for 10 min. The cells were then stained with DAPI and incubated for 15 min at 37°C in the dark. Finally, the cells were again washed with PBS, and the cells were observed under a fluorescence microscope (Nikon ECLIPSE Ti-S, Japan).

Determination of Apoptosis by Flow Cytometry and Annexin-V FITC/Propidium Iodide Staining

The prominent characteristic of apoptosis is the alteration in the distribution of phosphatidylserine on the two leaflets of the plasma membrane. The apoptosis induction was determined using the annexin V-FITC kit according to the manufacturer's protocol. In

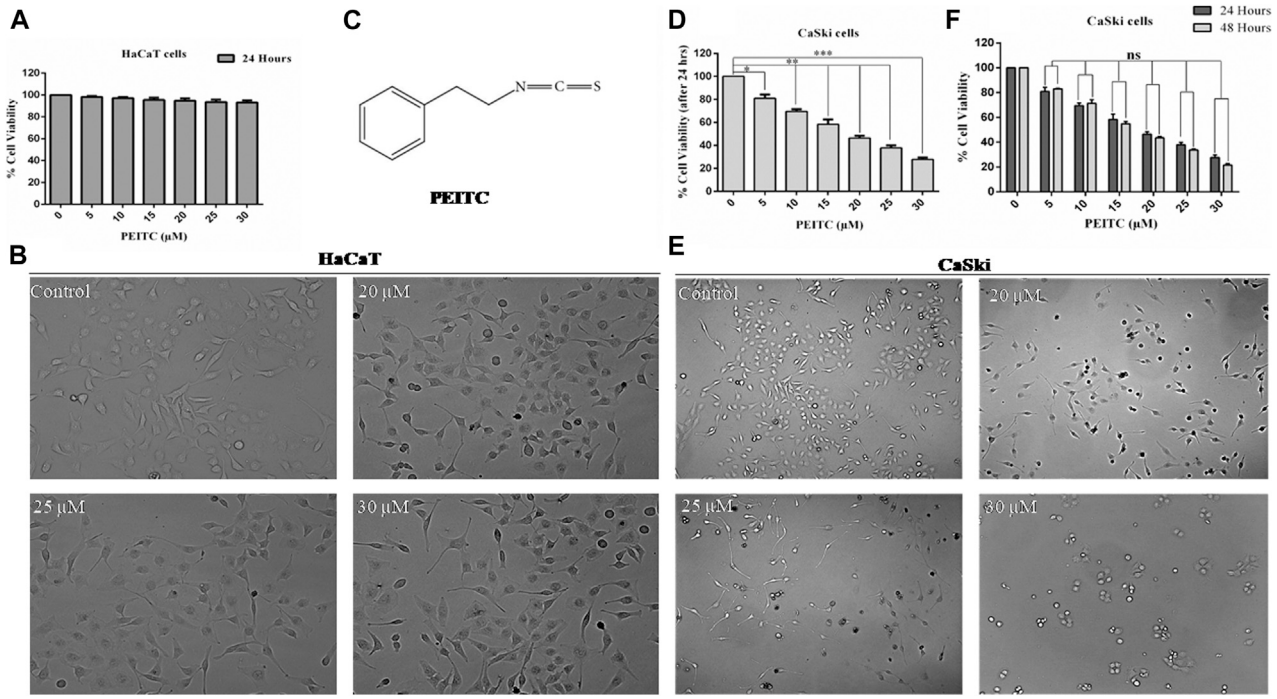

FIGURE 1 | Cell viability assay was performed to assess the effect of PEITC on HaCaT and CaSki cell lines. **(A)** PEITC exerted insignificant cytotoxic effects on HaCaT cells at various doses. **(B)** Morphological analysis showed that phenethyl isothiocyanate at doses of 20, 25, and 30 μM did not significantly alter the morphology of HaCaT 24 h after treatment. **(C)** Represents the structure of phenethyl isothiocyanate. **(D)** Phenethyl isothiocyanate resulted in significant cytotoxic effects in CaSki cells after 24 h of treatment in a dose-dependent manner when compared to the untreated control. **(E)** Cytotoxic effect of phenethyl isothiocyanate as analyzed by phase contrast microscopy. Similar to the cell viability result, phenethyl isothiocyanate sufficiently induced morphological changes in CaSki cells at 20, 25, and 30 μM after 24 h of treatment. **(F)** Inhibition of cell survival after 48 h of treatment with phenethyl isothiocyanate further increased as compared to that after 24 h in CaSki cells. The graphs represent ± SD of three independent experiments. The image is the representation of three independent experiments. *p value < 0.05 compared with the untreated control was considered statistically significant.

brief, the cells were washed with cold phosphate-buffered saline after 24 h of PEITC treatment and then incubated with 5 μl fluorochrome-conjugated annexin V for 15 min at room temperature. Thereafter, the cell suspension was centrifuged at 600 × g for 5 min and the supernatant was discarded, followed by incubation with 5 μl propidium iodide solution at room temperature for 15 min. Apoptotic cells were immediately analyzed by flow cytometry. Annexin V/PI staining was also performed in accordance with the previously described method (Mannarreddy et al., 2017). Briefly, the cells were treated with various concentrations of PEITC for a period of 24 h and then washed and fixed with methanol and acetic acid (3:1 v/v) for 10 min. The cells were incubated with Annexin V and PI for 30 min at room temperature in the dark and then immediately examined under a fluorescence microscope after washing with PBS.

Assay of Caspase-3, Caspase-8, and Caspase-9 Activities

Briefly, cells were seeded and allowed to grow for 24 h. The caspase activity in PEITC-treated and untreated cervical cancer cells was determined using caspase colorimetric assay kits. The cells were lysed in 50 μl ice-cold cell lysis buffer and centrifuged for 3 min at 8,000 × g after incubation for 10 min on ice to collect the supernatant. Then, 50 μl cell lysate was transferred into a 96-well plate, and 50 μl of reaction buffer containing 10 mM DTT was added. Thereafter, 5 μl of 4 mM DEVD-pNA substrate was transferred to each well and allowed to incubate for 1 h at 37°C. Finally, the absorbance was measured at 405 nm on a microtiter plate reader.

Determination of Effect of Caspase Inhibitors

To determine the effect of PEITC, the CaSki and HeLa cells were pretreated with 50 μM each of Z-DEVD-FMK (caspase-3 inhibitor), Z-IETD-FMK (caspase-8 inhibitor), and Z-LEHD-FMK (caspase-9 inhibitor) for 2 h. Then, cells were treated with various concentrations of PEITC for 24 h, and cell survival was determined using MTT assay as described above.

Determination of Mitochondrial Oxidative Stress

The oxidative stress in mitochondria is measured on the basis of the generation of peroxynitrite through dihydrorhodamine 123 (DHR123), a cell-permeable fluorogenic probe. DHR123 is oxidized into rhodamine 123 upon reacting with peroxynitrite

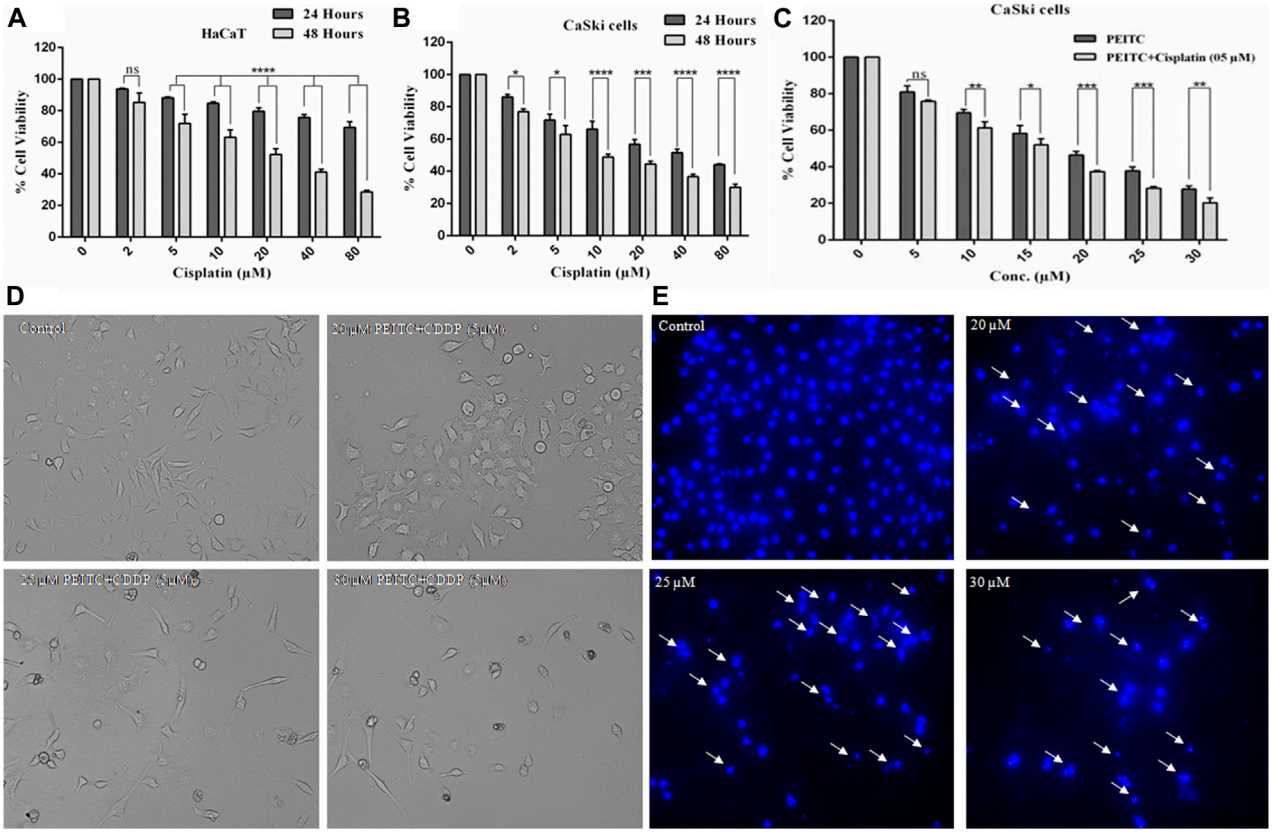

FIGURE 2 | (A) Cisplatin exerted cytotoxicity on the normal cell line (HaCaT). **(B)** Cisplatin-treated CaSki cells showed significant reduction in cell viability in a dose and time dependent manner. **(C)** Percent cell viability of CaSki cells exposed to various doses of PEITC (5-30 μM) accompanied with 5 μM cisplatin compared to individual PEITC-treatment (5-30 μM). **(D)** Combined doses of PEITC with sub-optimal concentration of cisplatin (5 μM) exerted significant cytotoxic effects on CaSki cells. **(E)** CaSki cells were incubated with different concentration of PEITC (20, 25 and 30 μM) for 48 h, then nuclear condensation and fragmentation (white arrows) was detected by fluorescence microscopy. The data represents mean ±SD of three independent experiments. The image is the representation of three independent experiments. *p value < 0.05 compared with the untreated control was considered statistically significant.

and localizes in the mitochondria, exhibiting green fluorescence (Sobreira et al., 1996). Following PEITC treatment on grown CaSki and HeLa cells for 24 h, 1.25 μM DHR123 was added and incubated for 30 min at 37°C in the dark. Subsequently, the cells were fixed and washed twice with PBS before being examined under the fluorescence microscope.

Determination of Intracellular ROS Level

The intracellular level of reactive oxygen species was measured using the DCF-DA method as described previously (Wasim and Chopra, 2018). To study the effect of PEITC, CaSki and HeLa cells were seeded into a 12-well plate and incubated for 24 h. The cells were exposed to various concentrations of PEITC for 24 h and then fixed and incubated with 10 μM DCF-DA for 30 min at 37°C, wrapped in aluminum foil. The cells were washed with PBS to remove the excessive DCF-DA, and images were examined under the fluorescence microscope.

Determination of Effect of an ROS Inhibitor, N-Acetylcysteine

We used an ROS inhibitor, N-acetylcysteine (NAC), to verify the intracellular ROS generation in PEITC-treated CaSki and HeLa cells. Briefly, the cells were incubated with 10 mM NAC for 2 h following the PEITC treatment for 24 h. Thereafter, 10 μM DCFH-DA was added and incubated for 30 min at 37°C in the dark. After washing with PBS, the images were captured using the fluorescence microscope. Additionally, we also checked the cell viability in the presence of NAC using MTT assay as described above.

Evaluation of Synergistic Interaction Between Phenethyl Isothiocyanate and Cisplatin Using Chou–Talalay's Method

The effect on cell viability of CaSki cells was determined using MTT cytotoxicity assay after 24 h of incubation, and the combination

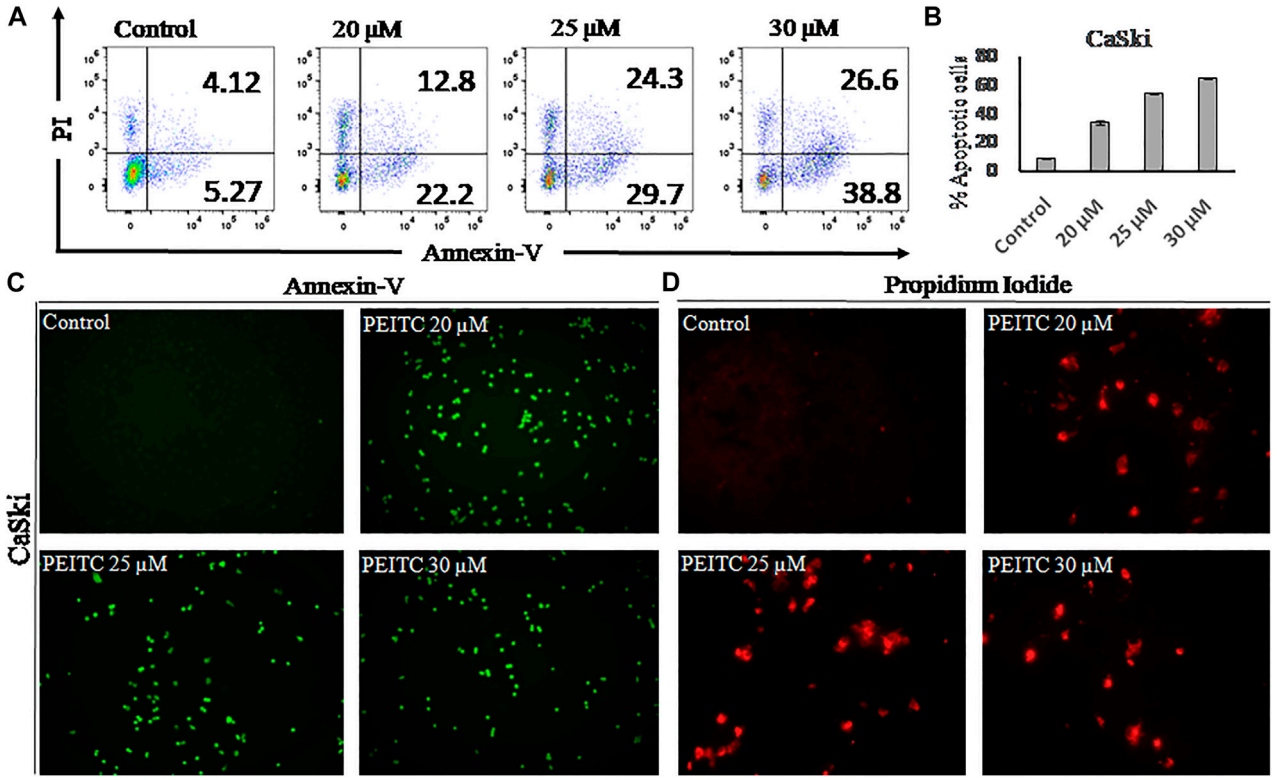

FIGURE 3 | (A) After 24 hours apoptosis induction was quantified in PEITC-treated CaSki cells by Annexin V-FITC kit using flow cytometry. **(B)** Apoptosis percentage in PEITC-treated CaSki cells was measured. CaSki cells were induced with different concentration of PEITC (20, 25 and 30 µM) for 24 h and fluorescent microscopic images of Annexin V-FITC/PI stained cells were captured to examine the induction of apoptosis in CaSki cells under fluorescent microscope. PI can bind with damaged nucleus of cancer cells and Annexin V-FITC binds with phosphatidylserine of the plasma membrane. (**C and D**) Control untreated CaSki cells appear non-fluorescent while the fluorescent bright green and red demonstrate induction of apoptosis in CaSki cells. The data represents mean ±SD of three independent experiments. The image is the representation of three independent experiments.

index (CI) values were calculated using Chou–Talalay's method (Chou and Talalay, 1983; Chou et al., 1994). The CI for the two drugs at IC_{50} and IC_{70} was calculated using the following equation:

$$CI = (D)_1/(Dx)_1 + (D)_2/(Dx)_2,$$

where $(Dx)_1$ and $(Dx)_2$ represent the lone concentrations of PEITC and cisplatin, respectively, which were required for x% inhibition and $(D)_1$ and $(D)_2$ are the concentrations of PEITC and cisplatin, respectively, used in the combination that together induced x% inhibition. The CI value quantitatively defines synergism (if CI < 1), additive effect (if CI = 1), and antagonism (if CI > 1).

Statistical Analysis

Statistical analysis was performed using GraphPad Prism 6.0 software. All the experiments presented here were performed in triplicate, and each experiment was repeated three times. The error bars for all the data indicate mean ± standard deviation (SD). The two groups were compared by one- and two-way ANOVA using Dunnett's and Tukey's multiple comparison tests, respectively. A p-value <0.05 was considered to be significant.

RESULTS

Phenethyl Isothiocyanate Exerted Insignificant Cytotoxic Effects on HaCaT Cells

The human keratinocytes (normal cell line HaCaT) were used for investigating phenethyl isothiocyanate cytotoxicity through MTT assay (viability) and phase contrast microscopy (morphological changes). As the findings show, exposure of phenethyl isothiocyanate resulted in negligible toxicity to normal cells (HaCaT) up to a dose of 30 µM for 24 h. Percentage of normal cell survival at doses of 20, 25, and 30 µM after 24 h was recorded as 94.78, 93.62, and 93.28%, respectively, which is statistically insignificant compared to the untreated control (**Figure 1A**). In addition, morphological analysis showed that phenethyl isothiocyanate at doses of 20, 25, and 30 µM did not significantly alter the morphology of HaCaT 24 h after treatment (**Figure 1B**). Consequently, the findings clearly endorse negligible cytotoxic effects of phenethyl isothiocyanate on normal cells. **Figure 1C** represents the structure of phenethyl isothiocyanate.

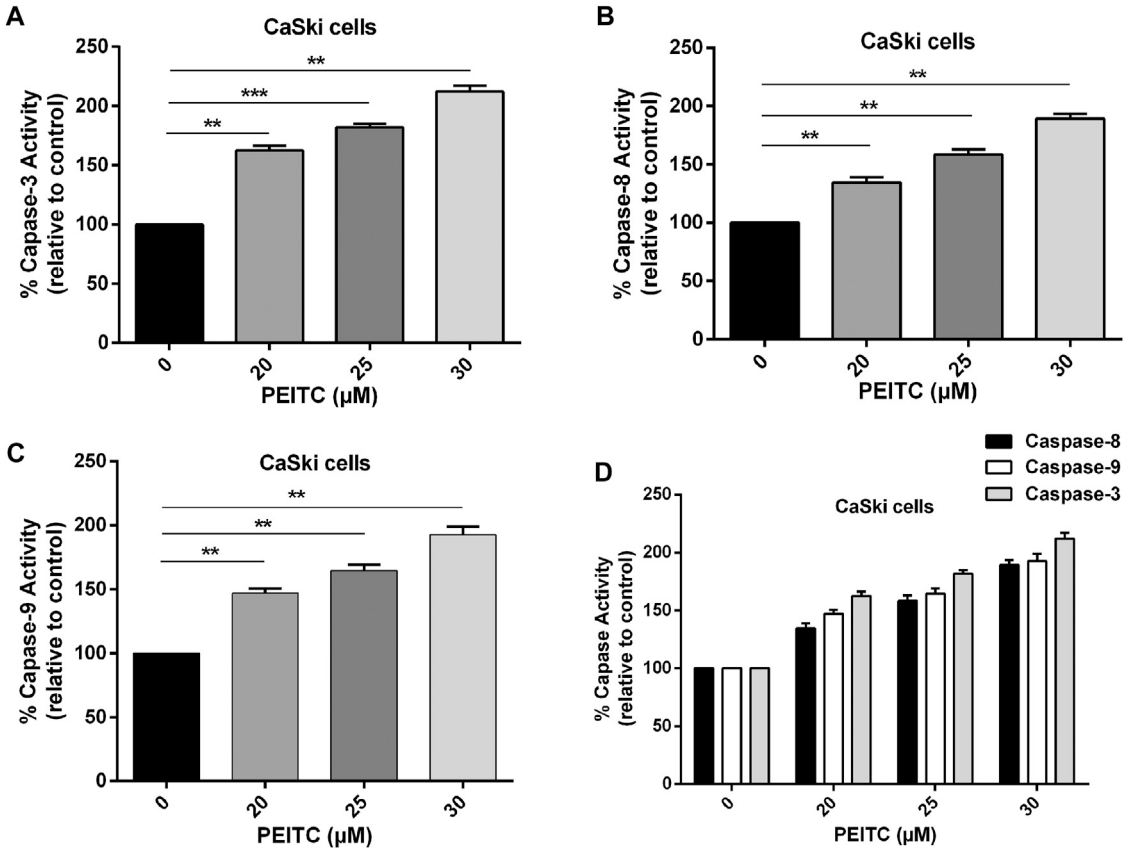

FIGURE 4 | Effect of PEITC on apoptosis induction as assessed by caspase-3, -8 and -9 activity assays. **(A-C)** PEITC-treatment (20, 25 and 30 μM) resulted in induction of apoptosis in CaSki cells through activation of caspase-3, -8 and -9 after 24 h. **(D)** Combined graph exhibiting activation of various cellular caspases in cervical cancer cells after PEITC-treatment. The data represents mean ±SD of three independent experiments. *p value < 0.05 compared with the untreated control was considered statistically significant.

Phenethyl Isothiocyanate Attenuated Cervical Cancer Cell Proliferation

Similarly, cell viability assay (MTT assay) was performed to assess the anticancerous potential of phenethyl isothiocyanate on CaSki and HeLa cells with various concentrations and incubation times, like 24 and 48 h. Phenethyl isothiocyanate treatment resulted in significant cytotoxic effects (i.e., decreased the cervical cancer cell viability) in a dose- and time-dependent manner when compared to the untreated control. After 24 h of phenethyl isothiocyanate treatment, the inhibition percent recorded for CaSki cells was around 19.08, 30.42, 41.68, 53.52, 62.13, and 72.27% at 5, 10, 15, 20, 25, and 30 μM, respectively, as compared to the untreated control (**Figure 1D**). Simultaneously, the cytotoxic effect of phenethyl isothiocyanate was also analyzed by phase contrast microscopy. Similar to the cell viability result, phenethyl isothiocyanate has sufficiently induced morphological changes in CaSki cells at 20, 25, and 30 μM after 24 h of treatment (**Figure 1E**). Moreover, inhibition of cell survival after 48 h of treatment with phenethyl isothiocyanate further increased as compared to that after 24 h (**Figure 1F**). Moreover, PEITC treatment exerted significant cytotoxicity in HeLa cells in a dose- and time-dependent manner. Thereafter, the morphological changes in PEITC-treated HeLa cells were analyzed by phase contrast microscopy. All the experimental data of HeLa cells are provided in **Supplementary Material**.

Cisplatin Attenuated Growth of Normal and Cervical Cancer Cells

To gain an understanding of the comparative cytotoxicity, cancer cell lines (CaSki and HeLa) and normal cells were treated with different doses of cisplatin over 24 and 48 h. The results of cell viability assay showed that cervical cancer cells and normal cells are similarly susceptible to cisplatin. After 48 h of cisplatin treatment, HaCaT cells showed 85.29, 71.95, 63.20, 52.25, 41.14, and 28.61% survival at the corresponding doses of 2, 5, 10, 20, 40, and 80 μM, respectively (**Figure 2A**). Briefly, after 24 h of treatment, the cell survival percent of CaSki cells at various doses of 2, 5, 10, 20, 40, and 80 μM was found to be 86, 71.75, 66.11, 56.81, 51.52, and 44.09%, respectively, as compared to the untreated control. On the other hand, after 48 h of exposure, the cell viability of cisplatin-treated CaSki cells was further reduced but not very significantly compared to that after 24 h, which was observed as 76.94, 62.85, 48.75, 44.43, 36.59, and 30.03% at the same doses of 2, 5, 10, 20, 40, and 80 μM, respectively (**Figure 2B**). Furthermore, cisplatin-treated HeLa cells also

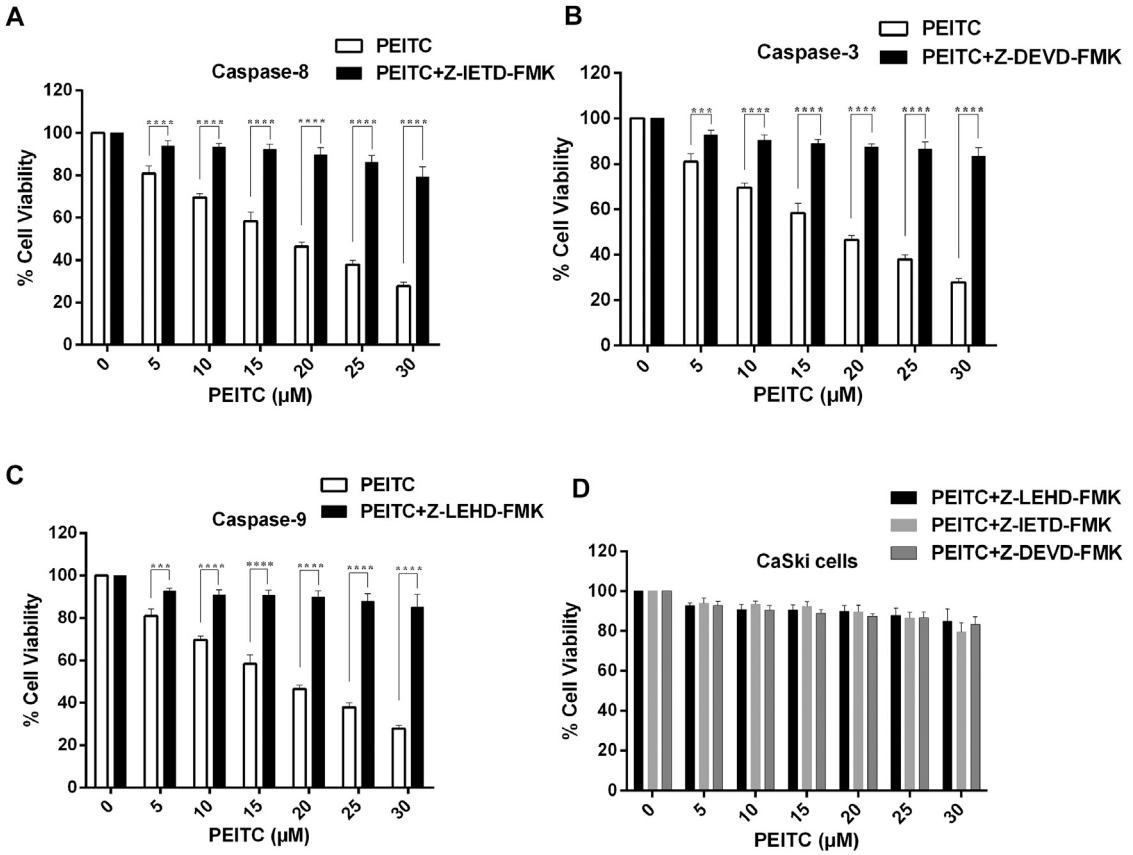

FIGURE 5 | Effect of PEITC on activation of caspases in CaSki cells as assessed in the presence of caspase inhibitors. Percent cell viability of PEITC-treated (20, 25 and 30 μM) CaSki cell was determined in the presence of caspase inhibitors by MTT assay. **(A)** Z-DEVD-FMK-caspase-3 inhibitor, **(B)** Z-IETD-FMK-caspase-8 inhibitor and **(C)** Z-LEHD-FMK-caspase-9 inhibitor. **(D)** Combined graph showing percent cell viability of PEITC-treated CaSki cells in the presence of caspase inhibitors. The data represents mean ±SD of three independent experiments. *p value < 0.05 compared with the untreated control was considered statistically significant.

showed cytotoxicity in a dose- and time-dependent manner (**Supplementary Material**).

Phenethyl Isothiocyanate Exerted Synergistic Effects With Cisplatin on CaSki Cells

Growth inhibitory effects of phenethyl isothiocyanate on the cervical cancer cells triggered a great interest in investigating the combined effects of phenethyl isothiocyanate with cisplatin on CaSki cells. The cervical cancer cells were grown and treated with a suboptimal dose of cisplatin (5 μM) combined with increasing doses of phenethyl isothiocyanate (5–30 μM), and cell viability was estimated using MTT assay. After 24 h of incubation, the result of a substantial decrease in proliferation, which was 24.21, 38.66, 48.02, 62.59, 71.81, and 79.9% at the concentrations of 2, 5, 10, 20, 40, and 80 μM of phenethyl isothiocyanate, respectively, in combination with 5 μM cisplatin, compared to phenethyl isothiocyanate alone, suggested that phenethyl isothiocyanate inhibits cell survival synergistically when combined with a suboptimal dose of cisplatin (**Figure 2C**). The combination index (CI) method of Chou–Talalay was used to ascertain the synergistic interaction between PEITC and cisplatin. The CI values at IC_{50} and IC_{70} were found to be 0.875 and 0.892, respectively. Both the values being less than one clearly shows the synergism between PEITC and cisplatin in inhibiting the growth of cancer cells. Moreover, morphological changes were also observed in cervical cancer cells exposed to phenethyl isothiocyanate combined with a suboptimal dose of cisplatin (5 μM) (**Figure 2D**). Similarly, HeLa cells were also treated with various doses of PEITC combined with a suboptimal dose of cisplatin (5 μM), followed by morphological analysis (**Supplementary Material**).

Phenethyl Isothiocyanate Induced Nuclear Fragmentation and Condensation in Cervical Cancer Cells

Mostly, apoptosis involvement is delineated through the assessment of prominent nuclear fragmentation and condensation. DAPI staining was performed to confirm whether the proliferation inhibition of phenethyl isothiocyanate–treated cervical cancer cells was due to apoptosis. The results indicated that phenethyl isothiocyanate

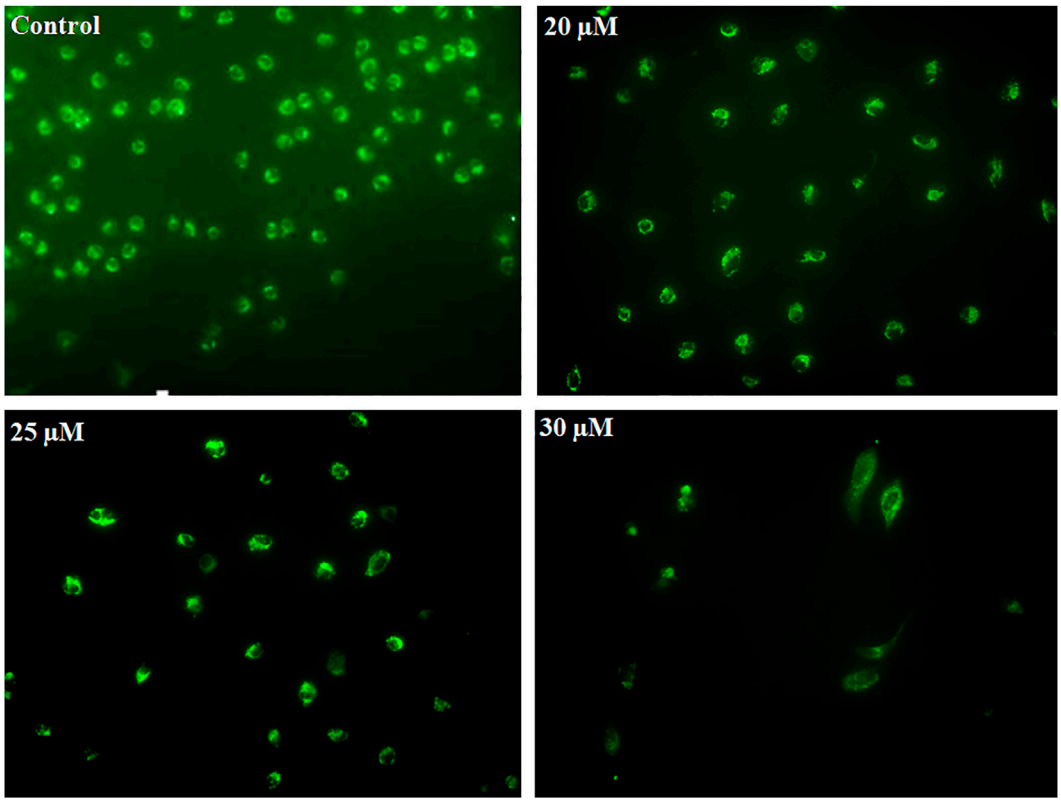

FIGURE 6 | CaSki cells were exposed to different concentration of PEITC (20, 25 and 30 μM) for 24 h. Then, cervical cancer cells were analyzed for mitochondrial ROS generation by fluorescence microscope using DHR123. The image is the representation of three independent experiments.

significantly induced nuclear changes at various doses (20, 25, and 30 μM) post treatment for 24 h. Phenethyl isothiocyanate induced nuclear fragmentation and condensation in cervical cancer cells in a dose-dependent manner, as indicated in the photomicrographs (**Figure 2E**). Thus, the results suggested that phenethyl isothiocyanate possesses apoptotic potential to attenuate the cervical cancer cell proliferation.

Phenethyl Isothiocyanate Induced Apoptosis in the Cervical Cancer Cells

Apoptosis is observed *via* the movement of phosphatidylserine from the inner leaflet to the outer leaflet of the plasma membrane. In order to check the apoptotic effect of phenethyl isothiocyanate on CaSki cells, we used the phosphatidylserine-specific membrane-impermeable dye annexin-V with the FITC tag and the nuclear staining dye PI. Therefore, to elaborate on the effect of PEITC on cervical cancer, CaSki and HeLa cells were treated with various doses of PEITC for 24 h, and then the cells were trypsinized and harvested for flow cytometry, pronouncing the apoptosis induction in cervical cancer cells (**Figures 3A,B**). The staining results of CaSki and HeLa cells (green fluorescence) showed substantial annexin V-FITC binding and showed a considerable apoptosis induction in the phenethyl isothiocyanate–treated cancer cells compared to the untreated control (**Figure 3C**). Furthermore, the red fluorescence observed in phenethyl isothiocyanate–administered CaSki and HeLa cells stipulates the PI stain of the nucleus in the apoptotic cells (**Figure 3D**).

Phenethyl Isothiocyanate Caused Activation of Caspases (Caspase-8, -9, and -3) in Cervical Cancer Cells

The role of caspases in phenethyl isothiocyanate–mediated apoptosis cells was investigated to gain insight at the molecular level. The caspases belong to the family of cystein proteases which exist as inactive zymogens in the cells. One of the key factors at the onset of apoptosis is a cascade of catalytic activation of caspases, which further leads to apoptosis. Particularly, caspase-8 and caspase-9 are known as initiator caspases of the extrinsic and intrinsic apoptosis pathways, respectively, while caspase-3 is the main executioner of apoptosis. So, we measured caspase activity in phenethyl isothiocyanate–treated and untreated cervical cancer cells. Phenethyl isothiocyanate–treated CaSki cells showed significant caspase activity in a concentration-dependent manner. The results indicated that phenethyl isothiocyanate administration caused increased caspase-3 activities in cervical cancer cells as 62.53, 81.89, and 112.06% at 20, 25, and 30 μM, respectively, as compared to the untreated control (**Figure 4A**). Likewise, a substantial dose-dependent increment in caspase-8 and caspase-9 activities was

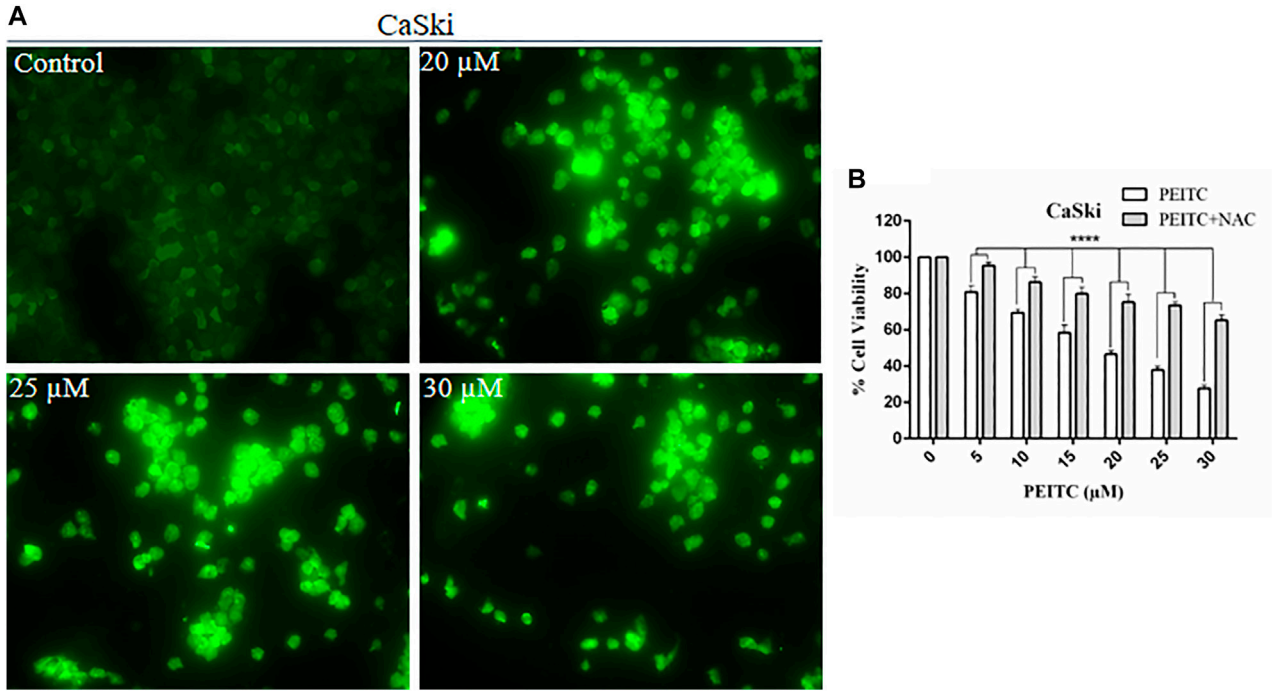

FIGURE 7 | Analysis of ROS generation using DC-FDA staining on CaSki cells treated with PEITC for 24 h and the images were captured by fluorescence microscopy. **(A)** PEITC treatment resulted in significant production of ROS in cervical cancer cells. **(B)** Percent cell viability of PEITC treated (20, 25 and 30 µM) CaSki cells was assessed in the presence of ROS inhibitor, NAC, by MTT assay. The data represents mean ±SD of three independent experiments. *p value < 0.05 compared with the untreated control was considered statistically significant.

observed in cervical cancer cells at the same doses as depicted in **Figures 4B–D**.

Caspase Inhibitors Attenuated Phenethyl Isothiocyanate–Mediated Apoptosis in Cervical Cancer Cells

We further studied the cell viability assay of the phenethyl isothiocyanate–mediated cytotoxic effect of CaSki and HeLa cells in order to understand the role of the caspase inhibitors (Z-DEVD-FMK, Z-IETD-FMK, and Z-LEHD-FMK for caspase-3, -8, and -9, respectively). We observed significant reduction in the inhibition percent of cell survival in phenethyl isothiocyanate–exposed cervical cancer cells which were pretreated with caspase inhibitors, as shown in **Figures 5A–D**. Phenethyl isothiocyanate mediated apoptosis due to caspase activation in cervical cancer cells, simultaneously; caspase inhibitors did not fully mitigate phenethyl isothiocyanate–induced cytotoxicity, indicating an additional function of the caspase-independent pathway.

Phenethyl Isothiocyanate Induced ROS Generation in Mitochondria of Cervical Cancer Cells

Early apoptosis is marked by the decreased mitochondrial membrane potential. Dihydrorhodamine 123 is a non-fluorescent molecule until it oxidizes to fluorescent rhodamine 123 in the presence of peroxynitrite, which is localized in the mitochondria and exhibits green fluorescence. After PEITC treatment, CaSki and HeLa cells were analyzed to determine the mitochondrial ROS generation. PEITC-treated cells were analyzed for peroxynitrite using a fluorescence microscope. PEITC-treated cervical cancer cells showed oxidation of dihydrorhodamine 123, which indicates the production of mitochondrial reactive oxygen species, particularly peroxynitrite. Decreased green fluorescence suggested that PEITC significantly exerted cytotoxic effects with increased concentration as cells undergo apoptosis (**Figure 6**).

Phenethyl Isothiocyanate Elevated Intracellular ROS Production in Cervical Cancer Cells

The cell death may be caspase-dependent or -independent, which is validated through intracellular reactive oxygen species production (ROS). Therefore, to explore the mechanism of action, we further investigated the ROS level in phenethyl isothiocyanate–treated and untreated CaSki and HeLa cells. Strong DCF-fluorescence in phenethyl isothiocyanate–treated CaSki cells showed an elevated level of ROS generation, as compared to the untreated control. Furthermore, the results of DCF-fluorescence also indicated that phenethyl isothiocyanate enhanced ROS generation in cervical cancer cells in a dose-dependent manner (20, 25, and 30 µM) (**Figure 7A**).

N-Acetylcysteine Suppressed Phenethyl Isothiocyanate–Mediated Cytotoxicity in Cervical Cancer Cells

Furthermore, to understand the effect of the ROS inhibitor N-acetylcysteine (NAC) on phenethyl isothiocyanate–mediated cytotoxic effects over CaSki and HeLa cells, we executed cell viability assay at different doses of PEITC. As discussed in the methodology section, cancer cells were treated with 10 mM NAC for 2 h, prior to phenethyl isothiocyanate treatment. The results of viability of NAC-pretreated cells at various doses of phenethyl isothiocyanate (5, 10, 15, 20, 25, and 30 μM) were observed to be 95.45, 86.27, 79.89, 75.20, 73.56, and 65.24%, which was comparatively more than that of the cells not treated with the ROS inhibitor, as depicted in **Figure 7B**. Thus, the results advised that intracellular ROS generation plays a crucial role in phenethyl isothiocyanate–mediated apoptosis in cervical cancer cells. At the same time, we also observed that the existence of an ROS inhibitor (NAC) was not fully successful in inhibiting phenethyl isothiocyanate cytotoxicity in CaSki and HeLa cells, suggesting the possibility of ROS-independent apoptosis pathways in phenethyl isothiocyanate–treated cervical cancer cells.

DISCUSSION

At present, the most considerable treatment strategies for cervical cancer are conventional approaches, which include chemotherapy, radiotherapy, and surgery. However, each of the conventional treatment strategies is associated with various complications, such as drug resistance, adverse side effects, low drug efficacy, and cancer recurrence. Formerly, several naturally occurring chemopreventive and chemotherapeutic plant products had been recognized; these trigger a great interest in searching for novel plant products which were reported to have high efficacy, target specificity, and low side effects.

Several recent studies have shown that isothiocyanates obtained from cruciferous plants can be effective in reducing the risk of many cancers as they can cause chemopreventive effects by involving various signaling pathways (Popolo et al., 2017; Abbaoui et al., 2018; Pan et al., 2018; Zhang et al., 2018).Previously, the effect of phenethyl isothiocyanate on KB and HEp-2 indicated growth inhibition and apoptosis induction, exhibited through death receptors 4 and 5(Huong et al., 2011). In the present study, we coherently sought to elucidate the effects of phenethyl isothiocyanate in combination with cisplatin on cervical cancer cells. The aim of the study is to minimize adverse effects and increase medication tolerance and efficacy of traditional standard drugs. It was found that when cervical cancer cells were treated with phenethyl isothiocyanate alone, the viability of cancer cells was significantly reduced in a dose-dependent manner, but in combination with a suboptimal concentration of cisplatin, the viability of cancer cells was further reduced. Phenethyl isothiocyanate and cisplatin together have more cytotoxicity effects than phenethyl isothiocyanate or cisplatin separately, and this indicates that there is an enhanced sensitization of phenethyl isothiocyanate when given in conjunction with the suboptimal dose of cisplatin. The results ascertain that there is synergy between phenethyl isothiocyanate and cisplatin and together they can be considered as a healthy chemical prevention combination in the management of cervical cancer. In conjunction with cell viability results, treatment with phenethyl isothiocyanate, or combination with cisplatin, the morphological examination has also advocated distortion, shrinkage, and detachment of the cervical cancer cells. Earlier *in vitro* experiments also showed the similar effect of phenethyl isothiocyanate on multiple cancer cell lines (Huong et al., 2012; Chen et al., 2013; Ma et al., 2017). On the contrary, the typical cytotoxicity of human keratinocytes does not display phenethyl isothiocyanate, as cisplatin therapy resulted in the cytotoxicity of the normal human keratinocytes.

Chemopreventive agents are capable of regulating the accelerated growth of cancer cells through activation of apoptosis (Braicu et al., 2020). Apoptosis induction can be marked by the fragmentation and condensation of the cell nucleus, inside and outside the membrane leaflets (Nagata, 2000; Saraste and Pulkki, 2000; Balasubramanian et al., 2007). To elucidate the plausible apoptotic mode of action of phenethyl isothiocyanate, nuclear staining and binding of FITC-annexin V with exposed phosphatidylserine were executed. The DAPI staining result indicated condensation and fragmentation of the nucleus, which suggest the induction of the apoptotic cell death in cervical cancer cells when grown in the presence of phenethyl isothiocyanate and cisplatin. The findings of the FITC-annexine V binding were subsequently shown to induce apoptosis in cervical cancer cells with the use of phenethyl isothiocyanate and cisplatin.

Cystein proteases are known to perform multifaceted functions, including apoptosis (Estaquier et al., 2012). Usually, a cascade of caspase activation takes place during apoptosis induction (Degterev et al., 2003). Caspases are synthesized as inactive zymogens (Stennicke et al., 2000), and their activation occurs in response to a particular death signal (Green and Llambi, 2015). The results of caspase activation suggested the involvement of caspase-3, caspase-9, and caspase-8 in apoptosis induction, and the considerable reduction of the cytotoxicity of phenethyl isothiocyanate in the presence of the caspase inhibitor confirmed the caspase-3 participation in execution of the apoptosis in phenethyl isothiocyanate–administered cervical cancer cells. The change in mitochondrial membrane potential during apoptosis is linked to mitochondrial disruption, which may lead to cytochrome c releasing into the cytosol (Gottlieb et al., 2003; Troiano et al., 2007). It has previously been shown that the plant extract has an anticancer activity by apoptosis, which was regulated by the modulation of the mitochondrial membrane potential mechanism and/or by the caspase-3–dependent pathway (Denning et al., 2002; Mantena et al., 2006; Lin et al., 2016; Jaudan et al., 2018). The results of our studies also showed that phenethyl isothiocyanate perturbed mitochondrial functioning, which suggested the involvement of cytochrome-c–dependent apoptosis in cervical cancer cells.

In different biological systems, free radicals are formed and persistently removed, such as reactive oxygen and reactive

nitrogen species, and they have been known to perform many critical roles (Pelicano et al., 2004). In cancer cells, the excessive production of ROS may be accompanied by oxidation of macromolecules including proteins, lipids, and nucleic acids. ROS production can be amplified by chemotherapeutic compounds to kill the cancer cells through ROS-mediated apoptosis, conferring the modulation of the redox status in cancer cells (Schumacker et al., 2006; Trachootham et al., 2009). We found that phenethyl isothiocyanate augmented intracellular ROS production in cervical cancer cells, which further triggered nucleus condensation and fragmentation, mitochondrial disruption, and apoptosis induction. Furthermore, phenethyl isothiocyanate–mediated amelioration of intracellular ROS generation was attenuated when cervical cancer cells were pretreated with NAC (ROS inhibitor), which further justifies the augmented ROS level as being due to cytotoxicity of phenethyl isothiocyanate. Therefore, it can be stated that plausibly phenethyl isothiocyanate alone and in combination with cisplatin could induce apoptosis in cervical cancer cells through the disruption of mitochondria and caspase activation by intracellular ROS generation.

CONCLUSION

Plant products have been used as chemotherapeutic and chemopreventive agents in various infectious and noninfectious diseases for decades. Several phytochemicals have been identified that have anti-inflammatory, antioxidant, and anticancer properties. The findings of this study have provided insights into the effects of phenethyl isothiocyanate on cervical cancer cells, either on its own or in combination with cisplatin, as can be seen from the growth inhibitions, mitochondrial damage, increased intracellular ROS development, and stimulation of caspases in apoptosis induction. Altogether, in the present study, we have observed that phenethyl isothiocyanate is an excellent compound for the management of cervical cancer. Therefore, we can state that employing phenethyl isothiocyanate could help in cervical cancer management if used in combination with the standard cancer drugs.

DATA AVAILABILITY STATEMENT

The original contributions presented in the study are included in the article/**Supplementary Material**; further inquiries can be directed to the corresponding author.

AUTHOR CONTRIBUTIONS

SS and NI conceived the idea. SS, ST, and MS performed the experiments. SS, ST, MS, NY, and NI analyzed the results. SS, ST, MS, and NI wrote the paper.

ACKNOWLEDGMENTS

SS and ST are thankful to the CSIR for the Senior Research Fellowship (SRF) and the UGC for the Women PDF, respectively. NY acknowledges grant support (1R01AR071157-01A1) from National Institute of Arthritis and Mucoskeletal and Skin Diseases.

SUPPLEMENTARY MATERIAL

The Supplementary Material for this article can be found online at: https://www.frontiersin.org/articles/10.3389/fphar.2021.673103/full#supplementary-material

REFERENCES

Abbaoui, B., Lucas, C. R., Riedl, K. M., Clinton, S. K., and Mortazavi, A. (2018). Cruciferous Vegetables, Isothiocyanates, and Bladder Cancer Prevention. *Mol. Nutr. Food Res.* 62 (18), 1800079. doi:10.1002/mnfr.201800079

Al-Otaibi, W. A., Alkhatib, M. H., and Wali, A. N. (2018). Cytotoxicity and Apoptosis Enhancement in Breast and Cervical Cancer Cells upon Coadministration of Mitomycin C and Essential Oils in Nanoemulsion Formulations. *Biomed. Pharmacother.* 106, 946–955. doi:10.1016/j.biopha.2018.07.041

Arbyn, M., Castellsagué, X., de Sanjosé, S., Bruni, L., Saraiya, M., Bray, F., et al. (2011). Worldwide burden of Cervical Cancer in 2008. *Ann. Oncol.* 22 (12), 2675–2686. doi:10.1093/annonc/mdr015

Balasubramanian, K., Mirnikjoo, B., and Schroit, A. J. (2007). Regulated Externalization of Phosphatidylserine at the Cell Surface. *J. Biol. Chem.* 282 (25), 18357–18364. doi:10.1074/jbc.m700202200

Braicu, C., Zanoaga, O., Zimta, A. A., Tigu, A. B., Kilpatrick, K. L., Bishayee, A., et al. (2020). Natural Compounds Modulate the Crosstalk between Apoptosis- and Autophagy-Regulated Signaling Pathways: Controlling the Uncontrolled Expansion of Tumor cells. *Semin. Cancer Biol.* S1044-579X (20), 30111–30115. doi:10.1016/j.semcancer.2020.05.015

Chauhan, S. C., Vannatta, K., Ebeling, M. C., Vinayek, N., Watanabe, A., Pandey, K. K., et al. (2009). Expression and Functions of Transmembrane Mucin MUC13 in Ovarian Cancer. *Cancer Res.* 69 (3), 765–774. doi:10.1158/0008-5472.can-08-0587

Chen, H.-J., Lin, C.-M., Lee, C.-Y., Shih, N.-C., Amagaya, S., Lin, Y.-C., et al. (2013). Phenethyl Isothiocyanate Suppresses EGF-Stimulated SAS Human Oral Squamous Carcinoma Cell Invasion by Targeting EGF Receptor Signaling. *Int. J. Oncol.* 43 (2), 629–637. doi:10.3892/ijo.2013.1977

Chou, T.-C., Motzer, R. J., Tong, Y., and Bosl, G. J. (1994). Computerized Quantitation of Synergism and Antagonism of Taxol, Topotecan, and Cisplatin against Human Teratocarcinoma Cell Growth: a Rational Approach to Clinical Protocol Design. *JNCI J. Natl. Cancer Inst.* 86, 1517–1524. doi:10.1093/jnci/86.20.1517

Chou, T.-C., and Talalay, P. (1983). Analysis of Combined Drug Effects: a New Look at a Very Old Problem. *Trends Pharmacol. Sci.* 4, 450–454. doi:10.1016/0165-6147(83)90490-x

Cohen, P. A., Jhingran, A., Oaknin, A., and Denny, L. (2019). Cervical Cancer. *The Lancet* 393 (10167), 169–182. doi:10.1016/s0140-6736(18)32470-x

Degterev, A., Boyce, M., and Yuan, J. (2003). A Decade of Caspases. *Oncogene* 22 (53), 8543–8567. doi:10.1038/sj.onc.1207107

Denning, M. F., Wang, Y., Tibudan, S., Alkan, S., Nickoloff, B. J., and Qin, J.-Z. (2002). Caspase Activation and Disruption of Mitochondrial Membrane Potential during UV Radiation-Induced Apoptosis of Human Keratinocytes Requires Activation of Protein Kinase C. *Cell Death Differ* 9 (1), 40–52. doi:10.1038/sj.cdd.4400929

Eifel, P. J. (2006). Chemoradiotherapy in the Treatment of Cervical Cancer. *Semin. Radiat. Oncol.* 16 (No. 3), 177–185. doi:10.1016/j.semradonc.2006.02.007

Estaquier, J., Vallette, F., Vayssiere, J.-L., and Mignotte, B. (2012). The Mitochondrial Pathways of Apoptosis. *Adv. Mitochondrial Med.* 942, 157–183. doi:10.1007/978-94-007-2869-1_7

Ferlay, J., Soerjomataram, I., Dikshit, R., Eser, S., Mathers, C., Rebelo, M., et al. (2015). Cancer Incidence and Mortality Worldwide: Sources, Methods and Major Patterns in GLOBOCAN 2012. *Int. J. Cancer* 136 (5), E359–E386. doi:10.1002/ijc.29210

Gottlieb, E., Armour, S. M., Harris, M. H., and Thompson, C. B. (2003). Mitochondrial Membrane Potential Regulates Matrix Configuration and Cytochrome C Release during Apoptosis. *Cel Death Differ* 10 (6), 709–717. doi:10.1038/sj.cdd.4401231

Green, D. R., and Llambi, F. (2015). Cell Death Signaling. *Cold Spring Harbor Perspect. Biol.* 7 (12), a006080. doi:10.1101/cshperspect.a006080

Hong, Y. H., Uddin, M., Jo, U., Kim, B., Suh, D. H., Kim, H. S., et al. (2015). ROS Accumulation by PEITC Selectively Kills Ovarian Cancer Cells via UPR-Mediated Apoptosis. *Front. Oncol.* 5, 167. doi:10.3389/fonc.2015.00167

Huong, L. D., Shim, J.-H., Choi, K.-H., Shin, J.-A., Choi, E.-S., Kim, H.-S., et al. (2011). Effect of β-Phenylethyl Isothiocyanate from Cruciferous Vegetables on Growth Inhibition and Apoptosis of Cervical Cancer Cells through the Induction of Death Receptors 4 and 5. *J. Agric. Food Chem.* 59 (15), 8124–8131. doi:10.1021/jf2006358

Huong, L., Shin, J.-A., Choi, E.-S., Cho, N.-P., Kim, H., Leem, D.-H., et al. (2012). β-Phenethyl Isothiocyanate Induces Death Receptor 5 to Induce Apoptosis in Human Oral Cancer Cells via P38. *Oral Dis.* 18 (5), 513–519. doi:10.1111/j.1601-0825.2012.01905.x

Jaudan, A., Sharma, S., Malek, S. N. A., and Dixit, A. (2018). Induction of Apoptosis by Pinostrobin in Human Cervical Cancer Cells: Possible Mechanism of Action. *PLoS One* 13 (2), e0191523. doi:10.1371/journal.pone.0191523

Kim, M. Y., Park, S.-J., Shim, J. W., Yang, K., Kang, H. S., and Heo, K. (2015). Naphthazarin Enhances Ionizing Radiation-Induced Cell Cycle Arrest and Apoptosis in Human Breast Cancer Cells. *Int. J. Oncol.* 46 (4), 1659–1666. doi:10.3892/ijo.2015.2857

Klee, M., Thranov, I., and Machin, Prof., D. (2000). The Patients' Perspective on Physical Symptoms after Radiotherapy for Cervical Cancer. *Gynecol. Oncol.* 76 (1), 14–23. doi:10.1006/gyno.1999.5642

Lin, M.-T., Lin, C.-L., Lin, T.-Y., Cheng, C.-W., Yang, S.-F., Lin, C.-L., et al. (2016). Synergistic Effect of Fisetin Combined with Sorafenib in Human Cervical Cancer HeLa Cells through Activation of Death Receptor-5 Mediated Caspase-8/caspase-3 and the Mitochondria-dependent Apoptotic Pathway. *Tumor Biol.* 37 (5), 6987–6996. doi:10.1007/s13277-015-4526-4

Ma, Y. S., Hsiao, Y. T., Lin, J. J., Liao, C. L., Lin, C. C., and Chung, J. G. (2017). Phenethyl Isothiocyanate (PEITC) and Benzyl Isothiocyanate (BITC) Inhibit Human Melanoma A375.S2 Cell Migration and Invasion by Affecting MAPK Signaling Pathway *In Vitro*. *Anticancer Res.* 37 (11), 6223–6234. doi:10.21873/anticanres.12073

Mannarreddy, P., Denis, M., Munireddy, D., Pandurangan, R., Thangavelu, K. P., and Venkatesan, K. (2017). Cytotoxic Effect of Cyperus Rotundus Rhizome Extract on Human Cancer Cell Lines. *Biomed. Pharmacother.* 95, 1375–1387. doi:10.1016/j.biopha.2017.09.051

Mantena, S. K., Sharma, S. D., and Katiyar, S. K. (2006). RETRACTED: Berberine Inhibits Growth, Induces G1arrest and Apoptosis in Human Epidermoid Carcinoma A431 Cells by Regulating Cdki-Cdk-Cyclin cascade, Disruption of Mitochondrial Membrane Potential and Cleavage of Caspase 3 and PARP. *Carcinogenesis* 27 (10), 2018–2027. doi:10.1093/carcin/bgl043

Moga, M., Dimienescu, O., Arvatescu, C., Mironescu, A., Dracea, L., and Ples, L. (2016). The Role of Natural Polyphenols in the Prevention and Treatment of Cervical Cancer-An Overview. *Molecules* 21 (8), 1055. doi:10.3390/molecules21081055

Moody, C. A., and Laimins, L. A. (2010). Human Papillomavirus Oncoproteins: Pathways to Transformation. *Nat. Rev. Cancer* 10 (8), 550–560. doi:10.1038/nrc2886

Nagata, S. (2000). Apoptotic DNA Fragmentation. *Exp. Cel. Res.* 256 (1), 12–18. doi:10.1006/excr.2000.4834

Pan, J. H., Abernathy, B., Kim, Y. J., Lee, J. H., Kim, J. H., Shin, E. C., et al. (2018). Cruciferous Vegetables and Colorectal Cancer Prevention through microRNA Regulation: A Review. *Crit. Rev. Food Sci. Nutr.* 58 (12), 2026–2038. doi:10.1080/10408398.2017.1300134

Pelicano, H., Carney, D., and Huang, P. (2004). ROS Stress in Cancer Cells and Therapeutic Implications. *Drug Resist. Updates* 7 (2), 97–110. doi:10.1016/j.drup.2004.01.004

Popolo, A., Pinto, A., Daglia, M., Nabavi, S. F., Farooqi, A. A., and Rastrelli, L. (2017). Two Likely Targets for the Anti-cancer Effect of Indole Derivatives from Cruciferous Vegetables: PI3K/Akt/mTOR Signalling Pathway and the Aryl Hydrocarbon Receptor. *Semin. Cancer Biol.* 46, 132–137. doi:10.1016/j.semcancer.2017.06.002

Ramirez, C. N., Li, W., Zhang, C., Wu, R., Su, S., Wang, C., et al. (2018). In Vitro-In Vivo Dose Response of Ursolic Acid, Sulforaphane, PEITC, and Curcumin in Cancer Prevention. *AAPS J.* 20 (1), 19. doi:10.1208/s12248-018-0190-0

Sak, K. (2014). Characteristic Features of Cytotoxic Activity of Flavonoids on Human Cervical Cancer Cells. *Asian Pac. J. Cancer Prev.* 15 (19), 8007–8018. doi:10.7314/apjcp.2014.15.19.8007

Saraste, A., and Pulkki, K. (2000). Morphologic and Biochemical Hallmarks of Apoptosis. *Cardiovasc. Res.* 45 (3), 528–537. doi:10.1016/s0008-6363(99)00384-3

Sarkar, R., Mukherjee, S., Biswas, J., and Roy, M. (2016). Phenethyl Isothiocyanate, by Virtue of its Antioxidant Activity, Inhibits Invasiveness and Metastatic Potential of Breast Cancer Cells: HIF-1α as a Putative Target. *Free Radic. Res.* 50 (1), 84–100. doi:10.3109/10715762.2015.1108520

Satyan, K. S., Swamy, N., Dizon, D. S., Singh, R., Granai, C. O., and Brard, L. (2006). Phenethyl Isothiocyanate (PEITC) Inhibits Growth of Ovarian Cancer Cells by Inducing Apoptosis: Role of Caspase and MAPK Activation. *Gynecol. Oncol.* 103 (1), 261–270. doi:10.1016/j.ygyno.2006.03.002

Schumacker, P. T. (2006). Reactive oxygen species in cancer cells: live by the sword, die by the sword. *Cancer cell* 10 (3), 175–176. doi:10.1016/j.ccr.2006.08.015

Sobreira, C., Davidson, M., King, M. P., and Miranda, A. F. (1996). Dihydrorhodamine 123 Identifies Impaired Mitochondrial Respiratory Chain Function in Cultured Cells Harboring Mitochondrial DNA Mutations. *J. Histochem. Cytochem.* 44 (6), 571–579. doi:10.1177/44.6.8666742

Stennicke, H. R., and Salvesen, G. S. (2000). Caspases–controlling Intracellular Signals by Protease Zymogen Activation. *Biochim. Biophys. Acta (BBA)-Protein Struct. Mol. Enzymol.* 1477 (1-2), 299–306. doi:10.1016/s0167-4838(99)00281-2

Trachootham, D., Alexandre, J., and Huang, P. (2009). Targeting Cancer Cells by ROS-Mediated Mechanisms: a Radical Therapeutic Approach? *Nat. Rev. Drug Discov.* 8 (7), 579–591. doi:10.1038/nrd2803

Troiano, L., Ferraresi, R., Lugli, E., Nemes, E., Roat, E., Nasi, M., et al. (2007). Multiparametric Analysis of Cells with Different Mitochondrial Membrane Potential during Apoptosis by Polychromatic Flow Cytometry. *Nat. Protoc.* 2 (11), 2719–2727. doi:10.1038/nprot.2007.405

Wasim, L., and Chopra, M. (2018). Synergistic Anticancer Effect of Panobinostat and Topoisomerase Inhibitors through ROS Generation and Intrinsic Apoptotic Pathway Induction in Cervical Cancer Cells. *Cell Oncol.* 41 (2), 201–212. doi:10.1007/s13402-017-0366-0

Xu, C., Shen, G., Chen, C., Gélinas, C., and Kong, A.-N. T. (2005). Suppression of NF-κB and NF-κB-Regulated Gene Expression by Sulforaphane and PEITC through IκBα, IKK Pathway in Human Prostate Cancer PC-3 Cells. *Oncogene* 24 (28), 4486–4495. doi:10.1038/sj.onc.1208656

Zhang, Z., Bergan, R., Shannon, J., Slatore, C. G., Bobe, G., and Takata, Y. (2018). The Role of Cruciferous Vegetables and Isothiocyanates for Lung Cancer Prevention: Current Status, Challenges, and Future Research Directions. *Mol. Nutr. Food Res.* 62 (18), 1700936. doi:10.1002/mnfr.201700936

Conflict of Interest: The authors declare that the research was conducted in the absence of any commercial or financial relationships that could be construed as a potential conflict of interest.

The reviewer FA declared a shared affiliation with several of the authors (MS and NY) to the handling editor at the time of the review.

Publisher's Note: All claims expressed in this article are solely those of the authors and do not necessarily represent those of their affiliated organizations, or those of the publisher, the editors and the reviewers. Any product that may be evaluated in this article, or claim that may be made by its manufacturer, is not guaranteed or endorsed by the publisher.

frontiers in Pharmacology

ORIGINAL RESEARCH
published: 03 August 2021
doi: 10.3389/fphar.2021.694762

A Polyphenol-Rich Extract of Olive Mill Wastewater Enhances Cancer Chemotherapy Effects, While Mitigating Cardiac Toxicity

Adriana Albini[1]‡, Marco M. G. Festa[1†], Nadja Ring[2†], Denisa Baci[1], Michael Rehman[2], Giovanna Finzi[3], Fausto Sessa[3,4], Serena Zacchigna[2,5], Antonino Bruno[6‡] and Douglas M. Noonan[7,8‡]*

[1]Laboratory of Vascular Biology and Angiogenesis, IRCCS MultiMedica, Milan, Italy, [2]Cardiovascular Biology Laboratory, International Centre for Genetic Engineering and Biotechnology, Trieste, Italy, [3]Department of Pathology, ASST Settelaghi, Varese, Italy, [4]Department of Medicine and Surgery, University of Insubria, Varese, Italy, [5]Department of Medicine, Surgery and Health Science, University of Trieste, Trieste, Italy, [6]Laboratory of Innate Immunity, Unit of Molecular Pathology, Biochemistry and Immunology, IRCCS MultiMedica, Milan, Italy, [7]Immunology and General Pathology Laboratory, Department of Biotechnology and Life Sciences, University of Insubria, Varese, Italy, [8]Unit of Molecular Pathology, Immunology and Biochemistry, IRCCS MultiMedica, Milan, Italy

OPEN ACCESS

Edited by:
Jamal Arif,
Shaqra University, Saudi Arabia

Reviewed by:
Krishnamurthi Kannan,
National Environmental Engineering Research Institute (CSIR), India
Arshad Mehmood,
Beijing Technology and Business University, China
Hamda Siddiqui,
The Institute of Liver and Biliary Sciences (ILBS), India

***Correspondence:**
Adriana Albini
adriana.albini@multimedica.it

†These authors share first authorship

‡These authors share last authorship

Specialty section:
This article was submitted to Pharmacology of Anti-Cancer Drugs, a section of the journal Frontiers in Pharmacology

Received: 13 April 2021
Accepted: 19 July 2021
Published: 03 August 2021

Citation:
Albini A, Festa MMG, Ring N, Baci D, Rehman M, Finzi G, Sessa F, Zacchigna S, Bruno A and Noonan DM (2021) A Polyphenol-Rich Extract of Olive Mill Wastewater Enhances Cancer Chemotherapy Effects, While Mitigating Cardiac Toxicity. Front. Pharmacol. 12:694762. doi: 10.3389/fphar.2021.694762

Cardiovascular toxicity remains one of the most adverse side effects in cancer patients receiving chemotherapy. Extra-virgin olive oil (EVOO) is rich in cancer preventive polyphenols endowed with anti-inflammatory, anti-oxidant activities which could exert protective effects on heart cells. One very interesting derivative of EVOO preparation is represented by purified extracts from olive mill waste waters (OMWW) rich in polyphenols. Here, we have investigated the anti-cancer activity of a OMWW preparation, named A009, when combined with chemotherapeutics, as well as its potential cardioprotective activities. Mice bearing prostate cancer (PCa) xenografts were treated with cisplatin, alone or in combination with A009. In an *in vivo* model, we found synergisms of A009 and cisplatin in reduction of prostate cancer tumor weight. Hearts of mice were analyzed, and the mitochondria were studied by transmission electron microscopy. The hearts of mice co-treated with A009 extracts along with cisplatin had reduced mitochondria damage compared to the those treated with chemotherapy alone, indicating a cardioprotective role. To confirm the *in vivo* results, tumor cell lines and rat cardiomyocytes were treated with cisplatin *in vitro*, with and without A009. Another frequently used chemotherapeutic agent 5-fluorouracil (5-FU), was also tested in this assay, observing a similar effect. In vitro, the combination of A009 with cisplatin or 5-FU was effective in decreasing prostate and colon cancer cell growth, while it did not further reduce growth of rat cardiomyocytes also treated with cisplatin or 5-FU. A009 cardioprotective effects towards side effects caused by 5-FU chemotherapy were further investigated, using cardiomyocytes freshly isolated from mice pups. A009 mitigated toxicity of 5-FU on primary cultures of mouse cardiomyocytes. Our study demonstrates that the polyphenol rich purified A009 extracts enhance the effect of chemotherapy *in vitro* and *in vivo,* but mitigates chemotherpy adverse effects on heart and on isolated cardiomyocytes. Olive mill waste water extracts could therefore represent a potential candidate for cardiovascular prevention in patients undergoing cancer chemotherapy.

Keywords: polyphenols, cardioncology, cardio protection, cardio prevention, cardiotoxicity, heart, cancer

INTRODUCTION

Cancer therapy has made remarkable advances for the treatment of solid and hematological tumors, leading to significant progresses in the reduction of tumor recurrences (Albini et al., 2010; Albini et al., 2012a; Angsutararux et al., 2015; Conway et al., 2015; Focaccetti et al., 2015; Curigliano et al., 2016; Polonsky and DeCara, 2019). Although the introduction of different antineoplastic agents in the clinic, such as monoclonal antibodies and tyrosine kinase inhibitors, has significantly augmented life expectancy (Senkus and Jassem, 2011), cardiovascular toxicity remains a major clinical concern, sometimes generating higher morbidity and mortality than tumor recurrences (Senkus and Jassem, 2011). Cardiovascular toxicities, defined as "toxicities affecting the heart", are among the most frequent undesirable effects of cancer chemotherapy. Major effects of chemotherapy-induced cardiovascular toxicities include arrythmias, myocardial ischemia, coronary artery diseases, hypertension, and myocardial dysfunctions (Polonsky and DeCara, 2019).

A major problem in the manifestation of clinically evident cardiotoxic events is the fact that they are often asymptomatic, and therefore negatively impact the cardiological prognosis of cancer patients, as well as significantly limits applicable treatment options (Albini et al., 2010 ; Albini et al., 2012a ; Angsutararux et al., 2015 ; Conway et al., 2015; Focaccetti et al., 2015; Curigliano et al., 2016; Polonsky and DeCara, 2019). In fact, even minor cardiac dysfunctions significantly restrict the choice of therapeutic programs, forcing the selection of those considered less aggressive and, as such, potentially less effective (Albini et al., 2010; Albini et al., 2012a; Angsutararux et al., 2015; Conway et al., 2015; Focaccetti et al., 2015; Curigliano et al., 2016; Polonsky and DeCara, 2019). Occurrence of chemotherapy-induced cardiotoxicity is continuously increasing, as a consequence of the growing number of patients undergoing chemotherapy and the introduction of new, more aggressive, anticancer drugs, often administered in combination with other toxic compounds (Albini et al., 2010; Albini et al., 2012a; Angsutararux et al., 2015; Conway et al., 2015; Focaccetti et al., 2015; Curigliano et al., 2016; Polonsky and DeCara, 2019).

This knowledge suggested that a strict dialogue between the oncologists and the cardiologists is necessary, when selecting the proper chemotherapy intervention, as well as cardiac monitoring in cancer patients, bringing to a new discipline termed cardio-oncology (Albini et al., 2010).

Mitochondria represent the metabolic engine, governing and sensing the cellular energy requirements during physiological and pathological conditions (Vringer and Tait, 2019; Missiroli et al., 2020). Cardiomyocytes strongly depend on mitochondria for energy requirements. The maintenance of mitochondrial membrane potential is crucial to supply gradients for ATP synthesis (Bhatti et al., 2017). Oxidative stress represents a major hallmark of age- and chronic inflammatory-related disorders and significantly impacts on mitochondrial functionality (Bhatti et al., 2017). Generation of reactive oxygen species (ROS) (Toric et al., 2019; Fiorentino et al., 2020; Li et al., 2020; Cocetta et al., 2021; Oruganti and Meriga, 2021; To and Cho, 2021) and mitochondrial damage are major drivers of chemotherapy-induced cardiotoxicities (Hahn et al., 2014; Ichikawa et al., 2014; Nitiss and Nitiss, 2014; Zhang et al., 2020).

Polyphenols can acts as anti-cancer agent when combined with chemotherapy (Albini et al., 2007; Albini et al., 2012b; Rossi et al., 2014; Bassani et al., 2016; Albini et al., 2019; Toric et al., 2019; Fiorentino et al., 2020; Li et al., 2020; Cocetta et al., 2021; Oruganti and Meriga, 2021; Sartori et al., 2021) and can exhibit cardio protective effects (Cheng et al., 2017; Zheng et al., 2018; Choy et al., 2019; Martínez-González et al., 2019; Poti et al., 2019; Atale et al., 2020). Polyphenols can overcome multidrug resistance (El-Readi et al., 2021). Chemotherapy with Doxorubicin associates with cardiovascular toxicities; polyphenols such as resveratrol and curcumin can abate this toxicity (Rezk et al., 2006; Shakibaei et al., 2014; Kalyanaraman, 2020). Polyphenols act as anti-oxidants, by contrasting the generation of ROS that drive cellular and mitochondrial damage.

It has been widely demonstrated that adherence to the Mediterranean diet is associated with reduced risk of developing cardiovascular diseases. In recent decades, numerous epidemiological and interventional studies have confirmed this observation, underlining the close relationship between the Mediterranean diet and cardiovascular diseases (Grosso et al., 2014; Billingsley and Carbone, 2018; Estruch et al., 2018). In this context, extra-virgin olive oil (EVOO), the most representative component of this diet, seems to be important in reducing the incidence of cardiovascular events, including myocardial infarction and stroke (Nocella et al., 2018). Current research on the beneficial effect of EVOO is focused on defining its protective effects against cardiovascular risk factors, such as inflammation, oxidative stress, coagulation, platelet aggregation, fibrinolysis, and endothelial or lipid dysfunction. A further approach is based on the modulation of conditions that predispose people to cardiovascular events, such as obesity, metabolic syndrome or type 2 diabetes mellitus, and chemotherapy (Estruch et al., 2018; Marcelino et al., 2019; Martínez-González et al., 2019; Mazzocchi et al., 2019; Nediani et al., 2019). The protective activity of EVOO results from the high levels of phenolic compounds, monounsaturated fatty acids (MUFA) and other minor compounds present in EVOO (Nocella et al., 2018).

Industrial EVOO processing is associated with the generation of large volume of liquid waste products, termed olive mill wastewater (OMWW) (El-Abbassi et al., 2012; Vougogiannopoulou et al., 2015). OMWW are rich in water soluble polyphenols, endowed with anti-bacterial, anti-antioxidant, cytoprotective activities, (Schaffer et al., 2010; Abu-Lafi et al., 2017; Belaqziz et al., 2017), thus representing a valid waste product to be repositioned in the market (Taticchi et al., 2019a; Taticchi et al., 2019b).

Here, we investigate the potential cardioprotective activities of a polyphenol-rich, EVOO-derived polyphenol extracts (A009), derived from olive mill wastewater (OMWW). A009-extracts have been reported to exhibit chemopreventive and angiopreventive properties, *in vitro* and *in vivo*, in different cancer types (Baci et al., 2019; Gallazzi et al., 2020).

We examined A009 effects on tumor growth, when combined with a chemotherapeutic agent and evaluated the effects of the

combination on the heart and cardiomyocytes, at both cellular and molecular level, using *in vivo* (mice bearing prostate tumors) and *in vitro* models.

MATERIALS AND METHODS

Chemicals

Cis-Diammine platinum dichloride (Cis-Pt) and 5-Fluorouracil (5FU), all purchased by SIGMA Aldrich were dissolved in dimethyl sulfoxide (DMSO) and used for *in vitro* experiments as detailed below. 3-(4,5-dimethylthiazol-2-yl)-2,5-diphenyltetrazolium bromide (MTT) was purchased by SIGMA Aldrich and resuspended at 5 mg/ml. A009 polyphenol -rich extract, derived from olive mill wastewater (OMWW) processing, were provided by Azienda Agricola fattoria La Vialla, Castiglion Fibocchi, Arezzo Italy.

Preparation of A009 Extracts

The A009 was obtained from the OMWW derived from the processing of EVOO. Extraction procedures and polyphenol quantification has been previously published (Bassani et al., 2016, Baci et al., 2019). The polyphenol composition is not altered, following different years of cultivars (Bassani et al., 2016; Baci et al., 2019). Polyphenol content of the A009 extract is showed in **Supplemental Table S1**, **Supplementary Figure S1** and has been published (Bassani et al., 2016, Baci et al., 2019).

Cell Line Culture and Maintenances

The human prostate cancer (PCa) cell lines DU-145, 22Rv1 and the colorectal cancer cell line HT29 (all purchased by ATCC) were maintained in RPMI 1640 medium, supplemented with 10% Fetal Bovine Serum (FBS) (Euroclone), 2 mM L-glutamine (Euroclone), 100 U/ml penicillin and 100 μg/ml streptomycin (Euroclone), at 37°C, 5% CO_2. The rat cardiomyocyte cell line H9C2 (PromoCell) was maintained in Myocyte Growth Medium plus Myocyte supplements mix (PromoCell), addition with 10% Fetal Bovine Serum (FBS) (Euroclone), 2 mM L-glutamine (Euroclone), 100 U/ml penicillin and 100 μg/ml streptomycin (Euroclone), at 37°C, 5% CO_2. Cells were routinely screened for eventual *mycoplasma* contaminations.

Detection of Cardioprotective Activities *in Vivo* Tumor Xenograft Models

We used a mouse model of prostate cancer to determine whether co-treatment with the chemotherapeutic agent cisplatin and A009 extract could exert a protective effect on the hearts of the treated animals. The effects of the A009 extracts in inhibiting prostate cancer (PCa) tumor cell growth was assessed using an *in vivo* xenograft model. 5-week-old male Nu/MRI nude mice (from Charles River) were used, with four animals per experimental group. Animals were housed in a conventional animal facility with 12:12 h light dark cycles and fed ad libitum. Animals were subcutaneously injected into the right flank with 2.5×10^6 22Rv1 cells or DU-145 cells, in a total volume of 300 μL, containing 50% serum free RMPI 1650, and 50% 10 mg/ml reduced growth factor Matrigel (Corning) with or without A009 (dilution 1:250). From day 0 animals received A009 daily (dilution 1:250), in the drinking water. When tumors were palpable, mice received Cisplatin, 7 mg/kg *i. p*, twice a week. At day 27, the tumor cell growth was stopped, tumors were excised, weighted and tumor volume was measured with a caliper and determined using the formula $(W^2 \times L)/2$. Hearts were surgically removed from animals and used for transmission electron microscopy analyses.

All the procedures involving the animals and their care were performed according to the institutional guidelines, in compliance with national and international law and guidelines for the use of animals in biomedical research and housed in pathogen-free conditions. All the procedures applied were approved by the local animal experimentation ethics committee (ID# #06_16 Noonan) of the University of Insubria and by the Italian Health Ministry (ID#225/2017-PR).

Transmission Electron Microscopy Analysis of Murine Hearts

Hearts were surgically excised from sacrified animals and extensively washed in PBS. Heart sections were obtained using a scalpel and then placed in fixing solution for TEM processing (2% PFA, 2% glutaraldehyde), finally post-fixed using 1% osmium tetroxide and embedded in an Epon-Araldite resin. Following exposure to uranyl acetate and lead citrate, thin sections were analyzed by TEM, using a Morgagni electron microscope (Philips) at 3500X magnification, to detect mitochondrial alterations in terms of morphology, size, organization, and quantity. The number of altered mitochondria per section, exhibiting altered morphology/shape, was counted using the ImageJ software.

Combination Effect of Chemotherapy and A009 on Cancer Cell Lines

To investigate whether the A009 extract could synergize with chemotherapy, the prostate cancer DU-145 cell line or the colorectal cancer HT-29 cell line were treated with Cis-Pt 100 μM or 5-FU 100 μM, respectively, alone or in combination with A009 L3 or L4 extracts, for 24–72 h. Detection of cell viability was determined by MTT (3-[4,5-dimethylthiazole-2-yl]-2,5-diphenyltetrazolium bromide) assay, on 3,000 cardiomyocytes/well, seeded into a 96 well plate.

Effects of A009 Extracts on Adult Rat Cardiomyocyte

To evaluate the effects of the A009 extracts on chemotherapy induced cardiotoxicity, after preliminary experiment to assess dosages, adult rat cardiomyocyte H9C2 cells were treated with 5-FU 100 μM or Cis-Pt 100 μM, alone or in combination with A009 L3 or L4 extracts, for 24–72 h. The schedule treatments included a prevention approach by pre-treating cardiomyocyte with A009 L3 and L4 extracts at T24 to T48 h, subsequently A009 L3 or L4 extracts were removed, and wells were auditioned with fresh medium containing Cis-Pt 100 μM or 5-Fu 100 μM. Detection of cell viability was determined by MTT assay descripted in 2.6.

TABLE 1 | Monitoring of healthy conditions during *in vivo* treatments.

	NT	Cisplatin (7 mg/kg)	A009 1:250	Cisplatin (7 mg/kg) + A009 1:250
Skin peeling	0 (10)	5 (9)	1 (10)	2 (10)
Dehydration	0 (10)	0 (9)	0 (10)	0 (10)
Alterations in water consumption	0 (10)	0 (9)	0 (10)	0 (10)
Alterations in food consumption	0 (10)	0 (9)	0 (10)	0 (10)
Urine	0 (10)	0 (9)	0 (10)	0 (10)
Feces	0 (10)	0 (9)	0 (10)	0 (10)

The healthy state on mice receiving single agent (A009, dilution 1:250) alone, or Cisplatin (7 mg/kg) alone, or the combinations of Cisplatin with the A009 extract was daily monitored. As readout of clinical parameters, the presence of skin peeling, dehydration, alterations of water and food consumption, alteration in solid (feces) and liquid (urine) dejections are showed. Data are presented as (number of events)/total animal per experimental conditions.

Isolation of Neonatal Murine Cardiomyocytes

Cardiomyocytes were isolated from neonatal C57/Bl6 mice at 2 days after birth as previously described, with minor modifications (Zacchigna et al., 2018). Briefly, hearts were removed and cleaned in calcium and bicarbonate-free Hanks' balanced salt solution with HEPES (CBFHH, containing 137 mM NaCl, 5.36 mM KCl, 0.81 mM $MgSO_4$ $7H_2O$, 5.55 mM dextrose, 0.44 mM KH_2PO_4, 0.34 mM Na_2HPO_4 $7H_2O$, and 20.06 mM HEPES). Excess blood and valves were removed, and hearts were diced. The tissue was then enzymatically digested using CBFHH supplemented with 1.75 mg/ml of Trypsin (BD Biosciences) and 20 mg/ml of DNAse I (Sigma). Tissue was digested for 3 h, with cells harvested into fetal bovine serum (FBS) every 10 min to stop the digestion. Cells were then filtered using a 40 μm cell strainer and pre-plated for 2 h to remove contaminating fibroblasts. Finally, cardiomyocytes were collected and seeded on tissue culture plates treated for primary cultures. Cells were cultured in Dulbecco's modified Eagle medium 4.5 g/L glucose (DMEM, Life Technologies) supplemented with 5% FBS, 20 mg/ml vitamin B12 (Sigma), 100 U/ml penicillin and 100 mg/ml streptomycin (Sigma).

Effects of A009 Extracts on Neonatal Murine-Derived Cardiomyocytes

To evaluate the effect of the A009 extract on cardiomyocyte viability *in vitro*, 30,000 cardiomyocytes/well were seeded into a 96 well plate. One day after plating, cells were treated with L3 and L4 A009 extracts, dilution of 1:800, for 24 h. On day 2, cells were treated with 4.6 μM of 5-Fluorouracil. Following 24 and 48 h, cells were fixed and stained using anti-Cardiac Troponin I antibody (Abcam, ab47003, dilution of 1:200) and Hoechst 33,342 (Invitrogen, H3570, dilution of 1:5000). The number of cardiomyocytes for each time point was counted in three independent experiments.

RESULTS

Cardioprotective Activities of A009 Extracts *in Vivo* Models of Cardiotoxicity Induced by Anticancer Drug

We used a mouse model of prostate cancer xenographt to determine the A009-extract effect on tumors and the hearts of mice treated with the chemotherapeutic agent cisplatin. During the treatment schedule, we did not observe behavioral changes, alterations in food intake, water consumption, or dejections by the animals included in all the experimental groups of the study (**Table 1**).

Animals receiving the different treatment did not show weight loss during the tumor cell growth kinetic (**Figure 1A**). Interesting, A009 also reduced the skin peeling induced by cisplatin treatments (from 5/9 mice to (2/10 mice) (**Table 1**). We found that the combination of cisplatin with the A009 extract synergized by further reducing the PCa cell tumor weight, as compared to the treatment with cisplatin alone (**Figure 1B**). The macroscopical/morphological inspection did not reveal detectable differences amongst the hearts of the various experimental groups (data not shown).

However ultrastructural analysis, using transmission electron microscopy (TEM), showed that animals treated with cisplatin which received also the A009 extract have a reduced number of damaged mitochondria (showing a rounder shape and having mitochondrial cristae better organized and higher in number), as compared to the hearts of mice treated with cisplatin only (**Figures 2A,B**). We also observed a more regular muscle myosin and actin fiber disposition in the hearts of animals treated with A009 and cisplatin as compared to those treated with cisplatin alone. Henatoxylin/Eosin analysis, by optical microscopy, showed no alterations of cardiomyocytes; inflammation and fibrosis were observed in hearts treated with cisplatin, nor in those treated with A009 with and without cisplatin. Therefore, it is confirmed that in these cases the electron microscopy data are the only ones able to demonstrate cellular suffering (in particular those relating to mitochondria).

A009 Activities Against Tumor Cell Lines and Heart Cell Lines

Cisplatin and 5-FU treatment in vitro decreased both prostate (**Figure 3A**) and colon cancer (**Figure 3B**) cell growth. The proliferation of the tumor cells treated with A009 was also significantly different from the control vehicle. A009 enhanced the effect of the cisplatin and 5-FU alone (**Figures 3A,B**, **Supplementary Figure S2**) on prostate and colon cancer cells. 5-FU and cisplatin were toxic for rat cardiomyocytes, while the A009 was not. Furthermore, A009 in combination with Cisplatin or 5FU did not enhance the growth reduction (**Figure 3C**)

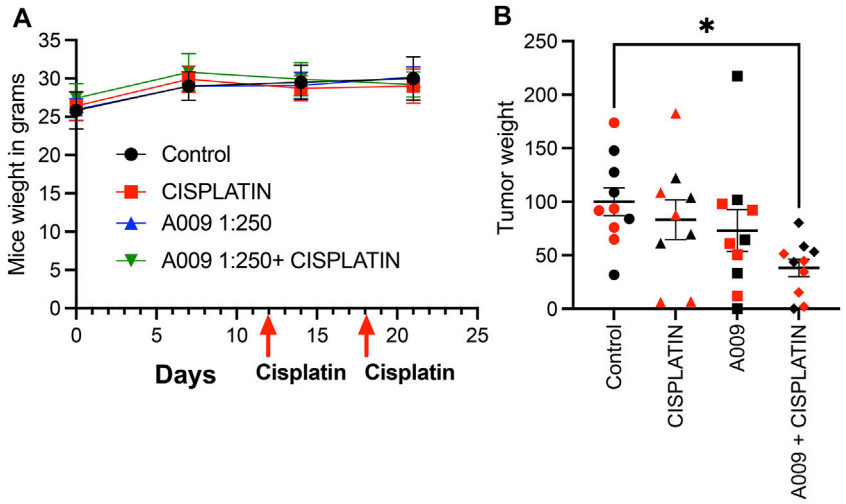

FIGURE 1 | Dietary administration of the A009 extract, in combination with chemotherapy, resulted in both synergism by reducing tumor weight. Dietary administration (drinking water) of A009 extracts synergizes with chemotherapy by reducing tumor weight *in vivo*. In panel **(A)** the red arrows indicate the day of administration dose of cisplatin (7 mg/kg), the mice weights did not change. In panel **(B)**, the effects of the combination of A009 extract with cisplatin (7 mg/kg), was determined by measuring the weight of the tumors excised from the orthotopic *in vivo* model of prostate cancer cells DU-145 (red), 22Rv1 (black), normalized to the control group tumor weight. Data are showed as mean ± SEM, one-way ANOVA, $^{*}p < 0.05$.

induced by the chemotherapics. Therefore, while A009 significantly decreased tumor cell proliferation and exhibited additive effect with cisplatin and 5-FU, it did not affect cardiomyocyte growth and it did not enhance toxicity of cisplatin and 5-FU (**Figure 3C**).

Protective Activities of A009 Extracts on Neonatal Murine Cardiomyocytes

We observed a cardioprotective effect of the A009 extracts on neonatal murine cardiomyocytes, following co-treatment with the chemotherapeutic drug 5-FU (**Figure 4**). The protective effect of the A009 extracts was studied by determining the number of viable cardiomyocytes, following 24 h (**Figure 2A**) and 48 h (**Figure 2B**) of treatment. At the early time point of 24 h, A009 showed a cardioprotective effect in basal conditions, and was slightly protective against 5-FU (**Figure 4A**). After 48 h, A009 was consistently cardioprotective also against 5-FU (**Figure 4B**).

DISCUSSION

Cardiovascular toxicities still remain a major challenge in clinical oncology (Albini et al., 2010; Senkus and Jassem, 2011; Albini et al., 2012a; Angsutararux et al., 2015; Conway et al., 2015). While chemotherapeutic agents efficiently target malignantly transformed cells, they simultaneously induce cell death of healthy cells (Albini et al., 2010; Senkus and Jassem, 2011; Albini et al., 2012a; Angsutararux et al., 2015; Conway et al., 2015). The cardiovascular system is the major off target of anti-neoplastic drugs (Albini et al., 2010; Senkus and Jassem, 2011; Albini et al., 2012a; Angsutararux et al., 2015; Conway et al., 2015). The patients treated with 5-FU can develop angina, acute myocardial infarction, Takotsubo and Raynaud's syndrome as adverse effects, while cisplatin receiving patients can show angina, acute myocardial infarction, hypertension, Raynaud's syndrome, Raynaud's Stroke or peripheral arterial disease (Herrmann et al., 2016) as side effects. Most of the studies on chemotherapy agents were performed *in vitro* in cardiomyocytes and *in vivo* on the heart (Ma et al., 2020; Kim and Choi, 2021).

Mimicking a scenario closer to the clinic, we tested the cardioprotective properties of the A009 extract in an *in vivo* murine model of prostate tumor xenograft treated with cisplatin, a chemotherapy agent associated with cardiotoxicity and mitotoxicity (Varga et al., 2015; Ma et al., 2020). C57/Bl6 tumor bearing mice mice treated with cisplatin for 1 week developed myocardial contractile dysfunction; transmission electron microscopy revealed ultrastructural abnormalities of the mitochondria (Ma et al., 2010; Varga et al., 2015). Mice subcutaneously injected with the DU-145 prostate cancer cell line, co-treated with A009 and the chemotherapeutic drug cisplatin, showed a reduced number of abnormal and damaged mitochondria, as compared to those treated with cisplatin alone. Mitochondria have an essential role in myocardial tissue homeostasis (Varga et al., 2015; Brown et al., 2017) and diverse chemical compounds and chemotherapy drugs have been known to directly or indirectly modulate cardiac mitochondrial function (Gogvadze et al., 2009; Gorini et al., 2018). Mitochondrial oxidative stress and dysfunctions are common mechanisms in cardiotoxic effects (Altena et al., 2009; El-Awady et al., 2011; Ichikawa et al., 2014; Nitiss and Nitiss, 2014; Dugbartey et al., 2016; Brown et al., 2017). Cisplatin was tested *in vitro* on DU145 prostate cancer cell lines, as well as on HT29 colonc cancer cells, alone or in combination with A009 and its effects compared to those on rat cardiomyocytes.

Most of the cytotoxic activities of chemotherapeutic agents on normal cells are due to the induction of exacerbated oxidative

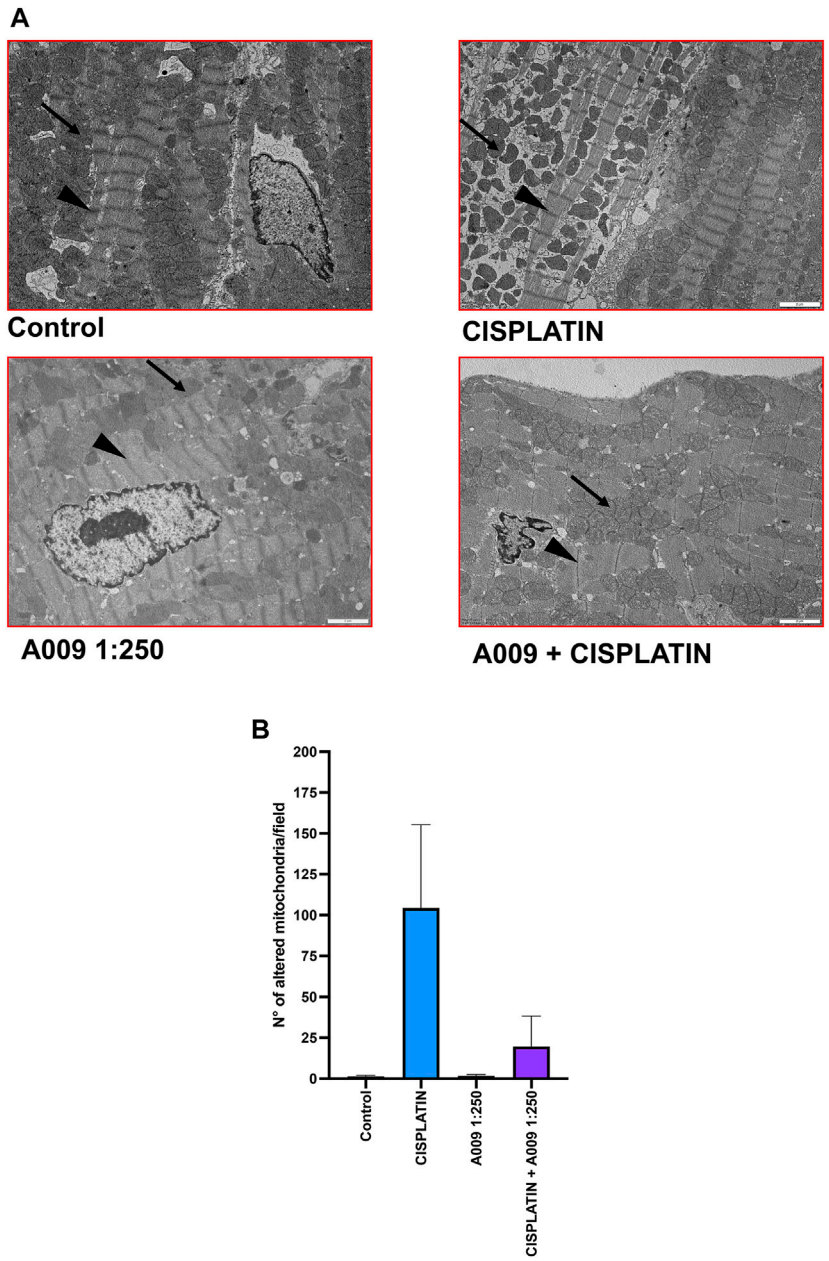

FIGURE 2 | A009 cardioprotective activities against cisplatin-induce cardiotoxicity *in vivo*. Mitochondria number, shape/morphology and color was monitored, by transmission electron microscopy (TEM) on hearts from mice treated with cisplatin alone (7 mg/kg), A009 extract (dilution 1:250, in drinking water) or the cisplatin-A009 extract combination. **(A)** representative TEM micrographs (arrows for the mitochondria, arrowheads for the z-line). **(B)** graph bars showing the count of altered mitochondria per experimental condition. Data are showed as mean ± SEM.

stress, through the generation of both ROS and reactive nitrogen species (RNS) (Angsutararux et al., 2015; Zhang et al., 2018). Agents such as anti-inflammatory, anti-oxidants, able to counteract these effects, can be used to reduce side effects by chemotherapeutics and can be easily tolerated by oncologic patients and administered by dietary regimen (Kaiserová et al., 2007; Vincent et al., 2013). Many dietary polyphenols demonstrate anti-oxidant and cytoprotective properties (Krajka-Kuźniak et al., 2009; Polk et al., 2013; Baranowska and Bartoszek, 2016; Sara et al., 2018). We tested the ability of a polyphenol-rich purified extract of OMWW, termed A009, to protect from cardiovascular damages induced by the anti-cancer agent cis-platin, in vivo and in vitro.

5-FU is also a common cancer chemotherapeutic agent. The 5-FU cytotoxic action on cardiomyocytes results in mitochondrial dysfunctions (Eskandari et al., 2015). ROS scavengers, anti-oxidants can prevent, mitochondrial permeability induced 5FU in this study (Eskandari et al., 2015). In a previous study, we demonstrated that

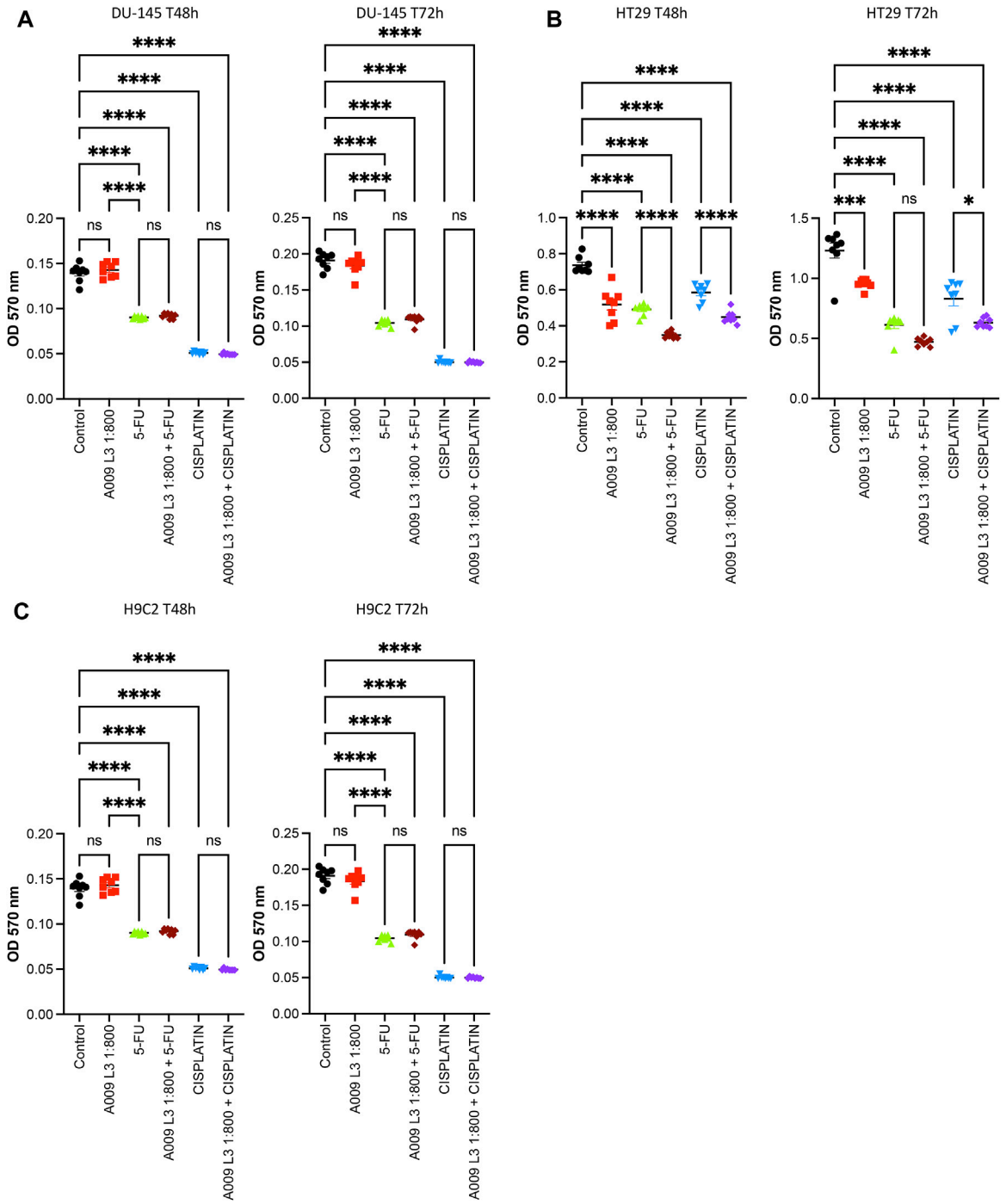

FIGURE 3 | Activities of A009 extracts combined with chemotherapy on tumor cells and cardiomyocytes. A009 (batch L3) deceases the proliferation rate of tumors cells *in vitro* [**(A)**: DU-145 PCa and **(B)**: HT29 CRC and has additive effects on the cisplatin and the 5-Fluorouracil (5FU) effects. The cardiomyocytes proliferation rate is not affected by A009 alone **(C)**, and reduced proliferation by 5FU and cisplatin is not further decreased by A009 *in vitro*. Control: vehicle control. Data are showed as mean ± SEM, one-way ANOVA, $*p < 0.05$, $**p < 0.01$, $***p < 0.001$, $****p < 0.0001$.

human cardiomyocytes exposed to 5-FU *in vitro* acquire a senescent phenotype and undergo autophagy (Focaccetti et al., 2015). While A009 significantly decreased tumor cell proliferation and had additive effect with cisplatin and 5-FU, it did not affect cardiomyocyte growth as single treatment and did not enhance toxicity of cisplatin and 5-FU. Based on these results, we investigated the effects of the A009 extracts also on fresh cardiomyocytes isolated from neonatal mice. In these experiments, we validated 5-FU

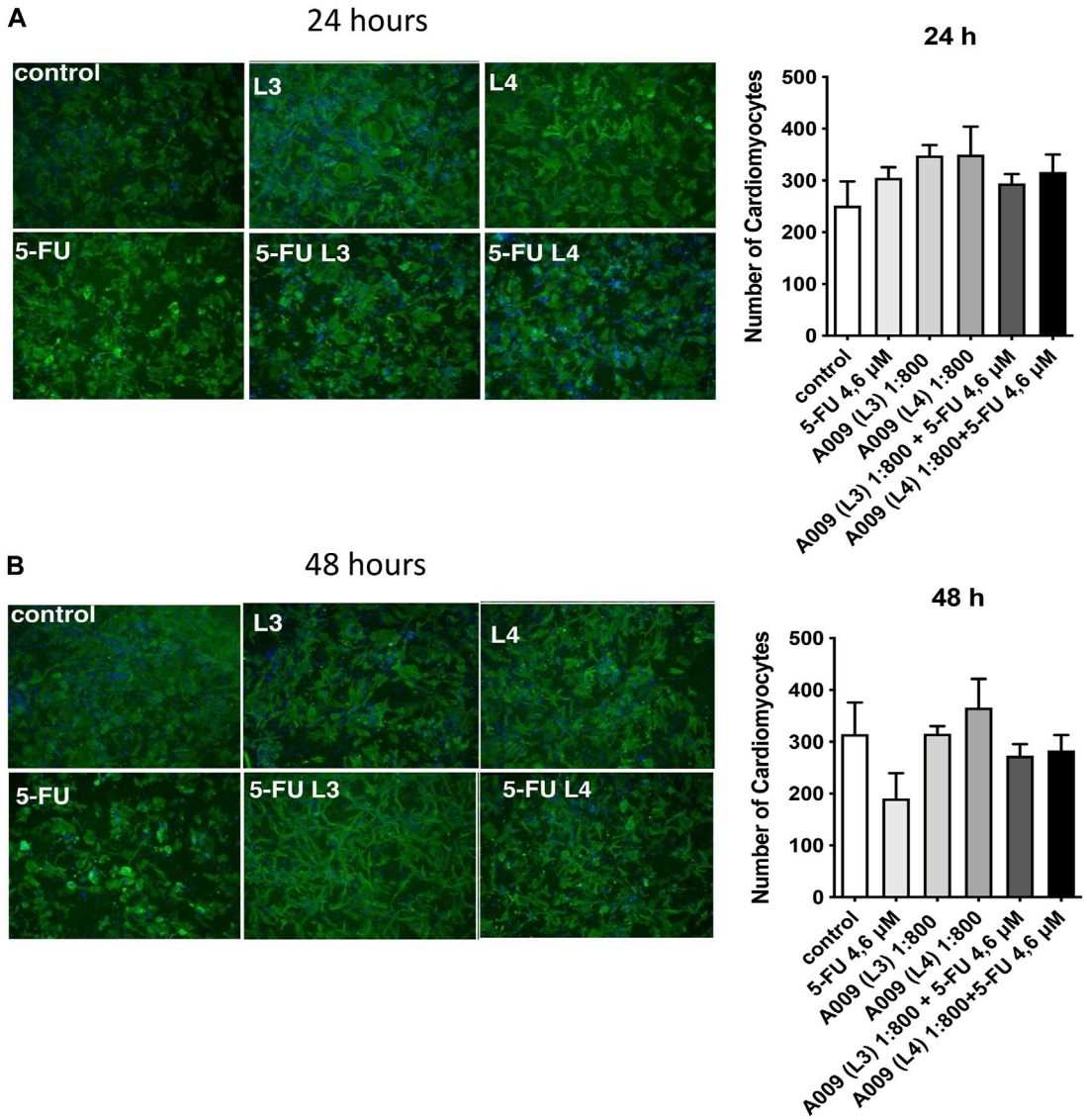

FIGURE 4 | Protective activities of A009 extracts on neonatal murine cardiomyocytes. The cardioprotective effects of the A009 extract on chemotherapy induced cardiotoxicities was assessed, *in vitro*, on neonatal murine cardiomyocytes. Neonatal murine cardiomyocytes were exposed for 24 h **(A)** and 48 h **(B)** to 5-FU (4.6 µM) alone, A009 extracts (dilution 1:800, batches L3 or L4) alone, or the combination of the 5-FU and A009 extracts (dilution 1:800, batches L3 or L4). Number of cardiomyocytes was not affected by 5FU after 24 h treatments, while the OMWW extract improved their number to a slight but significative percent. After 48 h 5FU strongly decreased cardiomyocyte number to 60%. A009 alone did not lower the quantity of cardiomyocytes, and even slightly increased it as in the 24 h (in the L4 formulation). Addition to L3 and L4 together with the cytotoxic drug counteracted 5FU effect at 48 h. Data are showed as mean ± SEM. 5-FU: 5-fluoro-Uracile; L3/L4: A009 batch extract; Control: vehicle control; 5-fluorouracil.

cardiotoxic activities (Albini et al., 2010; Polk et al., 2013; Angsutararux et al., 2015; Focaccetti et al., 2015; Sara et al., 2018). We observed that cardiomyocytes co-treated with the A009 extracts and the chemotherapeutic drug 5-FU exhibited less reduction of the number of cardiomyocytes, as compared with the drug alone. This rescue was maintained from 24 to 48 h of cardiomyocyte culture and treatment and potentially related to the antioxidant polyphenols present in the A009 extracts.

CONCLUSION

Here, we demonstrated that the A009 extracts, although additive in cancer therapy, do not have cardiotoxic effects, and can actually mitigate chemotherapy-induced cardiotoxicity. One of the effects, detected by transmission electron microscopy on hearts of treated mice, suggests mitochondrial protection and anti-oxidant capabilities of A009.

Our study demonstrates that a polyphenol rich purified OMWW extract can be placed as valid candidate for combination with chemotherapy (additive effects) while protecting the heart from chemotherapy-associated cardiovascular toxicities.

DATA AVAILABILITY STATEMENT

The raw data supporting the conclusions of this article will be made available by the authors, without undue reservation.

ETHICS STATEMENT

The animal study was reviewed and approved. All the procedures applied were approved by the local animal experimentation ethics committee (ID# #06_16 Noonan) of the University of Insubria and by the Italian Health Ministry (ID#225/2017-PR).

AUTHOR CONTRIBUTIONS

AA, AB, FS, SZ, and DN: Conceptualization. NR, MR, MF, DB, and GF: Performed the *in vitro* and *in vivo* experiments AB, DB, NR, MR, DN, and SZ. Analyzed data AB, DB, NR, MR, FS, DN, and SZ. Data curation AA, AB, SZ, and DN. AA, AB, and DN Supervised the project and the experimental procedures. All authors have read and agreed to the published version of the manuscript.

FUNDING

AB, received founds by the Italian Association for Cancer Research (AIRC), MFAG2019-ID-22818 and the Cariplo Foundation (ID-2019-1609). This work was supported by institutional funds and salaries. This work has been supported by Italian Ministry of Health Ricerca Corrente - IRCCS MultiMedica (AB, DN).

ACKNOWLEDGMENTS

We thank Paola Corradino for support in literature research and text editing.

SUPPLEMENTARY MATERIAL

The Supplementary Material for this article can be found online at: https://www.frontiersin.org/articles/10.3389/fphar.2021.694762/full#supplementary-material

REFERENCES

Abu-Lafi, S., Al-Natsheh, M. S., Yaghmoor, R., and Al-Rimawi, F. (2017). Enrichment of Phenolic Compounds from Olive Mill Wastewater and *In Vitro* Evaluation of Their Antimicrobial Activities. *Evid. Based Complement. Alternat Med.* 2017, 3706915. doi:10.1155/2017/3706915

Albini, A., Bassani, B., Baci, D., Dallaglio, K., Gallazzi, M., Corradino, P., et al. (2019). Nutraceuticals and "Repurposed" Drugs of Phytochemical Origin in Prevention and Interception of Chronic Degenerative Diseases and Cancer. *Cmc* 26, 973–987. doi:10.2174/0929867324666170920144130

Albini, A., Donatelli, F., Focaccetti, C., D'Elios, M. M., and Noonan, D. M. (2012a). Renal Dysfunction and Increased Risk of Cardiotoxicity with Trastuzumab Therapy: a New challenge in Cardio-Oncology. *Intern. Emerg. Med.* 7, 399–401. doi:10.1007/s11739-012-0845-2

Albini, A., Noonan, D. M., and Ferrari, N. (2007). Molecular Pathways for Cancer Angioprevention: Fig. 1. *Clin. Cancer Res.* 13, 4320–4325. doi:10.1158/1078-0432.ccr-07-0069

Albini, A., Pennesi, G., Donatelli, F., Cammarota, R., De Flora, S., and Noonan, D. M. (2010). Cardiotoxicity of Anticancer Drugs: the Need for Cardio-Oncology and Cardio-Oncological Prevention. *J. Natl. Cancer Inst.* 102, 14–25. doi:10.1093/jnci/djp440

Albini, A., Tosetti, F., Li, V. W., Noonan, D. M., and Li, W. W. (2012b). Cancer Prevention by Targeting Angiogenesis. *Nat. Rev. Clin. Oncol.* 9, 498–509. doi:10.1038/nrclinonc.2012.120

Altena, R., De Haas, E. C., Nuver, J., Brouwer, C. A. J., Van Den Berg, M. P., Smit, A. J., et al. (2009). Evaluation of Sub-acute Changes in Cardiac Function after Cisplatin-Based Combination Chemotherapy for Testicular Cancer. *Br. J. Cancer* 100, 1861–1866. doi:10.1038/sj.bjc.6605095

Angsutararux, P., Luanpitpong, S., and Issaragrisil, S. (2015). Chemotherapy-Induced Cardiotoxicity: Overview of the Roles of Oxidative Stress. *Oxid Med. Cel Longev* 2015, 795602. doi:10.1155/2015/795602

Atale, N., Yadav, D., Rani, V., and Jin, J. O. (2020). Pathophysiology, Clinical Characteristics of Diabetic Cardiomyopathy: Therapeutic Potential of Natural Polyphenols. *Front. Nutr.* 7, 564352. doi:10.3389/fnut.2020.564352

Baci, D., Gallazzi, M., Cascini, C., Tramacere, M., De Stefano, D., Bruno, A., et al. (2019). Downregulation of Pro-inflammatory and Pro-angiogenic Pathways in Prostate Cancer Cells by a Polyphenol-Rich Extract from Olive Mill Wastewater. *Int. J. Mol. Sci.* 20. doi:10.3390/ijms20020307

Baranowska, M., and Bartoszek, A. (2016). Antioxidant and Antimicrobial Properties of Bioactive Phytochemicals from cranberry. *Postepy Hig Med. Dosw* 70, 1460–1468. doi:10.5604/17322693.1227896

Bassani, B., Rossi, T., De Stefano, D., Pizzichini, D., Corradino, P., Macrì, N., et al. (2016). Potential Chemopreventive Activities of a Polyphenol Rich Purified Extract from Olive Mill Wastewater on colon Cancer Cells. *J. Funct. Foods* 27, 236–248. doi:10.1016/j.jff.2016.09.009

Belaqziz, M., Tan, S. P., El-Abbassi, A., Kiai, H., Hafidi, A., O'donovan, O., et al. (2017). Assessment of the Antioxidant and Antibacterial Activities of Different Olive Processing Wastewaters. *PLoS One* 12, e0182622. doi:10.1371/journal.pone.0182622

Bhatti, J. S., Bhatti, G. K., and Reddy, P. H. (2017). Mitochondrial Dysfunction and Oxidative Stress in Metabolic Disorders - A Step towards Mitochondria Based Therapeutic Strategies. *Biochim. Biophys. Acta (Bba) - Mol. Basis Dis.* 1863, 1066–1077. doi:10.1016/j.bbadis.2016.11.010

Billingsley, H. E., and Carbone, S. (2018). The Antioxidant Potential of the Mediterranean Diet in Patients at High Cardiovascular Risk: an In-Depth Review of the PREDIMED. *Nutr. Diabetes* 8, 13. doi:10.1038/s41387-018-0025-1

Brown, D. A., Perry, J. B., Allen, M. E., Sabbah, H. N., Stauffer, B. L., Shaikh, S. R., et al. (2017). Mitochondrial Function as a Therapeutic Target in Heart Failure. *Nat. Rev. Cardiol.* 14, 238–250. doi:10.1038/nrcardio.2016.203

Cheng, Y. C., Sheen, J. M., Hu, W. L., and Hung, Y. C. (2017). Polyphenols and Oxidative Stress in Atherosclerosis-Related Ischemic Heart Disease and Stroke. *Oxid Med. Cel Longev* 2017, 8526438. doi:10.1155/2017/8526438

Choy, K. W., Murugan, D., Leong, X. F., Abas, R., Alias, A., and Mustafa, M. R. (2019). Flavonoids as Natural Anti-inflammatory Agents Targeting Nuclear Factor-Kappa B (NFkappaB) Signaling in Cardiovascular Diseases: A Mini Review. *Front. Pharmacol.* 10, 1295. doi:10.3389/fphar.2019.01295

Cocetta, V., Quagliariello, V., Fiorica, F., Berretta, M., and Montopoli, M. (2021). Resveratrol as Chemosensitizer Agent: State of Art and Future Perspectives. *Int. J. Mol. Sci.* 22. doi:10.3390/ijms22042049

Conway, A., Mccarthy, A. L., Lawrence, P., and Clark, R. A. (2015). The Prevention, Detection and Management of Cancer Treatment-Induced Cardiotoxicity: a Meta-Review. *BMC Cancer* 15, 366. doi:10.1186/s12885-015-1407-6

Curigliano, G., Cardinale, D., Dent, S., Criscitiello, C., Aseyev, O., Lenihan, D., et al. (2016). Cardiotoxicity of Anticancer Treatments: Epidemiology, Detection, and Management. *CA: A Cancer J. Clinicians* 66, 309–325. doi:10.3322/caac.21341

Dugbartey, G. J., Peppone, L. J., and De Graaf, I. A. M. (2016). An Integrative View of Cisplatin-Induced Renal and Cardiac Toxicities: Molecular Mechanisms, Current Treatment Challenges and Potential Protective Measures. *Toxicology* 371, 58–66. doi:10.1016/j.tox.2016.10.001

El-Abbassi, A., Kiai, H., and Hafidi, A. (2012). Phenolic Profile and Antioxidant Activities of Olive Mill Wastewater. *Food Chem.* 132, 406–412. doi:10.1016/j.foodchem.2011.11.013

El-Awady, E.-S. E., Moustafa, Y. M., Abo-Elmatty, D. M., and Radwan, A. (2011). Cisplatin-induced Cardiotoxicity: Mechanisms and Cardioprotective Strategies. *Eur. J. Pharmacol.* 650, 335–341. doi:10.1016/j.ejphar.2010.09.085

El-Readi, M. Z., Al-Abd, A. M., Althubiti, M. A., Almaimani, R. A., Al-Amoodi, H. S., Ashour, M. L., et al. (2021). Multiple Molecular Mechanisms to Overcome Multidrug Resistance in Cancer by Natural Secondary Metabolites. *Front. Pharmacol.* 12, 658513. doi:10.3389/fphar.2021.658513

Eskandari, M. R., Moghaddam, F., Shahraki, J., and Pourahmad, J. (2015). A Comparison of Cardiomyocyte Cytotoxic Mechanisms for 5-fluorouracil and its Pro-drug Capecitabine. *Xenobiotica* 45, 79–87. doi:10.3109/00498254.2014.942809

Estruch, R., Ros, E., Salas-Salvadó, J., Covas, M.-I., Corella, D., Arós, F., et al. (2018). Primary Prevention of Cardiovascular Disease with a Mediterranean Diet Supplemented with Extra-Virgin Olive Oil or Nuts. *N. Engl. J. Med.* 378, e34. doi:10.1056/nejmoa1800389

Fiorentino, S., Uruena, C., Lasso, P., Prieto, K., and Barreto, A. (2020). Phyto-Immunotherapy, a Complementary Therapeutic Option to Decrease Metastasis and Attack Breast Cancer Stem Cells. *Front. Oncol.* 10, 1334. doi:10.3389/fonc.2020.01334

Focaccetti, C., Bruno, A., Magnani, E., Bartolini, D., Principi, E., Dallaglio, K., et al. (2015). Effects of 5-fluorouracil on Morphology, Cell Cycle, Proliferation, Apoptosis, Autophagy and ROS Production in Endothelial Cells and Cardiomyocytes. *PLoS One* 10, e0115686. doi:10.1371/journal.pone.0115686

Gallazzi, M., Festa, M., Corradino, P., Sansone, C., Albini, A., and Noonan, D. M. (2020). An Extract of Olive Mill Wastewater Downregulates Growth, Adhesion and Invasion Pathways in Lung Cancer Cells: Involvement of CXCR4. *Nutrients* 12, 903. doi:10.3390/nu12040903

Gogvadze, V., Orrenius, S., and Zhivotovsky, B. (2009). Mitochondria as Targets for Cancer Chemotherapy. *Semin. Cancer Biol.* 19, 57–66. doi:10.1016/j.semcancer.2008.11.007

Gorini, S., De Angelis, A., Berrino, L., Malara, N., Rosano, G., and Ferraro, E. (2018). Chemotherapeutic Drugs and Mitochondrial Dysfunction: Focus on Doxorubicin, Trastuzumab, and Sunitinib. *Oxid Med. Cel Longev* 2018, 7582730. doi:10.1155/2018/7582730

Grosso, G., Mistretta, A., Frigiola, A., Gruttadauria, S., Biondi, A., Basile, F., et al. (2014). Mediterranean Diet and Cardiovascular Risk Factors: a Systematic Review. *Crit. Rev. Food Sci. Nutr.* 54, 593–610. doi:10.1080/10408398.2011.596955

Hahn, V. S., Lenihan, D. J., and Ky, B. (2014). Cancer Therapy-Induced Cardiotoxicity: Basic Mechanisms and Potential Cardioprotective Therapies. *J. Am. Heart Assoc.* 3, e000665. doi:10.1161/jaha.113.000665

Herrmann, J., Yang, E. H., Iliescu, C. A., Cilingiroglu, M., Charitakis, K., Hakeem, A., et al. (2016). Vascular Toxicities of Cancer Therapies. *Circulation* 133, 1272–1289. doi:10.1161/circulationaha.115.018347

Ichikawa, Y., Ghanefar, M., Bayeva, M., Wu, R., Khechaduri, A., Prasad, S. V. N., et al. (2014). Cardiotoxicity of Doxorubicin Is Mediated through Mitochondrial Iron Accumulation. *J. Clin. Invest.* 124, 617–630. doi:10.1172/jci72931

Kaiserová, H., Šimůnek, T., Van Der Vijgh, W. J. F., Bast, A., and Kvasničková, E. (2007). Flavonoids as Protectors against Doxorubicin Cardiotoxicity: Role of Iron Chelation, Antioxidant Activity and Inhibition of Carbonyl Reductase. *Biochim. Biophys. Acta (Bba) - Mol. Basis Dis.* 1772, 1065–1074. doi:10.1016/j.bbadis.2007.05.002

Kalyanaraman, B. (2020). Teaching the Basics of the Mechanism of Doxorubicin-Induced Cardiotoxicity: Have We Been Barking up the Wrong Tree? *Redox Biol.* 29, 101394. doi:10.1016/j.redox.2019.101394

Kim, C.-W., and Choi, K.-C. (2021). Effects of Anticancer Drugs on the Cardiac Mitochondrial Toxicity and Their Underlying Mechanisms for Novel Cardiac Protective Strategies. *Life Sci.* 277, 119607. doi:10.1016/j.lfs.2021.119607

Krajka-Kuźniak, V., Szaefer, H., Ignatowicz, E., Adamska, T., Oszmiański, J., and Baer-Dubowska, W. (2009). Effect of Chokeberry (Aronia Melanocarpa) Juice on the Metabolic Activation and Detoxication of Carcinogenic N-Nitrosodiethylamine in Rat Liver. *J. Agric. Food Chem.* 57, 5071–5077. doi:10.1021/jf803973y

Li, K., Teng, C., and Min, Q. (2020). Advanced Nanovehicles-Enabled Delivery Systems of Epigallocatechin Gallate for Cancer Therapy. *Front. Chem.* 8, 573297. doi:10.3389/fchem.2020.573297

Ma, H., Jones, K. R., Guo, R., Xu, P., Shen, Y., and Ren, J. (2010). Cisplatin Compromises Myocardial Contractile Function and Mitochondrial Ultrastructure: Role of Endoplasmic Reticulum Stress. *Clin. Exp. Pharmacol. Physiol.* 37, 460–465. doi:10.1111/j.1440-1681.2009.05323.x

Ma, W., Wei, S., Zhang, B., and Li, W. (2020). Molecular Mechanisms of Cardiomyocyte Death in Drug-Induced Cardiotoxicity. *Front Cel Dev Biol.* 8, 434. doi:10.3389/fcell.2020.00434

Marcelino, G., Hiane, P. A., Freitas, K. C., Santana, L. F., Pott, A., Donadon, J. R., et al. (2019). Effects of Olive Oil and its Minor Components on Cardiovascular Diseases, Inflammation, and Gut Microbiota. *Nutrients* 11, 1826. doi:10.3390/nu11081826

Martínez-González, M. A., Gea, A., and Ruiz-Canela, M. (2019). The Mediterranean Diet and Cardiovascular Health. *Circ. Res.* 124, 779–798. doi:10.1161/circresaha.118.313348

Mazzocchi, A., Leone, L., Agostoni, C., and Pali-Scholl, I. (2019). The Secrets of the Mediterranean Diet. Does [Only] Olive Oil Matter? *Nutrients* 11, 2941. doi:10.3390/nu11122941

Missiroli, S., Genovese, I., Perrone, M., Vezzani, B., Vitto, V. a. M., and Giorgi, C. (2020). The Role of Mitochondria in Inflammation: From Cancer to Neurodegenerative Disorders. *J. Clin. Med.* 9. doi:10.3390/jcm9030740

Nediani, C., Ruzzolini, J., Romani, A., and Calorini, L. (2019). Oleuropein, a Bioactive Compound from Olea Europaea L., as a Potential Preventive and Therapeutic Agent in Non-communicable Diseases. *Antioxidants (Basel)* 8. doi:10.3390/antiox8120578

Nitiss, K. C., and Nitiss, J. L. (2014). Twisting and Ironing: Doxorubicin Cardiotoxicity by Mitochondrial DNA Damage. *Clin. Cancer Res.* 20, 4737–4739. doi:10.1158/1078-0432.ccr-14-0821

Nocella, C., Cammisotto, V., Fianchini, L., D'amico, A., Novo, M., Castellani, V., et al. (2018). Extra Virgin Olive Oil and Cardiovascular Diseases: Benefits for Human Health. *Endocr. Metab. Immune Disord. Drug Targets* 18, 4–13. doi:10.2174/1871530317666171114121533

Oruganti, L., and Meriga, B. (2021). Plant Polyphenolic Compounds Potentiates Therapeutic Efficiency of Anticancer Chemotherapeutic Drugs: A Review. *Emiddt* 21, 246–252. doi:10.2174/1871530320666200807115647

Polk, A., Vaage-Nilsen, M., Vistisen, K., and Nielsen, D. L. (2013). Cardiotoxicity in Cancer Patients Treated with 5-fluorouracil or Capecitabine: a Systematic Review of Incidence, Manifestations and Predisposing Factors. *Cancer Treat. Rev.* 39, 974–984. doi:10.1016/j.ctrv.2013.03.005

Polonsky, T. S., and Decara, J. M. (2019). Risk Factors for Chemotherapy-Related Cardiac Toxicity. *Curr. Opin. Cardiol.* 34, 283–288. doi:10.1097/hco.0000000000000619

Poti, F., Santi, D., Spaggiari, G., Zimetti, F., and Zanotti, I. (2019). Polyphenol Health Effects on Cardiovascular and Neurodegenerative Disorders: A Review and Meta-Analysis. *Int. J. Mol. Sci.* 20, 351. doi:10.3390/ijms20020351

Rezk, Y. A., Balulad, S. S., Keller, R. S., and Bennett, J. A. (2006). Use of Resveratrol to Improve the Effectiveness of Cisplatin and Doxorubicin: Study in Human Gynecologic Cancer Cell Lines and in Rodent Heart. *Am. J. Obstet. Gynecol.* 194, e23–e26. doi:10.1016/j.ajog.2005.11.030

Rossi, T., Gallo, C., Bassani, B., Canali, S., Albini, A., and Bruno, A. (2014). Drink Your Prevention: Beverages with Cancer Preventive Phytochemicals. *Pol. Arch. Med. Wewn* 124, 713–722. doi:10.20452/pamw.2560

Sara, J. D., Kaur, J., Khodadadi, R., Rehman, M., Lobo, R., Chakrabarti, S., et al. (2018). 5-fluorouracil and Cardiotoxicity: a Review. *Ther. Adv. Med. Oncol.* 10, 1758835918780140. doi:10.1177/1758835918780140

Sartori, R., Romanello, V., and Sandri, M. (2021). Mechanisms of Muscle Atrophy and Hypertrophy: Implications in Health and Disease. *Nat. Commun.* 12, 330. doi:10.1038/s41467-020-20123-1

Schaffer, S., Müller, W. E., and Eckert, G. P. (2010). Cytoprotective Effects of Olive Mill Wastewater Extract and its Main Constituent Hydroxytyrosol in PC12 Cells. *Pharmacol. Res.* 62, 322–327. doi:10.1016/j.phrs.2010.06.004

Senkus, E., and Jassem, J. (2011). Cardiovascular Effects of Systemic Cancer Treatment. *Cancer Treat. Rev.* 37, 300–311. doi:10.1016/j.ctrv.2010.11.001

Shakibaei, M., Buhrmann, C., Kraehe, P., Shayan, P., Lueders, C., and Goel, A. (2014). Curcumin Chemosensitizes 5-fluorouracil Resistant MMR-Deficient Human colon Cancer Cells in High Density Cultures. *PLoS One* 9, e85397. doi:10.1371/journal.pone.0085397

Taticchi, A., Selvaggini, R., Esposto, S., Sordini, B., Veneziani, G., and Servili, M. (2019a). Physicochemical Characterization of virgin Olive Oil Obtained Using an Ultrasound-Assisted Extraction at an Industrial Scale: Influence of Olive Maturity index and Malaxation Time. *Food Chem.* 289, 7–15. doi:10.1016/j.foodchem.2019.03.041

Taticchi, A., Urbani, S., Albi, E., Servili, M., Codini, M., Traina, G., et al. (2019b). *In Vitro* Anti-inflammatory Effects of Phenolic Compounds from Moraiolo Virgin Olive Oil (MVOO) in Brain Cells via Regulating the TLR4/NLRP3 Axis, *Molecules.* 24, 4523. doi:10.3390/molecules24244523

To, K. K. W., and Cho, W. C. S. (2021). Flavonoids Overcome Drug Resistance to Cancer Chemotherapy by Epigenetically Modulating Multiple Mechanisms. *Ccdt* 21, 289–305. doi:10.2174/1568009621666210203111220

Toric, J., Markovic, A. K., Brala, C. J., and Barbaric, M. (2019). Anticancer Effects of Olive Oil Polyphenols and Their Combinations with Anticancer Drugs. *Acta Pharm.* 69, 461–482. doi:10.2478/acph-2019-0052

Varga, Z. V., Ferdinandy, P., Liaudet, L., and Pacher, P. (2015). Drug-induced Mitochondrial Dysfunction and Cardiotoxicity. *Am. J. Physiology-Heart Circulatory Physiol.* 309, H1453–H1467. doi:10.1152/ajpheart.00554.2015

Vincent, D. T., Ibrahim, Y. F., Espey, M. G., and Suzuki, Y. J. (2013). The Role of Antioxidants in the Era of Cardio-Oncology. *Cancer Chemother. Pharmacol.* 72, 1157–1168. doi:10.1007/s00280-013-2260-4

Vougogiannopoulou, K., Angelopoulou, M., Pratsinis, H., Grougnet, R., Halabalaki, M., Kletsas, D., et al. (2015). Chemical and Biological Investigation of Olive Mill Waste Water - OMWW Secoiridoid Lactones. *Planta Med.* 81, 1205–1212. doi:10.1055/s-0035-1546243

Vringer, E., and Tait, S. W. G. (2019). Mitochondria and Inflammation: Cell Death Heats up. *Front. Cel Dev Biol.* 7, 100. doi:10.3389/fcell.2019.00100

Zacchigna, S., Martinelli, V., Moimas, S., Colliva, A., Anzini, M., Nordio, A., et al. (2018). Paracrine Effect of Regulatory T Cells Promotes Cardiomyocyte Proliferation during Pregnancy and after Myocardial Infarction. *Nat. Commun.* 9, 2432. doi:10.1038/s41467-018-04908-z

Zhang, J., Lei, W., Chen, X., Wang, S., and Qian, W. (2018). Oxidative Stress Response Induced by Chemotherapy in Leukemia Treatment. *Mol. Clin. Oncol.* 8, 391–399. doi:10.3892/mco.2018.1549

Zhang, X., Hu, C., Kong, C.-Y., Song, P., Wu, H.-M., Xu, S.-C., et al. (2020). FNDC5 Alleviates Oxidative Stress and Cardiomyocyte Apoptosis in Doxorubicin-Induced Cardiotoxicity via Activating AKT. *Cell Death Differ* 27, 540–555. doi:10.1038/s41418-019-0372-z

Zheng, J., Cheng, J., Zheng, S., Feng, Q., and Xiao, X. (2018). Curcumin, A Polyphenolic Curcuminoid with its Protective Effects and Molecular Mechanisms in Diabetes and Diabetic Cardiomyopathy. *Front. Pharmacol.* 9, 472. doi:10.3389/fphar.2018.00472

Conflict of Interest: The authors declare that the research was conducted in the absence of any commercial or financial relationships that could be construed as a potential conflict of interest.

Publisher's Note: All claims expressed in this article are solely those of the authors and do not necessarily represent those of their affiliated organizations, or those of the publisher, the editors and the reviewers. Any product that may be evaluated in this article, or claim that may be made by its manufacturer, is not guaranteed or endorsed by the publisher.

frontiers in Pharmacology

ORIGINAL RESEARCH
published: 06 August 2021
doi: 10.3389/fphar.2021.668348

Macleayins A From *Macleaya* Promotes Cell Apoptosis Through Wnt/β-Catenin Signaling Pathway and Inhibits Proliferation, Migration, and Invasion in Cervical Cancer HeLa Cells

Chunmei Sai*, Wei Qin, Junyu Meng, Li-Na Gao, Lufen Huang, Zhen Zhang, Huannan Wang, Haixia Chen and Chaohua Yan

College of Pharmacy, Jining Medical University, Rizhao, China

OPEN ACCESS

Edited by:
Raghuram Kandimalla, James Graham Brown Cancer Center, United States

Reviewed by:
Balaji Chandrasekaran, University of Louisville, United States
Saba Tufail, Aligarh Muslim University, India

****Correspondence:***
Chunmei Sai
saichunmei1980@163.com

Specialty section:
This article was submitted to Pharmacology of Anti-Cancer Drugs, a section of the journal Frontiers in Pharmacology

Received: *16 February 2021*
Accepted: *29 March 2021*
Published: *06 August 2021*

Citation:
Sai C, Qin W, Meng J, Gao L-N, Huang L, Zhang Z, Wang H, Chen H and Yan C (2021) Macleayins A From Macleaya *Promotes Cell Apoptosis Through Wnt/β-Catenin Signaling Pathway and Inhibits Proliferation, Migration, and Invasion in Cervical Cancer HeLa Cells. Front. Pharmacol. 12:668348. doi: 10.3389/fphar.2021.668348*

Macleayins A (MA), a novel compound, was isolated from *Macleaya cordata* (Willd.) R. Br. *and Macleaya microcarpa* (Maxim.) Fedde. The plant species are the member of *Papaveraceae* family and have been used traditionally for diverse therapeutic purposes. According to the reported studies, the chemical constituents, as well as crude extracts of these plants, could attenuate the proliferation of several cancer cell lines, such as HL-60, A549, HepG2, and MCF-7. The current study aimed to investigate the anticervical cancer activity of MA and its related molecular mechanism. Isolation of MA was carried out using various column chromatographic methods, and its structure was elucidated with ^{1}H NMR. The cytotoxicity of MA was determined against HeLa cell lines *via* CCK-8 assay. The cell proliferation, apoptosis, cell cycle, migration, and invasion were measured by EdU labeling, Annexin-V APC/7-AAD double staining, PI staining, and transwell assay, respectively. The protein expression levels of c-Myc, *β*-catenin, cyclin D1, and MMP-7 in the cells were evaluated by western blotting. The Wnt/β-catenin signaling cascade activation was verified using the Dual-Glo® Luciferase assay. We found that MA inhibited the growth of HeLa cells at 72 h (IC_{50} = 26.88 μM) *via* inducing apoptotic process, reduced the proliferation rate by 29.89%, and decreased the cells migration and invasion as compared to the untreated group. It arrested the cell cycle at the G1 phase and its treatment inhibited the expression of related proteins c-Myc, *β*-catenin, cyclin D1, and MMP-7 in the Wnt/β-catenin signaling cascade. Further, the Wnt/β-catenin signaling cascade activation in MA-treated HeLa cells was attenuated in a dose-dependent manner. These findings demonstrate the anticancer effects of MA on a mechanistic level, thus providing a basis for MA to become a potential candidate drug for resistance of cervical carcinoma.

Keywords: Macleayins A, *Macleaya*, anticervical cancer, Wnt/β-catenin cascade, proliferation, apoptosis, migration, invasion

INTRODUCTION

According to the report of Lancet Global Health 2019, about 570,000 cervical cancer cases and 311,000 cervical cancer deaths occurred in 2018 across the globe, with 106,000 cases and 48,000 deaths reported in China. Despite vaccination campaigns against human papillomavirus (HPV), cervical carcinoma has been considered to be one of the third most prevalent carcinomas in the world. Mostly, cervical carcinoma is found to be affecting women below the age of 45 years (Siegel et al., 2019; Arbyn et al., 2020; de Felice et al., 2021). According to the stage of disease at diagnosis, the treatment strategies of cervical carcinoma particularly comprised of surgery, chemotherapy, immunotherapy, radiotherapy, and locally targeted therapy (Liu et al., 2020a; de Felice et al., 2021). However, limited treatment options can be proposed in the case of recurrent or metastatic disease. Therefore, the research on invasion and metastasis of cervical cancer has been a hot topic in recent years. The patients are often treated with chemotherapy with or without bevacizumab, but survival time is still shorter (17 months) and associated with a rapid deterioration of quality of life due to toxicity profile. (Marchetti, et al., 2018; Marchetti et al., 2020). Therefore, researchers are currently focusing on investigating the candidate drugs with relatively low toxicity for overcoming cervical carcinoma. Epidemiology and animal experiments have shown that various natural ingredients can block the occurrence and development of tumors. Hence, it is not only of theoretical value but also of practical significance to search for antitumor drugs from plant active ingredients having high efficiency and low toxicity (Bich Ngoc et al., 2020).

Macleaya cordata (Willd.) R. Br. and *M. microcarpa* (Maxim.) Fedde. plant species are the members of the *Papaveraceae* family. Among *Papaveraceae*, the most commonly known and extensively studied species is *Macleaya cordata*. It is a perennial herb and is widely found in Japan, Northwest, and South China, whereas the origin of *M. microcarpa* is in central China (Chinese Academy of Sciences, Chinese Flora Chronicle Committee, 1998; Lin et al., 2020). As traditional medical herbs in China, the majority of studies have focused on *Macleaya* due to structurally diverse and biologically active alkaloids, and their various medicinal applications, such as antitumor, anti-inflammatory, antimicrobial, and insecticidal (Lin et al., 2017; Liu Y. et al., 2020; Nguyen et al., 2020). In China, *M. cordata* has also been used to treat cancer, including thyroid cancer and cervical cancer (Ke et al., 2017; Jiang et al., 2020).

Our previous results on the chemical constituents of *M. cordata* suggested that the new compound MA suppressed cell growth of many human cancer cells, including leukemia, lung, and liver cancer (Sai et al., 2015). The compound was again isolated as part of our ongoing research on the chemical constituents of *M. microcarpa*. The antitumor activity and mechanism of this compound were further studied and the obtained results revealed that MA inhibited the growth of the HeLa cell line in a concentration-dependent manner with an IC_{50} value of 26.88 μM. Previous reports have shown that the ingredients of *M. cordata* can induce and stabilize G-quadruplex made in the proximal promoter site of the *MYC* oncogene, thereby inhibiting the expression of MYC (Gao et al., 2020). The protein expressed by MYC works as a transcription factor and is associated with cell proliferation, metastasis, and apoptotic process. This transcription factor considerably contributes to the metastasis of tumors (Wang K.-B. et al., 2019). C-Myc was one of the key downstream target proteins in the Wnt signaling cascade (Ji et al., 2013). It has been revealed that Wnt/β-catenin signaling cascade activation in an abnormal manner triggers the initiation and progression of the tumor (Wang et al., 2018). Herein, we aim to explore the underlying mechanisms through which MA regulates the Wnt/β-catenin signaling cascade, causing decreased proliferation, invasion, metastasis, and induced apoptosis of cervical carcinoma cell lines.

MATERIALS AND METHODS

Plant Material

The *M. microcarpa* fruits were obtained from Xiaguan Town, Neixiang, Nanyang County (located in the southwest of Henan

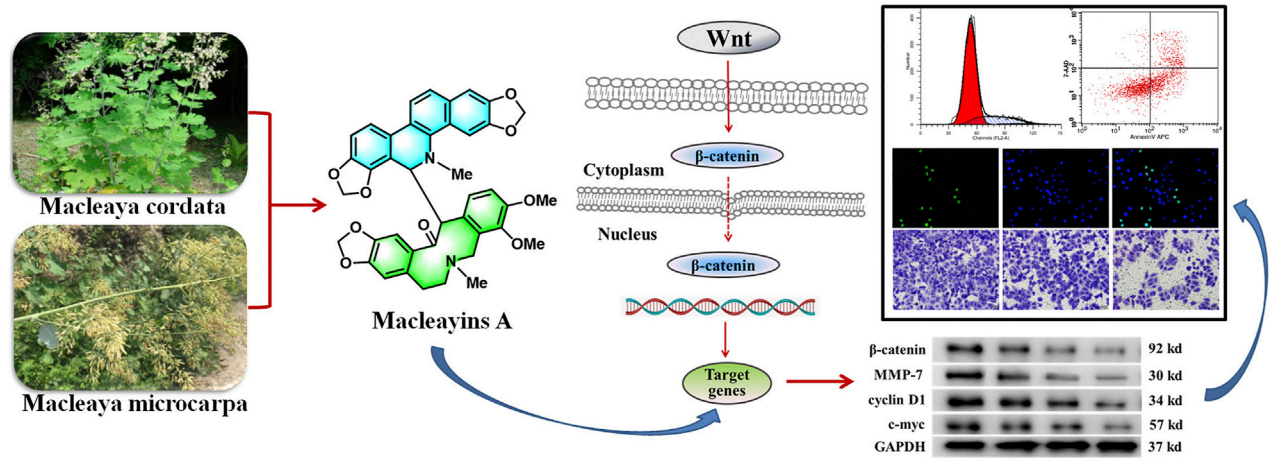

GRAPHICAL ABSTRACT |

province, China), following the national and institutional rules concerning biodiversity rights. The above plant sample was identified and the voucher sample (XGBLH-20170918) was preserved in the pharmaceutical experimental center, Jining Medical University, Rizhao, China.

Preparation of Phytochemical Constituent

The fruits of *M. microcarpa* were air-dried, followed by grinding into a coarse powder. The powder (15.0 Kg) was soaked (three times) in 95% ethanol (18 L) (Guanglian, China) for 7 days at around 20–22°C. The extracts were combined and filtered, followed by concentrating using a rotary evaporator (Yiheng, China). The obtained concentrated ethanolic extract was suspended in water, followed by extracting with petroleum ether (PE) (Fuyu, China), methylene chloride (CH_2Cl_2) (Yuandong, China), and n-BuOH (Fuyu, China). Then these diluted extracts were concentrated under vacuum to obtain PE, CH_2Cl_2, and *n*-BuOH extracts. DCM extract (365 g) was fractioned *via* silica gel column chromatography (CC) and eluted with PE (60–90°C)–ethyl acetate (100:5, 100:10, 100:20, 100:50, 1:1 and 0:100, v/v) to get six fractions (Fr.A-Fr.F). Fr.E was further separated by MCI gel (Mitsubishi, Japan) CC eluting with MeOH–H_2O (70:30, 80:20, 90:10, 100:0) to afford four subfractions (E1–E4). Subfraction E3 was purified using Sephadex LH-20 with CH_2Cl_2: MeOH (1:1) to yield compound 1 (40 mg).

The ^{1}H NMR spectra of compound 1 were measured on Bruker ARX-300 NMR spectrometers (Bruker, Switzerland). The TLC and NMR data of compound 1 were the same as MA, which was previously isolated from *M. cordata*. The structural identification of the new compound, i.e., MA, has been published in Organic Letters in 2015 by our team (Sai et al., 2015).

Cell Lines and Culture Medium

Cell lines, i.e., HeLa, SiHa (human cervical cancer), HepG2 (human liver cancer), and HFL-1 (human normal cells-human embryonic lung fibroblast) were procured from Jiangsu KeyGEN BioTECH Co., Ltd. (Nanjing, China). The HeLa, SiHa, and HepG2 cell lines were grown in 90% MEM medium, containing 10 percent of FBS. HFL-1 cells were cultured in 90% F-12K medium, containing 10% FBS. The cells incubation was carried out in humidified atmosphere (5% CO_2) at 37°C.

In Vitro Cytotoxicity Assay and Determination of IC_{50}

The cytotoxicity effect of MA was examined *via* CCK-8 assay (Wang X. et al., 2019). Cells were digested, counted, and prepared into cell suspension of 5.0×10^4 cells/mL. After that, 5.0×10^5 cells were seeded into 96-well microtiter plates, followed by incubating for 24 h in the presence of 5 percent CO_2 and 37°C temperature. The drug MA was diluted to different concentrations (100, 50, 25, 12.5, 6.25, 3.125, 1.56, 0.78, and 0.39 μM) with the complete medium; then, 100 μL of each MA dilution were added into each well. The negative control group was established. After 72 h of cultivation, following transfection, experimental wells were incubated with 10 μL/well of CCK-8 for 3 h. The absorbance was measured at a wavelength of 450 nm *via* a microplate reader (BioTek ELx800, United States). The following formula was employed to calculate the percent inhibition.

$$\text{Inhibition rate (\%)} = (\text{OD Negative control group} - \text{OD Experimental group})/\text{OD Negative control group} \times 100\%$$

The experiments were independently repeated three times. The cytotoxic ability of MA was assessed with IC_{50} obtained from probability unit weighted regression method using SPSS (Staffstical Package for the Social Science) 24.0. The results have been indicated as the mean ± SD.

Cell Proliferation Assay by EdU Labeling

The proliferation experiment on the HeLa cell line was performed *via* EdU labeling using keyFluor488Click-iT EdU Staining Proliferation Kit (KGA330, Jiangsu KeyGEN BioTECH Co., Ltd., China), following the provided instructions of the manufacturer (Li et al., 2019; Shao et al., 2020). Cell solution (1×10^4/ml, 200 μL) was seeded into a 96-well plate (Corning Incorporated 3599, United States). After 24 h of incubation (in the presence of 5 percent CO_2 and 37°C temperature), different concentrations (i.e., 0, 6.75, 13.5, and 27.0 μM) of MA-containing medium were added and cultured for 72 h. Next, the removal of media was carried out, followed by washing of cells *via* PBS twice. The addition of EDU solution (50 μM prepared with the medium) was carried out into each well, and then the incubation of cells was performed at 37°C and CO_2 (5%) for 2 h. The medium was discarded, followed by rewashing (twice) with PBS. Cell fixatives (i.e., PBS containing 4% paraformaldehyde, 50 μL) were added to each well and incubated for 0.5 h at approximately 20–22°C. Next, the fixative solution was discarded. Glycine (50 μL, 2 mg/ml) was added into each well and treated for 5 min in a decolorizing cradle (WH-2, Shanghai Huxi Analytical Instrument Factory, China) and then discarded. PBS (100 μL) was added to each well, washed with a decolorizing cradle for 5 min, and then discarded. 1 × Apollo® staining reaction solution (100 μL) was added to each well and incubated with a decolorizing cradle for 0.5 h at approximately 20–22°C in dark, and discarded. Penetrant (0.5% TritonX-100 PBS, 100 μL) was added, washed by decolorizing cradle for 2–3 times (10 min each time), and then discarded. 1 × Hoechst 33,342 reaction cocktail (100 μL) was added to each well and incubated in a decolorizing cradle for 30 min in dark at room temperature and then discarded. Images were visualized under a high-content cell imaging system (200×) (MD, United States) and combined *via* Adobe Photoshop, version 6.0. Furthermore, EdU-positive cells, as well as total cells, were calculated in each chamber. All experiments were repeated three times.

Cell Apoptosis Assay by Annexin-V APC/7-AAD Double Staining Method

Cell apoptosis was detected by Annexin-V APC/7-AAD double staining assay (Kong et al., 2019; Lin et al., 2019). HeLa cells in the logarithmic growth phase were digested and inoculated into

six-well cell culture plates (Corning Incorporated 3516, United States). The next day, after cells attached to the bottom of the plate, the underlined cells were treated with the corresponding drug-containing medium (0, 6.75, 13.5, 27.0 μM) at 37°C for 72 h. The cells were digested with 0.25% trypsin (without EDTA) and then washed twice with PBS (centrifugation at 1,000 rpm for 5 min), and 5×10^5 cells were collected. The cells were then resuspended in 500 μL of binding buffer. Finally, Annexin V–APC/7-AAD (KGA1024, Jiangsu KeyGEN BioTECH Co., Ltd., China) was added and mixed well at around 20–22°C for 15 min in the absence of light. The apoptotic process of the cells was evaluated *via* flow cytometry (Becton-Dickinson FACS Calibur, United States). All experiments were repeated thricely.

Cell Cycle Assay by a PI Staining Method

The cell cycle distribution in the presence of MA was measured by propidium iodide (PI) staining method using flow cytometry (Zhang et al., 2018). HeLa cells (5.0×10^4 cells/mL) were plated in 6-well plates, followed by 24 h incubation. The cells were then exposed to various concentrations (i.e., 0, 6.75, 13.5, and 27.0 μM) of MA at 37°C for 72 h. The cells were washed with PBS buffer and then collected and fixed with 70% EtOH for 24 h at −4°C. The fixed cells were rewashed *via* PBS, followed by 100 μL RNase-A exposure at 37°C for hrs., and, at the end, the cells were stained *via* 400 μL PI in the absence of light for 30 min at 4°C. The red fluorescence at the excitation wavelength of 488 nm was recorded by a flow cytometer (Becton-Dickinson FACS Calibur, United States). All experiments were repeated thricely.

Cell Migration and Invasion Assays

Cell migration and invasion abilities were evaluated using transwell chamber (Corning Incorporated 3422, United States) [in the absence of Matrigel for transwell migration assay/with Matrigel (BD 356234, United States) for transwell invasion assay] (Ji et al., 2013). The cells of logarithmic growth phase were digested and inoculated into a six-well plate. The next day, after the cells adhered to the wall, the serum was removed and the cells were starved in incomplete medium for 24 h. Place Matrigel adhesive at 4°C to melt overnight. Dilute the melted Matrigel glue twice with incomplete medium, add 30 μL diluted Matrigel in the upper chamber of transwell, and incubate at 37°C for 120 min to polymerize Matrigel into glue. Cells were digested and counted, and the cell density was adjusted to 1×10^5 cells/mL. The above was the Matrigel laminating process in cell invasion assay. The following were the same experimental procedures for cell migration and invasion. The following are the same experimental procedures for invasion and migration experiments. Cell suspension (100 μL) was added into the above chamber, and at the same time, 500 μL medium (comprised of FBS) was supplemented to each well of 24-well plate (Corning Incorporated 3514, United States) in the lower chamber. The plates were incubated for 24 h, followed by eliminating the upper membrane of cells *via* a cotton swab, and then transwell was removed, inverted, and air-dried, accordingly. Those migrated/invaded cells in the 24-well plates were fixed and stained with 500 μL of 0.1 percent crystal violet (Sigma C3886, United States), the chamber was plated in the dye, and the membrane was immersed in the dye for 30 min at 37°C and washed with PBS. The images of each well (containing cells) were taken and quantified in three random fields using an inverted biological microscope (at ×200 magnification, IX51, Olympus, Japan). Experiments were performed three times.

The Analysis of Protein Expression by Western Blotting

Western blotting was performed for analyzing protein expression (Zhang et al., 2013; Ma et al., 2018). The proteins were extracted by using the Whole Cell Lysis Assay KGP 250 (Jiangsu KeyGEN BioTECH Co., Ltd.), as suggested by the manufacturer. HeLa cells were harvested following treatment with macleayin A for 72 h. The proteins were extracted in lysis buffer. Protein quantification was evaluated *via* BCA Protein Assay Kit (KGA902, Jiangsu KeyGEN BioTECH Co., Ltd.). An SDS-PAGE was carried out for the separation of proteins, followed by electroblotting onto the NC membrane. Next, the membrane blockage was carried out by skimmed milk (5%) for 2 h. Membranes were incubated at 4°C for 24 h with the underlined primary antibodies: rabbit anti-β-catenin (1:5,000; Abcam; cat. no. ab32572), rabbit anti-c-Myc (1:1,000; Abcam; cat. no. ab32072), rabbit anti-cyclin D1 (1:10,000; Abcam; cat. no. ab134175), rabbit anti-MMP-7 (1:1,000; Abcam; cat. no. ab207299), and rabbit anti-GAPDH (1:5,000; cat. no. KGAA002; Jiangsu KeyGEN BioTECH Co., Ltd., China). GAPDH served as an internal control. Next, the membranes incubation was carried out with secondary antibodies, i.e., Goat Anti-Rabbit lgG HRP (KGAA35) at 25°C for 2 h. Enhanced chemiluminescence (ECL) detection system was employed for visualizing immunoreactivity. Imaging was carried out using Syngene G: Box Chemixr5 (Britain), and the grayscale of the results was examined *via* Gel-Pro32 software. All experiments were performed in triplicate.

Luciferase Assay

The culturing of HeLa cells (5×10^4 cells/well) was carried out in the presence of MA in 12-well plates. After overnight incubation, the underlined cells were cotransfected with Topflash firefly luciferase plasmid. Cells were transfected *via* Lipofectamine™ 3000 reagent. Next, the transfection of the cells was carried out for 24 h. After 72 h of MA treatment, cells were subjected to a luciferase-kit- (i.e., Dual-Glo® Luciferase assay kit, E2920, Promega) based assay according to the provided procedure of the manufacturer. The normalized firefly luciferase assay was evaluated as the quotient of firefly/Renilla luciferase activity. Experiments were performed in triplicate.

RESULTS

Analysis of Phytochemical Constituent Macleayins A

MA: This compound was obtained as a white powder with a molecular formula, i.e., $C_{41}H_{36}N_2O_9$. The underlined compound

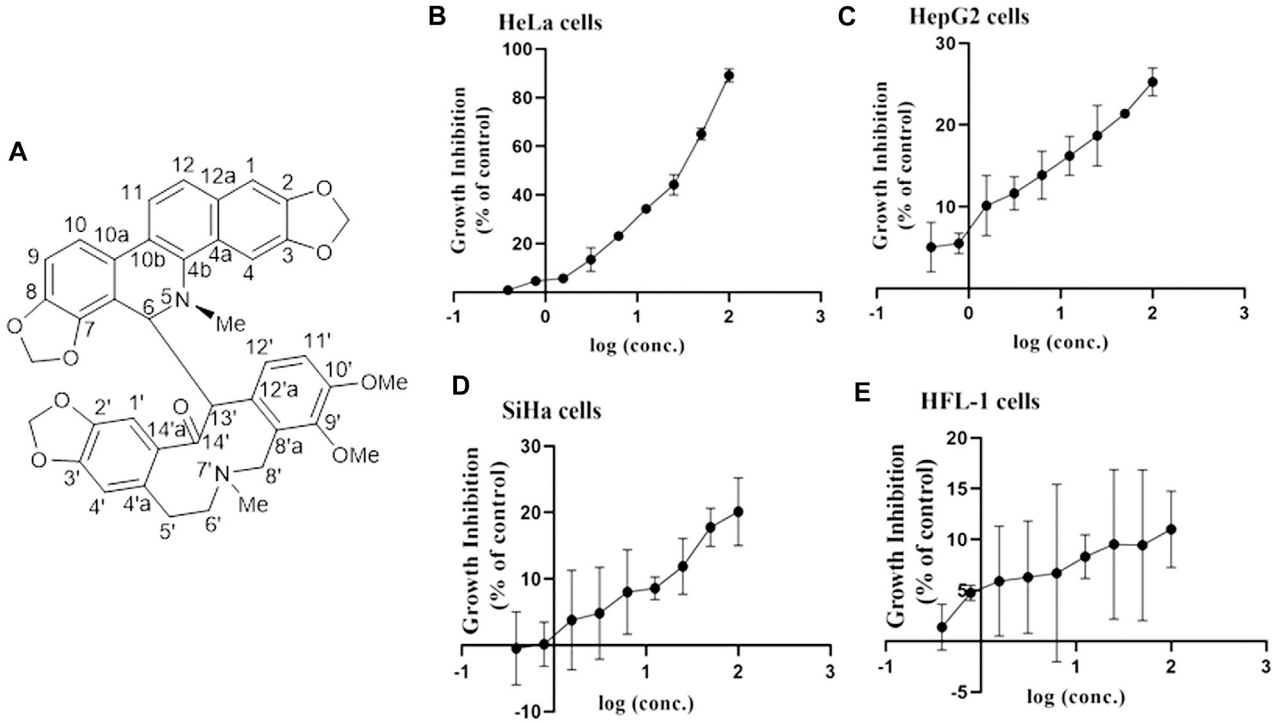

FIGURE 1 | Structure of MA and the association between inhibition of growth and MA concentrations on various cell lines. **(A)** Structure of MA. **(B)** HeLa cervical carcinoma cell line. **(C)** HepG2 liver carcinoma cell line. **(D)** SiHa cervical carcinoma cell line. **(E)** HFL-1 normal cell line. Each dot indicates the mean ± SD of triplicate experiments that were evaluated independently.

was observed as a dark speck under UV light with a wavelength of 254 nm by using silica gel TLC plates and Dragendorff's reagent. ^{1}H NMR (400 MHz, $CDCl_3$) δ: 7.01 (1H, s, H-1), 6.61 (1H, s, H-4), 4.81 (1H, d, J = 11.0 Hz, H-6), 6.57 (1H, br d, J = 7.7 Hz, H-9), 7.12 (1H, d, J = 8.1 Hz, H-10), 7.68 (1H, d, J = 8.6 Hz, H-11), 7.46 (1H, d, J = 8.6 Hz, H-12), 6.23 (1H, s, H-4′), 2.57 (1H, brs, H-5′a), 1.96 (1H, d, J = 16.3 Hz, H-5′b), 1.83 (1H, brs, H-6′a), 2.39 (1H, d, J = 12.6 Hz, H-6′b), 2.32 (1H, brs, H-8′a), 3.07 (1H, d, J = 13.4 Hz, H-8′b), 7.07 (1H, d, J = 8.5 Hz, H-11′), 7.52 (1H, brs, H-12′), 4.53 (1H, brs, H-13′), 2.49 (3H, s, 5-N-CH3), 1.52 (3H, s, 7′-N-CH3), 5.91 (1H, d, J = 1.1 Hz, 2,3-OCH2O-), 5.88 (1H, d, J = 1.1 Hz, 2,3-OCH2O-), 6.11 (1H, d, J = 1.5 Hz, 7,8-OCH2O-), 5.95 (1H, d, J = 1.3 Hz, 7,8-OCH2O-), 5.92 (1H, d, J = 1.5 Hz, 2′,3′-OCH2O-), 5.90 (1H, d, J = 1.5 Hz, 2′,3′-OCH2O-), 3.46 (3H, s, 9′-OCH3), 3.95 (3H, s, 10′-OCH3). The structure was shown in **Figure 1A**.

Cytotoxicity of Macleayins A

To investigate the antitumor activity of MA obtained from *M. microcarpa*, we first evaluated the cytotoxicity of candidate compound, i.e., MA, on different cancer cell lines. CCK-8 assay was employed to evaluate the effects of MA on the feasibility of HeLa, SiHa, HepG2, and HFL-1cells by exposing cells to various concentrations of MA, i.e., 0.39–100 μM for 72 h, respectively. The obtained results indicated that the viability of HeLa cells was considerably decreased than Siha and HepG2 cells in a dose-dependent manner, and MA had little effect on the viability of normal cell HFL-1, as depicted in **Figures 1B–E**. The IC_{50} value of MA against HeLa cells was 26.88 μM. Therefore, HeLa cells were selected for further studies on cancer and its associated mechanisms.

Effect of Macleayins A on Proliferation, Apoptosis, Migration, and Invasion of HeLa Cells

To further investigate the effects of MA on cervical carcinoma, various concentrations of MA were used and our results indicated an IC_{50} value of 27.0 μM against the HeLa cells. We have selected the various concentrations of MA, i.e., 6.75, 13.5, and 27.0 μM, for evaluating the effect of MA on the proliferation, apoptosis, invasion, and migration of the carcinoma cells. Furthermore, we examined whether the reduced number of HeLa cells by MA (in CCK-8 assays) was caused by inhibiting proliferation or inducing apoptosis. To detect and quantify the effect of MA on the attenuation of cells proliferation, EdU assay was used and the cell densities (treated with MA for 72 h) were monitored through high content cell imaging system and it has been revealed that MA inhibited EdU incorporated cell proportion in a concentration-dependent manner, as depicted in **Figures 2A,B**.

Activation of apoptotic cell death is considered an effective approach for the treatment of cancer cells (Bich Ngoc et al., 2020). The results of apoptosis assay (by Annexin-V APC/7-AAD double staining) revealed that the elevation in the concentration of MA considerably elevated the proportion of apoptotic cells (early as well as late apoptotic cells), i.e., 7.43, 23.83, 35.19, and 44.17% for 0, 6.75, 13.5, and 27 μM, accordingly, as depicted in **Figures 3A,B**.

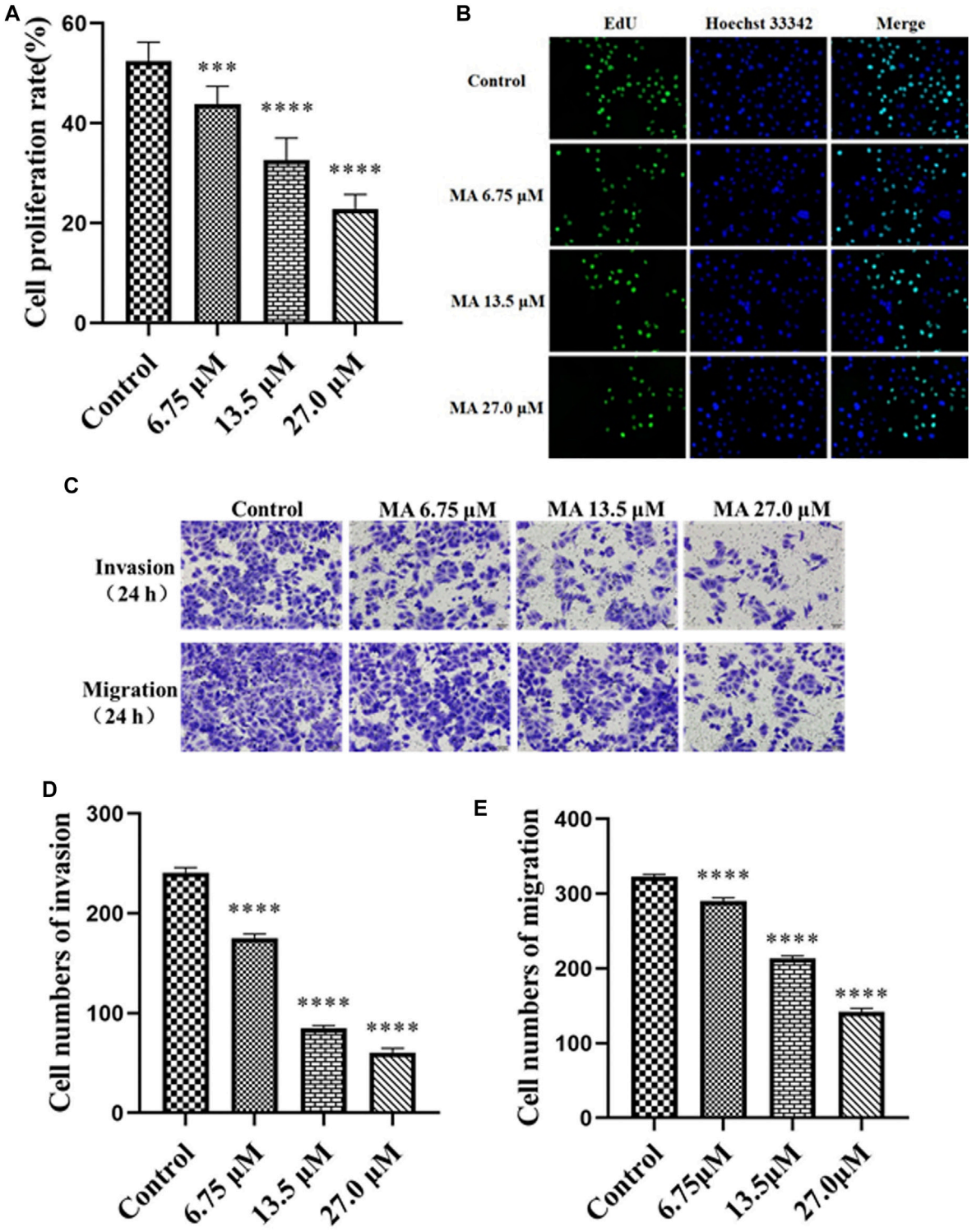

FIGURE 2 | MA inhibits the proliferation, invasion, and migration of HeLa cells. **(A)** The proliferation rate of cells treated with MA. **(B)** Images by EdU assay: cells DNA (blue) stained with Hoechst 33,342 (ab145597), green color revealed EdU/Hoechst-positive cells. **(C)** Images of cell invasion and migration by transwell assay. **(D)** The quantitative analysis of the cell invasion. **(E)** The quantitative analysis of the cell migration. Control represents the blank control group without any treatment. The results obtained from triplicate experiments (independent) are represented as mean ± SD (magnification ×200; relative to the control group, ***$p < 0.001$, **** $p < 0.0001$).

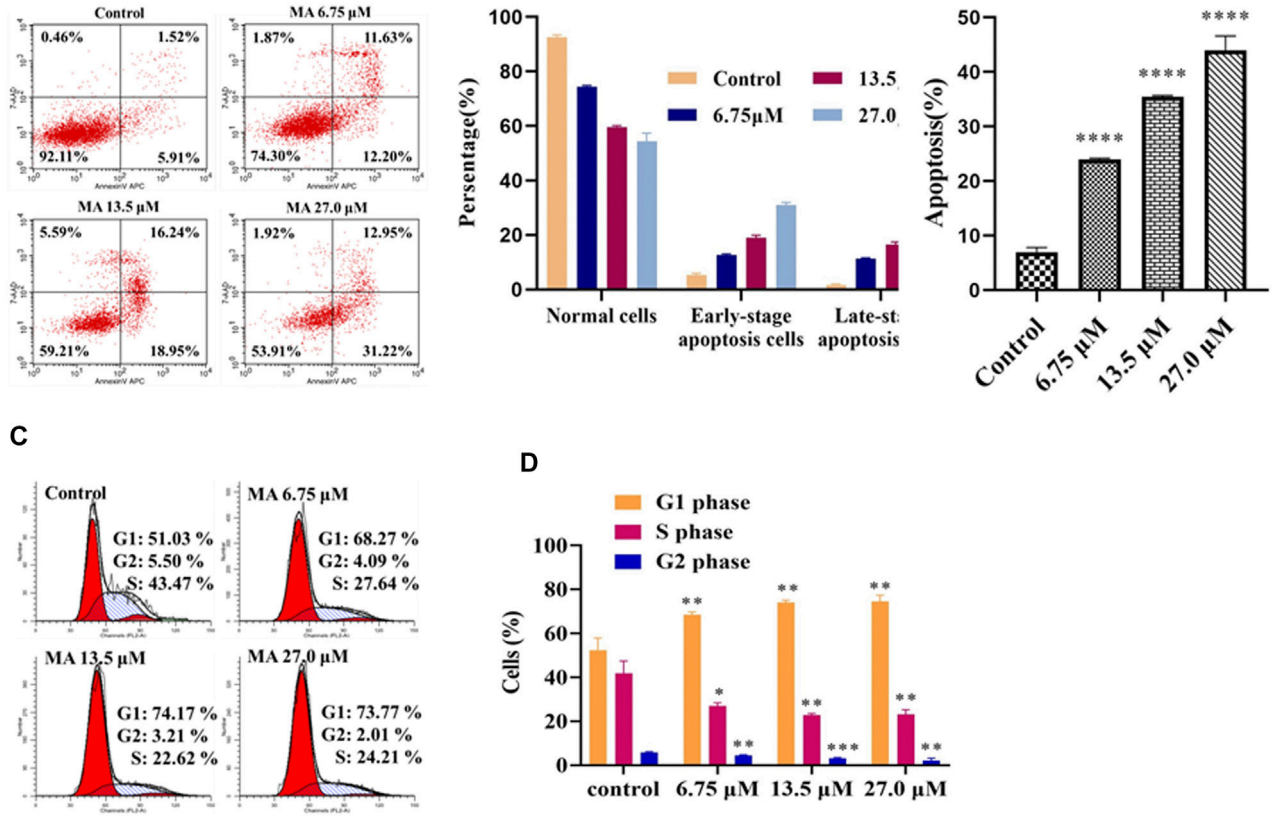

FIGURE 3 | MA enhanced the apoptotic process of HeLa cells and stimulated cell cycle arrest of HeLa cells in G0/G1 phase. **(A)** Apoptotic profile of cells treated with different concentrations of MA by Flow cytometer (Annexin-V APC/7-AAD). **Upper left** quadrant, naked nucleus cell; **upper right** quadrant, late apoptosis or necrotic cells; **lower left** quadrant, living cells; **lower right** quadrant, early apoptotic cell. **(B)** The quantitative analysis of the proportion of apoptosis was carried out. **(C)** Cell cycle distribution (left red, right red, oblique line, and white part indicate G1 phase cell, G2 phase cells, S phase cells, and total cells, accordingly). **(D)** The quantitative analysis of different phases has been indicated. The results obtained from triplicate experiments (independent) were represented as mean ± SD (relative to the control group, $^{*}p < 0.05$, $^{**}p < 0.01$, $^{***}p < 0.001$, $^{****}p < 0.0001$).

The underlined results suggested that MA induced apoptosis in HeLa cells. The above results also indicated that MA can suppress the proliferation of HeLa cells by activating the apoptotic process.

Tumor migration and invasion are necessary stages in tumorigenesis and are the most life-threatening features of cancer. The cervical cancer cells become metastatic, resulting in the migration and invasion to other tissues (Liang et al., 2016; Zhang et al., 2018). Next, we performed a transwell assay to investigate the effects of MA on HeLa cells migration and invasion. The obtained results revealed that the invasion and migration abilities of cells reduced post-MA exposure relative to the negative control group in a concentration-dependent manner, as depicted in **Figures 2C–E**. These results suggested that MA can inhibit invasion and migration in HeLa cells.

Macleayins A Stimulates G0/G1 Cell Cycle Arrest in HeLa Cells

The obtained results revealed that MA could stimulate the apoptotic process in HeLa cells. Next, we performed flow cytometry (*via* PI staining) to examine cell cycle arrest and to explore the inhibitory mechanism of cell growth. As shown in **Figure 3C**, the proportion of HeLa cells (not treated with MA) in the G1 phase was 51.03%. However, when these cells were exposed to MA, a considerable elevation was observed in the percentage of the underlined cells in a concentration-dependent manner, i.e., 68.27, 74.17, and 73.77% with 6.75, 13.5, and 27.0 μM, accordingly, as depicted in **Figure 3D**, while, in S-phase, a considerable downward trend was observed in these cells, which revealed that MA can block the cell cycle in the G1 phase.

Macleayins A Inhibits the Activation of Wnt/β-Catenin Signaling in Cervical Carcinoma

To further explore the effects of MA on the molecular mechanisms regarding the HeLa cells proliferation, apoptosis, migration, and invasion, we examined the expression of associated proteins. Western blot results showed that the protein expression levels of *β*-catenin, cyclin D1, MMP-7, and c-Myc prominently decreased after MA treatment in a dose-dependent manner (**Figures 4A,B**) which suggested the contribution of MA against the

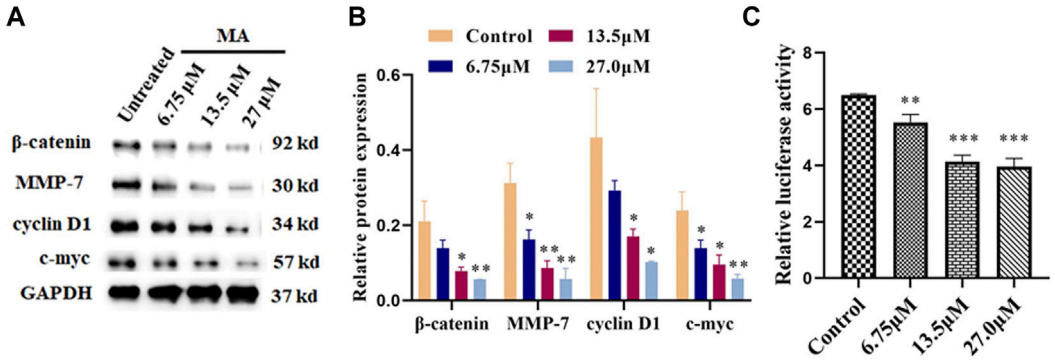

FIGURE 4 | MA inhibits the activation of Wnt/β-catenin signaling. **(A)** Western blotting images: MA decreases the protein expression levels of β-catenin, cyclin D1, MMP-7, and c-Myc. GAPDH was used as internal control. **(B)** Quantification of associated proteins. **(C)** MA decreases the luciferase activity of the Topflash firefly luciferase. The obtained results were expressed as means ± SD (n = 3) (relative to the control group, $^{*}p < 0.05$, $^{**}p < 0.01$, $^{***}p < 0.001$).

proliferation of cervical cancer cells through downregulating the expression level of the critical protein, i.e., β-catenin, cyclin D1, MMP-7, and c-Myc of Wnt/β-catenin signaling cascade.

Topflash reporter plasmid has been used to examine the level of β-catenin-mediated TCF/LEF transcription activity in the Wnt signaling cascade. Topflash is widely used to study Wnt signaling pathway (Liang et al., 2016; Xu et al., 2016). To further elucidate the direct effect of MA on Wnt/β-catenin signaling, luciferase activity was examined after cotransfection of Topflash luciferase plasmids for 12 h and HeLa cells treatment with MA for 72 h using a Dual-Glo Luciferase Assay System. As shown in **Figure 4C**, MA considerably decreased the luciferase activity of the Topflash firefly luciferase.

DISCUSSION

Cervical cancer is the fourth highly prevalent malignancy among women, and it has been an alarming disease due to its high rate of recurrence after surgery. (Liu M.-M. et al., 2020). Currently, the main treatments for cervical cancer include chemotherapy, immunotherapy, and surgical resection, while other approaches include traditional Chinese medicine (TCM). Many TCMs are having many medicinal functions that cause improvement in symptoms of cancer and decrease cancer metastasis and the risk of cancer recurrence. The effective natural products obtained from TCM have been revealed as an effective candidate against tumors (Yu et al., 2019; Yang et al., 2020). In addition, many natural products have been developed into antitumor drugs, such as paclitaxel, camptothecin, and vincristine. However, there is a need to explore their therapeutic targets and associated molecular mechanisms. Previous reports on *Macleaya* treatment of cervical cancer paid much attention to their alkaloids with anticancer activity (Jiang et al., 2020). MA is a new compound extracted from *M. cordata* and *M. microcarpa*. In our previous study, it has been revealed that MA could inhibit the growth of HL-60, A-549, MCF-7, and HeLa tumor cells, which indicated that it has potential anticancer effects. In this study, it has been revealed that MA has antitumor effects by regulating the Wnt/β-catenin signaling cascade; attenuating the proliferation, invasion, and metastasis of cervical cancer cell lines; and inducing apoptosis, which can provide a theoretical basis for evaluating potential new natural antitumor products.

In the current study, the results obtained from CCK-8 and EdU assay revealed that elevated concentrations of MA can attenuate the cancer cell proliferation through activating the apoptotic process of the HeLa cell, and the average ratio of the underlined cells apoptosis was elevated to 44%. The underlined effect was further validated by Annexin-V APC/7-AAD double staining. Early and late apoptotic cells were evaluated through flow cytometry by using Annexin V-labeled fluorescent dye APC and 7-AAD, accordingly. Therefore, the apoptosis rate in our experimental results refers to the sum of early and late apoptosis, namely the sum of apoptosis rates shown on the upper right and the lower right quadrant. It has been known that the molecular mechanism of apoptosis has been categorized into endogenous death receptor cascade and exogenous mitochondrial cascade, the core part of the apoptotic process in mitochondria. Many of their features make it possible to be used as targets to kill cancer cells (Wu et al. 2019). They are not only a sensor of the endogenous apoptotic pathway, but also act as an amplifier of apoptotic signals, allowing cell apoptosis to proceed quickly and efficiently. Up to date, the natural active products have been associated with apoptosis that exerts their antitumor effects by activating apoptosis and attenuating proliferation, invasion, and metastasis in target cells as well as tissues (Yang et al., 2017). C-Myc is an oncogene with malignant transformation, and c-Myc protein (transcription factor) has been considerably contributed to the differentiation, growth, and apoptotic process of the cell. C-Myc proto-oncogene amplification is closely related to tumor formation, development, and metastasis and is highly expressed in cervical cancer, breast cancer, gastric cancer, and other tumors (Souza et al., 2013). The main characteristic of the mitochondrial apoptotic cascade is the dysregulation of MMP. The reported studies have revealed that the MMP-7 expression has been closely associated with tumor invasion and metastasis (Sharma et al.,

2012; Liu Y. et al., 2020). In the current study, the obtained results of the transwell assay revealed that the migration, as well as invasion of HeLa cells, was effectively attenuated (malignant and invasive cell numbers decreased by 180 relative to the untreated group). Under MA treatment, we further verified that the protein expression levels of c-Myc and MMP-7 were inhibited with the increased concentration of MA (in a concentration-dependent manner) by western blot assay.

Based on the changes in cell DNA content, the growth and reproduction of proliferating cells can be divided into four stages: G1, S, G2, and M (mitosis) phase; these phases are collectively called the cell cycle (Niyonizigiye et al., 2019; Zhang et al., 2019). The proliferating cells in the tumor undergo changes in the cell cycle. Currently, researchers are trying to explore various therapeutic measures for tumor cell proliferation at different stages of the cell cycle (Sharma et al., 2012). The uncontrolled cell cycle is one of the obvious features of tumor cells, which was evaluated by identifying the inhibitory effect of MA treatment on the cell cycle *via* PI staining through flow cytometry. The obtained results revealed that the cell cycle of HeLa cells (exposed to MA) was arrested in the G1 phase (cells elevated by 22.15% than the group not exposed to MA). Cyclin D1 is a cell cycle machine and growth factor sensor that considerably contributes to the development of the G1 to S phase (Liu M.-M. et al., 2020). We analyzed the expression of a protein associated with the cell cycle arrest by western blotting and found that the expression of Cyclin D1 was reduced.

The Wnt signaling pathway is a complex pathway that regulates cell growth and proliferation (Xu, et al., 2016). The abnormal excitation of the pathway due to genetic mutation or increased stability can activate the abnormal expression of downstream target genes, including Cyclin, C-Myc, and MMP-7, which can lead to cell proliferation, inhibition of cell apoptosis, and tumor formation (Ji et al., 2013). Canonical Wnt/β-catenin pathway activates gene transcription through *β*-catenin (Zhang et al., 2013). Nuclear *β*-catenin turning on genes that promote cell division is a component of adherens junctions that interact with E-cadherin. *β*-Catenin (in free form) regulates the expression of genes by entering the nucleus. Abnormal expression or activation of *β*-catenin can cause a tumor. An elevated expression of *β*-catenin has been reported to increase the migration and invasiveness of tumor cells. Wnt signaling pathway is one of the signal transduction pathways that participate in the mechanism of tumorigenesis and has a key contribution in signal transduction, cell cycle, growth, migration, and apoptotic process, etc. (Yang et al., 2017). In this study, MA has been shown as a potential candidate against cervical cancer by suppressing the expression level of MMP-7, *β*-catenin, c-Myc, and cyclin D1 in Wnt signaling cascade. Topflash reporter plasmid has been used to determine the *β*-catenin-mediated TCF/LEF transcription activity in the Wnt signaling cascade and has been widely used to study Wnt signaling cascade (Xu et al., 2016). Therefore, we used the Topflash firefly luciferase plasmid (Sigma) through Dual Glo® luciferase reporter gene assay to further verify whether MA plays an anticervical cancer role by inhibiting the stimulation of Wnt/β-catenin cascade. The experimental results showed that MA significantly suppressed the luciferase activity of the Topflash firefly luciferase, which implied that MA can inhibit the triggering of the Wnt/β-catenin cascade. In short, our findings suggested that MA (from *Macleaya*) is a candidate natural product against cervical cancer that may delay the progression of cervical cancer through the Wnt/β-catenin signaling cascade; restrain the proliferation, migration, and invasion; and enhance the apoptotic process of cells.

In conclusion, MA, a bioactive compound of plant origin, can considerably attenuate the growth and development of cervical cancer cells, induce apoptosis, and cause cell cycle arrest in the G0/G1 phase which indicates its higher antitumor efficacy. Furthermore, the obtained results also revealed that the migration and invasion of cells were attenuated by MA exposure. Regarding the mechanism, MA might attenuate the proliferation of cells by downregulating the expression level of MMP-7, *β*-catenin, cyclin D1, and c-Myc and considerably attenuating apoptotic process in cervical cancer cells through Wnt/β-catenin signaling cascade. Thus, MA from *Macleaya* has been suggested as a potential candidate against cervical cancer.

DATA AVAILABILITY STATEMENT

The original contributions presented in the study are included in the article/**Supplementary Material**; further inquiries can be directed to the corresponding author.

AUTHOR CONTRIBUTIONS

CS and WQ designed the experiment study; CS, ZZ, HW, JM, HC, and CY performed the research; LH analyzed the data; CS wrote the paper; WQ and LG revised the paper.

FUNDING

The current study was partially sponsored by the National Natural Science Foundation of China (Grant No. 31800282), Natural Science Foundation of Shandong Province (Grant No. ZR2017LC003), and Jining Medical University National Natural Science Foundation Nurture Project (Grant No. JYP 201716).

ACKNOWLEDGMENTS

We thank all members of the Cell Laboratory for their support. We thank Jian'an Wang of the College of Pharmacy, Jining Medical University, for plant identification. We gratefully acknowledge Changshui Wang, Jining Life Science Center, for the NMR data measurements.

SUPPLEMENTARY MATERIAL

The Supplementary Material for this article can be found online at: https://www.frontiersin.org/articles/10.3389/fphar.2021.668348/full#supplementary-material

REFERENCES

Arbyn, M., Weiderpass, E., Bruni, L., de Sanjosé, S., Saraiya, M., Ferlay, J., et al. (2020). Estimates of Incidence and Mortality of Cervical Cancer in 2018: a Worldwide Analysis. *Lancet Glob. Health* 8 (2), E191–E203. doi:10.1016/s2214-109x(19)30482-6

Bich Ngoc, T. T., Hoai Nga, N. T., My Trinh, N. T., Thuoc, T. L., and Phuong Thao, D. T. (2020). Elephantopus Mollis Kunth Extracts Induce Antiproliferation and Apoptosis in Human Lung Cancer and Myeloid Leukemia Cells. *J. Ethnopharmacology* 263, 113222. doi:10.1016/j.jep.2020.113222

Chinese Academy of Sciences, Chinese Flora Chronicle Committee (1998). *Flora of China*. Beijing: Science and Technology Press.

de Felice, F., Giudice, E., Bolomini, G., Distefano, M. G., Scambia, G., Fagotti, A., et al. (2021). Pembrolizumab for Advanced Cervical Cancer: Safety and Efficacy. *Expert Rev. Anticancer Ther.* 21 (2), 221–228. doi:10.1080/14737140.2021.1850279

Gao, Y., Qin, W. W., Ge, Y. W., Sun, Y., Yan, Y. S., Zeng, Y., et al. (2020). Screening of G-Quadruplex Ligands from Macleaya Cordata Extract by Contrast Ultrafiltration with Liquid Chromatography-Mass Spectrometry and Molecular Docking. *Zhongguo Zhong Yao Za Zhi* 45 (16), 3908–3914. doi:10.19540/j.cnki.cjcmm.20200519.202

Ji, Q., Liu, X., Fu, X., Zhang, L., Sui, H., Zhou, L., et al. (2013). Resveratrol Inhibits Invasion and Metastasis of Colorectal Cancer Cells *via* MALAT1 Mediated Wnt/β-Catenin Signal Pathway. *Plos one* 8 (11), e78700. doi:10.1371/journal.pone.0078700

Jiang, C., Yang, H., Chen, X., Qiu, S., Wu, C., Zhang, B., et al. (2020). Macleaya Cordata Extracts Exert Antiviral Effects in Newborn Mice with Rotavirus-induced D-iarrhea *via* I-nhibiting the JAK2/STAT3 S-ignaling P-athway. *Exp. Ther. Med.* 20, 1137–1144. doi:10.3892/etm.2020.8766

Ke, W., Lin, X., Yu, Z., Sun, Q., and Zhang, Q. (2017). Molluscicidal Activity and Physiological Toxicity of Macleaya Cordata Alkaloids Components on Snail Oncomelania Hupensis. *Pestic. Biochem. Physiol.* 143, 111–115. doi:10.1016/j.pestbp.2017.08.016

Kong, L., Hu, W., Gao, X., Wu, Y., Xue, Y., Cheng, K., et al. (2019). Molecular Mechanisms Underlying Nickel Nanoparticle Induced Rat Sertoli-Germ Cells Apoptosis. *Sci. Total Environ.* 692, 240–248. doi:10.1016/j.scitotenv.2019.07.107

Li, J., Li, N., Yan, S., Lu, Y., Miao, X. Y., Miao, X., et al. (2019). Liraglutide Protects Renal Mesangial Cells against Hyperglycemia-mediated M-itochondrial A-poptosis by A-ctivating the ERK-Yap S-ignaling P-athway and U-pregulating Sirt3 E-xpression. *Mol. Med. Rep.* 19, 2849–2860. doi:10.3892/mmr.2019.9946

Liang, X., Li, H., Fu, D., Chong, T., Wang, Z., and Li, Z. (2016). MicroRNA-1297 Inhibits Prostate Cancer Cell Proliferation and Invasion by Targeting the AEG-1/Wnt Signaling Pathway. *Biochem. Biophysical Res. Commun.* 480, 208–214. doi:10.1016/j.bbrc.2016.10.029

Lin, C., Zhang, J., Lu, Y., Li, X., Zhang, W., Zhang, W., et al. (2018). NIT1 Suppresses Tumour Proliferation by Activating the TGFβ1-Smad2/3 Signalling Pathway in Colorectal Cancer. *Cell Death Dis.* 9, 263. doi:10.1038/s41419-018-0333-3

Lin, L., Li, X. Y., Liu, S. S., Qing, Z. X., Liu, X. B., Zeng, J. G., et al. (2020). Systematic Identification of Compounds in Macleaya Microcarpa by High-performance Liquid Chromatography/quadrupole Time-of-flight Tandem Mass Spectrometry Combined with Mass Spectral Fragmentation Behavior of Macleaya Alkaloids. *Rapid Commun. Mass. Spectrom.* 34 (9), 1–19. doi:10.1002/rcm.8715

Lin, L., Liu, Y.-C., Huang, J.-L., Liu, X.-B., Qing, Z.-X., Zeng, J.-G., et al. (2017). Medicinal Plants of the genus Macleaya (Macleaya cordata, Macleaya Microcarpa): A Review of Their Phytochemistry, Pharmacology, and Toxicology. *Phytotherapy Res.* 32, 19–48. doi:10.1002/ptr.5952

Liu, M.-M., Ma, R.-H., Ni, Z.-J., Thakur, K., Cespedes-Acuña, C. L., Wei, Z. J., et al. (2020a). Apigenin 7-O-Glucoside Promotes Cell Apoptosis through the PTEN/PI3K/AKT Pathway and Inhibits Cell Migration in Cervical Cancer HeLa Cells. *Food Chem. Toxicol.* 146, 111843. doi:10.1016/j.fct.2020.111843

Liu, Y., Wang, W., Che, F., Lu, Y., Li, A., Li, H., et al. (2020b). Isolation and Purification of Alkaloids from the Fruits of Macleaya Cordata by Ionic-liquid-modified High-speed Counter-current Chromatography. *J. Sep. Sci.* 43, 2459–2466. doi:10.1002/jssc.201901242

Ma, S., Deng, X., Yang, Y., Zhang, Q., Zhou, T., and Liu, Z. (2018). The lncRNA LINC00675 Regulates Cell Proliferation, Migration, and Invasion by Affecting Wnt/β-Catenin Signaling in Cervical Cancer. *Biomed. Pharmacother.* 108, 1686–1693. doi:10.1016/j.biopha.2018.10.011

Marchetti, C., De Felice, F., Di Pinto, A., Romito, A., Musella, A., Palaia, I., et al. (2018). Survival Nomograms after Curative Neoadjuvant Chemotherapy and Radical Surgery for Stage IB2-IIIB Cervical Cancer. *Cancer Res. Treat.* 50 (3), 768–776. doi:10.4143/crt.2017.141

Marchetti, C., Fagotti, A., Tombolini, V., Scambia, G., and De Felice, F. (2020). Survival and Toxicity in Neoadjuvant Chemotherapy Plus Surgery versus Definitive Chemoradiotherapy for Cervical Cancer: A Systematic Review and Meta-Analysis. *Cancer Treat. Rev.* 83, 101945. doi:10.1016/j.ctrv.2019.101945

Nguyen, D. T., Iqbal, J., Han, J., Pierens, G. K., Wood, S. A., Mellick, G. D., et al. (2020). Chemical Constituents from Macleaya Cordata (Willd) R. Br. And Their Phenotypic Functions against a Parkinson's Disease Patient-Derived Cell Line. *Bioorg. Med. Chem.* 28, 115732. doi:10.1016/j.bmc.2020.115732

Niyonizigiye, I., Ngabire, D., Patil, M. P., Singh, A. A., and Kim, G.-D. (2019). *In Vitro* induction of Endoplasmic Reticulum Stress in Human Cervical Adenocarcinoma HeLa Cells by Fucoidan. *Int. J. Biol. Macromolecules* 137, 844–852. doi:10.1016/j.ijbiomac.2019.07.043

Sai, C.-M., Li, D.-H., Xue, C.-M., Wang, K.-B., Hu, P., Pei, Y.-H., et al. (2015). Two Pairs of Enantiomeric Alkaloid Dimers from Macleaya Cordata. *Org. Lett.* 17, 4102–4105. doi:10.1021/acs.orglett.5b02044

Shao, B., Fu, X., Li, X., Li, Y., and Gan, N. (2020). RP11-284F21.9 Promotes Oral Squamous Cell Carcinoma Development *via* the miR-383-5p/MAL2 axis. *J. Oral Pathol. Med.* 49, 21–29. doi:10.1111/jop.12946

Sharma, C., Nusri, Q. E.-A., Begum, S., Javed, E., Rizvi, T. A., and Hussain, A. (2012). (-)-Epigallocatechin-3-Gallate Induces Apoptosis and Inhibits Invasion and Migration of Human Cervical Cancer Cells. *Asian Pac. J. Cancer Prev.* 13 (9), 4815–4822. doi:10.7314/APJCP.2012.13.9.4815

Siegel, R. L., Miller, K. D., and Jemal, A. (2019). Cancer Statistics, 2019. *CA A. Cancer J. Clin.* 69, 7–34. doi:10.3322/caac.21551

Souza, C. R. T., Leal, M. F., Calcagno, D. Q., Sozinho, E. K. C., Borges, B. N., Montenegro, R. C., et al. (2013). MYC Deregulation in Gastric Cancer and its Clinicopathological Implications. *Plos one* 8 (5), e64420. doi:10.1371/journal.pone.0064420

Wang, B., Tian, T., Kalland, K.-H., Ke, X., and Qu, Y. (2018). Targeting Wnt/β-Catenin Signaling for Cancer Immunotherapy. *Trends Pharmacol. Sci.* 39 (7), 648–658. doi:10.1016/j.tips.2018.03.008

Wang, K.-B., Elsayed, M. S. A., Wu, G., Deng, N., Cushman, M., and Yang, D. (2019a). Indenoisoquinoline Topoisomerase Inhibitors Strongly Bind and Stabilize the MYC Promoter G-Quadruplex and Downregulate MYC. *J. Am. Chem. Soc.* 141 (28), 11059–11070. doi:10.1021/jacs.9b02679

Wang, X., Li, H., and Shi, J. (2019b). LncRNA HOXA11-AS Promotes Proliferation and Cisplatin Resistance of Oral Squamous Cell Carcinoma by Suppression of miR-214-3p Expression. *Biomed. Res. Int.* 2019, 1–11. doi:10.1155/2019/8645153

Wu, X., Chen, H., Zhang, G., Wu, J., Zhu, W., Gu, Y., et al. (2019). MiR-212-3p Inhibits Cell Proliferation and Promotes Apoptosis by Targeting Nuclear Factor IA in Bladder Cancer. *J. Biosci.* 44, 80. doi:10.1007/s12038-019-9903-5

Xu, M., Wang, S., Song, Y., Yao, J., Huang, K., and Zhu, X. (2016). Apigenin Suppresses Colorectal Cancer Cell Proliferation, Migration and Invasion *via* Inhibition of the Wnt/β-Catenin Signaling Pathway. *Oncol. Lett.* 11, 3075–3080. doi:10.3892/ol.2016.4331

Yang, G., Shen, T., Yi, X., Zhang, Z., Tang, C., Wang, L., et al. (2018). Crosstalk between Long Non-coding RNA S and Wnt/β-catenin Signalling in Cancer. *J. Cell. Mol. Med.* 22, 2062–2070. doi:10.1111/jcmm.13522

Yang, T., Xu, R., Su, Q., Wang, H., Liu, F., Dai, B., et al. (2020). Chelerythrine Hydrochloride Inhibits Proliferation and Induces Mitochondrial Apoptosis in Cervical Cancer Cells *via* PI3K/BAD Signaling Pathway. *Toxicol. Vitro* 68, 104965. doi:10.1016/j.tiv.2020.104965

Yu, Y., Li, Z., Guo, R., Qian, J., Zhang, H., Zhang, J., et al. (2019). Ononin, Sec-O-β-D-Glucosylhamaudol and Astragaloside I: Antiviral lead Compounds Identified *via* High Throughput Screening and Biological Validation from Traditional Chinese Medicine Zhongjing Formulary. *Pharmacol. Res.* 145, 104248. doi:10.1016/j.phrs.2019.04.032

Zhang, D., Chen, Z.-g., Liu, S.-h., Dong, Z.-q., Dalin, M., Bao, S.-s., et al. (2013). Galectin-3 Gene Silencing Inhibits Migration and Invasion of Human Tongue Cancer Cells *In Vitro via* Downregulating β-catenin. *Acta Pharmacol. Sin.* 34, 176–184. doi:10.1038/aps.2012.150

Zhang, Y.-Y., Zhang, F., Zhang, Y.-S., Thakur, K., Zhang, J.-G., Liu, Y., et al. (2019). Mechanism of Juglone-Induced Cell Cycle Arrest and Apoptosis in Ishikawa Human Endometrial Cancer Cells. *J. Agric. Food Chem.* 67, 7378–7389. doi:10.1021/acs.jafc.9b02759

Zhang, Z.-F., Zhang, H.-R., Zhang, Q.-Y., Lai, S.-Y., Feng, Y.-Z., Zhou, Y., et al. (2018). High Expression of TMEM40 Is Associated with the Malignant Behavior and Tumorigenesis in Bladder Cancer. *J. Transl. Med.* 16, 9. doi:10.1186/s12967-017-1377-3

Conflict of Interest: The authors declare that the research was conducted in the absence of any commercial or financial relationships that could be construed as a potential conflict of interest.

Publisher's Note: All claims expressed in this article are solely those of the authors and do not necessarily represent those of their affiliated organizations, or those of the publisher, the editors and the reviewers. Any product that may be evaluated in this article, or claim that may be made by its manufacturer, is not guaranteed or endorsed by the publisher.

frontiers in Oncology

ORIGINAL RESEARCH
published: 18 August 2021
doi: 10.3389/fonc.2021.712824

Novel Butein Derivatives Repress DDX3 Expression by Inhibiting PI3K/AKT Signaling Pathway in MCF-7 and MDA-MB-231 Cell Lines

Shailima Rampogu[1,2†], Seong Min Kim[3†], Baji Shaik[4†], Gihwan Lee[1], Ju Hyun Kim[4], Gon Sup Kim[3], Keun Woo Lee[1] and Myeong Ok Kim[2*]*

[1] Division of Life Sciences, Division of Applied Life Science (BK21 Plus), Research Institute of Natural Science (RINS), Gyeongsang National University (GNU), Jinju, South Korea, [2] Division of Life Science and Applied Life Science (BK 21 Plus), College of Natural Sciences, Gyeongsang National University, Jinju, South Korea, [3] Research Institute of Life Science and College of Veterinary Medicine, Gyeongsang National University, Jinju, South Korea, [4] Department of Chemistry (BK 21 Plus), Research Institute of Natural Science (RINS), Gyeongsang National University, Jinju, South Korea

OPEN ACCESS

Edited by:
Raghuram Kandimalla, James Graham Brown Cancer Center, United States

Reviewed by:
Rajalakshmi Manikkam, Holy Cross College, India
Lalit Batra, University of Louisville, United States

***Correspondence:**
Myeong Ok Kim
mokim@gnu.ac.kr
Keun Woo Lee
kwlee@gnu.ac.kr

[†]These authors have contributed equally to this work

Specialty section:
This article was submitted to Pharmacology of Anti-Cancer Drugs, a section of the journal Frontiers in Oncology

Received: *21 May 2021*
Accepted: *10 June 2021*
Published: *18 August 2021*

Citation:
Rampogu S, Kim SM, Shaik B, Lee G, Kim JH, Kim GS, Lee KW and Kim MO (2021) Novel Butein Derivatives Repress DDX3 Expression by Inhibiting PI3K/AKT Signaling Pathway in MCF-7 and MDA-MB-231 Cell Lines. Front. Oncol. 11:712824. doi: 10.3389/fonc.2021.712824

Background: Breast cancer is one of the major causes of mortalities noticed in women globally. DDX3 has emerged as a potent target for several cancers, including breast cancer to which currently there are no reported or approved drugs.

Methods: To find effective cancer therapeutics, three compounds were computationally designed tweaking the structure of natural compound butein. These compounds were synthesized and evaluated for their anticancer property in MCF-7 and MDA-MB-231 cell lines targeting DDX3. The *in silico* molecular docking studies have shown that the compounds have occupied the binding site of the human DDX3 target. Furthermore, to investigate the cell viability effect of **3a**, **3b**, and **3c** on MCF-7 and MDA-MB-231 cell lines, the cell lines were treated with different concentrations of compounds for 24 and 48 h and measured using MTT assay.

Results: The cell viability results showed that the have induced dose dependent suppression of DDX3 expression. Additionally, **3b** and **3c** have reduced the expression of DDX3 in MCF-7 and MDA-MD-231 cell lines. **3b** or **3c** treated cell lines increased apoptotic protein expression. Both the compounds have induced the apoptotic cell death by elevated levels of cleaved PARP and cleaved caspase 3 and repression of the anti-apoptosis protein BCL-xL. Additionally, they have demonstrated the G2/M phase cell cycle arrest in both the cell lines. Additionally, **3c** decreased PI3K and AKT levels.

Conclusions: Our results shed light on the anticancer ability of the designed compounds. These compounds can be employed as chemical spaces to design new prospective drug candidates. Additionally, our computational method can be adapted to design new chemical scaffolds as plausible inhibitors.

Keywords: anticancer agents, butein, DDX3, cell cycle, apoptosis

INTRODUCTION

RNA helicases are a group of proteins possessing a unique motif, called the DEAD/H (Asp-Glu-Ala-Asp/His) (1). One of the members of the RNA helicase family, DDX3, demonstrates a wide range of roles in the process of cellular biogenesis that includes cell survival, cell-cycle regulation, cellular differentiation, and apoptosis (2). The genome of human encodes for two genes, namely DDX3X and DDX3Y. DDX3Y is present on Y-chromosome and demonstrates its role in male fertility. The gene DDX3X is present on the X-chromosome bands, p11.3– > p11.23 (2) and acts as a oncogene or tumor suppressor (1). DDX3 modulates the expression of genes at various levels. It takes part in transcriptional regulation of gene promoters, engages in splicing, performs the nuclear export of RNA, demonstrates a role in translational regulation (3). The structure of DDX3 is made up of 12 conserved motifs and two recA like domains. The X-ray structure of DDX3 was cocrystallized with the AMP located at the nucleotide-binding pocket (2). The residues from the Q motif, Arg202, and Gln207, hold the adenine group and the phosphate group is held by the P-loop residues, namely Gly227, Ser228, Gly229, Lys230, and Thr231 (2). This binding site has been exploited widely by the researchers to design and discover new chemical compounds (4–6).

DDX3 is a well-studied protein and is a known validated target to design and develop antiviral and anticancer drugs (7). DDX3 communicates with several viral and human proteins and their complexes *via* the RNA and demonstrates a double role in viral replication. Intriguingly, it works as a cofactor for viral replication and acts as a mediator of the innate immunity system (7). The association of DDX3 in cancer has been emerging in the recent times (8) and has demonstrated a significant role in progression of malignancies besides playing a key role in tumorigenesis to metastasis (8–17). Although the role of DDX3 is noticed in several cancers (1), in the current study, we focused on breast cancer targeting two cell lines, MCF-7 and MDA-MB-231, respectively.

DDX3 demonstrates an oncogenic role in breast cancer and upon its elevation may promote cell growth and proliferation (1, 10) and corresponds to distant metastasis (18), whose knockdown represses the tumor volume in vivo (19), thus demonstrating an oncogenic role in breast cancer (1). Several inhibitors were employed to target DDX3 in breast cancer. The combination of DDX3 and PARP inhibitors have brought about synthetic lethality noticed in BRCA1-proficient breast cancer (20). Another compound RK-33 has induced radiosensitization in breast cancer via the mitochondrial translation inhibition (21).

In the current investigation, we have used the butein derivatives to potentially target DDX3 in MCF-7 and MDA-MB-231 cell lines. Butein, a flavonoid, is known to have immense therapeutic potential (22), besides being an anticancer agent (23). In lung cancer cells, butein promotes apoptosis and represses the expression of cyclooxygenase-2 (24). It is reported that butein triggers the suppression of breast cancer growth by causing the reduction of the reactive oxygen species (ROS) production (25) and hindering the AKT phosphorylation. Furthermore, it was mechanistically noticed that butein elicits apoptosis by a series of mechanisms, thereby demonstrating the anti-proliferative activity (26) and can further act as aromatase inhibitor with the IC_{50} value of 3.7 μM (27). It also subsides the proliferative ability of the breast cancer cells by the formation of reactive oxygen species and regulation of ERK and p38 functions (26). Estrogen has been linked with the initiation and the progression of the disease. It was evidenced that butein could efficiently inhibit the aromatase when tested on MCF-7 cells with a minimum inhibitory concentration showing less than 5 μM (27). The purified phenolic-rich EtOAC fraction (PPEF) extracts of medicinal plant Rhus verniciflua Stokes (RVS) that contained butein, demonstrated apoptosis in breast cancer cell lines (28). Fibroblasts, the cockroaches of the human body (29), are found at all the stages of cancer, further playing a major role in promoting the growth of breast cancer. The phytochemical butein has inhibited the clonogenic growth of UACC-812, which was co-cultured with fibroblasts. Mechanistically, it can be speculated that the chalcone butein compound might intrude between the fibroblast and the breast cancer cells at as low as 2.5 μg/ml (30). It is evidenced that butein downregulates the CXC chemo receptor-4 (CXCR4) by transcriptional regulation demonstrated by the downregulation of mRNA expression, suppression of NF-κB activation, and suppression of chromatin immunoprecipitation activity, thereby hindering the process of metastasis (31). It was reported that butein repressed the formation of osteoclasts prompted by MDA-MB-231 cell lines (32).

Motivated by the aforementioned reports, in the current investigation, we have synthesized butein analogs and have tested them against MCF-7 and MDA-MB-231 cell lines, respectively. The primary objective of the study is to evaluate the anticancer potential of the new compounds and to assess their ability as DDX3 inhibitors.

METHODS

Preparation of the Parent Structure Butein

The butein structure was downloaded from the PubChem database (33) in the 2D format and was subsequently exported on to the *Discovery Studio v18* (hereinafter referred to as DS). The compound was minimized by employing the *Full Minimization* protocol accessible with DS.

Computational Designing of the Butein Compounds

Using the *Discovery Studio*, the B ring of butein was modified to obtain new structures as described in **Figure 1**, and three compounds were designed and synthesized.

Abbreviations: DEAD/H, Asp-Glu-Ala-Asp/His; BRCA1, breast cancer 1; CXCR4, CXC chemo receptor-4; CDK1, cyclin-dependent kinase 1; KCLB, Korean cell line bank; IC50, half-maximal inhibitory concentration; MD, molecular dynamics; PPEF, purified phenolic-rich EtOAC fraction; PARP, poly (ADP-ribose) polymerase; SEM, standard error of mean; TNFα, tumor necrosis factor alpha; THF, tetrahydrofuran; TBAF, tetrabutylammonium fluoride.

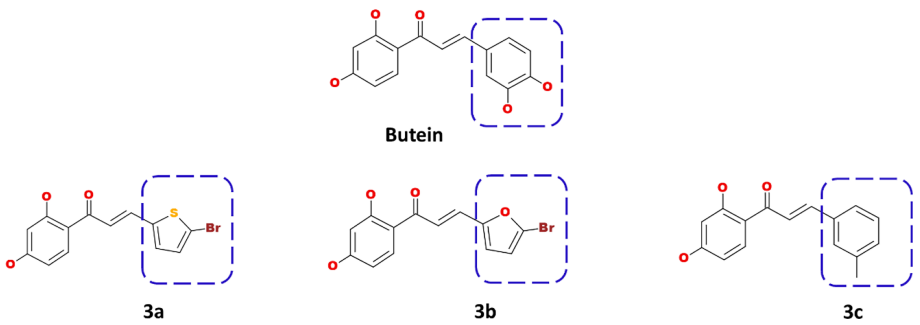

FIGURE 1 | Computational designing of butein compounds modifying the ring B as indicated in dotted box.

Binding Affinity Studies

To elucidate on their binding affinity toward the target DDX3, the molecular docking was performed using the CDOCKER program (34–37) available on DS. The CDOCKER utilized a CHARMm-based molecular dynamics (MD) strategy to dock ligands into a receptor-binding site. Correspondingly, *Random Ligand Conformations* are generated using high-temperature MD. These conformations are then translated into the binding site. The candidate poses are subsequently created using random rigid-body rotations followed by simulated annealing. A final minimization is then used to refine the ligand poses (34, 38).

The protein for the current study is the human DEAD-box RNA helicase DDX3X bearing the PDB code 2I4I cocrystallized with the AMP (39). The protein was initially prepared by initiating the *Clean Protein* tool available with the DS. Correspondingly, the heteroatoms and the water molecules were dislodged and were minimized using the *Minimization* tool available under the *Minimize and Refine Protein* protocol. The active site was marked for all the atoms and the residues around the cocrystallized AMP (39).

The synthesized butein-like compounds were docked into the active site of the protein permitting the generation of 50 conformers for each compound along with the butein compound. The best pose was selected from the largest cluster demonstrating a higher dock score, read according to the -CDOCKER interaction energy and the key residue interactions.

SYNTHESIS

Unless otherwise noted, all reactions were carried out under an atmosphere of argon in oven-dried flasks. All reagents and chemicals were purchased from Sigma Aldrich Co., TCI, or Alfa Aesar Co. Solvents, such as tetrahydrofuran (THF) and methylene chloride, were used after distillation following standard purification procedures. ^{1}H NMR spectra were recorded on a Bruker DRX-300 and chemical shifts (δ) for ^{1}H NMR spectra are given in ppm relative to TMS. Column chromatography was performed on Merck silica gel (40–63 mesh).

Synthesis of 1-(2,4-bis((tert-butyldimethylsilyl)oxy)phenyl)ethanone (2)

To a solution of 2′,4′-dihydroxyacetophenone (0.76 g, 5.0 mmol) in dry CH_2Cl_2 (5 mL) triethylamine (2.4 mL, 17.5 mmol) and 4-dimethylamino pyridine (0.06g, 0.5 mmol) were added, and then tertbutyldimethylsilyl chloride (2.11g, 14.0 mmol) dissolved in CH_2Cl_2 (9 mL) was added dropwise. After the completion of addition, the reaction mixture was allowed to stirred overnight at room temperature. The reaction mixture was quenched by the addition of water. The organic fractions were collected, and the aqueous phase was extracted with CH_2Cl_2. The combined organic fractions were washed with water and brine, dried over anhydrous $MgSO_4$, and concentrated under reduced pressure. The residue was purified by short column chromatography on silica gel using n-hexanes as the eluent to afford compound **2** (1.56 g, 82% yield) as a colorless oil; ^{1}H NMR (300 MHz, Chloroform-*d*) δ 7.62 (d, *J* = 8.6 Hz, 1H), 6.47 (dd, *J* = 8.6, 2.3 Hz, 1H), 6.32 (d, *J* = 2.3 Hz, 1H), 2.57 (s, 3H), 1.00 (s, 9H), 0.97 (s, 9H), 0.28 (s, 6H), 0.21 (s, 6H).

Synthesis of Chalcones (3a-3c)

To a solution of compound **2** (1.0 mmol) in dry THF (3 ml) under argon was added lithium diisopropylamide (LDA, 1.0 M, 1.1 ml, 1.1 mmol) dropwise at −78°C. The reaction mixture was allowed to warm to −20°C over 30 min, and then cooled to −78°C. The solution of substituted aldehyde (1.0 mmol) in dry THF (3 ml) was added dropwise at −78°C, and the resulting reaction mixture was allowed to warm to room temperature stirred overnight and then quenched by addition of sat. aqueous NH_4Cl. The organic fraction was collected, and the aqueous layer was extracted with diethyl ether. The combined organic fractions were washed with brine, dried over anhydrous $MgSO_4$, and evaporated under reduced pressure to afford the monohydroxy protected chalcones. The monohydroxy protected chalcones were purified by using CH_2Cl_2/MeOH as eluent.

The monohydroxy protected chalcone derivatives (0.2 mmol) were dissolved in THF (5 ml), and tetrabutylammonium fluoride (TBAF, 1.0 M, 0.4 mmol) was added. The resulting reaction mixture was stirred at room temperature for 30 min. and quenched by addition of water. The organic fraction was

collected, and the aqueous layer was extracted with ethyl acetate three times. The combined organic fractions were washed with brine, dried over anhydrous $MgSO_4$, and evaporated under reduced pressure. The residues were purified column chromatography on silica gel using CH_2Cl_2/MeOH as eluent to afford compounds **3a-3c** in 70% to 85% yields.

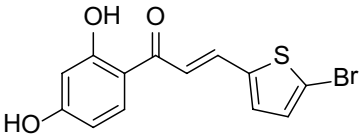

(*E*)-3-(5-bromothiophen-2-yl)-1-(2,4-dihydroxyphenyl)prop-2-en-1-one (3a)

The compound (**3a**) was synthesized by following the general procedure using monohydroxy-protected chalcone (0.10 g, 0.23 mmol) dissolved in THF (8 mL) and tetrabutylammonium fluoride (TBAF, 1.0 M, 0.46 mL, 0.46 mmol). The **3a** was purified using silica gel column CH_2Cl_2/MeOH 10: 1, v/v. Rf. Value = 0.5. Yellow solid (63 mg, 85%); ^{1}H NMR (300 MHz, Chloroform-*d*) δ 13.28 (s, 1H), 7.87 (dd, *J* = 15.1, 0.6 Hz, 1H), 7.75 (d, *J* = 8.5 Hz, 1H), 7.23 (d, *J* = 15.1 Hz, 1H), 7.12 (d, *J* = 3.9 Hz, 1H), 7.07 (d, *J* = 3.9 Hz, 1H), 6.46–6.40 (m, 2H), 5.53 (s, 1H).

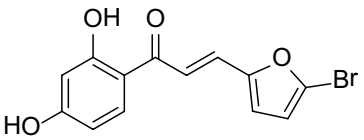

(*E*)-3-(5-bromofuran-2-yl)-1-(2,4-dihydroxyphenyl)prop-2-en-1-one (3b)

The compound (**3b**) was synthesized by following general procedure using monohydroxy-protected chalcone (0.10 g, 0.24 mmol) dissolved in THF (8 mL) and tetrabutylammonium fluoride (TBAF, 1.0 M, 0.48 mL, 0.48 mmol). The **3b** was purified using silica gel column CH_2Cl_2/MeOH 10: 1, v/v. Rf. Value =0.5. Yellow solid (52 mg, 70%); ^{1}H NMR (300 MHz, Chloroform-*d*) δ 13.34 (s, 1H), 7.84 (d, *J* = 8.5 Hz, 1H), 7.59–7.38 (m, 2H), 6.67 (d, *J* = 3.5 Hz, 1H), 6.48–6.40 (m, 3H), 5.30 (s, 1H).

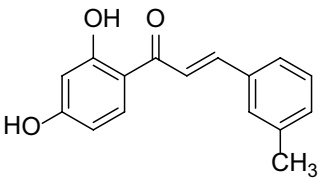

(*E*)-1-(2,4-dihydroxyphenyl)-3-(m-tolyl) prop-2-en-1-one (3c)

The compound (**3c**) was synthesized by following general procedure using monohydroxy protected chalcone (0.03 g, 0.08 mmol), was dissolved in THF (2 mL) and tetrabutylammonium fluoride (TBAF, 1.0 M, 0.16 mL, 0.16 mmol). The **3c** was purified using silica gel column CH_2Cl_2/MeOH 10: 1, v/v. Rf. Value = 0.5. Yellow solid (16 mg, 77%) (40); ^{1}H NMR (300 MHz, Chloroform-*d*) δ 13.36 (s, 1H), 7.90–7.83 (m, 2H), 7.56 (d, *J* = 15.5 Hz, 1H), 7.46 (d, *J* = 6.9 Hz, 2H), 7.23–7.35 (m, 2H), 6.47–6.41 (m, 2H), 5.47 (s, 1H), 2.41 (s, 3H); CAS. No. 1385668-91-6.

Cell Lines and Culture

Human MCF-7 and MDA-MB-231 cell lines were purchased from the Korean Cell Line Bank (KCLB, Seoul, Korea). The MCF-7 and MDA-MB-231 cell lines were maintained in RPMI-1640 medium (Gibco, Life Technologies, Carlsbad, CA, USA) containing 10% (v/v) fetal bovine serum (FBS, Gibco) and 1% penicillin–streptomycin (Gibco) at 37°C in a humidified atmosphere of 5% CO2 (41).

Cell Viability Assay

The cell viability assay was conducted as described before (42) the cells were seeded in 48 well, plated at a density of 5×10^4 cells in 500 µL medium per well for 16 h. The cultured cells were treated with various concentration for 24, 48, and 72 h. After incubation, the cells were added with 55 µl of 5 mg/ml 3-(4, 5-dimethylthiazol-2-yl)-2, 5-diphenyltetrazolium bromide (MTT; Duchefa Biochemie, Haarlem, The Netherlands) solution for 2 h, and the medium was removed, which was followed by lysis with DMSO. The absorbance at 570 nm was measured with PowerWave HT microplate spectrophotometer (BioTek, Winooski, VT, USA).

Western Blot Analysis

The Western blot analysis was performed as described before (43). After 48 h treatment of each compounds, the cells were lysed with RIPA buffer (50 mM Tris-HCl pH 7.5, 0.1% SDS, 1% Triton X-100, 150 mM NaCl, 0.5% Sodium deoxycholate, and 2 mM EDTA) containing protease/phosphatase inhibitor cocktail (Thermo Fisher Scientific, Waltham, MA, USA) at 4°C for 1 h. The supernatants were collected and quantified using BCA protein assay kit (Thermo Fisher Scientific) according to the manufacturer's instructions. To identify the molecular weight, we used Regular Range Protein marker (PM2510; SMOBIO Technology. Inc., Taiwan) and precisionplus protein dual color standard marker (Bio-Rad catalog no 1610374). Protein of 10–20 µg concentration was loaded on 8–12% sodium dodecyl sulfate polyacrylamide gel electrophoresis (SDS-PAGE), and then transferred to polyvinylidene difluoride membrane (PVDF, ATTO, Tokyo, Japan). The membranes were blocked with TBS-T buffer (Tris-buffered saline containing 0.1% Tween 20) containing 5% (w/v) skim milk power for 1 h at 25°C, and then incubated with primary antibodies for 16 h at 4°C. After incubation with the secondary antibody for 3 h at 25°C, the membranes was detected using Clarity™ Western ECL Blotting Substrates (Bio-Rad, Hercules, CA, USA).

Statistical Analysis

The data were expressed as mean ± standard error of mean (SEM) and analyzed by GraphPad Prism Version 4.0b (GraphPad Software Inc., La Jolla, CA, USA), for statistical significance using one-way analysis of variance (ANOVA). $p < 0.05$ was considered as statistically significant. All experiments were performed in triplicates.

RESULTS

Computational Designing of the Butein-Compounds

The prepared butein compound was used as the starting structure (parent structure) to computationally design new compounds. Subsequently, modifying the ring B has yielded three compounds as shown in **Figure 1**.

Binding Affinity Studies

The synthesized compounds were assessed for the binding affinity studies using the CDOCKER program. These compounds were docked into the ATP binding pocket of the DDX3 to understand their potentiality along with butein for comparative study. The results have shown that the modified compounds have demonstrated a better to comparable dock score than the parent compound butein as shown in **Table 1**.

Further, the compounds have shown interactions with the key residues positioning at the binding pocket as elucidated in **Figure 2**. The compound butein has formed hydrogen bond with the residue Arg202, as displayed in **Figure 3A**. Additionally, the key residue Tyr200 has formed the π-π stacked interaction. The **3a** has prompted hydrogen bond interactions with the residues, Thr201 and Gln207, as shown in **Figure 3B**, along with the π-π stacked interaction by Tyr200. The compound **3b** has interacted *via* hydrogen bonds with the residues, Thr231, Ala232, Gln281, and Glu285, respectively, as represented in **Figure 3C**. The key residue Tyr200 has participated by π-alkyl interaction holding the compound at the binding pocket. The compound **3c** has formed hydrogen bond interactions with the residues, Thr231, Ala232, and Gln281 residues. The residue Thr231 has formed two hydrogen bonds with the ligand as illustrated in **Figure 3D**. The key residue Tyr200 has demonstrated the π-π stacked interaction. Several other residues have clamped the ligands at the binding pocket as shown in **Supplementary 1A–C** respectively.

TABLE 1 | Molecular dock score of butein and its analogues with target DDX3.

Compound name	-CDOCKER Interaction Energy (kcal/mol)
Butein	33.23
3a	34.08
3b	34.07
3c	35.55

Synthesis of Chalcones

The syntheses of chalcones are illustrated in **Scheme 1**. All the chalcones were synthesized by aldol condensation reaction using an appropriate aldehyde and ketone as previously described in the literature method with modification. The dihydroxy ketone was protected by using TBSCl. Dihydroxy protected compound by reacting with aldehyde in the presence of LDA base resulted in the condensation product, which on desilylation by TBAF, the desired chalcones were obtained. The ^{1}H NMR spectrum data of the three compounds is provided as, **Supplementary Figures 2–4** for **3a**, **3b**, and **3c**, respectively.

Anti-Proliferative Effect of 3b and 3c

To evaluate the anti-proliferative effect of **3b** and **3c**, MTT assays were carried out on the MDA-MB-231 and MCF-7 representing the human breast cancer cell lines. **3b** and **3c** were treated with various concentration for 24, 48, and 72 h in the MDA-MB-231 and MCF-7, respectively. The cell viability on the MDA-MB-231 and MCF-7 cells was markedly decreased by **3b** and **3c** treatment

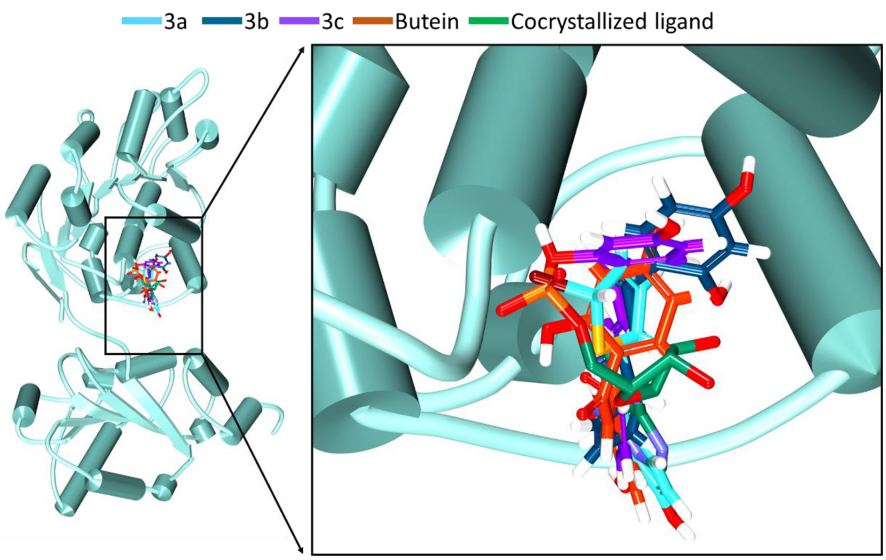

FIGURE 2 | Accommodation of the synthesized compounds at the ATP binding pocket of DDX3 in comparison with butein and the cocrystallized ligand. The new compounds have displayed a similar binding mode as that of the cocrystallized ligand.

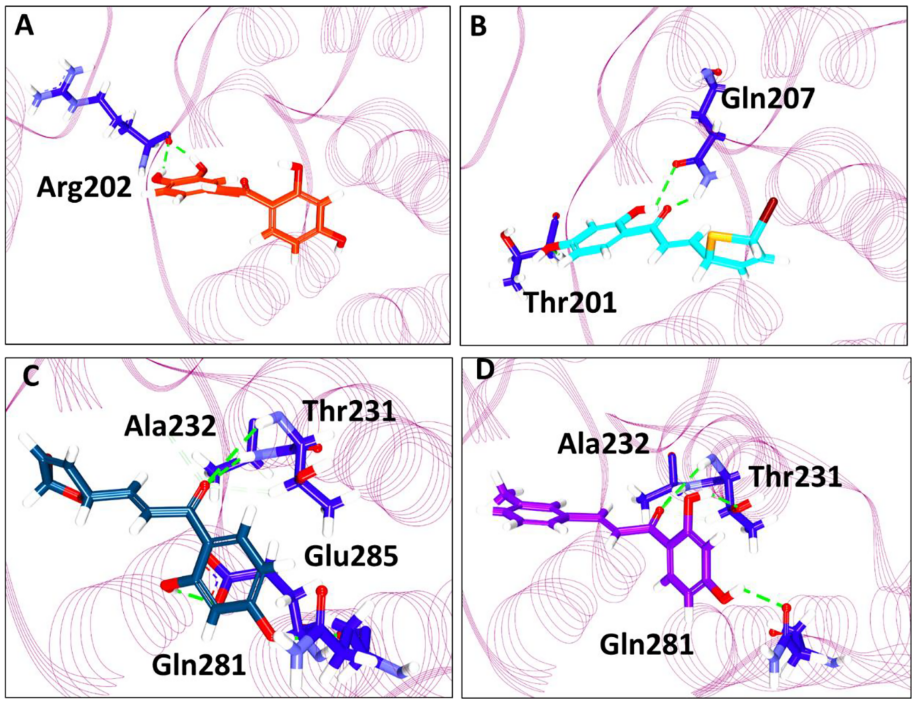

FIGURE 3 | Intermolecular interaction between the protein and the small molecules. **(A)** Interaction of compound butein. **(B)** Hydrogen bond interaction between DDX3 and **3a**. **(C)** Molecular interactions between **3b** and DDX3. **(D)** Hydrogen bond interaction of DDX3 and **3c**.

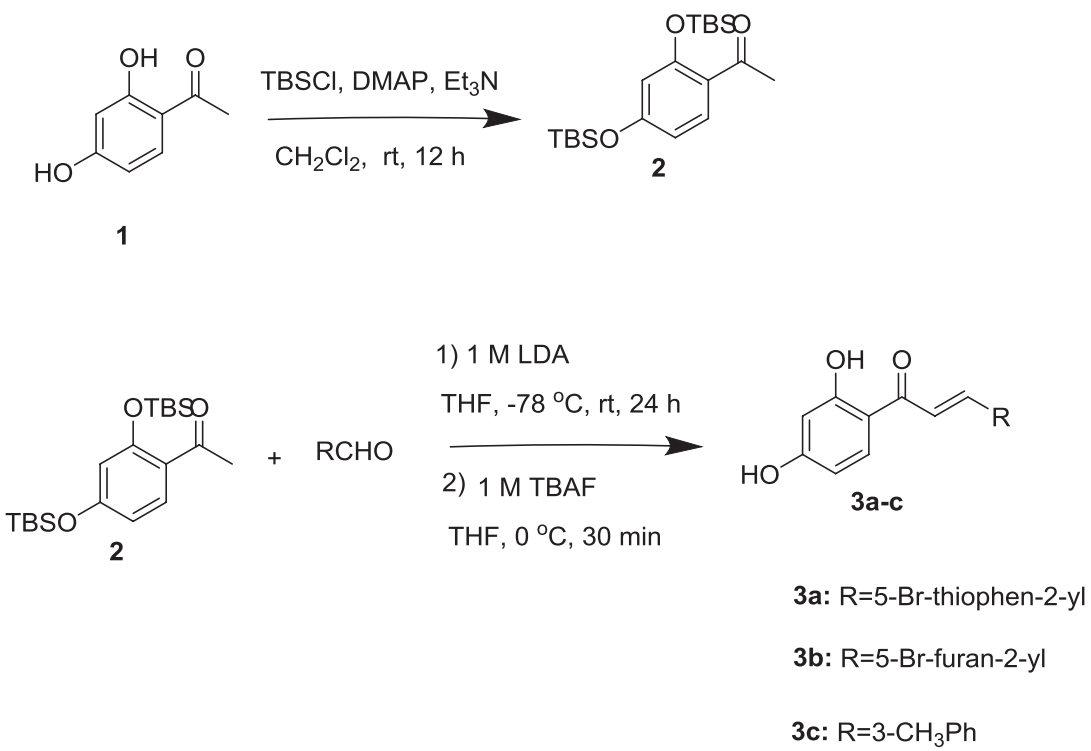

SCHEME 1 | Synthesis of chalcones.

in a dose- and time-dependent manner as shown in **Figures 4A, B**. The IC_{50} values of **3b** were recorded as 58.23 μM and 37.74 μM at 48 h in MCF-7 and MDA-MB-231 cell line, respectively. Also, IC_{50} values of **3c** were shown as 22.72 μM and 20.51 μM at 48 h in MCF-7 and MDA-MB-231 cell line, respectively. These results showed that **3b** and **3c** have anti-proliferative effect in both human cell lines. Therefore, we used 20 and 30 μM of **3a**, 25 and 50 μM of **3b**, and 10 and 20 μM of **3c** in our subsequent experiments.

Inhibition Effect of DDX3 Protein Level on 3b and 3c

Based on cell viability results, we also identified the DDX3 protein expression. The two cell lines, which include MCF-7 and MDA-MB-231 cells were treated with indicated concentration of **3a**, **3b**, or **3c**, respectively. The DDX3 protein expression was decreased dose-dependently in **3b** or **3c** treated MCF-7 and MDA-MB-231 cell lines as shown in **Figures 5A, B**, and **Supplementary Figure 5**. This data indicated that **3b** and **3c** could suppress DDX3 protein expression in MCF-7 and MDA-MB-231 cell lines. Since **3a** did not show any significant reduction of DDX3 expression, as shown in **Supplementary Figure 7**, we have not proceeded with the compound further.

Apoptosis and Cell Cycle Arrest Effect of 3b and 3c

To determine the cell death and cell cycle arrest effect on **3b** and **3c** in human breast cancer cell lines, we identified the apoptosis and cell cycle related protein expression in **3b** and **3c** treated MCF-7 and MDA-MB-231 cell lines. The apoptosis marker proteins, such as cleaved PARP and cleaved caspase 3 were increased, and anti-apoptosis protein, BCL-xL, was decreased in compound use to treat both cell lines, as shown **Figures 6A, B**, and **Supplementary Figure 6**. In addition, G2/M cell cycle arrest-related protein including CDK1 and cyclinB1, were inhibited in compound treated both cell lines. Those data

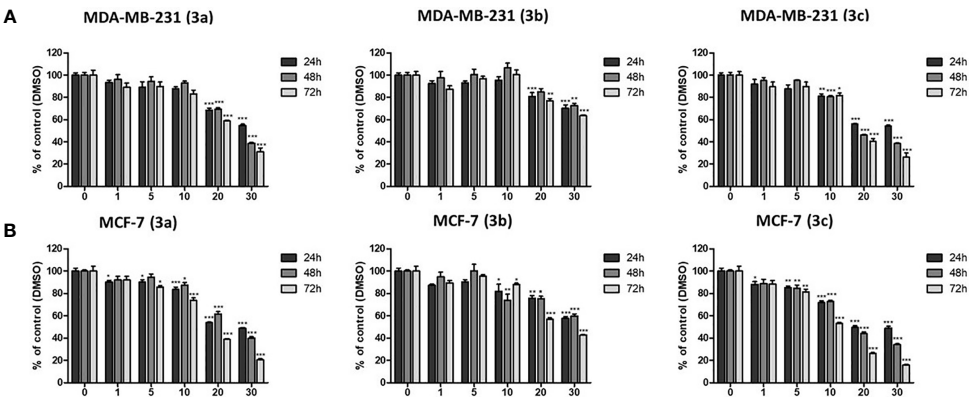

FIGURE 4 | The cytotoxic effects on **3a**, **3b**, and **3c** in MDA-MB-231, and MCF-7 cell lines. **(A)** The MDA-MB-231 and **(B)** MCF-7 cells were treated with each compounds as various concentrations (0–30 μM) for 24, 48, and 72 h. Then, the cell viability was measured by MTT assay. *$p < 0.05$ *vs*. untreated group; **$p < 0.01$ *vs*. untreated group; ***$p < 0.001$ *vs*. untreated group.

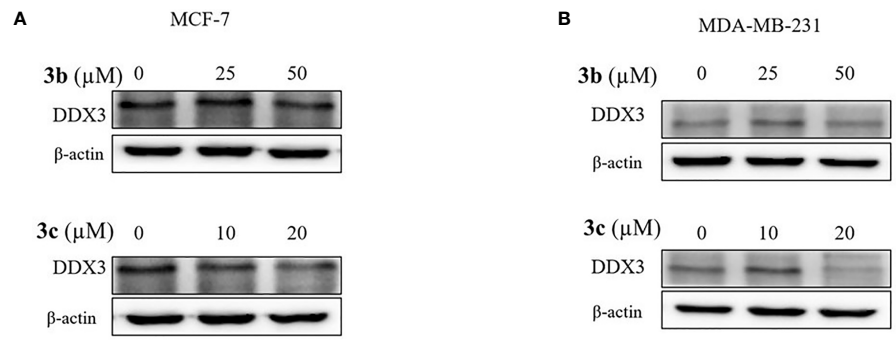

FIGURE 5 | DDX3 protein expression on **3b** and **3c** in MCF-7 and MDA-MB-231 cell lines. The **3b** and **3c** were treated with indicated concentration **(A)** MCF-7 **(B)** MDA-MB-231 cell lines for 48 h. Control group (0 μM) was treated with same amount of DMSO. Western blot analysis were conducted to identify the DDX3 protein expression. The β-actin protein was used as loading control.

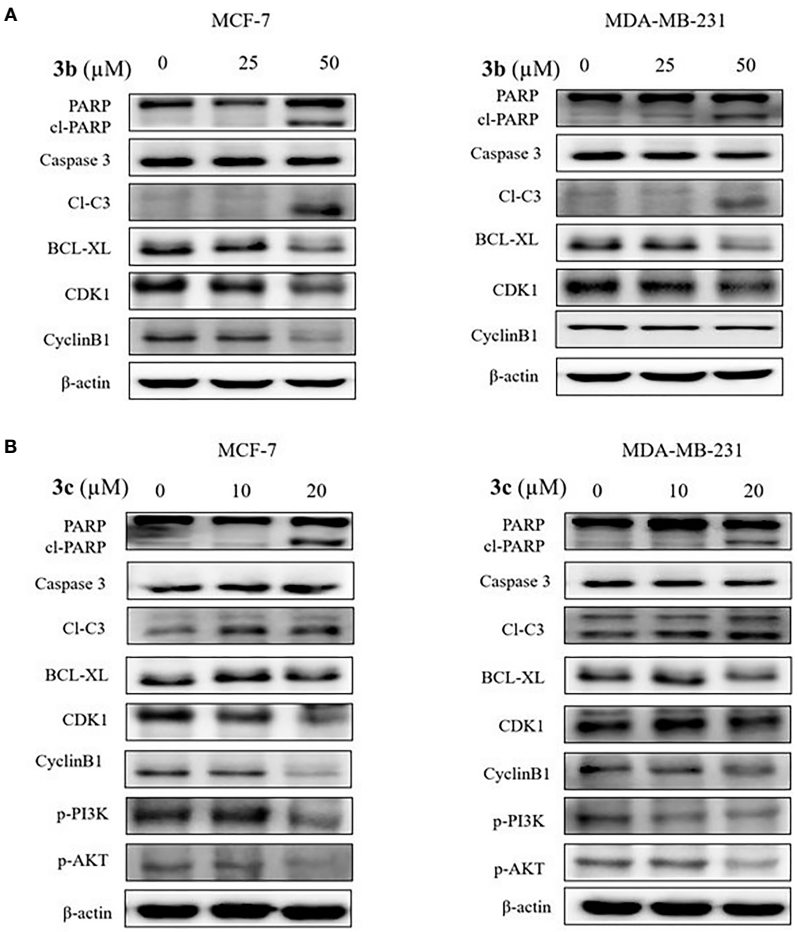

FIGURE 6 | The apoptotic cell death effects of **3b** and **3c** in MCF-7 and MDA-MB-231 cell lines. The indicated concentration of **3b** was treated in the MCF-7 and MDA-MB-231 cell lines for 48 h. **(A)** The indicated concentration of **3c** was treated in the MCF-7 and MDA-MB-231 cell lines for 48 h. **(B)** Control group (0 μM) was treated with same amount of DMSO. The apoptotic related protesins (PARP, cleaved PARP, cleaved caspase 3, BCL-XL), cell cycle related proteins (CDK1 and CyclineB1), p-PI3K and p-AKT expression levels were analyzed using Western blot. The β-actin protein was used as loading control.

suggest that **3b** and **3c** can induce apoptotic cell death and G2/M phase cell cycle arrest in MCF-7 and MDA-MB-231 cell lines, indicating anti-cancer effect, as shown in **Figures 6A, B**.

In addition, PI3K/AKT signaling pathway is an important intercellular signal involving apoptotic cell death and cell cycle arrest. Therefore, we examined the phosphorylated PI3K and AKT protein expression in the **3b** and **3c** treated human breast cancer cells. **3b** was not affective to PI3K/AKT protein change. The results showed that inhibition of PI3K and AKT activation was induced in the **3c** treated both cell lines, as shown in **Figure 6B**.

DISCUSSION

With an objective to find effective therapeutics to breast cancer, the current investigation has proceeded by tweaking the natural compound butein. Correspondingly, we have obtained three compounds. These three compounds, namely **3a**, **3b**, and **3c**, were docked into the active site of the protein target 2I4I to gain insights into the atomistic interactions. Alluringly, the three compounds have rendered an interaction with the key residue Tyr200, *via* π-π stalk interaction with **3a** and **3c**, whereas **3b** has prompted a π-alkyl interaction as shown in **Supplementary Figure 1**. Interaction with this residue is regarded to be potential as reported in previous reports (2, 4, 44). Additionally, it was reported that binding with Tyr200 phenyl ring and the imidazole-diazepine ring amplifies the binding (19). It was further noted that the compounds were accommodated at the binding pocket prompted by various residues.

To elucidate on their anti-proliferative activity in cancer cells, we proceeded with the *in vitro* MTT assay. This assay has shown a remarkable decline in the cell viability when compared with the untreated cells. The **3a** has shown an IC_{50} value of 27.44 and 26.06 μM in MCF-7 and MDA-MD-231 cell lines for 48 h, whereas the **3b** and **3c** have demonstrated 58.23 μM and 37.74 μM and 22.72 μM and 20.51 μM, respectively, in MCF-7 and MDA-MD-231 cell lines recorded at 48 hrs. Although, **3a** showed relatively stronger IC_{50} value, it has not repressed the DDX3 expression. This gives rise to the notion that **3a** might act on other

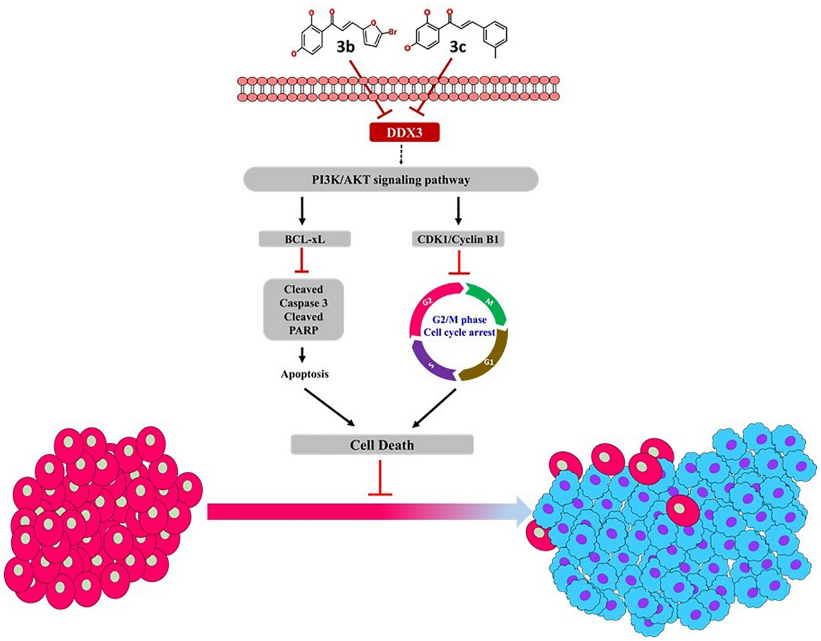

FIGURE 7 | Proposed mechanism of **3b** and **3c**.

target other than DDX3, while the **3b** and **3c** have decreased the expression of DDX3 in both the cell lines. This finding sheds light on the identification of new inhibitors against DDX3.

Fundamentally, the flavonoids promote the anticancer mechanism by instigating the apoptosis and cell cycle arrest (42). The apoptosis was studies by the expression of cleaved PARP and cleaved caspase 3 (42). Caspases broadly belong to the protease family that manifests specificity to aspartic acids. These caspases are pivotal players of apoptosis (42). Among the caspases, Caspase-8, -9, and -10 are called the instigators of apoptosis as they are capable of activating other caspases while the caspase-3, -6, and -7 are grouped as executioners because of their ability to cleave important substrates thereby killing the cell (45). One such substrate is the poly (ADP-Ribose) polymerase (PARP) that is instrumental in maintaining DNA stability and repair (45, 46). The PARP being cleaved into two fragments serves as an indication of functional caspase activation (45). Our identified compounds have triggered the elevation of the apoptosis marker protein, such as cleaved PARP and cleaved caspase 3.

The antiapoptosis protein (apoptosis inhibitor) is an eminent member of BCL-2 family of apoptosis regulators (47). This protein is elevated in certain cancers, and its role in particular to breast cancer corresponds to increased metastatic potential than the primary tumor growth (48, 49) and is a target against invasive cancer cells (50). Our finding has shown that the level of BCL-xL was downregulated by both the compounds in two cell lines. These results signify the ability of the compounds to induce apoptosis cell death.

We further extended our study to assess the effect of **3b** and **3c** on cell cycle. Cell cycle has four phases that transvers from quiescence (G0 phase) to proliferation (G1, S, G2, and M phases). The process of cell cycle occurs by the activation of cyclin-dependent kinase (CDK) and its corresponding cofactor the cyclins (51). Among the innumerable factors that are involved in the process, the activation of CDK-cyclin heterodimeric complexes are considered as the paramount steps. Furthermore, the activation of the kinases (CDKs) is closely governed by the binding to cyclins (51). Correspondingly, the cell cycle proteins, cyclin B1 and CDK1, are interconnected with the G2/M phase. The primary factor cyclin B1 switches on the mitosis could compose compound with CDK1 to adjust the G2/M phase (51). Our findings have demonstrated that **3b** and **3c** have arrested the G2/M phase and suppressed the proteins CDK1 and cyclin B1 (51). The corresponding downregulation of CDK1 and cyclin B1 may reduce the formation of CDK1-cyclin B1 complex, thereby leading to the arrest of G2/M phase. These findings put forth that **3b** and **3c** have arrested the G2/M phase by repressing the expression of proteins CDK1 and cyclin B1.

The phosphatidylinositol 3-kinase (PI3K)/protein kinase B (AKT) signaling pathway is believed to be associated with the modulation of several cellular physiological processes (52) and has an important role in the regulation of cell proliferation, the cell cycle and apoptosis (52). It is a well-known fact that inhibition of PI3K/AKT signal pathway favors the process of apoptosis in cancer cell (53, 54). Likewise, **3c** inhibited the expression level of PI3K and its downstream target AKT that is remarkably associated with cellular apoptosis. In a noteworthy observation, it was only **3c** that could inhibit the PI3K/AKT signal pathway. The proposed mechanism of inhibition is represented in **Figure 7**, and all the full blots are provided as **Supplementary Files**.

In conclusion, the present manuscript predominantly focuses on finding new therapeutics targeting DDX3. DDX3 is widely

noted target that is over expressed in several cancers. In here, the phytocompound butein has been modified at ring B position to obtain new derivatives. These new compounds have repressed DDX3 expression in two cell lines, illuminating their potential to target DDX3. Additionally, these compounds have arrested the cell cycle proteins and have shown apoptosis, remarkably extending their usability in cancer treatments. Taken together, we propose two butein derivatives as novel DDX3 inhibitors that can additionally serve as scaffolds for designing new compounds.

DATA AVAILABILITY STATEMENT

The original contributions presented in the study are included in the article/**Supplementary Material**. Further inquiries can be directed to the corresponding authors.

AUTHOR CONTRIBUTIONS

SR, GL, MK, and KL conceived the idea. SR and GL performed the computational designing and molecular docking. BS and JK have synthesized the compounds. SK and GK have performed the MTT assay and the western blot analysis. SR, BS, and SK wrote the manuscript. All authors contributed to the article and approved the submitted version.

FUNDING

This research was supported by the Bio & Medical Technology Development Program of the National Research Foundation (NRF) and funded by the Korean government (MSIT) (No. NRF-2018M3A9A7057263). This research was supported by the Neurological Disorder Research Program of the National Research Foundation (NRF) funded by the Korean Government (MSIT) (2020M3E5D9080660).

SUPPLEMENTARY MATERIAL

The Supplementary Material for this article can be found online at: https://www.frontiersin.org/articles/10.3389/fonc.2021.712824/full#supplementary-material

REFERENCES

1. He Y, Zhang D, Yang Y, Wang X, Zhao X, Zhang P, et al. A Double-Edged Function of DDX3, as an Oncogene or Tumor Suppressor, in Cancer Progression (Review). *Oncol Rep* (2018) 39:883–92. doi: 10.3892/or.2018.6203
2. Bol GM, Xie M, Raman V. DDX3, A Potential Target for Cancer Treatment. *Mol Cancer* (2015) 14:1–16. doi: 10.1186/s12943-015-0461-7
3. Ariumi Y. Multiple Functions of DDX3 RNA Helicase in Gene Regulation, Tumorigenesis, and Viral Infection. *Front Genet* (2014) 5:423. doi: 10.3389/fgene.2014.00423
4. Botlagunta M, Kollapalli B, Kakarla L, Gajarla SP, Gade SP, Dadi CL, et al. *In Vitro* Anti-Cancer Activity of Doxorubicin Against Human RNA Helicase, DDX3. *Bioinformation* (2016) 12:347–53. doi: 10.6026/97320630012347
5. Bol GM, Vesuna F, Xie M, Zeng J, Aziz K, Gandhi N, et al. Targeting DDX 3 With a Small Molecule Inhibitor for Lung Cancer Therapy. *EMBO Mol Med* (2015) 7:648–69. doi: 10.15252/emmm.201404368
6. Rampogu S, Kim SM, Son M, Baek A, Park C, Lee G, et al. A Computational Approach With Biological Evaluation: Combinatorial Treatment of Curcumin and Exemestane Synergistically Regulates Ddx3 Expression in Cancer Cell Lines. *Biomolecules* (2020) 10(6):857. doi: 10.3390/biom10060857
7. Kukhanova MK, Karpenko IL, Ivanov AV. DEAD-Box RNA Helicase DDX3: Functional Properties and Development of DDX3 Inhibitors as Antiviral and Anticancer Drugs. *Molecules* (2020) 25(4):1015. doi: 10.3390/molecules25041015
8. Mo J, Liang H, Su C, Li P, Chen J, Zhang B. DDX3X: Structure, Physiologic Functions and Cancer. *Mol Cancer* (2021) 20:38. doi: 10.1186/s12943-021-01325-7
9. Chang PC, Chi CW, Chau GY, Li FY, Tsai YH, Wu JC, et al. DDX3, a DEAD Box RNA Helicase, Is Deregulated in Hepatitis Virus-Associated Hepatocellular Carcinoma and Is Involved in Cell Growth Control. *Oncogene* (2006) 25:1991–2003. doi: 10.1038/sj.onc.1209239
10. Botlagunta M, Vesuna F, Mironchik Y, Raman A, Lisok A, Winnard P, et al. Oncogenic Role of DDX3 in Breast Cancer Biogenesis. *Oncogene* (2008) 27:3912–22. doi: 10.1038/onc.2008.33
11. Wu DW, Lin PL, Cheng YW, Huang CC, Wang L, Lee H. DDX3 Enhances Oncogenic KRAS-Induced Tumor Invasion in Colorectal Cancer *Via* the β-Catenin/ZEB1 Axis. *Oncotarget* (2016) 7:22687–99. doi: 10.18632/oncotarget.8143
12. Wu DW, Lee MC, Wang J, Chen CY, Cheng YW, Lee H. DDX3 Loss by p53 Inactivation Promotes Tumor Malignancy *Via* the MDM2/Slug/E-cadherin Pathway and Poor Patient Outcome in Non-Small-Cell Lung Cancer. *Oncogene* (2014) 33:1515–26. doi: 10.1038/onc.2013.107
13. Liang S, Yang Z, Li D, Miao X, Yang L, Zou Q, et al. The Clinical and Pathological Significance of Nectin-2 and DDX3 Expression in Pancreatic Ductal Adenocarcinomas. *Dis Markers* (2015) 2015:379568. doi: 10.1155/2015/379568
14. Miao X, Yang Z-L, Xiong L, Zou Q, Yuan Y, Li J, et al. Nectin-2 and DDX3 Are Biomarkers for Metastasis and Poor Prognosis of Squamous Cell/Adenosquamous Carcinomas and Adenocarcinoma of Gallbladder. *Int J Clin Exp Pathol* (2013) 6:179–90. doi: 10.3109/07357907.2012.756113
15. Chen HH, Yu HI, Yang MH, Tarn WY. Ddx3 Activates Cbc-eIF3–Mediated Translation of uORF-Containing Oncogenic mRNAs to Promote Metastasis in HNSCC. *Cancer Res* (2018) 78(16):4512–23. doi: 10.1158/0008-5472.CAN-18-0282
16. Phung B, Cieśla M, Sanna A, Guzzi N, Beneventi G, Cao Thi Ngoc P, et al. The X-Linked Ddx3x RNA Helicase Dictates Translation Reprogramming and Metastasis in Melanoma. *Cell Rep* (2019) 27:3573–86. doi: 10.1016/j.celrep.2019.05.069
17. Brandimarte L, Pierini V, Di Giacomo D, Borga C, Nozza F, Gorello P, et al. New MLLT10 Gene Recombinations in Pediatric T-Acute Lymphoblastic Leukemia. *Blood* (2013) 121:5064–7. doi: 10.1182/blood-2013-02-487256
18. Heerma van Voss MR, Schrijver WAME, ter Hoeve ND, Hoefnagel LD, Manson QF, van der Wall E, et al. The Prognostic Effect of DDX3 Upregulation in Distant Breast Cancer Metastases. *Clin Exp Metastasis* (2017) 34:85–92. doi: 10.1007/s10585-016-9832-8
19. Xie M, Vesuna F, Botlagunta M, Bol GM, Irving A, Bergman Y, et al. NZ51, a Ring-Expanded Nucleoside Analog, Inhibits Motility and Viability of Breast Cancer Cells by Targeting the RNA Helicase DDX3. *Oncotarget* (2015) 6:29901–13. doi: 10.18632/oncotarget.4898
20. Heerma van Voss MR, Brilliant JD, Vesuna F, Bol GM, van der Wall E, van Diest PJ, et al. Combination Treatment Using DDX3 and PARP Inhibitors Induces Synthetic Lethality in BRCA1-Proficient Breast Cancer. *Med Oncol* (2017) 34(3):33. doi: 10.1007/s12032-017-0889-2
21. Heerma van Voss MR, Vesuna F, Bol GM, Afzal J, Tantravedi S, Bergman Y, et al. Targeting Mitochondrial Translation by Inhibiting DDX3: A Novel Radiosensitization Strategy for Cancer Treatment. *Oncogene* (2017) 34:63. doi: 10.1038/onc.2017.308

22. Padmavathi G, Roy NK, Bordoloi D, Arfuso F, Mishra S, Sethi G, et al. Butein in Health and Disease: A Comprehensive Review. *Phytomedicine* (2017) 25:118–27. doi: 10.1016/j.phymed.2016.12.002
23. Bordoloi D, Monisha J, Roy NK, Padmavathi G, Banik K, Harsha C, et al. An Investigation on the Therapeutic Potential of Butein, A Tretrahydroxychalcone Against Human Oral Squamous Cell Carcinoma. *Asian Pac J Cancer Prev* (2019) 20:3437–46. doi: 10.31557/APJCP.2019.20.11.3437
24. Li Y, Ma C, Qian M, Wen Z, Jing H, Qian D. Butein Induces Cell Apoptosis and Inhibition of Cyclooxygenase-2 Expression in A549 Lung Cancer Cells. *Mol Med Rep* (2014) 9:763–7. doi: 10.3892/mmr.2013.1850
25. Cho SG, Woo SM, Ko SG. Butein Suppresses Breast Cancer Growth by Reducing a Production of Intracellular Reactive Oxygen Species. *J Exp Clin Cancer Res* (2014) 33(1):51. doi: 10.1186/1756-9966-33-51
26. Yang L-H, Ho Y-J, Lin J-F, Yeh C-W, Kao S-H, Hsu L-S. Butein Inhibits the Proliferation of Breast Cancer Cells Through Generation of Reactive Oxygen Species and Modulation of ERK and p38 Activities. *Mol Med Rep* (2012) 6:1126–32. doi: 10.3892/mmr.2012.1023
27. Wang Y, Chan FL, Chen S, Leung LK. The Plant Polyphenol Butein Inhibits Testosterone-Induced Proliferation in Breast Cancer Cells Expressing Aromatase. *Life Sci* (2005) 77:39–51. doi: 10.1016/j.lfs.2004.12.014
28. Jin Hye K, Chan Hwa J, Bo-Hyoung J, Ho Yeon G, Jong-Hyeong P, You-Kyung C, et al. Selective Cytotoxic Effects on Human Cancer Cell Lines of Phenolic-Rich Ethyl-Acetate Fraction From Rhus Verniciflua Stokes. *Am J Chin Med* (2009) 37:609–20. doi: 10.1142/S0192415X09007090
29. Kalluri R. The Biology and Function of Fibroblasts in Cancer. *Nat Rev Cancer* (2016) 16:582–98. doi: 10.1038/nrc.2016.73
30. Samoszuk M, Tan J, Chorn G. The Chalcone Butein From Rhus Verniciflua Stokes Inhibits Clonogenic Growth of Human Breast Cancer Cells Co-Cultured With Fibroblasts. *BMC Complement Altern Med* (2005) 5:5. doi: 10.1186/1472-6882-5-5
31. Chua AWL, Hay HS, Rajendran P, Shanmugam MK, Li F, Bist P, et al. Butein Downregulates Chemokine Receptor CXCR4 Expression and Function Through Suppression of NF-κb Activation in Breast and Pancreatic Tumor Cells. *Biochem Pharmacol* (2010) 80:1553–62. doi: 10.1016/j.bcp.2010.07.045
32. Sung B, Cho SG, Liu M, Aggarwal BB. Butein, a Tetrahydroxychalcone, Suppresses Cancer-Induced Osteoclastogenesis Through Inhibition of Receptor Activator of Nuclear Factor-Kappab Ligand Signaling. *Int J Cancer* (2011) 129:2062–72. doi: 10.1002/ijc.25868
33. Kim S, Chen J, Cheng T, Gindulyte A, He J, He S, et al. PubChem 2019 Update: Improved Access to Chemical Data. *Nucleic Acids Res* (2019) 47: D1102–9. doi: 10.1093/nar/gky1033
34. Wu G, Robertson DH, Brooks CL, Vieth M. Detailed Analysis of Grid-Based Molecular Docking: A Case Study of CDOCKER - A Charmm-Based MD Docking Algorithm. *J Comput Chem* (2003) 24:1549–62. doi: 10.1002/jcc.10306
35. Rampogu S, Gajula RG, Lee G, Kim MO, Lee KW. Unravelling the Therapeutic Potential of Marine Drugs as SARS-CoV-2 Inhibitors: An Insight From Essential Dynamics and Free Energy Landscape. *Comput Biol Med* (2021) 135:104525. doi: 10.1016/j.compbiomed.2021.104525
36. Rampogu S, Lee KW. Old Drugs for New Purpose—Fast Pace Therapeutic Identification for SARS-CoV-2 Infections by Pharmacophore Guided Drug Repositioning Approach. *Bull Korean Chem Soc* (2021) 212–26. doi: 10.1002/bkcs.12171
37. Rampogu S, Lee KW. Pharmacophore Modelling-Based Drug Repurposing Approaches for SARS-CoV-2 Therapeutics. *Front Chem* (2021) 9:636362. doi: 10.3389/fchem.2021.636362
38. Rampogu S, Lee G, Kulkarni AM, Kim D, Yoon S, Kim MO, et al. Computational Approaches to Discover Novel Natural Compounds for SARS-CoV-2 Therapeutics. *ChemistryOpen* (2021) 10:593–9. doi: 10.1002/open.202000332
39. Högbom M, Collins R, van den Berg S, Jenvert RM, Karlberg T, Kotenyova T, et al. Crystal Structure of Conserved Domains 1 and 2 of the Human DEAD-Box Helicase DDX3X in Complex With the Mononucleotide Amp. *J Mol Biol* (2007) 372:150–9. doi: 10.1016/j.jmb.2007.06.050
40. Ameta KL, Rathore NS, Kumar B. Synthesis of Some Novel Chalcones and Their Facile One-Pot Conversion to 2-Aminobenzene-1, 3-Dicarbonitriles Using Malononitrile. *Analele Univ Bucuresti Chim* (2011) 20(1):15–24.
41. Lee JH, Lee HJ, Sim DY, Jung JH, Kim KR, Kim SH. Apoptotic Effect of Lambertianic Acid Through AMPK/FOXM1 Signaling in MDA-MB231 Breast Cancer Cells. *Phyther Res* (2018) 32:1755–63. doi: 10.1002/ptr.6105
42. Kim SM, Ha SE, Lee HJ, Rampogu S, Vetrivel P, Kim HH, et al. Sinensetin Induces Autophagic Cell Death Through p53-Related Ampk/Mtor Signaling in Hepatocellular Carcinoma Hepg2 Cells. *Nutrients* (2020) 12(8):2462. doi: 10.3390/nu12082462
43. Kim SM, Vetrivel P, Ha SE, Kim HH, Kim JA, Kim GS. Apigetrin Induces Extrinsic Apoptosis, Autophagy and G2/M Phase Cell Cycle Arrest Through PI3K/AKT/mTOR Pathway in AGS Human Gastric Cancer Cell. *J Nutr Biochem* (2020) 83:108427. doi: 10.1016/j.jnutbio.2020.108427
44. Lin TC. DDX3X Multifunctionally Modulates Tumor Progression and Serves as a Prognostic Indicator to Predict Cancer Outcomes. *Int J Mol Sci* (2020) 21 (1):281. doi: 10.3390/ijms21010281
45. Puig B, Tortosa A, Ferrer I. Cleaved Caspase-3, Caspase-7 and Poly (ADP-Ribose) Polymerase Are Complementarily But Differentially Expressed in Human Medulloblastomas. *Neurosci Lett* (2001) 306:85–8. doi: 10.1016/S0304-3940(01)01873-0
46. Parsons JL, Dianova II, Allinson SL, Dianov GL. Poly(ADP-Ribose) Polymerase-1 Protects Excessive DNA Strand Breaks From Deterioration During Repair in Human Cell Extracts. *FEBS J* (2005) 272:2012–21. doi: 10.1111/j.1742-4658.2005.04628.x
47. Youle RJ, Strasser A. The BCL-2 Protein Family: Opposing Activities That Mediate Cell Death. *Nat Rev Mol Cell Biol* (2008) 9:47–59. doi: 10.1038/nrm2308
48. Martin SS, Ridgeway AG, Pinkas J, Lu Y, Reginato MJ, Koh EY, et al. A Cytoskeleton-Based Functional Genetic Screen Identifies Bcl-xL as an Enhancer of Metastasis, But Not Primary Tumor Growth. *Oncogene* (2004) 23:4641–5. doi: 10.1038/sj.onc.1207595
49. Fernández Y, España L, Mañas S, Fabra A, Sierra A. Bcl-x(L) Promotes Metastasis of Breast Cancer Cells by Induction of Cytokines Resistance. *Cell Death Differ* (2000) 7:350–9. doi: 10.1038/sj.cdd.4400662
50. Keitel U, Scheel A, Thomale J, Halpape R, Kaulfuß S, Scheel C, et al. Bcl-Xl Mediates Therapeutic Resistance of a Mesenchymal Breast Cancer Cell Subpopulation. *Oncotarget* (2014) 5:11778–91. doi: 10.18632/oncotarget.2634
51. Shi-Yong G, Jun L, Xiao-Ying Q, Nan Zhu Y-BJ. Downregulation of Cdk1 and CyclinB1 Expression Contributes to Oridonin-Induced Cell Cycle Arrest at G2/M Phase and Growth Inhibition in SGC-7901 Gastric Cancer Cells. *Asian Pac J Cancer Prev* (2014) 15:6437–41. doi: 10.7314/APJCP.2014.15.15.6437
52. Shi X, Wang J, Lei Y, Cong C, Tan D, Zhou X. Research Progress on the PI3K/AKT Signaling Pathway in Gynecological Cancer (Review). *Mol Med Rep* (2019) 19:4529–35. doi: 10.3892/mmr.2019.10121
53. Hussain AR, Al-Rasheed M, Manogaran PS, Al-Hussein KA, Platanias LC, Al Kuraya K, et al. Curcumin Induces Apoptosis *Via* Inhibition of PI3′-kinase/AKT Pathway in Acute T Cell Leukemias. *Apoptosis* (2006) 11:245–54. doi: 10.1007/s10495-006-3392-3
54. Park HS, Park KIl, Lee DH, Kang SR, Nagappan A, et al. Polyphenolic Extract Isolated From Korean Lonicera Japonica Thunb. Induce G2/M Cell Cycle Arrest and Apoptosis in HepG2 Cells: Involvements of PI3K/Akt and MAPKS. *Food Chem Toxicol* (2012) 50:2407–16. doi: 10.1016/j.fct.2012.04.034

Conflict of Interest: The authors declare that the research was conducted in the absence of any commercial or financial relationships that could be construed as a potential conflict of interest.

Publisher's Note: All claims expressed in this article are solely those of the authors and do not necessarily represent those of their affiliated organizations, or those of the publisher, the editors and the reviewers. Any product that may be evaluated in this article, or claim that may be made by its manufacturer, is not guaranteed or endorsed by the publisher.

Advantages of publishing in Frontiers

OPEN ACCESS
Articles are free to read for greatest visibility and readership

FAST PUBLICATION
Around 90 days from submission to decision

HIGH QUALITY PEER-REVIEW
Rigorous, collaborative, and constructive peer-review

TRANSPARENT PEER-REVIEW
Editors and reviewers acknowledged by name on published articles

Frontiers
Avenue du Tribunal-Fédéral 34
1005 Lausanne | Switzerland

Visit us: www.frontiersin.org
Contact us: frontiersin.org/about/contact

REPRODUCIBILITY OF RESEARCH
Support open data and methods to enhance research reproducibility

DIGITAL PUBLISHING
Articles designed for optimal readership across devices

FOLLOW US
@frontiersin

IMPACT METRICS
Advanced article metrics track visibility across digital media

EXTENSIVE PROMOTION
Marketing and promotion of impactful research

LOOP RESEARCH NETWORK
Our network increases your article's readership